Analysis of Steel Frames with Deformable Beam-to-Column Connections

by
Mario J. Scerbo

A Thesis
Submitted to the Faculty of Graduate Studies in
Partial Fulfillment of the Requirements
for the Degree of

MASTER OF SCIENCE

September 1996

National Library
of Canada

Acquisitions and
Bibliographic Services Branch

395 Wellington Street
Ottawa, Ontario
K1A 0N4

Bibliothèque nationale
du Canada

Direction des acquisitions et
des services bibliographiques

395, rue Wellington
Ottawa (Ontario)
K1A 0N4

Your file Votre référence

Our file Notre référence

The author has granted an irrevocable non-exclusive licence allowing the National Library of Canada to reproduce, loan, distribute or sell copies of his/her thesis by any means and in any form or format, making this thesis available to interested persons.

L'auteur a accordé une licence irrévocable et non exclusive permettant à la Bibliothèque nationale du Canada de reproduire, prêter, distribuer ou vendre des copies de sa thèse de quelque manière et sous quelque forme que ce soit pour mettre des exemplaires de cette thèse à la disposition des personnes intéressées.

The author retains ownership of the copyright in his/her thesis. Neither the thesis nor substantial extracts from it may be printed or otherwise reproduced without his/her permission.

L'auteur conserve la propriété du droit d'auteur qui protège sa thèse. Ni la thèse ni des extraits substantiels de celle-ci ne doivent être imprimés ou autrement reproduits sans son autorisation.

ISBN 0-612-16266-4

Canada

Name _____

Dissertation Abstracts International and *Masters Abstracts International* are arranged by broad, general subject categories. Please select the one subject which most nearly describes the content of your dissertation or thesis. Enter the corresponding four-digit code in the spaces provided.

SUBJECT TERM

CIVIL ENGINEERING

SUBJECT CODE 0543

UMI

Subject Categories

THE HUMANITIES AND SOCIAL SCIENCES

COMMUNICATIONS AND THE ARTS
Architecture 0729
Art History 0377
Cinema 0900
Dance 0378
Design and Decorative Arts 0389
Fine Arts 0357
Information Science 0723
Journalism 0391
Landscape Architecture 0390
Library Science 0399
Mass Communications 0708
Music 0413
Speech Communication 0459
Theater 0465

EDUCATION
General 0515
Administration 0514
Adult and Continuing 0516
Agricultural 0517
Art 0273
Bilingual and Multicultural 0282
Business 0688
Community College 0275
Curriculum and Instruction 0727
Early Childhood 0518
Elementary 0524
Educational Psychology 0525
Finance 0277
Guidance and Counseling 0519
Health 0680
Higher 0745
History of 0520
Home Economics 0278
Industrial 0521
Language and Literature 0279
Mathematics 0280
Music 0522
Philosophy of 0998
Physical 0523
Reading 0535
Religious 0527
Sciences 0714
Secondary 0533
Social Sciences 0534
Sociology of 0340
Special 0529
Teacher Training 0530
Technology 0710
Tests and Measurements 0288
Vocational 0747

LANGUAGE, LITERATURE AND LINGUISTICS
Language
- General 0679
- Ancient 0289
- Linguistics 0290
- Modern 0291
- Rhetoric and Composition 0681

Literature
- General 0401
- Classical 0294
- Comparative 0295
- Medieval 0297
- Modern 0298
- African 0316
- American 0591
- Asian 0305
- Canadian (English) 0352
- Canadian (French) 0355
- Caribbean 0360
- English 0593
- Germanic 0311
- Latin American 0312
- Middle Eastern 0315
- Romance 0313
- Slavic and East European 0314

PHILOSOPHY, RELIGION AND THEOLOGY
Philosophy 0422
Religion
- General 0318
- Biblical Studies 0321
- Clergy 0319
- History of 0320
- Philosophy of 0322

Theology 0469

SOCIAL SCIENCES
American Studies 0323
Anthropology
- Archaeology 0324
- Cultural 0326
- Physical 0327

Business Administration
- General 0310
- Accounting 0272
- Banking 0770
- Management 0454
- Marketing 0338

Canadian Studies 0385
Economics
- General 0501
- Agricultural 0503
- Commerce-Business 0505
- Finance 0508
- History 0509
- Labor 0510
- Theory 0511

Folklore 0358
Geography 0366
Gerontology 0351
History
- General 0578
- Ancient 0579
- Medieval 0581
- Modern 0582
- Church 0330
- Black 0328
- African 0331
- Asia, Australia and Oceania 0332
- Canadian 0334
- European 0335
- Latin American 0336
- Middle Eastern 0333
- United States 0337

History of Science 0585
Law 0398
Political Science
- General 0615
- International Law and Relations 0616
- Public Administration 0617

Recreation 0814
Social Work 0452
Sociology
- General 0626
- Criminology and Penology 0627
- Demography 0938
- Ethnic and Racial Studies 0631
- Individual and Family Studies 0628
- Industrial and Labor Relations 0629
- Public and Social Welfare 0630
- Social Structure and Development 0700
- Theory and Methods 0344

Transportation 0709
Urban and Regional Planning 0999
Women's Studies 0453

THE SCIENCES AND ENGINEERING

BIOLOGICAL SCIENCES
Agriculture
- General 0473
- Agronomy 0285
- Animal Culture and Nutrition 0475
- Animal Pathology 0476
- Fisheries and Aquaculture 0792
- Food Science and Technology 0359
- Forestry and Wildlife 0478
- Plant Culture 0479
- Plant Pathology 0480
- Range Management 0777
- Soil Science 0481
- Wood Technology 0746

Biology
- General 0306
- Anatomy 0287
- Animal Physiology 0433
- Biostatistics 0308
- Botany 0309
- Cell 0379
- Ecology 0329
- Entomology 0353
- Genetics 0369
- Limnology 0793
- Microbiology 0410
- Molecular 0307
- Neuroscience 0317
- Oceanography 0416
- Plant Physiology 0817
- Veterinary Science 0778
- Zoology 0472

Biophysics
- General 0786
- Medical 0760

EARTH SCIENCES
Biogeochemistry 0425
Geochemistry 0996
Geodesy 0370
Geology 0372
Geophysics 0373
Hydrology 0388
Mineralogy 0411
Paleobotany 0345
Paleoecology 0426
Paleontology 0418
Paleozoology 0985
Palynology 0427
Physical Geography 0368
Physical Oceanography 0415

HEALTH AND ENVIRONMENTAL SCIENCES
Environmental Sciences 0768
Health Sciences
- General 0566
- Audiology 0300
- Dentistry 0567
- Education 0350
- Administration, Health Care 0769
- Human Development 0758
- Immunology 0982
- Medicine and Surgery 0564
- Mental Health 0347
- Nursing 0569
- Nutrition 0570
- Obstetrics and Gynecology 0380
- Occupational Health and Safety 0354
- Oncology 0992
- Ophthalmology 0381
- Pathology 0571
- Pharmacology 0419
- Pharmacy 0572
- Public Health 0573
- Radiology 0574
- Recreation 0575
- Rehabilitaion and Therapy 0382
- Speech Pathology 0460
- Toxicology 0383

Home Economics 0386

PHYSICAL SCIENCES
Pure Sciences
Chemistry
- General 0485
- Agricultural 0749
- Analytical 0486
- Biochemistry 0487
- Inorganic 0488
- Nuclear 0738
- Organic 0490
- Pharmaceutical 0491
- Physical 0494
- Polymer 0495
- Radiation 0754

Mathematics 0405
Physics
- General 0605
- Acoustics 0986
- Astronomy and Astrophysics 0606
- Atmospheric Science 0608
- Atomic 0748
- Condensed Matter 0611
- Electricity and Magnetism 0607
- Elementary Particles and High Energy 0798
- Fluid and Plasma 0759
- Molecular 0609
- Nuclear 0610
- Optics 0752
- Radiation 0756

Statistics 0463

Applied Sciences
Applied Mechanics 0346
Computer Science 0984
Engineering
- General 0537
- Aerospace 0538
- Agricultural 0539
- Automotive 0540
- Biomedical 0541
- Chemical 0542
- Civil 0543
- Electronics and Electrical 0544
- Environmental 0775
- Industrial 0546
- Marine and Ocean 0547
- Materials Science 0794
- Mechanical 0548
- Metallurgy 0743
- Mining 0551
- Nuclear 0552
- Packaging 0549
- Petroleum 0765
- Sanitary and Municipal 0554
- System Science 0790

Geotechnology 0428
Operations Research 0796
Plastics Technology 0795
Textile Technology 0994

PSYCHOLOGY
General 0621
Behavioral 0384
Clinical 0622
Cognitive 0633
Developmental 0620
Experimental 0623
Industrial 0624
Personality 0625
Physiological 0989
Psychobiology 0349
Psychometrics 0632
Social 0451

THE UNIVERSITY OF MANITOBA

FACULTY OF GRADUATE STUDIES

COPYRIGHT PERMISSION

ANALYSIS OF STEEL FRAMES WITH DEFORMABLE BEAM-TO-COLUMN CONNECTIONS

BY

MARIO J. SCERBO

A Thesis/Practicum submitted to the Faculty of Graduate Studies of the University of Manitoba in partial fulfillment of the requirements for the degree of

MASTER OF SCIENCE

Mario J. Scerbo © 1996

Permission has been granted to the LIBRARY OF THE UNIVERSITY OF MANITOBA to lend or sell copies of this thesis/practicum, to the NATIONAL LIBRARY OF CANADA to microfilm this thesis/practicum and to lend or sell copies of the film, and to UNIVERSITY MICROFILMS INC. to publish an abstract of this thesis/practicum..

This reproduction or copy of this thesis has been made available by authority of the copyright owner solely for the purpose of private study and research, and may only be reproduced and copied as permitted by copyright laws or with express written authorization from the copyright owner.

Abstract

The behaviour of steel frames may be significantly affected by the moment versus rotational deformation behaviour of its beam-to-column connections. Connection behaviour is generally non-linear and difficult to model analytically. The factors affecting connection behaviour are discussed as well as the factors affecting frame behaviour. Analytical models that are applicable to a general set of connection geometries are not yet available. Nor are empirical models based on the more than 300 available experimentally measured connection M-ϕ data sets. Thus, the most practical method to model connection behaviour is to curve-fit the experimental moment-rotation data for various specimens. 274 sets of experimental data are curve-fitted using a powerful six parameter function. This representation of connection M-ϕ behaviour is suitable for incorporation into a frame analysis computer program that accounts for non-linear frame behaviour. To obtain a graphical illustration of the range of connection behaviour, envelopes of connection M-ϕ curves for several common connection types are superimposed on the Eurocode3 connection classification boundaries. Connections often account for a significant part of the construction cost of a steel frame and many geometric options are afforded the designer. A standardized set of connection geometries and a connection designation system that may ultimately reduce construction costs are proposed in this study. A structural analysis computer program that accounts for connection deformation is used to examine the effects of connection behaviour on overall frame behaviour. A sensitivity study is conducted on a three bay, three story frame to illustrate the effect of connection behaviour on overall frame behaviour.

Acknowledgments

I would like to express my gratitude and respect to Dr. Glenn Morris for his guidance throughout this study. NSERC (National Science and Engineering Research Council of Canada) provided financial assistance for part of this study. I would like to thank my family and friends for their encouragement and support.

Table of Contents

Abstract ii
Acknowledgments iii
List of Tables vii
List of Figures ix
Nomenclature xi
1. Introduction 1
  1.1 Background 1
  1.2 Assumptions and Limitations 2
  1.3 Scope of Study 3
  1.4 Objective 5
2. Summary of Connection Behaviour and Research 6
  2.1 Connection Behaviour 6
    2.1.1 Force-Deformation Behaviour 6
    2.1.2 Factors Affecting Connection Behaviour 7
  2.2 Connection Research 9
    2.2.1 Studies of the Behaviour of Bare Steel Connections 10
    2.2.2 Composite Connections 10
    2.2.3 Cyclic Loading 11
    2.2.4 Effect of Connection Behaviour on Frame Behaviour 11
  2.3 Modeling M-ϕ Behaviour Using Curve Fitting Techniques 14
    2.3.1 Analytical Functions 14
    2.3.2 Statistical Methods 16
    2.3.3 Parametric Studies 17
  2.4 Classification Systems for Connections 17
    2.4.1 Typical Moment-Rotation Behaviour 17
    2.4.2 Bjorhovde Classification System 18
    2.4.3 Eurocode3 Classification System 19
    2.4.4 Bijlaard Classification System 19
3. Comparison and Analysis of Curve Fitting Functions 27
  3.1 Introduction 27
  3.2 Ramberg-Osgood Function 27
    3.2.1 Characteristics of the Ramberg-Osgood Function 27
    3.2.2 Derivatives of the Ramberg-Osgood Function 28
    3.2.3 Shortcomings of the Ramberg-Osgood Function 29
  3.3 Richard-Abbott Function 30
    3.3.1 Characteristics of the Richard-Abbott Function 30
    3.3.2 Derivatives of the Richard-Abbott Function 30
    3.3.3 Shortcomings of the Richard-Abbott Function 32
  3.4 Modified Richard-Abbott Function 33
    3.4.1 Characteristics of the Modified Richard-Abbott Function 33
    3.4.2 Capabilities of the Modified Function 33
    3.4.3 Effect of the Shape Parameters, n_1 and n_2 35

Table of Contents (cont.)

3.4.4 Derivatives of the Modified Function 35
3.4.5 Observations from Derivative Plots 36
3.4.5.1 Richard-Abbott Function Behaviour 36
3.4.5.2 Reversal of Curvature 37
3.4.5.3 Two Points of Maximum Negative Curvature 38
4. Curve Fitting and Classification of Connection M-ϕ Data 58
4.1 Modeling of Connection Behaviour 58
4.2 Modeling of Connection Data by Curve-Fitting 59
4.2.1 Curve Fitting Function 59
4.2.2 Types of Connections Included in the Study 59
4.2.3 Eurocode3 Classification System 60
4.2.3.1 Classification of Connections 60
4.2.3.2 Normalizing the Modified Function Parameters 61
4.2.4 Curve Fitting of Connection Data 62
4.3 Envelopes of M-ϕ Curves 63
5. Standardization of Connections 98
5.1 Reasons For Standardizing Connections 98
5.1.1 Introduction 98
5.1.2 Cost of Construction 98
5.1.3 Implementation Into A Frame Analysis Program 98
5.2 Summary Of Current Standardization Practice 99
5.2.1 Canada 99
5.2.2 United States 100
5.2.3 Australia 100
5.3 Standardization 100
5.3.1 General 100
5.3.2 Connection Geometry 102
5.3.2.1 Single Web Angle Connection 102
5.3.2.2 Single Plate Connection 104
5.3.2.3 Double Web Angle Connection 106
5.3.2.4 Header Plate Connection 107
5.3.2.5 Top and Seat Angle Connection 109
5.3.2.6 Flush End Plate Connection 110
5.3.2.7 Top and Seat Angles with Double Web Angle Connection 112
5.3.2.8 Extended End Plate Connection 112
5.4 Recommendations for Future Testing 114
6. Analysis of Flexibly Connected Steel Frames using Micro-Computer Programming 129
6.1 Modeling of the Structure 129
6.1.1 Structural Layout 129
6.1.2 Coordinate System 129
6.1.3 Assumptions and Idealizations 130
6.2 Element Stiffness Matrices 131

Table of Contents (cont.)

6.2.1 Column Stiffness Matrix....131
6.2.2 Beam Stiffness Matrix....133
6.3 Assembly of Structure Stiffness Matrix....135
6.4 Model of Connection Behaviour....137
6.5 Analysis Procedure to Account for Non-Linear Connection Behaviour....137
6.6 Computer Program for PC with DOS: FLEXFRM2....138
6.6.1 Introduction....138
6.6.2 Data Input....138
6.6.3 Program Output....141
7. Analysis of Three-Dimensional Frames using FLEXFRM2....147
7.1 Introduction....147
7.2 Example 1: Program Verification....147
7.3 Sensitivity Study....148
7.3.1 Flexible Connections:....149
7.3.2 Semi-Rigid Connections:....149
7.3.3 Rigid Connections....150
7.4 Summary of Effects of Connection Behaviour on Overall Frame Behaviour....151
8. Conclusions / Recommendations....157
8.1 Conclusions....157
8.1.1 Modeling Connection Behaviour....157
8.1.2 Classification and Standardization of Connections....158
8.1.3 Computer Analysis and Results....158
8.2 Recommendations for Further Study....159
References....161
Appendix A....167

List of Tables

Table 2.1 Summary of Connection Tests 20
Table 4.1 Geometric Parameters for Single Web Angle Connections 66
Table 4.2 Geometric Parameters for Single Plate Connections 66
Table 4.3 Geometric Parameters for Double Web Angle Connections 67
Table 4.4 Geometric Parameters for Top and Seat Angle Connections 68
Table 4.5 Geometric Parameters for Top and Seat Angle Connections with Double Web Angles 69
Table 4.6 Geometric Parameters for Header Plate Connections 70
Table 4.7 Geometric Parameters for Flush End Plate Connections 70
Table 4.8 Geometric Parameters for Extended End Plate Connections 71
Table 4.9 Geometric Parameters for Extended End Plate Connections 72
Table 4.10 Plastic moment and rotation for the beams using in the M-ϕ tests 73
Table 4.11 Non-dimensional curve fitting parameters for single web angle connections 74
Table 4.12 Non-dimensional curve fitting parameters for side plate connections 74
Table 4.13 Non-dimensional curve fitting parameters for double web angle connections 75
Table 4.14 Non-dimensional curve fitting parameters for top and seat angle connections 76
Table 4.15 Non-dimensional curve fitting parameters for top and seat angle connections with double web angles 77
Table 4.16 Non-dimensional curve fitting parameters for header plate connections 77
Table 4.17 Non-dimensional curve fitting parameters for flush end plate connections ... 78
Table 4.18 Non-dimensional curve fitting parameters for extended end plate connections 79
Table 4.19 M-ϕ data for Lipson: AA-2/1 (1968) 85
Table 4.20 M-ϕ data for Lipson: P1-2/1 (1968) 86
Table 4.21 M-ϕ data for Thompson: A1-1 alt a (1968) 87
Table 4.22 M-ϕ data for Sommer: Test 5 (1969) 88
Table 4.23 M-ϕ Data for Marley: A-1/4-1 (1982) 89
Table 4.24 M-ϕ Data for Ostrander: Test 1 (1970) 90
Table 4.25 M-ϕ data for Azizinamini: 8S1 (1985) 91
Table 4.26 M-ϕ data for Ioannides: Test 1 (1978) 92
Table 4.27 Summary of connection behaviour 93
Table 5.1 Standardized options for SWA connections (100 x 75) 116
Table 5.2 Geometric parameters for SWA tests that resemble standard designations 116
Table 5.3 Modified Richard-Abbott parameters for standardized SWA connections 116
Table 5.4 Standard options for SP connections (90 mm width) 117
Table 5.5 Geometric parameters for SPC tests that resemble standard designations 117
Table 5.6 Modified Richard-Abbott parameters for Standardized SP connections 117
Table 5.7 CISC standard gauges for DWA connections 118
Table 5.8 Standard options for DWA connections (100 x 100) 118
Table 5.9 Geometric parameters for DWA tests that resemble standard designations ... 118
Table 5.10 Modified Richard-Abbott parameters for standardized DWA connections .. 119
Table 5.11 Standard Options for HP connections 120

List of Tables (cont.)

Table 5.12 Geometric parameters for HP tests that resemble standard designations 120
Table 5.13 Modified Richard-Abbott parameters for standardized HP connections 120
Table 5.14 Standard dimensions for TSA connections 121
Table 5.15 Geometric parameters for TSA tests that resemble standard designations ...121
Table 5.16 Modified Richard-Abbott parameters for standardized TSA connections....121
Table 5.17 Standard Dimensions for FEP connections 122
Table 5.18 Geometric parameters for FEP tests that resemble standard designations....122
Table 5.19 Modified Richard-Abbott parameters for standardized FEP connections 122
Table 5.20 Standard designations for TSA/DWA connections 123
Table 5.21 Geometric parameters for TSA/DWA tests that resemble standard designations.....123
Table 5.22 Modified Richard-Abbott parameters for standardized TSA/DWA connections 123
Table 5.23 Standard dimensions for EEP connections 124
Table 5.24 Geometric parameters for EEP tests that resemble standard designations ...124
Table 5.25 Modified Richard-Abbott parameters for standardized EEP connections 125
Table 7.1 End moments for typical flexible connections.....154
Table 7.2 End moments for typical semi-rigid connections 155
Table 7.3 End moments for typical rigid connections 156

List of Figures

Figure 2.1 Force and Deformation Components of a Connection 22
Figure 2.2 Planar View of Moment-Rotation Characteristic 22
Figure 2.3 Typical Connection Types 23
Figure 2.4 M-ϕ Relationship for Cyclic Loading 24
Figure 2.5 Curve Fitting Models 24
Figure 2.6 Moment-Rotation Curves for Typical Connection Types 25
Figure 2.7 Bjorhovde Classification System 25
Figure 2.8 Eurocode3 Classification System 26
Figure 3.1 Effect of shape parameter, n, on the Ramberg-Osgood Function 40
Figure 3.2 Effect of slope parameter, S_o, on the Ramberg-Osgood Function 40
Figure 3.3 Effect of reference moment, M_o, on the Ramberg-Osgood Function 40
Figure 3.4 Ramberg-Osgood properties for n=2, n=4 and n=8 41
Figure 3.5 Richard-Abbott Function; Effect of shape parameter, n 42
Figure 3.6 Richard-Abbott Function; Effect of S_p, negative curve 42
Figure 3.7 Richard-Abbott Function; Effect of S_p, positive curve 42
Figure 3.8 Properties of the Richard-Abbott Function 43
Figure 3.9 Bi-linear Richard-Abbott Function for large n 44
Figure 3.10 Spike in Curvature Diagram for large values of n 44
Figure 3.11 Richard-Abbott Function with Positive Curvature 44
Figure 3.12 Effect of ϕ_u on Modified Function; S_o=5, S_p=0.5, M_o=1, n_1=2, n_2=1 45
Figure 3.13 Five types of curves with a reversal of curvature 45
Figure 3.14 Two Points of Maximum Curvature 45
Figure 3.15 Effect of n_1 on Modified Function; S_o=5, S_p=0.5, M_o=1, ϕ_u=1, n_2=1 46
Figure 3.16 Effect of n_1 on final asymptote for positive n_2 46
Figure 3.17 Effect of shape parameters n_1 and n_2 47
Figure 3.18 Effect of shape parameters n_1 and n_2 for small values 48
Figure 3.19 Modified Function: Type 1 49
Figure 3.20 Modified Function: Type 2 50
Figure 3.21 Modified Function: Type 3 51
Figure 3.22 Modified Function: Type 4 52
Figure 3.23 Modified Function: Type 5 53
Figure 3.24 Two Points of Maximum Curvature: Equal Magnitude 54
Figure 3.25 Two Points of Maximum Curvature: Greater at Origin 55
Figure 3.26 Two Points of Maximum Curvature: Greater at ϕ_u 56
Figure 3.27 Maximum Curvature at Origin with intermediate "hump" 57
Figure 4.1 Single Web Angle Connection 80
Figure 4.2 Single Plate Connection 80
Figure 4.3 Double Web Angle Connection 81
Figure 4.4 Top and Seat Angle Connection 81
Figure 4.5 Top and Seat Angles with Double Web Angle Connections 82
Figure 4.6 Header Plate Connection 83
Figure 4.7 Flush End Plate Connection 83

List of Figures (cont.)

Figure 4.8 Extended End Plate Connection 84
Figure 4.9 M-ϕ behaviour of Lipson: AA-2/1 85
Figure 4.10 M-ϕ behaviour of Lipson: P1-2/1 86
Figure 4.11 M-ϕ behaviour of Thompson: A1-1 alt a 87
Figure 4.12 M-ϕ behaviour of Sommer: Test 5 88
Figure 4.13 M-ϕ behaviour of Marley: A-1/4-1 89
Figure 4.14 M-ϕ behaviour of Ostrander: Test 1 90
Figure 4.15 M-ϕ behaviour for Azizinamini: 8S1 91
Figure 4.16 M-ϕ behaviour for Ioannides: Test 1 92
Figure 4.17 Classification boundaries for Single Web/Side Plate Connection 94
Figure 4.18 Classification boundaries for Double Web Angle Connection 94
Figure 4.19 Classification boundaries for Header Plate Connection 95
Figure 4.20 Classification boundaries for Top and Seat Angle Connection 95
Figure 4.21 Classification boundaries for Flush End Plate Connection 96
Figure 4.22 Classification boundaries for Top and Seat Angle Connection with Double Web Angles 96
Figure 4.23 Classification boundaries for Extended End Plate Connection 97
Figure 5.1 Standardized SWA connection 126
Figure 5.2 Standardized SP connection 126
Figure 5.3 Standardized DWA connection 126
Figure 5.4 Standardized HP connection 127
Figure 5.5 Standardized TSA connection 127
Figure 5.6 Standardized FEP connection 127
Figure 5.7 Standardized EEP connection 128
Figure 6.1 Typical Frame Structure 142
Figure 6.2 Typical Column Element showing Joint Forces and Displacements 142
Figure 6.3 Typical Beam Element showing Joint Forces and Displacements 143
Figure 6.4 Master-Slave Joint End Forces and Displacements 143
Figure 6.5 Idealized Cyclic Moment-Rotation Behaviour 144
Figure 6.6 Modification of Connection Flexibility Using Secant Stiffness 144
Figure 6.7 Typical Structure in Orthogonal View showing Bracing Elements 145
Figure 6.8 Joint Load Vectors 146
Figure 7.1 One Bay Frame: Example 1 152
Figure 7.2 M-ϕ Curves for Connections in Example 1 152
Figure 7.3 Braced Frame: Example 2 153

Nomenclature

A	member cross-sectional area
a	distance of concentrated load from A end of beam AB
b	length of beam AB
D_A	displacement vector at A for beam AB
D_{Lo}	out-of-plane displacement vector
D_{li}	in-plane displacement vector
E	modulus of elasticity
G	shearing modulus
I_1	torsional constant
I_{yy}	second moment of area about principal axis y-y of cross-section
K_{AA}	stiffness matrix at A for beam AB
K_D	first order elastic stiffness matrix
K_G	geometric stiffness matrix
m_1	torsional moment about X_1-axis
m_2	bending moment about X_2-axis
M_o	connection reference moment of Richard-Abbott function
M_p	beam plastic moment
n	shape parameter of various curve-fitting functions
n_1, n_2	shape parameters of modified Richard-Abbott function
p_1	force component in X_1 direction
P_A^F	fixed end force vector at A end for beam AB
p_{A2}	force component at A for beam AB
P_{B1}^F	fixed end force vector in X_1 direction at B end of beam AB
P_{Uo}	out-of-plane force vector
P_{vi}	in-plane force vector
S_B	connection stiffness at B end
S_o	initial slope parameter of Richard-Abbott function
S_p	final slope parameter of Richard-Abbott function

Nomenclature (cont.)

δ_{A1} displacement in X_1 direction at A end of beam AB

ϕ_1 connection rotation about X_1-axis

ϕ_o reference rotation of connection of Richard-Abbott

ϕ_u ultimate rotation of modified Richard-Abbott function

1. Introduction

1.1 Background

The beams and columns of a typical steel building frame generally exhibit linear, elastic behaviour at service load levels and somewhat beyond. Conversely, typical beam-to-column connects display nonlinear behaviour accompanied by plastic deformation that often begins at low load levels. There are numerous studies to indicate that nonlinear connection behaviour may significantly influence frame stiffness and internal force distribution (Huang and Morris, 1993; Ang and Morris, 1984). Nevertheless, because connection behaviour is difficult to predict accurately and because non-linear structural analysis is more complex than traditional linear analysis methods, Canadian steel design specifications mandate that beam-to-column connections be treated as either "rigid" for continuous construction or "pinned" for simple construction (CSA 1989).

The significant measure of connection behaviour is the relationship between the flexural moment, M, applied to the connection by the beam framing into it and the resulting rotational deformation, ϕ, in the connection. Thus, connection behaviour is usually defined by the moment-rotation, or M-ϕ, relationship. Various attempts to predict the moment-rotation behaviour of typical connection types have been made. "Standardized" functions expressed in terms of the connection geometric parameters (Nethercott, 1990) work well only for a limited range of connection types and geometries.

For economic reasons the steel industries in several counties have attempted to standardize the geometries of steel beam-to-column connections. The unified European code, Eurocode3 (1990), includes a classification system that describes a connection in terms of its strength and stiffness. In Canada, there is some degree of standardization. This is in the form of limiting thickness, gauge, pitch, etc. to several nominal dimensions.

Thus, standardization exists for the geometric parameters but not for the overall connection. If there were a standard menu of connection types, a single designation would define all of the pertinent parameters for each connection. Thus, it would be possible to have a menu of standard connections analogous to the menu of standard W-sections found in the Handbook of Steel Construction (CISC, 1993).

If this limited menu were adopted, the number of connection geometries encountered in design would be relatively small. Thus, it would be possible to develop reliable M-ϕ test data for all of the standard connections in the menu. These data could then be curve-fitted using a reliable function. One such function is a modified version of the Richard-Abbott function (Dong, 1994). The curve-fitting parameters of this function could then be incorporated in a computer program that analyzes frames with non-linear connection behaviour.

This thesis incorporates the elements described above. That is, a standardized designation system for 8 typical connection types is proposed, the versatility of the modified Richard-Abbott function is demonstrated and the available experimental data are curve-fitted to this function. All that is required is to acquire more test data for connection geometries that match the proposed standard designations and to curve fit them.

The benefit of such an approach will be improved economy because of standard connection components and possibly greater safety through more realistic modeling of steel frame structures.

1.2 Assumptions and Limitations

The curve-fitting portion of this study is limited to the available experimental data. No laboratory testing was done as part of this study.

The computer program used in this study is modified from an existing program (Ang, 1983; Huang, 1994). The assumptions and limitations of that computer program fall into three categories:

1. Assumptions and limitations relating to individual members:
    a) all members are prismatic and straight
    b) buckling of individual members is ignored
    c) columns are either rigid or pinned at their base
    d) all members behave linearly elastically
    e) floors act as rigid diaphragms for resisting in-plane forces
    f) small deflection theory is employed except when calculating column stiffness matrices
    g) the effect of column panel zone deformation is ignored.

2. Assumptions and limitations relating to the connections:
    a) connections are located at the intersection of the beam and column centre lines
    b) only the flexural moment-rotation behaviour is considered
    c) dimensions of the connections are assumed to be negligible.

3. Assumptions and limitations related to the whole structure:
    a) while only static loading is considered, sequential, non-proportional loading systems can be accommodated
    b) lateral loads are applied at floor levels only.

1.3 Scope of Study

A summary of connection force-deformation behaviour and the factors that affect it is presented. The history of connection research is summarized, with reference to the following specific topics:

i) bare steel connections,

ii) composite connections,

iii) cyclic loading and

iv) the effect of connection behaviour on frame behaviour.

The various curve-fitting approaches that have been used are described and connection classification systems are described.

Three mathematical functions suitable for modelling connection M-ϕ behaviour are analyzed and compared. These are the Ramberg-Osgood, the Richard-Abbott and the modified Richard-Abbott functions. The capability, weaknesses and benefits of each function are discussed in detail.

The approach that is used to model the moment-rotation behaviour of connections using all of the available test data and a powerful curve fitting function, the modified Richard-Abbott function, is described. The experimental data are curve-fitted and classified using the Eurocode3 classification system and envelopes are presented that allow designers to develop a "feel" for the range of strength and stiffness of a given connection type.

A menu of standard connections for eight commonly used connection types is presented. A justification for the use of standard connections is presented as well as a summary of current standardization practice in Canada, Australia and the United States. Standard connection geometries are presented for the following types:

i) single web angle connection,

ii) single plate connection,

iii) double web angle connection,

iv) header plate connection,

v) top and seat angle connection,

vi) flush end plate connection,

vii) top and seat angles with double web angle connection and

viii) extended end plate connection.

A methodology for the analysis of flexibly connected steel frames is given. The structural model used in the study is described, the element and structural stiffness matrices are assembled and the analysis procedure accounting for non-linear connection behaviour is presented. The computer program that performs the analysis is introduced and the program input and output are described.

Example structures are analyzed using the program. A typical structure is analyzed using connections whose M-ϕ curves correspond to the upper and lower boundary of moment-rotation behaviour of the standardized connection types described above. The goal of this approach is to demonstrate how sensitive frame behaviour is to the range of M-ϕ behaviour for connections of the same type.

1.4 Objective

The actual moment-rotation behaviour of all connections is between the two extremes: fully rigid and pinned. The ultimate moment capacity of connections is also highly variable. Canadian steel design specifications mandate that beam-to-column connections be treated as either "rigid" for continuous construction or "pinned" for simple construction (CSA 1989). The computer analysis program developed in this study permits the non-linearity of connections to be accounted for when analyzing frames. Thus, if dependable moment-rotation behaviour were available for a standard set of connection geometries it would be simple for designers to analyze steel framed structures more accuratey. Thus, the objective of this thesis is to demonstrate that the non-linear behaviour of beam-to-column connections in steel frames can be accounted for in design with minimal effort.

2. Summary of Connection Behaviour and Research

2.1 Connection Behaviour

2.1.1 Force-Deformation Behaviour

Figure 2.1 shows a typical beam-to-column connection in a steel building frame. It experiences, at most, six force components: beam axial force, p_1, vertical and horizontal shear components, p_2 and p_3, torsional moment, m_1 and bending moments, m_2 and m_3, and six corresponding deformation components: three linear deformations, δ_1, δ_2 and δ_3 and three rotational deformations, ϕ_1, ϕ_2 and ϕ_3.

The in-plane deformations, δ_1, δ_3 and ϕ_2 are negligibly small because each floor can be assumed to act as a rigid diaphragm. They and the corresponding force components, p_1, p_3 and m_2 are thus normally ignored in frame analysis. Rigid diaphragm behaviour is assumed because the floor beams are bonded to the slab that is assumed to have infinite in-plane stiffness. The torsional stiffness of the typical connection is much greater than that of the typical W-section. Therefore, the torsional moment, m_1 and the torsional deformation, ϕ_1, are small and are usually ignored. It is commonly assumed that the shearing deformation, δ_2, and the shearing force, p_2, have negligible effect on the behaviour of the frame.

Thus, it has been the usual practice to consider only the flexural moment, m_3 and the corresponding rotational deformation, ϕ_3, when analyzing the force-deformation behaviour of connections. The relationship between these two components is commonly referred to as the M-ϕ, or moment-rotation, behaviour of the connection. Figure 2.2 shows an elevation view of a beam-to-column connection loaded by flexural moment, M, which produces a corresponding rotational deformation, ϕ, assumed to be concentrated in the connection. For analysis purposes, the beams and columns are usually modeled as

line elements and the connection deformation is assumed to be concentrated at the beam end - that is to say at the beam-to-column intersections.

2.1.2 Factors Affecting Connection Behaviour

The seven commonly used beam-to-column connection types shown in Figure 2.3 (a) through (h) are considered in this study. They are respectively:

1. Single Web Angle/ Side Plate Connection,
2. Double Web Angle Connection,
3. Header Plate Connection,
4. Top and Seat Angle Connection,
5. Top and Seat Angle Connection with Double Web Angles,
6. Flush End Plate Connection and
7. Extended End Plate Connection.

The moment-rotation behaviour of a typical connection is intermediate between the two extremes; rigid and pinned. At the serviceability limit state almost all connections display non-linear behaviour. According to Chen and Lui (1986) the five factors that contribute most significantly to non-linear behaviour in connections are:

1. bolt slip, even at service load levels, for snug tightened bolts,
2. localized yielding in flexure of the connection elements and the beam and column in the vicinity of the connection,
3. localized yielding due to bearing stresses between the connected elements,
4. local bucking of the webs and flanges of the beam or column,
5. deformation of the connection which can cause the initial geometry to be altered significantly.

All connections are able to develop some moment resistance. Lewitt et al. (1969) demonstrated that connections which are traditionally considered to behave as pinned can develop as much as twenty percent of the moment resistance of the connected beam.

For all connection types, the M-ϕ behaviour depends largely on the following factors (Jones et. al., 1982; Morris and Packer, 1987):

1. bolt size and material properties
2. gage of the fasteners to the face of the column
3. angle or plate thickness
4. depth of the beam
5. length of the angle or plate
6. presence or absence of column stiffeners
7. thickness of column flange or web
8. material properties of the beam, column and connection

Below is a summary of the effect of the specific geometric parameters on each connection (Morris and Packer, 1987).

(a) Web Angle Connections

Angle thickness and length, the number of beam web bolts and the thickness of the column flange have the most significant effect on the M-ϕ behaviour of web angle connections most significantly. For double web angle connections the gage distance of the column-flange bolts also affects the M-ϕ behaviour.

(b) Side Plate Connection

Side plate connections are similar to web angle connections except that the end of the plate is welded to the column flange. Plate thickness and length, the number of beam web bolts and the thickness of the beam web have the most significant effect on the M-ϕ behaviour of side plate connections.

(c) Header Plate Connection

Plate thickness has the primarily effect on the M-ϕ behaviour of header plate connections. The length and the gage of column flange bolts also have a small affect on the

connection's behaviour. The connection is welded to the web of the beam and bolted to the flange of the column.

(d) Top and Seat Angle Connection

The thickness of the angle and the distance from the heel of the angle to the column-flange bolts have the most significant effect on M-ϕ behaviour for top and seat angle connections. Top and seat angle connections can be fully bolted or bolted to the beam and welded to the column.

(e) Flush End Plate Connection

Plate thickness, the distance from the tension flange to the first row of bolts and the gage of the end-plate to column-flange bolts have the greatest effect on M-ϕ behaviour of flush end plate connections. The presence of column web stiffeners can increase moment capacity. Flush end plates have a relatively large moment capacity because the plate is welded to the flanges and the web of the beam.

(f) Extended End Plate Connection

The M-ϕ behaviour for the extended end plate connection is similar to that of the flush end plate connection except that the longer moment arm produced by extending the plate increases the initial stiffness and the moment capacity. Therefore, the plate thickness, the distance from the outside the beam flange to the first row of bolts inside the beam flange and the gage of the end-plate to column-flange bolts also affect the M-ϕ behaviour for extended end plates. Extended end plate connections are welded similarly to flush end plate connections.

2.2 Connection Research

Connection research has focused on the load testing of various connection types and the construction of theoretical models to predict the observed M-ϕ behaviour. The first

systematic theoretical, analytical and experimental treatment of connections was presented by Graham et al. (1959).

2.2.1 Studies of the Behaviour of Bare Steel Connections

Batho and Rowan (1934) and Rathburn (1935) conducted tests on riveted connections attempting to verify their models of connection behaviour. Horne (1958) and L.G. Johnson (1959) tested welded connections. They proposed simple design rules based on observed failure patterns. Munse (1959) and Schultz (1959) tested bolted connections using high strength bolts under static and dynamic loading. Johnson et al. (1960), Charlton (1960) and Sherbourne (1961) tested bolted connections in the plastic range. Lewitt, Chesson and Munse (1966) predicted moment-rotation curves based on available experimental data. Sommer (1969) performed tests on double web angles and header plate connections. N. Krishnamurthy (1978) analyzed the effect of prying action on bolted connections.

Since 1930 there have been approximately 300 tests of beam-to-column connections for which the complete sets of moment-rotation data are available. A summary of moment-rotation tests, indicating the connection type, researchers and the number of specimens, is presented in Table 2.1. There have been many more tests on connections but the complete moment-rotation data are not available for them.

2.2.2 Composite Connections

The behaviour of composite beam-to-column connections has attracted recent interest. In composite connections the beam is attached to the concrete slab by shear studs. The stiffness differs from that of a bare steel connection because the concrete slab adds to the flexural stiffness of the beam. There is a limited amount of test data for composite connections. Therefore, a model of the moment-rotation behaviour of composite connections is not yet available.

Johnson and Hope-Gill (1970) tested composite beam-to-column connections. Van Dalen and Godoy (1981) made comparisons between similar composite and bare steel connections. Leon et al. (1987) conducted full scale tests of composite beam-to-column connections. Bernuzzi et al. (1991) tested composite connections under monotonic and cyclic loading. The results of this research indicate that the presence of reinforcing steel around the column gives the connection a much higher moment capacity than would be the case for non-composite construction.

Because of the increasing use of composite connections in practice it is desirable for more research to be conducted in this area to demonstrate the impact of composite connections on frame behaviour.

2.2.3 Cyclic Loading

Wind or seismic loading may cause fluctuations, or even reversals, in the moment applied to a connection. Cyclic loading tests of several connection types have revealed the type of M-ϕ behaviour illustrated in Figure 2.4. The unloading portion of the curve can be approximated as the double mirror image of the initial loading curve. The unloading stiffness is thus approximately equal to the initial loading stiffness.

Because researchers have concentrated on monotonic loading there are few research results available on the cyclic behaviour of connections. However, cyclic loading M-ϕ data presented by H. Krawinkler et al. (1981) suggest that the unloading branch of the M-ϕ curve approximates a double mirror image of the loading branch.

2.2.4 Effect of Connection Behaviour on Frame Behaviour

Deformations of connections contribute to frame displacements which affect the internal force distribution and amplify lateral displacements. The effect of deformable connections on frame behaviour can be more significant than that of axial and direct shearing deformations in beams and columns and even "P-Δ effects", yet, connection

behaviour is accounted for only crudely in most design specifications. The Canadian Standards Association, CSA standard CAN 3-S16.1-M-89 Limit States Design of Steel Structures, recognizes two construction types for steel frames: continuous and simple construction. The American Institute of Steel Construction, AISC standard (LRFD) Load and Resistance Factor Design specification (AISC, 1986) also recognize two construction types: fully-restrained and partially restrained. While the AISC recognizes deformable connections it gives little guidance on how to design for them. On the other hand, the European specification, Eurocode3 (1990), requires connection behaviour to be accounted for explicitly and accurately.

Connection deformation contributes to lateral drift, amplifying the P-Δ effect, thus affecting stability. This is shown in the work of Ang and Morris (1984), Bijlaard and Zoetmeijar (1986), Lindsey (1987), Kishi and Chen (1989).

Perfectly pinned connections transfer no moment to the columns but connections with even a small amount of stiffness may transfer significant moment. Ackroyd (1987) showed by analyzing frames under gravity load that the assumption of pinned connections can lead to over-design of beams and under-design of columns. Batho and Rowan (1934) concluded that savings in beam weights can be achieved by taking into account the end restraint provided by connections.

As a frame is loaded progressively the stiffness of the connections gradually decreases. This affects the end restraint provided to the columns and therefore their effective lengths. Because column strength depends on the effective length, connection behaviour affects the strength of the column it is connected to.

Analyzing frames assuming non-linear connections under non-proportional loading yields different results compared to those obtained assuming rigid or pinned connections. This is due to residual internal forces that leave permanent deformations after the removal of

lateral load. Deirline (1991) showed that after the elastic "shake down" state is achieved further cycling of the wind load produces smaller subsequent wind drifts.

The behaviour of connections subject to cyclic loading also affects frame behaviour. Identical connections at different locations of a frame may be at different stages of loading. Therefore, one connection may be at its initial loading stage while another connection is unloading.

Batho and Rowan (1930) proposed a beam line method to predict frame behaviour. J.F. Baker (1931) and J.C. Rathburn (1935) proposed a slope-deflection and modified moment distribution method. Lothers (1950) published a paper that presented elastic restraint equations.

In the 1960's the use of high speed computers permitted frames to be analyzed using the direct stiffness method and matrix algebra. Goble (1963) and Le Messurier (1974) proposed computerized methods that assume linearly elastic connections with varying rigidities. Fry (1971) used Sommer's method to model connection behaviour and account for it in a planar frame analysis program. Bose (1972) formulated a finite element model to investigate the effect of geometric parameters on connection behaviour and derived simple design equations for the strength and stability of column webs. Moncarz and Gersle (1981) analyzed frames under non-proportional loading. Ang and Morris (1983) created a three-dimensional frame analysis program that incorporated non-linear connection behaviour. Huang and Morris (1993) created a similar three-dimensional frame analysis program, permitting non-proportional loading, for use with micro-computers.

By the 1970's the research became more specific. Romstad and Subramanian (1970) studied frame buckling using bi-linear approximations to the moment-rotation behaviour. Dawe et al. (1974) analyzed the effect of eccentric loading. Driscoll (1976; 1982) proposed methods to account for loss of end restraint due to stiffness reduction of loaded

connections. Jones, Kirby and Nethercot (1979) analyzed the effect of semi-rigid end restraint on the strength of steel columns.

2.3 Modeling M-ϕ Behaviour Using Curve Fitting Techniques

2.3.1 Analytical Functions

One approach to the modeling of connection behaviour has been to curve fit experimentally-measured moment-rotation data for a given connection to an analytical function. As illustrated in Figure 2.5, the simplest types of models are linear models such as the ones proposed by Rathburn (1936), Monforton and Wu (1963) and Lightfoot and LeMesurier (1974) and a bi-linear model proposed by Tarpy and Cardinal (1981). A number of analytical functions have been proposed, such as: the Ramberg-Osgood function (1943), the Richard-Abbott function (1975), the exponential model by Lui and Chen (1986), the power model by Kishi and Chen (1990) and the modified Richard-Abbott function by Dong (1993).

For the linear model shown in Figure 2.5 the stiffness of the connection is assumed to be constant throughout its loading range. This model does not represent how the connection stiffness is gradually degraded as load increases. Thus, it does not represent the connection behaviour adequately as it approaches its ultimate limit state.

The bi-linear model, also shown in Figure 2.5, addresses this limitation by using a second straight line with a reduced slope at a particular transition moment. This model is not suitable for connection types that have non-linear moment-rotation behaviour throughout their entire range.

Kishi and Chen (1990) developed the following three-parameter power function, plotted in Figure 2.5 to model moment-rotation data based on initial stiffness and ultimate moment capacity:

$$M = \frac{R_{ki}\phi}{\left(1+\left(\frac{\phi}{\phi_o}\right)^n\right)^{1/n}} \qquad 2.1$$

where: R_{ki} is the initial connection stiffness,

n defines the sharpness of the curve,

ϕ_o is the plastic rotation.

The plastic rotation is defined as a ratio of the ultimate moment capacity, M_u and the initial connection stiffness, R_{ki}. The function has no final slope parameter. Therefore, it cannot be made asymptotic to a specific final slope. This model allows the initial stiffness to be obtained directly.

While Ramberg and Osgood (1943) developed their three-parameter function to model stress-strain data, the function has been used also to model moment-rotation curves. Ang and Morris (1984) used it in the following form to model connection behaviour in a three dimensional frame analysis program:

$$\frac{\phi}{\phi_o} = \frac{KM}{M_o}\left[1+\left(\frac{KM}{M_o}\right)^{n-1}\right] \qquad 2.2$$

where: M_o is a reference moment value and

K is a dimensionless scaling factor.

This function has the same weakness as the Kishi-Chen function in that it has no final slope parameter.

The Richard-Abbott function (1975) shown in Figure 2.5 is more accurate and versatile than the Ramberg-Osgood function. This function requires four parameters to describe its shape. Attiogbe and Morris (1988) used the following form of the function to model moment-rotation behaviour.

$$\frac{M}{M_o}=\frac{\phi}{\phi_o}\left[\frac{\left(1-S_p\frac{\phi_o}{M_o}\right)}{\left(1+\left|\left(\frac{1}{\phi_o}-\frac{S_p}{M_o}\right)\phi\right|^n\right)^{1/n}}+S_p\frac{\phi_o}{M_o}\right] \qquad 2.3$$

where: S_p defines the final slope of the curve.

The parameter, S_p gives the Richard-Abbott function the advantage of having a final asymptote.

The modified Richard-Abbott function developed by Dong (1993) has the form shown in Eq. 2.4.

$$\frac{M}{M_o}=\frac{\phi}{\phi_o}\left[\frac{\left(1-S_p\frac{\phi_o}{M_o}\right)}{\left(\left(\frac{\phi_u-|\phi|}{\phi_u}\right)^{n_1}+\left|\left(\frac{1}{\phi_o}-\frac{S_p}{M_o}\right)\phi\right|^{n_2}\right)^{1/n_2}}+S_p\frac{\phi_o}{M_o}\right] \qquad 2.4$$

In addition the four Richard-Abbott parameters it uses shape parameter, n_1 and an ultimate rotational deformation, ϕ_u. The additional parameters give the modified function more versatility than the Richard-Abbott function. The modified function allows for reversals of curvature and can be made tangent to the final slope at a specific abscissa.

2.3.2 Statistical Methods

Statistical methods such as least-squares and the cubic B-spline methods have been used to curve fit M-ϕ data. The least-squares regression model requires minimizing the sum of the squared deviations of data points from the regression line. However, because the regression line may peak and trough within the range of the function, this method may produce inaccurate connection tangent stiffnesses. The cubic B-spline method proposed by Jones et al. (1971;1982) involves dividing the M-ϕ data into a number of subsets. A cubic B-spline curve is then fitted to each subset. The continuities of the first and second

derivative must be enforced at the boundaries between the subsets. The disadvantage of this method is that is requires a large number of parameters to define the resultant moment-rotation function.

2.3.3 Parametric Studies

Parametric studies, where the curve-fitting function parameters are expressed in terms of the geometric parameters of the connection have been attempted. Examples of such parametric models are polynomial functions by Sommer (1969), Frye and Morris (1975) and Radziminski (1988). These parametric models have not been successful for the wide range of possible connection geometries.

Sommer (1969) developed a parametric method in which moment-rotation data for double web angle connections were curve-fitted to a polynomial function expressed in terms of the beam depth, the angle thickness and the bolt gage. Frye and Morris (1975) used all of the available moment-rotation data sets to derive "standardized" polynomial functions for the seven commonly used connection types. Radziminski et al. (1988) used a similar polynomial function to generate moment-rotation curves for top and seat angle connections with double web angles. Sommer's procedure was used by Ang and Morris (1984) to express the Ramberg-Osgood function parameters in terms of the important connection parameters.

2.4 Classification Systems for Connections

2.4.1 Typical Moment-Rotation Behaviour

As illustrated in Figure 2.6, the common connection types exhibit a wide range of initial stiffnesses and ultimate moment capacities. The moment-rotation curve for a perfectly rigid connection would lie along the vertical axis while that for a perfectly pinned connection would lie along the horizontal axis. As the figure shows, all of the moment-rotation curves are non-linear and fall between the two extremes: rigid and pinned. For

design purposes it would be desirable to have a method of classifying a connection in terms of stiffness and strength. That would permit an initial analysis based on assumed classes of connections. Bjorhovde et al. (1988) and Bijlaard et al (1991) have proposed classification systems. A connection classification system is also described in the European Community design code Eurocode3 (1990).

2.4.2 Bjorhovde Classification System

Figure 2.7 shows the classification system proposed by Bjorhovde et al. This system considers three connection characteristics: initial stiffness, strength and ductility. A connection is classified as rigid, semi-rigid or flexible depending on its initial stiffness. The boundaries between the three classifications are bi-linear. The vertical axis is defined as a ratio between the applied moment, M and the plastic moment of the beam section, M_p. The horizontal axis is defined as a ratio between the rotational deformation, ϕ and the plastic rotation, ϕ_p that is defined as the ratio between the initial slope, S_o and the plastic moment, M_p. The initial slope is a function of the effective beam length, L_e that corresponds to the initial connection stiffness, S_o and the flexural rigidity, EI:

$$S_o = \frac{EI}{L_e} \qquad 2.5$$

The effective length is expressed as a multiple of the beam depth, d:

$$L_e = \alpha d \qquad 2.6$$

Therefore, the initial connection stiffness is defined as:

$$S_o = \frac{EI}{\alpha d} \qquad 2.7$$

As indicated, flexible connections fall below the boundary defined by α=10 and may transfer a maximum of 20% of the beam plastic moment, M_p. The rigid connection boundary is defined by α=2 and the connections transfers greater than 70% of M_p. Semi-rigid connections transfer between 20% and 70% of M_p, with an initial stiffness between the rigid and flexible boundaries. The rotational deformation that is required is defined by the ductility demand, which is based on test data.

2.4.3 Eurocode3 Classification System

The Eurocode3 (1990) Clause 6.96 defines connections in terms of strength and stiffness. Figure 2.8 illustrates the Eurocode3 classification system. The vertical axis is the normalized moment, M/M_p. The horizontal axis is the normalized rotation, ϕ/ϕ_p, where ϕ_p is the plastic rotation, defined as:

$$\phi_p = \frac{M_p L_b}{EI_b} \qquad 2.8$$

where: L_b is the length of the beam and

I_b is the moment of inertial of the beam.

Connections are classified as rigid, semi-rigid or nominally pinned. The system uses two tri-linear boundaries to define the rigid-semi-rigid boundary: one for braced frames and the other for unbraced frames. The nominally pinned region defines very flexible connections and is bounded by a straight line. A connection is designated full-strength if its maximum moment resistance equals or exceeds the plastic moment capacity of the beam and partial strength if it does not. The code mentions the need to check the ductility requirement of the connection but offers little guidance. Clause 6.9.7.3 states that the procedures used to calculate rotation capacity must be verified by test data. However, Clause 6.9.6.3 (4) states that when the moment resistance of the connection exceeds the plastic moment resistance of the beam by twenty percent the rotational capacity need not be checked.

2.4.4 Bijlaard Classification System

The classification system proposed by Bijlaard et al. (1991) is a combination of two systems described above. Like the Eurocode3 system it distinguishes between braced and unbraced frames but the connection stiffness is expressed in terms of the ratio of the flexural rigidity, EI, and the length, L, of the beam.

Table 2.1 Summary of Connection Tests

Type	Author	# of Tests
Single Web Angle	Lipson (1968)	30
Single Web Angle	Lipson (1977)	43
Single Web Angle	Lipson et al (1980)	33
Web Side Plate	Thompson et al (1970)	12
Web Side Plate	Richard et al (1982)	4
Double Web Angle	Batho et al (1934)	3
Double Web Angle	Rathburn (1936)	7
Double Web Angle	Hechtman et al (1947)	4
Double Web Angle	Bell et al (1958)	4
Double Web Angle	Munse et al (1959)	4
Double Web Angle	Lewitt et al (1969)	6
Double Web Angle	Sommer (1969)	4
Double Web Angle	Thompson et al (1970)	48
Double Web Angle	Bergguist (1977)	3
Double Web Angle	Bennetts et al (1978)	2
Double Web Angle	Birkemoe et al (1978)	2
Double Web Angle	Mansell et al (1981)	8
Double Web Angle	Bose (1981)	1
Double Web Angle	Ricles et al (1982)	8
Double Web Angle	Wing et al (1982)	12
Double Web Angle	Bjorhovde (1984)	10
Double Web Angle	Redwood et al (1984)	20
Double Web Angle	Radziminski (1987)	18
Double Web Angle	Janss et al (1987)	4
Double Web Angle	Davison et al (1987)	8
Double Web Angle	Onuah et al (1987)	20
Double Web Angle	Rauscher et al (1990)	24
Double Web Side Plate	Pham et al (1982)	5
Double Web Side Plate	Aggarwal et al (1986)	8
Double Web Side Plate	Patrick et al (1986)	16
Top and Seat Angles	Rathburn (1934)	5
Top and Seat Angles	Batho et al (1936)	10
Top and Seat Angles	Hechtmann et al (1947)	12
Top and Seat Angles	Maxwell (1981)	12
Top and Seat Angles	Bose (1981)	1
Top and Seat Angles	Van Dalen et al (1982)	1
Top and Seat Angles	Marley et al (1982)	26
Top and Seat Angles	Hotz (1983)	37
Top and Seat Angles	Janss et al (1987)	4
Top and Seat Angles	Davison et al (1987)	3
T & S with DWA	Batho et al (1934)	2
T & S with DWA	Young et al (1934)	4
T & S with DWA	Rathburn (1936)	18
T & S with DWA	Hechtman et al (1947)	1
T & S with DWA	Zoetemeijer (1974)	4
T & S with DWA	Azizinamini et al (1985)	20
T & S with DWA	Davison et al (1987)	2
Flush End Plate	Ostrander (1970)	24

Table 2.1 Summary of Connection Tests (cont.)

Type	Author	# of Tests
Flush End Plate	Zoetemeijer (1974)	6
Flush End Plate	Zoetemeijer et al (1975)	12
Flush End Plate	Bose (1981)	1
Flush End Plate	Morris et al (1981)	4
Flush End Plate	Mann et al (1981)	6
Flush End Plate	Zoetemeijer (1981)	23
Flush End Plate	Phillips et al (1981)	5
Flush End Plate	Jenkins et al (1984)	3
Flush End Plate	Davison et al (1987)	5
Flush End Plate	Kukreti et al (1987)	8
Header Plate	Sommer (1969)	20
Header Plate	Benetts et al (1978)	2
Header Plate	Pham et al (1982)	7
Header Plate	Kennedy et al (1984)	8
Header Plate	Davison et al (1987)	1
Extended End Plate	Sherbourne (1961)	5
Extended End Plate	Johnson et al (1960)	1
Extended End Plate	Bailey (1970)	26
Extended End Plate	Surtees et al (1970)	6
Extended End Plate	Zoetemeijer (1974)	8
Extended End Plate	Packer et al (1977)	5
Extended End Plate	Ioannides (1978)	6
Extended End Plate	Dews (1979)	3
Extended End Plate	Grundy et al (1980)	2
Extended End Plate	Johnstone et al (1981)	8
Extended End Plate	Zoetemeijer (1981)	10
Extended End Plate	Zoetemeijer (1981)	5
Extended End Plate	Tarpy et al (1981)	16
Extended End Plate	Bahia et al (1981)	20
Extended End Plate	Moore et al (1981)	4
Extended End Plate	Jenkins et al (1984)	3
Extended End Plate	Zoetemeijer et al (1984)	4
Extended End Plate	Aggarwal et al (1985)	6
Extended End Plate	Zandonini et al (1985)	18
Extended End Plate	Janss et al (1987)	4
Extended End Plate	Davison et al (1987)	6
Extended End Plate	Kalyonov et al (1989)	4
Extended End Plate	Chasten et al (1992)	7
Extended End Plate	Ghobarah et al (1992)	4

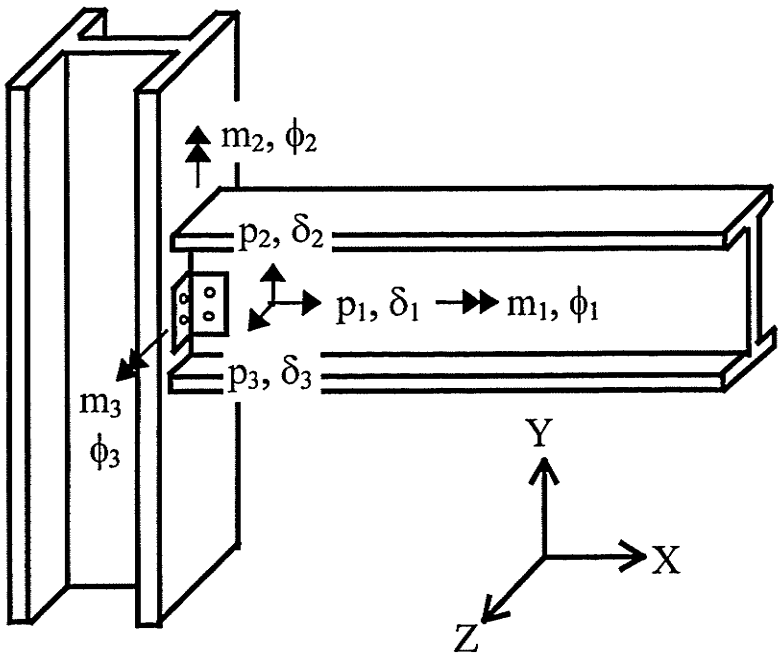


Figure 2.1 Force and Deformation Components of a Connection

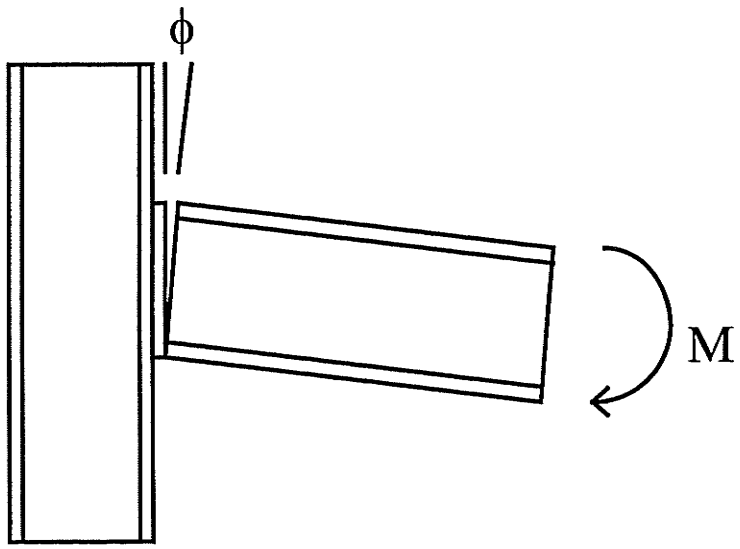


Figure 2.2 Planar View of Moment-Rotation Characteristic

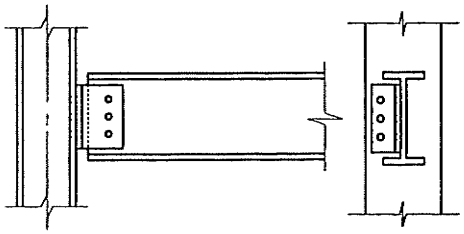


Figure 2.3 (a) Single Web Angle Connection Connection

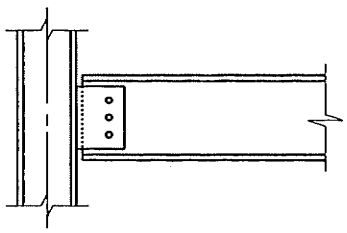


Figure 2.3 (b) Side Plate

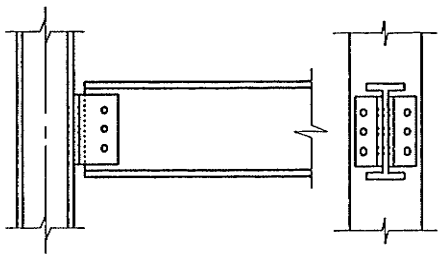


Figure 2.3 (c) Double Web Angle Connection

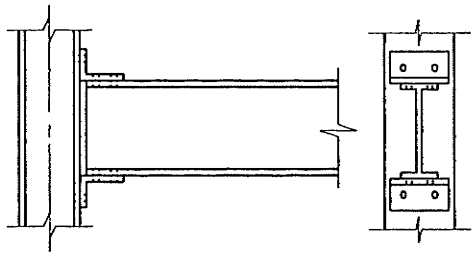


Figure 2.3 (d) Top and Seat Angle Connection

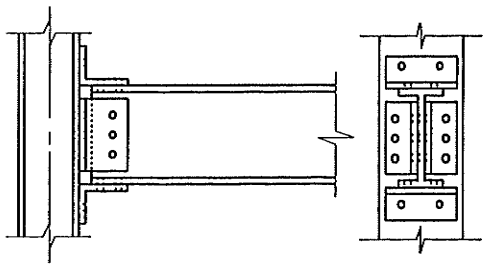


Figure 2.3 (e) Top and Seat Angle Connection with Double Web Angles

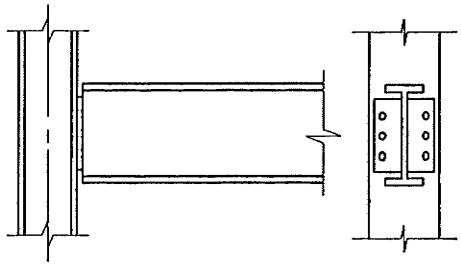


Figure 2.3 (f) Header Plate Connection

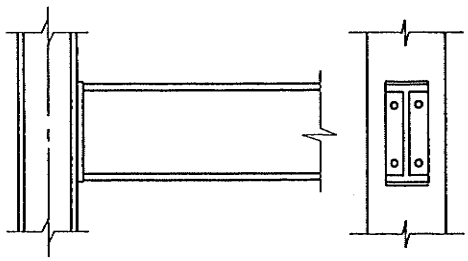


Figure 2.3 (g) Flush End Plate Connection

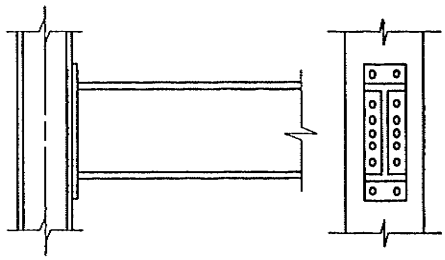


Figure 2.3 (h) Extended End Plate Connection

Figure 2.3 Typical Connection Types

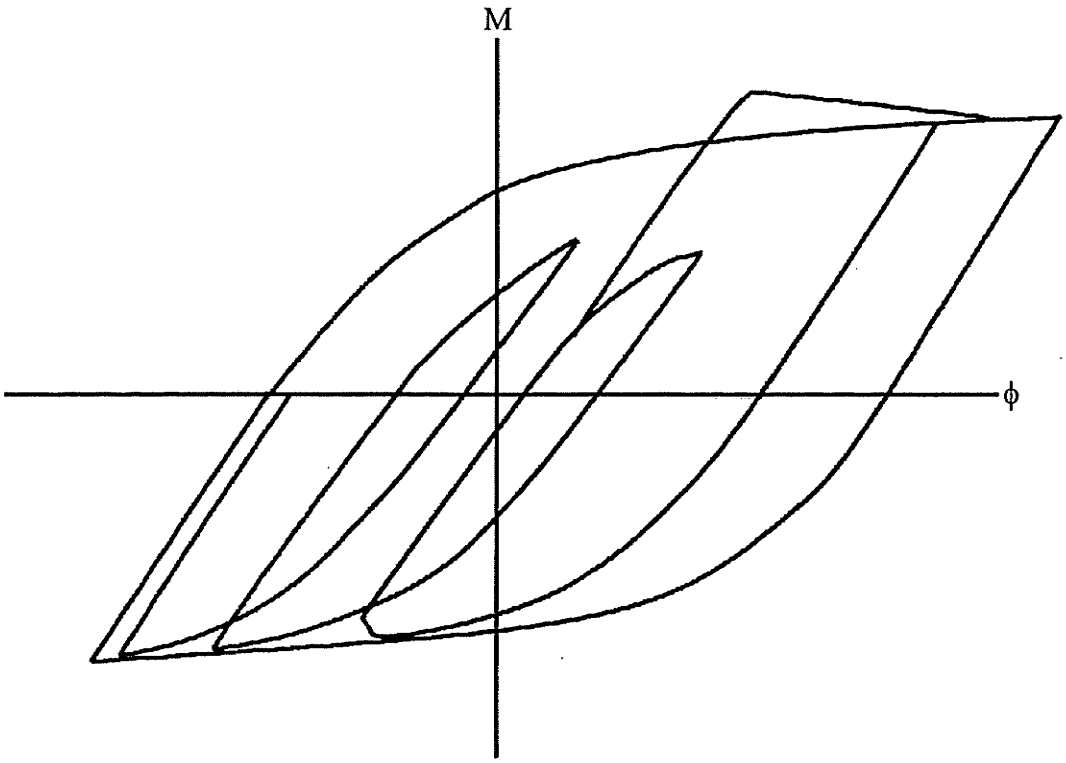


Figure 2.4 M-ϕ Relationship for Cyclic Loading

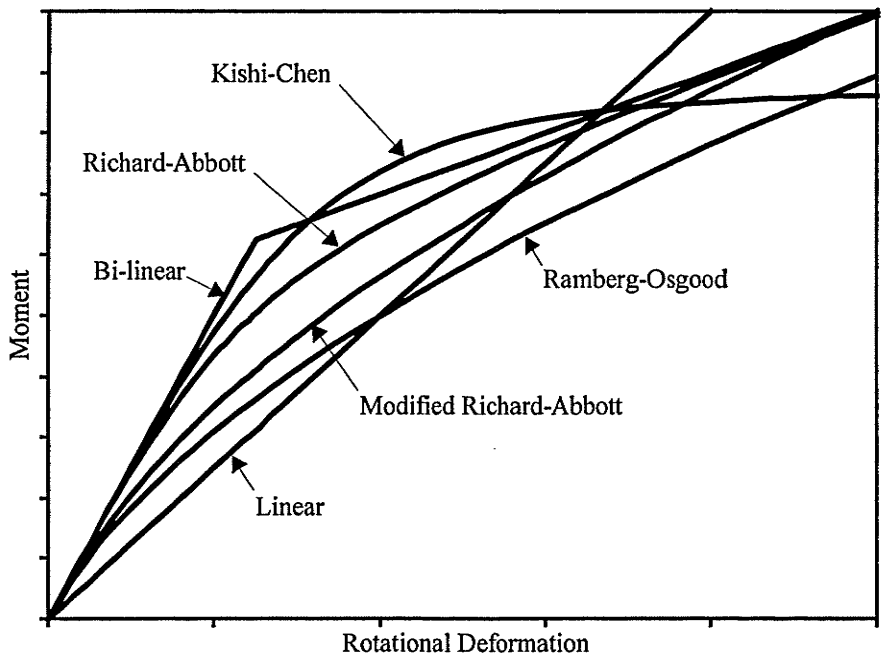


Figure 2.5 Curve Fitting Models

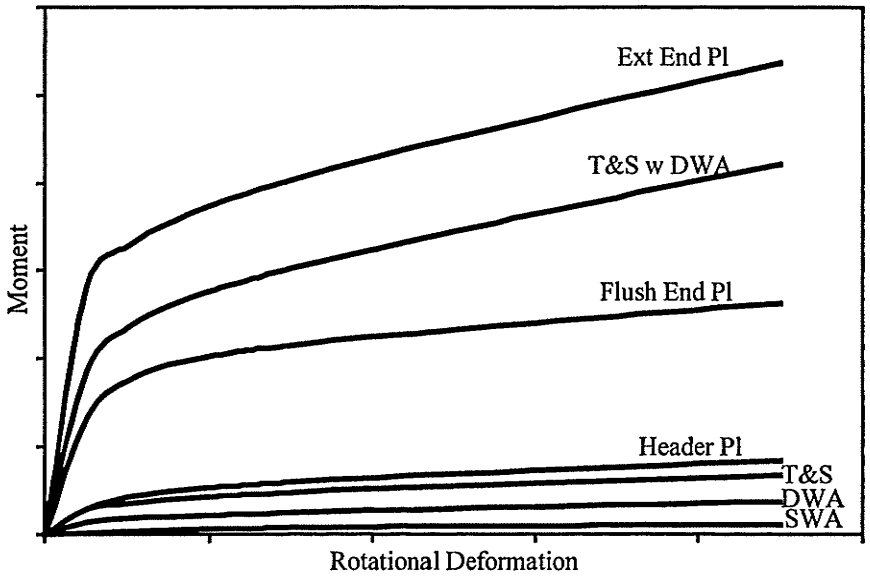


Figure 2.6 Moment-Rotation Curves for Typical Connection Types

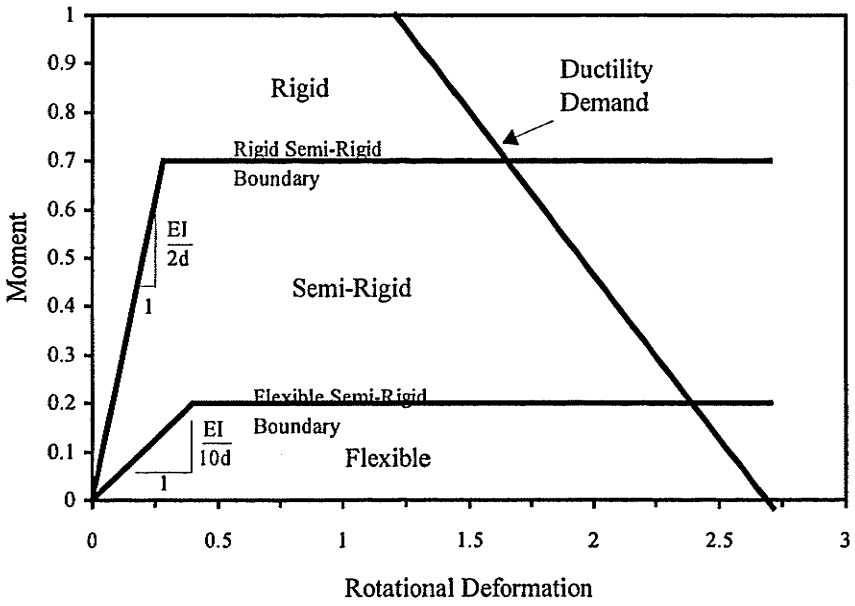


Figure 2.7 Bjorhovde Classification System

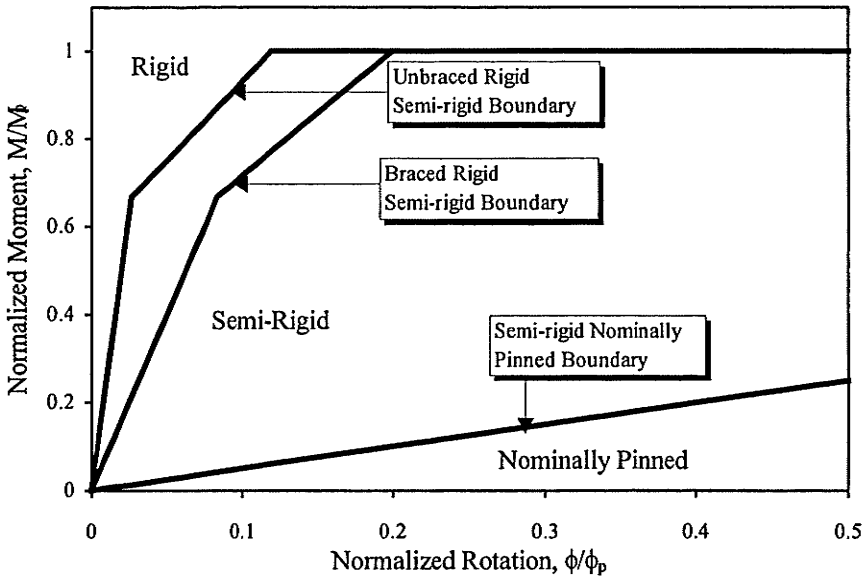


Figure 2.8 Eurocode3 Classification System

3. Comparison and Analysis of Curve Fitting Functions

3.1 Introduction

In this chapter three of the most versatile curve fitting functions that have been used to model connection M-ϕ data are analyzed and compared. The three functions are the Ramberg-Osgood (1943), the Richard-Abbott (1975) and the modified Richard-Abbott function (Dong, 1994). They are compared on the basis of their ability to model various shapes of curves and the modified Richard-Abbott function is shown to be more versatile than the other two. The first and second derivatives of these functions were derived using the Mathematica 2.2.2 computer software (1994). These derivatives permit an analysis of the slopes and curvatures of the functions, and the locating of points of maximum curvature, regions of little or no curvature and points of reversal of curvature.

3.2 Ramberg-Osgood Function

3.2.1 Characteristics of the Ramberg-Osgood Function

The Ramberg-Osgood function uses three parameters to describe it: M_o, S_o and n. Rotational deformation, ϕ is expressed as a function of the applied moment, M. The form of the Ramberg-Osgood function is as follows:

$$\phi = f(M) = \frac{M}{S_o}\left(1+\left(\frac{M}{M_o}\right)^{n-1}\right) \qquad 3.1$$

where: M_o is a reference moment,

S_o is the slope parameter and

n is a shape parameter.

Plots of the Ramberg-Osgood function for three different values of the shape parameter, n are presented in Figure 3.1. The figure demonstrates that the slope parameter, S_o, is the initial slope of the plot only when n=1. The initial slope of the plot increases as the shape

parameter, n, increases. Thus, for values of n greater than one the slope parameter does not define the initial slope of the plot. When n=1 the curvature is zero and curvature increases as n increases.

Figure 3.2 illustrates the effect of the slope parameter, S_o, on plots of the function. Increasing S_o while holding M_o and n constant results in an increase in the slope of the plot and an increase in the magnitude of the moment. Increasing the reference moment, M_o does not result in a steeper plot but does increase the magnitude of the moment as Figure 3.3 illustrates.

3.2.2 Derivatives of the Ramberg-Osgood Function

In Equation 3.1, the rotational deformation, ϕ is expressed in terms of the applied moment, M. In order to develop expressions for the first and second derivatives of the M-ϕ function it is most convenient to express moment as a function of rotational deformation. To that end, the derivatives were determined using the following equations:

$$M'(\phi) = \frac{1}{\phi'(M)} \qquad 3.2$$

$$M''(\phi) = \frac{1}{\phi'(M'(\phi))} \qquad 3.3$$

Then, using the Mathematica software, derivatives were computed as follows:

The first derivative (slope) was

$$M'(\phi) = \left[\frac{1}{S_o}\left(1+\left(\frac{M}{M_o}\right)^{n-1}\right)+\frac{(1-n)M_o}{S_o M_o}\left(1+\left(\frac{M}{M_o}\right)^{n-2}\right)\right]^{-1} \qquad 3.4$$

The second derivative (curvature) was

$$M''(\phi) = \frac{\frac{2(n-1)}{M_o S_o}\left(1+\left(\frac{M}{M_o}\right)^{n-2}\right)+\frac{M(n-2)(n-1)}{M_o{}^2 S_o}\left(1+\left(\frac{M}{M_o}\right)^{n-3}\right)}{\left[\frac{1}{S_o}\left(1+\left(\frac{M}{M_o}\right)^{n-1}\right)+\frac{(n-1)M}{M_o S_o}\left(\frac{M}{M_o}\right)^{n-2}\right]^2} \qquad 3.5$$

As illustrated in Figure 3.4 (a), when n is greater than one the Ramberg-Osgood plot is concave downward. Figures 3.4 (b) and (c) show plots of the slope and the curvature, respectively of the Ramberg-Osgood curves in Figure 3.4 (a). The slope and curvature confirm the fact that as parameter n increases, the Ramberg-Osgood curves become increasingly sharp. It can be seen from Figure 3.4 (c) that the location of maximum curvature migrates away from the origin as the parameter n increases and that the magnitude of the curvature decreases rapidly as rotational deformation increases.

3.2.3 Shortcomings of the Ramberg-Osgood Function

The shortcomings of the Ramberg-Osgood Function include the following:

1. The function does a poor job of fitting curves that are approximately bi-linear. As illustrated by the plots in Figure 3.1, while the curvature increases as n increases, the curve takes on an increasingly "round" shape.
2. The initial slope, S_o, cannot be explicitly specified since the shape parameter, n, affects the initial slope of the curve.
3. A "final slope" for a Ramberg-Osgood curve cannot be specified.
4. Although it is most convenient to have M expressed as a function of ϕ, in the Ramberg-Osgood function ϕ is expressed as a function of M.
5. The Ramberg-Osgood plots with negative curvature (concave down) can have only one point of maximum curvature. Thus, the function cannot accurately fit data that require multiple points of maximum curvature .

3.3 Richard-Abbott Function

3.3.1 Characteristics of the Richard-Abbott Function

Defined in terms of four parameters, the Richard-Abbott function plots a curve that expresses M as a function of ϕ, as follows:

$$M(\phi) = \frac{(S_o - S_p)\phi}{\left(1+\left(\frac{(S_o - S_p)\phi}{M_o}\right)^n\right)^{1/n}} + S_p\phi \qquad 3.6$$

where: M_o is a reference moment,

S_o is the initial slope of the plot,

S_p is the slope of a final asymptote line, and

n is a shape parameter.

As illustrated in Figure 3.5, the function plots as a curve that has an initial tangent slope, S_o, and is asymptotic to a final asymptote line at a large value of ϕ. M_o is the moment at which the final asymptote line crosses the vertical axis. The final asymptote is defined by $M=M_o+S_p\phi$. The figure illustrates the effect of variation in the shape parameter, n, on the shape and sharpness of the curve. As n increases, the curvature of the plot increases and the curve approaches a bi-linear shape.

Figure 3.6 demonstrates that parameter S_p defines the slope of the final asymptote and thus the slope of the "tail" of the curve. Figure 3.7 demonstrates that when S_o is smaller than S_p and M_o is negative the curve is concave upward.

3.3.2 Derivatives of the Richard-Abbott Function

The derivatives of the Richard-Abbott function in Equation 3.6, derived using the Mathematica software, are as follows:

The first derivative is

$$M'(\phi) = S_p - \frac{(S_o - S_p)^2 \phi}{M_o}\left(\frac{(S_o - S_p)\phi}{M_o}\right)^{n-1}\left(1+\left(\frac{(S_o - S_p)\phi}{M_o}\right)^{n}\right)^{-\left(\frac{1}{n}+1\right)} + \frac{(S_o - S_p)}{\left(1+\left(\frac{(S_o - S_p)\phi}{M_o}\right)^{n}\right)^{\frac{1}{n}}} \quad 3.7$$

The second derivative is

$$M''(\phi) = n\phi\left(1+\frac{1}{n}\right)\frac{(S_o - S_p)^3}{{M_o}^2}\left(\frac{(S_o - S_p)\phi}{M_o}\right)^{2n-2}\left(1+\left(\frac{(S_o - S_p)\phi}{M_o}\right)^{n}\right)^{-\left(2+\frac{1}{n}\right)} + (1-n)\frac{(S_o - S_p)^3}{{M_o}^2}\left(\frac{(S_o - S_p)\phi}{M_o}\right)^{n-2}\left(1+\left(\frac{(S_o - S_p)\phi}{M_o}\right)^{n}\right)^{-\left(1+\frac{1}{n}\right)} - \frac{2(S_o - S_p)^2}{M_o}\left(\frac{(S_o - S_p)\phi}{M_o}\right)^{n-1}\left(1+\left(\frac{(S_o - S_p)\phi}{M_o}\right)^{n}\right)^{-\left(1+\frac{1}{n}\right)} \quad 3.8$$

Depending on the choice of the four curve fitting parameters the Richard-Abbott function can produce the following four types of curve:

1. negative curvature with point of maximum curvature at origin, $0<n\leq 1$, $S_o>S_p$ and $M_o>0$
2. negative curvature with point of maximum curvature away from origin, $n>1$, $S_o>S_p$ and $M_o>0$
3. positive curvature with point of maximum curvature at origin, $0<n\leq 1$, $S_o<S_p$ and $M_o<0$
4. positive curvature with point of maximum curvature away from origin, $n>1$, $S_o<S_p$ and Mo<0

Figure 3.8 (a), (b) and (c) show plots of the Richard-Abbott function and its first and second derivatives, for the case where $S_o > S_p$ and for five different values of n. Figure 3.8 (b) confirms that as n increases the initial portion of the curve approaches the initial asymptote more and more closely. Figure 3.8 (c) demonstrates that as n increases from 0.5 to 8.0, the point of maximum curvature migrates from the origin to a point with an abscissa of approximately M_o/ S_o, the abscissa of the break point on the corresponding bi-linear curve.

Figure 3.9 shows the nearly perfect bi-linear shape of the Richard-Abbott function for n=30. Figure 3.10 shows the curvature diagrams corresponding to a range of n values between 10 and 60. As n becomes larger the "spike" in the curvature diagram becomes increasingly pronounced and the magnitude of the maximum curvature increases.

For concave upward curves, such as those shown in Figure 3.11, as n increases through positive values the point of maximum curvature again migrates from the origin to an abscissa corresponding to the intersection of the initial tangent line and the final asymptote line. It has been observed that the characteristics of the Richard-Abbott curves with positive curvature are similar to those of corresponding ones with negative curvature.

3.3.3 Shortcomings of the Richard-Abbott Function

The shortcomings of the Richard-Abbott function include the following:

1. The function does not model well curves that have a "rounded" shape. Curves with a somewhat rounded shape approach the final asymptote line only at large ϕ values and the curve is not very close to the final asymptote line.
2. The function can have only one point of maximum curvature. Thus, it cannot model curves with a reversal of curvature.

3.4 Modified Richard-Abbott Function

3.4.1 Characteristics of the Modified Richard-Abbott Function

The Modified Richard-Abbott function, presented in Eq. 3.9, is defined in terms of the six parameters, S_o, S_p, M_o, ϕ_u, n_1 and n_2.

$$M = \frac{(S_o - S_p)\phi}{\left(\left(\frac{\phi_u - \phi}{\phi_u}\right)^{n_1} + \left(\frac{(S_o - S_p)\phi}{M_o}\right)^{n_2}\right)^{1/n_2}} + S_p\phi \qquad 3.9$$

where: S_o, S_p and M_o are as defined for the Richard-Abbott function,

n_2 corresponds to n in the latter,

ϕ_u is the "ultimate" rotational deformation, and

n_1 is an additional shape parameter.

3.4.2 Capabilities of the Modified Function

When the shape parameter, n_1 is zero Equation 3.9 reduces to the Richard-Abbott function. Thus, while the Modified function can duplicate the Richard-Abbott function, because it incorporates two additional parameters it is more versatile than the latter in the following significant ways:

1. Whereas the Richard-Abbott curve approaches the final asymptote only at a large ϕ value, the plot of the Modified function is tangent to the latter line at abscissa ϕ_u.
2. The function can model curves that have a reversal of curvature.
3. The function can model curves that have two points of maximum curvature.

Since the Modified function approaches the final asymptote tangentially at a specific point this line can be referred to as the final tangent line. Figure 3.12 shows plots of the Modified function approaching the final tangent line at three different values of ϕ_u. Shown in the figure are the initial tangent line and the final tangent line. By changing the value of the ultimate rotation, ϕ_u, the point at which the curve contacts the final tangent

line can be controlled. The top curve shows the function for ϕ_u=0.5, the middle curve for ϕ_u=0.75 and the lower curve for ϕ_u=1.

Figure 3.13 shows the following five types of curves that the Modified function is capable of modeling:

Type 1- Curves where the initial slope, S_o is greater than zero, the final slope, S_p is smaller than S_p and is greater than zero, the shape parameter n_1 is negative and the shape parameter n_2 is positive.

Modified Parameters: S_o=5, S_p=0.1, M_o=0.5, ϕ_u=1, n_1=-5 and n_2=1

Type 2- Curves where the initial slope, S_o is small, the final slope, S_p is negative and the shape parameters n_1 and n_2 are positive.

Modified Parameters: S_o=0.1, S_p=-0.1, M_o=0.5, ϕ_u=1, n_1=10 and n_2=1

Type 3- Curves where the initial slope, S_o equals zero, the final slope, S_p is positive, the shape parameter n_1 is greater than two and the shape parameter n_2 is positive.

Modified Parameters: S_o=0, S_p=1, M_o=-0.5, ϕ_u=1, n_1=5 and n_2=1

Type 4- Curves where the initial slope, S_o is greater than the final slope, S_p, the shape parameter n_1 and n_2 is positive.

Modified Parameters: S_o=2, S_p=0.1, M_o=0.1, ϕ_u=1, n_1=10 and n_2=5

Type 5- Curves where the initial slope, S_o is positive, the final slope, S_p is less than S_o, the shape parameter n_1 is between zero and one and the shape parameter n_2 is greater than 0.2.

Modified Parameters: S_o=3, S_p=0.1, M_o=0.5, ϕ_u=1, n_1=0.5 and n_2=0.5

Figure 3.14 illustrates a plot of the Modified function that has two points of maximum curvature. The maxima are located at the extremes: at the origin and at the abscissa ϕ_u. By adjusting the values of the various parameters the relative magnitudes of the maximum curvature at the two locations can be adjusted.

3.4.3 Effect of the Shape Parameters, n_1 and n_2

The parameter n_1 controls how quickly the curve approaches the final tangent line. Figure 3.15 shows the Modified function for n_1=0.5, 1, and 2. As shown in the figure increasing the magnitude of the shape parameter, n_1 causes the function to approach the final tangent line more quickly.

Figure 3.16 shows how the shape parameter, n_1 causes a downward shift in the final asymptote. Negative values of the parameter n_1 cause the curve to "tail downward". As the shape parameter n_1 becomes more negative the curve approaches a Type 1 curve with reversal of curvature.

When n_2 is negative the plot of the curve approaches the final tangent line from above instead of below and is characterized as a "hump" over the final tangent line. Figure 3.17 (a) shows how n_1 interacts with n_2 to affect the shape of the hump. Increasing the magnitude of n_2 also affects the shape of the hump as illustrated in Figure 3.17 (b).

Figure 3.18 (a) and (b) shows that as n_1 and n_2 become smaller the plot of the Modified function becomes flatter, yet the function is required to contact the final tangent line at the ultimate rotation, ϕ_u. Type 5 curves with reversal of curvature use this feature of the Modified function.

3.4.4 Derivatives of the Modified Function

The first and second derivatives of the Modified function, obtained using the Mathematica software are the following:

The first derivative, or slope, is

$$M'(\phi) = S_p + \frac{S_o - S_p}{\left(\left(\frac{\phi_u - \phi}{\phi_u}\right)^{n_1} + \left(\frac{(S_o - S_p)\phi}{M_o}\right)^{n_2}\right)^{1/n_2}}$$

$$-\frac{1}{n_2}\left(\frac{(S_o - S_p)\phi\left(\left(n_2\left(\frac{S_o - S_p}{M_o}\right)\left(\frac{(S_o - S_p)\phi}{M_o}\right)^{n_2 - 1}\right) - \left(\frac{1}{n_2\phi_u}\right)\left(\frac{\phi_u - \phi}{\phi_u}\right)^{n_1 - 1}\right)}{\left(\left(\frac{\phi_u - \phi}{\phi_u}\right)^{n_1} + \left(\frac{(S_o - S_p)\phi}{M_o}\right)^{n_2}\right)^{1 + 1/n_2}}\right) \quad 3.10$$

The second derivative, or curvature, is

$$M''(\phi) = \left(\left(\frac{\phi_u - \phi}{\phi_u}\right)^{n_1} + \left(\frac{(S_o - S_p)\phi}{M_o}\right)^{n_2}\right)^{2 - 1/n_2}$$

$$-\frac{(S_o - S_p)\phi}{n_2}\left(\frac{(n_1^2 - n_1)}{\phi_u^2}\left(\frac{\phi_u - \phi}{\phi_u}\right)^{n_1 - 2} + \frac{\left(n_2^2 - n_2\right)(S_o - S_p)^2}{M_o^2}\left(\frac{(S_o - S_p)\phi}{M_o}\right)^{n_2 - 2}\right) *$$

$$\left(\left(\frac{\phi_u - \phi}{\phi_u}\right)^{n_1} + \left(\frac{(S_o - S_p)\phi}{M_o}\right)^{n_2}\right)^{-1 - 1/n_2}$$

$$-2n_2(S_o - S_p)\left(\frac{n_2(S_o - S_p)}{M_o}\left(\frac{(S_o - S_p)\phi}{M_o}\right)^{1/n_2 - 1} - \frac{n_1}{\phi_u}\left(\frac{\phi_u - \phi}{\phi_u}\right)^{n_1 - 1}\right) * \quad 3.11$$

$$\left(\left(\frac{\phi_u - \phi}{\phi_u}\right)^{n_1} + \left(\frac{(S_o - S_p)\phi}{M_o}\right)^{n_2}\right)^{-1 - 1/n_2}$$

3.4.5 Observations from Derivative Plots

3.4.5.1 Richard-Abbott Function Behaviour

Because the Modified function is a generalized form of the Richard-Abbott function it can plot all of the curves described in the section describing the Richard-Abbott function. Therefore, the Modified function can have a point of maximum curvature at the origin

and at a location defined by the reference rotational deformation, $\phi_o=M_o/S_o$. Thus, the function can model curves that possess a bi-linear or nearly bi-linear shape.

3.4.5.2 Reversal of Curvature

Figures 3.19 (a), (b) and (c) show the plot of the function and its derivatives for a Type 1 curve. The curve starts from the origin with maximum negative curvature, Figure 3.19 (c). The maximum negative slope, Figure 3.19 (b), corresponds to a rotational deformation of approximately 0.4. This indicates the point of inflection on the curve, Figure 3.19 (a). The maximum positive curvature is at a rotational deformation of approximately 0.6. The magnitude of the maximum positive curvature is less than one percent of the maximum negative curvature. At the ultimate rotation, ϕ_u there is zero curvature. At the ultimate rotation the curve is parallel to the final tangent line but is shifted down by the reference moment, M_o.

Figures 3.20 (a), (b) and (c) show a plot of the function and its derivatives for a Type 2 curve. This curve reaches a point of maximum slope, Figure 3.20 (b), at a rotational deformation of approximately 0.2. This corresponds to the point of inflection in the curve, Figure 3.20 (c). For this curve the points of maximum positive and negative curvature are at rotational deformations of approximately 0.12 and 0.29 respectively. These curvatures are equal in magnitude. Beyond a rotational deformation of 0.6 there is zero curvature and the curve is tangent to the final tangent line.

Figures 3.21 (a), (b) and (c) show a plot of the function and its derivatives for a Type 3 curve. For this curve, the maximum negative curvature is at the origin and the maximum positive curvature is at a rotational deformation of approximately 0.3, Figure 3.21 (c). The magnitudes of these two values are equal. The point of inflection corresponding to the maximum slope, Figure 3.21 (b), is located at a rotational deformation of approximately 0.13. The curvature drops to zero at a rotational deformation of 0.8 and the curve is tangent to the final tangent line.

Figures 3.22 (a), (b) and (c) show a plot of the function and its derivatives for a Type 4 curve. This curve has three points of maximum curvature, Figure 3.22 (c). There is one point of maximum negative curvature between two points of maximum positive curvature. The curvature is mathematically undefined at the origin. The first point of maximum positive curvature is at a rotational deformation of 0.1 and the second at a rotational deformation of 0.75. Between these two points there is a region of negative curvature. This region appears as a "hump" on the function plot, Figure 3.22 (a), which rises above the final tangent line. Thus, the curve approaches this line tangentially from above instead of below.

Figures 3.23 (a), (b) and (c) show a plot of the function and its derivatives for a Type 5 curve. This curve starts from the origin with maximum negative curvature, Figure 3.23 (c). There is nearly zero curvature between a rotational deformation of 0.2 and 0.8. Thus, the curve is linear in this region with a slope of approximately 0.35, Figure 3.23 (b). Near the ultimate rotation, ϕ_u the curvature becomes positive and reaches a maximum at ϕ_u, Figure 3.23 (c).

3.4.5.3 Two Points of Maximum Negative Curvature

The Modified function also permits curves which have two points of maximum negative curvature: the first at the origin and the second at the ultimate rotation, ϕ_u. When n_1 is between 1 and 2 and n_2 is between 0 and 1 the case of two maximum curvatures is achieved. The interaction between the initial slope and the two shape parameters controls the relative magnitude of the maximum curvatures.

Figures 3.24 (a), (b) and (c) show the function and its derivatives for a curve in which the two maximum curvature points are approximately equal in magnitude. The parameters for this type of curve are: S_o=5, S_p=0, M_o=1, ϕ_u=1, n_1=1.5 and n_2=2.

Figures 3.25 (a), (b) and (c) show the function and its derivatives for a curve in which the magnitude of curvature at the origin is larger than that at the ultimate rotation. To

achieve this increased curvature at the origin the initial slope, S_o is increased. The initial slope for this plot is S_o=5. The other parameters are equal to those used in Figure 3.24.

Figures 3.26(a), (b) and (c) show the function and its derivatives for a curve in which the higher magnitude of curvature is at the ultimate rotation. In this case the initial slope, S_o is decreased. The initial slope for this plot is S_o=3 with the other parameters equal to the ones used in Figure 3.24.

Figures 3.27 (a), (b) and (c) show the effect of increasing the magnitude of the shape parameter n_1. Increasing n_1 to 3 and keeping the other curve fitting parameters similar to those used in Figure 3.24 causes the plot, Figure 3.27 (a), to possess negative curvature in the middle region of the curve. This is evident by the slight "hump" in the curvature diagram, Figure 3.27 (c). Decreasing the parameter n_1 creates double curvature in the plot. For n_1 less than zero the plot will be Type 1, Figure 3.15, and for n_1 between zero and one the plot will be Type 5, Figure 3.23.

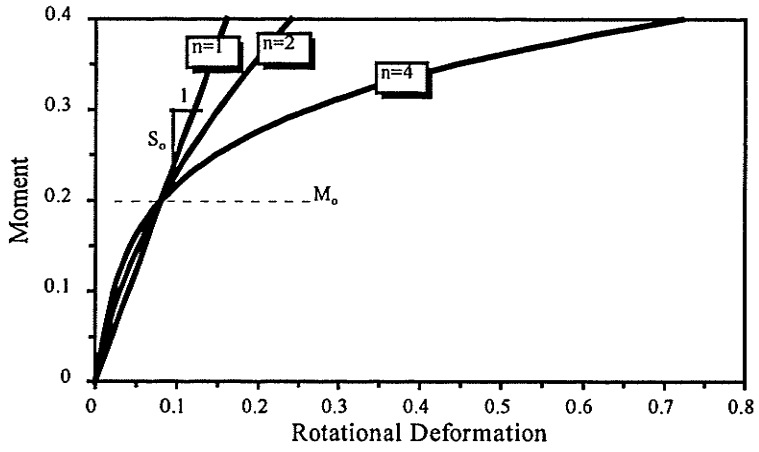


Figure 3.1 Effect of shape parameter, n, on the Ramberg-Osgood Function

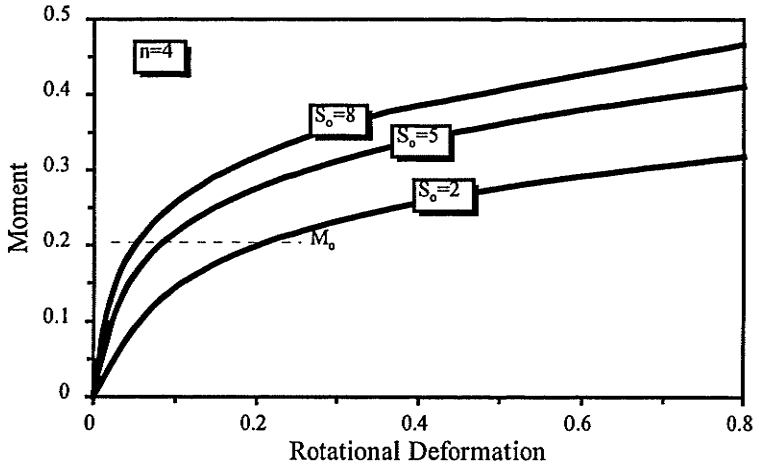


Figure 3.2 Effect of slope parameter, S_o, on the Ramberg-Osgood Function

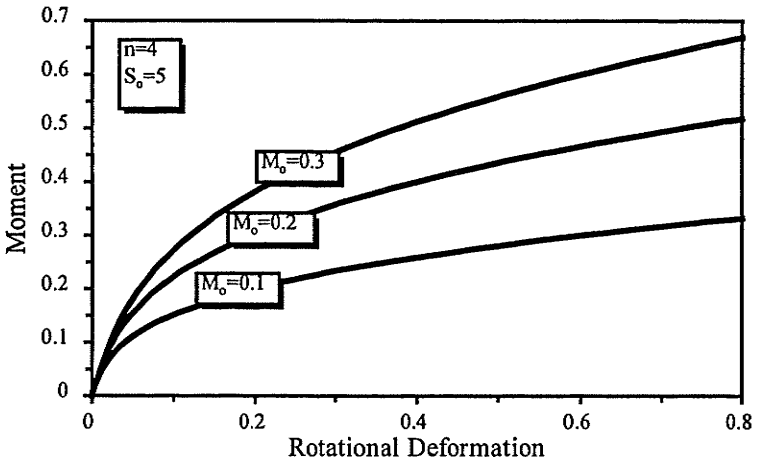


Figure 3.3 Effect of reference moment, M_o, on the Ramberg-Osgood Function

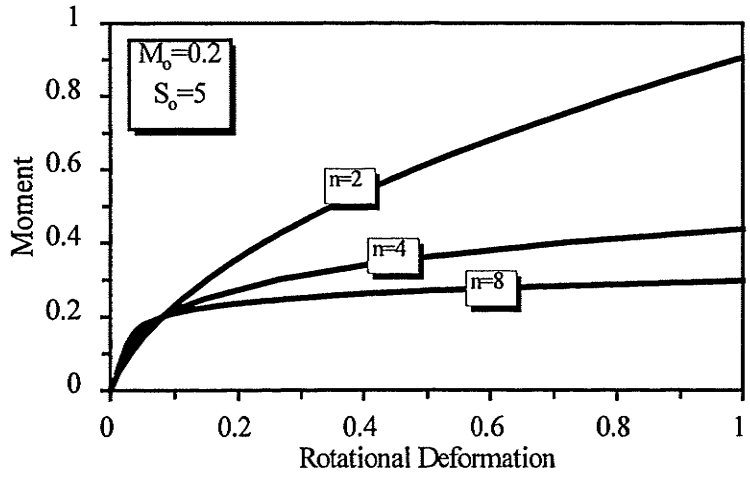


Figure 3.4 (a) Ramberg-Osgood Function for n=2, n=4 and n=8

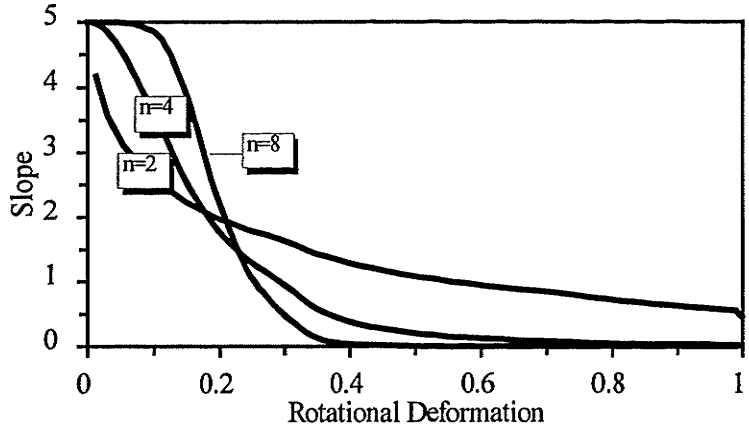


Figure 3.4 (b) Slope of Ramberg-Osgood Function for n=2, n=4 and n=8

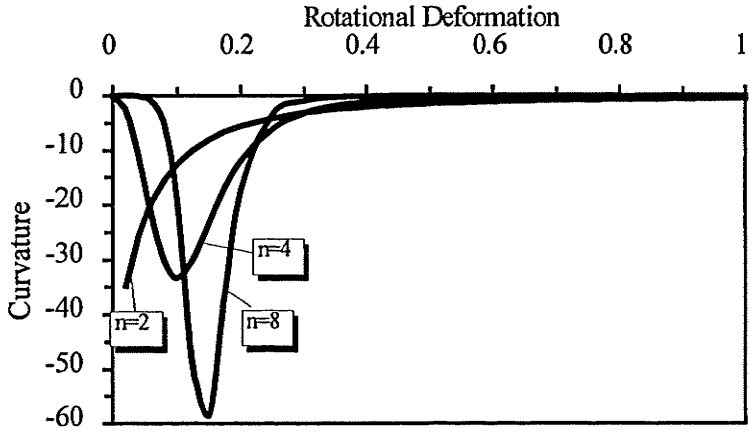


Figure 3.4.(c) Curvature of Ramberg-Osgood Function for n=2, n=4 and n=8

Figure 3.4 Ramberg-Osgood properties for n=2, n=4 and n=8

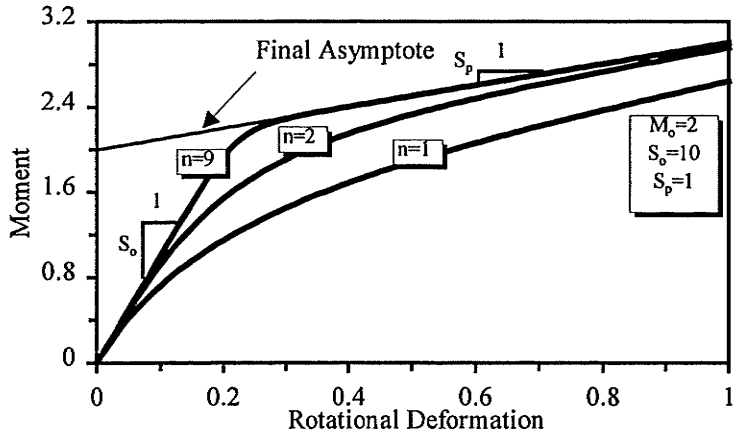


Figure 3.5 Richard-Abbott Function; Effect of shape parameter, n

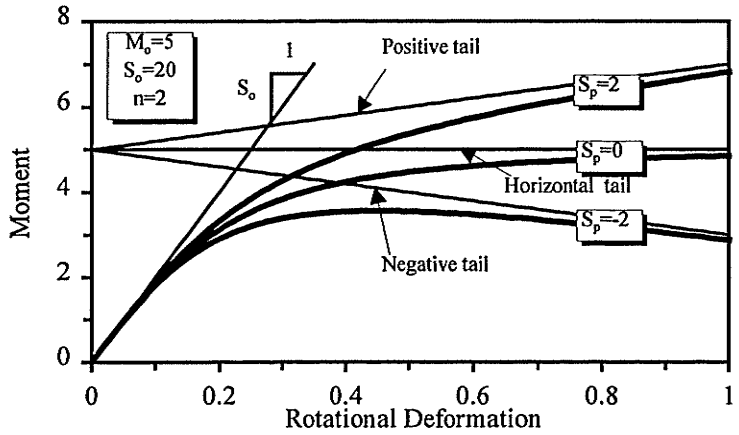


Figure 3.6 Richard-Abbott Function; Effect of S_p, negative curve

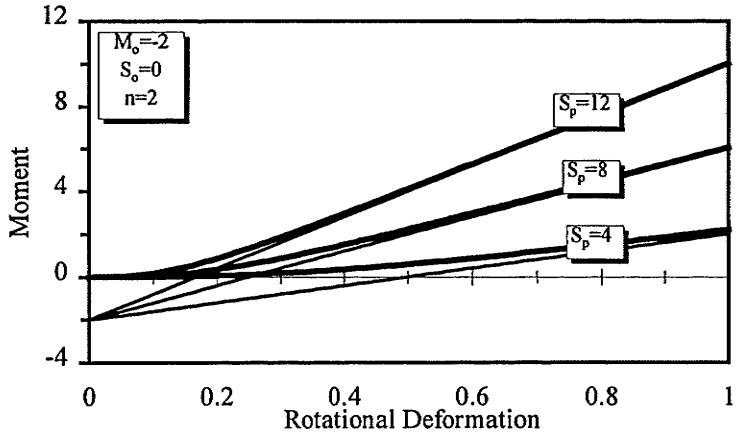


Figure 3.7 Richard-Abbott Function; Effect of S_p, positive curve

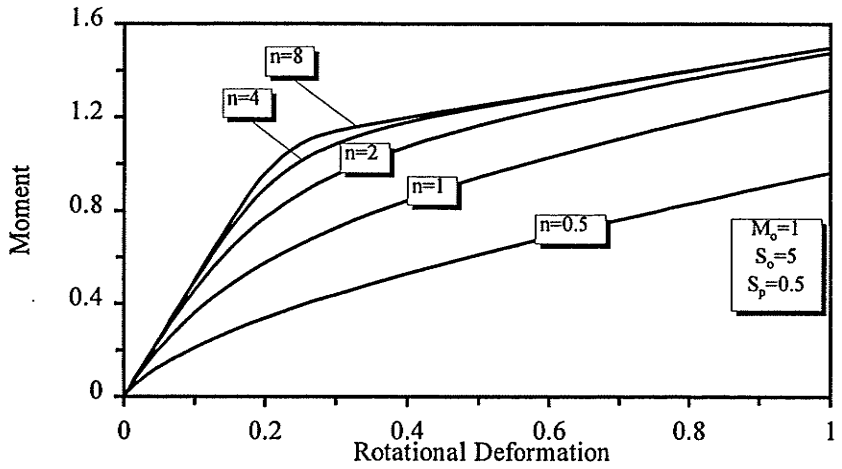


Figure 3.8 (a) Richard-Abbott Function with Negative Curvature

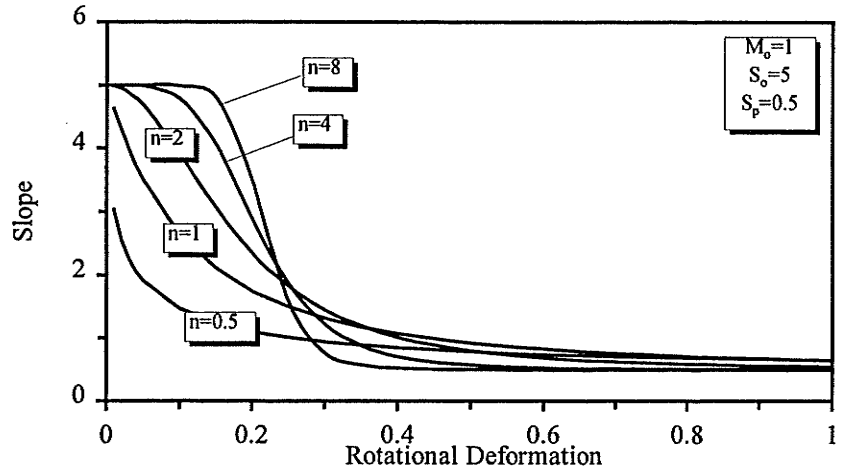


Figure 3.8 (b) Slope of Richard-Abbott Function with Negative Curvature

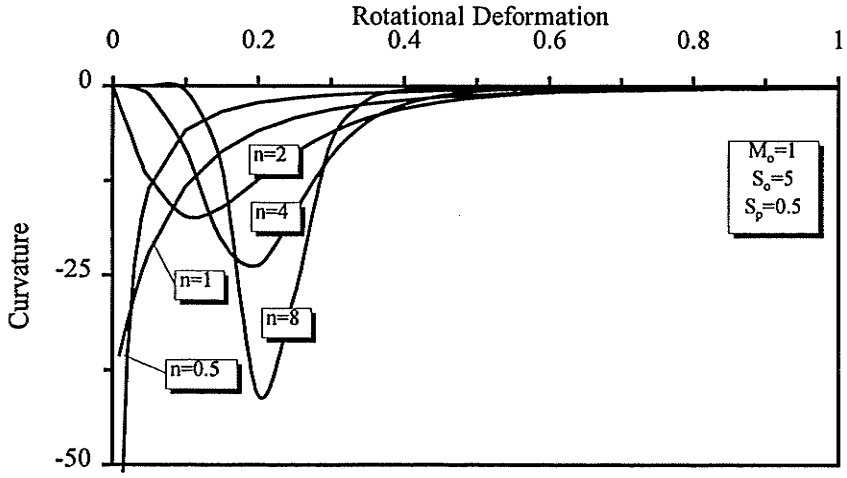


Figure 3.8 (c) Curvature of Richard-Abbott Function with Negative Curvature

Figure 3.8 Properties of the Richard-Abbott Function

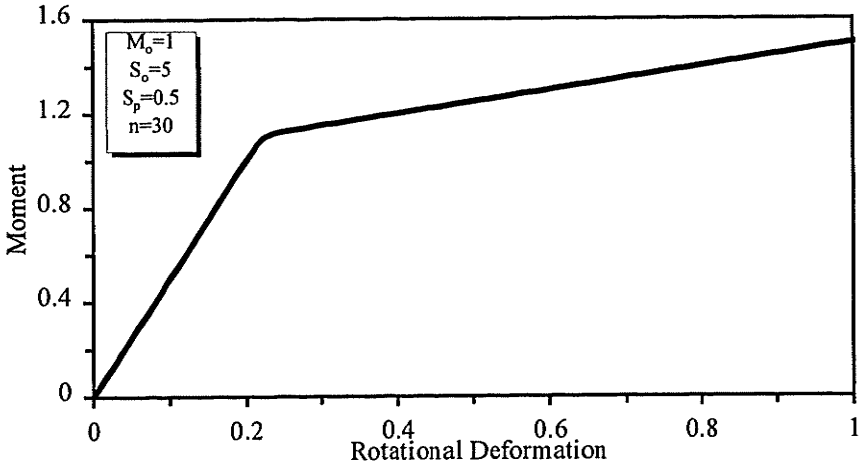


Figure 3.9 Bi-linear Richard-Abbott Function for large n

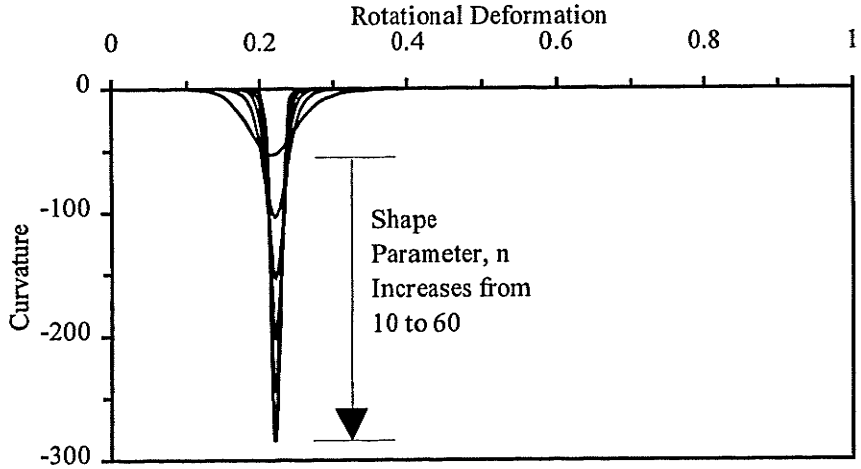


Figure 3.10 Spike in Curvature Diagram for large values of n

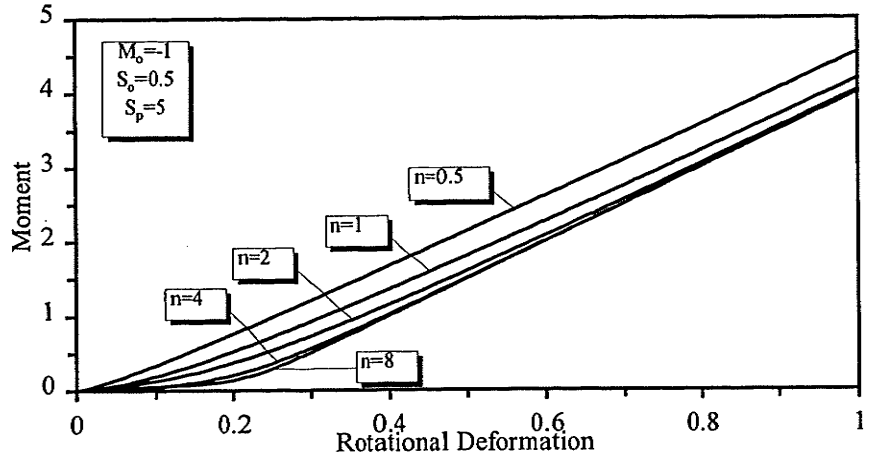


Figure 3.11 Richard-Abbott Function with Positive Curvature

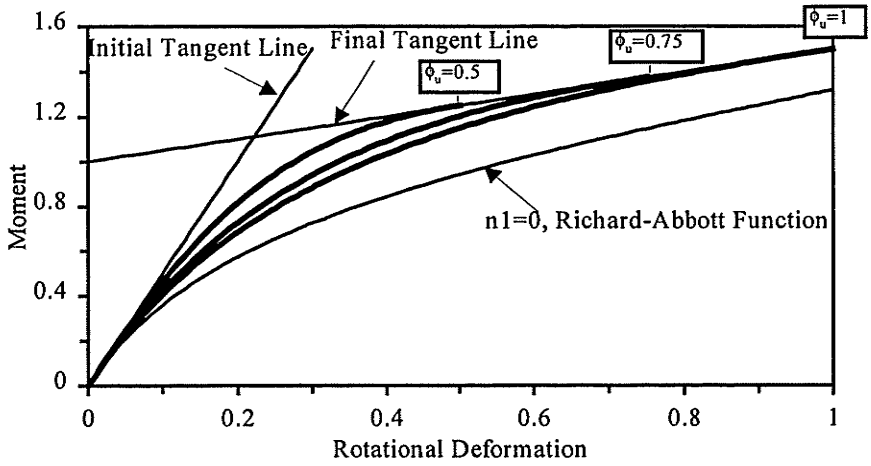


Figure 3.12 Effect of ϕ_u on Modified Function; S_o=5, S_p=0.5, M_o=1, n_1=2, n_2=1

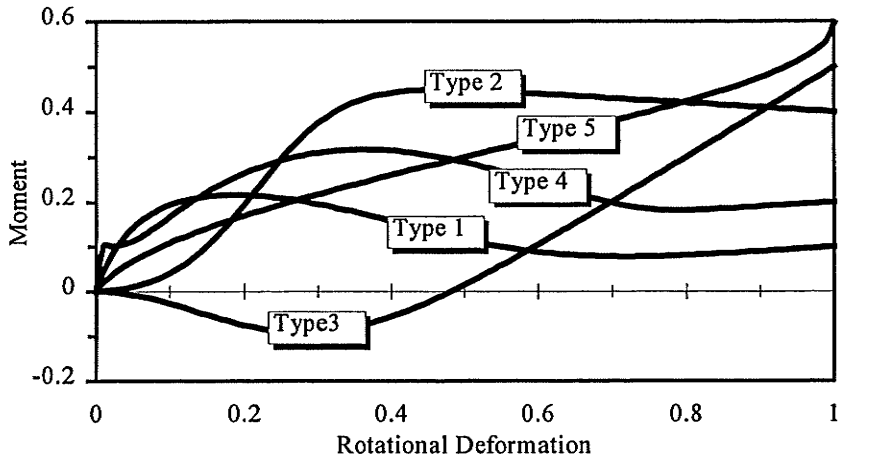


Figure 3.13 Five types of curves with a reversal of curvature

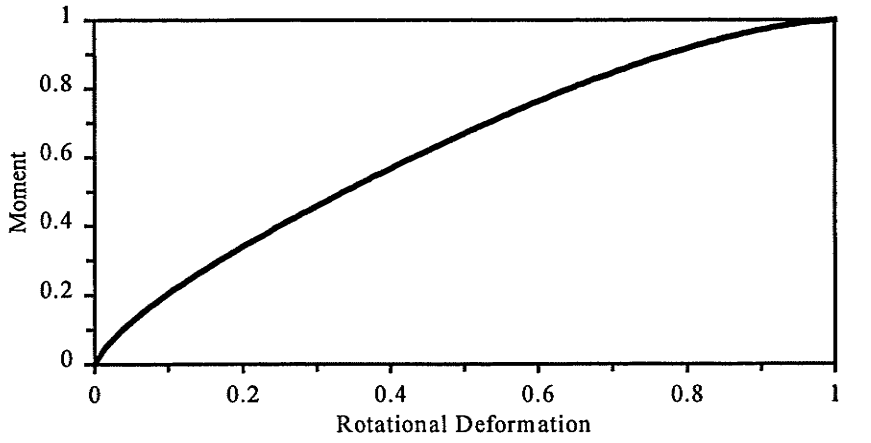


Figure 3.14 Two Points of Maximum Curvature

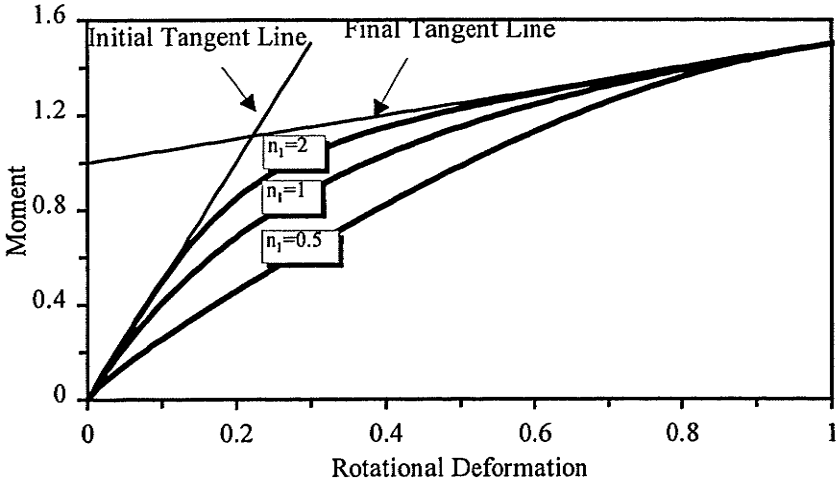


Figure 3.15 Effect of n_1 on Modified Function; S_o=5, S_p=0.5, M_o=1, ϕ_u=1, n_2=1

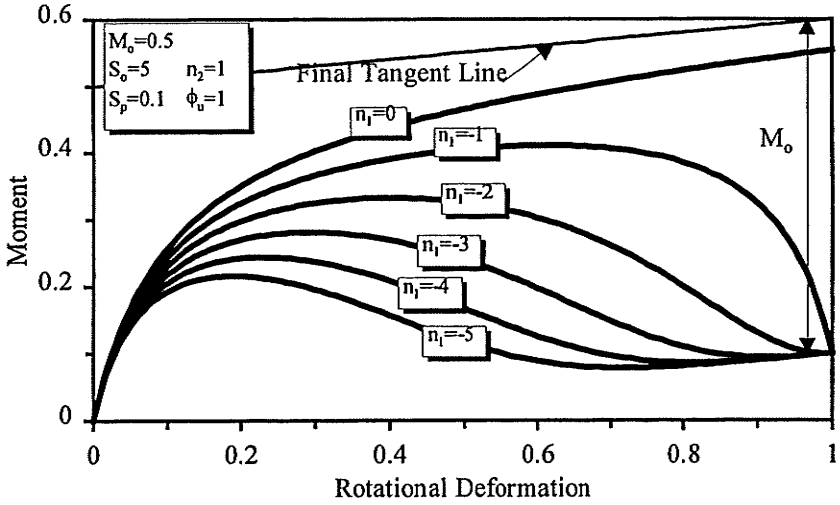


Figure 3.16 Effect of n_1 on final asymptote for positive n_2

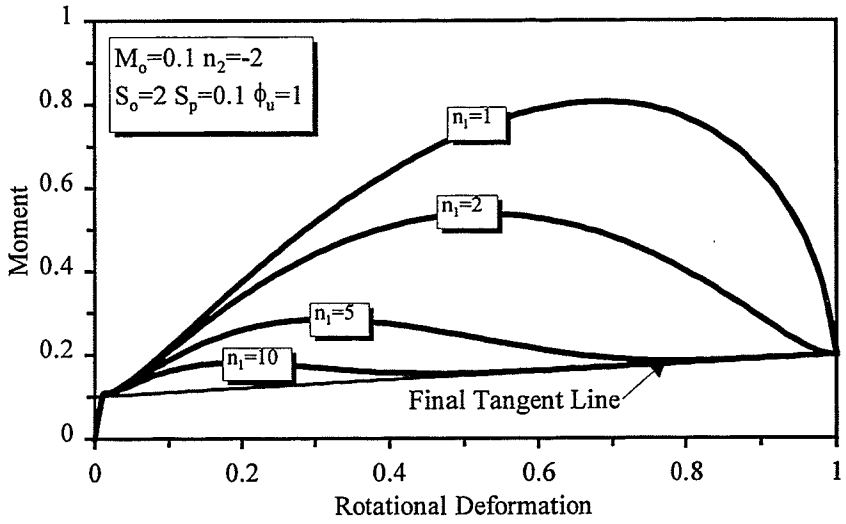


Figure 3.17(a) Effect of shape parameter, n_1 for negative n_2

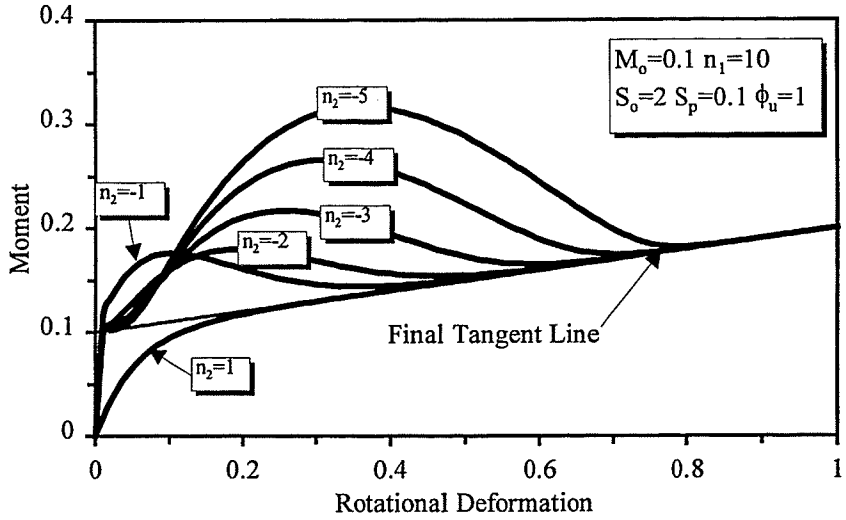


Figure 3.17(b) Effect of shape parameter, n_2 for positive n_1

Figure 3.17 Effect of shape parameters n_1 and n_2

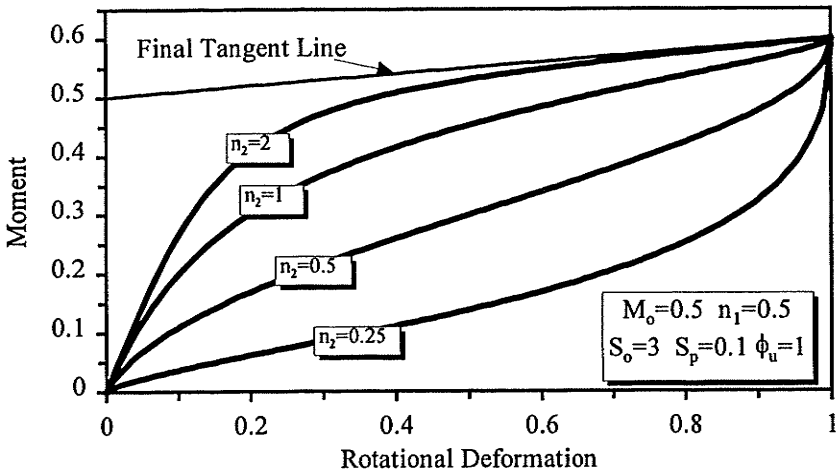


Figure 3.18 (a) Effect of shape parameter, n_2 for small n_1

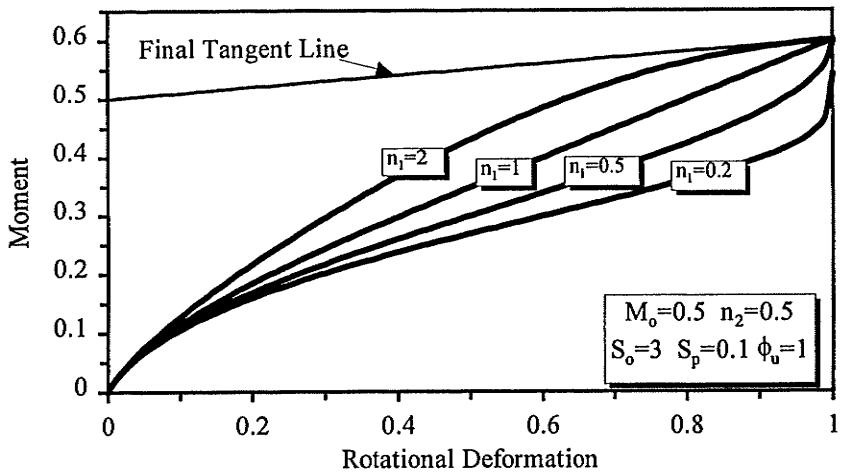


Figure 3.18 (b) Effect of shape parameter, n_1 for small n_2

Figure 3.18 Effect of shape parameters n_1 and n_2 for small values

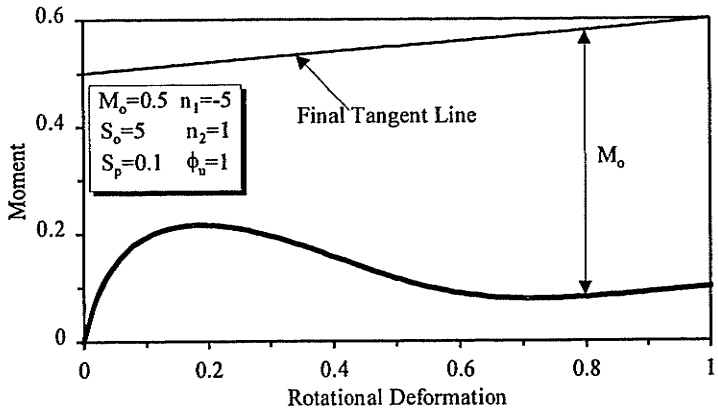


Figure 3.19 (a) Type 1 Reversal of Curvature

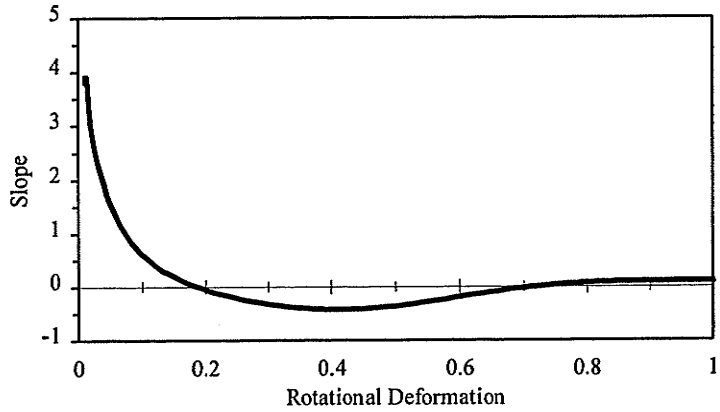


Figure 3.19 (b) Slope Type 1 Reversal of Curvature

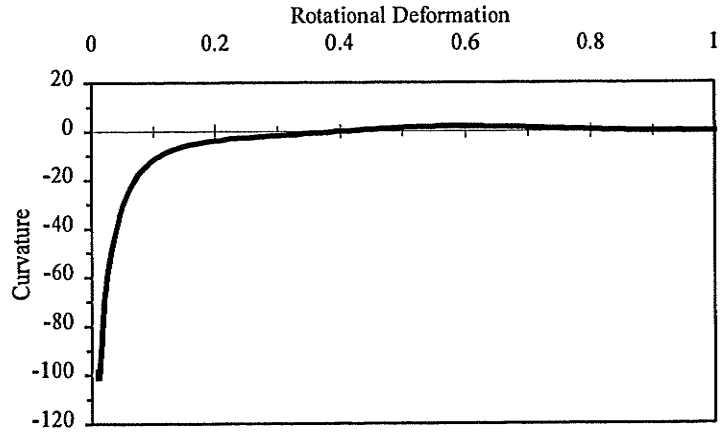


Figure 3.19 (c) Curvature of Type 1 Reversal of Curvature

Figure 3.19 Modified Function: Type 1

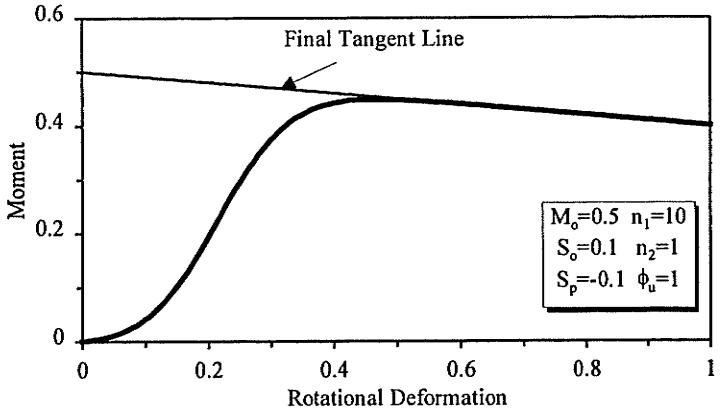


Figure 3.20 (a) Type 2 Reversal of Curvature

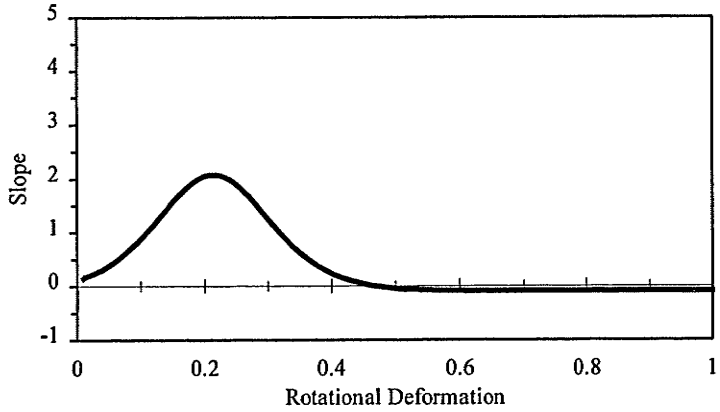


Figure 3.20 (b) Slope Type 2 Reversal of Curvature

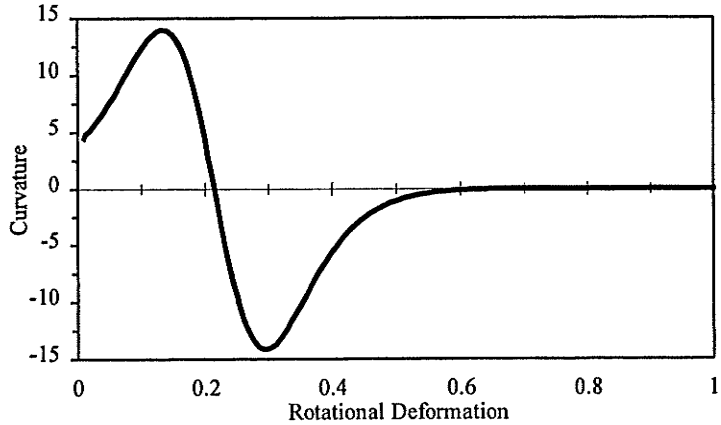


Figure 3.20 (c) Curvature of Type 2 Reversal of Curvature

Figure 3.20 Modified Function: Type 2

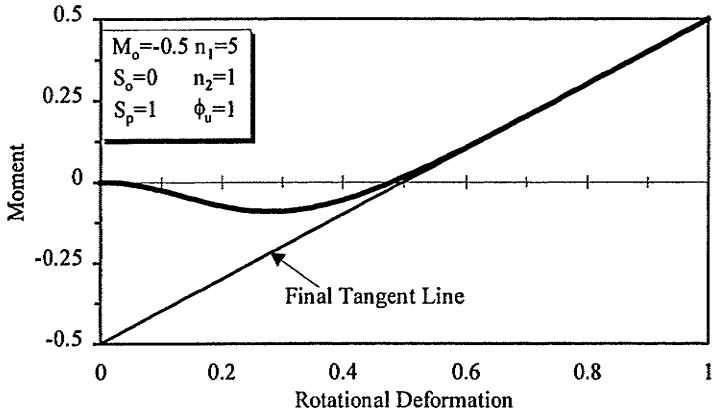


Figure 3.21 (a) Type 3 Reversal of Curvature

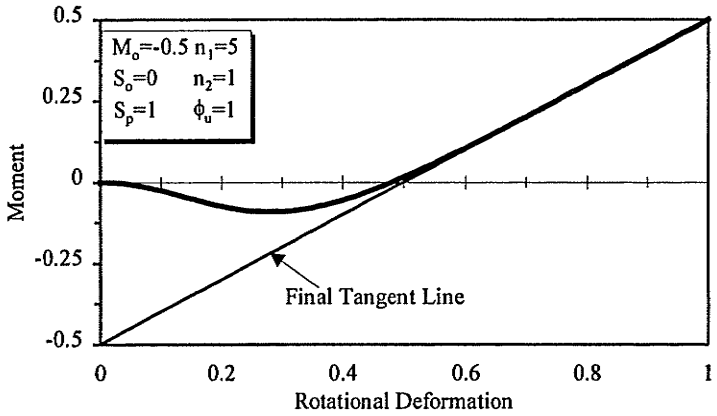


Figure 3.21 (b) Slope Type 3 Reversal of Curvature

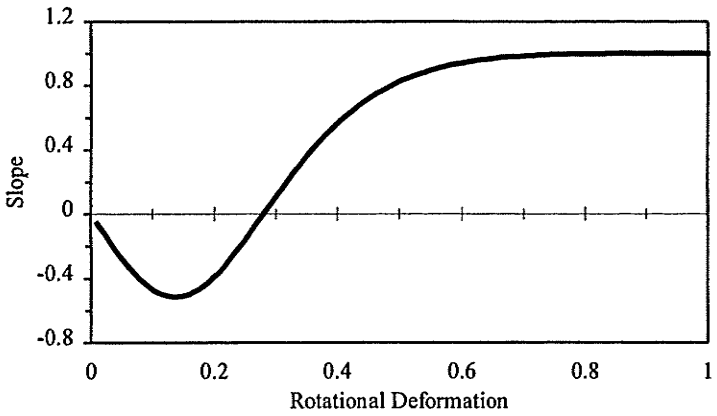


Figure 3.21 (c) Curvature of Type 3 Reversal of Curvature

Figure 3.21 Modified Function: Type 3

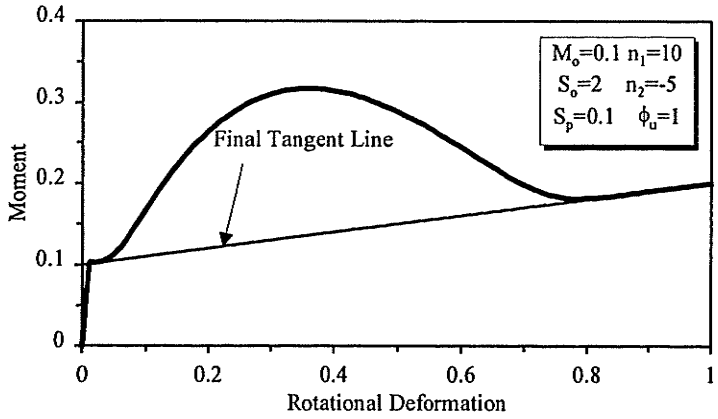


Figure 3.22 (a) Type 4 Reversal of Curvature

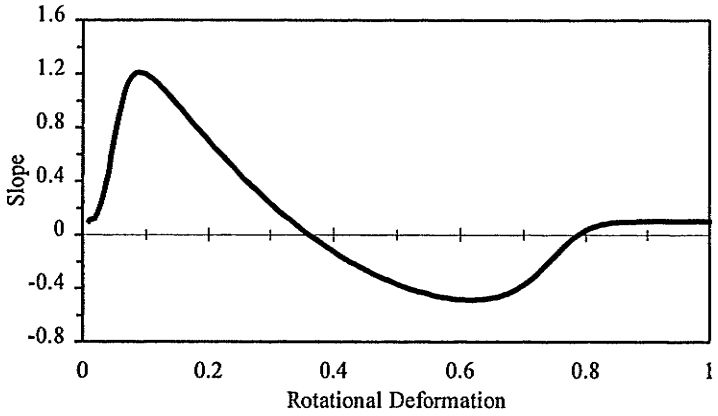


Figure 3.22 (b) Slope Type 4 Reversal of Curvature

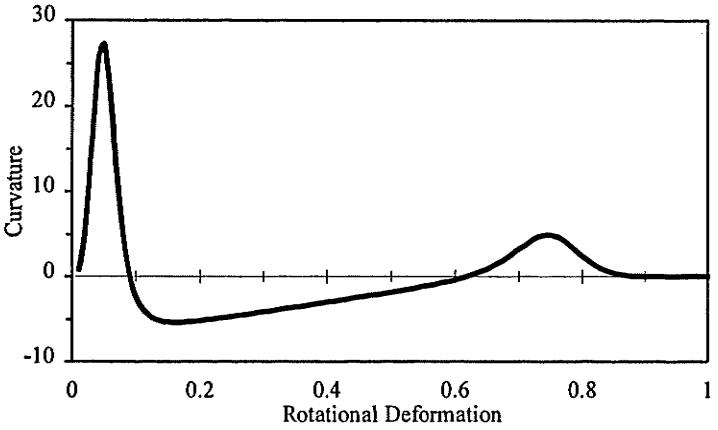


Figure 3.22 (c) Curvature of Type 4 Reversal of Curvature

Figure 3.22 Modified Function: Type 4

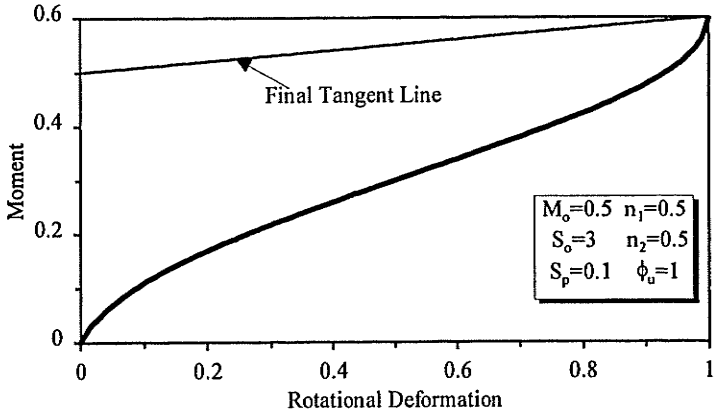


Figure 3.23 (a) Type 2 Reversal of Curvature

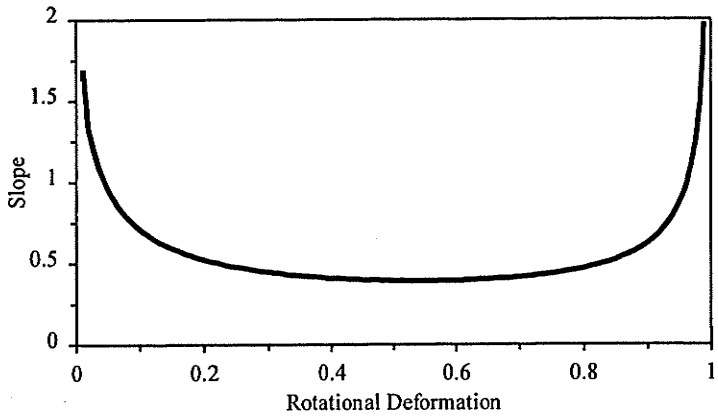


Figure 3.23 (b) Slope Type 2 Reversal of Curvature

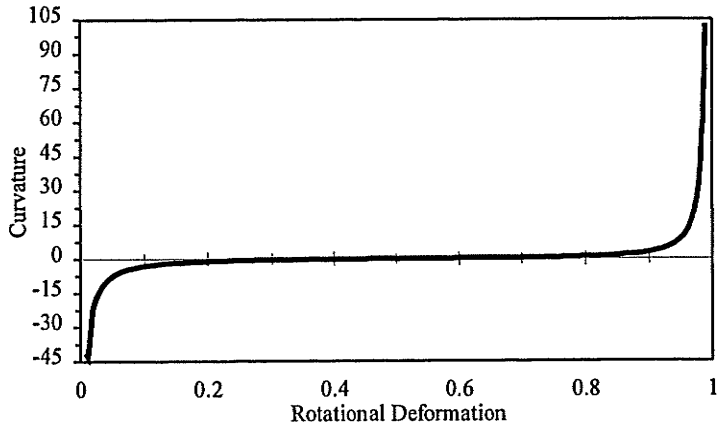


Figure 3.23 (c) Curvature of Type 5 Reversal of Curvature

Figure 3.23 Modified Function: Type 5

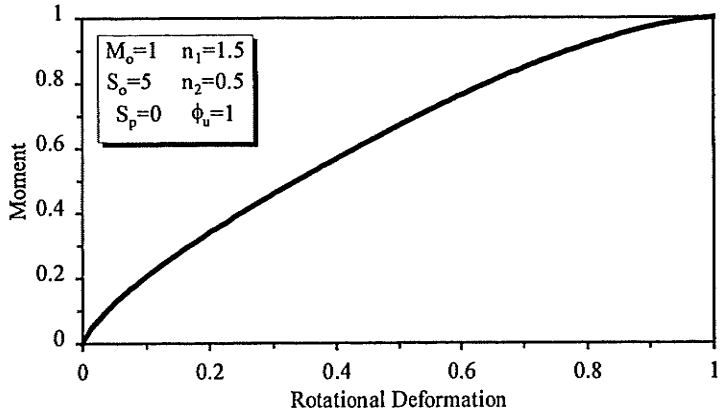


Figure 3.24 (a) Plot of Function

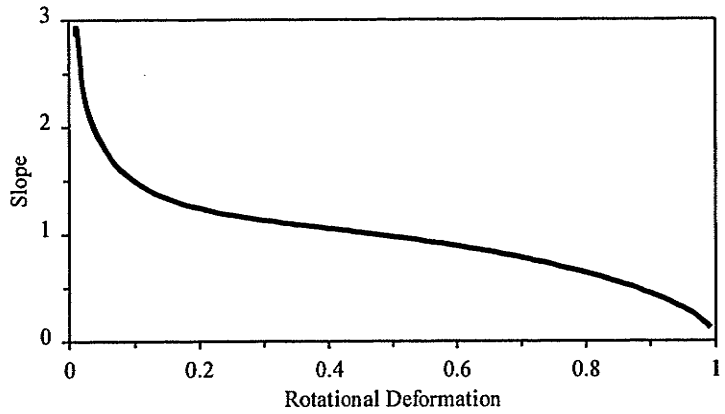


Figure 3.24 (b) Slope of Function

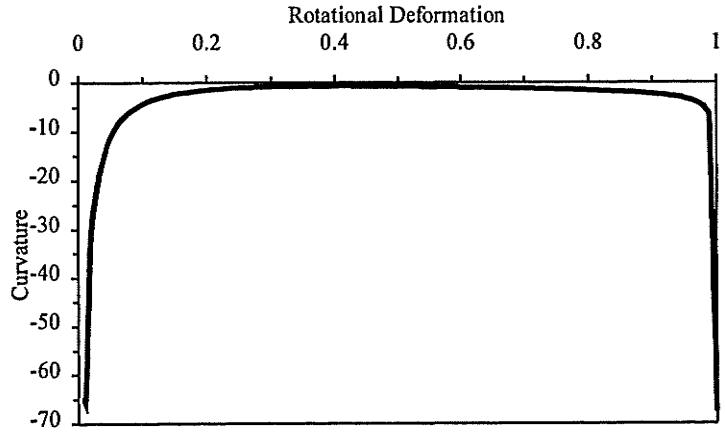


Figure 3.24 (c) Curvature of Function

Figure 3.24 Two Points of Maximum Curvature: Equal Magnitude

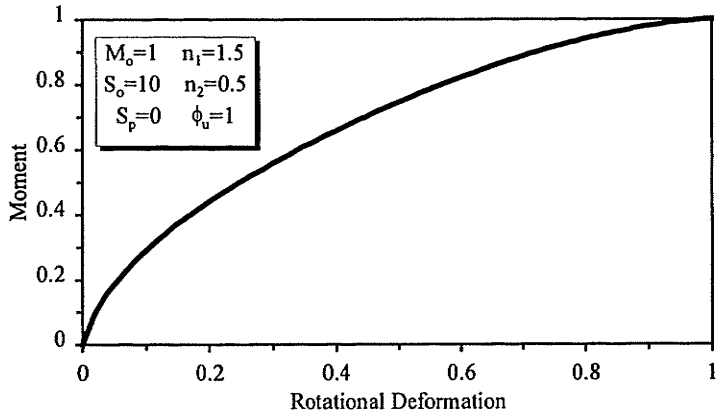


Figure 3.25 (a) Plot of Function

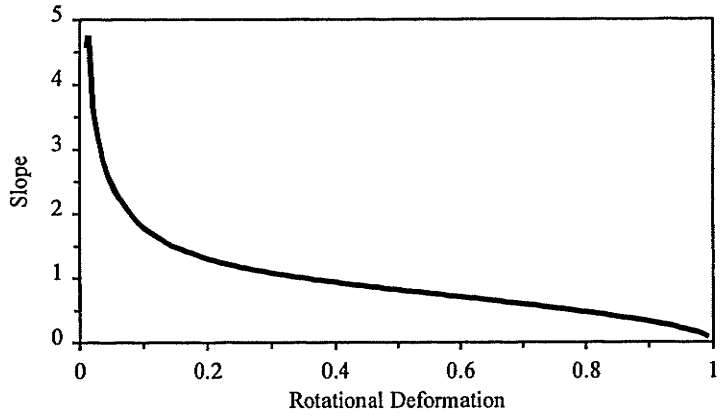


Figure 3.25 (b) Slope of Function

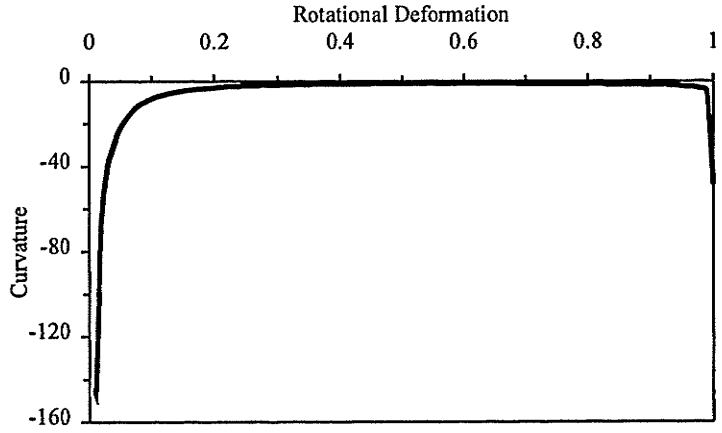


Figure 3.25 (c) Curvature of Function

Figure 3.25 Two Points of Maximum Curvature: Greater at Origin

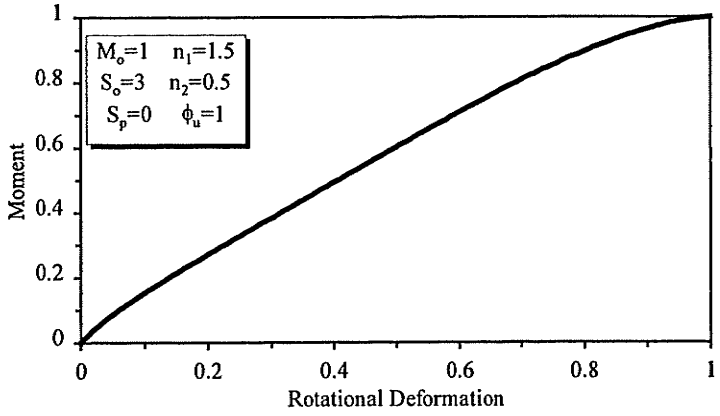


Figure 3.26 (a) Plot of Function

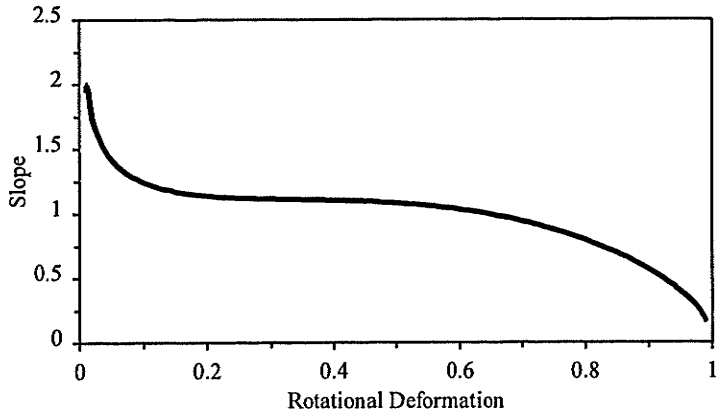


Figure 3.26 (b) Slope of Plot

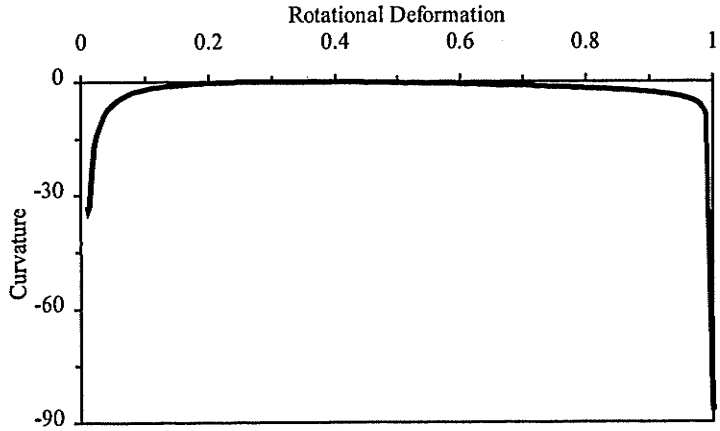


Figure 3.26 (c) Curvature of Plot

Figure 3.26 Two Points of Maximum Curvature: Greater at ϕ_u

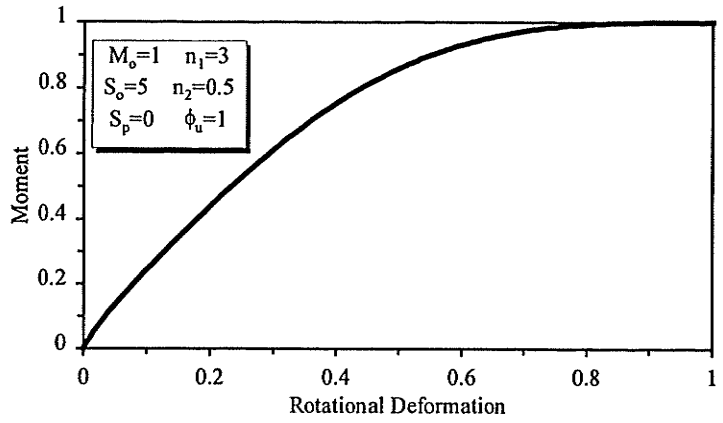


Figure 3.27 (a) Plot of Function

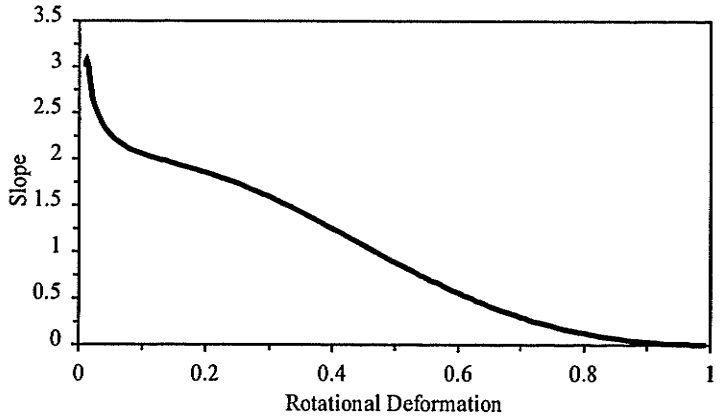


Figure 3.27 (b) Slope of Function

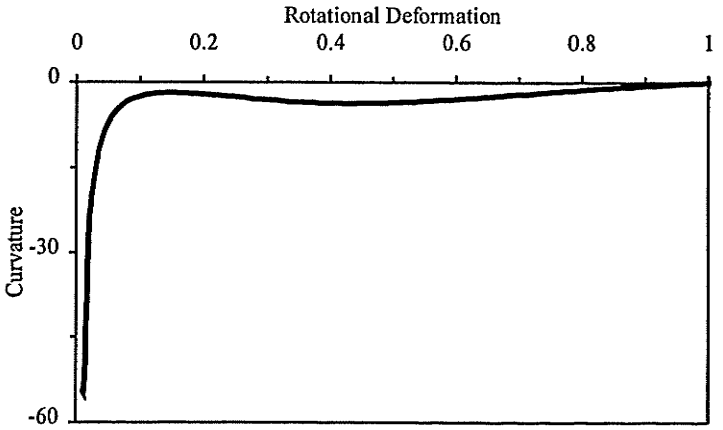


Figure 3.27 (c) Curvature of Function

Figure 3.27 Maximum Curvature at Origin with intermediate "hump"

4. Curve Fitting and Classification of Connection M-ϕ Data

4.1 Modeling of Connection Behaviour

A number of methods have been used to predict beam-to-column connection behaviour. They include finite element models (Krishnamurthy et. al., 1979; Tarpy and Cardinal, 1981; Maxwell et. al., 1981; Patel and Chen, 1984) and yield line models (Packer and Morris, 1977). Other approaches have involved modeling or measuring the behaviour of individual elements that make up the connection and then assembling them to form the connection (Sherbourne, 1961; Douty and McGuire, 1965; Kennedy et. al., 1981; Richard et. al., 1980; Kennedy and Hafez, 1984). Because of factors such as bolt slip, that are difficult to model, none of the above-mentioned approaches have provided accurate behaviour prediction models for a wide range of connection types and geometries.

Using all of the available experimental M-ϕ data, attempts have been made to curve fit the data and develop M-ϕ functions expressed in terms of the connection geometric parameters (Sommer, 1969; Frye and Morris, 1975; Altman et. al., 1982; Ang and Morris, 1984; Attiogbe et. al., 1989). While these empirical functions have generally been accurate for those connection geometries on which they were based, they have not worked well for other connection geometries.

Thus, the most practical way to develop an accurate, concise M-ϕ behaviour model for a given connection is to measure its M-ϕ behaviour experimentally and to curve-fit the M-ϕ data to a versatile function. The modified Richard-Abbott function described in the previous chapter is an excellent one for the purpose.

4.2 Modeling of Connection Data by Curve-Fitting

4.2.1 Curve Fitting Function

In order to incorporate the nonlinear M-ϕ behavior of a variety of connection geometries into a frame analysis computer program it is necessary to express that behavior in a very compact form. Using the modified Richard-Abbott function, the M-ϕ behavior of any connection can be expressed in terms of the six parameters of the function. Thus, if the modified Richard-Abbott function and the six parameters for a set of connections are incorporated into the program, the M-ϕ behavior of any of those connections can be generated.

Kishi and Chen (1986) compiled and digitized the M-ϕ data from approximately 300 connection tests - almost all of the tests for which the data were available. In this study the data from 260 of the tests were curve fitted to the modified Richard-Abbott function, and the six curve fitting parameters were computed in each case. The data for 14 additional double web angle connection specimens tested by Onuah (1988) were similarly curve fitted.

4.2.2 Types of Connections Included in the Study

The seven connection types include are:

1. Single Web Angle/ Side Plate Connection,
2. Double Web Angle Connection,
3. Header Plate Connection,
4. Top and Seat Angle Connection,
5. Top and Seat Angle Connection with Double Web Angles,
6. Flush End Plate Connection and
7. Extended End Plate Connection

Detailed sketches of the seven connection types, illustrating their significant dimensions and geometric parameters, are shown in Figure 4.1 through Figure 4.8. The values of the

geometric parameters for the 260 M-ϕ data sets from the Kishi-Chen database and the 14 from Onuah's tests are presented in Tables 4.1 to 4.9.

4.2.3 Eurocode3 Classification System

4.2.3.1 Classification of Connections

A simple plot of the M-ϕ behaviour of a connection is not very useful to a designer. A "feel" for the connection strength and stiffness is required. The Eurocode3 classification system for connections, described in Chapter 2, is an effective way to establish this "feel" as it shows the connection behaviour superimposed on a common template: the classification boundaries. Using this system the designer can ascertain a connection's strength and stiffness characteristics at a glance.

In the Eurocode3 connection classification system the connection moments and rotational deformations are expressed in non-dimensional form. As expressed in Clause 6.9.6 of Eurocode3 Design of Steel Structures (1990 Draft), the non-dimensional connection moment is expressed as a fraction of the plastic moment, M_p of the connected beam, as follows

$$\overline{m} = \frac{M}{M_p} \qquad 4.1$$

where M is the moment applied to the connection.

The normalized rotational deformation of the connection is derived as follows. The total rotational deformation along a beam of span L_b under a constant bending moment M, is

$$\phi_b = \frac{L_b}{EI_b} M \qquad 4.2.$$

where E = modulus of elasticity and

I_b = second moment of area of the beam.

Thus, ignoring contained plastic flow, the total rotational deformation, ϕ_p, when the constant moment just reaches the beam plastic moment, M_p, is

$$\phi_p = \frac{L_b}{EI_b} M_p \qquad 4.3.$$

Assuming a typical beam span-to-depth ratio of 20, the expression for the total plastic rotational deformation becomes

$$\phi_p = \frac{20d}{EI_b} M_p \qquad 4.4.$$

The normalized rotational deformation is then the rotational deformation, ϕ, in the connection, expressed as a fraction of the total plastic rotational deformation in the beam, as follows

$$\overline{\phi} = \frac{\phi}{\phi_p} \qquad 4.5.$$

The beam plastic moments, M_p, and plastic rotational deformations, ϕ_p, are presented in Table 4.10 for all of the 274 connection specimens considered.

4.2.3.2 Normalizing the Modified Function Parameters

In order to superimpose the connection M-ϕ plots onto the plots of the Eurocode3 connection classification boundaries, the curve fitting parameters for the modified Richard-Abbott function must be normalized using the appropriate M_p and ϕ_p values presented in Table 4.10. The following formulae were used to normalize the parameters.

$$\overline{S}_o = \frac{\phi_p}{M_p} S_o$$

$$\overline{S}_p = \frac{\phi_p}{M_p} S_p \qquad 4.6.$$

$$\overline{M}_o = \frac{M_o}{M_p}$$

$$\overline{\phi}_u = \frac{\phi_u}{\phi_p}$$

Because the shape parameters n_1 and n_2 are non-dimensional they did not need to be modified. Using Eq. 4.6, the modified Richard-Abbott function can be expressed in either dimensional or non-dimensional form.

4.2.4 Curve Fitting of Connection Data

A least-squares curve-fitting program was used to fit the 274 sets of experimental data to the modified Richard-Abbott function. Tables 4.11 to 4.18 show the normalized versions of the curve fitting parameters for all 274 data sets.

For purposes of illustration, the experimentally measured M-ϕ data for the following 8 connection specimens, representing the connection types indicated, are presented in Tables 4.19 through 4.26.

1.	S.L. Lipson:	AA-2/1	Single Web Angle Connection
2.	S.L. Lipson:	P1-2/1	Side Plate Connection
3.	L.E. Thompson et. al.:	A1-1 alt (a)	Double Web Angle Connection
4.	W.H. Sommer:	Test 5	Header Plate Connection
5.	M.J. Marley:	A-1/4-1	Top and Seat Angle Connection
6.	J.R. Ostrander:	Test 1	Flush End Plate Connection
7.	A. Azizinamini et. al.:	8S1	Top and Seat Angle with Double Web Angle Connection
8.	S.A. Ioannides:	Test 1	Extended End Plate Connection

Juxtaposed with the tables are plots of the data and corresponding modified Richard-Abbott functions, and plots of the function superimposed on the Eurocode3 connection classification boundaries. The plots are presented in figures 4.9 and through 4.16. Some of the M-ϕ data plots, such as that for the Lipson: P1-2/1 specimen in Figure 4.10 (a), have an ascending branch at large rotational deformation. That branch, which occurs for connections to beam webs, corresponds to a moment increase when, as a result of large connection deformation, the bottom flange of the beam comes into contact with the

column. The connection deformation at which contact occurs is well beyond the serviceability limit state and thus the ascending branch can be ignored.

The M-ϕ data and their plots and the plots of M-ϕ curves superimposed on the Eurocode3 connection classification boundaries for all 274 connection specimens considered are presented in Appendix A.

4.3 Envelopes of M-ϕ Curves

To help establish a "feel" for connection behaviour a graphical representation of the ranges of force-deformation behaviour exhibited by the various connection types is presented in this section. Envelopes of the M-ϕ curves for the common connection types are shown in Figure 4.17 through 4.23. The shaded area in each figure represents the range of M-ϕ curves for the particular connection type. Because they span the range of practical geometries the envelopes indicate the practical ranges of connection strength and stiffness. The normalized connection rotational deformation corresponding to CAN/CSA S16.1-M89 beam deflection and column drift limits at the serviceability limit state is approximately 0.35. Except for 41 of the connections, most of them falling within the "rigid" classification, all of the 274 connections considered have rotational deformation capacities in excess of that limit.

The single web angle connection is the most flexible type and the M-ϕ curves for that type fall almost entirely within the "nominally pinned" classification. Nonetheless, as illustrated in Figure 4.17, single web angle connections may resist as much as 10 percent of the beam plastic moment, M_p.

As illustrated in Figure 4.18, the M-ϕ curves for double web angle connections straddle the boundary between the "nominally pinned" and "semi-rigid" regions. Double web

angle connections are approximately twice as stiff as single web angle connections and the strongest ones resist almost 20 percent of the beam plastic moment, M_p.

The envelope of M-ϕ curves for header plate connections is shown in Figure 4.19. It can be seen that at the upper boundary of the envelope, header plate connections are marginally stiffer and stronger than double web angle connections, the strongest ones exhibiting maximum moments in excess of 20 percent of the beam plastic moment, M_p. Header plate connections span a wider range of stiffness and strength than do double web angle connections.

As illustrated in Figure 4.20, the M-ϕ curves for top and seat angle connections occupy the lower third of the "semi-rigid" classification. The stiffest of the top and seat angle connections are in the "rigid" region for braced frames and they resist between 10 and 40 percent of the beam plastic moment, M_p at a rotational deformation corresponding to the serviceability limit state.

Flush end plate connections are both stiffer and stronger than top and seat angle connections. As illustrated in Figure 4.21, their moment resistance at the serviceability limit state ranges from 20 to 60 percent of the beam plastic moment. The stiffest of the connections fall within the "rigid" classification for braced frames.

As shown in Figure 4.22, top and seat angle connections with double web angles exhibit a wide range of initial stiffnesses. Their ultimate moment resistance range from 20 to almost 80 percent of the beam plastic moment. The stiffest of these connections have initial stiffnesses in the "rigid" range for both braced and unbraced frames.

Extended end plate connections, for which the envelope of M-ϕ curves is shown in Figure 4.23, are extremely stiff and strong. Their initial stiffnesses range from approximately the middle of the "semi-rigid" classification to the top third of the "rigid" classification. In terms of strength, they range from 60 to approximately 125 percent of the beam plastic

moment. The probable reason for connection strengths of more than 100 percent of the beam M_p is beam yield strengths in excess of the specified minimum.

The ranges of behavior for the various connection types are summarized in Table 4.27. The three aspects of behavior included in the table are: resistance range, as a percentage of the beam plastic moment, M_p, stiffness range, expressed in terms of the Eurocode3 classification system, and rotational deformation capacity, expressed as the percentage of connections which have a normalized rotational capacity of less than the serviceability limit of 0.35.

Table 4.1 Geometric Parameters for Single Web Angle Connections

Author	Test ID	Angle Size	Lp	d	gb	gc	c	p	nb	nc	db
S.L. Lipson	AA-2/1	100x90x6	140	44	57	65	32	76	1x2	1x2	20
S.L. Lipson	AA-2/2	100x90x6	140	44	57	65	32	76	1x2	1x2	20
S.L. Lipson	AA-3/1	100x90x6	216	44	57	65	32	76	1x3	1x3	20
S.L. Lipson	AA-3/2	100x90x6	216	44	57	65	32	76	1x3	1x3	20
S.L. Lipson	AA-4/1	100x90x6	292	44	57	65	32	76	1x4	1x4	20
S.L. Lipson	AA-4/2	100x90x6	292	44	57	65	32	76	1x4	1x4	20
S.L. Lipson	AA-5/1	100x90x6	368	44	57	65	32	76	1x6	1x6	20
S.L. Lipson	AA-5/2	100x90x6	368	44	57	65	32	76	1x6	1x6	20
S.L. Lipson	AA-6/1	100x90x6	445	44	57	65	32	76	1x6	1x6	20
S.L. Lipson	AA-6/2	100x90x6	445	44	57	65	32	76	1x6	1x6	20
S.L. Lipson	BB-4/1	100x90x8	292	44	57	65	32	76	1x4	1x4	20
S.L. Lipson	BB-4/2	100x90x8	292	44	57	65	32	76	1x4	1x4	20
S.L. Lipson	B2-4	100x90x8	292	44	57	65	32	76	1x4	1x4	20
S.L. Lipson	B3-4	100x90x8	292	44	57	65	32	76	1x4	1x4	20
S.L. Lipson	C-4	125x90x8	292	44	57	49	32	76	1x4	1x4	20
S.L. Lipson	D-4	100x90x8	292	44	57	49	32	76	1x4	1x4	20
S.L. Lipson	G-2/1	100x90x6	121	206	64	-	32	57	1x2	-	20
S.L. Lipson	G-3/1	100x90x6	203	165	64	-	44	57	1x3	-	20
S.L. Lipson	G-4/1	100x90x6	305	124	64	-	57	57	1x4	-	20
S.L. Lipson	G-5/1	100x90x6	368	83	64	-	70	57	1x5	-	20

Table 4.2 Geometric Parameters for Single Plate Connections

Author	Test ID	Thickness	Lp	d	gb	c	pb	nb	db
S.L Lipson	P1-2/1	6	140	197	64	32	76	1x2	20
S.L Lipson	P1-2/2	6	140	197	64	32	76	1x2	20
S.L Lipson	P1-3/1	6	216	159	64	32	76	1x3	20
S.L Lipson	P1-3/2	6	216	159	64	32	76	1x3	20
S.L Lipson	P1-4/1	6	292	121	64	32	76	1x4	20
S.L Lipson	P1-4/2	6	292	121	64	32	76	1x4	20
S.L Lipson	P1-5/1	6	368	83	64	32	76	1x5	20
S.L Lipson	P1-5/2	6	368	83	64	32	76	1x5	20
S.L Lipson	P1-6/1	6	445	44	64	32	76	1x6	20
S.L Lipson	P1-6/2	6	445	44	64	32	76	1x6	20
L.E. Thompson et. al.	F-1 alt a	16	292	-	57	-	76	2x -	20
L.E. Thompson et. al.	F-1 alt b	16	292	-	57	-	76	2x -	20
L.E. Thompson et. al.	G-1 alt a	16	292	-	57	-	76	2x -	20
L.E. Thompson et. al.	G-1 alt b	16	292	-	57	-	76	2x -	20
L.E. Thompson et. al.	H-1 alt a	16	292	-	57	-	76	2x -	20
L.E. Thompson et. al.	H-1 alt b	16	292	-	57	-	76	2x -	20
L.E. Thompson et. al.	F-2-1 alt a	16	292	-	57	-	76	2x -	20
L.E. Thompson et. al.	F-2-1 alt b	16	292	-	57	-	76	2x -	20
L.E. Thompson et. al.	F-2-2 alt a	16	292	-	57	-	76	2x -	20
L.E. Thompson et. al.	F-2-2 alt b	16	292	-	57	-	76	2x -	20
L.E. Thompson et. al.	F-2-3 alt a	16	292	-	57	-	76	2x -	20
L.E. Thompson et. al.	F-2-3 alt b	16	292	-	57	-	76	2x -	20
R.M. Richard et. al.	RGKL2	6	154	-	-	-	76	1x2	20
R.M. Richard et. al.	RGKL3	6	229	-	-	-	76	1x3	20
R.M. Richard et. al.	RGKL5	6	381	-	-	-	76	1x5	20
R.M. Richard et. al.	RGKL7	6	546	-	-	-	76	1x7	22

Table 4.3 Geometric Parameters for Double Web Angle Connections

Author	Test ID	Angle Size	Lp	d	gb	gc	c	p	nb	nc	db
C.W. Lewitt et. al.	FK-4AB-M	150x100x10	292	83	89	53	32	76	2x4	2x4	20
B. Bose	B-1	150x90x15	400	28	90	60	50	75	2x -	1x5	20
L.E. Thompson	A1-1 alt (a)	100x90x8	292	-	57	65	-	-	- x2	- x -	20
L.E. Thompson	A1-1 alt (b)	100x90x8	292	-	57	65	-	-	- x2	- x -	20
L.E. Thompson	A1-2 alt (a)	100x90x8	292	-	57	65	-	-	- x2	- x -	20
L.E. Thompson	A1-2 alt (b)	100x90x8	292	-	57	65	-	-	- x2	- x -	20
L.E. Thompson	A1-3 alt (a)	100x90x8	292	-	57	65	-	-	- x2	- x -	20
L.E. Thompson	A1-3 alt (b)	100x90x8	292	-	57	65	-	-	- x2	- x -	20
L.E. Thompson	B1-1 alt (a)	100x90x13	292	-	57	65	-	-	- x2	- x -	20
L.E. Thompson	B1-1 alt (b)	100x90x13	292	-	57	65	-	-	- x2	- x -	20
L.E. Thompson	B1-2 alt (a)	100x90x13	292	-	57	65	-	-	- x2	- x -	20
L.E. Thompson	B1-2 alt (b)	100x90x13	292	-	57	65	-	-	- x2	- x -	20
L.E. Thompson	B1-3 alt (a)	100x90x13	292	-	57	65	-	-	- x2	- x -	20
L.E. Thompson	B1-3 alt (b)	100x90x13	292	-	57	65	-	-	- x2	- x -	20
L.E. Thompson	D1-1 alt (a)	100x90x10	292	-	57	46	-	-	- x2	- x -	20
L.E. Thompson	D1-1 alt (b)	100x90x10	292	-	57	46	-	-	- x2	- x -	20
L.E. Thompson	D1-2 alt (a)	100x90x10	292	-	57	46	-	-	- x2	- x -	20
L.E. Thompson	D1-2 alt (b)	100x90x10	292	-	57	46	-	-	- x2	- x -	20
L.E. Thompson	D1-3 alt (a)	100x90x10	292	-	57	46	-	-	- x2	- x -	20
L.E. Thompson	D1-3 alt (b)	100x90x10	292	-	57	46	-	-	- x2	- x -	20
L.E. Thompson	E1-1 alt (a)	100x90x13	292	-	57	46	-	-	- x2	- x -	20
L.E. Thompson	E1-1 alt (b)	100x90x13	292	-	57	46	-	-	- x2	- x -	20
L.E. Thompson	E1-2 alt (a)	100x90x13	292	-	57	46	-	-	- x2	- x -	20
L.E. Thompson	E1-2 alt (b)	100x90x13	292	-	57	46	-	-	- x2	- x -	20
L.E. Thompson	E1-3 alt (a)	100x90x13	292	-	57	46	-	-	- x2	- x -	20
L.E. Thompson	E1-3 alt (b)	100x90x13	292	-	57	46	-	-	- x2	- x -	20
L.E. Thompson	A2-1 alt (a)	100x90x8	292	-	57	65	-	-	- x2	- x -	20
L.E. Thompson	A2-1 alt (b)	100x90x8	292	-	57	65	-	-	- x2	- x -	20
L.E. Thompson	A2-2 alt (a)	100x90x8	292	-	57	65	-	-	- x2	- x -	20
L.E. Thompson	A2-2 alt (b)	100x90x8	292	-	57	65	-	-	- x2	- x -	20
L.E. Thompson	A2-3 alt (a)	100x90x8	292	-	57	65	-	-	- x2	- x -	20
L.E. Thompson	A2-3 alt (b)	100x90x8	292	-	57	65	-	-	- x2	- x -	20
L.E. Thompson	B2-1 alt (a)	100x90x8	292	-	57	46	-	-	- x2	- x -	20
L.E. Thompson	B2-1 alt (b)	100x90x8	292	-	57	46	-	-	- x2	- x -	20
L.E. Thompson	B2-2 alt (a)	100x90x8	292	-	57	46	-	-	- x2	- x -	20
L.E. Thompson	B2-2 alt (b)	100x90x8	292	-	57	46	-	-	- x2	- x -	20
L.E. Thompson	B2-3 alt (a)	100x90x8	292	-	57	46	-	-	- x2	- x -	20
L.E. Thompson	B2-3 alt (b)	100x90x8	292	-	57	46	-	-	- x2	- x -	20
L.E. Thompson	C2-1 alt (a)	100x90x13	292	-	57	65	-	-	- x2	- x -	20
L.E. Thompson	C2-1 alt (b)	100x90x13	292	-	57	65	-	-	- x2	- x -	20
L.E. Thompson	C2-2 alt (a)	100x90x13	292	-	57	65	-	-	- x2	- x -	20
L.E. Thompson	C2-2 alt (b)	100x90x13	292	-	57	65	-	-	- x2	- x -	20
L.E. Thompson	C2-3 alt (a)	100x90x13	292	-	57	65	-	-	- x2	- x -	20
L.E. Thompson	C2-3 alt (b)	100x90x13	292	-	57	65	-	-	- x2	- x -	20
L.E. Thompson	D2-1 alt (a)	100x90x13	292	-	57	46	-	-	- x2	- x -	20
L.E. Thompson	D2-1 alt (b)	100x90x13	292	-	57	46	-	-	- x2	- x -	20
L.E. Thompson	D2-2 alt (a)	100x90x13	292	-	57	46	-	-	- x2	- x -	20
L.E. Thompson	D2-2 alt (b)	100x90x13	292	-	57	46	-	-	- x2	- x -	20
L.E. Thompson	D2-3 alt (a)	100x90x13	292	-	57	46	-	-	- x2	- x -	20
L.E. Thompson	D2-3 alt (b)	100x90x13	292	-	57	46	-	-	- x2	- x -	20
W.H. Sommer	Test 21	90x75x10	229	38/187	-	47	38	76	-	1x3	20
W.H. Sommer	Test 22	90x75x10	305	38/187	-	47	38	76	-	1x3	20
W.H. Sommer	Test 23	100x75x10	381	38/187	-	64	38	76	-	1x5	20
W.H. Sommer	Test 24	100x75x10	457	38/111	-	64	38	76	-	1x6	20
C. Onuah	A01B	100x100x10	390	-	-	65	-	80	1x5	1x5	20
C. Onuah	A02	100x100x8	390	-	-	65	-	80	1x5	1x5	20
C. Onuah	A03	100x100x12	390	-	-	65	-	80	1x5	1x5	20
C. Onuah	A04	100x100x10	390	-	-	65	-	80	1x5	1x5	20
C. Onuah	A07	100x90x10	390	-	-	60	-	80	1x5	1x5	20
C. Onuah	A08	100x75x10	390	-	-	45	-	80	1x5	1x5	20
C. Onuah	A10	100x100x8	230	-	-	65	-	80	1x3	1x3	20
C. Onuah	A13	100x100x12	230	-	-	65	-	80	1x3	1x3	20
C. Onuah	A14	100x100x12	230	-	-	65	-	80	1x3	1x3	20
C. Onuah	A15	100x100x8	310	-	-	65	-	80	1x4	1x4	20
C. Onuah	A16	100x100x10	390	-	-	65	-	80	1x5	1x5	20
C. Onuah	A18	100x100x8	470	-	-	65	-	80	1x6	1x6	20
C. Onuah	A19	100x100x12	470	-	-	65	-	80	1x6	1x6	20

Table 4.4 Geometric Parameters for Top and Seat Angle Connections

Author	Test ID	Angle Size	l	t	nt	nt'	ns	ns'	db
M.J. Marley	A-1/4-1	100x100	125	6	2x1	2x1	2x1	2x1	20
M.J. Marley	A-1/4-2	100x100	125	6	2x1	2x1	2x1	2x1	20
M.J. Marley	B-1/4-1	100x100	125	6	2x1	2x1	2x1	2x1	20
M.J. Marley	B-1/4-2	100x100	125	6	2x1	2x1	2x1	2x1	20
M.J. Marley	C1-1/4-2	100x100	125	6	2x1	2x1	2x1	2x1	20
M.J. Marley	C2-1/4-1	100x100	125	6	2x1	2x1	2x1	2x1	20
M.J. Marley	C2-1/4-2	100x100	125	6	2x1	2x1	2x1	2x1	20
M.J. Marley	D1-1/4-1	100x100	125	6	2x1	2x1	2x1	2x1	20
M.J. Marley	D1-1/4-2	100x100	125	6	2x1	2x1	2x1	2x1	20
M.J. Marley	D2-1/4-1	100x100	125	6	2x1	2x1	2x1	2x1	20
M.J. Marley	D2-1/4-2	100x100	125	6	2x1	2x1	2x1	2x1	20
M.J. Marley	D3-1/4-1	100x100	125	6	2x1	2x1	2x1	2x1	20
M.J. Marley	D3-1/4-2	100x100	125	6	2x1	2x1	2x1	2x1	20
M.J. Marley	A-1/2-1	100x100	125	13	2x1	2x1	2x1	2x1	20
M.J. Marley	B-1/2-1	100x100	125	13	2x1	2x1	2x1	2x1	20
M.J. Marley	B-1/2-2	100x100	125	13	2x1	2x1	2x1	2x1	20
M.J. Marley	C1-1/2-1	100x100	125	13	2x1	2x1	2x1	2x1	20
M.J. Marley	C1-1/2-2	100x100	125	13	2x1	2x1	2x1	2x1	20
M.J. Marley	C2-1/2-1	100x100	125	13	2x1	2x1	2x1	2x1	20
M.J. Marley	C2-1/2-2	100x100	125	13	2x1	2x1	2x1	2x1	20
M.J. Marley	D1-1/2-1	100x100	125	13	2x1	2x1	2x1	2x1	20
M.J. Marley	D1-1/2-2	100x100	125	13	2x1	2x1	2x1	2x1	20
M.J. Marley	D2-1/2-1	100x100	125	13	2x1	2x1	2x1	2x1	20
M.J. Marley	D2-1/2-2	100x100	125	13	2x1	2x1	2x1	2x1	20
M.J. Marley	D3-1/2-1	100x100	125	13	2x1	2x1	2x1	2x1	20
M.J. Marley	D3-1/2-2	100x100	125	13	2x1	2x1	2x1	2x1	20
S.M. Maxwell et. al.	A1	150x90	150	10	2x2	2x1	2x2	2x1	M20
S.M. Maxwell et. al.	A2	150x90	200	10	2x2	2x1	2x2	2x1	M20
S.M. Maxwell et. al.	A3	150x90	150	10	2x2	2x1	2x2	2x1	M20
S.M. Maxwell et. al.	A4	150x90	200	10	2x2	2x1	2x2	2x1	M20
S.M. Maxwell et. al.	B1	150x90	150	12	2x2	2x1	2x2	2x1	M20
S.M. Maxwell et. al.	B2	150x90	200	12	2x2	2x1	2x2	2x1	M20
S.M. Maxwell et. al.	B3	150x90	150	12	2x2	2x1	2x2	2x1	M20
S.M. Maxwell et. al.	B4	150x90	200	12	2x2	2x1	2x2	2x1	M20
S.M. Maxwell et. al.	C1	150x90	150	15	2x2	2x1	2x2	2x1	M20
S.M. Maxwell et. al.	C2	150x90	200	15	2x2	2x1	2x2	2x1	M20
S.M. Maxwell et. al.	C3	150x90	150	15	2x2	2x1	2x2	2x1	M20
S.M. Maxwell et. al.	C4	150x90	200	15	2x2	2x1	2x2	2x1	M20

Table 4.5 Geometric Parameters for Top and Seat Angle Connections with Double Web Angles

		Flange Dimensions												Web Dimensions									
Author	Test ID	Angle Size	L_f	t_f	g	g'	q	r	pf	nt	nt'	ns	ns'	Angle Size	L_w	t_w	d	gb	gc	c	p	nb	nc	db
A. Azizinamini et. al.	8S1	150x100	150	10	89	51	70	89	64	2x2	2x1	2x2	2x1	100x90	140	6	35	51	67	32	76	1x2	1x2	20
A. Azizinamini et. al.	8S2	150x90	150	10	89	51	70	89	64	2x2	2x1	2x2	2x1	100x90	140	6	35	51	67	32	76	1x2	1x2	20
A. Azizinamini et. al.	8S3	150x90	200	8	89	51	70	89	64	2x2	2x1	2x2	2x1	100x90	140	6	35	51	67	32	76	1x2	1x2	20
A. Azizinamini et. al.	8S4	150x150	150	10	89	114	70	89	64	2x2	2x1	2x2	2x1	100x90	140	6	35	51	67	32	76	1x2	1x2	20
A. Azizinamini et. al.	8S5	150x100	200	10	89	64	70	140	64	2x2	2x1	2x2	2x1	100x90	140	6	35	51	67	32	76	1x2	1x2	20
A. Azizinamini et. al.	8S6	150x100	150	8	64	51	70	89	64	2x2	2x1	2x2	2x1	100x90	140	6	35	51	67	32	76	1x2	1x2	20
A. Azizinamini et. al.	8S7	150x100	150	10	89	64	70	89	64	2x2	2x1	2x2	2x1	100x90	140	6	35	51	67	32	76	1x2	1x2	20
A. Azizinamini et. al.	8S8	150x90	150	8	89	51	70	89	64	2x2	2x1	2x2	2x1	100x90	140	6	35	51	67	32	76	1x2	1x2	20
A. Azizinamini et. al.	8S9	150x90	150	10	89	51	70	89	64	2x2	2x1	2x2	2x1	100x90	140	6	35	51	67	32	76	1x2	1x2	20
A. Azizinamini et. al.	8S10	150x90	150	13	89	51	70	89	64	2x2	2x1	2x2	2x1	100x90	140	6	35	51	67	32	76	1x2	1x2	20
A. Azizinamini et. al.	14S1	150x100	200	10	89	64	89	140	64	2x2	2x1	2x2	2x1	100x90	215	6	71	51	67	32	76	1x3	1x3	20
A. Azizinamini et. al.	14S2	150x100	200	10	89	64	89	140	64	2x2	2x1	2x2	2x1	100x90	215	6	71	51	67	32	76	1x3	1x3	20
A. Azizinamini et. al.	14S3	150x100	200	10	89	64	89	140	64	2x2	2x1	2x2	2x1	100x90	140	6	110	51	67	32	76	1x2	1x2	20
A. Azizinamini et. al.	14S4	150x100	200	10	89	64	89	140	64	2x2	2x1	2x2	2x1	100x90	215	10	71	51	67	32	76	1x3	1x3	20
A. Azizinamini et. al.	14S5	150x100	200	10	89	64	89	140	64	2x2	2x1	2x2	2x1	100x90	215	6	71	51	67	32	76	1x3	1x3	20
A. Azizinamini et. al.	14S6	150x100	200	13	89	64	89	140	64	2x2	2x1	2x2	2x1	100x90	215	6	71	51	67	32	76	1x3	1x3	20
A. Azizinamini et. al.	14S8	150x100	200	16	89	64	89	140	64	2x2	2x1	2x2	2x1	100x90	215	6	71	51	67	32	76	1x3	1x3	20
A. Azizinamini et. al.	14S9	150x100	200	13	89	64	89	140	64	2x2	2x1	2x2	2x1	100x90	215	6	71	51	67	32	76	1x3	1x3	20
A. Azizinamini et. al.	14WS1	150x100	200	10	-	64	-	140	-	-	2x1	-	-	100x90	215	6	71	-	67	32	76	-	1x3	20
A. Azizinamini et. al.	14WS2	150x100	200	13	-	64	-	140	-	-	2x1	-	-	100x90	215	6	71	-	67	32	76	1x2	1x2	20

Table 4.6 Geometric Parameters for Header Plate Connections

Author	Test ID	Thickness	Lp	c	p	lt	lc	g	n	db
W.H. Sommer	Test 5	6	381	38	76	38	35	102	2x5	20
W.H. Sommer	Test 6	6	229	38	76	38	340	102	2x3	20
W.H. Sommer	Test 7	6	305	38	76	38	264	102	2x4	20
W.H. Sommer	Test 8	6	381	38	76	38	187	102	2x5	20
W.H. Sommer	Test 9	6	457	38	76	38	111	102	2x6	20
W.H. Sommer	Test 10	10	229	38	76	38	187	102	2x3	20
W.H. Sommer	Test 11	10	305	38	76	38	111	102	2x4	20
W.H. Sommer	Test 12	10	381	38	76	38	35	102	2x5	20
W.H. Sommer	Test 13	10	229	38	76	38	340	102	2x3	20
W.H. Sommer	Test 14	10	305	38	76	38	264	102	2x4	20
W.H. Sommer	Test 15	10	381	38	76	38	187	140	2x5	20
W.H. Sommer	Test 16	10	457	38	76	38	111	140	2x6	20
W.H. Sommer	Test 17	10	457	38	76	38	264	140	2x4	20
W.H. Sommer	Test 18	6	381	38	76	38	187	140	2x5	20
W.H. Sommer	Test 19	13	305	38	76	38	264	140	2x4	20
W.H. Sommer	Test 20	13	381	38	76	38	187	140	2x5	20
W.H. Sommer	Test 25	6	305	38	76	38	111	102	2x4	20
W.H. Sommer	Test 26	6	229	38	76	38	187	102	2x3	20
W.H. Sommer	Test 27	6	229	38	76	38	38	102	2x3	20
W.H. Sommer	Test 28	6	152	38	76	38	114	102	2x2	20

Table 4.7 Geometric Parameters for Flush End Plate Connections

Author	Test ID	Thickness	Li	c	p	g	nt	nc	db
J.R. Ostrander	Test 1	13	127	13	64	89	2x1	2x1	20
J.R. Ostrander	Test 3	10	127	13	64	89	2x1	2x1	20
J.R. Ostrander	Test 4	6	127	13	64	89	2x1	2x1	20
J.R. Ostrander	Test 9	20	127	13	64	89	2x1	2x1	20
J.R. Ostrander	Test 11	10	178	13	64	102	2x1	2x1	20
J.R. Ostrander	Test 12	13	178	13	64	102	2x1	2x1	20
J.R. Ostrander	Test 13	16	178	13	64	102	2x1	2x1	20
J.R. Ostrander	Test 17	10	178	13	64	102	2x1	2x1	20
J.R. Ostrander	Test 18	13	178	13	64	102	2x1	2x1	20
J.R. Ostrander	Test 19	16	178	13	64	102	2x1	2x1	20
J.R. Ostrander	Test 23	16	178	13	64	102	2x1	2x1	20
J.R. Ostrander	Test 2	13	127	13	64	89	2x1	2x1	20
J.R. Ostrander	Test 5	13	127	13	64	89	2x1	2x1	20
J.R. Ostrander	Test 6	10	127	13	64	89	2x1	2x1	20
J.R. Ostrander	Test 7	6	127	13	64	89	2x1	2x1	20
J.R. Ostrander	Test 8	6	127	13	64	89	2x1	2x1	20
J.R. Ostrander	Test 10	10	127	13	64	89	2x1	2x1	20
J.R. Ostrander	Test 14	10	178	13	64	102	2x1	2x1	20
J.R. Ostrander	Test 15	13	178	13	64	102	2x1	2x1	20
J.R. Ostrander	Test 16	16	178	13	64	102	2x1	2x1	20
J.R. Ostrander	Test 20	10	178	13	64	102	2x1	2x1	20
J.R. Ostrander	Test 21	13	178	13	64	102	2x1	2x1	20
J.R. Ostrander	Test 22	16	178	13	64	102	2x1	2x1	20
J.R. Ostrander	Test 24	16	178	13	64	102	2x1	2x1	20

Table 4.8 Geometric Parameters for Extended End Plate Connections

Author	Test ID	Thickness	Lp	p	g	nt	nc	ni	db
J.R. Bailey	Test A1-L	25	422	114	102	2x2	2x1	2x1	22
J.R. Bailey	Test A1-R	19	422	111	102	2x2	2z1	2z1	16
J.R. Bailey	Test A2-L	19	422	111	102	2x2	2z1	2z1	16
J.R. Bailey	Test A2-R	19	422	111	102	2x2	2x1	2x1	20
J.R. Bailey	Test A3-L	19	422	111	102	2x2	2x1	2x1	20
J.R. Bailey	Test A3-R	19	422	111	102	2x2	2x1	2x1	20
J.O. Surtees et. al.	Test C1	19	406	114	89	2x1	2x1	2x1	20
J.O. Surtees et. al.	Test C2	19	489	114	89	2x1	2x1	2x1	20
J.O. Surtees et. al.	Test C3	19	489	114	89	2x1	2x1	2x1	25
J.O. Surtees et. al.	Test C4	25	489	114	89	2x1	2x1	2x1	25
J.O. Surtees et. al.	Test C5	25	489	114	89	2x1	2x1	2x1	25
J.R. Bailey	Test B4-L	32	422	114	102	2x2	2x1	2x1	22
J.R. Bailey	Test B4-R	32	422	114	102	2x2	2x1	2x1	22
J.R. Bailey	Test B5-L	25	422	108	102	2x2	2x1	2x1	20
J.R. Bailey	Test B5-R	25	422	108	102	2x2	2x1	2x1	20
J.R. Bailey	Test B6-L	35	422	110	102	2x2	2x1	2x1	25
J.R. Bailey	Test B6-R	35	422	110	102	2x2	2x1	2x1	25
J.R. Bailey	Test B7-L	32	422	114	102	2x2	2x1	2x1	25
J.R. Bailey	Test B7-R	32	422	114	102	2x2	2x1	2x1	25
J.R. Bailey	Test B8-L	19	422	114	102	2x2	2x1	2x1	20
J.R. Bailey	Test B8-R	19	422	114	102	2x2	2x1	2x1	20
J.R. Bailey	Test C9-L	19	422	114	102	2x2	2x1	2x1	16
J.R. Bailey	Test C9-R	19	422	114	102	2x2	2x1	2x1	16
J.R. Bailey	Test C10-L	21	422	114	102	2x2	2x1	2x1	20
J.R. Bailey	Test C10-R	21	422	114	102	2x2	2x1	2x1	20
J.R. Bailey	Test C11-L	22	422	108	102	2x2	2x1	2x1	16
J.R. Bailey	Test C11-R	22	422	108	102	2x2	2x1	2x1	16
J.R. Bailey	Test C12-L	27	422	111	102	2x2	2x1	2x1	22
J.R. Bailey	Test C12-R	27	422	111	102	2x2	2x1	2x1	22
J.R. Bailey	Test C13-L	32	422	117	102	2x2	2x1	2x1	25
J.R. Bailey	Test C13-R	32	422	117	102	2x2	2x1	2x1	25
J.G. Surtees et. al.	Test C6	29	610	152	152	2x2	- x -	- x -	29
N.D. Johnstone et. al.	Test 1-L	32	570	178	140	2x2	2x2	- x -	30
N.D. Johnstone et. al.	Test 1-R	32	570	178	140	2x2	2x2	- x -	30
N.D. Johnstone et. al.	Test 2-L	32	570	178	140	2x2	2x2	- x -	30
N.D. Johnstone et. al.	Test 2-R	32	570	178	140	2x2	2x2	- x -	30
N.D. Johnstone et. al.	Test 3-L	24	517	102	140	2x2	2x2	- x -	24
N.D. Johnstone et. al.	Test 3-R	24	517	102	140	2x2	2x2	- x -	24
N.D. Johnstone et. al.	Test 4-L	16	530	115	140	2x2	2x2	- x -	24
N.D. Johnstone et. al.	Test 4-R	16	530	115	140	2x2	2x2	- x -	24

Table 4.9 Geometric Parameters for Extended End Plate Connections[1]

Author	Test ID	Thickness	li	ct	cc	pt	pc	pit	pi	pic	gt	gt2	gi	gc	nt	nc	ni	db
S.A. Ioannides	Test 1	16	260	44	44	89	89	-	-	-	140	-	-	140	2x2	2x2	- x -	20
S.A. Ioannides	Test 2	19	356	41	41	95	95	-	-	-	140	-	-	140	2x2	2x2	- x -	22
S.A. Ioannides	Test 3	22	260	44	44	89	89	-	-	-	140	-	-	140	2x2	2x2	- x -	25
S.A. Ioannides	Test 4	22	260	44	44	89	89	-	-	-	140	-	-	140	2x2	2x2	- x -	20
S.A. Ioannides	Test 5	32	356	41	41	95	95	-	-	-	140	-	-	140	2x2	2x2	- x -	20
R.J. Dews	Test 1	25	249	46	46	89	89	-	-	-	140	-	-	140	2x2	2x2	- x -	20
R.J. Dews	Test 2	25	252	46	46	89	89	-	-	-	140	-	-	140	2x2	2x2	- x -	20
J.A. Packer et. al.	Test J1	15	151	40	32	97	49	-	-	-	86	-	-	86	2x2	2x1	- x -	M16
J.A. Packer et. al.	Test J2	15	151	40	32	97	49	-	-	-	86	-	-	86	2x2	2x1	- x -	M16
J.A. Packer et. al.	Test J3	15	151	40	32	97	49	-	-	-	86	-	-	86	2x2	2x1	- x -	M16
P. Grundy et. al.	T1	25	581	38	-	95	48	-	-	-	89	64	-	152	4x2	2x1	- x -	22
P. Grundy et. al.	T2	25	581	38	-	95	48	-	-	-	89	64	-	152	4x2	2x1	- x -	22
L.G. Johnson et. al.	Test 5	13	340	-	-	95	48	-	-	-	89	-	102	89	2x2	2x1	2x1	20
A.N. Sherbourne	Test A1	32	279	38	19	89	44	64	76	64	102	-	102	102	2x2	2x1	2x3	20
A.N. Sherbourne	Test A2	32	279	38	19	89	48	64	76	64	102	-	102	102	2x2	2x1	2x3	20
A.N. Sherbourne	Test A3	19	279	38	19	89	48	64	76	64	102	-	102	102	2x2	2x1	2x3	20
A.N. Sherbourne	Test B1	25	305	38	25	127	64	76	76	76	102	-	102	102	2x2	2x1	2x3	22
A.N. Sherbourne	Test B2	19	305	38	25	127	102	76	76	76	102	-	102	102	2x2	2x1	2x3	22

Notes: 1. Additional geometric parameters recorded for these tests

Table 4.10 Plastic moment and rotation for the beams using in the M-ϕ tests

Section Designation	Country	Beam Depth d (mm)	Plastic Modulus z_x (10^3 mm^3)	Moment of Inertia I_x (10^6 mm^4)	Plastic Moment M_p (kN-m)	Plastic Rotation ϕ_p (rads)
W130 X 24	Canada	127	157	8.87	47	0.0677
W 130 X 24	Canada	127	190	10.9	57	0.0664
254 X 102 UB22	U.K.	254	261.5	28.6	78	0.0697
10 X 4 UB17	U.K.	257	305	34.0	91	0.0690
8 X 5¼ UB20	U.K.	207	315	28.8	94	0.0678
W200 X 31	Canada	210	334	31.3	100	0.0672
10 X 4 UB19	U.K.	260	352	40.0	106	0.0687
12 X 5 UB25	U.K.	304	392	71.4	117	0.0500
10 X 4½ RSJ25	U.K.	254	401	50.9	120	0.0601
W250 X 33	Canada	258	426	49.1	128	0.0672
W360 X 33	Canada	349	544	82.8	163	0.0688
12 X 5 UB32	U.K.	310	567	65.5	170	0.0806
W310 X 39	Canada	310	610	84.9	183	0.0669
14 X 5 UB26	U.K.	353	649	101	195	0.0683
12 X 5 RSJ32	U.K.	305	695	92.0	208	0.0690
W410 X 39	Canada	399	724	125	217	0.0691
W310 X 52	Canada	317	837	118	251	0.0675
12 X 6½ UB26	U.K.	311	844	117	253	0.0673
W360 X 57	Canada	358	1008	160	302	0.0676
15 X 5 RSJ42	U.K.	381	1068	178	321	0.0686
W460 X 52	Canada	450	1090	212	327	0.0694
15 X 6 UB40	U.K.	385	1106	186	332	0.0685
14 X 6¾ UB45	U.K.	364	1211	195	363	0.0679
457 X 191 X 67	U.K.	454	1469	293	441	0.0683
W460 X 67	Canada	454	1496	299	449	0.0680
18 X 6 UB55	U.K.	465	1798	362	539	0.0694
W460 X 82	Canada	460	1830	370	549	0.0683
W460 X 89	Canada	464	2016	410	605	0.0684
W610 X 82	Canada	599	2196	562	659	0.0702
W530 X 92	Canada	533	2360	554	708	0.0681
W610 X 101	U.K.	603	2900	764	870	0.0687
W610 X 113	U.K.	608	3277	874	983	0.0683
610 UB113	Australia	607	3283	873	985	0.0685
310 UB46	New Zealand	307	721	99.2	216	0.0668

Table 4.11 Non-dimensional curve fitting parameters for single web angle connections

Author	Test ID	ϕ_u	M_o	S_o	S_p	n_1	n_2
S.L. Lipson	AA-2/1	0.722	0.00212	0.00541	0.000481	1.731	0.816
S.L. Lipson	AA-2/2	0.501	0.00054	0.00724	0.00437	7.955	0.342
S.L. Lipson	AA-3/1	0.815	0.00487	0.0214	0.00378	1.216	2.097
S.L. Lipson	AA-3/2	0.323	0.00307	0.0308	0.0191	-0.032	1.480
S.L. Lipson	AA-4/1	0.962	0.00838	0.0408	0.00701	5.541	1.317
S.L. Lipson	AA-4/2	0.791	0.00991	0.0837	0.00870	1.234	1.310
S.L. Lipson	AA-5/1	0.751	0.0203	0.135	0.0158	1.362	1.823
S.L. Lipson	AA-5/2	0.774	0.0265	0.389	0.0311	2.611	1.305
S.L. Lipson	AA-6/1	0.446	0.0202	0.231	0.0281	1.854	1.247
S.L. Lipson	AA-6/2	0.576	0.0384	0.437	0.0269	0.421	1.297
S.L. Lipson	BB-4/1	0.965	0.0159	0.0847	0.00668	0.257	1.718
S.L. Lipson	BB-4/2	0.753	0.0118	0.103	0.0150	3.700	0.987
S.L. Lipson	B2-4	0.343	0.0126	0.127	0.0159	2.067	1.118
S.L. Lipson	B3-4	0.548	0.0149	0.110	0.0117	-0.011	2.408
S.L. Lipson	C-4	0.229	0.0175	0.585	0.0299	3.274	0.744
S.L. Lipson	D-4	0.213	0.0166	0.334	0.0310	1.396	1.288
S.L. Lipson	G-2/1	0.475	0.00773	0.184	-0.000371	11.099	12.626
S.L. Lipson	G-3/1	0.426	0.0117	0.362	0.0162	-0.559	4.817
S.L. Lipson	G-4/1	0.307	0.0188	0.765	0.0171	17.674	0.834
S.L. Lipson	G-5/1	0.476	0.0255	0.887	0.0586	-0.210	2.718

Table 4.12 Non-dimensional curve fitting parameters for side plate connections

Author	Test ID	ϕ_u	M_o	S_o	S_p	n_1	n_2
S.L. Lipson	P1-2/1	0.350	0.00800	0.151	-0.0004	0.500	1.500
S.L. Lipson	P1-2/2	0.530	0.00730	0.133	-0.00225	3.767	1.220
S.L. Lipson	P1-3/1	0.506	0.0185	0.584	0.0161	0.313	1.385
S.L. Lipson	P1-3/2	0.430	0.0119	0.467	0.00359	7.667	1.004
S.L. Lipson	P1-4/1	0.587	0.0222	0.623	0.0325	0.157	1.033
S.L. Lipson	P1-4/2	0.588	0.0214	0.576	0.0334	0.168	1.071
S.L. Lipson	P1-5/1	0.488	0.0590	1.302	0.0275	0.008	1.500
S.L. Lipson	P1-5/2	0.350	0.0239	1.613	0.0794	25.280	1.077
S.L. Lipson	P1-6/1	0.406	0.0558	2.308	0.116	0.083	1.998
S.L. Lipson	P1-6/2	0.424	0.0653	2.530	0.0935	24.954	1.938
L.E. Thompson et. al.	F-1 alt a	0.633	0.0719	1.232	0.0397	0.080	2.208
L.E. Thompson et. al.	F-1 alt b	0.605	0.0748	1.437	0.0404	-0.172	2.474
L.E. Thompson et. al.	G-1 alt a	0.890	0.0860	1.211	0.0167	0.193	1.284
L.E. Thompson et. al.	G-1 alt b	1.051	0.112	1.413	0.00665	0.383	0.814
L.E. Thompson et. al.	H-1 alt a	0.563	0.0641	1.308	0.0577	0.100	2.068
L.E. Thompson et. al.	H-1 alt b	0.435	0.0745	1.308	0.0144	-0.071	2.485
L.E. Thompson et. al.	F-2-1 alt a	0.616	0.0594	1.253	0.0751	1.040	0.768
L.E. Thompson et. al.	F-2-1 alt b	0.688	0.0404	1.002	0.0937	0.316	0.674
L.E. Thompson et. al.	F-2-2 alt a	0.647	0.0781	3.339	0.0578	0.652	0.658
L.E. Thompson et. al.	F-2-2 alt b	0.818	0.102	1.412	0.0575	1.267	0.767
L.E. Thompson et. al.	F-2-3 alt a	0.847	0.0558	2.174	0.0989	0.962	0.500
L.E. Thompson et. al.	F-2-3 alt b	0.825	0.0282	2.174	0.143	-20.982	3.696
R.M. Richard et. al.	RGKL2	0.911	0.00496	0.073	0.00386	13.099	1.649
R.M. Richard et. al.	RGKL3	0.958	0.0211	0.375	0.00252	-0.008	0.910
R.M. Richard et. al.	RGKL5	0.949	0.0847	2.573	0.0121	3.509	0.784
R.M. Richard et. al.	RGKL7	0.962	0.187	2.303	0.0225	1.027	1.279

Table 4.13 Non-dimensional curve fitting parameters for double web angle connections

Author	Test ID	ϕ_u	M_O	S_o	S_p	n_1	n_2
C.W. Lewitt et. al.	FK-4AB-M	1.082	0.0550	1.085	0.0321	7.690	0.857
B. Bose	B-1	0.132	0.0961	3.178	0.8540	-0.028	2.779
L.E. Thompson	A1-1 alt a	0.852	0.0214	0.155	0.0229	0.005	114.943
L.E. Thompson	A1-1 alt b	0.639	0.0207	0.138	0.0207	0.005	188.679
L.E. Thompson	A1-2 alt a	0.622	0.0275	0.401	0.0266	1.093	1.927
L.E. Thompson	A1-2 alt b	0.798	0.0334	0.381	0.0180	-0.007	1.545
L.E. Thompson	A1-3 alt a	0.723	0.0269	0.533	0.0243	-0.038	1.763
L.E. Thompson	A1-3 alt b	0.709	0.0263	0.604	0.0233	0.655	1.416
L.E. Thompson	B1-1 alt a	0.732	0.0594	1.139	0.0242	5.065	0.921
L.E. Thompson	B1-1 alt b	0.828	0.0609	1.302	0.0203	3.376	1.168
L.E. Thompson	B1-2 alt a	0.800	0.0410	1.315	0.0345	-0.133	1.801
L.E. Thompson	B1-2 alt b	0.976	0.0370	1.256	0.0104	-0.049	2.623
L.E. Thompson	B1-3 alt a	1.057	0.0749	1.341	0.0069	0.419	1.069
L.E. Thompson	B1-3 alt b	1.355	0.0770	1.341	0.0023	2.029	0.764
L.E. Thompson	D1-1 alt a	0.617	0.0446	0.843	0.0101	-0.026	1.626
L.E. Thompson	D1-1 alt b	0.515	0.0440	0.854	0.0122	4.042	0.926
L.E. Thompson	D1-2 alt a	1.026	0.0563	0.827	0.0071	1.834	1.097
L.E. Thompson	D1-2 alt b	0.728	0.0565	0.814	0.0083	1.977	1.088
L.E. Thompson	D1-3 alt a	0.822	0.0436	0.880	0.0214	0.263	1.315
L.E. Thompson	D1-3 alt b	0.721	0.0357	0.739	0.0276	-0.127	2.222
L.E. Thompson	E1-1 alt a	0.657	0.0509	1.848	0.0353	30.946	0.699
L.E. Thompson	E1-1 alt b	0.732	0.0602	1.848	0.0295	18.308	0.861
L.E. Thompson	E1-2 alt a	0.575	0.0358	1.574	0.0423	0.507	5.831
L.E. Thompson	E1-2 alt b	0.807	0.0444	1.349	0.0303	0.253	1.080
L.E. Thompson	E1-3 alt a	0.743	0.0530	2.041	0.0364	34.079	0.772
L.E. Thompson	E1-3 alt b	0.754	0.0520	2.041	0.0364	-0.069	1.865
L.E. Thompson	A2-1 alt a	1.346	0.0255	0.393	0.0119	1.373	0.679
L.E. Thompson	A2-1 alt b	1.230	0.0277	0.288	0.0113	1.823	0.667
L.E. Thompson	A2-2 alt a	1.371	0.0327	0.564	0.0102	0.551	0.773
L.E. Thompson	A2-2 alt b	1.053	0.0319	0.393	0.0138	0.144	1.185
L.E. Thompson	A2-3 alt a	1.090	0.0190	0.208	0.0161	-0.028	1.980
L.E. Thompson	A2-3 alt b	0.984	0.0227	0.179	0.0109	0.847	0.907
L.E. Thompson	B2-1 alt a	0.902	0.0348	0.472	0.0263	1.542	0.455
L.E. Thompson	B2-1 alt b	0.693	0.0160	0.608	0.0283	88.465	0.282
L.E. Thompson	B2-2 alt a	0.452	0.0177	0.720	0.0129	-0.547	5.181
L.E. Thompson	B2-2 alt b	0.903	0.0080	0.317	0.0455	12.927	-1.679
L.E. Thompson	B2-3 alt a	0.786	0.0056	0.878	0.0574	24.503	-1.617
L.E. Thompson	B2-3 alt b	0.487	0.0173	0.581	0.0506	-1.232	9.814
L.E. Thompson	C2-1 alt a	0.893	0.0166	1.174	0.0385	0.179	1.133
L.E. Thompson	C2-1 alt b	0.743	0.0374	0.774	0.0333	0.812	0.836
L.E. Thompson	C2-2 alt a	0.667	0.0170	4.402	0.0525	43.358	0.967
L.E. Thompson	C2-2 alt b	0.710	0.0413	0.880	0.0280	0.004	0.989
L.E. Thompson	C2-3 alt a	0.641	0.0137	1.181	0.0754	-15.743	2.278
L.E. Thompson	C2-3 alt b	0.762	0.0292	0.944	0.0509	-0.023	1.202
L.E. Thompson	D2-1 alt a	0.762	0.0507	1.387	0.0461	0.002	0.561
L.E. Thompson	D2-1 alt b	0.814	0.0621	1.040	0.0154	1.437	0.490
L.E. Thompson	D2-2 alt a	0.479	0.0071	1.332	0.0463	41.685	-4.695
L.E. Thompson	D2-2 alt b	0.613	0.0193	1.997	0.0685	78.157	0.670
L.E. Thompson	D2-3 alt a	0.600	0.0233	2.241	0.0531	0.786	0.511
L.E. Thompson	D2-3 alt b	0.557	0.0450	1.494	0.0352	0.444	1.000
W.H. Sommer	Test 21	0.793	0.0684	0.375	0.0603	-0.070	3.175
W.H. Sommer	Test 22	1.052	0.1660	1.009	0.0569	2.046	1.451
W.H. Sommer	Test 23	0.985	0.0700	0.518	0.0458	-0.006	2.214
W.H. Sommer	Test 24	1.024	0.0972	0.749	0.0073	3.375	1.797
C. Onuah	A01B	1.157	0.1380	3.271	0.0691	0.419	0.893
C. Onuah	A02	1.068	0.1080	1.090	0.0815	-0.061	2.290
C. Onuah	A03	0.804	0.1590	1.392	0.0780	0.525	2.027
C. Onuah	A04	1.042	0.1180	0.906	0.0703	9.483	1.548
C. Onuah	A07	0.922	0.0714	1.215	0.1550	1.955	1.172
C. Onuah	A08	1.235	0.1360	1.765	0.1030	2.393	1.105
C. Onuah	A10	1.365	0.6500	0.850	0.0550	-3.000	1.500
C. Onuah	A11	0.938	0.1050	1.500	0.0625	1.000	1.000
C. Onuah	A13	1.133	0.0750	0.900	0.0300	1.000	1.000
C. Onuah	A14	1.055	0.0723	0.743	0.0763	-1.007	0.961
C. Onuah	A15	1.168	0.0750	2.500	0.0800	1.000	1.000
C. Onuah	A16	0.979	0.0589	1.155	0.0760	22.815	1.459
C. Onuah	A18	0.700	0.0675	2.650	0.1350	-2.175	2.108
C. Onuah	A19	0.510	0.0889	1.090	0.2350	16.501	0.994

Table 4.14 Non-dimensional curve fitting parameters for top and seat angle connections

Author	Test ID	ϕ_u	M_o	S_o	S_p	n_1	n_2
M.J. Marley	A-1/4-1	0.640	0.0891	1.915	0.0513	4.310	0.722
M.J. Marley	A-1/4-2	0.316	0.0752	1.542	0.0891	2.040	0.772
M.J. Marley	B-1/4-1	0.256	0.0875	21.381	0.0886	2.242	0.543
M.J. Marley	B-1/4-2	0.448	0.0577	3.771	0.103	0.335	1.109
M.J. Marley	C1-1/4-2	0.669	0.102	3.661	0.0310	0.742	0.791
M.J. Marley	C2-1/4-1	0.731	0.0902	4.839	0.0483	1.023	0.728
M.J. Marley	C2-1/4-2	0.727	0.0972	2.056	0.0397	0.522	0.860
M.J. Marley	D1-1/4-1	0.545	0.0808	0.791	0.0679	1.821	1.979
M.J. Marley	D1-1/4-2	0.740	0.0873	0.802	0.0392	2.636	0.988
M.J. Marley	D2-1/4-1	0.547	0.0903	1.107	0.0677	0.007	1.184
M.J. Marley	D2-1/4-2	0.476	0.0842	2.518	0.105	0.004	0.709
M.J. Marley	D3-1/4-1	0.431	0.0805	1.168	0.0186	1.345	0.978
M.J. Marley	D3-1/4-2	0.744	0.0708	0.401	0.0334	-0.045	2.845
M.J. Marley	A-1/2-1	0.607	0.317	2.793	0.192	2.240	1.439
M.J. Marley	B-1/2-1	0.610	0.320	9.951	0.167	3.819	0.685
M.J. Marley	B-1/2-2	0.310	0.276	7.155	0.261	2.459	0.883
M.J. Marley	C1-1/2-1	0.538	0.365	5.647	0.162	1.657	1.017
M.J. Marley	C1-1/2-2	0.567	0.371	17.768	0.217	-0.013	0.747
M.J. Marley	C2-1/2-1	0.560	0.333	11.298	0.178	2.267	0.739
M.J. Marley	C2-1/2-2	0.595	0.333	3.598	0.157	1.948	1.065
M.J. Marley	D1-1/2-1	0.598	0.376	5.388	0.174	0.001	1.526
M.J. Marley	D1-1/2-2	0.616	0.353	9.450	0.217	3.374	0.906
M.J. Marley	D2-1/2-1	0.715	0.376	17.691	0.114	0.245	1.133
M.J. Marley	D2-1/2-2	0.552	0.400	4.943	0.102	1.863	1.115
M.J. Marley	D3-1/2-1	0.650	0.363	7.795	0.133	2.758	0.836
M.J. Marley	D3-1/2-2	0.631	0.409	4.346	0.0948	0.454	1.203
S.M. Maxwell	A1	0.143	0.0825	5.165	0.458	0.007	1.180
S.M. Maxwell	A2	0.145	0.143	3.800	0.409	1.858	0.895
S.M. Maxwell	A3	0.143	0.143	2.939	0.270	1.723	0.928
S.M. Maxwell	A4	0.143	0.146	3.745	0.612	1.733	0.890
S.M. Maxwell	B1	0.145	0.0907	3.188	0.786	2.169	1.021
S.M. Maxwell	B2	0.148	0.113	2.448	0.778	1.685	1.510
S.M. Maxwell	B3	0.145	0.144	2.555	0.545	2.429	1.127
S.M. Maxwell	B4	0.143	0.144	2.877	0.721	2.747	0.702
S.M. Maxwell	C1	0.145	0.145	2.458	0.845	-0.012	4.143
S.M. Maxwell	C2	0.146	0.268	2.492	0.0253	1.989	0.927
S.M. Maxwell	C3	0.137	0.154	3.462	0.761	1.402	1.290
S.M. Maxwell	C4	0.124	0.255	3.815	0.0973	1.708	0.922

Table 4.15 Non-dimensional curve fitting parameters for top and seat angle connections with double web angles

Author	Test ID	ϕ_u	M_o	S_o	S_p	n_1	n_2
A. Azizinamini et. al.	8S1	0.642	0.325	5.594	0.187	0.544	1.232
A. Azizinamini et. al.	8S2	0.450	0.443	18.068	0.0645	2.362	0.849
A. Azizinamini et. al.	8S3	0.624	0.387	8.402	0.254	2.836	1.223
A. Azizinamini et. al.	8S4	0.645	0.161	1.261	0.088	2.375	1.233
A. Azizinamini et. al.	8S5	0.637	0.315	6.923	0.190	4.793	0.993
A. Azizinamini et. al.	8S6	0.643	0.238	4.395	0.147	1.638	1.023
A. Azizinamini et. al.	8S7	0.640	0.350	3.485	0.200	-0.250	2.416
A. Azizinamini et. al.	8S8	0.628	0.345	4.665	0.250	1.750	1.348
A. Azizinamini et. al.	8S9	0.612	0.395	8.600	0.250	1.594	1.043
A. Azizinamini et. al.	8S10	0.402	0.555	41.254	0.463	0.307	0.993
A. Azizinamini et. al.	14S1	0.495	0.195	7.105	0.162	7.528	0.792
A. Azizinamini et. al.	14S2	0.477	0.270	11.809	0.250	9.685	0.638
A. Azizinamini et. al.	14S3	0.497	0.175	3.199	0.191	6.474	0.924
A. Azizinamini et. al.	14S4	0.486	0.235	5.584	0.209	4.096	1.202
A. Azizinamini et. al.	14S5	0.475	0.250	13.798	0.305	13.361	0.556
A. Azizinamini et. al.	14S6	0.480	0.330	6.352	0.190	1.166	1.262
A. Azizinamini et. al.	14S8	0.455	0.465	14.760	0.335	2.810	1.231
A. Azizinamini et. al.	14S9	0.470	0.305	6.276	0.220	6.510	0.999
A. Azizinamini et. al.	14WS1	0.485	0.294	9.115	0.155	2.251	0.758
A. Azizinamini et. al.	14WS2	0.452	0.415	35.440	0.145	2.875	0.570

Table 4.16 Non-dimensional curve fitting parameters for header plate connections

Author	Test ID	ϕ_u	M_o	S_o	S_p	n_1	n_2
W.H. Sommer	Test 5	0.847	0.0952	1.729	0.115	4.800	1.972
W.H. Sommer	Test 6	0.342	0.0055	0.0823	0.059	-10.923	8.979
W.H. Sommer	Test 7	0.279	0.0200	0.517	0.0662	5.682	0.389
W.H. Sommer	Test 8	0.397	0.0555	0.750	0.045	1.000	1.500
W.H. Sommer	Test 9	0.487	0.0720	1.129	0.105	1.982	1.477
W.H. Sommer	Test 10	0.350	0.0574	0.684	0.0734	2.795	1.206
W.H. Sommer	Test 11	0.689	0.106	2.804	0.106	11.461	0.791
W.H. Sommer	Test 12	0.607	0.203	2.443	0.0978	2.348	1.244
W.H. Sommer	Test 13	0.398	0.0177	0.208	0.0786	3.109	0.919
W.H. Sommer	Test 14	0.457	0.0561	0.420	0.0609	1.159	3.920
W.H. Sommer	Test 15	0.563	0.0663	0.841	0.0470	4.659	0.968
W.H. Sommer	Test 16	0.754	0.0997	1.571	0.0758	3.671	1.289
W.H. Sommer	Test 17	0.354	0.0121	0.146	0.0430	1.665	5.871
W.H. Sommer	Test 18	0.397	0.0198	0.209	0.0554	1.103	2.623
W.H. Sommer	Test 19	0.669	0.0573	0.443	0.0353	2.233	1.282
W.H. Sommer	Test 20	0.695	0.0917	1.074	0.0508	0.978	1.816
W.H. Sommer	Test 25	0.613	0.0241	0.264	0.0348	2.111	1.543
W.H. Sommer	Test 26	0.310	0.0105	0.222	0.0267	4.485	1.430
W.H. Sommer	Test 27	0.440	0.0753	0.674	0.0659	2.437	1.286
W.H. Sommer	Test 28	0.553	0.0170	0.226	0.0555	1.455	0.832

Table 4.17 Non-dimensional curve fitting parameters for flush end plate connections

Author	Test ID	ϕ_u	M_o	S_o	S_p	n_1	n_2
J.R. Ostrander	Test 1	0.818	0.402	4.781	0.107	0.752	1.518
J.R. Ostrander	Test 3	0.781	0.353	5.588	0.0990	2.111	1.055
J.R. Ostrander	Test 4	0.538	0.167	2.794	0.127	-0.017	1.892
J.R. Ostrander	Test 9	0.879	0.441	10.070	0.113	-0.027	1.337
J.R. Ostrander	Test 11	0.799	0.283	4.855	0.141	2.192	1.350
J.R. Ostrander	Test 12	0.781	0.393	7.767	0.144	-0.038	1.635
J.R. Ostrander	Test 13	0.574	0.422	4.854	0.220	3.101	1.120
J.R. Ostrander	Test 17	1.116	0.331	4.854	0.0280	0.366	1.093
J.R. Ostrander	Test 18	1.005	0.373	2.987	0.0506	0.463	1.376
J.R. Ostrander	Test 19	0.660	0.317	4.730	0.110	2.702	1.117
J.R. Ostrander	Test 23	0.356	0.436	7.767	0.327	2.562	1.194
J.R. Ostrander	Test 2	0.750	0.453	6.103	0.130	2.916	1.222
J.R. Ostrander	Test 5	1.517	0.468	5.588	0.0839	-0.017	1.665
J.R. Ostrander	Test 6	1.092	0.416	8.748	0.0602	0.631	0.961
J.R. Ostrander	Test 7	0.751	0.229	3.105	0.0686	0.047	1.244
J.R. Ostrander	Test 8	0.660	0.188	5.588	0.119	1.007	1.057
J.R. Ostrander	Test 10	0.718	0.518	21.653	0.191	5.485	0.758
J.R. Ostrander	Test 14	0.699	0.294	9.710	0.196	8.248	0.402
J.R. Ostrander	Test 15	0.362	0.430	9.709	0.267	1.325	1.120
J.R. Ostrander	Test 16	0.443	0.533	12.945	0.207	0.019	1.530
J.R. Ostrander	Test 20	1.040	0.300	3.530	0.0876	-0.012	1.808
J.R. Ostrander	Test 21	0.987	0.415	3.884	0.0931	0.375	1.325
J.R. Ostrander	Test 22	0.621	0.379	7.767	0.145	0.117	1.421
J.R. Ostrander	Test 24	0.272	0.518	13.485	0.374	-0.024	1.735

Table 4.18 Non-dimensional curve fitting parameters for extended end plate connections

Author	Test ID	ϕ_u	M_o	S_o	S_p	n_1	n_2
S.A. Ioannides	Test 1	0.367	0.435	10.391	0.635	2.800	1.900
S.A. Ioannides	Test 2	0.320	0.555	66.779	0.785	0.267	1.049
S.A. Ioannides	Test 3	0.168	0.411	50.001	0.382	1.176	0.758
S.A. Ioannides	Test 4	0.611	0.641	33.610	0.458	0.345	0.969
S.A. Ioannides	Test 5	0.563	0.668	16.400	0.429	1.295	0.945
R.J. Dews	Test 1	1.117	0.534	2.531	0.222	2.921	2.021
R.J. Dews	Test 2	0.877	0.432	4.196	0.407	2.741	4.574
A.N. Sherbourne	Test A1	0.197	0.953	23.500	0.368	0.303	2.166
J.R. Bailey	Test A1-L	0.504	1.123	4.911	0.204	5.284	1.086
J.R. Bailey	Test A1-R	0.455	1.214	13.573	0.0213	1.141	1.670
J.R. Bailey	Test A2-L	0.378	1.500	8.054	-0.0532	7.241	0.946
J.R. Bailey	Test A2-R	0.414	1.263	11.641	0.483	8.734	1.080
J.R. Bailey	Test A3-L	0.306	1.471	7.413	-0.0469	4.629	1.010
J.R. Bailey	Test A3-R	0.359	1.559	15.557	-0.0898	0.024	2.953
J.O. Surtees et. al.	Test C1	0.172	0.584	21.546	1.907	2.486	0.820
J.O. Surtees et. al.	Test C2	0.582	1.031	13.100	0.311	10.503	0.525
J.O. Surtees et. al.	Test C3	0.584	1.211	16.729	-0.0539	5.480	1.555
J.O. Surtees et. al.	Test C4	0.584	1.069	7.458	0.386	4.591	9.609
J.O. Surtees et. al.	Test C5	0.584	1.057	14.897	0.616	0.193	2.007
J.A. Packer et. al.	Test J1	1.253	1.237	13.597	0.166	-0.010	1.074
J.A. Packer et. al.	Test J2	0.830	0.694	6.243	0.319	1.419	1.231
J.A. Packer et. al.	Test J3	0.886	0.741	6.243	0.257	1.183	1.210
P. Grundy et. al.	T1	0.069	0.643	25.232	4.942	-0.040	3.410
P. Grundy et. al.	T2	0.080	0.854	24.241	1.703	1.786	2.653
A.N. Sherbourne	Test A2	0.356	1.882	97.800	0.000	0.632	0.852
A.N. Sherbourne	Test A3	0.477	1.602	49.417	0.985	1.083	1.971
A.N. Sherbourne	Test B1	0.899	1.581	56.857	0.402	-0.033	1.327
A.N. Sherbourne	Test B2	0.518	1.721	129.715	0.203	0.498	0.930
L.G. Johnson et. al.	Test 5	0.199	0.752	14.319	0.822	3.356	1.149
J.R. Bailey	B4-L	0.346	1.303	14.973	0.457	6.041	1.313
J.R. Bailey	B4-R	0.317	1.156	18.869	0.870	8.552	1.243
J.R. Bailey	B5-L	0.634	1.068	9.015	0.161	8.208	1.282
J.R. Bailey	B5-R	0.672	1.101	21.494	0.0954	8.667	1.056
J.R. Bailey	B6-L	0.580	0.915	5.272	0.416	8.050	1.036
J.R. Bailey	B6-R	0.685	1.035	8.241	0.216	6.707	1.381
J.R. Bailey	B7-L	0.717	1.022	6.876	0.170	7.585	1.474
J.R. Bailey	B7-R	0.551	1.148	8.208	0.0224	4.668	1.433
J.R. Bailey	B8-L	0.263	1.046	19.278	0.676	9.283	1.219
J.R. Bailey	B8-R	0.418	1.023	5.728	0.366	6.257	1.030
J.R. Bailey	C9-L	0.174	0.598	7.871	1.482	2.661	2.724
J.R. Bailey	C9-R	0.315	0.828	7.088	0.0816	3.217	1.528
J.R. Bailey	C10-L	0.196	0.971	25.400	1.549	1.730	1.911
J.R. Bailey	C10-R	0.263	1.176	19.848	0.303	0.442	1.848
J.R. Bailey	C11-L	0.114	0.642	14.445	1.449	3.687	0.548
J.R. Bailey	C11-R	0.087	0.490	9.541	2.907	0.932	6.572
J.R. Bailey	C12-L	0.499	1.089	7.638	0.221	4.270	1.425
J.R. Bailey	C12-R	0.701	1.289	12.357	0.0685	2.171	1.856
J.R. Bailey	C13-L	0.247	0.831	8.923	0.319	2.860	0.784
J.R. Bailey	C13-R	0.299	0.868	13.754	0.0242	2.471	0.816
J.G. Surtees et. al.	Test C6	0.577	1.027	18.943	0.233	18.135	0.447
N.D. Johnstone et. al.	Test 1-L	1.114	1.195	48.622	0.107	6.378	0.736
N.D. Johnstone et. al.	Test 1-R	0.569	1.181	33.458	0.255	-0.019	1.426
N.D. Johnstone et. al.	Test 2-L	1.195	1.131	11.771	0.191	11.045	1.536
N.D. Johnstone et. al.	Test 2-R	0.542	1.057	19.732	0.239	3.980	0.813
N.D. Johnstone et. al.	Test 3-L	0.867	1.130	13.590	0.138	-0.029	1.211
N.D. Johnstone et. al.	Test 3-R	0.542	0.905	15.268	0.365	2.080	0.943
N.D. Johnstone et. al.	Test 4-L	1.535	1.292	22.605	-0.019	1.205	0.634
N.D. Johnstone et. al.	Test 4-R	0.651	0.822	4.707	0.149	2.014	1.354

Angle Size Designation: A x B x t
where: A is the length of the angle along beam
B is the length of the angle along column
t is the thickness of the angle

Geometric Parameters:
Lp = angle height
d = distance from the top/bottom edge of the angle to the compression/tension flange of the beam
gb = distance from the angle's heel to the center of bolt holes in leg adjacent to the beam web face
gc = distance from the angle's heel to the center of bolt holes in leg adjacent to the column face
c = distance from the centre of upper/lower fastener holes to the top/bottom edge of the angle in the beam web
p = distance between two rows of fasteners in the beam web/column
nb = total number of fasteners in the beam
nc = total number of fasteners in the column

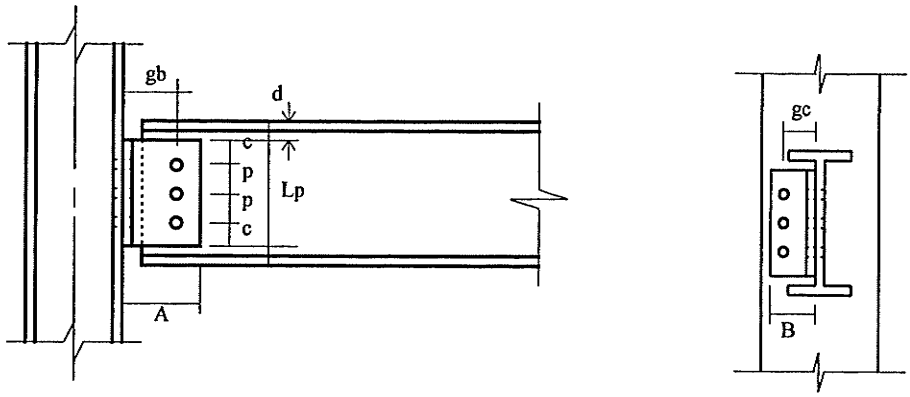


Figure 4.1 Single Web Angle Connection

Geometric Parameters:
Lp = angle height
d = distance from top/bottom edge of the angle to the compression/tension flange of the beam
t = thickness of plate
gb = distance from the angle's heel to the centre of bolt holes in leg adjacent to the beam web face
c = distance from the centre of upper/lower fastener holes to the top/bottom edge of the angle in the beam web
pb = distance between two rows of fasteners in the beam web
nb = total number of fasteners in the beam

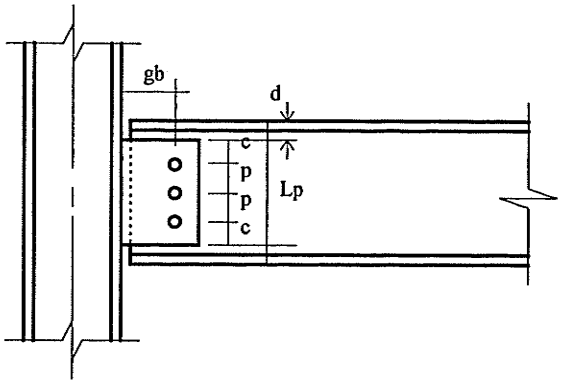


Figure 4.2 Single Plate Connection

Angle Size Designation: A x B x t

where: A is the length of the angle leg along beam
B is the length of the angle leg along column
t is the thickness of the angle

Geometric Parameters:

Lp = angle height
d = distance from the top/bottom edge of the angle to the compression/tension flange of the beam
gb = distance from the angle's heel to the center of bolt holes in leg adjacent to the beam web face
gc = distance from the angle's heel to the center of bolt holes in leg adjacent to the column face
c = distance from the centre of upper/lower fastener holes to the top/bottom edge of the angle in the beam web
p = distance between two rows of fasteners in the beam web/column
nb = total number of fasteners in the beam
nc = total number of fasteners in the column
qb = distance between two lines of fasteners in the beam web
qc = distance between two lines of fasteners in the column

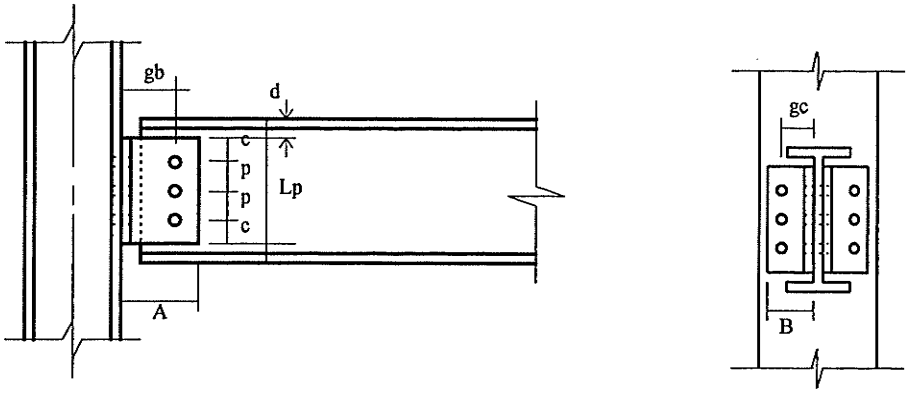


Figure 4.3 Double Web Angle Connection

Angle Size Designation: A x B x t x L

where: A is the length of the angle leg along beam
B is the length of the angle leg along column
t is the thickness of the angle
L is the width of the angle

Geometric Parameters:

nt = total number of fasteners in the tension beam flange
nt' = total number of fasteners in leg adjacent to the column face in tension side
ns = total number of fasteners in the compression beam flange
ns' = total number of fasteners in leg adjacent to the column face in compression side
l = width of angle
t = thickness of angle

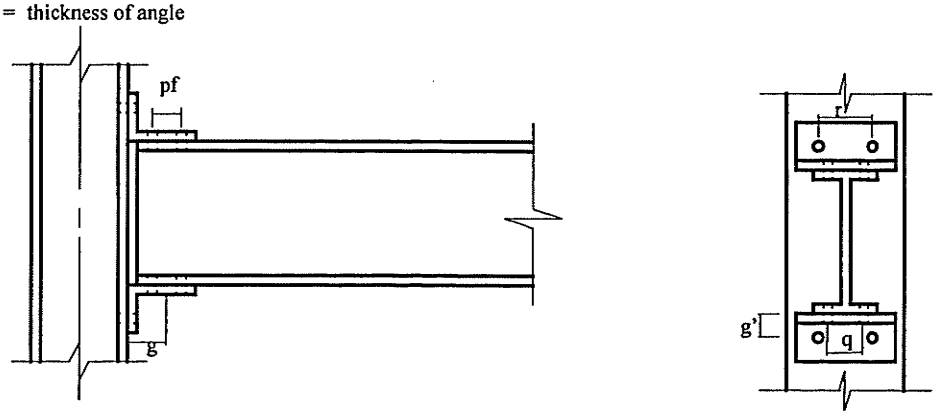


Figure 4.4 Top and Seat Angle Connection

Angle Size Designation: Flange Angles: $A_f \times B_f \times t_f \times L_f$

Web Angles: $A_W \times B_W \times t_W \times L_W$

where: A_f is the length of the flange angle leg along beam
B_f is the length of the flange angle leg along column
t_f is the thickness of the flange angle
L_f is the width of the flange angle

A_W is the length of the web angle leg along beam
B_W is the length of the web angle leg along column
t_W is the thickness of the web angle
L_W is the width of the web angle

Geometric Parameters:

Flange Angles:

g = gage from the top/seat angle's heel to the center of the fastener holes in leg on/under tension/compression flange of the beam
g' = gage from the top/seat angle's heel to the center of the fastener holes in leg adjacent to the column face
q = distance between two inner lines of fasteners in leg seating/under the tension/compression beam flange
r = distance between two inner lines of fasteners in leg adjacent to the column face in tension/compression side
r2 = distance between outer and inner line of fasteners in leg adjacent to the column face in tension/compression side where the fastener line number exceeds 3
pf = distance between two rows of fasteners
nt = total number of fasteners in the tension beam flange
nt' = total number of fasteners in leg adjacent to the column face in tension side
ns = total number of fasteners in the compression beam flange
ns' = total number of fasteners in leg adjacent to the column face in compression side

Web Angles:

d = distance from the top/bottom edge of the web angle to the compression/tension flange of the beam
gb = distance from the web angle's heel to the center of bolt holes in leg adjacent to the beam web face
gc = distance from the web angle's heel to the center of bolt holes in leg adjacent to the column face
c = distance from the centre of upper/lower fastener holes to the top/bottom edge of the web angle in the beam web
pw = distance between two rows of fasteners in the beam web/column
nb = total number of fasteners in the beam
nc = total number of fasteners in the column
qb = distance between two lines of fasteners in the beam web
qc = distance between two lines of fasteners in the column

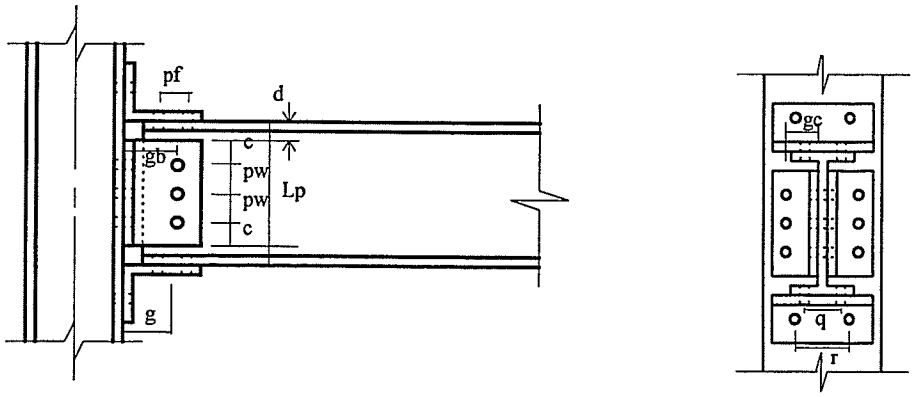


Figure 4.5 Top and Seat Angles with Double Web Angle Connections

Geometric Parameters:

lp = length of plate
c = distance from center of upper/lower fasteners holes to the top/bottom edge of the plate
p = distance between two rows of fasteners
lt = distance from the tension beam flange to the top edge of the plate
lc = distance from the compression beam flange to the bottom edge of the plate
g = distance between two lines of fasteners

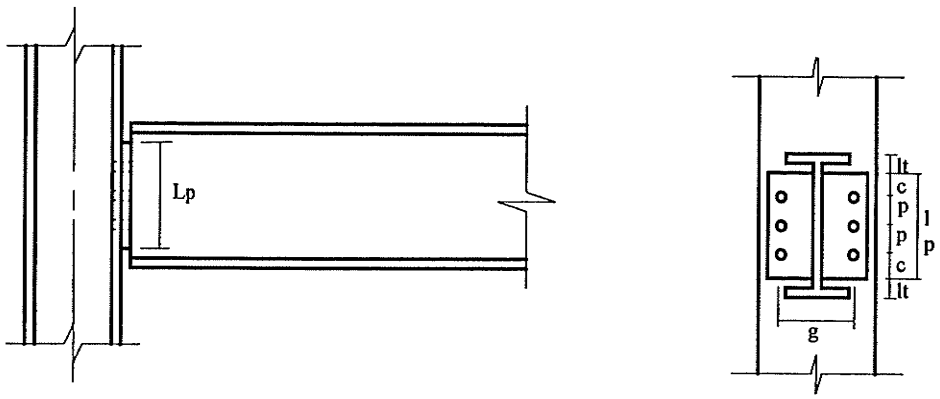


Figure 4.6 Header Plate Connection

Geometric Parameters:

li = distance from the center of tension side fastener holes to the center of the compression side edge of the plate
c = distance from the end of the plate to the tension/compression flange of the beam
p = distance from the tension/compression flange to the center of the row of tension/compression side fasteners
g = distance between two lines of fasteners
nt = total number of tension fasteners
nc = total number of compression fasteners

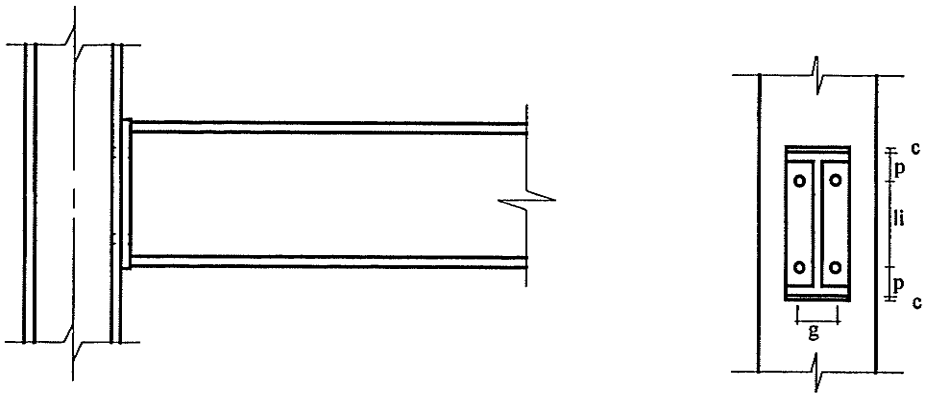


Figure 4.7 Flush End Plate Connection

Geometric Parameters:

li = distance from the center of the lower tension side fastener holes to the center of the upper compression side fastener holes
ct = distance from the tension side edge of plate to the center of the outer tension side fastener holes
cc = distance from the outer row of fasteners on the compression side to the compression side edge of plate
pt = distance between two rows of tension side fasteners
pc = distance between two rows of compression side fasteners
gt = distance between two inner lines of tension side fasteners
gt2 = distance from the outer line to the inner line of tension side fasteners where the fastener line number exceeds 3
gc = distance between two inner lines of compression side fasteners
gi = distance between two inner lines of central fasteners
pi = distance between the two inner rows of the central fasteners
pit = distance from the inner row of fasteners on the tension side to the upper row of the central fasteners
pic = distance from the inner row of fasteners on the compression side to the lower row of the central fasteners
nt = total number of fasteners on the tension side of the inner fasteners
nc = total number of fasteners on the compression side of the inner fasteners
ni = total number of inner fasteners

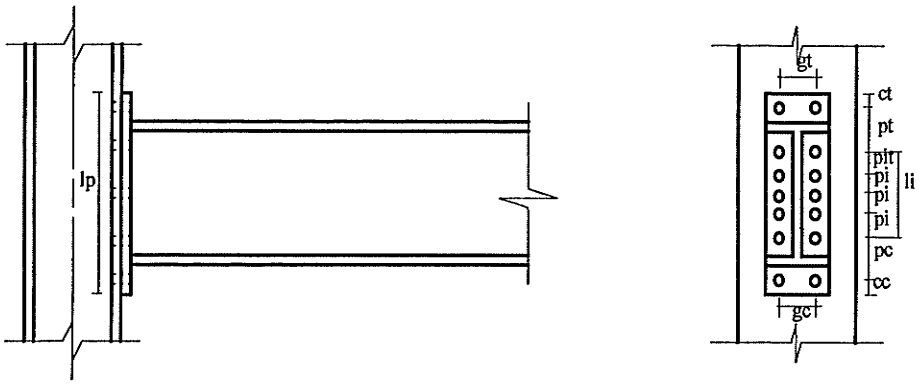


Figure 4.8 Extended End Plate Connection

Table 4.19 M-ϕ data for Lipson: AA-2/1 (1968)

Moment, M kN-m	Rotation, ϕ radians	Moment, M kN-m	Rotation, ϕ radians
0	0	1.59	0.0370
0.0840	0.00138	1.63	0.0392
0.168	0.00276	1.67	0.0415
0.218	0.00360	1.71	0.0435
0.269	0.00444	1.75	0.0456
0.319	0.00528	1.75	0.0474
0.369	0.00612	1.75	0.0492
0.417	0.00723		
0.465	0.00834		
0.531	0.0096		
0.597	0.0108		
0.660	0.0124		
0.722	0.0140		
0.797	0.0157		
0.872	0.0173		
0.947	0.0190		
1.01	0.0206		
1.07	0.0222		
1.14	0.0237		
1.21	0.0252		
1.29	0.0266		
1.37	0.0280		
1.42	0.0302		
1.48	0.0323		
1.54	0.0347		

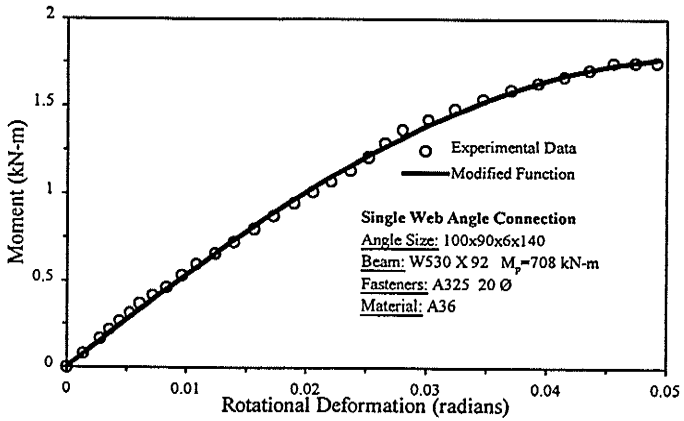


Figure 4.9 (a) M-ϕ curve for Lipson: AA-2/1

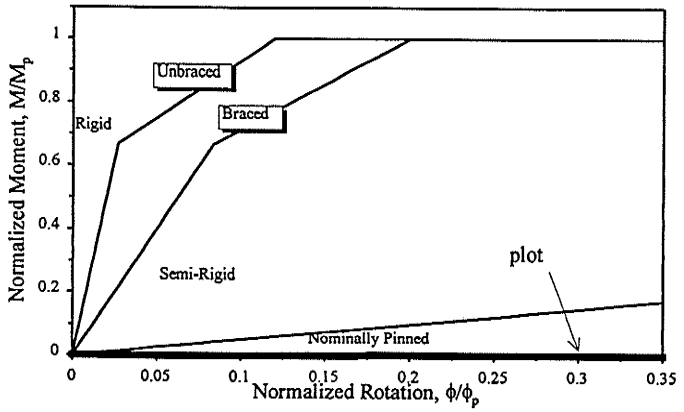


Figure 4.9 (b) Eurocode3 Classification of Lipson: AA-2/1

Figure 4.9 M-ϕ behaviour of Lipson: AA-2/1

Table 4.20 M-ϕ data for Lipson: P1-2/1 (1968)

Moment, M kN-m	Rotation, ϕ radians	Moment, M kN-m	Rotation, ϕ radians
0	0	4.79	0.0132
0.2408	0.00014	4.76	0.0146
0.482	0.00028	4.74	0.0160
0.722	0.00043	4.71	0.0174
0.963	0.00057	4.71	0.0186
1.204	0.00071	4.70	0.0197
1.445	0.00085	4.70	0.0209
1.688	0.00109	4.70	0.0220
1.931	0.00134	4.77	0.0233
2.175	0.0016	4.84	0.0245
2.418	0.0018	5.00	0.0254
2.612	0.0022	5.16	0.0263
2.806	0.0026	5.35	0.0273
2.999	0.0029	5.55	0.0283
3.252	0.0034		
3.505	0.0039		
3.69	0.0044		
3.88	0.0049		
4.07	0.0054		
4.27	0.0062		
4.48	0.0071		
4.59	0.0083		
4.70	0.0095		
4.73	0.0108		
4.76	0.0120		

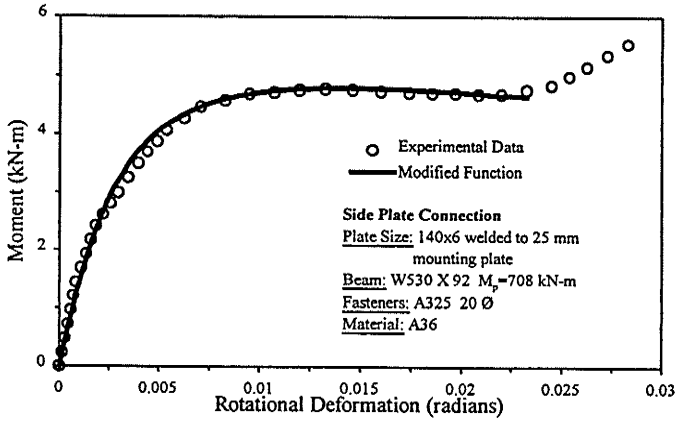


Figure 4.10 (a) M-ϕ curve for Lipson: P1-2/1

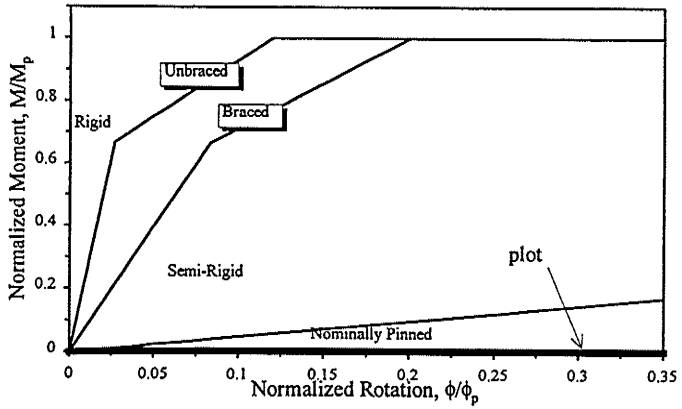


Figure 4.10 (b) Eurocode3 Classification of Lipson: P1-2/1

Figure 4.10 M-ϕ behaviour of Lipson: P1-2/1

Table 4.21 M-ϕ data for Thompson: A1-1 alt a (1968)

Moment, M kN-m	Rotation, ϕ radians	Moment, M kN-m	Rotation, ϕ radians
0	0	39.45	0.09905
2.77	0.00172	41.53	0.1002
5.54	0.00343	43.60	0.1014
8.31	0.00515	45.68	0.1026
11.1	0.00687	47.76	0.1030
13.84	0.00858	49.83	0.1034
16.61	0.01030	51.91	0.1038
18.44	0.01530	53.99	0.1041
19.83	0.02065	56.06	0.1051
21.22	0.02600	58.14	0.1060
22.61	0.03135	60.22	0.1073
24.00	0.03670	62.29	0.1086
25.27	0.04205	64.37	0.1118
26.54	0.04740	66.44	0.1149
27.80	0.05275		
29.07	0.05810		
29.49	0.06342		
29.90	0.06874		
30.32	0.07406		
30.73	0.07938		
31.15	0.08470		
32.18	0.08975		
33.22	0.09480		
35.30	0.09635		
37.38	0.09790		

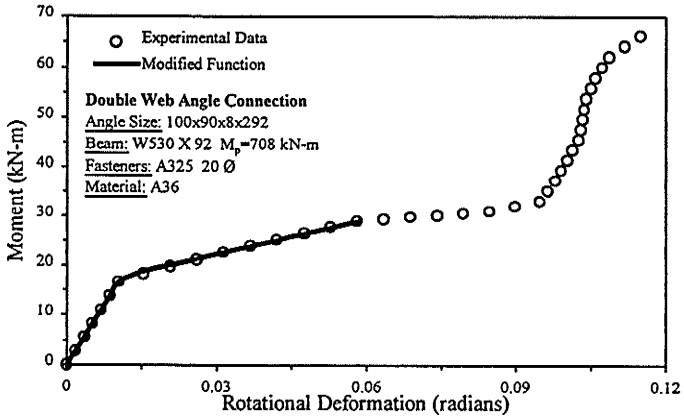


Figure 4.11 (a) M-ϕ curve for Thompson: A1-1 alt a

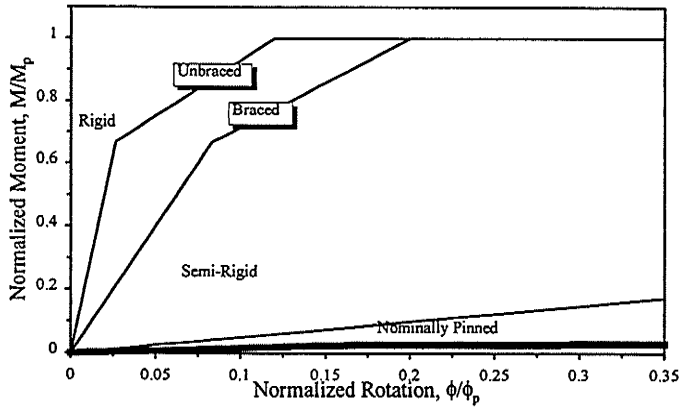


Figure 4.11 (b) Eurocode3 Classification of Thompson: A1-1 alt a

Figure 4.11 M-ϕ behaviour of Thompson: A1-1 alt a

Table 4.22 M-ϕ data for Sommer: Test 5 (1969)

Moment, M kN-m	Rotation, ϕ radians	Moment, M kN-m	Rotation, ϕ radians
0	0	90.96	0.06160
2.10	0.00020	93.68	0.06330
4.84	0.00040	96.39	0.06470
7.56	0.00080	99.10	0.06610
13.0	0.00110	105.7	0.06880
18.42	0.00140	111.2	0.07100
23.90	0.00205	115.5	0.07290
29.38	0.00270	119.8	0.07480
33.45	0.00360	123.7	0.07690
37.52	0.00450	127.7	0.07900
43.79	0.00865	132.8	0.08295
50.06	0.01280	137.9	0.08690
54.18	0.01700	140.7	0.08995
58.31	0.02120	143.5	0.09300
61.40	0.02520	145.2	0.09605
64.49	0.02920	146.9	0.09910
67.57	0.03320		
70.81	0.03687		
74.05	0.04053		
77.29	0.04420		
79.48	0.04757		
81.66	0.05093		
83.85	0.05430		
86.67	0.05760		
89.38	0.06010		

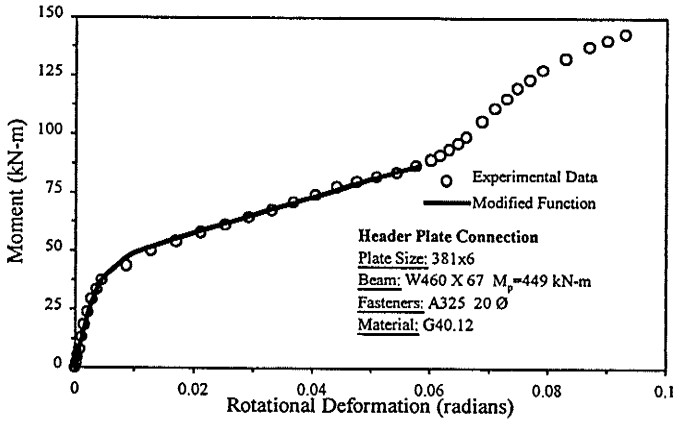


Figure 4.12 (a) M-ϕ curve for Sommer Test 5

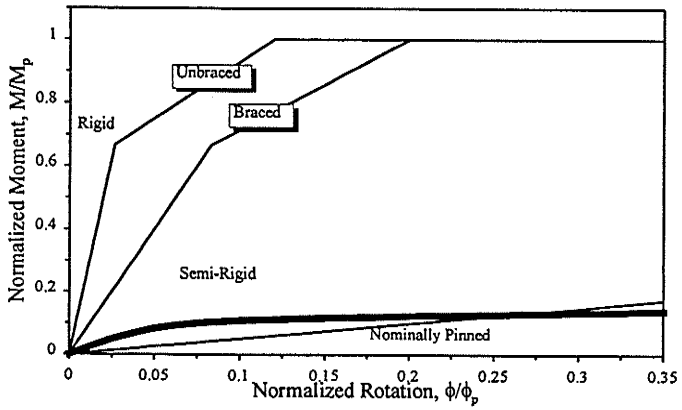


Figure 4.12 (b) Eurocode3 Classification of Sommer: Test 5

Figure 4.12 M-ϕ behaviour of Sommer: Test 5

Table 4.23 M-ϕ Data for Marley: A-1/4-1 (1982)

Moment, M kN-m	Rotation, ϕ radians	Moment, M kN-m	Rotation, ϕ radians
0	0	4.90	0.02130
0.20	0.00015	5.01	0.02340
0.40	0.00030	5.08	0.02525
0.65	0.00065	5.15	0.02710
0.9	0.00100	5.19	0.02840
1.15	0.00140	5.24	0.02970
1.40	0.00180	5.31	0.03140
1.62	0.00225	5.38	0.03310
1.84	0.00270	5.45	0.03465
2.08	0.00330	5.51	0.03620
2.32	0.00390	5.57	0.03785
2.56	0.00445	5.63	0.03950
2.80	0.00500	5.70	0.04140
3.08	0.00600	5.76	0.04330
3.37	0.00700	5.76	0.04330
3.56	0.00810		
3.75	0.00920		
3.96	0.01060		
4.06	0.01170		
4.17	0.01280		
4.27	0.01390		
4.37	0.01500		
4.55	0.01690		
4.78	0.01870		
4.84	0.02000		

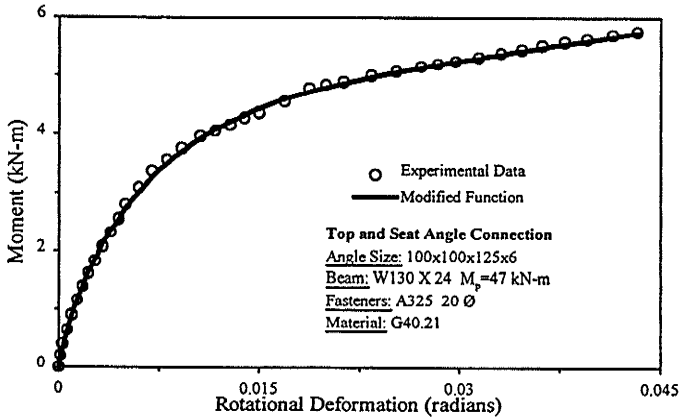


Figure 4.13 (a) M-ϕ curve for Marley: A-1/4-1

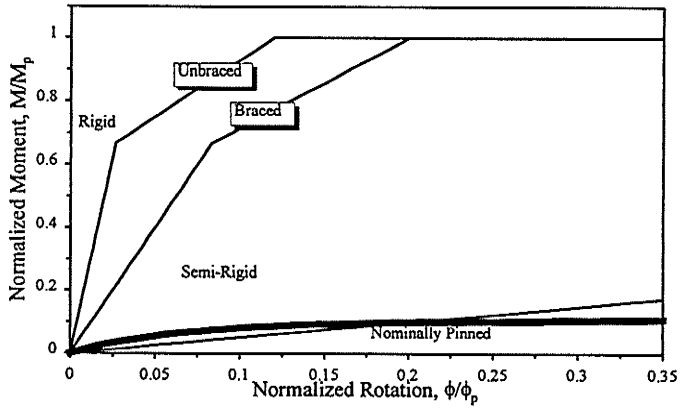


Figure 4.13 (b) Eurocode3 Classification of Marley: A-1/4-1

Figure 4.13 M-ϕ behaviour of Marley: A-1/4-1

Table 4.24 M-ϕ Data for Ostrander: Test 1 (1970)

Moment, M kN-m	Rotation, ϕ radians	Moment, M kN-m	Rotation, ϕ radians
0	0	56.16	0.02910
2.71	0.00030	56.78	0.03155
5.31	0.00060	57.40	0.03400
7.97	0.00085	58.03	0.03645
10.6	0.00110	58.65	0.03890
13.28	0.00140	59.19	0.04158
15.93	0.00170	59.74	0.04427
18.59	0.00205	60.29	0.04695
21.24	0.00240	60.83	0.04963
23.90	0.00295	61.38	0.05232
26.55	0.00350	61.92	0.05500
29.21	0.00430		
31.87	0.00510		
34.52	0.00605		
37.18	0.00700		
39.83	0.00835		
42.49	0.00970		
45.14	0.01165		
47.80	0.01360		
49.42	0.01577		
51.04	0.01793		
52.66	0.02010		
53.53	0.02235		
54.41	0.02460		
55.29	0.02685		

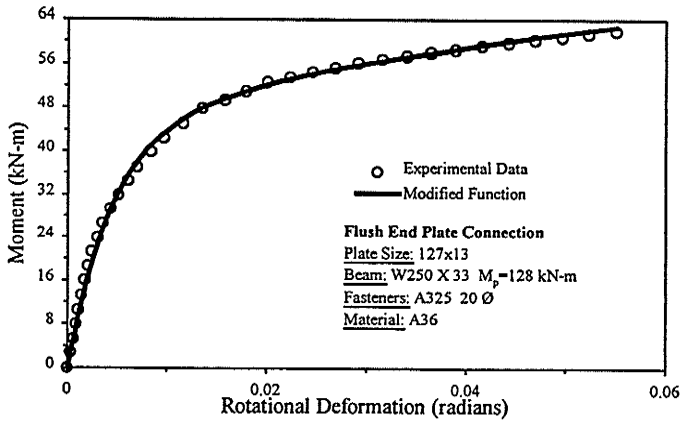


Figure 4.14 (a) M-ϕ curve for Ostrander: Test 1

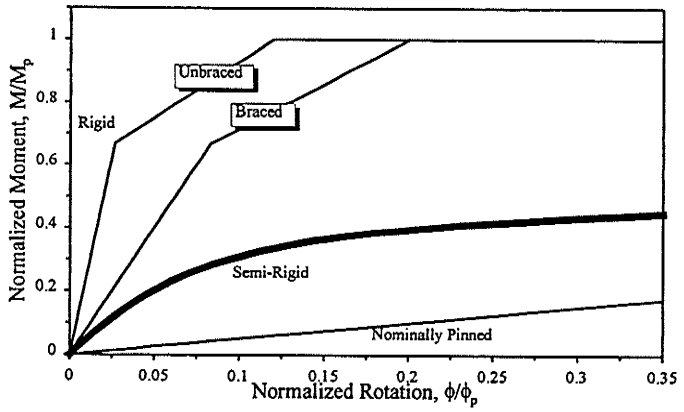


Figure 4.14 (b) Eurocode3 Classification of Ostrander: Test 1

Figure 4.14 M-ϕ behaviour of Ostrander: Test 1

Table 4.25 M-ϕ data for Azizinamini: 8S1 (1985)

Moment, M kN-m	Rotation, ϕ radians	Moment, M kN-m	Rotation, ϕ radians
0	0	33.89	0.01737
1.96	0.00023	34.59	0.01853
3.18	0.00038	35.35	0.02006
4.39	0.00053	36.12	0.02159
5.7	0.00076	36.85	0.02314
6.98	0.00100	37.58	0.02470
8.95	0.00132	38.06	0.02593
10.34	0.00151	38.54	0.02717
11.74	0.00170	39.06	0.02843
13.50	0.00209	39.57	0.02969
14.87	0.00242	39.97	0.03103
16.23	0.00276	40.37	0.03236
17.39	0.00310	40.82	0.03369
18.56	0.00344	41.27	0.03501
19.67	0.00385	41.59	0.03605
20.78	0.00426	41.9	0.03709
22.81	0.00514	42.27	0.03824
24.71	0.00643	42.63	0.03938
26.57	0.00793	42.87	0.04035
28.17	0.00960		
29.86	0.01131		
30.74	0.01263		
31.63	0.01395		
32.41	0.01508		
33.19	0.01621		

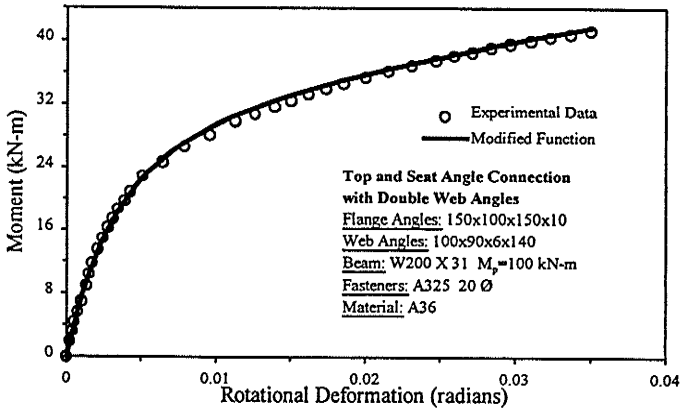


Figure 4.15 (a) M-ϕ curve for Azizinamini: 8S1

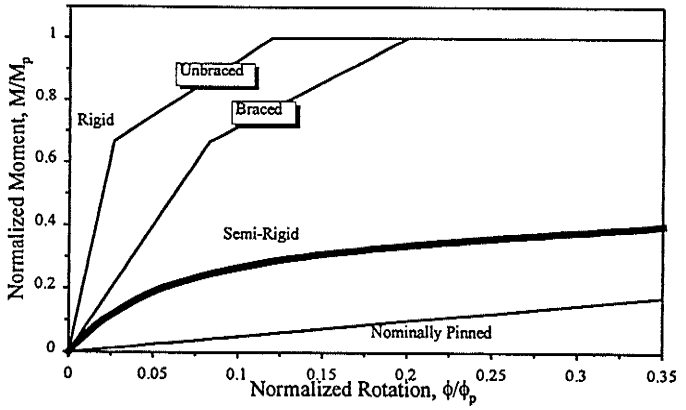


Figure 4.15 (b) Eurocode3 Classification of Azizinamini: 8S1

Figure 4.15 M-ϕ behaviour for Azizinamini: 8S1

Table 4.26 M-ϕ data for Ioannides: Test 1 (1978)

Moment, M kN-m	Rotation, ϕ radians	Moment, M kN-m	Rotation, ϕ radians
0	0	92.70	0.01444
4.71	0.00019	94.91	0.01569
9.41	0.00038	97.12	0.01693
14.12	0.00057	98.66	0.01794
18.67	0.00079	100.2	0.01894
23.21	0.00100	101.7	0.01995
27.75	0.00121	103.3	0.02095
31.53	0.00136	104.6	0.02202
35.31	0.00151	105.9	0.02310
39.08	0.00165	107.1	0.02417
43.60	0.00184	108.4	0.02524
48.11	0.00202		
52.55	0.00240		
56.25	0.00272		
59.95	0.00304		
64.55	0.00363		
69.33	0.00476		
72.96	0.00585		
76.59	0.00698		
78.99	0.00786		
81.38	0.00873		
83.45	0.00971		
85.52	0.01069		
88.01	0.01194		
90.49	0.01319		

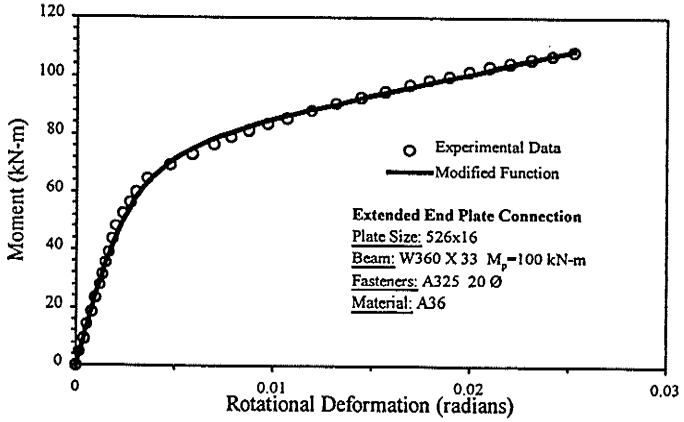


Figure 4.16 (a) M-ϕ curve for Ioannides: Test 1

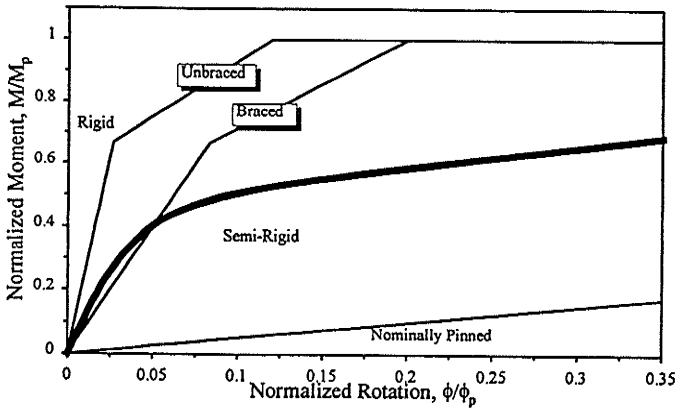


Figure 4.16 (b) Eurocode3 Classification of Ioannides: Test 1

Figure 4.16 M-ϕ behaviour for Ioannides: Test 1

Table 4.27 Summary of connection behaviour

Connection Type	Resistance (% of M_p)	Stiffness Range (Eurocode3 classification)	Rotational Capacity (% of tests with $\phi_u < 0.35$)	
Single Web Angle Connection	less than 10%	nominally pinned - semi-rigid	25%	(4 of 16)
Side Plate Connection	less than 10%	nominally pinned - semi-rigid	0%	(0 of 30)
Double Web Angle Connection	1-10%	nominally pinned - semi-rigid	1%	(1 of 68)
Header Plate Connection	1-20%	nominally pinned - semi-rigid	0%	(0 of 20)
Top and Seat Angle Connection	5-30%	semi-rigid - rigid (braced)	39%	(15 of 38)
Flush End Plate Connection	10-50%	semi-rigid - rigid (braced)	13%	(3 of 24)
Top and Seat Angle Connection with Double Web Angles	10-60%	semi-rigid - rigid (unbraced)	0%	(0 of 20)
Extended End Plate Connections	50-100%	semi-rigid - rigid (unbraced)	31%	(18 of 58)

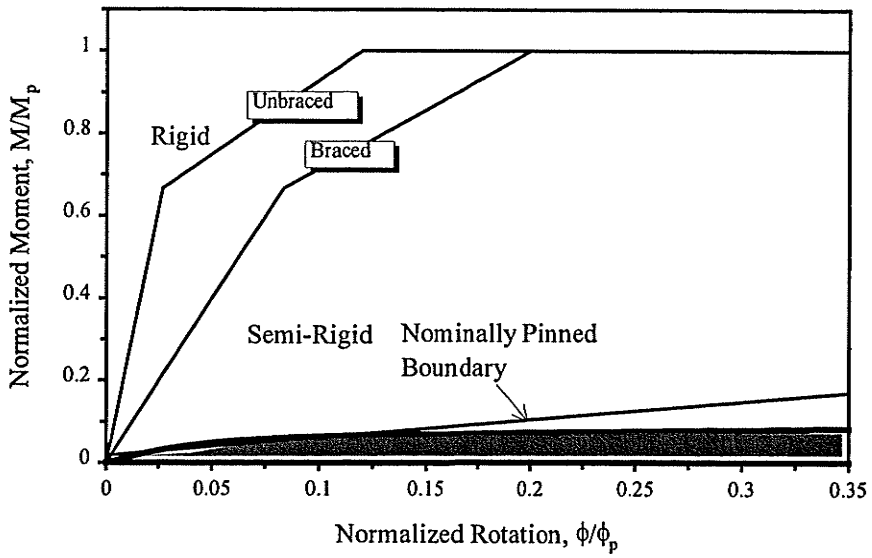


Figure 4.17 Classification boundaries for Single Web/Side Plate Connection

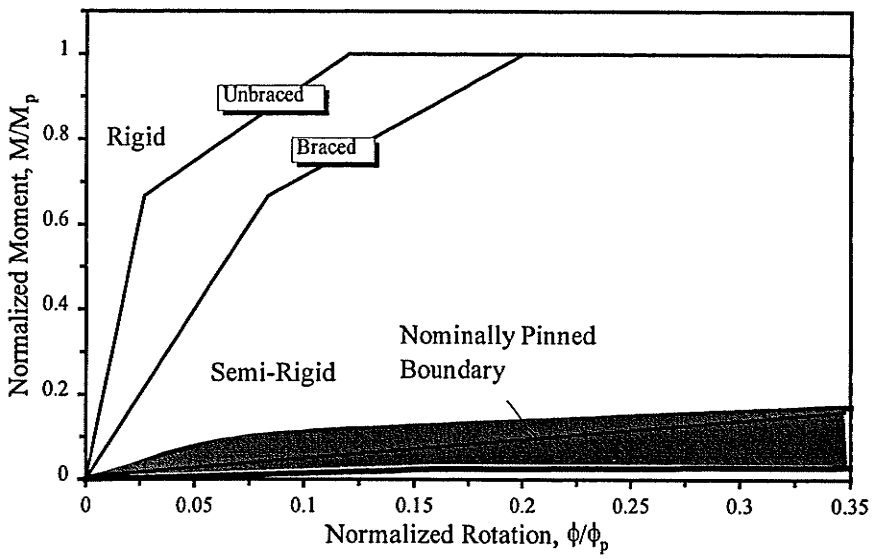


Figure 4.18 Classification boundaries for Double Web Angle Connection

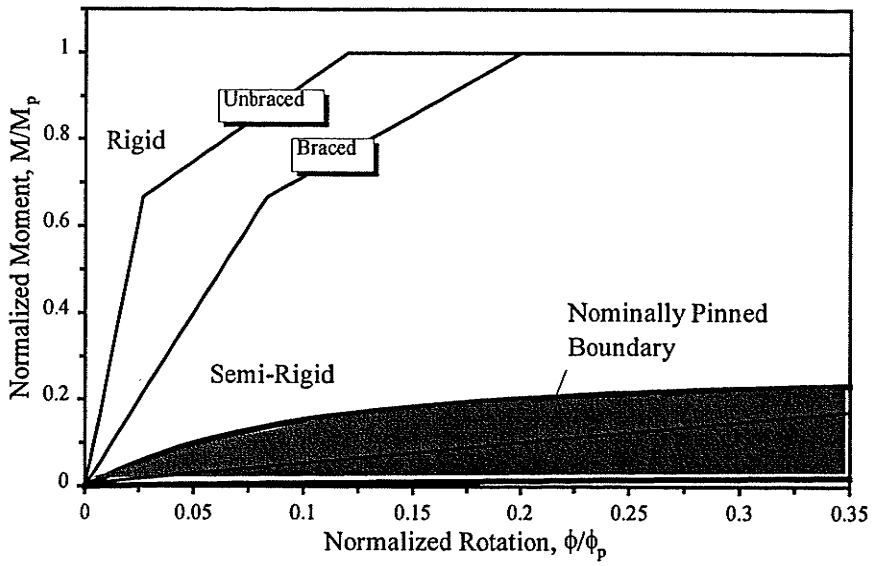


Figure 4.19 Classification boundaries for Header Plate Connection

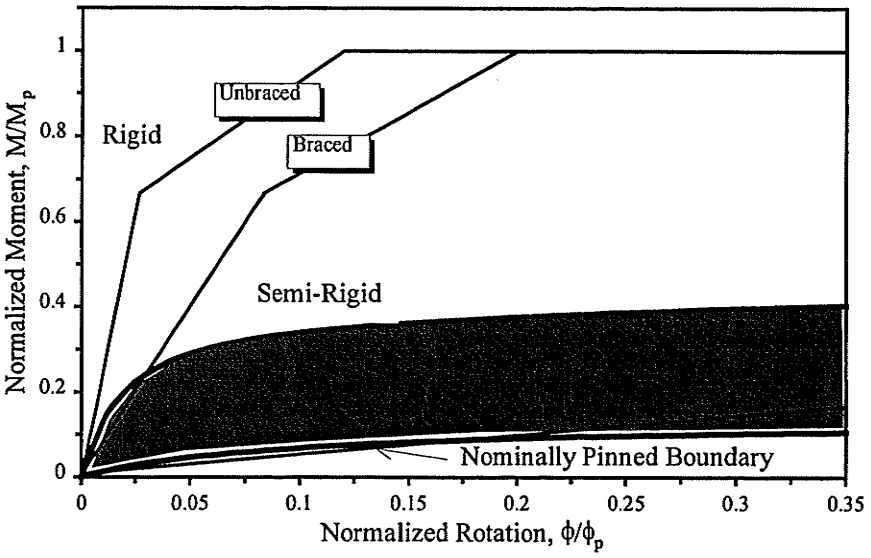


Figure 4.20 Classification boundaries for Top and Seat Angle Connection

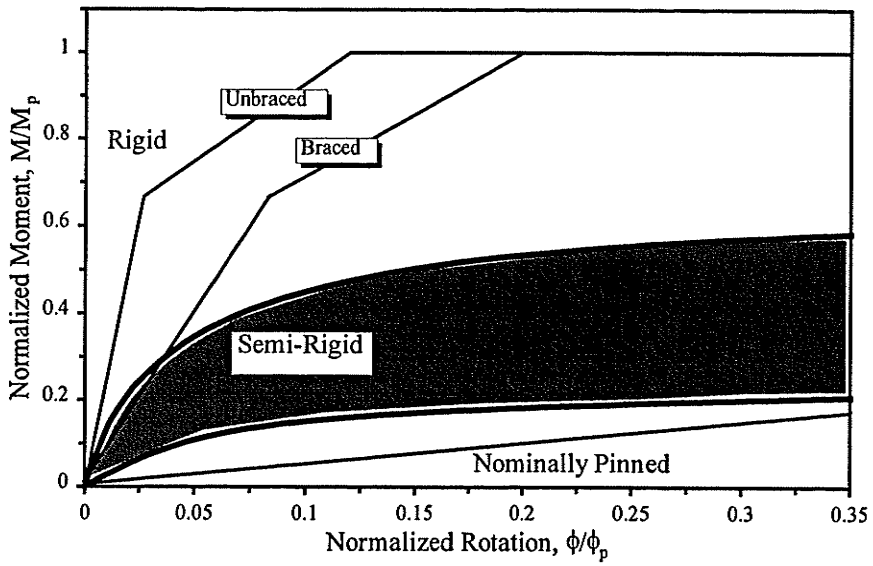


Figure 4.21 Classification boundaries for Flush End Plate Connection

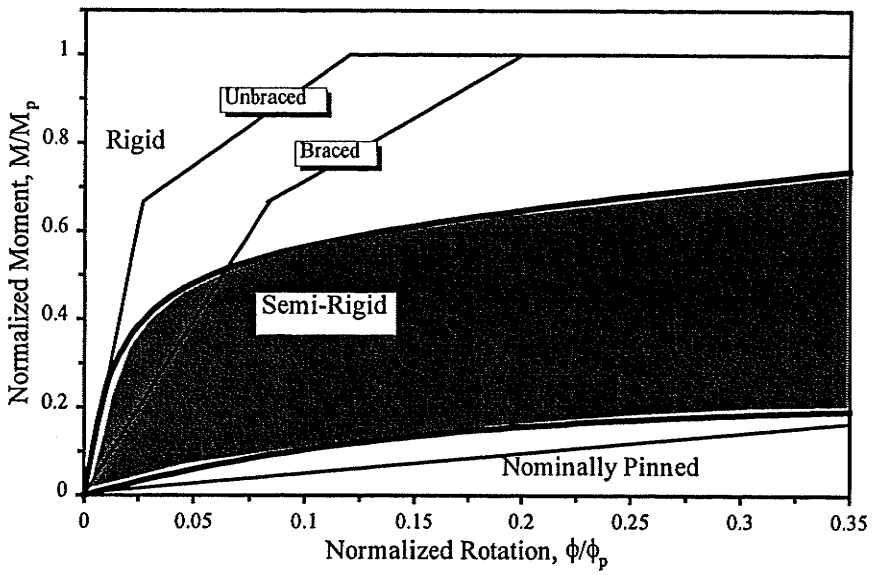


Figure 4.22 Classification boundaries for Top and Seat Angle Connection with Double Web Angles

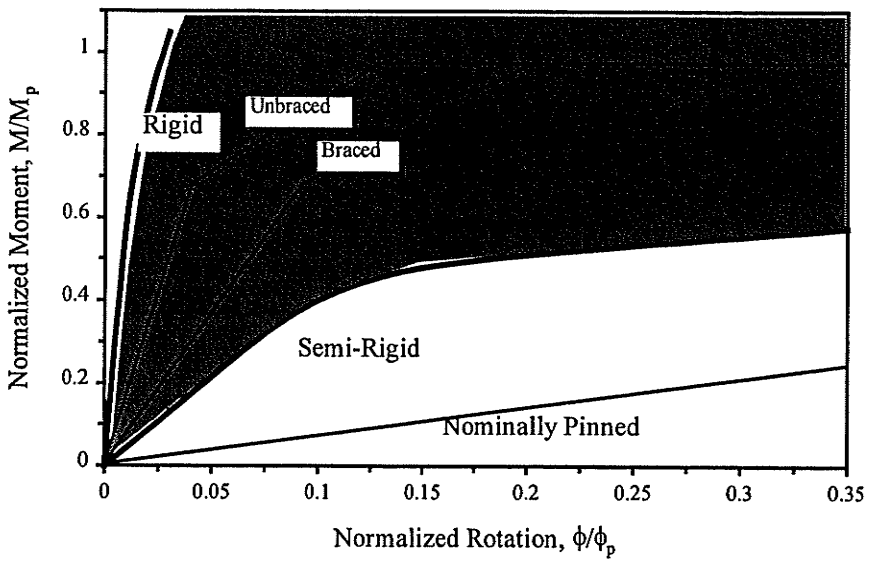


Figure 4.23 Classification boundaries for Extended End Plate Connection

5. Standardization of Connections

5.1 Reasons For Standardizing Connections

5.1.1 Introduction

Standardization of beam-to-column connections is well advanced in Australia, and in recent years, there has been a move toward standardization in Canada and the United States. In the latter two countries, steel design handbooks, published by the steel industries, that deal specifically with connections incorporate some standardization. Some fabricators in Britain and Europe produce standard connection geometries but no national or international standard exists.

5.1.2 Cost of Construction

Because they are labour intensive, connections often account for a significant part of the construction cost of a steel frame. Also, for each connection type, there are several options such as bolts size, strength and spacing, and plate or angle thickness and length. This requires fabricators to stock a variety of angle sizes, plate thicknesses, etc. Standardization of connection components can cut costs significantly. Other benefits of standardization are the following:

1. It reduces the risk of using the wrong connection components in the field
2. It requires workers to handle fewer different types of connections thereby simplifying construction
3. It requires minimal detailing effort by designers and draftspersons since standard connection details could simply be "called up" into drawings.

5.1.3 Implementation Into A Frame Analysis Program

Once a standardized menu of connection geometries is established, the experimental M-ϕ curve corresponding to each standardized connection type is curve fitted to the modified

Richard-Abbott function. The curve-fitting parameters are then incorporated into a database that can be incorporated into or read by a structural analysis program that can accommodate non-linear connection behaviour. Presumably, there may be gaps in the program's connection database corresponding to the connections for which there are no reliable experimental data. Over time, researchers can conduct tests and the resulting experimental data can be curve-fitted to the modified Richard-Abbott function. Eventually, all of the gaps in the connection database would be filled. Then, analysis of any steel frame structure using any of the standard connection types in the database will be possible using the computer program.

In this chapter, the following steps are used in the standardization approach:

1. develop a limited menu of standard connection geometries (standard gages, material thickness, lengths of connecting plates or angles) using the Canadian, American and the Australian standardized initiatives as a guide;
2 compare the standard menu with the existing experimental data to determine for which standard connection types there are moment-rotation data;
3. attempt to use interpolation or extrapolation to obtain M-ϕ curves for the standard connections in the menu for which experimental data are not available; and
4. make recommendations for experimental testing for the standard connections for which there are no experimental data

5.2 Summary Of Current Standardization Practice

5.2.1 Canada

The Canadian Institute of Steel Construction handbook (CISC, 1991) contains tables of recommended component sizes and capacities for several common connection types. Included are standard dimensions and sizes for single web angle, double web angle, header plate and top and seat angle connections. CISC has also published a handbook titled Standardized Shear Connections (CISC, 1994) which covers non-moment-resistant connections. This handbook incorporates a connection designation system and design

tables. It makes no attempt to standardize typical moment resistant connections such as flush and extended end plate connections.

5.2.2 United States

The American Institute of Steel Construction specification "Load and Resistance Factor Design" (AISC-LRFD, 1986) contains a detailed description of connection geometries. The AISC Handbook of Steel Construction (AISC, 1986) contains tables of recommended component sizes for several common connection types. These include connection capacity tables that incorporate standard gages, pitches, etc. AISC has also published a handbook on shear connections (AISC, 1994) which covers non-moment resistant connections. Most North American fabricators base their connection details on these standards.

5.2.3 Australia

The Australian Institute of Steel Construction (AISC, 1991) has done the most to promote standardization of connections. The Standardized Structural Connection manual (1991) covers standardization of parameters and connection components, and incorporates a connection designation system. It includes suggested steel grades, weld types and sizes, and bolt types and diameters. This manual covers both shear and moment resistant connections.

5.3 Standardization

5.3.1 General

Standardized Beam, Column and Connection Material Properties

The CISC Handbook of Steel Construction (CISC, 1991) defines CAN/CSA G40.21-M 300W as the standard weldable steel normally specified for building construction. Since the purpose of this study is to investigate the behaviour of steel building frames, G40.21-M 300W is the recommended material standard for beams and columns that are fastened together by the connections described in this chapter. The CISC Standardized Shear Connections Handbook (CISC, 1994) also recommends CAN/CSA G40.21-M 300W for non-moment-resistant beam-to-column connections. Thus, the proposed standardized

material for all connections is CAN/CSA G40.21-M 300W. Currently, the CISC Handbook contains tables that give the factored bearing resistance of bolts for several connection details and material properties. Since connections would have only one standard material designation the Handbook could use one table for design of bolt bearing resistance.

Standardized Bolt Material Properties and Size

Section 3 of the CISC Handbook contains bolt data for both metric (SI) series and Imperial series bolts. The material properties for metric series bolts are based on ASTM Specifications A325M and A490M and for the Imperial series on ASTM Specifications A325, A490 and A307. The CISC Standardized Shear Connections (CISC, 1991) manual discusses the reluctance of bolt producers to stock both metric and Imperial sizes. Bolt manufacturers usually only stock the Imperial sizes because they sell to both U.S. and Canadian clients. However, all U.S. Federal Government agencies are to convert to SI and target dates are in place. Therefore, before long, the inclination will be for North American bolt producers to produce metric sized bolts exclusively.

The recommended standardized bolt designation and the recommended standard bolt sizes are selected based on the metric series. For flexible and semi-rigid connections (single and double web angle, header plate and top and seat angle connections) the standard bolt size is M20-A325M. The moment resistant connections are classified as either ductile or non-ductile. The ductile types of connections are flush end plate and extended end plate connections with a thin plate (t = 16 mm). For ductile connections the standard bolts size is M20 A325M and for non-ductile connections (t = 28 mm) the standard bolt size is M24-A325M. The A490M designation, which is approximately 25 % stronger, is not selected in the standardization scheme because of its limited use and higher costs.

Standardized Welds

The electrode classification that matches G40.21 Grade 300 steel is E 480 XX. The CISC Handbook also contains tables of resistances for weld groups based on E 480 XX. This is also the electrode chosen in the Standardized Structural Connections manual published by the Australian Institute of Steel Construction (1991). Since E 480 XX is the preferred choice, it is the proposed standardized electrode classification selected.

The CISC Handbook contains no standardization for the size of the fillet welds. However, the AISC Standardized Structural Connections manual includes two standardized fillet weld sizes; 6mm and 8mm. In this study, 8mm is the choice as the standardized fillet weld size.

5.3.2 Connection Geometry

The purpose of this study is to limit the number of possible geometries for each connection type. The benefit of this would be lower costs and simpler detailing because of standardized component sizes. The approach used is to review the existing standardization in the North American and Australian codes and to further limit the recommended options. For example, if three angle sizes are given for a certain connection type, one of the three is chosen as the standardized angle. The slight increase in cost for extra material is offset by a reduction in the fabrication cost and detailing effort required. This is because fewer types of connections are specified to the manufacturer and catalogued standard details are more simple to specify into drawings.

5.3.2.1 Single Web Angle Connection

Current Practice

The CISC Handbook presents standard angle sizes and geometries for single web angle connections. There is one angle size designation; 100 x 75 and three angle thicknesses; 6, 8 and 10 mm. There is only one choice for gauge, pitch and end distances. The gauge distance, g, defined as the distance from the centre of the beam web to the centre of the bolt group along the column flange, and the gauge distance g_1, defined as the distance from the column face to the centre of the bolt group along the length of the beam, are both 65 mm. The pitch, defined as the distance between two rows of bolts, is 80 mm.

The end distance, c, defined as the distance from the edge of the plate to the centre-line of the nearest bolt is 35 mm. Four options are given for the bolt diameter; two metric, M20 and M22 and two Imperial, 3/4 and 7/8. The maximum number of bolts per vertical line is 8.

Selected Standardized Geometry

Although the CISC Handbook presents standard component sizes for single web angle connections, there are still many combinations of options available to the designer. It is the purpose of this study to limit these options. Thus, the following standardized component geometry is recommended:

Angle Size: 100 x 75

$t = 10$ mm

$g = g_1 = 65$ mm

$p = 80$ mm

$c = 35$ mm

d_b = M20 A325M

L = 150, 310, 470 or 630 mm

n = 1x2, 1x4, 1x6 or 1x8

In this case, the larger value of thickness and the smaller bolt diameter are the standardized selections. The smaller bolt diameter is used because web angle connections are not permitted to transfer appreciable moment. An angle thickness of 10 mm is selected because the shear plane tends to cross bolt threads for thinner angles, thus reducing bolt capacity. Table 5.1 shows the four standardized designations and the corresponding angle lengths and bolt layout. Figure 5.1 shows a diagram of the standardized single web angle connection. Thus, a single web angle connection is specified simply by its length preceded by the initials of the connection type. For example, a SWA-310 is a 100 x 75 single web angle connection fabricated from G40.21-

M 300W steel with angle thickness, gauges, pitch and bolt diameter as defined above. It has one line of four ASTM A325 bolts.

Available Experimental Data

The tests for the single web angle connection are by S.L. Lipson (1968). Table 5.2 lists the geometric parameters for each test specimen that closely resembles those from the standardized designation. Angle lengths of 140, 292 and 445 mm match the first three standard designations. There are no tests for SWA-630. Gauge distance, pitch and bolt data are very close to the standard designations. All of the test specimens uses 6 or 8 mm thick angles compared to 10 mm for the standardized connection. By analyzing the curve-fitting data the increase in M_o, S_o and S_p is approximately 50% for each 2 mm increase in angle thickness. Thus, the modified Richard-Abbott parameters listed in Table 5.3 are extrapolated from the available curve-fitting data.

5.3.2.2 Single Plate Connection

Current Practice

The current North American manuals do not give standard details for single plate connections. The CISC Standardized Shear Connections manual (CISC, 1994) expresses concern that single plate connections possess excessive stiffness and stress concentrations at the top of the welds. One way in which flexibility is achieved is by deformation of the plate or the beam web around the bolt holes. The manual describes a knife angle connection that is similar to the side plate connection. For this type of connection a pair of angles are shop welded to the flange of the column and the beam web is field bolted to the outstanding legs of the angles.

The single plate connection is standardized in the Australian Standardized Structural Connections Handbook (1991). The standard plate thickness is 10 mm. Two alternative bolt patterns are given:

1) a single line of bolts to the supported beam web, and
2) two lines of bolts to the supported beam web.

The standard plate widths for alternative one and alternative two are 70 mm and 180 mm respectively. For alternative two the gauge, g, between the two lines of bolts is 70 mm. The end distances, c, for options one and two are 35 mm and 55 mm respectively. For both options the pitch, p, is 70 mm. The connection is welded to the flange of the column with 6 or 8 mm fillet welds and fastened to the beam web with M22 bolts. The maximum number of bolts per vertical line is 9.

Selected Standardized Geometry

The selected standardized geometry for the single plate connection is chosen by employing the Australian standardization but using the North American standard detail dimensions. By selecting a single line of bolts as the standard, one standard plate width is chosen. Thus, the following standardized component geometry is recommended:

L_p = 150, 310, 470 or 690 mm
Plate Width = 90 mm
Plate Thickness = 10 mm
g = 65 mm
p = 80 mm
d_b = M20 A325M
n = 1x2, 1x4, 1x6 or 1x8
Weld Size = 8 mm

The gauge distances and the pitch are selected to reflect the North American standards. The relatively small plate thickness and bolt size are selected to ensure flexible M-ϕ behaviour. Table 5.4 shows the four standardized designations, plate length and bolt layout. Figure 5.2 shows a diagram of the single plate connection.

Available Experimental Data

The experimental tests for single plate connections that match the standard designations are by S.L. Lipson (1968) and R.M. Richard (1982). Table 5.5 lists the geometric parameters for the tests that closely resemble the standard designations. As with the

single web angle connection the only parameter that significantly varies from the standard designation is the plate thickness. Therefore, a similar approach is taken: extrapolating the curve-fitting parameters which are listed in Table 5.6.

5.3.2.3 Double Web Angle Connection

Current Practice

The standard dimensions for double web angle connections presented in the CISC handbook are similar to those of the single web angle connection except that three angle sizes are specified instead of one. The three angle sizes are: 100 x 100, 90 x 90 and 75 x 75. Because three angle sizes are given the gauge distances vary according to the length of the corresponding angle leg. For this reason three gauges, g, defined as the distance between the two vertical lines of bolts along the column flange and gauge, g_1, defined as for the single web angle connection, must be specified. Table 5.7 shows how g and g_1 vary with angle size. The maximum number of bolts per vertical line is 13. The angle thicknesses, pitch, end distance and bolt diameter are the same as for single web angle connections.

Selected Standardized Geometry

The following standardized component geometry using the single angle size of 100 x 100 is recommended:

Angle Size: 100 x 100

$t = 10$ mm

$g = 130$ mm

$g_1 = 65$ mm

$p = 80$ mm

d_b = M20 A325M

$L_p = 150, 310, 470, 630, 790$ or 950 mm

n = 1x2, 1x4, 1x6 or 1x8

A single angle size is specified to limit the number of possible combinations. Table 5.8 shows the six standardized designations and the corresponding angle lengths and bolt layouts. There are two extra designations to accommodate the larger number of bolts per vertical line allowed by CISC for double web angles. Figure 5.3 shows a diagram of the standardized double web angle connection.

Available Experimental Data

The tests whose specimens closely resemble DWA-310 and DWA-470 are by C. Onuah (1988). Table 5.9 lists geometric parameters for these test specimens. All of the geometric parameters are similar to the standard parameters except for the angle thickness. For DWA-310 one test specimen that resembles the standard designation is available, A15. Test specimen A15 uses a 10 mm plate. For DWA-470 two test specimens that resemble the standard one are available, A18 and A19. Specimen A18 uses an 8 mm plate while test A19 uses a 12 mm plate. Table 5.10 lists the modified Richard-Abbott parameters for the standard double web angle connections. Curve-fitting parameters for DWA-310 are obtained directly from the curve-fitting data while for DWA-470 the parameters are interpolated for an angle thickness of 10 mm. The remaining modified Richard-Abbott parameters are extrapolated from the available curve-fitting data.

5.3.2.4 Header Plate Connection

Current Practice

The Canadian (CISC,1991), American (AISC-LRFD, 1986) and Australian (AISC, 1991) handbooks all contain standard details for the commonly used header plate connection. The CISC handbook gives four standard plate thicknesses: 6, 7, 8 and 10 mm and three standard gauges: 80, 100 and 150 mm. The pitch and end distance is 80 mm and 35 mm respectively. Three possible fillet welds: 5, 6 and 8 mm and two bolt sizes: M20 and M22 are given. The maximum number of bolts is 8.

Selected Standardized Geometry

The following standardized component geometry with four plate sizes is recommended:

Plate Size: 150 x 170, 310 x 170, 470 x 220 or 630 x 220

t = 10 mm

p = 80 mm

c = 35 mm

Weld Size = 8 mm

d_b = M20-A325M

g = 100 or 150 mm

n = 2x2, 2x4, 2x6 or 2x8

L_p = 150, 310, 470 or 630 mm

Table 5.11 shows the four standardized designations and the corresponding plate sizes, gauges and bolt layouts. The number in the designation defines the length of the plate. For HPC-150 and HPC-310 the width of the plate is 170 mm, which corresponds to a gauge distance of 100 mm. For HPC-470 and HPC-630 the width of the plate is 220 mm which corresponds to a gauge distance of 150 mm. Figure 5.4 shows a diagram of the standardized header plate connection.

Available Experimental Data

Four tests by W. H. Sommer (1969) have geometric parameters that resemble the first three standardized header plate connections. Table 5.12 lists the test specimens that match the standard designations. Test 28 corresponds to HP-150 except for the plate thickness which is only 6 mm compared to 10 mm for the standard designation. Therefore, the curve-fitting data are extrapolated for HP-150. Tests 11 and 14 match HP-310, Test 16 matches HP-470 and no test data are available for HP-630. Thus, the curve-fitting data are obtained directly for HP-310 and HP-470 and extrapolated for HP-610. Table 5.13 lists the modified Richard-Abbott parameters for the standardized header plate connections.

5.3.2.5 Top and Seat Angle Connection

Current Practice

The Fourth Edition of the CISC handbook (CISC, 1987) recommends six standard top and seat angle sizes: 90 x 90, 100 x 90, 100 x 100, 125 x 100, 150 x 150 and 200 x 100. These recommendations do not appear in the Fifth Edition of the CISC handbook (CISC, 1991). There are five standard angle thicknesses of 8, 10, 13, 16 and 20 mm and two standard angle lengths of 180 and 230 mm. The gauge distances corresponding to these two angle lengths are 100 and 130 mm.

The U.S., AISC-LRFD handbook also presents a number of angle choices. These are: 100 x 90, 125 x 90, 150 x 100, 180 x 100 and 200 x 100. Angle lengths are 152 and 203 mm. No standard gauges are given but, three standard pitches between bolt rows are specified. They are: 60, 70 and 80 mm.

The Australian, AISC handbook, gives one standard angle size: 150 x 90 and limited dimension options are: t = 12 mm, L_p = 180 mm, g = 90 mm and p = 90 mm.

Selected Standardized Geometry

The following standardized component geometry, with two angle sizes, is recommended:

Angle Size: 100 x 100 or 150 x150
t = 13 mm
c = 35 mm
d_b = M20-A325M
g = 100 or 130 mm
p = 0 or 60 mm
n = 2x1 or 2x2
L_p = 180 or 230 mm

Table 5.14 shows the two standard designations and the corresponding dimensions and bolt layout. The first designation, TSA-180, uses a 100 x 100 angle with one row of bolts

each on the beam web and column flange. The number 180 in the designation corresponds to the length of the angle. The gauge distance between the two lines of bolts is 100 mm and the pitch is zero since there is only one row. The second designation, TSA-230, uses a 150 x 150 angle with two rows of bolts. The extra row of bolts, with a pitch of 60 mm, is used because the larger angle size can accommodate them. Figure 5.5 shows a diagram of the standardized top and seat angle connection.

Available Experimental Data

Table 5.15 lists the specimens tested by M.J. Marley (1982) which resemble the standard top and seat angle connections. Several specimens resemble TSA-180 and none resemble TSA-230. Thus, Table 5.16 lists the modified Richard-Abbott parameters obtained directly for TSA-180 and estimated for TSA-230.

5.3.2.6 Flush End Plate Connection

Current Practice

The CISC does not provide standard dimensions for this type of connection because it is typically a semi-rigid type connection and requires special attention in the analysis stage. The header plate connection described in the CISC handbook offers standard pitch and gauge distances that may be used as standard dimensions for flush end plate connections.

The Australian handbook does not explicitly standardize the dimensions for flush end plate connections. However, it standardizes bolted beam-to-column moment end plate connections. These are shown in the handbook as extended end plate connections.

Selected Standardized Geometry

The following five standardized connection geometries with varying plate sizes are proposed using a blend of the CISC details for end plate connections and the AISC specifications for moment connections:

Plate Size: 300 x 170, 500 x 170, 700 x 220, 900 x 220 or 1200 x 220

t = 13 or 16 mm

g = 100 or 150 mm

p_f = 80 mm

c = 35 mm

Weld Size = 8 mm

d_b = M20-A325M

n = 2x2

Table 5.17 shows the standardized designations and the corresponding plate sizes, thickness and gauge distances. The number in the designation corresponds to the length of the plate. The first two standard connections, FEP-300 and FEP-500, use a plate width of 170 mm, which corresponds to a gauge distance of 100 mm. The plate thickness for these two connection types is 13 mm. The final three standard connections, FEP-700, FEP-900 and FEP-1200, use a plate width of 220 mm which corresponds to a gauge distance of 150 mm. The plate thickness for these three types is 16 mm. Figure 5.6 shows a diagram of the standardized flush end plate connection.

Available Experimental Data

The tests for flush end plate connections are by J.R. Ostrander (1970). Table 5.18 lists the specimens that are used to obtain the curve-fitting parameters. All of the specimens are for a single plate size. They are arranged by matching the plate thickness to the standard designation which uses the similar thickness. For FEP-300 and FEP-500 the specimens use a plate thickness of 13 mm and for FEP-700, FEP-900 and FEP-1200 the specimens use a plate thickness of 16 mm. It is assumed that the moment-rotation curves for the standard flush end plates of similar thickness will be similar. If more data were available the actual moment-rotation data could be used for each standard connection. Table 5.19 lists the modified Richard-Abbott parameters for the standardized flush end plate connection.

5.3.2.7 Top and Seat Angles with Double Web Angle Connection

Current Practice

The CISC handbook shows an "optional location" for a clip angle in the section describing stiffened seated beam connections. The Australian handbook gives standard dimensions for an angle seat connection with a single web angle connection. These are similar to those describes for simple angle seat and single web angle connections.

Selected Standardized Geometry

Top and seat angles with double web angle connections are a combination of two connection types described previously. Thus, they can be assembled by combining the respective menus for double web angle connections and for top and seat angle connections. There are twelve possible connection geometries of this type since there are two options for top and seat angle connections and six options for double web angle connections. However, as illustrated in the CISC handbook, a small angle is typically placed at the top portion of the beam. Thus, Table 5.20 gives a list of the proposed combinations using TS-180 and TS-230 and only DWA-150 and DWA-310.

Available Experimental Data

Tests for the top and seat angle with double web angle connections are by A. Azizinamini (1985). Table 5.21 lists three specimens that have geometric parameters that are reasonably close to the standard designations. No specimen exactly matches any of the standard designations. Thus, Table 5.22 lists the modified Richard-Abbott parameters which are estimated from the available experimental data.

5.3.2.8 Extended End Plate Connection

Current Practice

In Canada, no standardization exists for this type of connection. However, the Australian Standardized Structural Connections manual (AISC, 1985) contains standard details of moment resisting end plate connections that serve as a guide. The distance, p_f, defined as the pitch between the two lines of bolts on either side of the beam flange, is 130 mm.

The gauge distance is 70 or 90 mm and the end distance is 50 mm. The standard plate thicknesses are: 28 and 32 mm and the standard bolt diameters are: M20 and M24.

Additional information is found in the Steel Construction Institute's Draft Report on Connection Standardization: A Review of International Practice in the Field of Moment Connections (SCI, 1993). In a private communication A. Hughes (1993) suggests that extended end plate connections need to be standardized in two classes: ductile and non-ductile. The main difference between the two classes is the failure mode. A ductile connection is assumed to act as a plastic hinge while a non-ductile one cannot. This is something that is not covered in the AISC Standardized Connections Manual and it is felt that the Australian standardized moment resisting connections may possess limited ductility because of their large plate thicknesses of 28 and 32 mm. Hughes also states that M20 bolts may not perform well in moment resisting connections and that M24 bolts may be the practical choice.

Selected Standardized Geometry

Based on the discussion above the recommended standard dimensions for extended end plate connections are the following:

Plate Size: 490 x 170, 650 x 220, 810 x 220, 970 x 220 or 1290 x 220

p_f = 130 mm (pitch of bolts across beam flange)

p_i = 80 mm (pitch of bolts in the central part of the plate)

g = 100 or 150 mm

n_t = 2x2 (total number of tension bolts)

n_c = 2x2 (total number of compression bolts)

n_i = 2x1, 2x2 or 2x3 (total number of inner bolts)

c = 35 mm

Weld Size = 8 mm

t = 16 mm, d_b = M20-A325M (ductile connections)

t = 28 mm, d_b = M24-A325M (non-ductile connections)

Table 5.23 shows the standardized designations and the corresponding plate sizes, gauge distances and numbers of inner bolts. Five standard plate sizes are proposed. There are two standard designations for each standard plate size: one for a ductile connection (t = 16 mm and d_b = M20) and the other for a non-ductile connection (t = 28 mm and d_b = M24). Figure 5.7 shows a diagram of the standard extended end plate connection.

Available Experimental Data

The experimental test specimens that resemble the standard designations are presented in Table 5.24. The tests are by several different authors. The specimen from Test 4 by N.D. Johnstone (1981) and from Test 1 by S.A. Ioannides (1978) match EEP-490D. Test A1 and C12 by J.R. Bailey (1970) and Test C4 and C5 by J.O. Surtees (1970) match EEP-490ND. Two tests by S.A. Ioannides (1978) match EEP-650. Test 2 corresponds to EEP-650D and Test 5 corresponds to EEP-650ND. Tests T1 and T2 by P. Grundy (1980) match EEP-970ND. There are no available tests for EEP-810D, EEP-810ND, EEP-970D, EEP-1290D and EEP-1290ND. Table 5.25 lists the modified Richard-Abbott parameters for the standard extended end plate connections. The curve-fitting parameters for the standard connections with matching experimental data are obtained directly while for the other connections the curve-fitting parameters are estimated.

5.4 Recommendations for Future Testing

It is recommended that experimental testing of the moment-rotation behaviour for all of the proposed standardized connections be conducted. Enough tests must be conducted to provide a statistically significant representation of the behaviour of each standard connection. This will provide designers with accurate M-ϕ behaviour for every standard connection type. Presently, there are not enough data available to know how accurate the M-ϕ curves are.

A suggested strategy for the order in which connections are tested should be to test the most commonly used connection types and geometries first. Specifically, the most

popular connections and the those exhibiting semi-rigid behaviour should be tested first. Second, the remaining connections for which there are no M-ϕ data should be tested. Finally, the remainder of the connections should be tested.

Table 5.1 Standardized options for SWA connections (100 x 75)

	Standardized Options (mm)	
Designation	L	n
SWA-150	150	1x2
SWA-310	310	1x4
SWA-470	470	1x6
SWA-630	630	1x8

Table 5.2 Geometric parameters for SWA tests that resemble standard designations

		Geometric Parameters (mm)							
Designation	Test I.D.	Angle Size	L	t	g	p	c	d_b	n
SWA-150	Lipson: AA-2/1 Lipson: AA-2/2	100 x 90	140	6	65	76	32	¾" - A325	1x2
SWA-310	Lipson: AA-4/1	100 x 90	292	6	65	76	32	¾" - A325	1x4
	Lipson: AA-4/2			6	65	76	32	¾" - A325	1x4
	Lipson: BB-4/1			8	65	76	32	¾" - A325	1x4
	Lipson: BB-4/2			8	65	76	32	¾" - A325	1x4
	Lipson: B2-4			8	65	76	32	¾" - A325	1x4
	Lipson: B3-4			8	65	76	32	¾" - A325	1x4
SWA-470	Lipson: AA-6/1 Lipson: AA-6.2	100 x 90	445	6	65	76	32	¾" - A325	1x6
SWA-630	-	-	-	-	-	-		-	-

Table 5.3 Modified Richard-Abbott parameters for standardized SWA connections

	Normalized Richard-Abbott Parameters #					
Designation	$\overline{\phi_u}$	$\overline{M_o}$	$\overline{S_o}$	$\overline{S_p}$	n_1	n_2
SWA-150	0.612	0.00389	0.0191	0.00669	4.843	0.579
SWA-310	0.727	0.0224	0.169	0.0185	2.131	1.476
SWA-470	0.511	0.0858	1.007	0.0756	1.138	1.272
SWA-630	0.617	0.163	3.071	0.259	2.584	1.109

Notes: # Extrapolated from experimental data

Table 5.4 Standard options for SP connections (90 mm width)

	Standardized Options (mm)	
Designation	L_p	n
SP-150	150	1x2
SP-310	310	1x4
SP-470	470	1x6
SP-630	630	1x8

Table 5.5 Geometric parameters for SPC tests that resemble standard designations

		Geometric Parameters (mm)						
Designation	Test I.D.	L_p	t	g	p	c	d_b	n
SP-150	Richard: RGKL2	152		-		-		
	Lipson: P1-2/1	140	6	64	76	32	¾" - A325	1x2
	Lipson: P1-2/2	140		64		32		
SP-310	Lipson: P1-4/1	292	6	64	76	32	¾" - A325	1x4
	Lipson: P1-4/2							
SP-470	Lipson: P1-6/1	445	6	64	76	32	¾" - A325	1x6
	Lipson: P1-6.2							
SP-630	Richard: RGKL7	546	6	-	76	-	¾" - A325	1x7

Table 5.6 Modified Richard-Abbott parameters for Standardized SP connections

	Normalized Richard-Abbott Parameters #					
Designation	$\overline{\phi_u}$	$\overline{M_o}$	$\overline{S_o}$	$\overline{S_p}$	n_1	n_2
SP-150	0.597	0.0198	0.359	0.00110	2.134	1.456
SP-310	0.588	0.0638	1.807	0.0905	0.163	1.052
SP-470	0.415	0.177	3.02	0.131	12.5	1.968
SP-630	0.962	0.234	6.94	0.0618	1.027	1.279

Notes: # Extrapolated from experimental data

Table 5.7 CISC standard gauges for DWA connections

Angle Size	g (mm)	g_1 (mm)
100 x100	140	65
90 x 90	130	60
75 x 75	100	45

Table 5.8 Standard options for DWA connections (100 x 100)

	Standardized Options (mm)	
Designation	L_p	n
DWA-150	150	1x2
DWA-310	310	1x4
DWA-470	470	1x6
DWA-630	630	1x8
DWA-790	790	1x10
DWA-950	950	1x12

Table 5.9 Geometric parameters for DWA tests that resemble standard designations

		Geometric Parameters (mm)								
Designation	Test I.D.	Angle Size	L	t	g	g_1	p	c	d_b	n
DWA-150	-	-	-	-	-	-	-	-	-	-
DWA-310	Onuah: A15	100 x 100	310	10	65	130	80	-	¾" - A325	1x4
DWA-470	Onuah: A18 Onuah: A19	100 x 100	470	8 12	65	130	80	-	¾" - A325	1x6
DWA-630	-	-	-	-	-	-	-	-	-	-
DWA-790	-	-	-	-	-	-	-	-	-	-
DWA-950	-	-	-	-	-	-	-	-	-	-

Table 5.10 Modified Richard-Abbott parameters for standardized DWA connections

	Normalized Richard-Abbott Parameters					
Designation	$\overline{\phi_u}$	$\overline{M_o}$	$\overline{S_o}$	$\overline{S_p}$	n_1	n_2
DWA-150 #	0.862	0.0230	1.158	0.0390	3.056	3.409
DWA-310 §	1.168	0.0472	1.592	0.125	-1.051	5.267
DWA-470 §	0.555	0.0714	2.032	0.211	7.163	1.551
DWA-630 #	0.862	0.0956	2.472	0.297	3.056	3.409
DWA-790 #	0.862	0.120	2.912	0.383	3.056	3.409
DWA-950 #	0.862	0.144	3.352	0.469	3.056	3.409

Notes: # Extrapolated from experimental data
§ Obtained directly from test data

Table 5.11 Standard Options for HP connections

	Standardized Options (mm)		
Designation	Plate Size (length x width)	g	n
HP-150	150 x 170	100	2x2
HP-310	310 x 170	100	2x4
HP-470	470 x 220	150	2x6
HP-630	630 x 220	150	2x8

Table 5.12 Geometric parameters for HP tests that resemble standard designations

		Geometric Parameters (mm)						
Designation	Test I.D.	Plate Size	t	g	p	c	d_b	n
HP-150	Sommer: Test 28	152 x -	6	102	76	38	¾" - A325	2x2
HP-310	Sommer: Test 11 Sommer: Test 14	305 x -	10	102	76	38	¾" - A325	2x4
HP-470	Sommer: Test 16	457 x -	10	140	76	38	¾" - A325	2x6
HP-630	-	-	-	-	-	-	-	-

Table 5.13 Modified Richard-Abbott parameters for standardized HP connections

	Normalized Richard-Abbott Parameters					
Designation	$\overline{\phi_u}$	$\overline{M_o}$	$\overline{S_o}$	$\overline{S_p}$	n_1	n_2
HP-150 #	0.553	0.0510	0.678	0.0694	1.455	0.832
HP-310 §	0.573	0.0811	1.612	0.0835	6.310	2.356
HP-470 §	0.754	0.0997	1.571	0.0758	3.671	1.289
HP-630 #	0.627	0.118	1.964	0.0762	3.812	1.492

Notes: # Extrapolated from experimental data
§ Obtained directly from test data

Table 5.14 Standard dimensions for TSA connections

	Standardized Options (mm)					
Designation	Angle Size	L_p	g	p	n_b	n_c
TSA-180	100 x 100	180	100	0	2x1	2x1
TSA-230	150 x 150	230	130	60	2x2	2x2

Table 5.15 Geometric parameters for TSA tests that resemble standard designations

		Geometric Parameters (mm)				
Designation	Test I.D.	Angle Size	t	L	d_b	n
TSA-180	Marley: A1-2/1 Marley: B1-2/1 Marley: B1-2/2 Marley: C1-1/2-1 Marley: C1-1/2-2 Marley: C2-1/2-1 Marley: C2-1/2-2 Marley: D1-1/2-1 Marley: D1-1/2-2 Marley: D2-1/2-1 Marley: D2-1/2-2 Marley: D3-1/2-1 Marley: D3-1/2-2	100 x 100	13	125	¾" - A325	2x1
TSA-230	-	-	-	-	-	-

Table 5.16 Modified Richard-Abbott parameters for standardized TSA connections

	Normalized Richard-Abbott Parameters					
Designation	$\overline{\phi_u}$	$\overline{M_o}$	$\overline{S_o}$	$\overline{S_p}$	n_1	n_2
TSA-180 §	0.557	0.353	8.29	0.167	1.77	1.02
TSA-230 †	0.557	0.441	10.4	0.209	1.77	1.02

Notes: † Estimated
§ Obtained directly from test data

Table 5.17 Standard Dimensions for FEP connections

	Standardized Options (mm)		
Designation	Plate Size (length x width)	t	g
FEP-300	300 x 170	13	100
FEP-500	500 x 170	13	100
FEP-700	700 x 220	16	150
FEP-900	900 x 220	16	150
FEP-1200	1200 x 220	16	150

Table 5.18 Geometric parameters for FEP tests that resemble standard designations

		Geometric Parameters (mm)						
Designation	Test I.D.	Plate Size	t	g	p_f	c	d_b	n
FEP-300 FEP-500	Ostrander: Test 12	332 x -	13	102	64	-	¾" - A325	2x
	Ostrander: Test 15							2
	Ostrander: Test 21							
FEP-700 FEP-900 FEP-1200	Ostrander: Test 13	332 x -	16	102	64	-	¾" - A325	2x
	Ostrander: Test 16							2
	Ostrander: Test 19							
	Ostrander: Test 22							
	Ostrander: Test 23							
	Ostrander: Test 24							

Table 5.19 Modified Richard-Abbott parameters for standardized FEP connections

	Normalized Richard-Abbott Parameters §					
Designation	$\overline{\phi_u}$	$\overline{M_o}$	$\overline{S_o}$	$\overline{S_p}$	n_1	n_2
FEP-300 FEP-500	0.710	0.413	7.120	0.168	0.554	1.360
FEP-700 FEP-900 FEP-1200	0.488	0.434	8.591	0.230	1.413	1.353

Notes: § Obtained directly from test data

Table 5.20 Standard designations for TSA/DWA connections

Standardized Designations		
Designation	Top and Seat Angle	Double Web Angle
TS-180/DWA-150	TS-180	DWA-150
TS-180/DWA-310	TS-180	DWA-310
TS-230/DWA-150	TS-230	DWA-150
TS-230/DWA-310	TS-230	DWA-310

Table 5.21 Geometric parameters for TSA/DWA tests that resemble standard designations

		Geometric Parameters (mm)					
		Web Angles			Top and Seat Angles		
Designation	Test I.D.	Angle Size	t	L	Angle Size	t	L
TS-180/DWA-150 TS-180/DWA-310 TS-230/DWA-150 TS-230/DWA-310	Azizinamini: 14S2 Azizinamini: 14S6 Azizinamini: 14S9	100 x 90	6	215	150 x 90	13	200

Table 5.22 Modified Richard-Abbott parameters for standardized TSA/DWA connections

	Normalized Richard-Abbott Parameters †					
Designation	$\overline{\phi_u}$	$\overline{M_o}$	$\overline{S_o}$	$\overline{S_p}$	n_1	n_2
TS-180/DWA-150	0.477	0.310	8.15	0.257	5.787	0.966
TS-180/DWA-310	0.477	0.341	8.97	0.217	5.787	0.966
TS-230/DWA-150	0.477	0.388	10.2	0.217	5.787	0.966
TS-230/DWA-310	0.477	0.419	11.0	0.217	5.787	0.966

Notes: † Estimated

Table 5.23 Standard dimensions for EEP connections

Designation	Standardized Options (mm)		
	Plate Size (length x width)	g	n_i
EEP-490D, EEP-490ND	490 x 170	100	2x1
EEP-650D, EEP-650ND	650 x 220	150	2x2
EEP-810D, EEP-810ND	810 x 220	150	2x3
EEP-970D, EEP-970ND	970 x 220	150	2x3
EEP-1290D, EEP-1290ND	1290 x 220	150	2x3

Table 5.24 Geometric parameters for EEP tests that resemble standard designations

Designation	Test I.D.	Geometric Parameters (mm)						
		Plate Size	t	g	p_f	p_i	d_b	n_{total}
EEP-490D	Johnstone: Test 4	530 x -	16	115	140	-	M24 G8.8	2x4
	Ioannides: Test 1	526 x -	16	89	140	-	¾" - A325	2x4
EEP-490ND	Bailey: Test A1	422 x -	25	102	114	-	7/8" -	2x8
	Bailey: Test C12	422 x -	27	102	111	-	7/8" -	2x8
	Surtees: Test C4	489 x -	25	89	114	-	1" -	2x6
	Surtees: Test C5	489 x -	25	89	114	-	1" -	2x6
EEP-650D	Ioannides: Test 2	628 x -	19	95	140	-	7/8" A325	2x4
EEP-650ND	Ioannides: Test 5	628 x -	32	95	140	-	7/8" A325	2x4
EEP-810D	-	-	-	-	-	-	-	-
EEP-810ND	-	-	-	-	-	-	-	-
EEP-970D	-	-	-	-	-	-	-	-
EEP-970ND	Grundy: T1 Grundy: T2	943 x -	25	95	89	-	7/8	2x10
EEP-1290D	-	-	-	-	-	-	-	-
EEP-1290ND	-	-	-	-	-	-	-	-

Table 5.25 Modified Richard-Abbott parameters for standardized EEP connections

Designation	Normalized Richard-Abbott Parameters					
	$\overline{\phi_u}$	$\overline{M_o}$	$\overline{S_o}$	$\overline{S_p}$	n_1	n_2
EEP-490D §	0.367	0.435	12.6	0.255	2.01	1.30
EEP-490ND §	0.554	0.555	12.6	0.253	2.94	2.94
EEP-650D #	0.320	0.555	12.6	0.785	0.267	1.05
EEP-650ND §	0.563	0.668	16.4	0.429	1.295	0.945
EEP-810D #	0.563	0.668	18.0	0.429	1.295	0.945
EEP-810ND #	0.563	0.711	20.0	0.429	1.295	0.945
EEP-970D #	0.0745	0.711	22.0	3.32	1.295	0.945
EEP-970ND §	0.0745	0.749	24.7	3.32	0.873	3.03
EEP-1290D #	0.0745	0.936	26.0	3.32	0.873	3.03
EEP-1290ND #	0.0745	0.950	28.0	3.32	0.873	3.03

Notes: # Extrapolated from experimental data
§ Obtained directly from test data

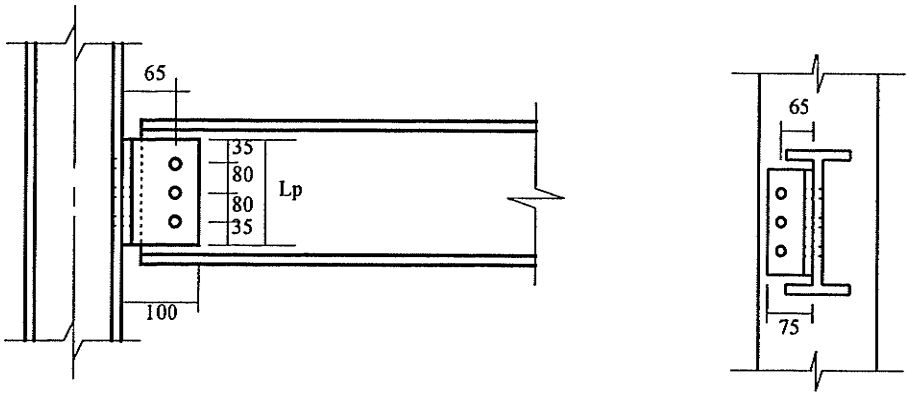


Figure 5.1 Standardized SWA connection

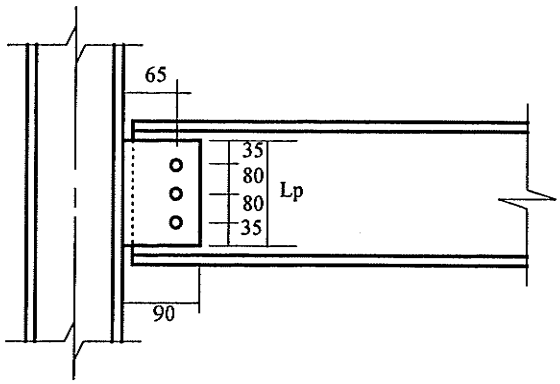


Figure 5.2 Standardized SP connection

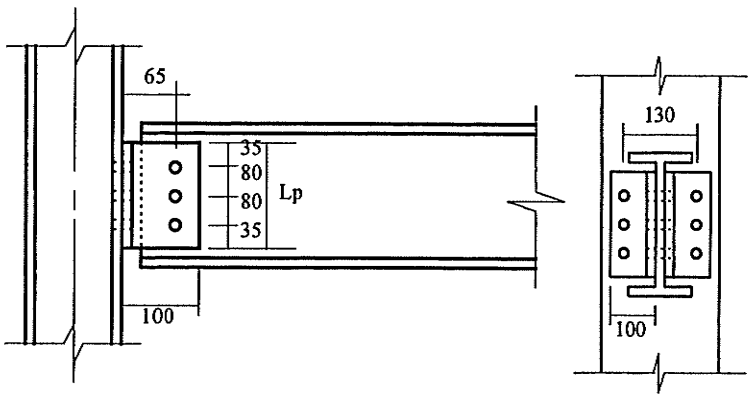


Figure 5.3 Standardized DWA connection

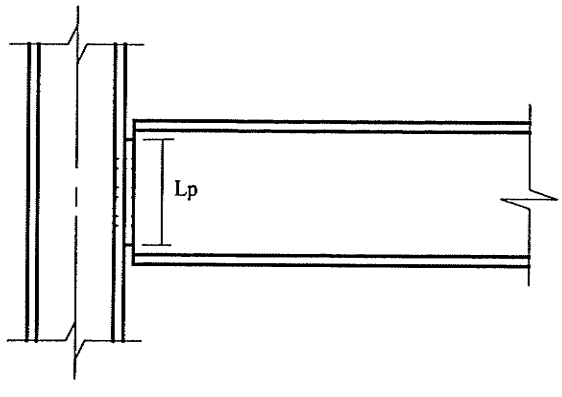


Figure 5.4 Standardized HP connection

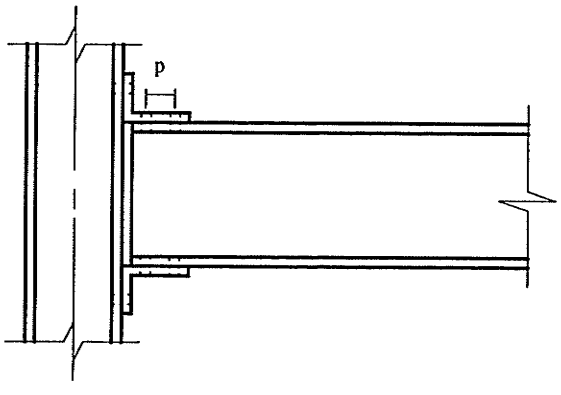


Figure 5.5 Standardized TSA connection

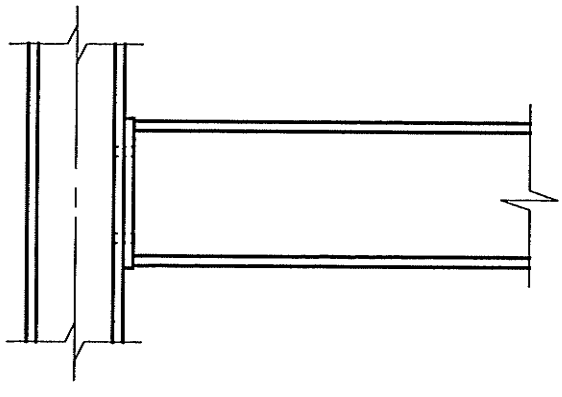


Figure 5.6 Standardized FEP connection

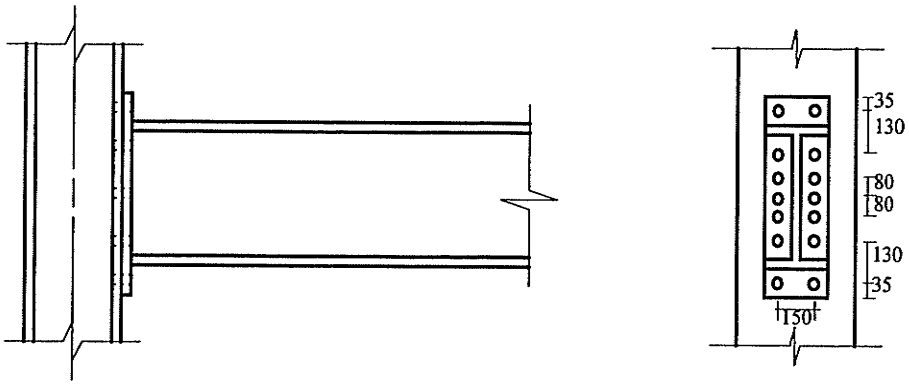


Figure 5.7 Standardized EEP connection

6. Analysis of Flexibly Connected Steel Frames using Micro-Computer Programming

6.1 Modeling of the Structure

6.1.1 Structural Layout

Figure 6.1 shows a typical frame that the program developed for this study can analyze. Although the program does not require the structure to be symmetrical, because of the symmetry of the structure, the layout shown decreases the amount of data the user is required to input into the analysis program. The number of stories, the number of bays in each direction, the storey heights and the bay lengths provide the required information to generate the joint coordinates and member connectivity of the structure.

6.1.2 Coordinate System

To model the structure and the loading, two coordinate systems are used. A global system, with vertical and horizontal axes, is used for the joint coordinates, joint loads and the joint displacements. Figure 6.1 shows how the global coordinate system applies to the whole structure. Load or displacement vectors corresponding to the global system are identified by a prime superscript (ie. D_E' is a displacement vector at joint E, expressed in the global coordinate system). Each member in the structure is assumed to have a direction and thus a local coordinate system associated with it. Consider member AB in Figure 6.1 to have a direction from A to B with its local X_1-axis coincident with the member axis and its X_2 and X_3 axes in the direction of the principal axes of the cross-section. The member loadings and end forces are expressed in the local coordinate system of a given member. The absence of a prime in a load or displacement vector indicates the local coordinate system is being used.

6.1.3 Assumptions and Idealizations

Each floor level is assumed to act as a rigid diaphragm that resists in-plane forces and the floor beams provide restraint for out-of-plane forces. Composite action between the beams and the floor diaphragm is not considered.

The behaviour of the beam-to-column connections is accounted for in the beam stiffness matrices and fixed-end-force vectors. The connections are assumed to have negligible size and are assumed to lie at floor level. The connections experience flexural rotational deformation only and are assumed to permit no direct shearing deformation, axial deformation or torsional deformation. Furthermore, since each floor level is assumed to be a rigid in-plane diaphragm, the stiffness of the connections with respect to displacement components in the plane of the floor are assumed to be infinite.

Using the above idealization only three independent degrees of freedom are considered for each joint; two rotations, ϕ_1' and ϕ_3' and translation δ_2'. These are the out-of-plane displacements. There are three more displacements at each joint; translations δ_1', δ_3' and ϕ_2'. These are in-plane displacements and are associated with the rigid body displacements of the floor diaphragm. Thus, for each floor level with n joints there are 3n out-of-plane displacements plus 3 in-plane displacements for a total of 3n+3 independent displacement components.

The beam and column elements are assumed to be linear-elastic and in general, the connections have non-linear M-ϕ behaviour. An iterative analysis procedure involving repeated cycles of linear analysis and connection stiffness modification is performed, the linear connection stiffnesses being modified to reflect their non-linear behaviour.

6.2 Element Stiffness Matrices

6.2.1 Column Stiffness Matrix

Figure 6.2 shows a typical column modeled as a line elements with end forces and displacement components as shown. The stiffness matrix expressed in the local coordinate system is resolved into two contributions as follows:

$$K = K_D + K_G \qquad (6.1)$$

where: K_D is the first order elastic stiffness matrix and

K_G is the geometric stiffness matrix.

The geometric stiffness matrix accounts for the effect of axial load on the bending stiffness of the column.

The stiffness matrix can be expressed in partitioned form:

$$\begin{bmatrix} P_U \\ P_L \end{bmatrix} = \begin{bmatrix} K_{UU} & K_{UL} \\ K_{LU} & K_{LL} \end{bmatrix} \begin{bmatrix} D_U \\ D_L \end{bmatrix} \qquad (6.2)$$

where subscripts U and L refer to the joints at the upper and lower ends of the column respectively. In Eq. 6.2, the force vectors at the upper and lower end of the column are:

$$P_U = [\, p_{U1}\ p_{U2}\ p_{U3}\ m_{U1}\ m_{U2}\ m_{U3} \,]^T \qquad (6.3)$$

and

$$P_L = [\, p_{L1}\ p_{L2}\ p_{L3}\ m_{L1}\ m_{L2}\ m_{L3} \,]^T \qquad (6.4)$$

respectively, and the displacement vectors at the upper and lower ends are:

$$D_U = [\, \delta_{U1}\ \delta_{U2}\ \delta_{U3}\ \theta_{U1}\ \theta_{U2}\ \theta_{U3} \,]^T \qquad (6.5)$$

and

$$P_U = [\ \delta_{L1}\ \delta_{L2}\ \delta_{L3}\ \theta_{L1}\ \theta_{L2}\ \theta_{L3}\ ]^T \qquad (6.6)$$

respectively.

The partitioned column stiffness matrix (Ang and Morris, 1984; Chen and Lui, 1990) is:

$$K_{UU} = \begin{bmatrix} \frac{AE}{L} & 0 & 0 & 0 & 0 & 0 \\ 0 & \frac{12EI_3}{L^3} & 0 & 0 & 0 & -\frac{6EI_3}{L^2} \\ 0 & 0 & \frac{12EI_2}{L^3} & 0 & \frac{6EI_2}{L^2} & 0 \\ 0 & 0 & 0 & \frac{GI_1}{L} & 0 & 0 \\ 0 & 0 & \frac{6EI_2}{L^2} & 0 & \frac{4EI_2}{L} & 0 \\ 0 & -\frac{6EI_3}{L^2} & 0 & 0 & 0 & \frac{4EI_3}{L} \end{bmatrix} + \begin{bmatrix} 0 & 0 & 0 & 0 & 0 & 0 \\ 0 & -\frac{6P_1}{5L} & 0 & 0 & 0 & \frac{P_1}{10} \\ 0 & 0 & -\frac{6P_1}{5L} & 0 & -\frac{P_1}{10} & 0 \\ 0 & 0 & 0 & 0 & 0 & 0 \\ 0 & 0 & -\frac{P_1}{10} & 0 & -\frac{2p_1L}{15} & 0 \\ 0 & \frac{P_1}{10} & 0 & 0 & 0 & -\frac{2p_1L}{15} \end{bmatrix} \qquad (6.7)$$

$$K_{UL} = \begin{bmatrix} -\frac{AE}{L} & 0 & 0 & 0 & 0 & 0 \\ 0 & -\frac{12EI_3}{L^3} & 0 & 0 & 0 & -\frac{6EI_3}{L^2} \\ 0 & 0 & -\frac{12EI_2}{L^3} & 0 & \frac{6EI_2}{L^2} & 0 \\ 0 & 0 & 0 & -\frac{GI_1}{L} & 0 & 0 \\ 0 & 0 & -\frac{6EI_2}{L^2} & 0 & \frac{2EI_2}{L} & 0 \\ 0 & \frac{6EI_3}{L^2} & 0 & 0 & 0 & \frac{2EI_3}{L} \end{bmatrix} + \begin{bmatrix} 0 & 0 & 0 & 0 & 0 & 0 \\ 0 & \frac{6P_1}{5L} & 0 & 0 & 0 & \frac{P_1}{10} \\ 0 & 0 & \frac{6P_1}{5L} & 0 & -\frac{P_1}{10} & 0 \\ 0 & 0 & 0 & 0 & 0 & 0 \\ 0 & 0 & \frac{P_1}{10} & 0 & \frac{p_1L}{30} & 0 \\ 0 & -\frac{P_1}{10} & 0 & 0 & 0 & \frac{p_1L}{30} \end{bmatrix} \qquad (6.8)$$

$$K_{LU} = K_{UL}^T \qquad (6.9)$$

and

$$K_{LL}=\begin{bmatrix} \frac{AE}{L} & 0 & 0 & 0 & 0 & 0 \\ 0 & \frac{12EI_3}{L^3} & 0 & 0 & 0 & \frac{6EI_3}{L^2} \\ 0 & 0 & \frac{12EI_2}{L^3} & 0 & -\frac{6EI_2}{L^2} & 0 \\ 0 & 0 & 0 & \frac{GI_1}{L} & 0 & 0 \\ 0 & 0 & -\frac{6EI_2}{L^2} & 0 & \frac{4EI_2}{L} & 0 \\ 0 & \frac{6EI_3}{L^2} & 0 & 0 & 0 & \frac{4EI_3}{L} \end{bmatrix}+\begin{bmatrix} 0 & 0 & 0 & 0 & 0 & 0 \\ 0 & -\frac{6P_1}{5L} & 0 & 0 & 0 & -\frac{P_1}{10} \\ 0 & 0 & -\frac{6P_1}{5L} & 0 & \frac{P_1}{10} & 0 \\ 0 & 0 & 0 & 0 & 0 & 0 \\ 0 & 0 & \frac{P_1}{10} & 0 & -\frac{2p_1L}{15} & 0 \\ 0 & -\frac{P_1}{10} & 0 & 0 & 0 & -\frac{2p_1L}{15} \end{bmatrix} \tag{6.10}$$

where: I_1 = column torsional constant

I_2 = column moment of inertia about X_2

I_3 = column moment of inertia about X_3

E = modulus of elasticity

G = shearing modulus

A = column cross-sectional area

L = column length

p_1 = column axial force.

6.2.2 Beam Stiffness Matrix

A typical beam with constant-stiffness connections at each end is shown in Figure 6.3. Assuming that the beam is bonded to the floor diaphragm the axial and horizontal shearing forces and deformations and bending moment and curvature about vertical axes can be assumed to be negligible. Therefore, only three degrees of freedom are considered at each end of the beam. The stiffness matrix for the beam plus connection is as follows:

$$\begin{bmatrix} P_B \\ P_A \end{bmatrix}=\begin{bmatrix} K_{BB} & K_{BA} \\ K_{AB} & K_{AA} \end{bmatrix}\begin{bmatrix} D_B \\ D_A \end{bmatrix} \tag{6.11}$$

where the member end force vectors at ends A and B are

$$P_B = [\, p_{B2}\ m_{B1}\ m_{B3} \,]^T \tag{6.12}$$

and

$$P_A = [\, p_{A2}\ m_{A1}\ m_{A3} \,]^T \tag{6.13}$$

and the member displacement vectors at ends A and B are

$$D_B = [\, \delta_{B2}\ \phi_{B1}\ \phi_{B3} \,]^T \tag{6.14}$$

and

$$D_A = [\, \delta_{A2}\ \phi_{A1}\ \phi_{A3} \,]^T \tag{6.15}$$

The submatrices of the partitioned stiffness matrix are as follows (Ang and Morris, 1984)

$$K_{BB} = \begin{bmatrix} S1 & 0 & -S2 \\ 0 & S3 & 0 \\ -S2 & 0 & S4 \end{bmatrix} \tag{6.16}$$

$$K_{BA} = \begin{bmatrix} -S1 & 0 & -S5 \\ 0 & -S3 & 0 \\ S2 & 0 & S7 \end{bmatrix} \tag{6.17}$$

$$K_{AB} = K_{BA}^{\ T} \tag{6.18}$$

and

$$K_{AA} = \begin{bmatrix} S1 & 0 & S5 \\ 0 & S3 & 0 \\ S5 & 0 & S6 \end{bmatrix} \tag{6.19}$$

where

$$S1 = \frac{12EI}{L^3}\beta_1, \quad S2 = \frac{6EI}{L^2}\beta_2, \quad S3 = \frac{GI_1}{L}, \quad S4 = \frac{4EI}{L}\beta_5, \quad S5 = \frac{6EI}{L^2}\beta_2, \quad S4 = \frac{4EI}{L}\beta_4, \quad S7 = \frac{2EI}{L}\beta$$

and

$$\beta = \frac{3}{4\left(1+\frac{3EI}{S_A L}\right)\left(1+\frac{3EI}{S_B L}\right)-1}, \quad \beta_1 = \beta\left(1+\frac{EI(S_A+S_B)}{S_A S_B L}\right), \quad \beta_2 = \beta\left(1+\frac{2EI}{S_B L}\right), \quad \beta_3 = \beta\left(1+\frac{2EI}{S_A L}\right)$$

$$\beta_4 = \beta\left(1+\frac{3EI}{S_B L}\right), \quad \beta_5 = \beta\left(1+\frac{2EI}{S_A L}\right).$$

S_A and S_B in the above expressions are the linear stiffnesses for the beam-to-column connections at ends A and B respectively.

6.3 Assembly of Structure Stiffness Matrix

To assemble the stiffness matrix for the complete structure, the stiffness coefficients for the individual column and beam elements must be computed and incorporated into the overall stiffness matrix. The member stiffness matrices must be transformed from the local coordinate system to the global coordinate system.

A master-slave joint procedure (Ang and Morris, 1983) is used for the columns to minimize the number of degrees of freedom at each joint from six to three. The assumption that the floors act as rigid in-plane diaphragms makes this possible. Figure 6.4 shows a typical column element UL between two floors. The end joints for all of the columns are considered to be "slave" joints. At the floor level being considered the in-plane forces and displacements for each column end are translated to a common "master" joint. Figure 6.4 illustrates the "master-slave" joint relationship. Joints V and M are master joints for the upper and lower floor level and they lie on an arbitrarily chosen vertical axis. Joints U and L are the upper and lower slave joints of a typical column

between the two floor levels. The in-plane and out-of-plane components of the member end force and displacement vectors can be partitioned and the force-displacement relationship for the typical column is expressed as follows:

$$\begin{bmatrix} P'_{Uo} \\ P'_{Vi} \\ P'_{Lo} \\ P'_{Mi} \end{bmatrix} = \begin{bmatrix} K'_{UU} & K'_{UV} & K'_{UL} & K'_{UM} \\ K'_{VU} & K'_{VV} & K'_{VL} & K'_{VM} \\ K'_{LU} & K'_{LV} & K'_{LL} & K'_{LM} \\ K'_{MU} & K'_{MV} & K'_{ML} & K'_{MM} \end{bmatrix} \begin{bmatrix} D'_{Uo} \\ D'_{Vi} \\ D'_{Lo} \\ D'_{Mi} \end{bmatrix} \tag{6.20}$$

The subscripts i and o in Eq. 6.20 refer to the in-place and out-of-plane force and displacement components, respectively. The stiffness submatrices relating out-of-plane force-displacement must be transformed from the local coordinate system as follows:

$$K'_{LL} = RK_{LLoo}R^T \tag{6.21}$$

where: R = rotation transformation from the local system to the global system and

K_{LLoo} = local column stiffness out-of-plane submatrix.

The following transformation is made for the in-plane stiffness submatrices:

$$K'_{MM} = T_{ML}K_{LLii}T_{ML}^T \tag{6.22}$$

where: T_{ML} = combined rotation-translation transformation from the local system at L to the global system at M and

K_{LLii} = local column stiffness in-plane submatrix.

Finally, the following transformation is required to relate in-plane force-displacement to the out-of-plane force-displacement:

$$K'_{ML} = T_{ML}K_{LUio}R^T \tag{6.23}$$

where: K_{LUio}= local column stiffness submatix relating in-plane force-displacement components at L to out-of-plane force-displacement components at U.

6.4 Model of Connection Behaviour

The behaviour of a connection subjected to cyclic loading can be idealized using five separate functions shown in Figure 6.5 (Huang and Morris, 1993). Function 1 is the initial loading curve and is modeled by the modified Richard-Abbott function (Eq. 3.9). Function 2 models the moment-rotation behaviour after a moment reversal at point "a". When point "b" is intersected Function 3 is invoked. This function is a double-mirror image of the modified Richard-Abbott function. If the moment reverses again at point "c" Function 4 with the same initial slope as Function 2 is applicable. Once point "d" is reached Function 5, the modified Richard-Abbott function displaced from the origin to point "d" on the curve is used.

6.5 Analysis Procedure to Account for Non-Linear Connection Behaviour

The stiffness matrix for a typical column depends on its axial force. The stiffness matrix for a typical beam depends on its connection moments. As a result, the overall structure stiffness matrix is affected by the internal forces in the structure. To account for this, an iterative procedure involving repeated cycles of analysis using linear connections is used. Figure 6.6 illustrates how the procedure is applied at a typical connection. The non-linear connection behaviour is modeled using the modified Richard-Abbott function, $f(\phi)$. For the first cycle of analysis the function is replaced by a linear function with a slope S_1 that is equal to the initial tangent to $f(\phi)$. This is done for all of the connections in the structure a linear analysis of the structure is performed and the moments at all connections are computed. Say M_1 is the moment at the typical connection. The rotation, ϕ_1, is the connection rotational deformation for a constant stiffness connection subjected

to moment, M_1. The adjusted rotation, ϕ_1', can be computed from $f(\phi)$ using the moment M_1 computed from the linear analysis. A second cycle of analysis is performed using S_2 as the connection stiffness yielding a second set of connection moments. Because S_2 is smaller than S_1 the moment M_2 computed in the second analysis is smaller in magnitude. A second adjusted rotation, ϕ_2', can be computed from $f(\phi)$ using the moment M_2. The above procedure is repeated until the linear rotations are sufficiently close to the nonlinear rotations computed using $f(\phi)$.

6.6 Computer Program for PC with DOS: FLEXFRM2

6.6.1 Introduction

The Fortran program developed for this study is modified from a program written for a mainframe computer (Ang and Morris, 1983) using the Ramberg-Osgood function to model connection behaviour. The program employs an in-core, constant band width equation solver. The program was adapted to PC with DOS using the Richard-Abbott function and the program was updated to account for sequential loading (Huang and Morris, 1993).

The program interface is now more "user friendly" and the modified Richard-Abbott function is used to model connection behaviour. The program is designed to work with the SI system of units.

6.6.2 Data Input

The data input is interactive as the user is prompted for the required information. The user can input data to the program from the keyboard or from input files created with a text editor or from previous program runs. Figure 6.7 shows the layout of a typical structure the program is designed to analyze. The data are entered in blocks as follows:

i) Structural Data (input file: STSPEC.IN)

- number of stories
- number of bays in the X-direction
- number of bays in the Z-direction
- number of bracing elements
- number of braced bays

ii) Connection Types and Loading Information (input file: STSPEC2.IN)

- type of connections (constant stiffness or non-linear)
- number of loaded joints
- number of uniformly loaded beams
- number of beams with concentrated loads
- include P-Δ effects in analysis

iii) Structural Dimensions (input file: DIMENS.IN)

- master node coordinates (m)
- height of each storey (m)
- length of each bay in the X-direction and the Z-direction (m)

iv) Material Properties and Member Information (input file: MAT.IN)

- Young's modulus (MPa)
- shear modulus (MPa)
- number of beam types
- number of column types

v) Beam and Column Section Properties (input files: BMPROP.IN and COLPROP.IN)

- torsional constant (mm^3)
- moment of inertia about Y'-axis (mm^4)
- moment of inertia about Z'-axis (mm^4)
- cross-sectional area (mm^2)

vi) Beam and Column Types in the Structure (input files: BMTYP.IN and COLTYP.IN)

- the beam and column number and joint incidences are displayed for each beam and column
- the user is prompted to input the beam and column type for each member in the structure

vii) Bracing Properties (input files: BRAPROP.IN)

- number of bracing elements types
- cross-sectional area (mm^2) for each type

viii) Bracing Types and Incidence (input files: BRAINID.IN and BRAIDNO.IN)

- bracing member type and incidence (lower joint and upper joint)

ix) Connection Properties

(input files: Linear - LCTYP.IN and LCPROP.IN
Non-linear - NLCTYP.IN and NLCPROP.IN)

- number of connection types
- Linear: connection stiffness (kN-m/rad) for each type
- Non-linear: Modified Richard-Abbott parameters for each type

units: S_o and S_p (kN-m/rad)

ϕ_o and ϕ_u (radians)

- start and end type of connection for each beam in the structure

x) Joint Loading Information (input file: LOADOFJO.IN)

- enter joint number and the joint load vector (see Figure 6.8 for the distinction between master node in-plane joint loads and out-of-plane joint loads) units: forces (kN) ; moments (kN-m)

xi) Uniform Loading Information (input file: UNIFORML.IN)

- input beam number and uniform load (kN/m) with positive direction being upward

xii) Concentrated Loading Information (input file: CONCENTR.IN)

- input beam number
- distance from start end (m)
- concentrated load (kN) with positive direction being upward

xiii) Support Conditions (input file: SUPPORT.IN)

- input support condition for each column base (0=fixed, 1=pinned about X, 2=pinned about Z, 3=pinned about X and Z)

6.6.3 Program Output

The program sends the output to a file called RESULTS.OUT. This includes a summary of all the input data and analysis results. These include final joint displacements, member end forces and connection moments and rotational deformations.

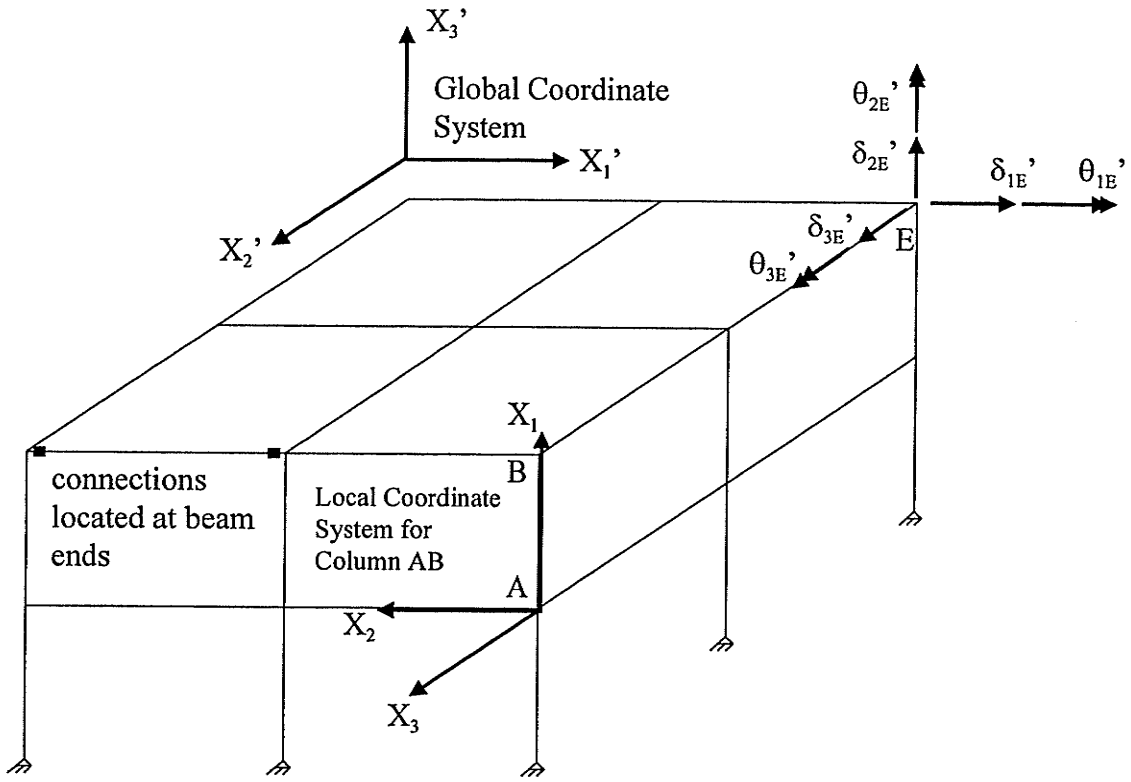


Figure 6.1 Typical Frame Structure

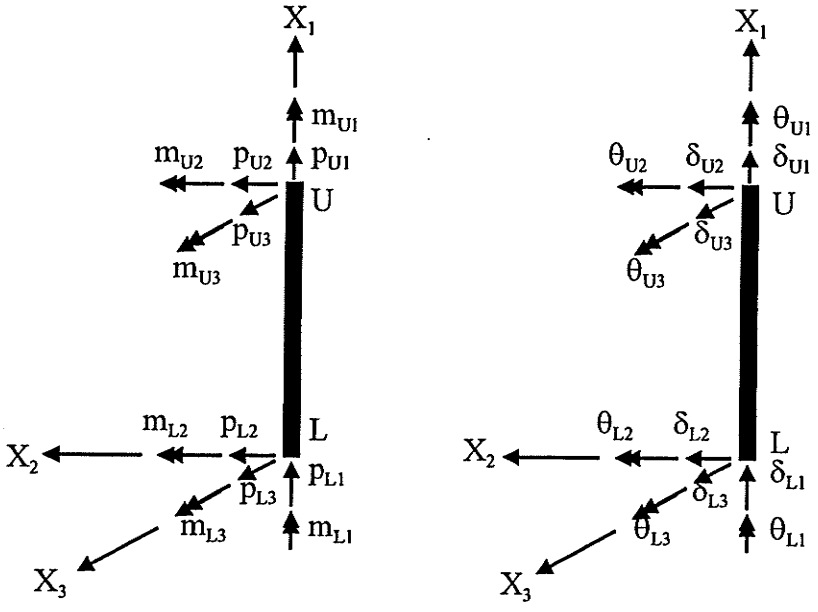


Figure 6.2 Typical Column Element showing joint forces and displacements

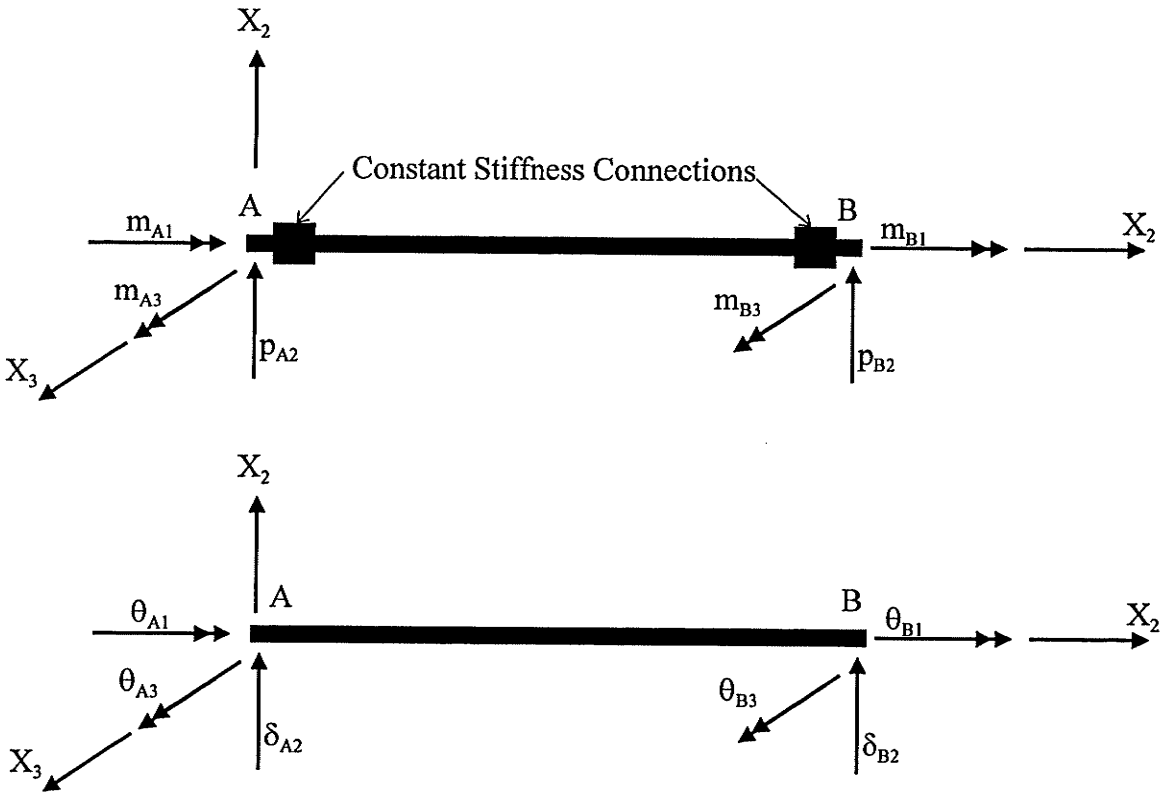


Figure 6.3 Typical Beam Element showing joint forces and displacements

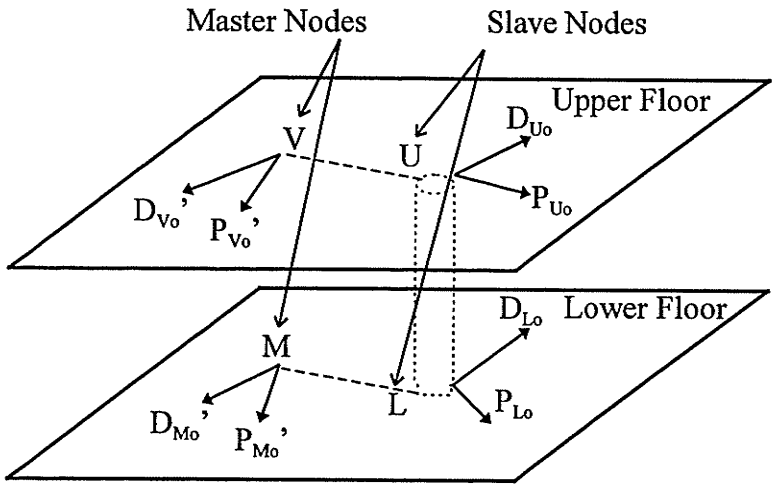


Figure 6.4 Master-Slave Joint End Forces and Displacement

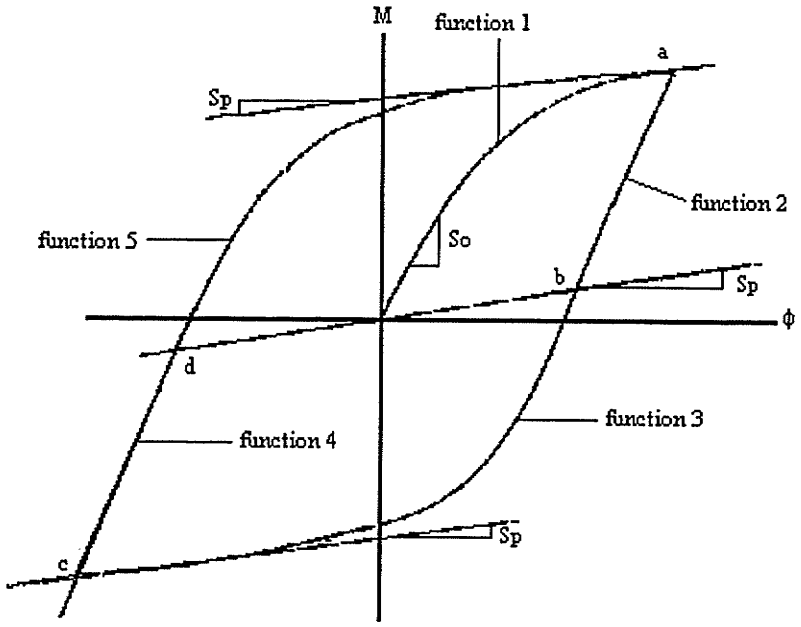


Figure 6.5 Idealized Cyclic Moment-Rotation Behaviour

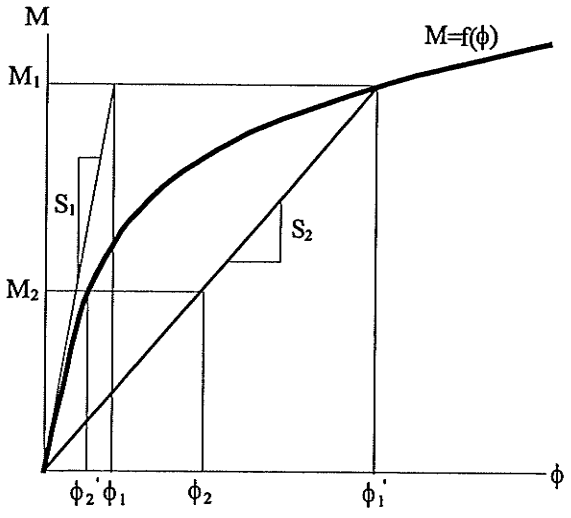


Figure 6.6 Modification of Connection Flexibility Using Secant Stiffness

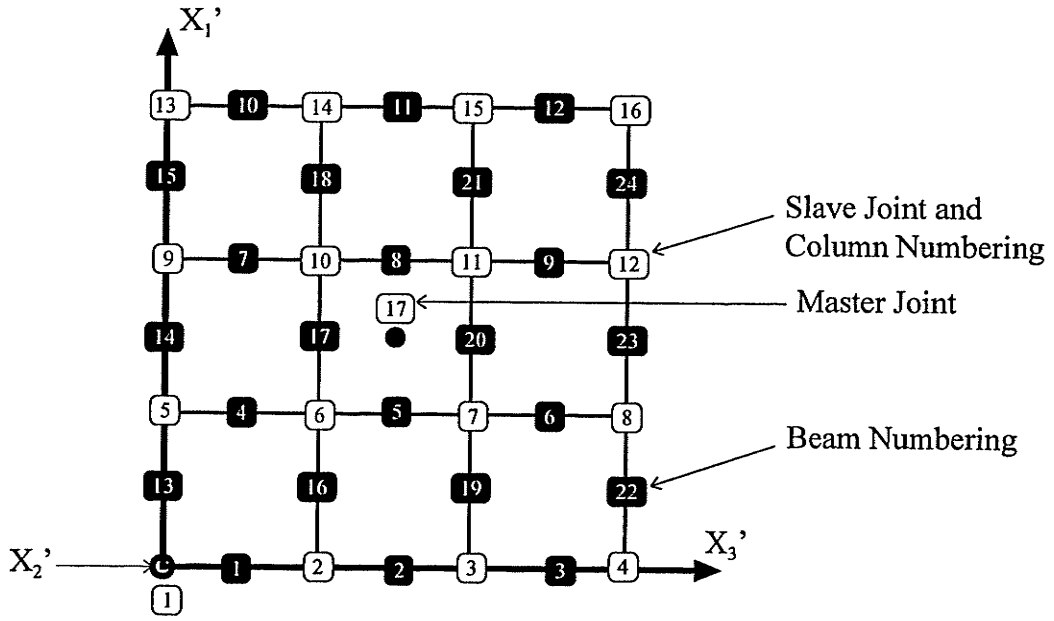


Figure 6.7 (a) Beam, Column and Joint Numbering in Storey Level 1

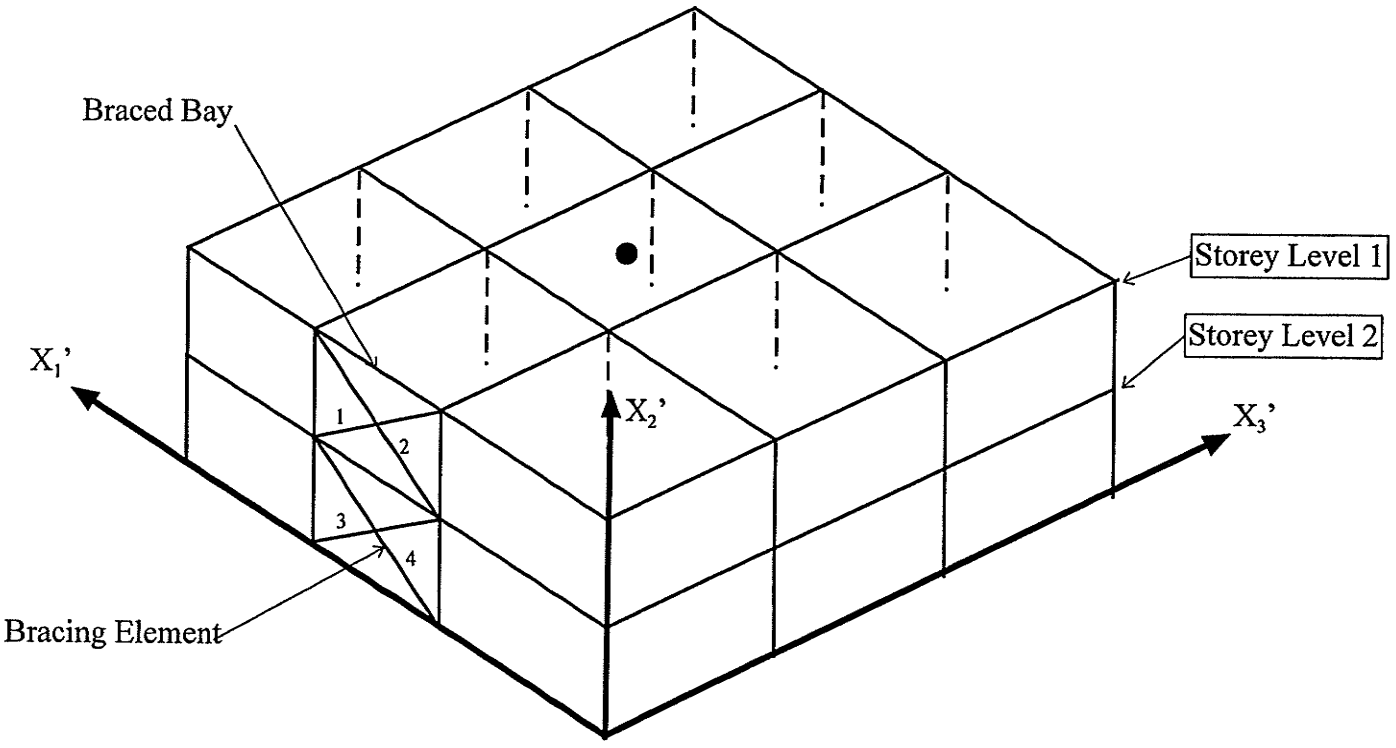


Figure 6.7 (b) Typical Structure in Orthoganal View showing Bracing Elements

Figure 6.7 Typical Structure

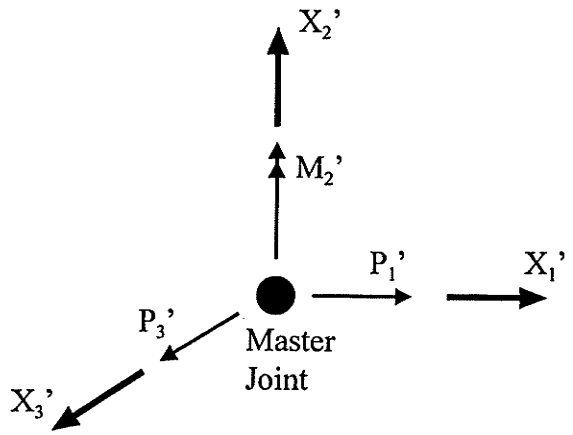


Figure 6.8 (a) Master Joint Loads

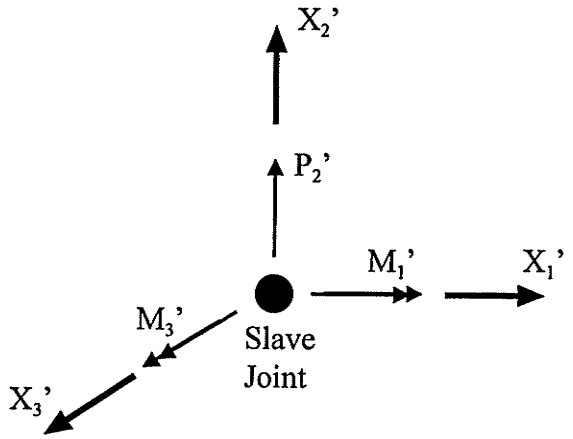


Figure 6.8 (b) Slave Joint Loads

Figure 6.8 Joint Load Vectors

7. Analysis of Three-Dimensional Frames using FLEXFRM2

7.1 Introduction

In this chapter, examples are presented to illustrate the effects of connection behaviour on overall frame behaviour. To simplify the presentation of information simple plane frames are analyzed instead of three dimensional frames. To verify the validity of FLEXFRM2 a one bay frame is analyzed and the results are compared to those reported in other studies. A sensitivity study is then conducted on a three bay, three story frame to illustrate the relationship between the range of connection behaviour and overall frame behaviour.

7.2 Example 1: Program Verification

To verify the validity of FLEXFRM2, the pinned based, unbraced frame with geometry shown in Figure 7.1 with a uniform gravity load of 28 kN/m on the beam is analyzed. Three separate analysies are performed with beam-to-column connections modeled as follows:

Case 1: linear with connection stiffness exceeding the fully rigid boundary specified by Eurocode3,

Case 2: nonlinear with initial connection stiffness corresponding to the Eurocode3 rigid semi-rigid boundary and connection moment resistance equal to 55% of the beam plastic moment and

Case 3: linear with connection stiffness corresponding to the Eurocode3 nominally pinned boundary.

The assumed connection behaviour is shown in Figure 7.2.

The frame is analyzed for the three cases described above and the beam end moments for each analysis are presented in Figure 7.1. The beam end moments from a previous study (Huang, 1993) are also shown. In this study, the connections are modeled similarly to case two described above. The end moment of 91.38 kN-m compares favourably to 89.5 kN-m from Huang's study.

7.3 Sensitivity Study

Connections are typically grouped into three classes; flexible, semi-rigid and rigid. Typically, web angle and header plate connections comprise flexible connections. Top and seat angle and flush end plate connections comprise semi-rigid connections. Extended end plate connections comprise rigid connections.

To illustrate the relationship between the M-ϕ behaviour of a connection and overall frame behaviour the braced three bay, three storey frame shown in Figure 7.2 is analyzed. Connections whose M- ϕ behaviour falls on the lower and upper boundary of the connection envelopes presented in Figures 4.17-4.23 are used. The frame is also analyzed for a connection that fall somewhere between the two extremes This frame is similar to one analyzed by Zaremba (1986). To examine the effects of connection behaviour on the beam and column end moments the beams are subjected to the following uniform gravity loads:

Beams 1 - 3: 42.6 kN/m

Beams 4 - 9: 80.5 kN/m.

7.3.1 Flexible Connections:

The frame was analyzed three times, assuming three connection types; one on the lower boundary of the flexible connection behaviour envelope, the second approximately in the middle and the third on the upper boundary. The test specimens whose modified Richard-Abbott parameters are used in the frame analysis program are as follows:

Lower boundary:	Lipson AA-2/1	Single web angle connection
Intermediate:	Onuah A19	Double web angle connection
Upper boundary:	Sommer Test 12	Header plate connection

The beam and column end moments for the frame analyzed for each of the three flexible connections are shown in Table 7.1. The end moments for the frame modeled using connections on the lower boundary are very close to zero as expected. Thus, for typical connections near the lower boundary, the assumption of pin ended beam-to-column connections is valid. However, for connections that are intermediate between the upper boundary and the lower boundary for flexible connections this assumption may not be valid. The magnitude of end moments can exceed 35% of the beam mid-span static moment, $wl^2/8$. Thus, assuming that the connection behaves as a pinned end may result in an overestimation of beam end moment and an underestimation of column moments. This can result in an unconservative design.

7.3.2 Semi-Rigid Connections:

The frame was analyzed three times, assuming three connection types; one on the lower boundary of the semi-rigid connection behaviour envelope, the second approximately in the middle and the third on the upper boundary. The test specimens whose modified Richard-Abbott parameters are used in the frame analysis program are as follows:

Lower boundary:	Marley D 2/1-2/1	Top and seat angle connection
Intermediate:	Ostrander Test 10	Flush end plate connection

Upper boundary:	Azzinamini 8S10	Top and seat angles with double web angle connection

The beam and column end moments for the frame analyzed for each of the three semi-rigid connections described above are shown in Table 7.2. Evidently the frame end moments are not very sensitive to the type of semi-rigid connection used. The maximum increase in end moments between the lower and upper boundary is about 10%. However, the end moments for the frame analyzed with semi-rigid connections can be as much 70% of the beam static mid-span moment.

7.3.3 Rigid Connections

The frame was analyzed three times, assuming three connection types; one on the lower boundary of the rigid connection behaviour envelope, the second approximately in the middle and the third on the upper boundary. The test specimens whose modified Richard-Abbott parameters are used in the frame analysis program for rigid connections are as follows:

Lower boundary:	Dews Test 2	Extended End Plate connection
Intermediate:	Ioannides Test 1	Extended End Plate connection
Upper boundary:	Sherbourne Test A2	Extended End Plate connection

The beam and column end moments for the frame analyzed for each of the three rigid connections described above are shown in Table 7.3. It appears that the maximum end moments are only marginally larger in magnitude that those on the upper boundary for semi-rigid connections such as top and seat angles with double web angles. Also, the range of magnitude of end moments appears to be slightly larger for rigid connections than for semi-rigid connections. The maximum increase in end moments between the lower and upper boundary for rigid connections is about 65%.

7.4 Summary of Effects of Connection Behaviour on Overall Frame Behaviour

Some flexible connections, such as single web angle connections, can be modeled as pinned connections in frame analysis. For stronger and stiffer flexible connections, such as double web angle and header plate connections this assumption may not be valid and can yield unconservative results. It appears that frame end moments are not sensitive to the type of semi-rigid connection used but that semi-rigid connections can transmit significantly higher end moments than typical flexible connections. Rigid connections appear to have a larger range of behaviour than for semi-rigid connections.

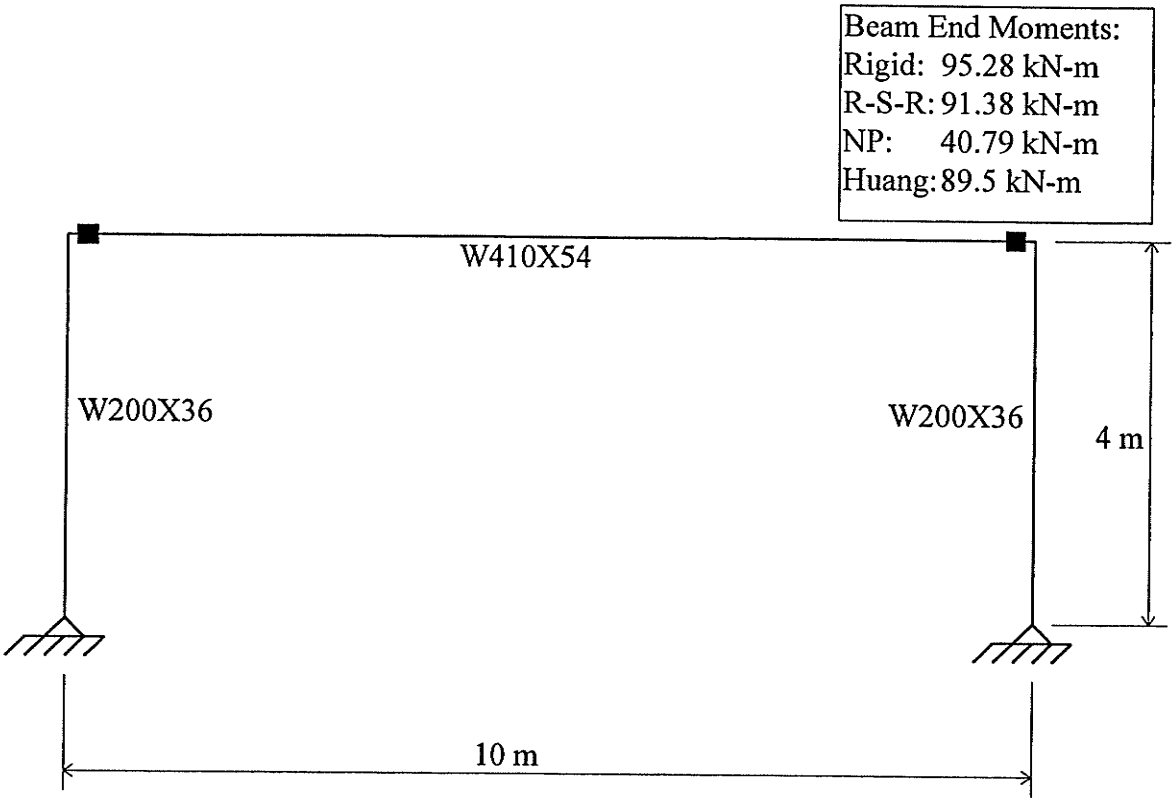


Figure 7.1 One Bay Frame: Example 1

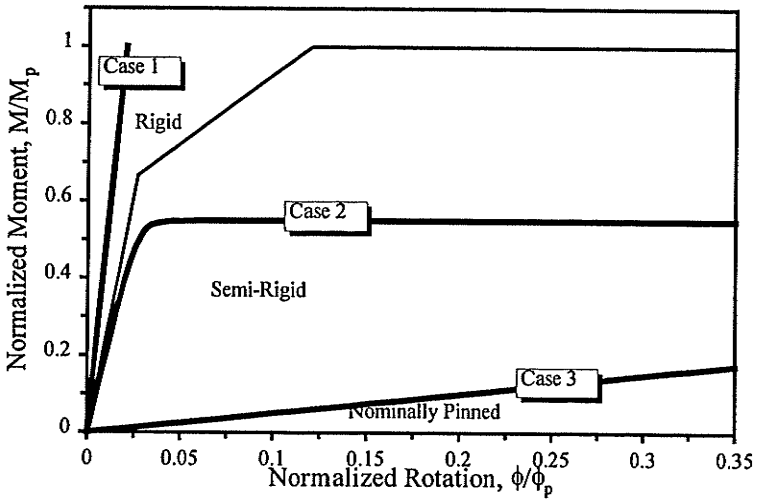


Figure 7.2 M-ϕ Curves for Connections in Example 1

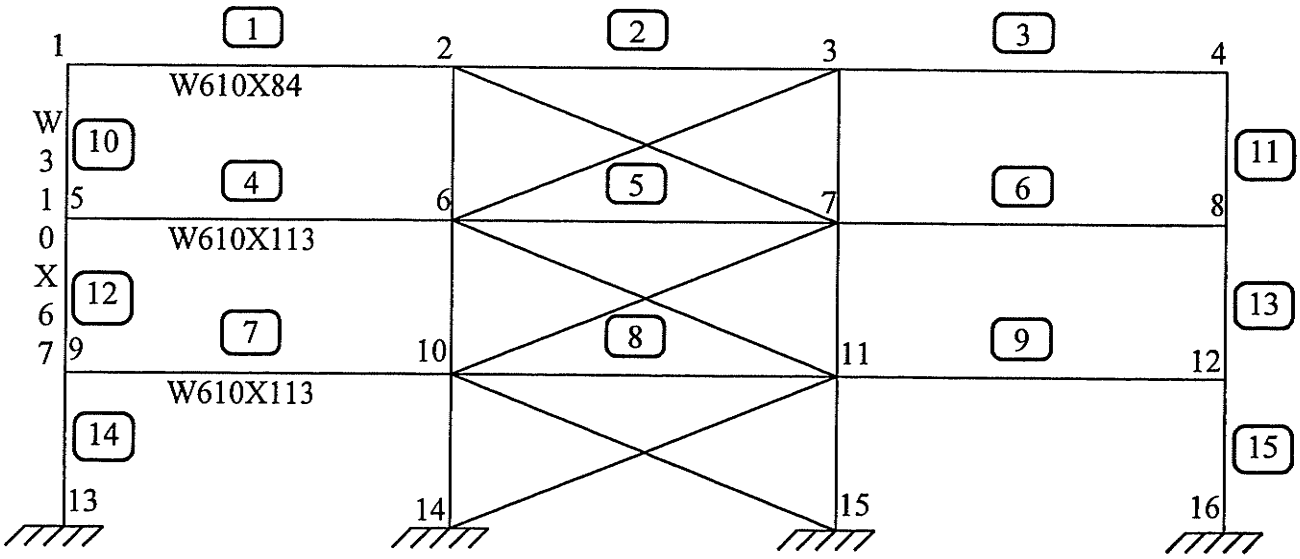


Figure 7.3 Braced Frame: Example 2

Table 7.1 End moments for typical flexible connections

Member #	Joints	End Moments (kN-m) Lower Boundary	Middle Boundary	Upper Boundary
1	1	0.79	49.26	56.64
	2	-0.76	-111.67	-187.42
2	2	0.78	110.71	183.93
	3	-0.78	-110.71	-183.93
3	3	0.76	111.67	187.42
	4	-0.79	-49.26	-56.64
4	5	1.51	106.96	125.07
	6	-1.46	-211.66	-357.28
5	6	1.49	209.19	349.02
	7	-1.49	-209.19	-349.02
6	7	1.46	211.66	357.28
	8	-1.51	-106.96	-125.07
7	9	1.50	95.97	110.52
	10	-1.47	-213.32	-360.09
8	10	1.49	210.43	351.88
	11	-1.49	-210.43	-351.88
9	11	1.47	213.32	360.09
	12	-1.50	-95.97	-110.52
10	1	-0.79	-49.23	-56.61
	5	-0.74	-51.52	-60.18
11	4	0.79	49.23	56.61
	8	0.74	51.52	60.18
12	5	-0.77	-55.36	-64.80
	9	-0.86	-56.91	-65.84
13	8	0.77	55.36	64.80
	12	0.86	56.91	65.84
14	9	-0.63	-38.98	-44.59
	13	-0.32	-19.49	-22.29
15	12	0.63	38.98	44.59
	16	0.32	19.49	22.29

Table 7.2 End moments for typical semi-rigid connections

Member #	Joints	End Moments (kN-m) Lower Boundary	Middle Boundary	Upper Boundary
1	1	55.96	55.59	54.66
	2	-355.24	-364.84	-387.03
2	2	344.82	354.00	375.19
	3	-344.82	-354.00	-375.19
3	3	355.24	364.84	387.03
	4	-55.96	-55.59	-54.66
4	5	124.74	123.94	121.88
	6	-674.91	-693.24	-735.67
5	6	650.71	668.05	708.18
	7	-650.71	-668.05	-708.18
6	7	674.91	693.24	735.67
	8	-124.74	-123.94	-121.88
7	9	108.42	107.64	105.68
	10	-679.89	-689.33	741.00
8	10	657.46	675.03	715.67
	11	-657.46	-675.03	-715.67
9	11	679.89	698.33	741.00
	12	-108.42	-107.64	-105.68
10	1	-55.93	-55.56	-54.63
	5	-60.09	-59.71	-58.74
11	4	55.93	55.56	54.63
	8	60.09	59.71	58.74
12	5	-64.56	-64.14	-63.05
	9	-64.87	-64.42	-63.27
13	8	64.56	64.14	63.05
	12	64.87	64.42	63.27
14	9	-43.45	-43.13	-42.32
	13	-21.73	-21.56	-21.16
15	12	43.45	43.13	42.32
	16	21.73	21.56	21.16

Table 7.3 End moments for typical rigid connections

Member #	Joints	End Moments (kN-m) Lower Boundary	Middle Boundary	Upper Boundary
1	1	58.03	57.03	53.94
	2	-243.01	-322.67	-402.67
2	2	237.37	313.67	390.13
	3	-237.37	-313.67	-390.13
3	3	243.01	322.67	402.67
	4	-58.03	-57.03	-53.94
4	5	128.77	127.03	120.28
	6	-460.97	-612.72	-765.60
5	6	447.81	591.82	736.47
	7	-447.81	-591.82	-736.47
6	7	460.97	612.72	765.60
	8	-128.77	-127.03	-120.28
7	9	113.02	110.69	104.17
	10	-464.53	-617.31	-771.09
8	10	451.94	597.81	744.32
	11	-451.94	-597.81	-744.32
9	11	464.53	617.31	771.09
	12	-113.02	-110.69	-104.17
10	1	58.00	-57.00	-53.91
	5	-61.97	-61.17	-57.98
11	4	58.00	57.00	53.91
	8	61.97	61.17	57.98
12	5	-66.70	-65.77	-62.21
	9	-67.45	-61.19	-62.38
13	8	66.70	65.77	62.21
	12	67.45	66.19	62.38
14	9	-45.47	-44.40	-41.70
	13	-22.74	-22.20	-20.85
15	12	45.47	44.40	41.70
	16	22.74	22.20	20.85

8. Conclusions / Recommendations

8.1 Conclusions

8.1.1 Modeling Connection Behaviour

It is shown in this and other studies that connection force-deformation behaviour contributes significantly to overall frame behaviour. Several factors such as bolt slip, localized yielding, local bucking and geometric effects contribute significantly to the non-linear behaviour of connections.

Attempts to develop connection behaviour models that are accurate for all possible combinations of connection parameters have been largely unsuccessful. Thus, the most practical method to model connection behaviour is to curve-fit the experimental moment-rotation data for various specimens.

The characteristics of three curve-fitting functions were analyzed and compared. These are the Ramberg-Osgood function (1943), the Richard-Abbott function (1975) and the modified Richard-Abbott function (Dong, 1994). The modified Richard-Abbott function was found to be superior for three reasons; it is capable of plotting curves that are tangent to the initial and final slope lines, it permits two points of maximum curvature and it can plot curves with reversals of curvature.

274 sets of experimental data have been curve-fitted using the six parameter modified Richard-Abbott function. The moment-rotation behaviour of a connection specimen can be described fully and compactly using only the six parameters. This makes the function ideal for incorporating into a structural analysis program that accounts for non-linear connection behaviour. The moment-rotation behaviour can be input by simply entering the six curve-fitting parameters for each connection type.

8.1.2 Classification and Standardization of Connections

A simple plot of the moment-rotation behaviour of a connection is not very useful to a designer. Therefore, the Eurocode3 (1990) classification boundaries have been superimposed on the normalized moment-rotation plots for each specimen. This provides a quantitative way of comparing the relative strength and stiffness of different connection specimens. Envelopes of M-ϕ behaviour of the typical connections types have been superimposed on the classification boundaries to help designers establish a "feel" for the behaviour of a connection.

Connections often account for a significant part of the construction cost of a steel frame. Standardization of connection components can cut costs significantly because for each connection type, there are several options such as bolts size, strength and spacing, and plate or angle thickness and length. This requires fabricators to stock a variety of angle sizes, plate thicknesses, etc. In the interest of economy, the steel industries in several countries have already begun the task of standardizing the geometries of beam-to-column connections. Given the current trend toward a global economy and the internationalization of standards, a logical strategy is to standardize structural steel connection geometries internationally. A standardized designation system has been proposed in this study. Laboratory testing of the "standard" connection geometries can be performed to develop accurate moment-rotation data. These data can then be curve-fitted and the curve-fitting parameters incorporated into a structural analysis program.

8.1.3 Computer Analysis and Results

A structural analysis computer program that accounts for connection deformation using the modified Richard-Abbott function was used to examine the effects of connection behaviour on overall frame behaviour. The program accounts for the non-linear behaviour of connections by performing repeated cycles of analysis assuming linear connection behaviour. After each cycle the computed end moments are compared the

"exact" end moments using the modified Richard-Abbott function. Connection stiffnesses are then modified and the structural stiffness matrix updated. The analysis is repeated until end moments for the linear analysis converge to the "exact" values.

A sensitivity study was conducted on a three bay, three story frame to illustrate the relationship between the range of connection behaviour on overall frame behaviour. The range of behaviour of three classes of connections; flexible, semi-rigid and rigid was used in the analysis. Results show that flexible connections that fall near the lower boundary of moment-rotation behaviour, such as single web angle connections, can justifiably be modeled as pinned connections in frame analysis. However, for stronger and stiffer flexible connections, such as double web angle and header plate connections this assumption may not be valid. This can result in an underestimation of column moments and therefore, an unconservative design. For semi-rigid connections it appears that frame end moments are not sensitive to the type connection used but that they can transmit significantly higher end moments than can flexible connections. Rigid connections appear to have a larger range of behaviour than for semi-rigid connections.

8.2 Recommendations for Further Study

Elastic and inelastic buckling of structural members and overall structural stability were not considered. The computer analysis program could be extended to account for these effects.

There is a limited amount of test data for composite beam-to-column connections. Therefore, an extensive database of the moment-rotation data for composite connections is not yet available. Because of the increasing use of composite connections in practice it is desirable for more research to be conducted in this area to demonstrate the impact of composite connections on frame behaviour. Attempts to standardize composite connections should be made.

It is recommended that experimental testing of the moment-rotation behaviour for all the proposed standardized connections be conducted. Enough tests must be conducted to provide a statistically significant representation of the behaviour of each standard connection. This will supply designers will accurate M-ϕ behaviour for every standard connection type. Presently, there are not enough data available to know how accurate the M-ϕ curves are.

References

Ackroyd, M.H., 1987, "Design of Flexibly-Connected Unbraced Steel Building Frames", Joint Flexibility in Steel Frames, Elsevier Publishers Ltd., New York, NY, pp. 261-286.

Altman W.G., Azizinamini A., Bradburn J.H. and Radziminski J.B., 1982, "Moment Rotation Characteristics of Semi-Rigid Steel Beam-Column Connections", Structural Research Studies, Department of Civil Engineering, University of South Carolina, Columbia, SC.

American Institute of Steel Construction, 1986, "Load and Resistance Factor Design Specifications for Structural Steel Buildings", Chicago, USA.

Ammerman Douglas J. and Leon Roberto T., 1987, "Behaviour of Semi-Rigid Composite Connections", Engineering Journal/ American Institute of Steel Construction, Second quarter, pp.12-21.

Ang, K.M. and Morris, G.A., 1984, "Analysis of Three-Dimensional Frames with Flexible Beam-Column Connections", Canadian Journal of Civil Engineers, Vol. 11, No. 2, pp 245-254.

Ang, K.M., 1984, "Analysis of Three-Dimensional Frames with Flexible Beam-Column Connections", M. Sc. Thesis, University of Manitoba, Winnipeg, Canada.

Asteneh Abolhassan, Nader Marwan N. and Malik Lincoln, 1989, "Cyclic Behaviour of Double Angle Connections", Journal of Structural Engineering, Vol. 115, No. 5, May, pp. 1101-1118.

Attiogbe, E. and Morris, G.A., 1991, "Moment-Rotation Functions for Steel Connections", Journal of Structural Engineering, American Society of Civil Engineers, Vol. 117, No. 6, pp. 1703-1718.

Attiogbe, E. and Morris, G.A. and Onuah, C., 1989, "Standardization of Moment-Rotation Curves", Proceedings of the Twelfth Canadian Congress of Applied Mechanics, Carleton University, Ottawa, Canada.

Australian Institute of Steel Construction, 1985, "Standardized Structural Connections (Third Edition)", Australian Institute of Steel Construction, Milsons Point, Australia.

Bertero Vitelmo V., Popov Egor P. and Krawinkler Helmut, 1972, "Beam-Column Subassemblages Under Repeated Loading", Journal of the Structural Division, Vol. 98, No. st5, May, pp. 1137-1159.

Bijlaard, F.S.K. and Snijder, H.H., 1988, "Influence of Semi-Rigid and Partial Strength Joints on the Behaviour of Frames", Connections in Steel Frames, Elsevier Publishers Ltd., New York, NY. pp. 280-290.

Bijlaard, F.S.K. and Zoetmeyer, P., 1986, "Influence of Joint Characteristics on the Structural Response of Frames", Proceedings of the International Conference on Steel Structures, Budva.

Bijlaard, F.S.K. and Steenhuis, C.M., 1991, "Prediction of the Influence of the Connection Behaviour on the Strength, Deformations and Stability of Frames by Classification of Connections", Proceedings of the Second International Workshop - Connections in Steel Structures: Behaviour, Strength and Design, Pittsburgh, Pennsylvania.

Bjorhovde Reidar, 1984, Effect of End Restraint on Column Strength - Practical Applications", Engineering Journal, American Institute of Steel Construction, First Quarter, pp. 1-13.

Bjorhovde R., Colson, A. and Brozzetti, J., 1990, "Classification System for Beam-to-Column Connections", Journal of Structural Engineering, American Society of Civil Engineers, Vol. 116, No. 11. pp. 3059-3076.

Canadian Institute of Steel Construction, 1991, "Handbook of Steel Construction", Canadian Institute of Steel Construction, Willowdale, Ontario.

Canadian Standard Association, 1989, "Steel Structures for Buildings", CSA Standard CAN3-S16.1-M89, Canadian Standard Association, Rexdale, Ontario, Canada.

Chen, W.F., and Kishi, N., 1989, "Semirigid Steel Beam-to-Column Connections; Data Base and Modeling", Journal of Structural Engineering, American Society of Civil Engineers, Vol. 115, No. 1, pp. 105-119.

Chen, W.F., and Kishi, N., 1986, "Data Base of Steel Beam-to-Column Connections", School of Civil Engineering, Purdue University, West Lafayette, IN.

Chen, W.F. and Lui, E.M., 1991, "Stability Design of Steel Frames", CRC Press, Boca Raton, Ann Arbor, Boston, London, pp. 253-271.

Chen, W.F. and Lui, E.M., 1990, "Structural Stability", Elsevier Science Publishing Co. Inc., New York, pp. 235-272.

Deierlein G.G., 1991, "An Inelastic Analysis and Design System for Steel Frames with Partially Restrained Connections", Proceeding of Second International Workshop - Connections in Steel Structures: Behaviour, Strength and Design, Pittsburgh, Pennsylvania.

Dhillon, B.S. and Abdel-Majid, S., 1990, "Interaction Analysis and Design of Flexibly Connected Frames", Computers and Structures, Vol. 36, No. 2, pp. 189-202.

Dong, Q., 1994, "Microcomputer Analysis of Reinforced Concrete Flat-Plate Structures Subjected to Lateral Loading", M. Sc. Thesis, University of Manitoba, Winnipeg, Canada.

Douty, R.T. and McGuire, W., 1965, "High Strength Bolted Moment Connections", Journal of the Structural Division, ASCE, Vol. 91, No. ST2, April, pp. 101-128.

Driscoll, G.C., 1976, "Effective Length of Columns with Semi-Rigid Connections", Engineering Journal, American Institute of Steel Construction, Fourth Quarter, pp. 109-115.

Driscoll, G.C. and Beedle, L.S., 1982, "Suggestions for Avoiding Beam-to-Column Web Connection Failure", Engineering Journal, American Institute of Steel Construction, First Quarter, 1982, pp. 16-19.

EUROCODE3 3, 1990, Editorial Group - EUROCODE3 3, "Design of Steel Structures", Edited draft issue.

Frank W. and Stockwell, J.R., 1974, "Yield Line Analysis of Column Webs with Welded Beam Connections", Engineering Journal, American Institute of Steel Construction, First Quarter, pp. 12-17.

Frye, M.J. and Morris, G.A., 1975, "Analysis of Flexibly Connected Steel Frames", Canadian Journal of Civil Engineers, Vol. 2, No. 3, pp. 280-291.

Ghobarah, A., Korol, R.M. and Osman, A., 1992, "Cyclic Behaviour of Extended End-Plate Joints", Journal of Structural Engineering, American Society of Civil Engineers, Vol. 118, No. 5, pp. 1333-1353.

Huang, J., 1993, "Behaviour of Flexibly Connected Steel Frames", M. Sc. Thesis, University of Manitoba, Winnipeg, Canada.

Huang, J. and Morris, G.A., 1991, "Analysis of Flexibly Connected Frames Under Non-Proportional Loading", Proceedings of Second International Workshop - Connections in Steel Structures: Behaviour, Strength and Design, Pittsburgh, Pennsylvania.

Huang, J. and Morris, G.A., 1993, "Sensitivity of Steel Frames to Connection Deformation", CSCE Anual Conference, Fredericton, NB, June 9-12.

Jones, S.W., Kirby, P.A. and Nethercot, D.A., 1981, "Modeling of Semi-Rigid Connection Behaviour and its Influence on Steel Column Behaviour", Joints in Structural Steelwork, John Wiley and Sons, New York, NY, pp. 5.74-5.87.

Julian, O.G. and Lawrence, L.S., 1959, "Notes on J and L Nomographs for Determination of Effective Lengths", unpublished

Kennedy, D.J.L. and Hafez, M.A., 1984, "A Study of End Plate Connections for Steel Beams", Canadian Journal of Civil Engineers, Vol. 11, No. 2, pp. 139-149.

Kennedy, N.A., Vinnakota, S. and Sherbourne, A.N., 1981, "The Slit-Tee Analogy in Bolted Splices and Beam-Column Connections", Joints in Structural Steelwork, John Wiley and Sons, New York, NY, pp. 2.138-2.157.

Krawinkler Helmut and Popov Egor P., 1982, "Seismic Behaviour of Moment Connections and Joints", Journal of the Structural Division, Vol. 108, No. st2, February, pp. 373-391.

Krishnamurty, N., Huang, H.T., Jeffrey, P.K. and Avery, L.K., 1979, "Analytical M-Theta Curves for End Plate Connections", Journal of the Structural Division, ASCE, Vol. 105, No. st1, January, pp. 133-145.

Leon, R.T., Ammerman, D.J. and Galambos, T.V., 1984, "Strength and Stiffness of Semi-Rigid Composite Connections", Preliminary Report to American Institute of Steel Construction.

Leon, R.T., Ammerman, D.J., Lin, J. and McCauley, R.D., 1987, "Semi-Rigid Composite Steel Frames", Engineering Journal, American Institute of Steel Construction, Fourth Quarter, pp. 147-155.

Leon, R.T. and Ammerman, D.J., 1990, "Semi-Rigid Composite Connections for Gravity Loads", Engineering Journal, American Institute of Steel Construction, First Quarter, pp. 1-11.

Lie, Han Ay, 1992, "Standardization of Steel Beam-to-Column Connections", M. Eng. Thesis, University of Manitoba, Winnipeg, Canada.

Lindsey, S.D., 1987, "Design of Frames with PR Connections", Joint Flexibility in Steel Frames, Elsevier Publishers Ltd., New York, NY, pp. 251-260.

Lui, E.M. and Chen, W.F., 1987, "Steel Frames with Flexible Joints", Joint Flexibility in Steel Frames, Elsevier Publishers Ltd., New York, NY, pp. 2.49-2.69.

Maxwell, S.M., Jenkins, W.M. and Howlett, J.H., 1981, "A Theoretical Approach to the Analysis of Connection Behaviour", Joints in Structural Steelwork, Proceedings of the International Conference in Cleveland, 1981, John Wiley and Sons, pp. 2.49-2.69.

Moncarz, P. and Gerstle, K.H., 1981, "Steel Frames with Nonlinear Connections", Journal of the Structural Division, American Society of Civil Engineers, Vol. 107, No. st8.

Morris, G.A., Huang, J. and Scerbo, M.J., 1994, "Accounting for Connection Behaviour in Steel Frame Design", Canadian Society for Civil Engineers, Annual Conference, Proceedings, Vol. 2, pp. 11-20.

Morris, G.A., Scerbo, M.J. and Polyzois, D., 1994, "A Comparison of Two Versatile Curve-Fitting Functions", Paper submitted to the Canadian Congress of Applied Mechanics, 1995 CANCAM Conference, Victoria, Canada.

Nethercot, D.A., 1985, "Steel Beam to Column Connections - A Review of Test Data", CIRIA, London.

Krishnamuthy, N.,1980, "Modeling and Prediction of Steel Bolted Connections Behaviour", Computers and Structures, Vol. 11, pp. 75-82.

Onuah, C.C., 1988, "Moment-Rotation Behaviour of Double Web Angle Connections", M. Sc. Thesis, University of Manitoba, Winnipeg, Canada.

Packer, J.A. and Morris, L.J., 1977, "A Limit State Design Method for the Tension Region of Bolted Beam-Column Connections", The Structural Engineer, October 1977, Vol. 5, No. 10, pp. 446-458.

Patel, K.V. and Chen, W.F., 1984, "Nonlinear Analysis of Steel Moment Connections", Journal of Structural Engineering, American Society of Civil Engineers, Vol. 110, No. 8, pp. 1861-1874.

Popov, E.P. and Bertero, V.V., 1973, "Cyclic Loading of Steel Beams and Connections", Journal of the Structural Division, Vol. 99, No. st6, June, pp. 1189-1204.

Popov, E.P. and Pinkney, B., 1969, "Cyclic Yield Reversal in Steel Building Connections", Journal of the Structural Division, Vol. 95, No. st3, March, pp. 327-353.

Ramberg, W. and Osgood. W.R., 1943, "Description of Stress-Strain Curves by Three Parameters", NACA Technical Paper, No. 902.

Richard, R.M., Gillett, P.E., Kreigh, J.D. and Lewis, B.A., 1980, "The Analysis and Design of Single Plate Framing Connections", Engineering Journal, AISC, Second Quarter, pp. 38-52.

Richard, R.M. and Abbott, B.J., 1975, "Versatile Elastic-Plastic Stress-Strain Formula", Journal of the Engineering Mechanics Division, Proceedings of the American Society of Civil Engineers, Vol. 101, No. EM4, pp. 511-515.

Ricles, J.M. and Yura, J.A., 1983, "Strength of Double-Row Bolted-Web Connections", Journal of Strucural Engineering, Vol. 109, No. 1, January, pp. 126-141.

Sherbourne, A.N. and Murthy, N.S., 1978, "Computer Simulation of Column Webs in Structural Steel Connections", Computers and Structures, Vol. 8, pp.479-490.

Sherbourne, A.N., 1961, "Bolted Beam to Column Connections", The Structural Engineer, 39, June 1961, pp. 203-210.

Sommer, W.H., 1969, "Behaviour of Welded Header Plate Connections", M. Sc. Thesis, University of Toronto.

Steel Construction Institute, 1993, "Draft Report, Connection Standardization, A Review of International Practice in the Field of Moment Connections", The Steel Construction Institute, Silwood Park Ascot Berks, U.K.

Tarpy, T.S. and Cardinal, J.W.,1981, "Behaviour of Semi-Rigid Beam-to-Column End Plate Connections", Joints in Structural Steelwork, John Wiley and Sons, New York, NY, pp. 2.3-2.25.

Tsai Keh-Chyuan and Popov, Egor P., 1990, "Cyclic Behaviour of End-Plate Moment Connections", Journal of Structural Engineering, Vol. 116, No. 11, November, pp. 2917-2930.

Van Dalen, K. and Goboy, H., 1982, "Strength and Rotational Behaviour of Composite Beam-Column Connections", Canadian Journal of Civil Engineers, Vol. 9, No. 2, pp. 313-322.

Zaremba, C., 1986, "Simplified Computer Analysis of Flexibly Connected Steel Frames", Unpublished Report, Ryan-Biggs Associates, Troy, NY, September, 16p.

Appendix A

Table A.1 M-ϕ data for Lipson: AA-2/1 (1968)

Moment, M kN-m	Rotation, ϕ radians	Moment, M kN-m	Rotation, ϕ radians
0	0	1.631	0.0392
0.084	0.0014	1.669	0.0415
0.168	0.0028	1.708	0.0435
0.218	0.0036	1.747	0.0456
0.269	0.0044	1.750	0.0474
0.319	0.0053	1.752	0.0492
0.369	0.0061		
0.417	0.0072		
0.465	0.0083		
0.531	0.0096		
0.597	0.0108		
0.660	0.0124		
0.722	0.0140		
0.797	0.0157		
0.872	0.0173		
0.947	0.0190		
1.010	0.0206		
1.073	0.0222		
1.136	0.0237		
1.213	0.0252		
1.290	0.0266		
1.367	0.0280		
1.424	0.0302		
1.482	0.0323		
1.538	0.0347		
1.593	0.0370		

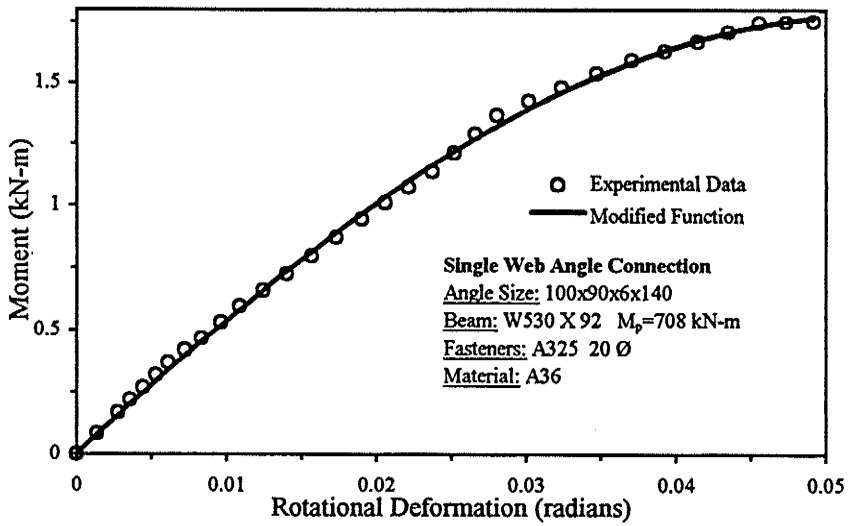


Figure A.1 (a) M-ϕ curve for Lipson: AA-2/1

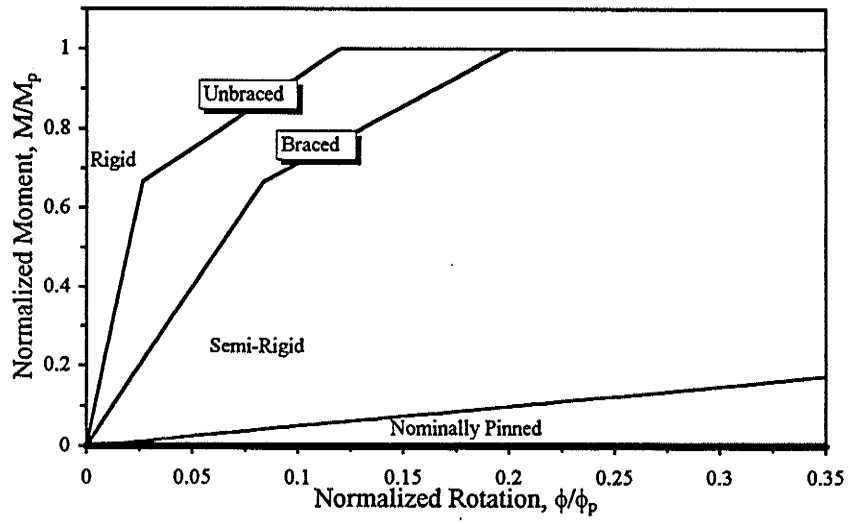


Figure A.1 (b) Eurocode3 Classification of Lipson: AA-2/1

Table A.2 M-ϕ data for Lipson: AA-2/2 (1968)

Moment, M kN-m	Rotation, ϕ radians	Moment, M kN-m	Rotation, ϕ radians
0	0	1.716	0.0268
0.052	0.0006	1.732	0.0278
0.104	0.0013	1.748	0.0289
0.173	0.0022	1.833	0.0302
0.243	0.0031	1.917	0.0315
0.312	0.0040		
0.381	0.0048		
0.464	0.0057		
0.546	0.0066		
0.628	0.0075		
0.698	0.0083		
0.768	0.0092		
0.837	0.0100		
0.905	0.0110		
0.973	0.0121		
1.042	0.0131		
1.087	0.0145		
1.132	0.0159		
1.198	0.0171		
1.264	0.0183		
1.331	0.0195		
1.398	0.0206		
1.466	0.0216		
1.534	0.0227		
1.617	0.0242		
1.700	0.0257		

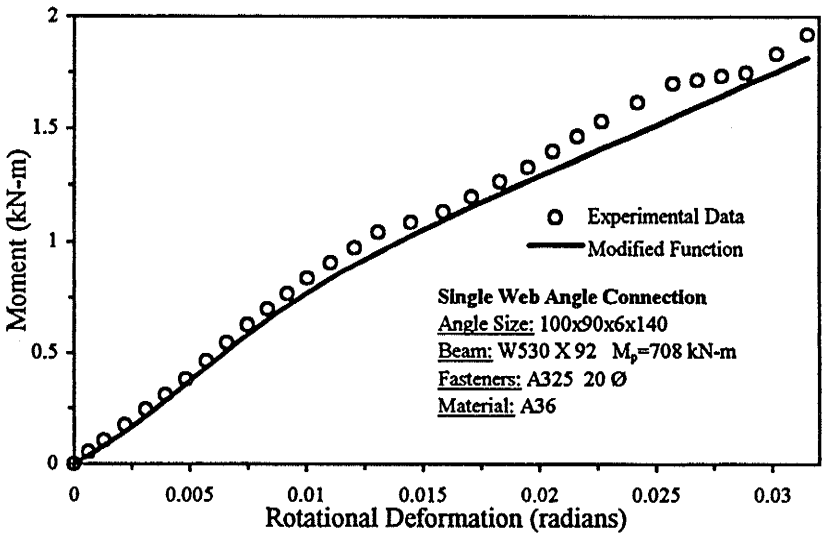


Figure A.2 (a) M-ϕ curve for Lipson: AA-2/2

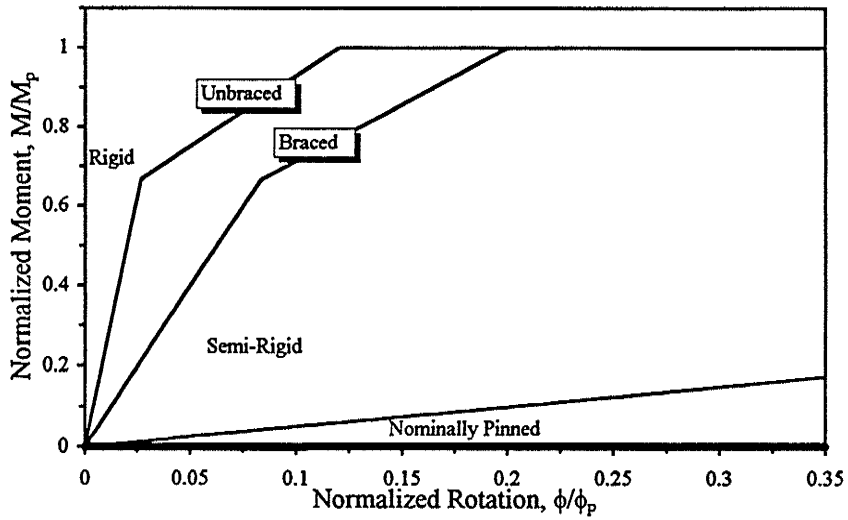


Figure A.2 (b) Eurocode3 Classification of Lipson: AA-2/2

Table A.3 M-ϕ data for Lipson: AA-3/1 (1968)

Moment, M kN-m	Rotation, ϕ radians	Moment, M kN-m	Rotation, ϕ radians
0	0	5.020	0.0392
0.244	0.0010	5.138	0.0413
0.487	0.0020	5.256	0.0434
0.751	0.0030	5.377	0.0451
1.015	0.0039	5.497	0.0469
1.277	0.0050	5.576	0.0490
1.540	0.0061	5.655	0.0512
1.801	0.0073		
2.062	0.0086		
2.341	0.0099		
2.620	0.0113		
2.841	0.0127		
3.062	0.0141		
3.262	0.0156		
3.463	0.0172		
3.643	0.0188		
3.823	0.0205		
4.002	0.0221		
4.182	0.0238		
4.263	0.0257		
4.344	0.0276		
4.481	0.0297		
4.618	0.0318		
4.740	0.0334		
4.861	0.0351		
4.940	0.0372		

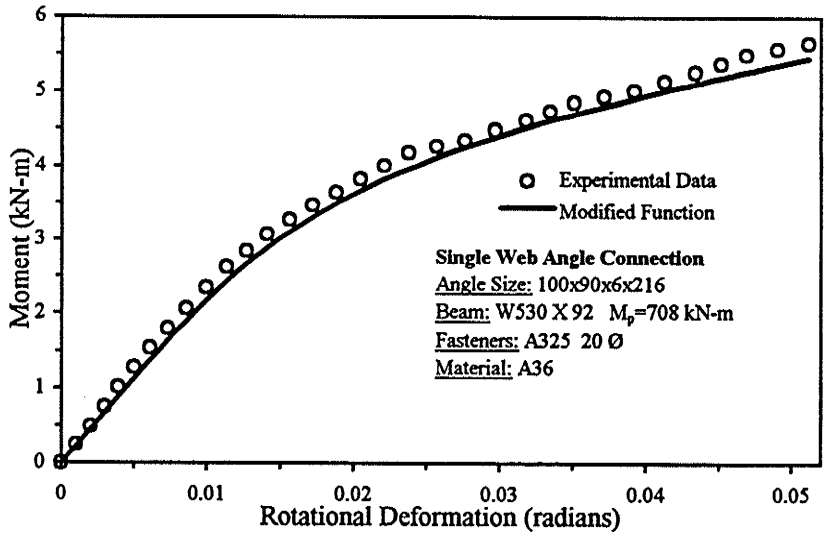


Figure A.3 (a) M-ϕ curve for Lipson: AA-3/1

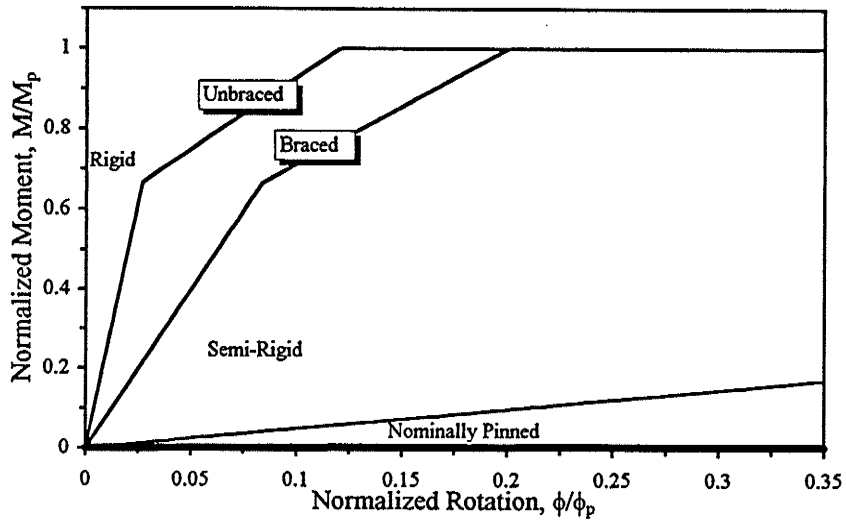


Figure A.3 (b) Eurocode3 Classification of Lipson: AA-3/1

Table A.4 M-ϕ data for Lipson: AA-3/2 (1968)

Moment, M kN-m	Rotation, ϕ radians	Moment, M kN-m	Rotation, ϕ radians
0	0	5.226	0.0185
0.227	0.0007	5.412	0.0194
0.454	0.0013	5.598	0.0203
0.680	0.0020		
0.882	0.0025		
1.084	0.0031		
1.286	0.0037		
1.513	0.0043		
1.740	0.0049		
1.967	0.0055		
2.168	0.0061		
2.369	0.0068		
2.570	0.0074		
2.833	0.0084		
3.096	0.0094		
3.271	0.0101		
3.445	0.0108		
3.620	0.0115		
3.833	0.0122		
4.046	0.0130		
4.260	0.0137		
4.395	0.0145		
4.530	0.0154		
4.665	0.0162		
4.852	0.0169		
5.039	0.0177		

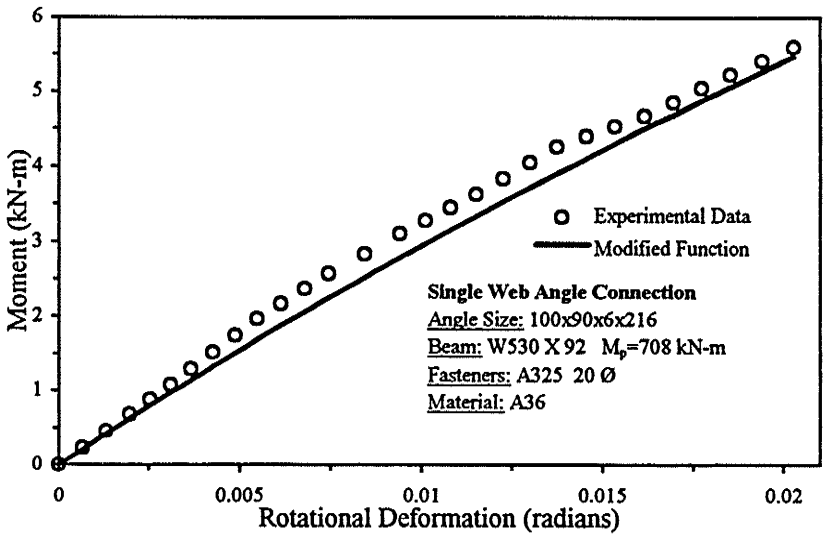


Figure A.4 (a) M-ϕ curve for Lipson: AA-3/2

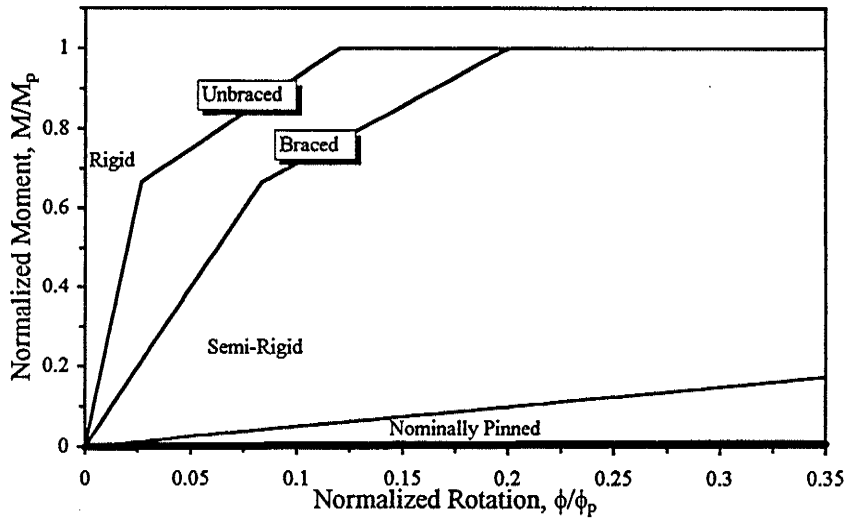


Figure A.4 (b) Eurocode3 Classification of Lipson: AA-3/2

Table A.5 M-ϕ data for Lipson: AA-4/1 (1968)

Moment, M kN-m	Rotation, ϕ radians	Moment, M kN-m	Rotation, ϕ radians
0	0	8.108	0.0287
0.374	0.0008	8.292	0.0305
0.689	0.0014	8.476	0.0323
1.004	0.0020	8.653	0.0342
1.297	0.0024	8.829	0.0360
1.589	0.0028	8.991	0.0379
2.039	0.0036	9.152	0.0399
2.563	0.0047	9.305	0.0419
2.871	0.0052	9.459	0.0439
3.178	0.0058	9.582	0.0458
3.477	0.0065	9.706	0.0477
3.777	0.0071	9.867	0.0495
4.151	0.0081	10.029	0.0514
4.525	0.0090	10.233	0.0544
4.817	0.0099	10.407	0.0570
5.108	0.0109	10.570	0.0583
5.392	0.0118	10.716	0.0604
5.676	0.0128		
5.951	0.0141		
6.227	0.0154		
6.762	0.0184		
7.021	0.0201		
7.281	0.0219		
7.510	0.0236		
7.740	0.0253		
7.924	0.0270		

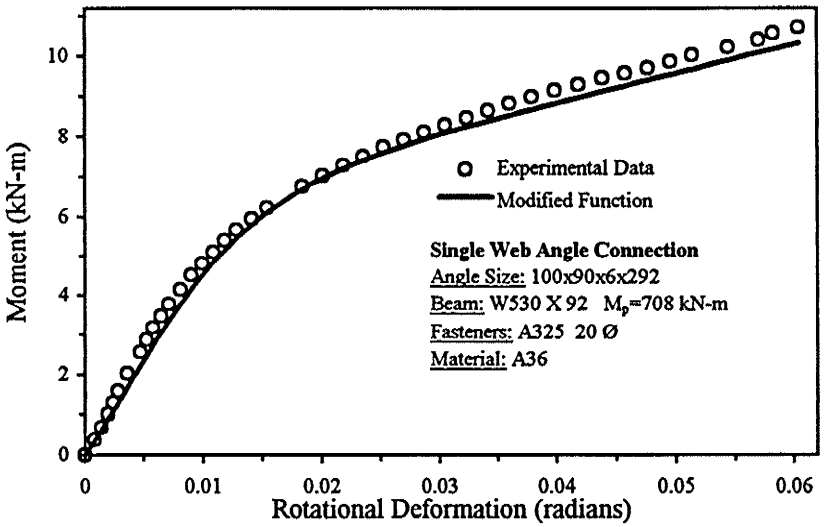


Figure A.5 (a) M-ϕ curve for Lipson: AA-4/1

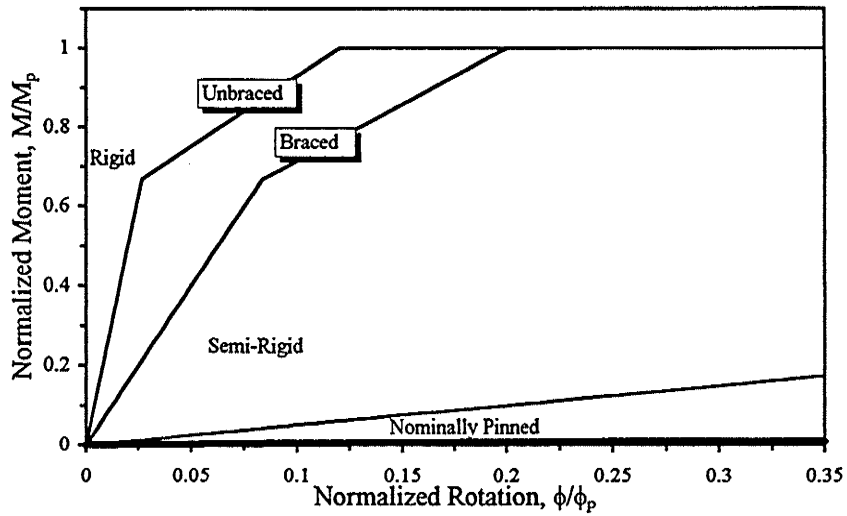


Figure A.5 (b) Eurocode3 Classification of Lipson: AA-4/1

Table A.6 M-ϕ data for Lipson: AA-4/2 (1968)

Moment, M kN-m	Rotation, ϕ radians	Moment, M kN-m	Rotation, ϕ radians
0	0	8.844	0.0241
0.451	0.0005	9.038	0.0254
0.751	0.0008	9.247	0.0268
1.052	0.0010	9.455	0.0282
1.593	0.0016	9.686	0.0300
1.924	0.0020	9.917	0.0318
2.254	0.0024	10.117	0.0334
2.615	0.0030	10.318	0.0351
2.975	0.0035	10.526	0.0370
3.290	0.0040	10.734	0.0389
3.606	0.0045	10.927	0.0407
3.928	0.0053	11.120	0.0425
4.251	0.0060	11.320	0.0445
4.760	0.0073	11.520	0.0465
5.331	0.0085	11.676	0.0481
5.645	0.0094	11.831	0.0497
5.960	0.0103		
6.275	0.0114		
6.589	0.0125		
6.911	0.0137		
7.233	0.0148		
7.502	0.0162		
7.770	0.0177		
8.233	0.0202		
8.442	0.0215		
8.651	0.0228		

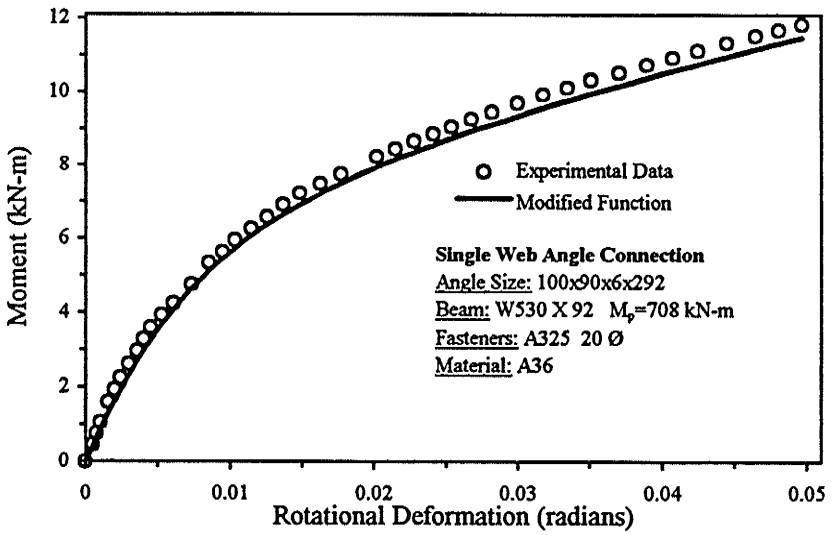


Figure A.6 (a) M-ϕ curve for Lipson: AA-4/2

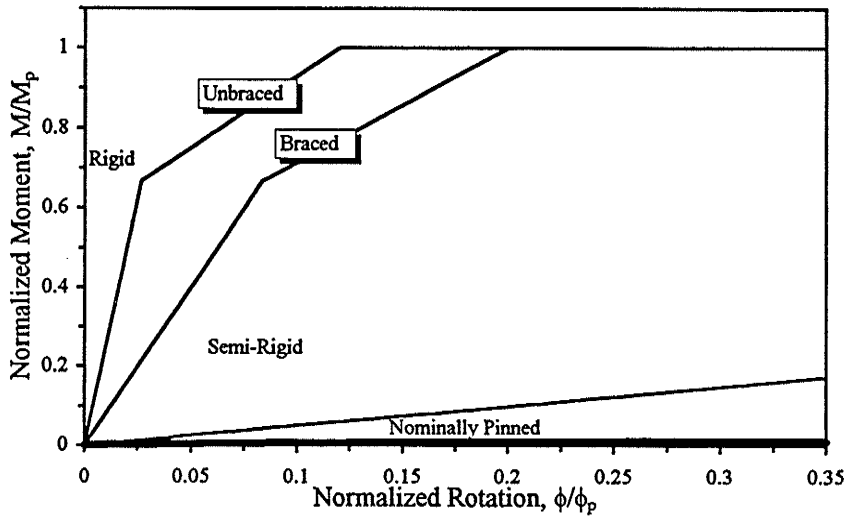


Figure A.6 (b) Eurocode3 Classification of Lipson: AA-4/2

Table A.7 M-ϕ data for Lipson: AA-5/1 (1968)

Moment, M kN-m	Rotation, ϕ radians	Moment, M kN-m	Rotation, ϕ radians
0	0	18.097	0.0246
0.839	0.0006	18.622	0.0263
1.677	0.0011	19.147	0.0280
2.516	0.0017	19.642	0.0301
3.286	0.0022	20.137	0.0321
4.057	0.0027	20.553	0.0344
4.879	0.0031	20.969	0.0366
5.702	0.0036	21.229	0.0382
6.446	0.0041	21.488	0.0397
7.190	0.0046	21.747	0.0413
8.011	0.0053	22.015	0.0429
8.831	0.0059	22.282	0.0445
9.471	0.0066	22.526	0.0458
10.110	0.0072	22.771	0.0472
10.748	0.0081		
11.386	0.0089		
11.971	0.0098		
12.556	0.0106		
13.568	0.0127		
14.151	0.0139		
14.733	0.0151		
15.312	0.0165		
15.892	0.0180		
16.546	0.0197		
17.199	0.0215		
17.648	0.0230		

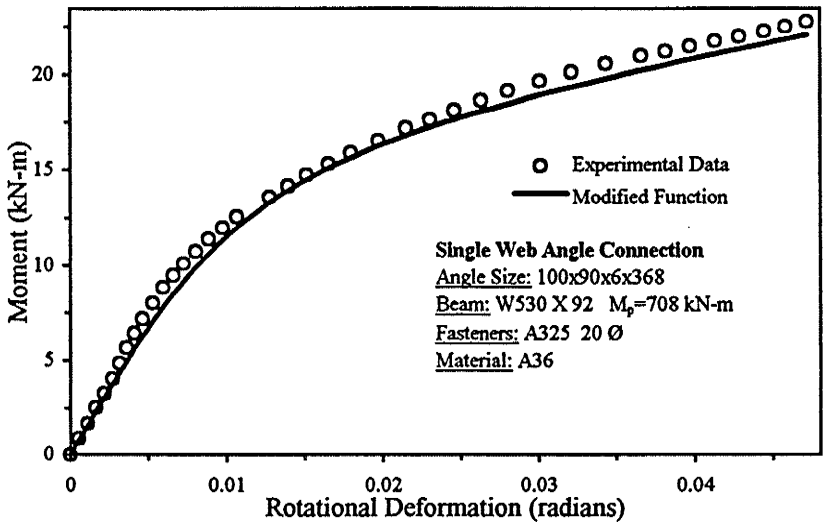


Figure A.7 (a) M-ϕ curve for Lipson: AA-5/1

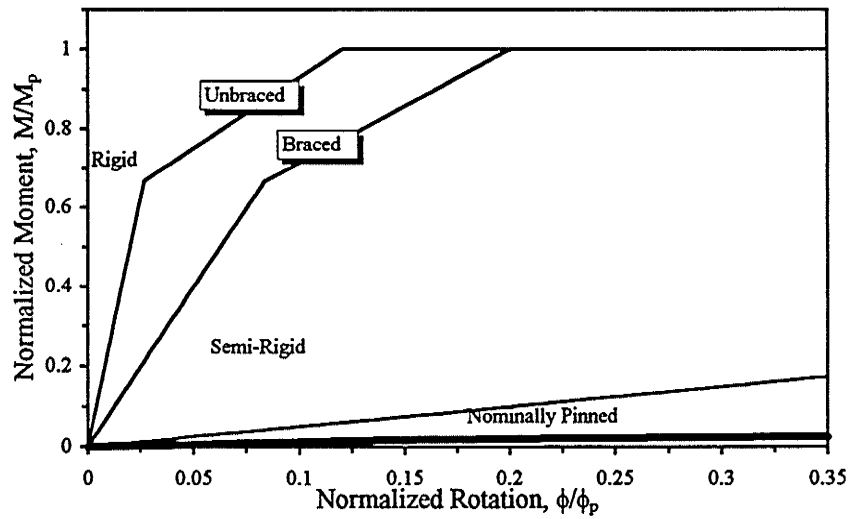


Figure A.7 (b) Eurocode3 Classification of Lipson: AA-5/1

Table A.8 M-ϕ data for Lipson: AA-5/2 (1968)

Moment, M kN-m	Rotation, ϕ radians	Moment, M kN-m	Rotation, ϕ radians
0	0	27.564	0.0249
1.134	0.0003	28.290	0.0269
2.269	0.0005	29.016	0.0288
3.971	0.0008	29.716	0.0307
5.362	0.0013	30.416	0.0326
6.805	0.0017	31.038	0.0346
7.783	0.0020	31.659	0.0366
8.761	0.0024	32.231	0.0385
9.867	0.0029	32.802	0.0404
10.973	0.0033	33.272	0.0421
12.079	0.0038	33.743	0.0438
13.185	0.0042	34.618	0.0462
14.134	0.0049	35.493	0.0486
15.083	0.0055		
16.773	0.0068		
18.104	0.0079		
19.275	0.0094		
20.545	0.0112		
21.455	0.0129		
22.241	0.0142		
23.028	0.0154		
23.809	0.0170		
24.591	0.0186		
25.397	0.0203		
26.204	0.0220		
26.884	0.0234		

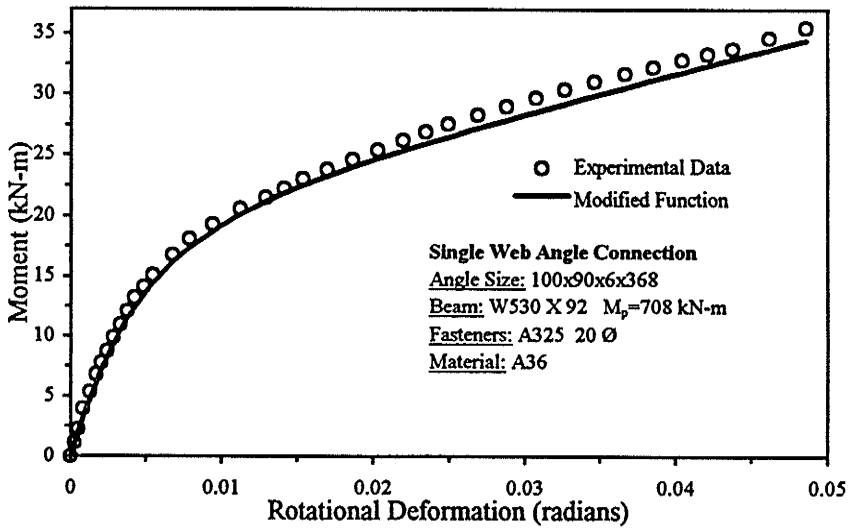


Figure A.8 (a) M-ϕ curve for Lipson: AA-5/2

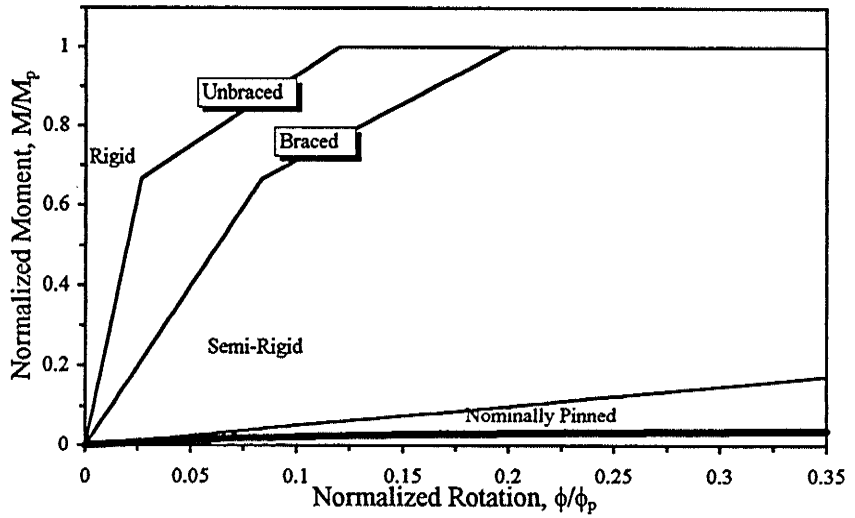


Figure A.8 (b) Eurocode3 Classification of Lipson: AA-5/2

Table A.9 M-ϕ data for Lipson: AA-6/1 (1968)

Moment, M kN-m	Rotation, ϕ radians	Moment, M kN-m	Rotation, ϕ radians
0	0	19.820	0.0186
0.859	0.0003	20.206	0.0196
1.718	0.0007	20.592	0.0205
2.577	0.0010	20.978	0.0215
3.479	0.0014	21.480	0.0229
4.380	0.0018	21.982	0.0243
5.203	0.0022	22.357	0.0254
6.026	0.0027	22.731	0.0266
6.927	0.0031	22.956	0.0273
7.828	0.0036	23.181	0.0280
8.599	0.0041		
9.370	0.0045		
10.063	0.0050		
10.756	0.0055		
11.604	0.0061		
12.451	0.0067		
13.063	0.0075		
13.676	0.0083		
14.800	0.0095		
15.437	0.0104		
16.074	0.0113		
16.708	0.0124		
17.342	0.0136		
18.027	0.0148		
18.711	0.0161		
19.266	0.0174		

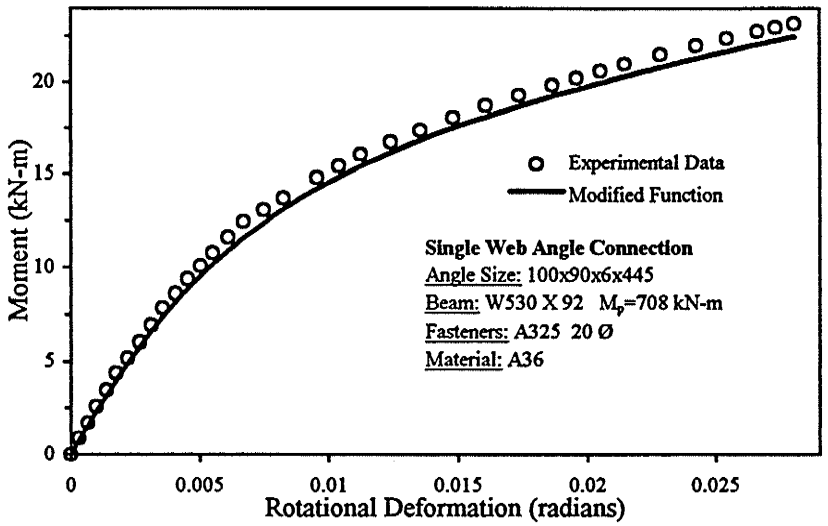


Figure A.9 (a) M-ϕ curve for Lipson: AA-6/1

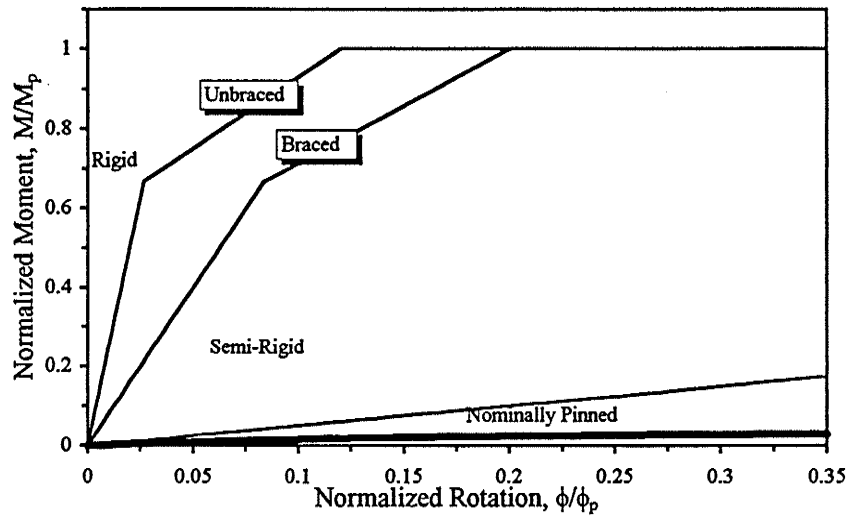


Figure A.9 (b) Eurocode3 Classification of Lipson: AA-6/1

Table A.10 M-ϕ data for Lipson: AA-6/2 (1968)

Moment, M kN-m	Rotation, ϕ radians	Moment, M kN-m	Rotation, ϕ radians
0	0	28.904	0.0172
1.674	0.0003	29.814	0.0187
3.348	0.0007	30.597	0.0200
5.101	0.0009	31.380	0.0214
6.131	0.0012	32.059	0.0228
7.160	0.0014	32.738	0.0242
8.318	0.0018	33.364	0.0256
9.476	0.0021	33.990	0.0271
10.581	0.0025	34.692	0.0287
11.687	0.0029	35.395	0.0303
12.637	0.0033	36.121	0.0320
13.587	0.0037	36.847	0.0337
14.666	0.0041	37.192	0.0350
15.745	0.0046	37.538	0.0362
16.719	0.0051		
17.694	0.0056		
18.770	0.0063		
19.845	0.0070		
20.868	0.0078		
21.890	0.0086		
22.936	0.0096		
23.981	0.0106		
24.895	0.0118		
25.809	0.0130		
26.901	0.0144		
27.993	0.0158		

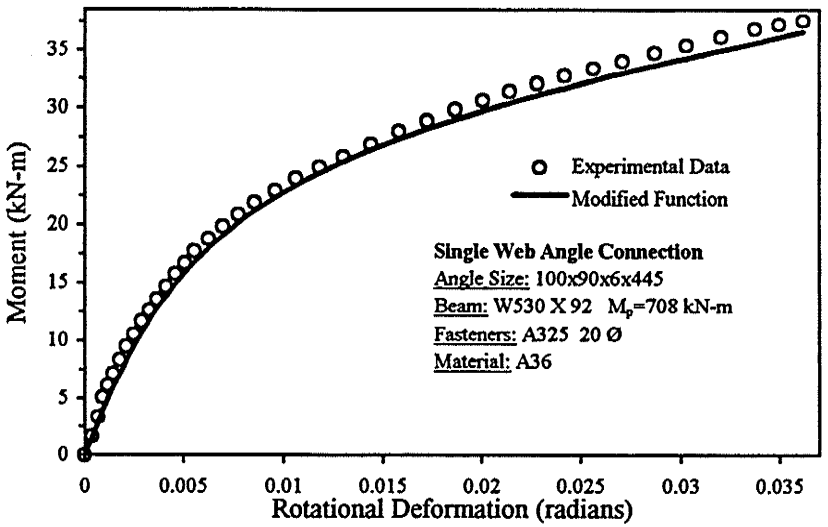


Figure A.10 (a) M-ϕ curve for Lipson: AA-6/2

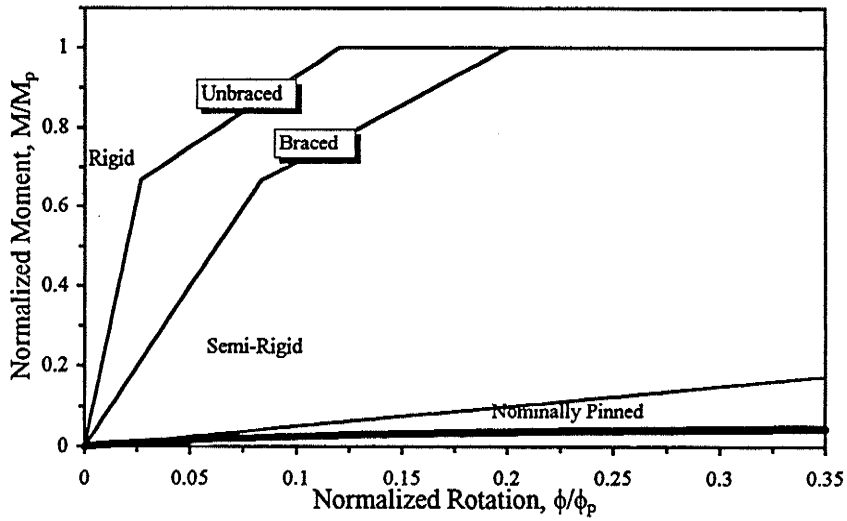


Figure A.10 (b) Eurocode3 Classification of Lipson: AA-6/2

Table A.11 M-ϕ data for Lipson: BB-4/1 (1968)

Moment, M kN-m	Rotation, ϕ radians	Moment, M kN-m	Rotation, ϕ radians
0	0	12.742	0.0323
0.525	0.0006	13.023	0.0346
1.095	0.0010	13.305	0.0369
1.755	0.0019	13.630	0.0397
2.430	0.0024	13.955	0.0425
3.120	0.0032	14.198	0.0451
3.517	0.0036	14.441	0.0478
3.914	0.0041	14.677	0.0503
4.319	0.0046	14.913	0.0527
4.724	0.0050	15.082	0.0548
5.474	0.0060	15.251	0.0568
6.133	0.0071	15.390	0.0587
6.687	0.0083	15.529	0.0606
7.405	0.0100		
7.838	0.0111		
8.272	0.0123		
8.750	0.0138		
9.228	0.0153		
9.668	0.0168		
10.109	0.0183		
10.825	0.0212		
11.160	0.0229		
11.495	0.0246		
11.792	0.0262		
12.089	0.0279		
12.416	0.0301		

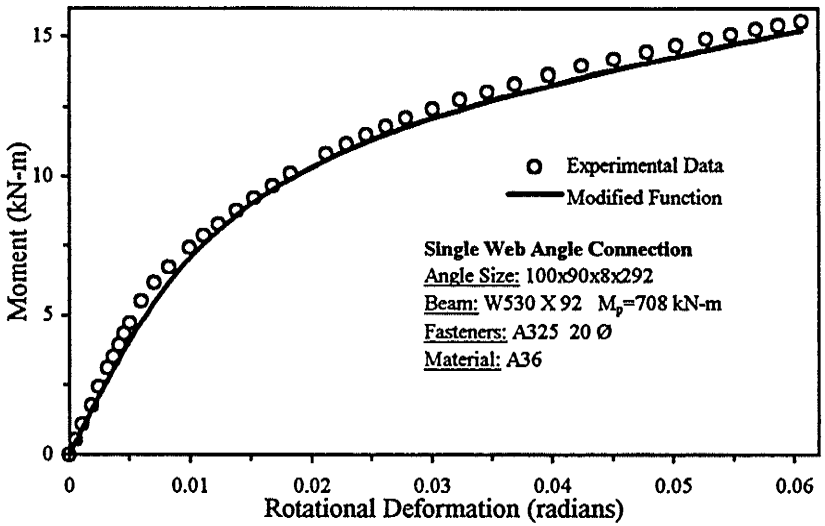


Figure A.11 (a) M-ϕ curve for Lipson: BB-4/1

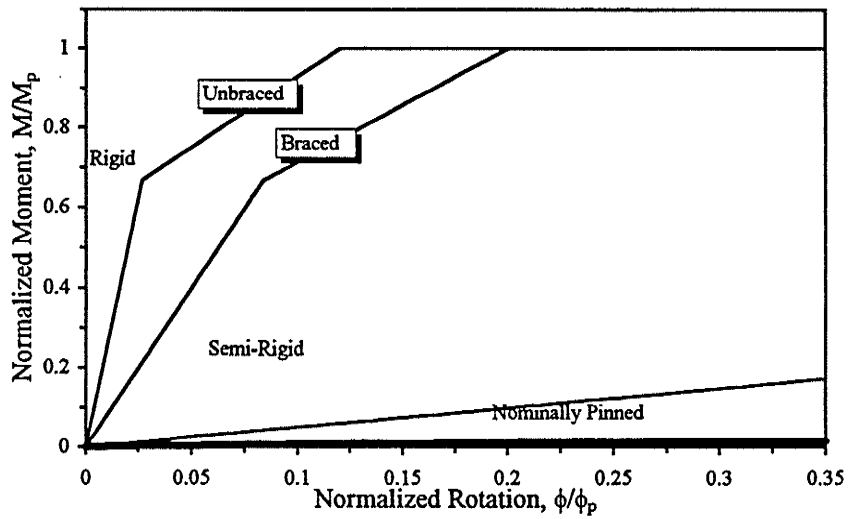


Figure A.11 (b) Eurocode3 Classification of Lipson: BB-4/1

Table A.12 M-ϕ data for Lipson: BB-4/2 (1968)

Moment, M kN-m	Rotation, ϕ radians	Moment, M kN-m	Rotation, ϕ radians
0	0	13.284	0.0297
0.480	0.0004	13.642	0.0316
1.035	0.0010	14.000	0.0335
1.560	0.0016	14.387	0.0357
2.356	0.0023	14.775	0.0379
3.046	0.0030	15.018	0.0395
3.721	0.0038	15.261	0.0411
4.134	0.0043	15.504	0.0427
4.546	0.0047	15.899	0.0450
5.281	0.0057	16.293	0.0473
6.031	0.0066		
6.706	0.0077		
7.515	0.0092		
7.949	0.0101		
8.383	0.0111		
8.795	0.0122		
9.207	0.0133		
9.655	0.0146		
10.104	0.0159		
10.493	0.0173		
10.881	0.0188		
11.255	0.0202		
11.629	0.0216		
12.031	0.0236		
12.434	0.0255		
12.859	0.0276		

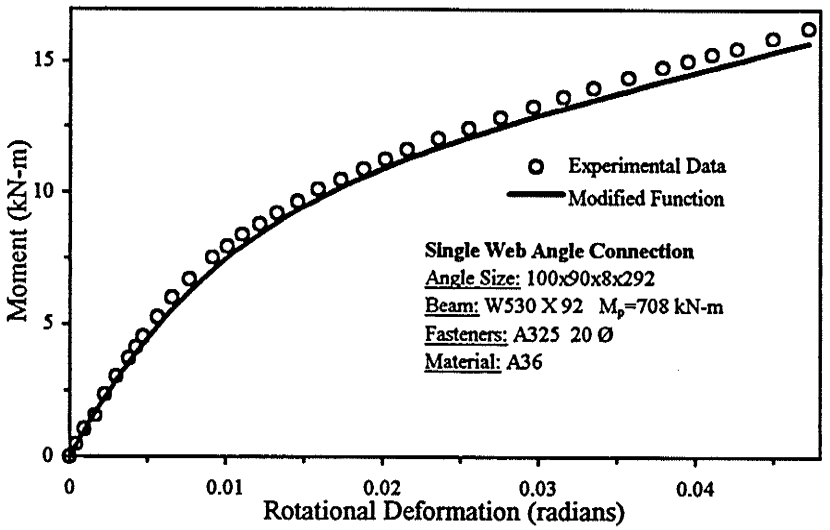


Figure A.12 (a) M-ϕ curve for Lipson: BB-4/2

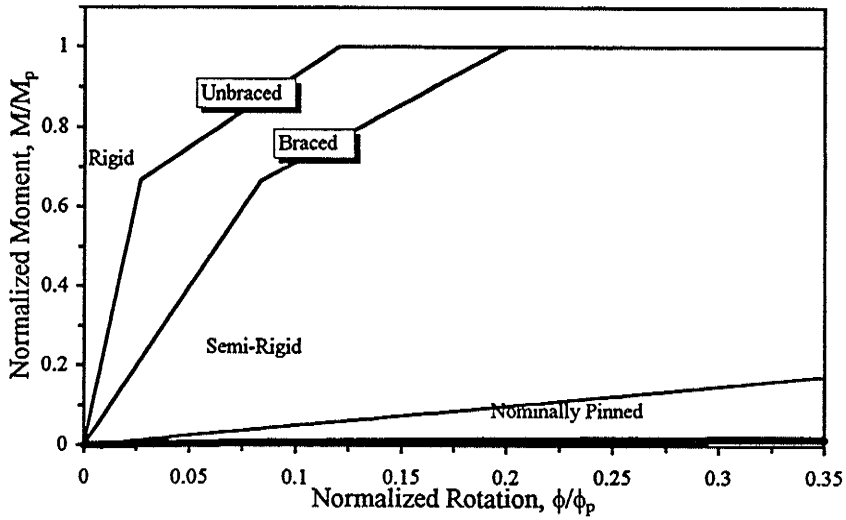


Figure A.12 (b) Eurocode3 Classification of Lipson: BB-4/2

Table A.13 M-ϕ data for Lipson: B2-4 (1968)

Moment, M kN-m	Rotation, ϕ radians	Moment, M kN-m	Rotation, ϕ radians
0	0	10.825	0.0132
0.346	0.0002	11.117	0.0140
0.692	0.0005	11.312	0.0147
1.278	0.0010	11.507	0.0154
1.616	0.0011	11.701	0.0162
1.955	0.0013	11.895	0.0171
2.331	0.0016	12.045	0.0180
2.707	0.0019	12.194	0.0189
3.120	0.0022	12.353	0.0198
3.533	0.0026	12.512	0.0207
3.857	0.0028	12.671	0.0215
4.180	0.0031		
4.563	0.0035		
4.946	0.0039		
5.427	0.0044		
5.908	0.0050		
6.359	0.0055		
6.809	0.0060		
7.320	0.0067		
7.831	0.0074		
8.349	0.0082		
8.867	0.0090		
9.362	0.0100		
9.858	0.0110		
10.195	0.0116		
10.533	0.0123		

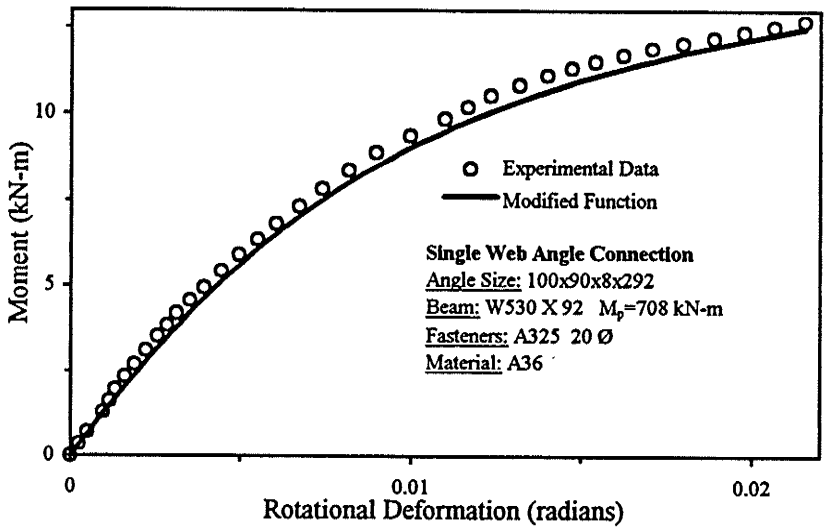


Figure A.13 (a) M-ϕ curve for Lipson: B2-4

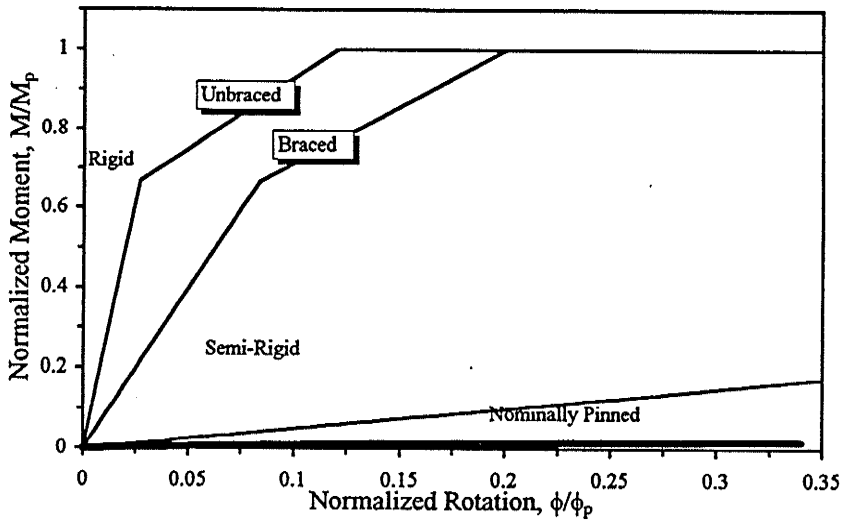


Figure A.13 (b) Eurocode3 Classification of Lipson: B2-4

Table A.14 M-ϕ data for Lipson: B3-4 (1968)

Moment, M kN-m	Rotation, ϕ radians	Moment, M kN-m	Rotation, ϕ radians
0	0	12.207	0.0179
0.601	0.0005	12.521	0.0194
1.338	0.0012	12.774	0.0207
1.743	0.0016	13.028	0.0220
2.149	0.0021	13.266	0.0234
2.810	0.0027	13.505	0.0248
3.502	0.0032	13.678	0.0260
4.005	0.0036	13.852	0.0271
4.509	0.0040	14.026	0.0283
4.967	0.0044	14.271	0.0299
5.426	0.0048	14.517	0.0315
6.162	0.0055	14.703	0.0330
6.568	0.0059	14.888	0.0344
6.973	0.0063		
7.492	0.0070		
8.010	0.0076		
8.385	0.0083		
8.760	0.0089		
9.188	0.0097		
9.615	0.0106		
10.028	0.0114		
10.440	0.0122		
10.807	0.0133		
11.174	0.0143		
11.534	0.0154		
11.893	0.0165		

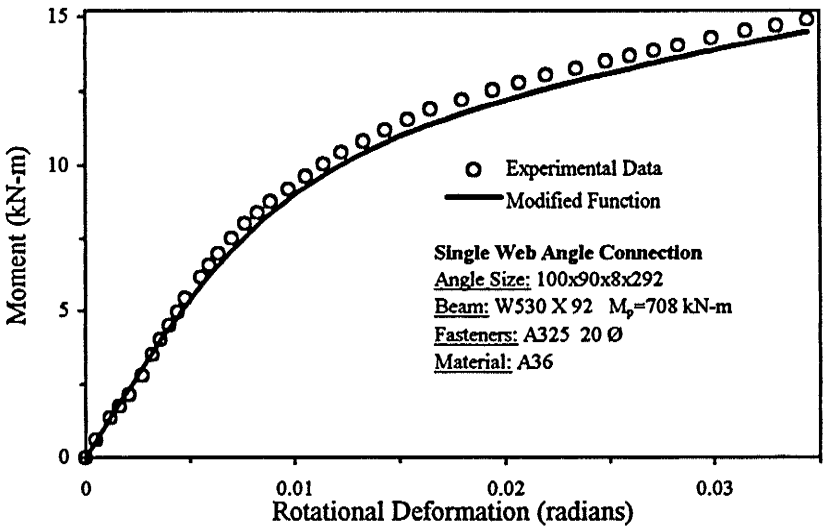


Figure A.14 (a) M-ϕ curve for Lipson: B3-4

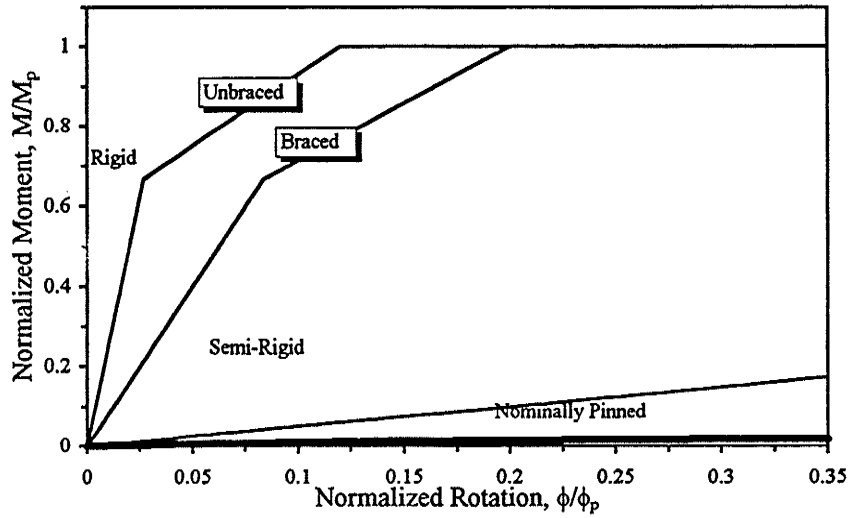


Figure A.14 (b) Eurocode3 Classification of Lipson: B3-4

Table A.15 M-ϕ data for Lipson: C-4 (1968)

Moment, M kN-m	Rotation, ϕ radians	Moment, M kN-m	Rotation, ϕ radians
0	0	15.052	0.0088
0.746	0.0001	15.317	0.0093
1.492	0.0002	15.581	0.0099
2.238	0.0003	15.871	0.0105
2.899	0.0007	16.160	0.0111
3.560	0.0010	16.450	0.0118
4.251	0.0012	16.670	0.0124
4.942	0.0013	16.891	0.0131
5.633	0.0014	17.111	0.0137
6.489	0.0017	17.332	0.0144
6.985	0.0018		
7.480	0.0019		
8.276	0.0023		
8.824	0.0026		
9.372	0.0030		
10.228	0.0033		
10.671	0.0037		
11.113	0.0040		
11.571	0.0045		
12.028	0.0049		
12.538	0.0054		
13.048	0.0059		
13.528	0.0066		
14.008	0.0072		
14.398	0.0077		
14.788	0.0083		

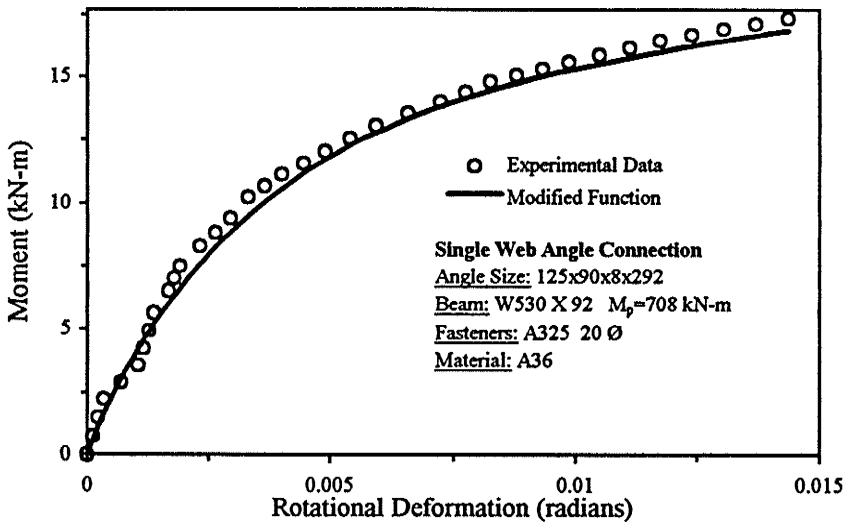


Figure A.15 (a) M-ϕ curve for Lipson: C-4

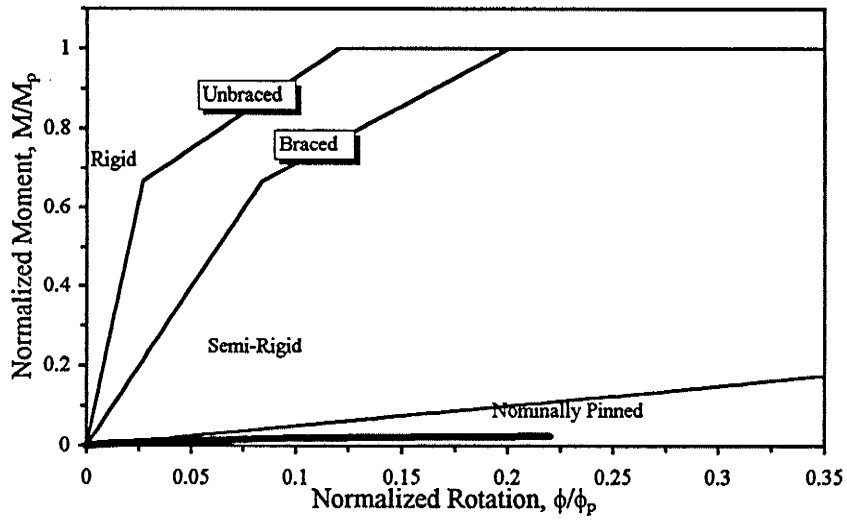


Figure A.15 (b) Eurocode3 Classification of Lipson: C-4

Table A.16 M-ϕ data for Lipson: D-4 (1968)

Moment, M kN-m	Rotation, ϕ radians	Moment, M kN-m	Rotation, ϕ radians
0	0	14.544	0.0092
0.748	0.0002	14.884	0.0097
1.496	0.0004	15.113	0.0102
2.244	0.0006	15.342	0.0107
3.012	0.0009	15.571	0.0112
3.779	0.0012	15.800	0.0117
4.254	0.0013	15.995	0.0123
4.728	0.0014	16.190	0.0129
5.353	0.0016	16.385	0.0134
5.978	0.0019		
6.467	0.0020		
6.957	0.0022		
7.528	0.0025		
8.100	0.0029		
8.650	0.0032		
9.199	0.0035		
9.816	0.0038		
10.433	0.0042		
11.005	0.0048		
11.577	0.0054		
12.080	0.0060		
12.584	0.0065		
13.010	0.0071		
13.436	0.0077		
13.862	0.0082		
14.203	0.0087		

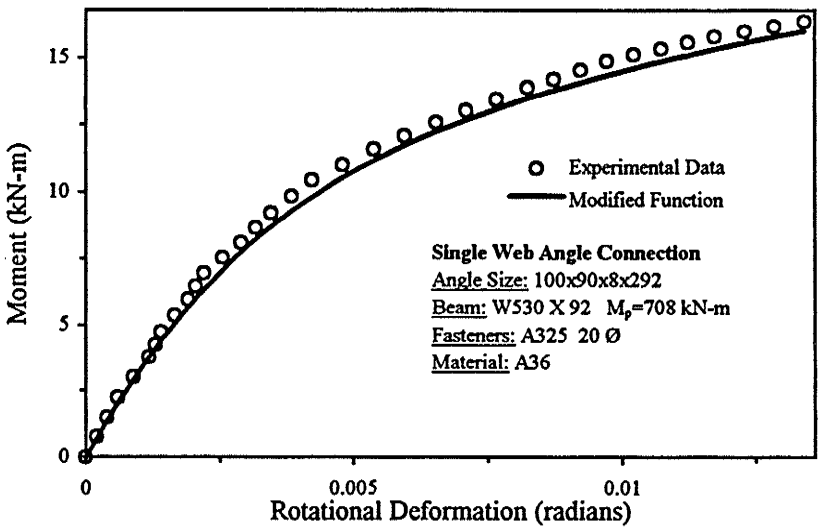


Figure A.16 (a) M-ϕ curve for Lipson: D-4

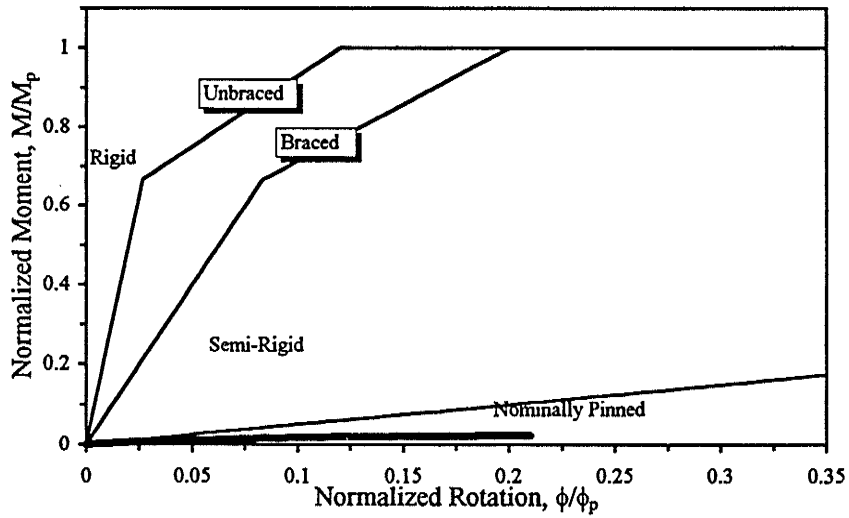


Figure A.16 (b) Eurocode3 Classification of Lipson: D-4

Table A.17 M-ϕ data for Lipson: G-2/1 (1968)

Moment, M kN-m	Rotation, ϕ radians	Moment, M kN-m	Rotation, ϕ radians
0	0	5.532	0.0059
0.255	0.0001	5.508	0.0068
0.510	0.0002	5.251	0.0076
0.765	0.0004	5.057	0.0090
1.020	0.0005	5.026	0.0101
1.275	0.0006	5.172	0.0104
1.530	0.0007	5.318	0.0107
1.752	0.0008	5.519	0.0118
1.975	0.0009	5.554	0.0127
2.197	0.0010	5.589	0.0135
2.420	0.0011	5.602	0.0144
2.642	0.0012	5.615	0.0153
2.881	0.0013	5.381	0.0167
3.120	0.0014	5.349	0.0179
3.359	0.0015	5.317	0.0190
3.597	0.0017	5.335	0.0204
3.817	0.0018	5.352	0.0219
4.037	0.0019	5.394	0.0231
4.257	0.0020	5.435	0.0244
4.477	0.0021	5.401	0.0256
4.726	0.0022	5.366	0.0269
4.975	0.0023	5.364	0.0279
5.184	0.0025	5.361	0.0289
5.392	0.0026	5.359	0.0298
5.510	0.0039		
5.521	0.0049		

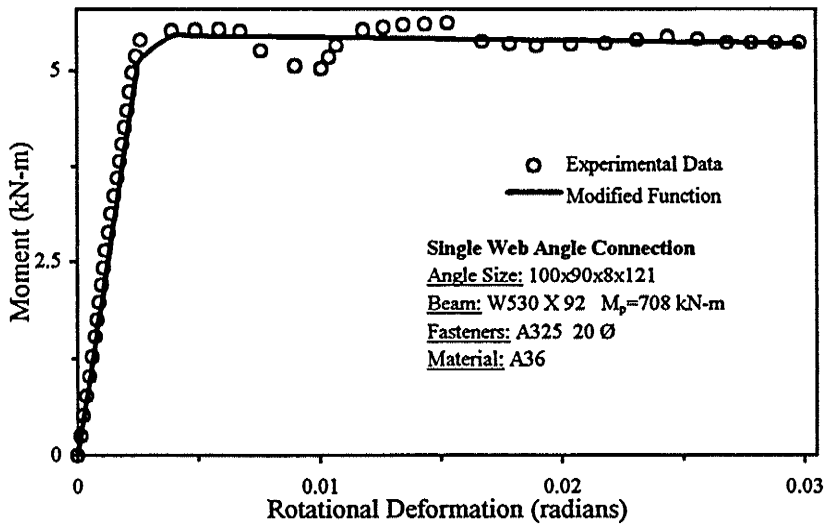


Figure A.17 (a) M-ϕ curve for Lipson: G-2/1

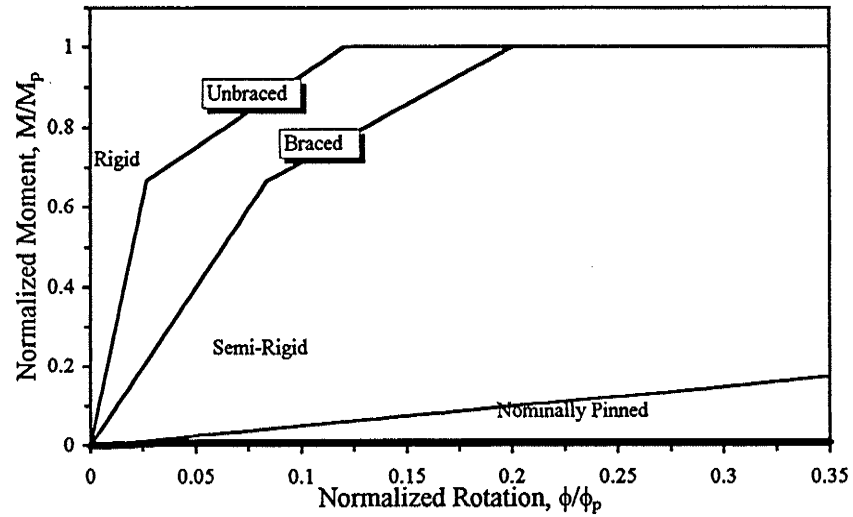


Figure A.17 (b) Eurocode3 Classification of Lipson: G-2/1

Table A.18 M-ϕ data for Lipson: G-3/1 (1968)

Moment, M kN-m	Rotation, ϕ radians	Moment, M kN-m	Rotation, ϕ radians
0	0	10.491	0.0115
0.576	0.0001	10.547	0.0130
1.153	0.0003	10.703	0.0143
1.729	0.0004	10.860	0.0156
2.306	0.0006	11.023	0.0167
2.882	0.0007	11.185	0.0178
3.459	0.0008	11.421	0.0191
4.073	0.0010	11.657	0.0203
4.687	0.0012	11.705	0.0214
5.301	0.0014	11.752	0.0224
5.823	0.0016	11.878	0.0235
6.346	0.0018	12.004	0.0245
6.869	0.0020	12.224	0.0256
7.404	0.0023	12.444	0.0267
7.939	0.0025	12.879	0.0278
8.473	0.0028	13.314	0.0288
8.929	0.0031	13.749	0.0299
9.385	0.0034		
9.917	0.0037		
10.292	0.0042		
10.471	0.0047		
10.490	0.0054		
10.575	0.0065		
10.660	0.0076		
10.548	0.0088		
10.435	0.0101		

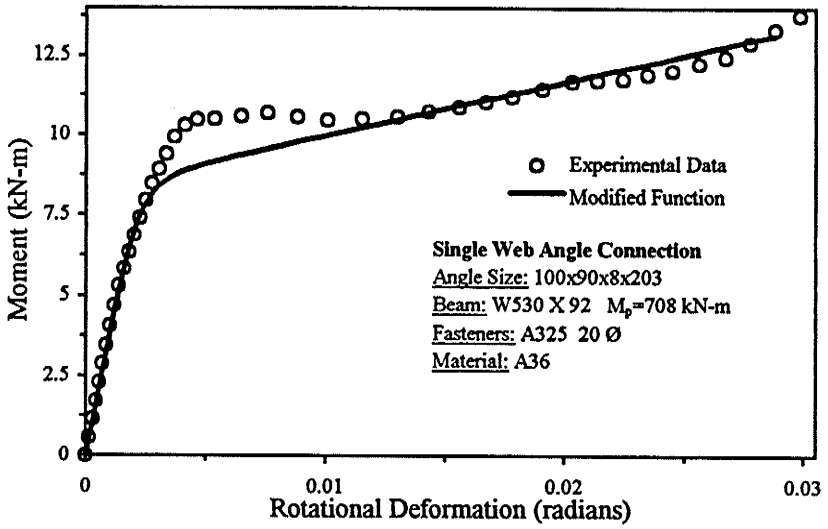


Figure A.18 (a) M-ϕ curve for Lipson: G-3/1

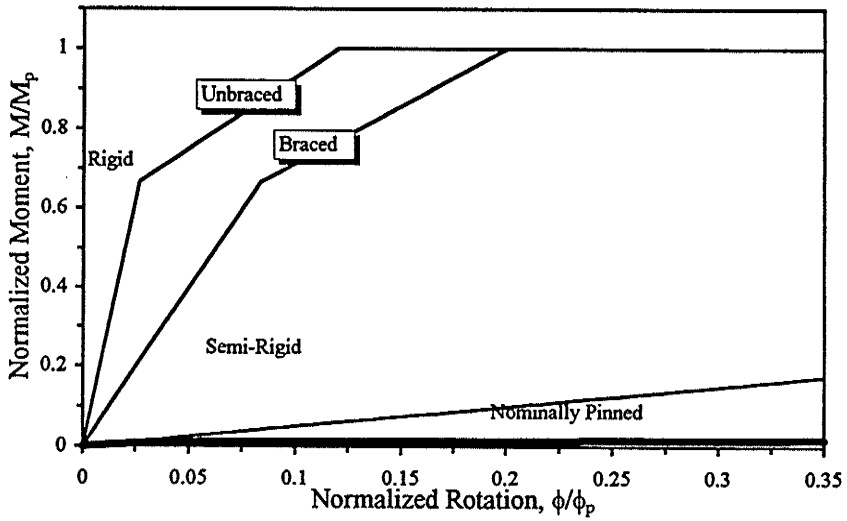


Figure A.18 (b) Eurocode3 Classification of Lipson: G-3/1

Table A.19 M-ϕ data for Lipson: G-4/1 (1968)

Moment, M kN-m	Rotation, ϕ radians	Moment, M kN-m	Rotation, ϕ radians
0	0	15.609	0.0124
0.996	0.0001	15.719	0.0133
1.992	0.0002	15.829	0.0142
2.988	0.0003	15.853	0.0154
3.984	0.0005	15.876	0.0166
4.980	0.0006	16.079	0.0177
5.907	0.0007	16.269	0.0185
6.833	0.0008	16.459	0.0193
7.616	0.0009	16.875	0.0204
8.399	0.0011	17.290	0.0214
9.182	0.0013	17.823	0.0225
9.934	0.0014	18.356	0.0235
10.685	0.0015	19.155	0.0247
11.489	0.0019	19.953	0.0259
12.292	0.0022	20.561	0.0270
13.402	0.0027	21.169	0.0281
14.430	0.0033	21.781	0.0291
14.993	0.0040	22.393	0.0300
15.324	0.0046		
15.228	0.0053		
15.110	0.0067		
15.102	0.0077		
15.093	0.0087		
15.218	0.0097		
15.343	0.0108		
15.476	0.0116		

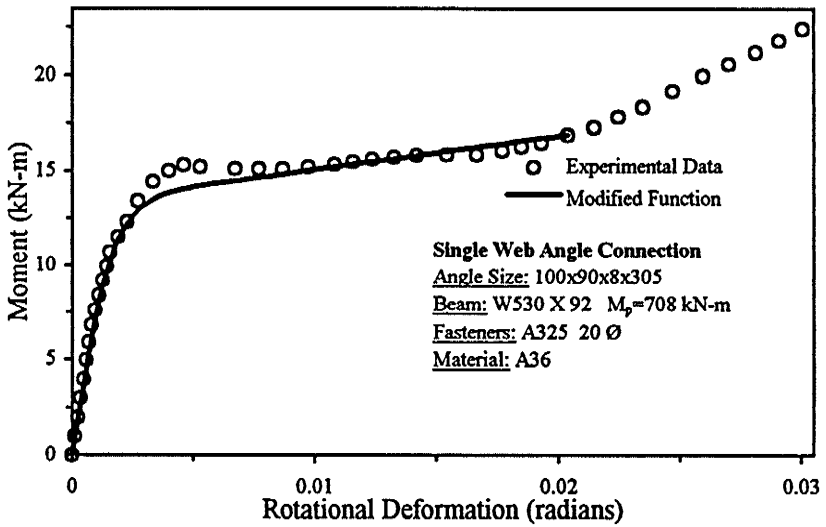


Figure A.19 (a) M-ϕ curve for Lipson: G-4/1

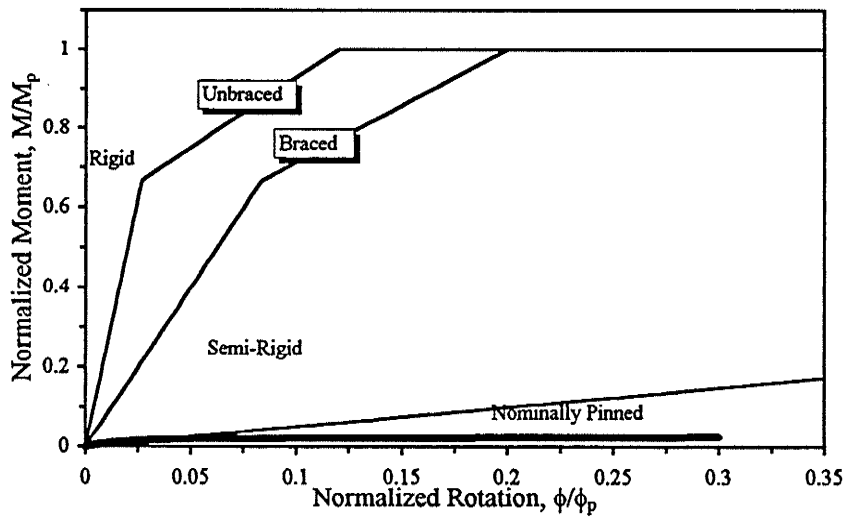


Figure A.19 (b) Eurocode3 Classification of Lipson: G-4/1

Table A.20 M-ϕ data for Lipson: G-5/1 (1968)

Moment, M kN-m	Rotation, ϕ radians	Moment, M kN-m	Rotation, ϕ radians
0	0	28.551	0.0163
1.854	0.0002	29.488	0.0174
3.708	0.0004	30.425	0.0185
5.562	0.0006	31.111	0.0198
7.222	0.0007	31.798	0.0211
8.882	0.0009	32.484	0.0224
10.290	0.0011	33.302	0.0236
11.697	0.0014	34.119	0.0249
12.835	0.0015	34.937	0.0261
13.973	0.0017	35.779	0.0274
15.106	0.0020	36.621	0.0286
16.239	0.0024	37.463	0.0299
17.544	0.0028		
18.850	0.0032		
20.014	0.0038		
21.178	0.0044		
21.671	0.0048		
22.004	0.0054		
22.521	0.0062		
23.038	0.0071		
23.717	0.0085		
24.396	0.0098		
25.098	0.0110		
25.801	0.0122		
26.504	0.0133		
27.528	0.0148		

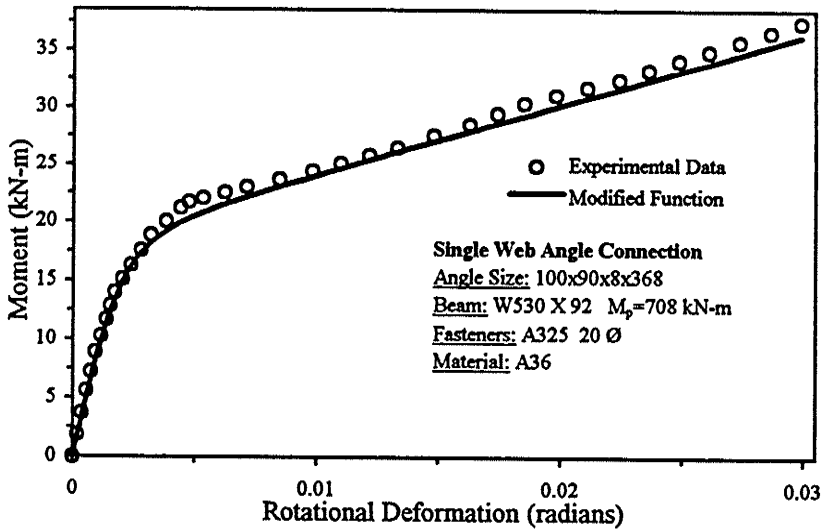


Figure A.20 (a) M-ϕ curve for Lipson: G-5/1

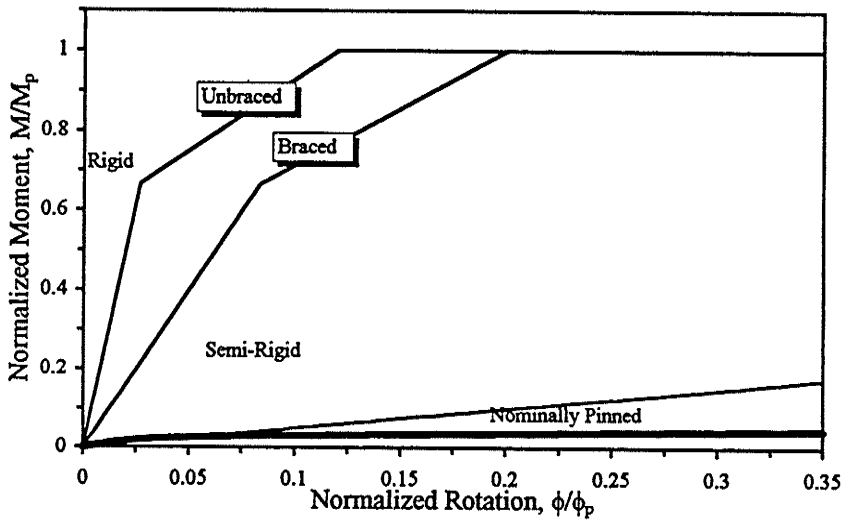


Figure A.20 (b) Eurocode3 Classification of Lipson: G-5/1

Table A.21 M-ϕ data for Lipson: P1-2/1 (1968)

Moment, M kN-m	Rotation, ϕ radians	Moment, M kN-m	Rotation, ϕ radians
0	0	4.763	0.0146
0.241	0.0001	4.737	0.0160
0.481	0.0003	4.711	0.0174
0.722	0.0004	4.707	0.0186
0.963	0.0006	4.703	0.0197
1.204	0.0007	4.699	0.0209
1.444	0.0009	4.695	0.0220
1.688	0.0011	4.765	0.0233
1.931	0.0013	4.835	0.0245
2.175	0.0016	4.996	0.0254
2.418	0.0018	5.158	0.0263
2.612	0.0022	5.353	0.0273
2.805	0.0026	5.548	0.0283
2.999	0.0029		
3.251	0.0034		
3.504	0.0039		
3.694	0.0044		
3.883	0.0049		
4.072	0.0054		
4.274	0.0062		
4.475	0.0071		
4.585	0.0083		
4.695	0.0095		
4.726	0.0108		
4.758	0.0120		
4.789	0.0132		

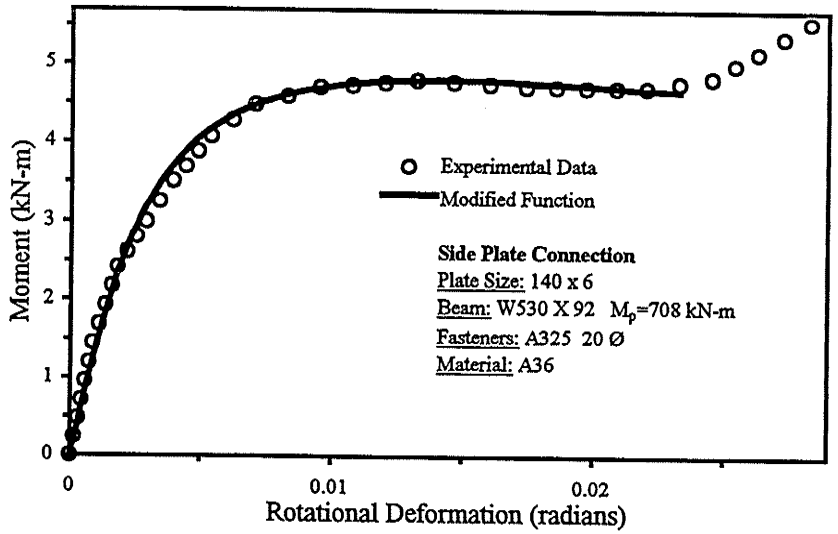


Figure A.21 (a) M-ϕ curve for Lipson: P1-2/1

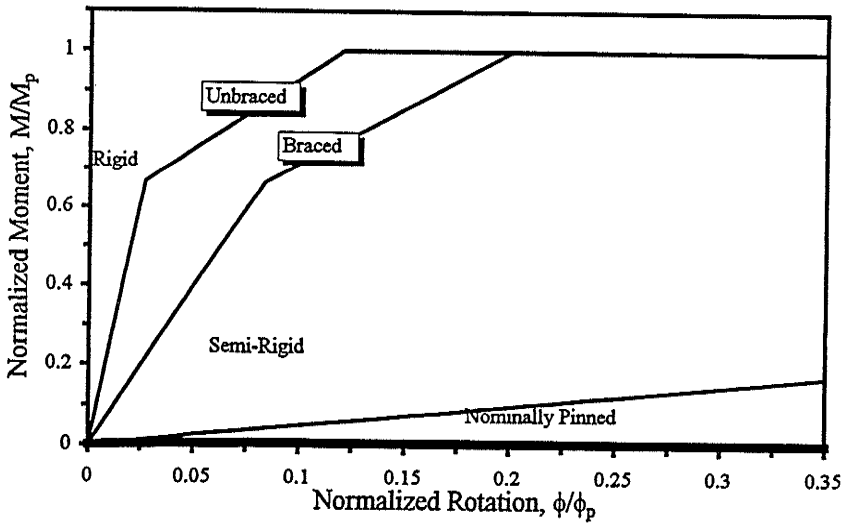


Figure A.21 (b) Eurocode3 Classification of Lipson: P1-2/1

Table A.22 M-ϕ data for Lipson: P1-2/2 (1968)

Moment, M kN-m	Rotation, ϕ radians	Moment, M kN-m	Rotation, ϕ radians
0	0	4.603	0.0205
0.212	0.0001	4.556	0.0229
0.424	0.0003	4.509	0.0253
0.635	0.0004	4.462	0.0278
0.847	0.0006	4.388	0.0305
1.059	0.0007	4.314	0.0333
1.284	0.0009	4.357	0.0360
1.509	0.0011	4.341	0.0383
1.735	0.0013	4.539	0.0405
1.960	0.0015	4.737	0.0426
2.182	0.0018	4.934	0.0447
2.403	0.0020	5.004	0.0468
2.625	0.0023	5.074	0.0489
2.826	0.0026	5.145	0.0510
3.026	0.0030	5.063	0.0536
3.226	0.0033	4.982	0.0563
3.427	0.0036	4.901	0.0589
3.669	0.0043		
3.912	0.0050		
4.149	0.0059		
4.387	0.0067		
4.612	0.0088		
4.679	0.0110		
4.747	0.0131		
4.699	0.0156		
4.651	0.0180		

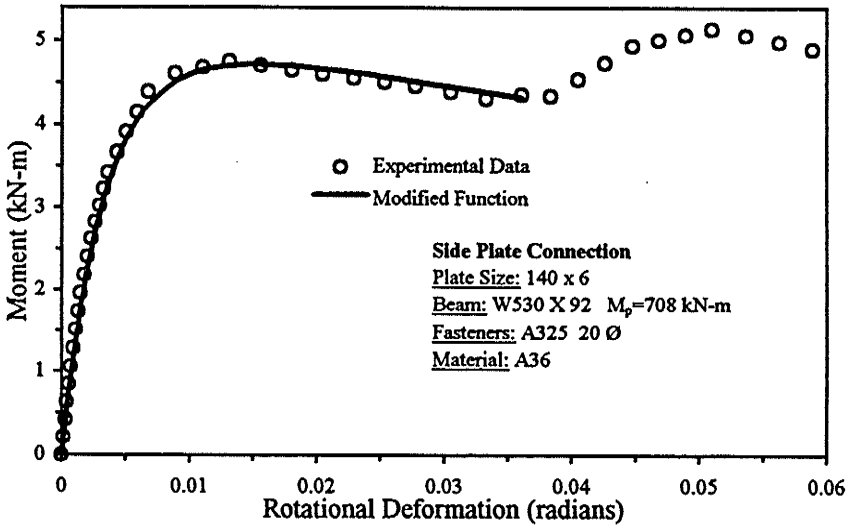


Figure A.22 (a) M-ϕ curve for Lipson: P1-2/2

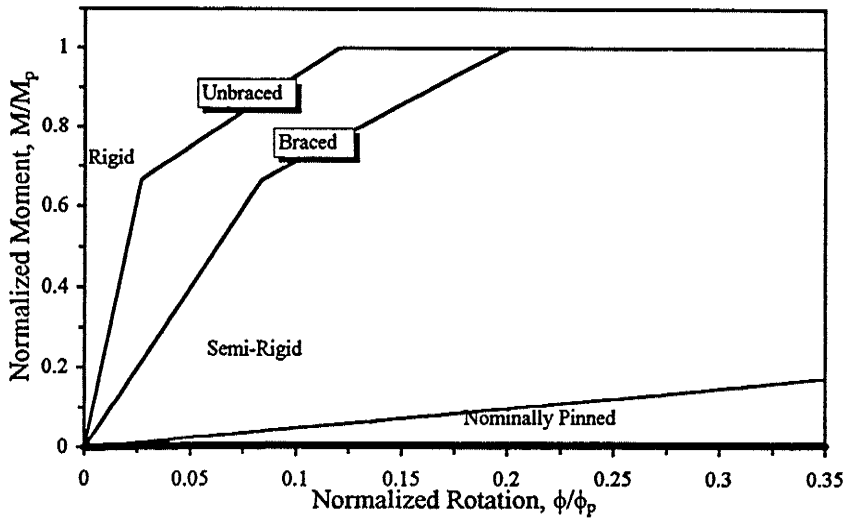


Figure A.22 (b) Eurocode3 Classification of Lipson: P1-2/2

Table A.23 M-ϕ data for Lipson: P1-3/1 (1968)

Moment, M kN-m	Rotation, ϕ radians	Moment, M kN-m	Rotation, ϕ radians
0	0	15.077	0.0148
0.756	0.0001	15.293	0.0160
1.511	0.0002	15.510	0.0171
2.267	0.0003	15.828	0.0183
3.023	0.0005	16.147	0.0195
3.779	0.0006	16.465	0.0207
4.545	0.0008	16.758	0.0219
5.311	0.0011	17.051	0.0231
6.117	0.0013	17.343	0.0243
6.923	0.0015	17.611	0.0255
7.497	0.0018	17.879	0.0267
8.070	0.0020	18.147	0.0278
8.720	0.0022	18.384	0.0292
9.370	0.0025	18.621	0.0305
9.860	0.0029	18.858	0.0318
10.351	0.0032		
11.251	0.0041		
11.771	0.0047		
12.292	0.0053		
12.796	0.0064		
13.301	0.0074		
13.719	0.0087		
14.138	0.0100		
14.379	0.0112		
14.620	0.0124		
14.861	0.0136		

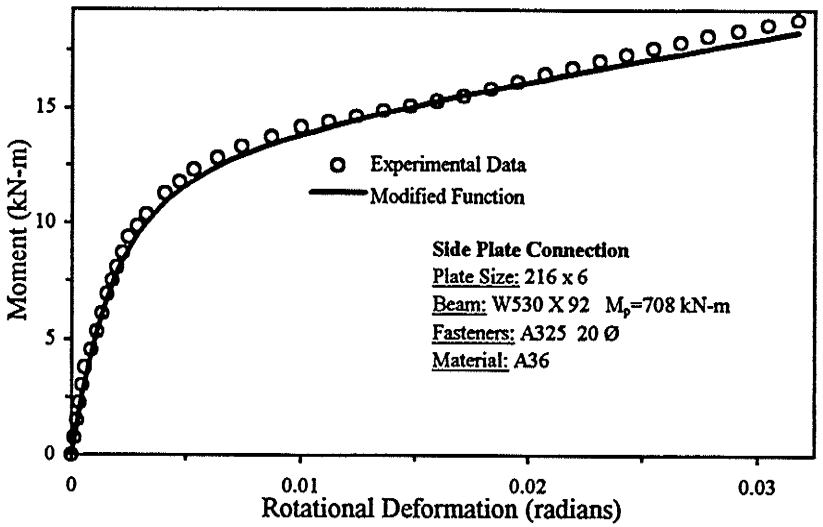


Figure A.23 (a) M-ϕ curve for Lipson: P1-3/1

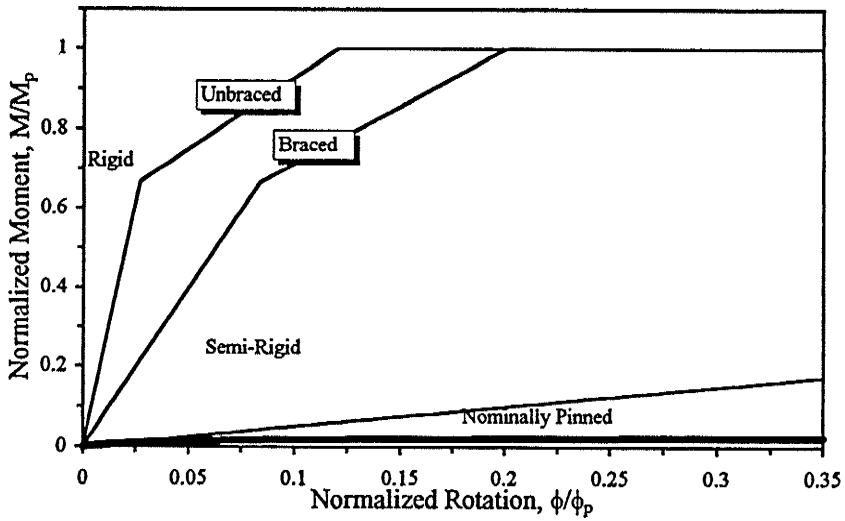


Figure A.23 (b) Eurocode3 Classification of Lipson: P1-3/1

Table A.24 M-ϕ data for Lipson: P1-3/2 (1968)

Moment, M kN-m	Rotation, ϕ radians	Moment, M kN-m	Rotation, ϕ radians
0	0	10.590	0.0374
0.828	0.0002	11.050	0.0397
1.656	0.0003	11.509	0.0420
2.484	0.0005	12.024	0.0439
3.311	0.0006	12.538	0.0457
3.869	0.0009	13.091	0.0476
4.427	0.0012	13.643	0.0495
4.984	0.0016	14.476	0.0522
5.662	0.0021	15.308	0.0549
6.339	0.0027	15.983	0.0577
7.167	0.0034	16.682	0.0598
7.614	0.0039		
8.060	0.0044		
8.719	0.0055		
8.767	0.0063		
8.815	0.0088		
8.862	0.0114		
8.910	0.0139		
8.957	0.0165		
9.005	0.0190		
9.116	0.0217		
9.227	0.0243		
9.338	0.0270		
9.549	0.0297		
9.761	0.0325		
10.175	0.0349		

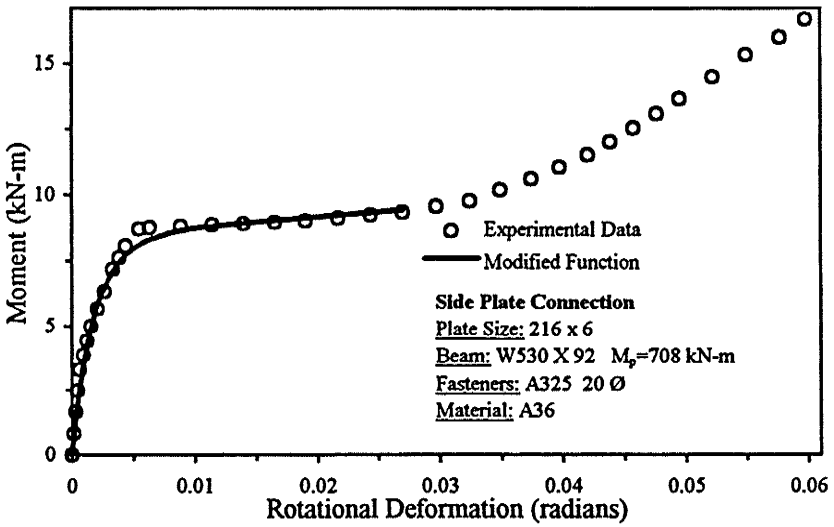


Figure A.24 (a) M-ϕ curve for Lipson: P1-3/2

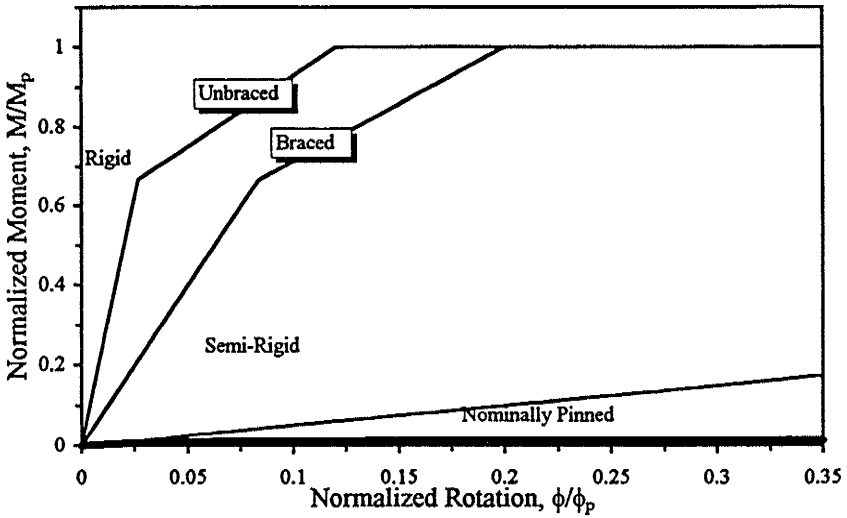


Figure A.24 (b) Eurocode3 Classification of Lipson: P1-3/2

Table A.25 M-ϕ data for Lipson: P1-4/1 (1968)

Moment, M kN-m	Rotation, ϕ radians	Moment, M kN-m	Rotation, ϕ radians
0	0	22.291	0.0225
1.297	0.0002	23.257	0.0237
2.594	0.0004	24.222	0.0248
3.891	0.0006	25.055	0.0261
5.188	0.0007	25.889	0.0273
6.485	0.0009	26.723	0.0285
7.409	0.0011	27.295	0.0298
8.333	0.0013	27.868	0.0311
9.101	0.0015	28.440	0.0324
9.869	0.0018	28.980	0.0339
11.242	0.0024	29.520	0.0354
12.460	0.0030	30.060	0.0369
13.353	0.0041		
13.995	0.0056		
14.260	0.0068		
14.525	0.0080		
14.836	0.0094		
15.147	0.0108		
15.457	0.0122		
15.876	0.0134		
16.295	0.0147		
17.021	0.0160		
17.748	0.0174		
18.753	0.0185		
19.758	0.0196		
21.025	0.0211		

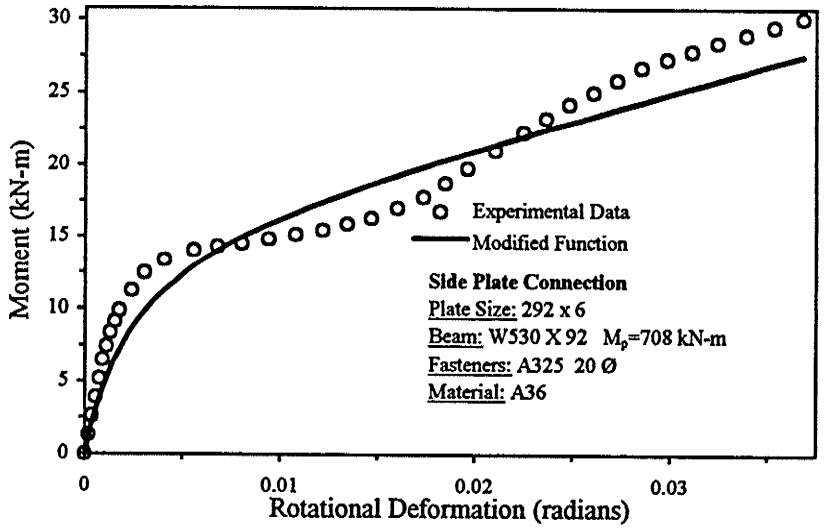


Figure A.25 (a) M-ϕ curve for Lipson: P1-4/1

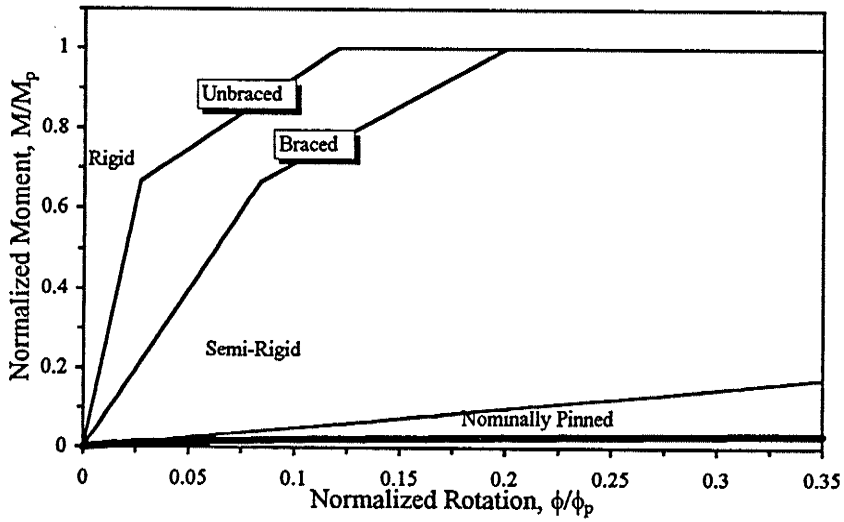


Figure A.25 (b) Eurocode3 Classification of Lipson: P1-4/1

Table A.26 M-ϕ data for Lipson: P1-4/2 (1968)

Moment, M kN-m	Rotation, ϕ radians	Moment, M kN-m	Rotation, ϕ radians
0	0	21.936	0.0222
1.281	0.0002	22.954	0.0234
2.562	0.0004	24.249	0.0251
3.843	0.0006	25.545	0.0268
5.124	0.0008	26.385	0.0282
6.405	0.0010	27.225	0.0296
7.673	0.0013	27.899	0.0313
8.941	0.0017	28.573	0.0330
9.706	0.0020	29.067	0.0343
10.472	0.0022	29.561	0.0356
11.922	0.0029	30.055	0.0369
12.828	0.0036		
13.638	0.0048		
14.215	0.0059		
14.468	0.0075		
14.579	0.0087		
14.690	0.0098		
14.956	0.0110		
15.222	0.0122		
15.789	0.0137		
16.355	0.0151		
16.935	0.0162		
17.515	0.0173		
18.708	0.0186		
19.901	0.0199		
20.919	0.0211		

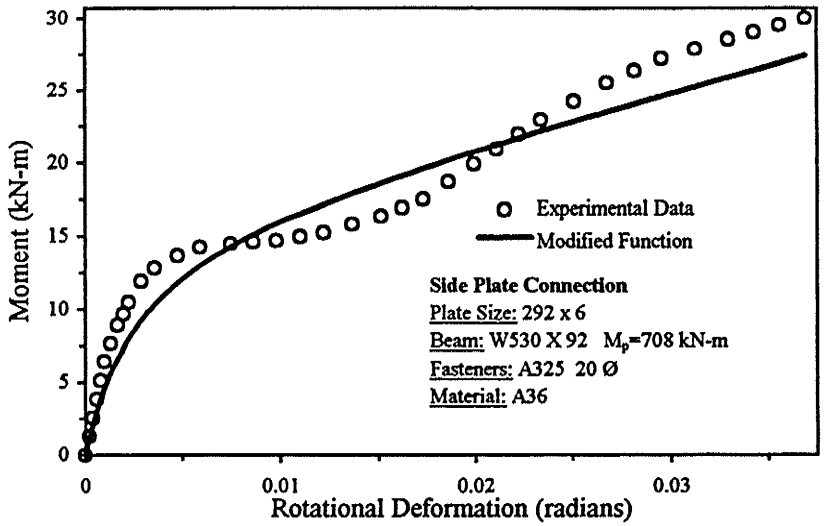


Figure A.26 (a) M-ϕ curve for Lipson: P1-4/2

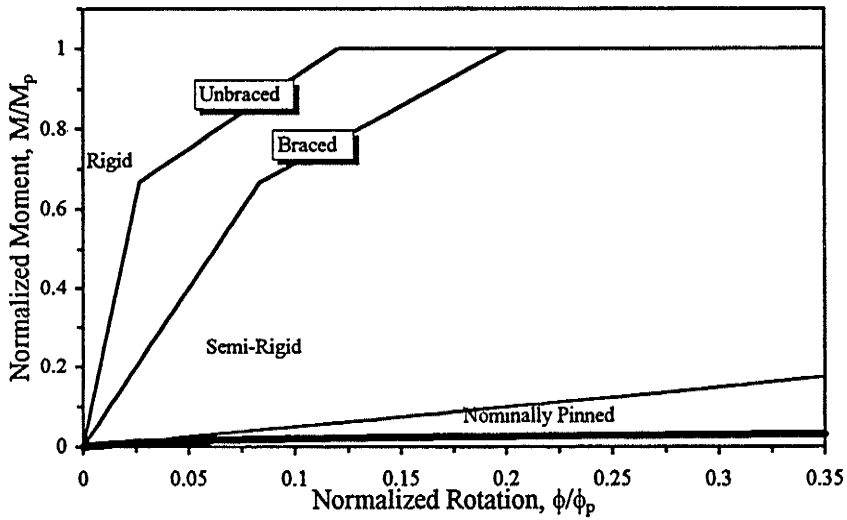


Figure A.26 (b) Eurocode3 Classification of Lipson: P1-4/2

Table A.27 M-ϕ data for Lipson: P1-5/1 (1968)

Moment, M kN-m	Rotation, ϕ radians	Moment, M kN-m	Rotation, ϕ radians
0	0	45.269	0.0175
2.354	0.0002	45.898	0.0187
4.707	0.0003	46.527	0.0198
7.061	0.0005	47.147	0.0212
9.414	0.0006	47.768	0.0227
11.768	0.0008	48.388	0.0241
13.597	0.0010	48.788	0.0251
15.427	0.0012	49.188	0.0262
17.257	0.0014	49.588	0.0273
19.319	0.0016	49.933	0.0284
21.381	0.0018	50.279	0.0295
23.442	0.0020	50.625	0.0307
25.906	0.0025		
28.369	0.0031		
30.899	0.0039		
33.429	0.0048		
35.557	0.0060		
37.685	0.0072		
38.920	0.0084		
40.154	0.0097		
40.940	0.0108		
41.727	0.0119		
42.514	0.0130		
43.223	0.0141		
43.931	0.0152		
44.640	0.0163		

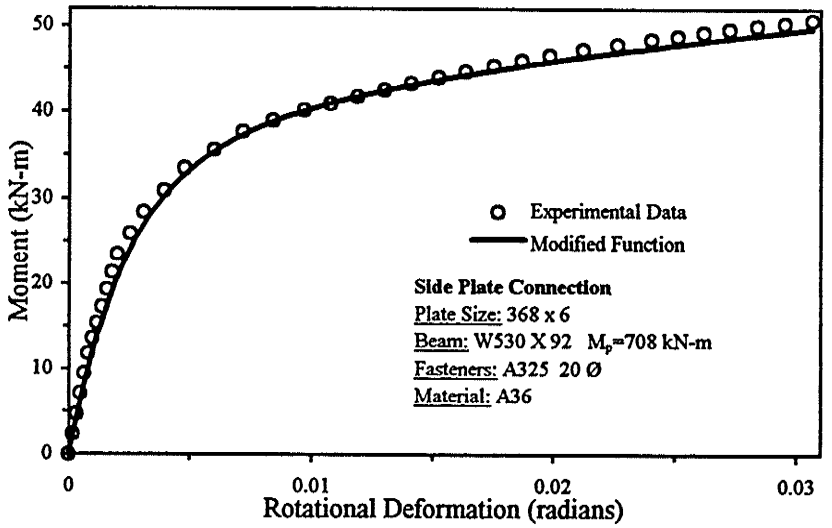


Figure A.27 (a) M-ϕ curve for Lipson: P1-5/1

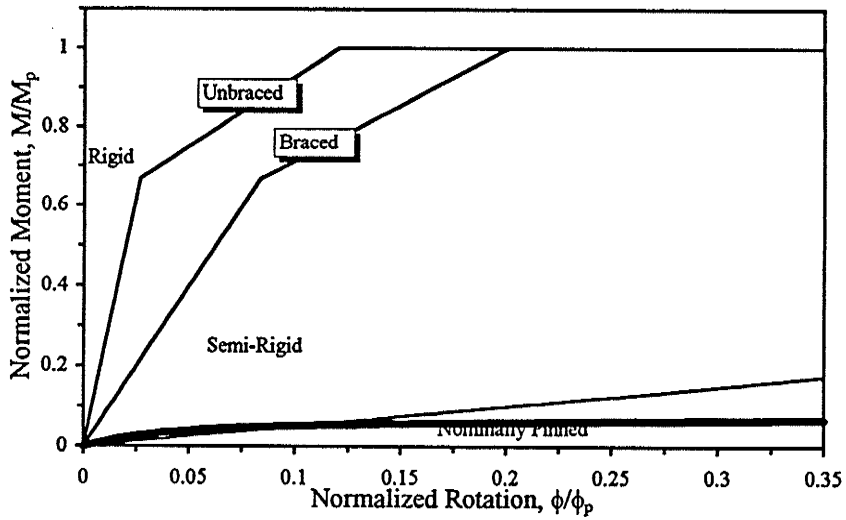


Figure A.27 (b) Eurocode3 Classification of Lipson: P1-5/1

Table A.28 M-ϕ data for Lipson: P1-5/2 (1968)

Moment, M kN-m	Rotation, ϕ radians	Moment, M kN-m	Rotation, ϕ radians
0	0	35.517	0.0237
2.498	0.0001	36.970	0.0243
4.996	0.0003	38.563	0.0252
7.494	0.0004	40.829	0.0269
9.992	0.0005	43.095	0.0286
11.768	0.0008	44.935	0.0302
13.545	0.0010	46.776	0.0319
15.322	0.0012	47.780	0.0330
17.243	0.0017	48.784	0.0342
19.165	0.0022	49.882	0.0360
21.086	0.0027	50.035	0.0371
22.736	0.0033	50.189	0.0381
24.385	0.0038		
26.663	0.0051		
27.096	0.0060		
27.111	0.0077		
27.217	0.0090		
27.324	0.0103		
27.430	0.0116		
27.788	0.0135		
28.145	0.0153		
28.786	0.0169		
29.428	0.0184		
30.760	0.0201		
32.864	0.0220		
34.064	0.0231		

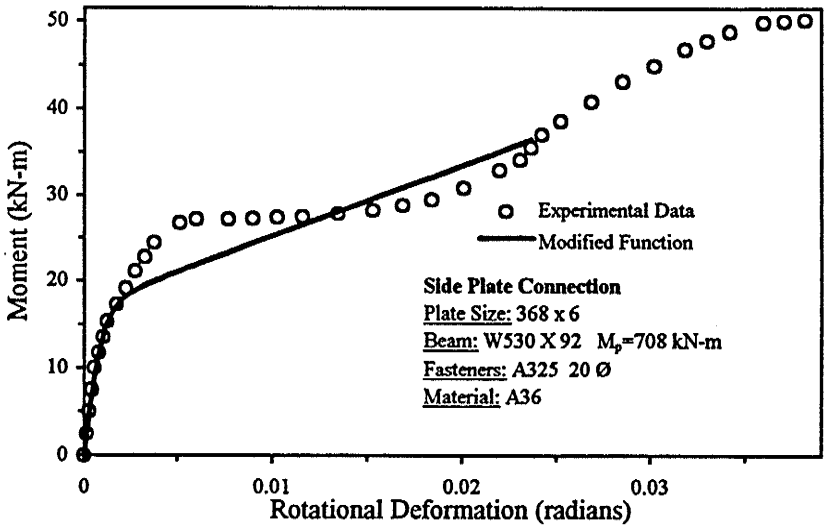


Figure A.28 (a) M-ϕ curve for Lipson: P1-5/2

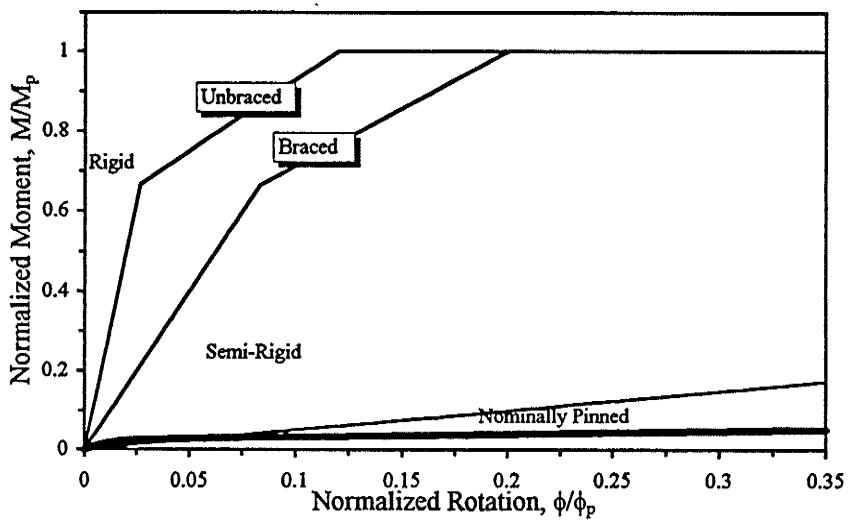


Figure A.28 (b) Eurocode3 Classification of Lipson: P1-5/2

Table A.29 M-ϕ data for Lipson: P1-6/1 (1968)

Moment, M kN-m	Rotation, ϕ radians	Moment, M kN-m	Rotation, ϕ radians
0	0	54.732	0.0138
3.737	0.0001	56.184	0.0146
7.474	0.0003	58.949	0.0157
11.211	0.0004	61.713	0.0168
14.949	0.0006	63.743	0.0178
18.686	0.0007	65.773	0.0188
21.215	0.0009	67.187	0.0196
23.745	0.0011	68.601	0.0204
26.275	0.0013	69.871	0.0213
29.142	0.0015	71.141	0.0222
32.010	0.0017	72.410	0.0230
34.019	0.0020	74.007	0.0243
36.029	0.0023	75.603	0.0255
38.426	0.0026		
40.737	0.0033		
42.119	0.0038		
43.260	0.0047		
44.627	0.0058		
45.575	0.0066		
46.523	0.0074		
47.810	0.0086		
49.096	0.0098		
49.777	0.0105		
50.458	0.0111		
51.600	0.0120		
53.279	0.0130		

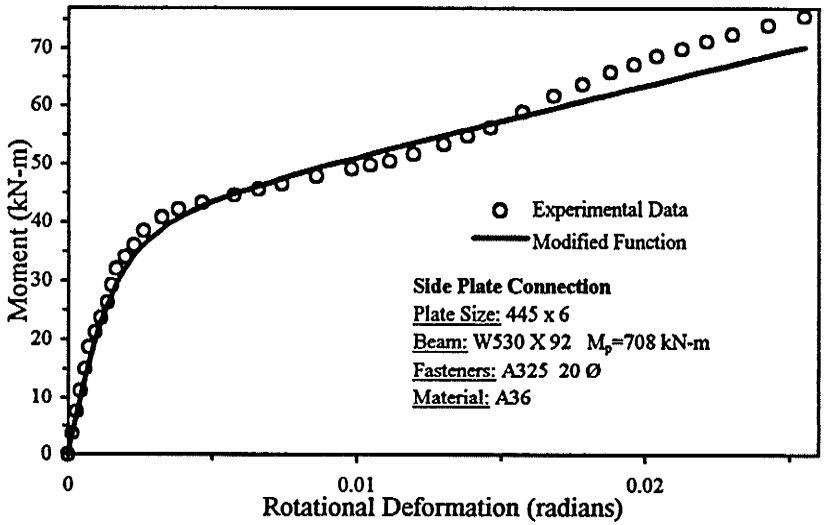


Figure A.29 (a) M-ϕ curve for Lipson: P1-6/1

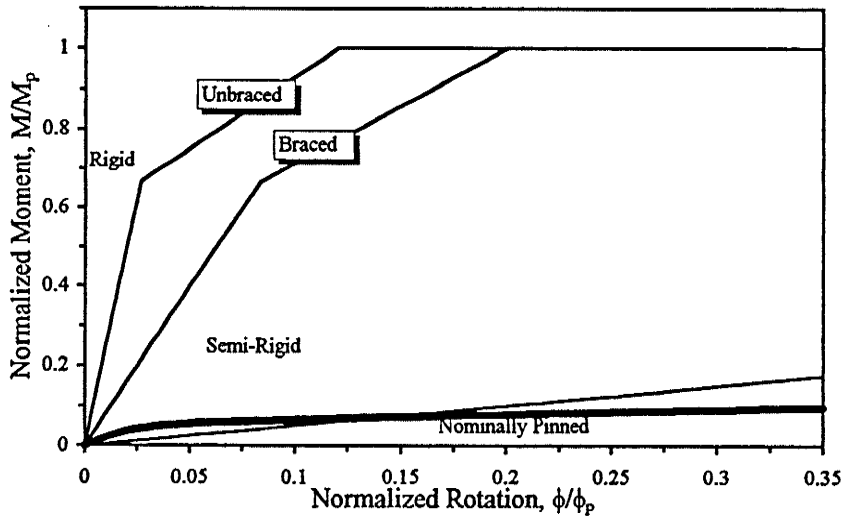


Figure A.29 (b) Eurocode3 Classification of Lipson: P1-6/1

Table A.30 M-ϕ data for Lipson: P1-6/2 (1968)

Moment, M kN-m	Rotation, ϕ radians	Moment, M kN-m	Rotation, ϕ radians
0	0	59.414	0.0125
3.114	0.0001	61.780	0.0138
6.228	0.0002	63.337	0.0149
9.342	0.0003	64.894	0.0160
12.455	0.0004	65.900	0.0170
15.569	0.0005	66.905	0.0180
19.212	0.0006	67.911	0.0189
22.854	0.0007	69.115	0.0202
26.496	0.0007	70.319	0.0214
30.139	0.0008	71.346	0.0225
33.781	0.0009	72.373	0.0236
36.359	0.0011	73.399	0.0248
38.936	0.0014	74.419	0.0257
41.514	0.0016	75.438	0.0266
44.910	0.0021		
47.300	0.0026		
49.436	0.0038		
50.228	0.0045		
51.020	0.0053		
51.385	0.0061		
51.749	0.0069		
52.151	0.0077		
52.552	0.0086		
53.369	0.0098		
54.820	0.0106		
56.270	0.0113		

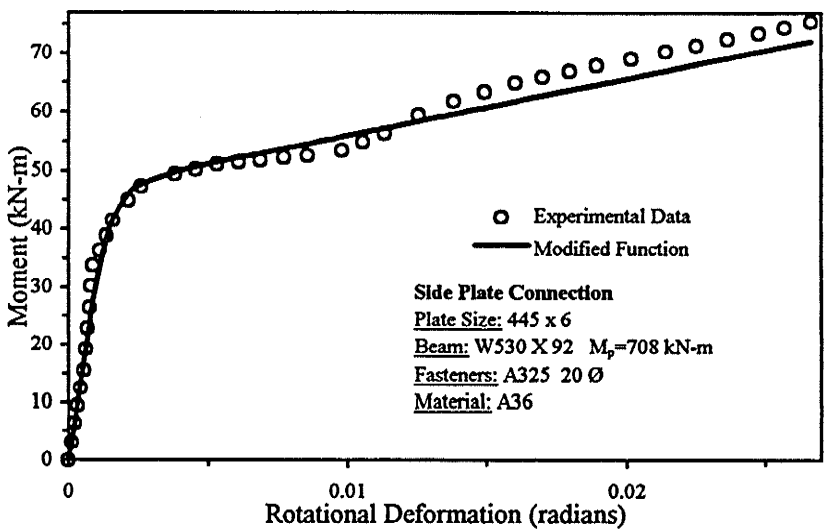


Figure A.30 (a) M-ϕ curve for Lipson: P1-6/2

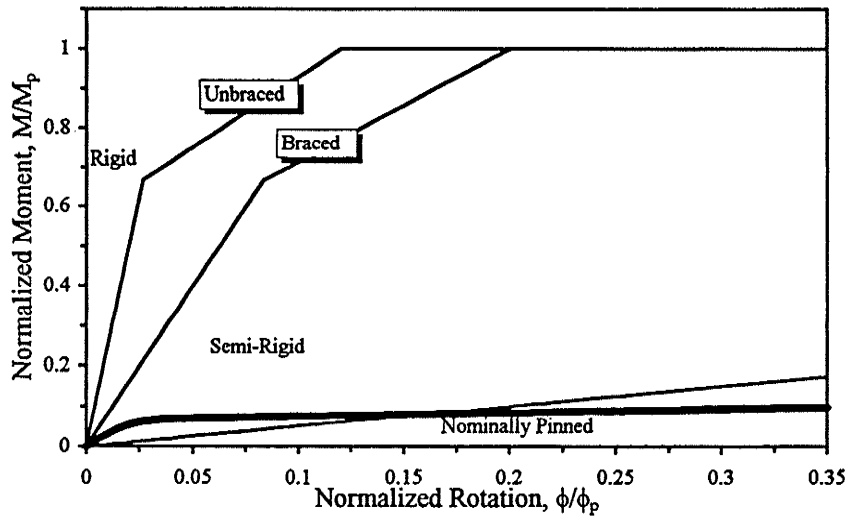


Figure A.30 (b) Eurocode3 Classification of Lipson: P1-6/2

Table A.31 M-ϕ data for Thompson: F-1 alt a (1970)

Moment, M kN-m	Rotation, ϕ radians	Moment, M kN-m	Rotation, ϕ radians
0	0	69.840	0.0426
4.858	0.0004	70.504	0.0454
9.716	0.0007	71.168	0.0483
13.909	0.0011	71.833	0.0511
18.103	0.0014	74.324	0.0530
21.758	0.0018	76.815	0.0549
25.412	0.0021	82.961	0.0557
29.938	0.0027	89.106	0.0565
34.464	0.0032	95.667	0.0573
38.159	0.0038	102.227	0.0581
41.854	0.0043	108.289	0.0589
46.006	0.0051	114.351	0.0597
49.826	0.0066	119.874	0.0605
51.903	0.0090	125.397	0.0612
53.979	0.0113	129.300	0.0618
55.363	0.0134	133.203	0.0623
56.747	0.0156	139.099	0.0631
58.131	0.0177		
59.169	0.0208		
60.207	0.0238		
61.591	0.0261		
62.975	0.0285		
64.359	0.0308		
66.435	0.0339		
68.511	0.0369		
69.175	0.0397		

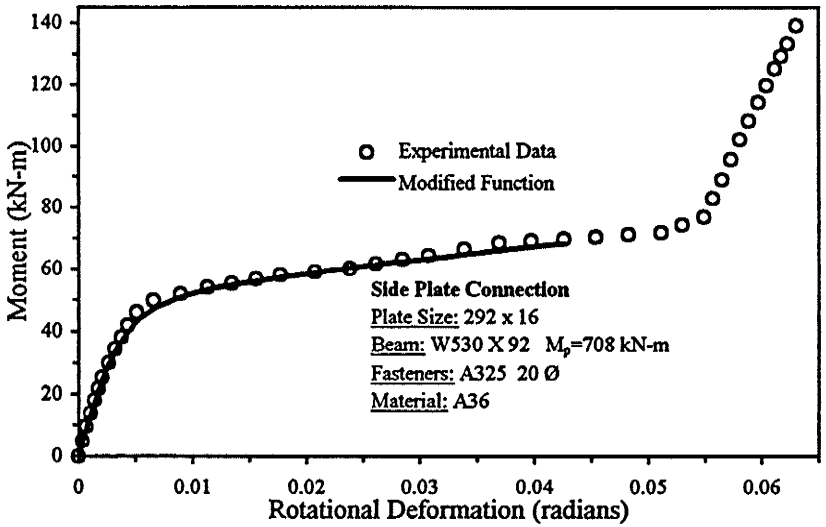


Figure A.31 (a) M-ϕ curve for Thompson: F-1 alt a

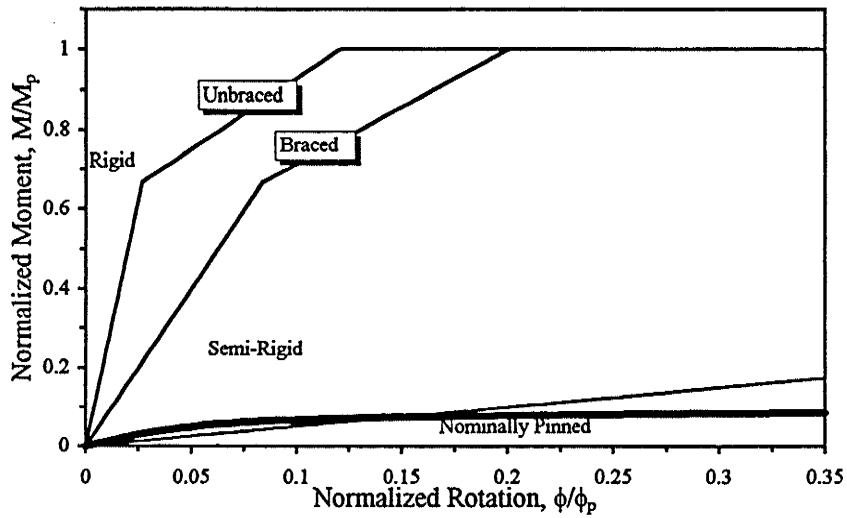


Figure A.31 (b) Eurocode3 Classification of Thompson: F-1 alt a

Table A.32 M-ϕ data for Thompson: F-1 alt b (1970)

Moment, M kN-m	Rotation, ϕ radians	Moment, M kN-m	Rotation, ϕ radians
0	0	74.740	0.0442
4.858	0.0003	75.259	0.0472
9.716	0.0006	75.777	0.0502
13.909	0.0009	76.296	0.0532
18.103	0.0012	76.815	0.0562
21.758	0.0015	79.930	0.0589
25.412	0.0018	83.044	0.0616
29.938	0.0023	88.919	0.0625
34.464	0.0027	94.795	0.0634
38.159	0.0032	101.625	0.0642
41.854	0.0036	108.456	0.0649
45.840	0.0043	114.020	0.0656
49.826	0.0050	119.583	0.0663
56.055	0.0065	124.566	0.0670
60.207	0.0096	129.549	0.0677
60.726	0.0126	135.278	0.0691
61.245	0.0155	139.099	0.0712
61.764	0.0185		
62.284	0.0214		
62.976	0.0240		
63.667	0.0265		
64.359	0.0291		
65.743	0.0321		
67.127	0.0350		
68.511	0.0380		
71.625	0.0411		

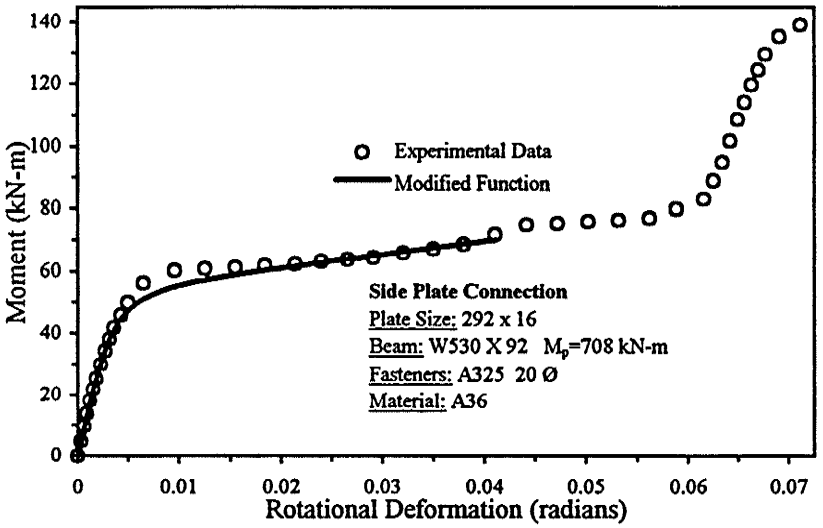


Figure A.32 (a) M-ϕ curve for Thompson: F-1 alt b

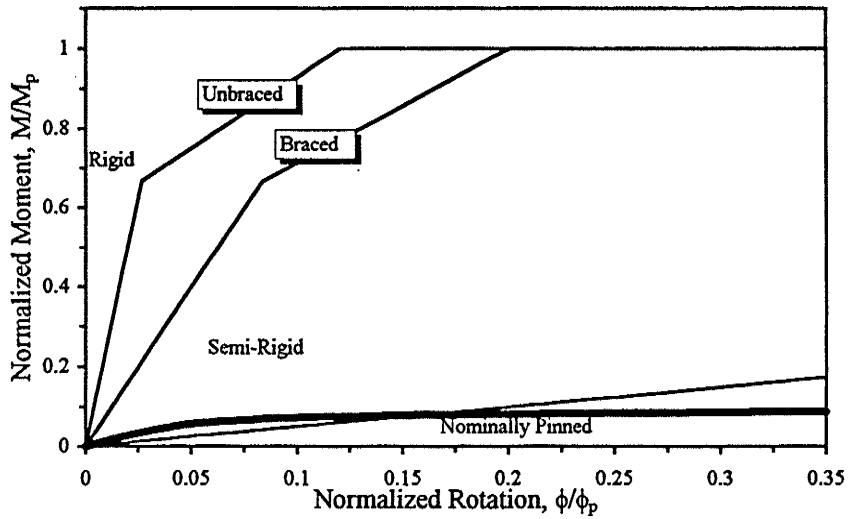


Figure A.32 (b) Eurocode3 Classification of Thompson: F-1 alt b

Table A.33 M-ϕ data for Thompson: G-1 alt a (1970)

Moment, M kN-m	Rotation, ϕ radians	Moment, M kN-m	Rotation, ϕ radians
0	0	74.221	0.0532
4.775	0.0004	74.740	0.0559
9.550	0.0007	79.390	0.0593
13.744	0.0011	84.041	0.0627
17.937	0.0014	88.276	0.0633
21.924	0.0018	92.512	0.0639
25.910	0.0022	97.079	0.0644
29.979	0.0027	101.646	0.0650
34.047	0.0031	106.214	0.0655
38.283	0.0039	111.653	0.0663
42.519	0.0047	117.093	0.0671
45.675	0.0062	118.545	0.0697
47.460	0.0094	119.998	0.0723
49.245	0.0125		
50.823	0.0159		
52.401	0.0192		
53.979	0.0226		
55.723	0.0257		
57.466	0.0287		
60.456	0.0318		
63.446	0.0350		
66.435	0.0381		
69.549	0.0415		
72.664	0.0449		
73.183	0.0477		
73.702	0.0504		

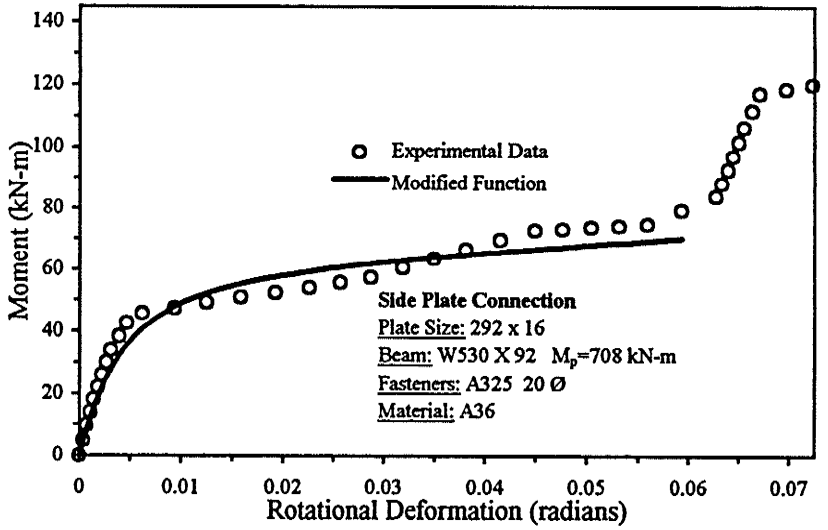


Figure A.33 (a) M-ϕ curve for Thompson: G-1 alt a

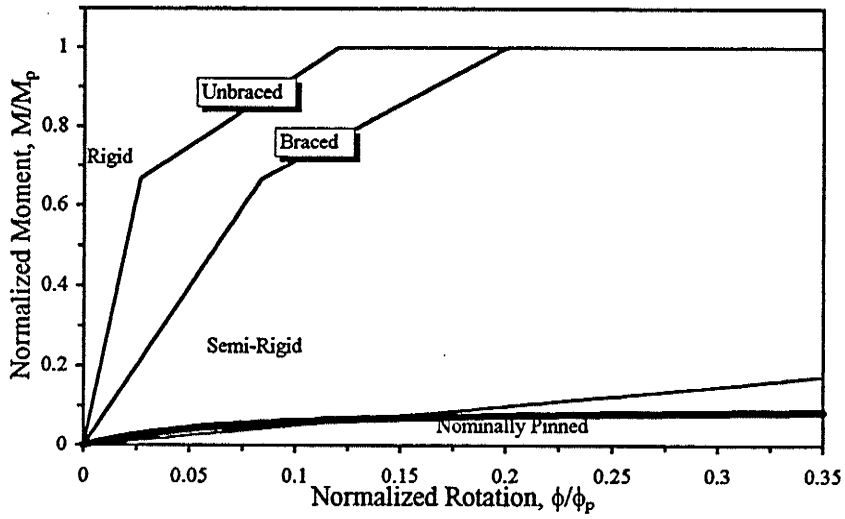


Figure A.33 (b) Eurocode3 Classification of Thompson: G-1 alt a

Table A.34 M-ϕ data for Thompson: G-1 alt b (1970)

Moment, M kN-m	Rotation, ϕ radians	Moment, M kN-m	Rotation, ϕ radians
0	0	79.972	0.0492
4.775	0.0003	83.044	0.0527
9.550	0.0006	83.293	0.0560
13.744	0.0009	83.542	0.0594
17.937	0.0012	83.791	0.0627
21.924	0.0015	84.041	0.0660
25.910	0.0018	88.276	0.0665
29.979	0.0023	92.512	0.0669
34.047	0.0027	97.660	0.0674
38.283	0.0033	102.809	0.0679
42.519	0.0039	107.957	0.0685
45.675	0.0046	113.105	0.0690
47.460	0.0081	116.552	0.0696
49.245	0.0116	119.998	0.0701
50.428	0.0144		
51.612	0.0171		
52.796	0.0199		
53.979	0.0226		
55.142	0.0250		
56.304	0.0274		
57.466	0.0298		
62.989	0.0331		
68.511	0.0364		
71.307	0.0395		
74.103	0.0426		
76.899	0.0457		
79.97168688	0.0492		
83.043975	0.0527		
83.29310693	0.056025		
83.54223885	0.05935		
83.79137078	0.062675		

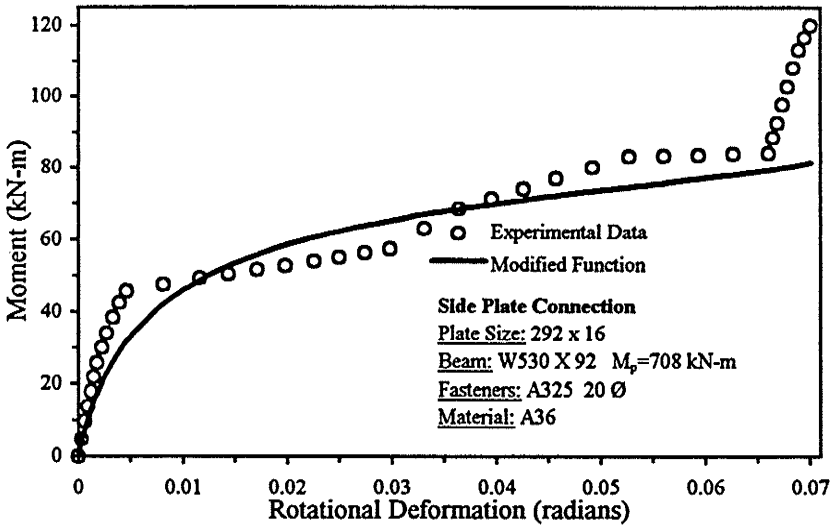


Figure A.34 (a) M-ϕ curve for Thompson: G-1 alt b

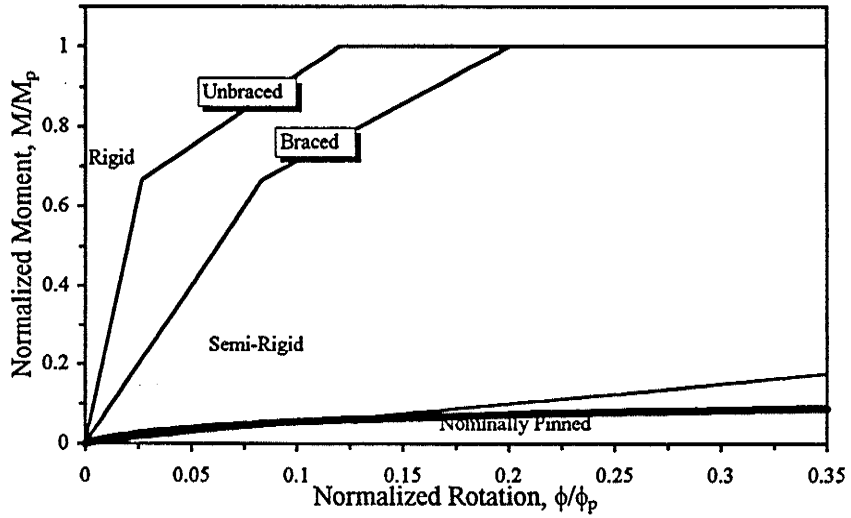


Figure A.34 (b) Eurocode3 Classification of Thompson: G-1 alt b

Table A.35 M-ϕ data for Thompson: H-1 alt a (1970)

Moment, M kN-m	Rotation, ϕ radians	Moment, M kN-m	Rotation, ϕ radians
0	0	68.511	0.0328
2.948	0.0002	69.514	0.0354
5.896	0.0004	70.516	0.0379
10.090	0.0007	72.628	0.0396
13.537	0.0010	74.740	0.0413
18.020	0.0014	75.072	0.0439
22.173	0.0018	75.404	0.0465
26.242	0.0023	75.736	0.0490
30.186	0.0027	76.068	0.0516
34.047	0.0032	78.892	0.0521
38.283	0.0039	83.127	0.0526
42.104	0.0046	86.448	0.0529
44.512	0.0052	89.770	0.0532
46.920	0.0058	92.365	0.0535
47.944	0.0081	94.960	0.0538
48.968	0.0103		
49.992	0.0126		
51.819	0.0140		
53.647	0.0153		
55.142	0.0177		
56.637	0.0200		
58.422	0.0219		
60.207	0.0237		
62.324	0.0259		
64.442	0.0280		
66.477	0.0304		

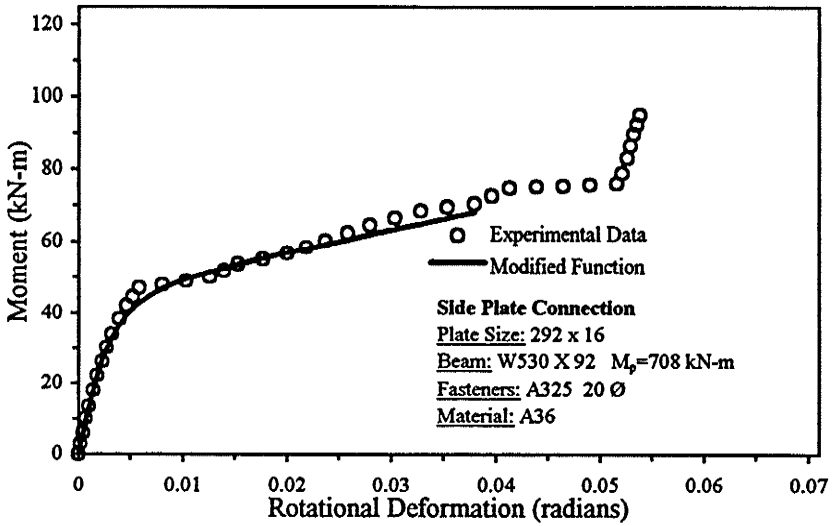


Figure A.35 (a) M-ϕ curve for Thompson: H-1 alt a

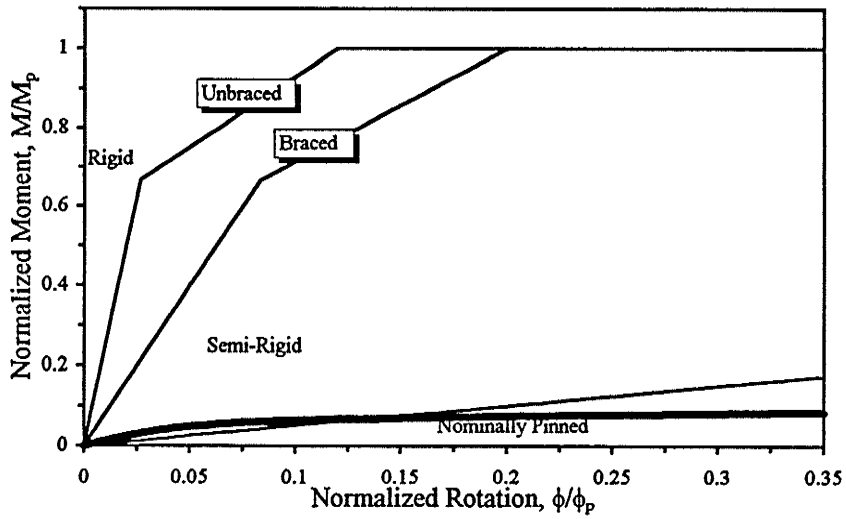


Figure A.35 (b) Eurocode3 Classification of Thompson: H-1 alt a

Table A.36 M-ϕ data for Thompson: H-1 alt b (1970)

Moment, M kN-m	Rotation, ϕ radians	Moment, M kN-m	Rotation, ϕ radians
0	0	71.625	0.0398
2.948	0.0002	74.740	0.0429
5.896	0.0004	76.816	0.0454
10.090	0.0007	78.892	0.0480
13.537	0.0010	80.968	0.0505
18.020	0.0014	81.508	0.0538
22.173	0.0017	82.047	0.0572
26.242	0.0021	82.587	0.0605
30.186	0.0025	83.127	0.0638
34.047	0.0029	85.120	0.0657
38.283	0.0034	88.691	0.0676
42.104	0.0039	92.262	0.0694
44.512	0.0044	94.960	0.0723
46.920	0.0048		
49.992	0.0057		
53.647	0.0089		
54.145	0.0120		
54.644	0.0150		
55.142	0.0181		
55.640	0.0212		
56.138	0.0242		
56.637	0.0273		
59.584	0.0295		
62.532	0.0316		
65.521	0.0341		
68.511	0.0366		

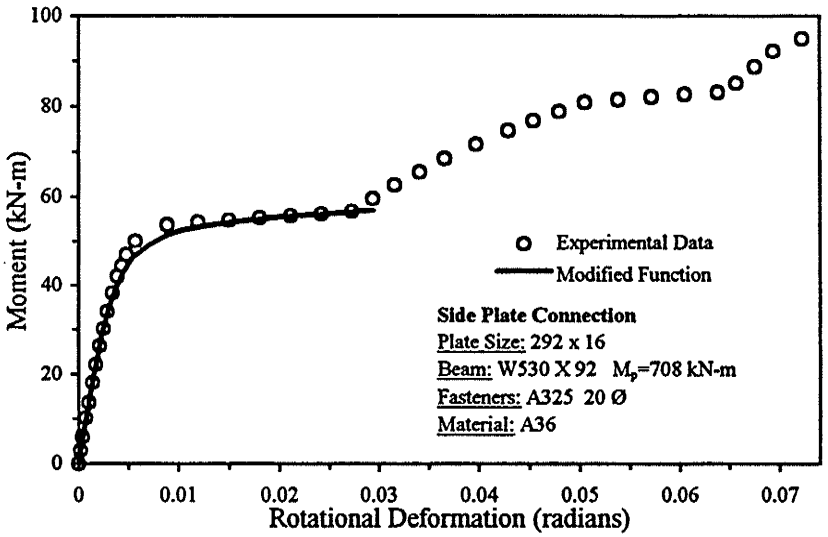


Figure A.36 (a) M-ϕ curve for Thompson: H-1 alt b

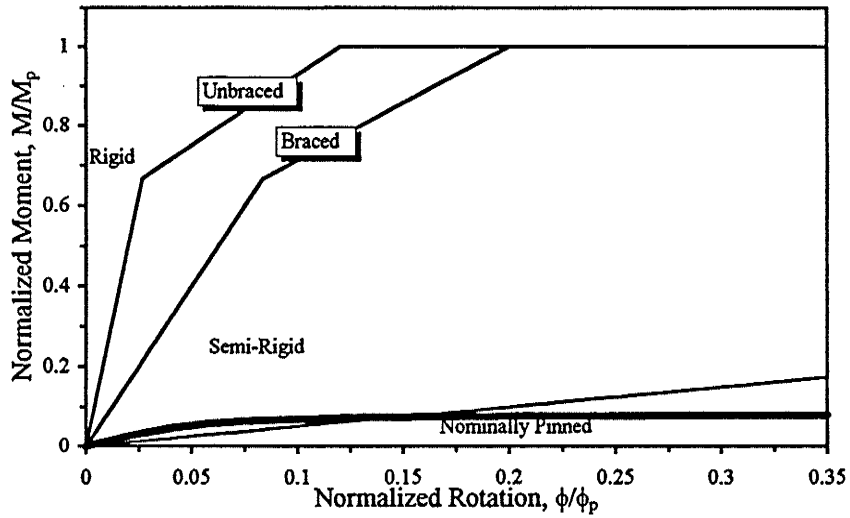


Figure A.36 (b) Eurocode3 Classification of Thompson: H-1 alt b

Table A.37 M-ϕ data for Thompson: F-2-1 alt a (1970)

Moment, M kN-m	Rotation, ϕ radians	Moment, M kN-m	Rotation, ϕ radians
0	0	88.940	0.0613
5.647	0.0004	95.667	0.0632
9.468	0.0007	105.632	0.0654
13.287	0.0011	115.182	0.0654
17.024	0.0018	125.230	0.0668
21.259	0.0029	133.285	0.0679
24.996	0.0045	141.756	0.0691
29.066	0.0063	149.729	0.0703
33.135	0.0085	158.282	0.0717
37.619	0.0106	166.088	0.0731
42.186	0.0127	174.376	0.0751
45.840	0.0149	182.697	0.0773
49.826	0.0171	190.752	0.0799
54.394	0.0201	199.720	0.0831
58.213	0.0229	207.942	0.0868
62.366	0.0262		
66.103	0.0297		
68.642	0.0327		
71.182	0.0357		
73.721	0.0387		
78.892	0.0413		
81.633	0.0436		
84.373	0.0458		
85.515	0.0497		
86.657	0.0536		
87.798	0.0574		

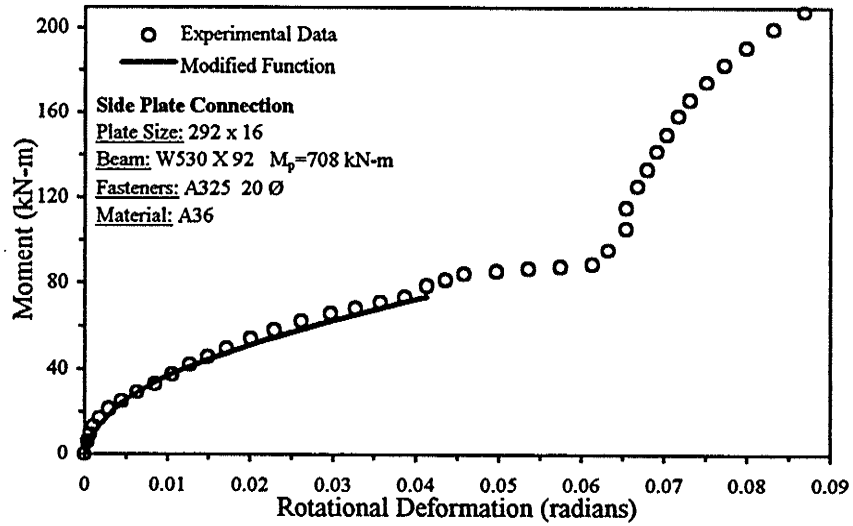


Figure A.37 (a) M-ϕ curve for Thompson: F-2-1 alt a

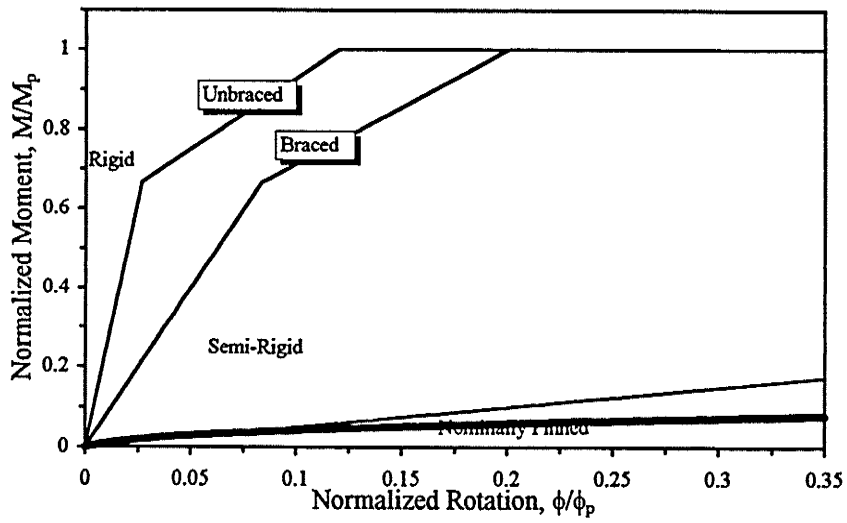


Figure A.37 (b) Eurocode3 Classification of Thompson: F-2-1 alt a

Table A.38 M-ϕ data for Thompson: F-2-1 alt b (1970)

Moment, M kN-m	Rotation, ϕ radians	Moment, M kN-m	Rotation, ϕ radians
0	0	93.985	0.0698
5.647	0.0005	95.667	0.0748
9.468	0.0008	105.632	0.0785
13.287	0.0012	115.182	0.0785
17.024	0.0017	125.230	0.0799
21.259	0.0030	133.285	0.0810
23.128	0.0062	141.756	0.0823
24.996	0.0094	149.729	0.0837
29.066	0.0134	158.282	0.0852
33.135	0.0162	166.088	0.0868
37.619	0.0203	174.376	0.0888
42.186	0.0230	182.697	0.0910
45.840	0.0248	190.752	0.0935
49.826	0.0265	199.720	0.0969
54.394	0.0288	207.942	0.1008
58.213	0.0311		
62.366	0.0332		
66.103	0.0357		
69.912	0.0395		
73.721	0.0432		
78.892	0.0461		
81.633	0.0487		
84.373	0.0513		
88.940	0.0547		
90.622	0.0597		
92.304	0.0648		

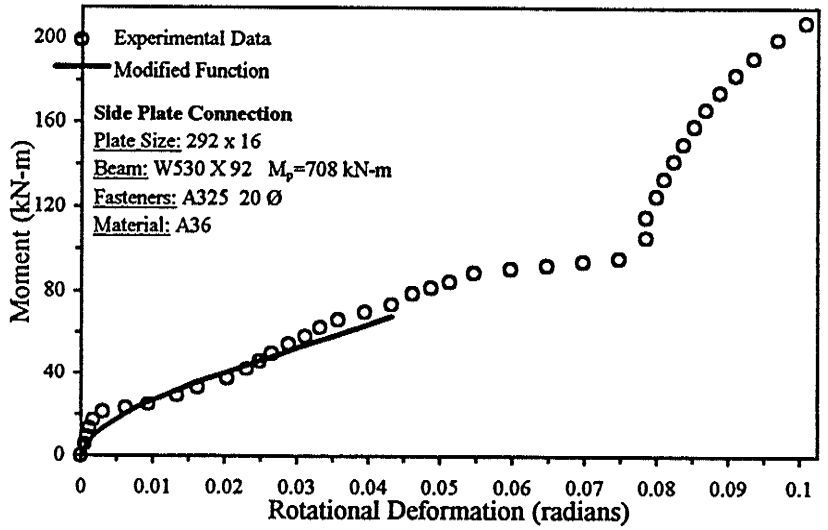


Figure A.38 (a) M-ϕ curve for Thompson: F-2-1 alt b

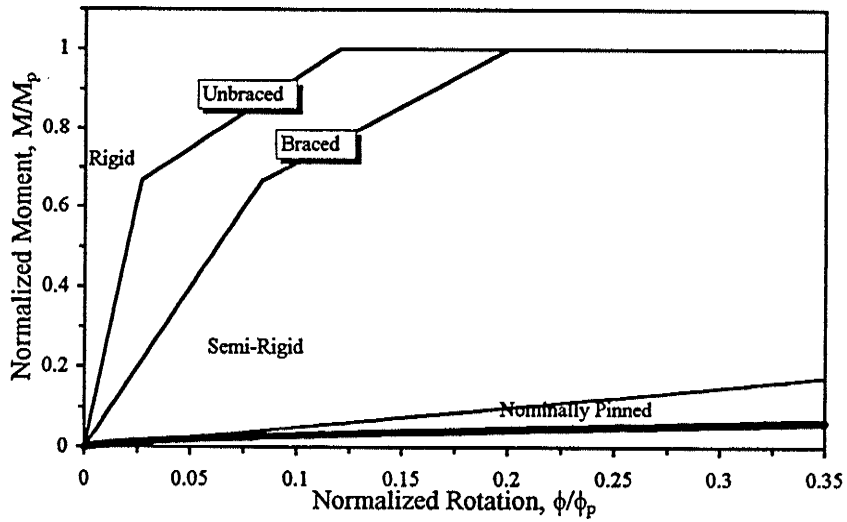


Figure A.38 (b) Eurocode3 Classification of Thompson: F-2-1 alt b

Table A.39 M-ϕ data for Thompson: F-2-2 alt a (1970)

Moment, M kN-m	Rotation, ϕ radians	Moment, M kN-m	Rotation, ϕ radians
0	0	142.171	0.0538
5.812	0.0001	148.067	0.0549
13.702	0.0008	153.963	0.0560
21.591	0.0014	160.275	0.0574
29.481	0.0023	166.587	0.0587
37.204	0.0044	172.649	0.0603
41.563	0.0080	178.711	0.0618
45.923	0.0115	187.015	0.0643
49.992	0.0143	195.319	0.0662
54.062	0.0171	203.458	0.0694
58.173	0.0201	207.610	0.0712
62.284	0.0230	212.095	0.0733
66.436	0.0258	215.914	0.0752
70.588	0.0286	220.233	0.0780
75.903	0.0321	224.219	0.0811
78.283	0.0364	228.704	0.0853
80.664	0.0406	230.032	0.0897
83.044	0.0449		
89.064	0.0465		
95.085	0.0480		
104.221	0.0491		
110.657	0.0498		
117.093	0.0505		
123.362	0.0513		
129.631	0.0520		
135.901	0.0529		

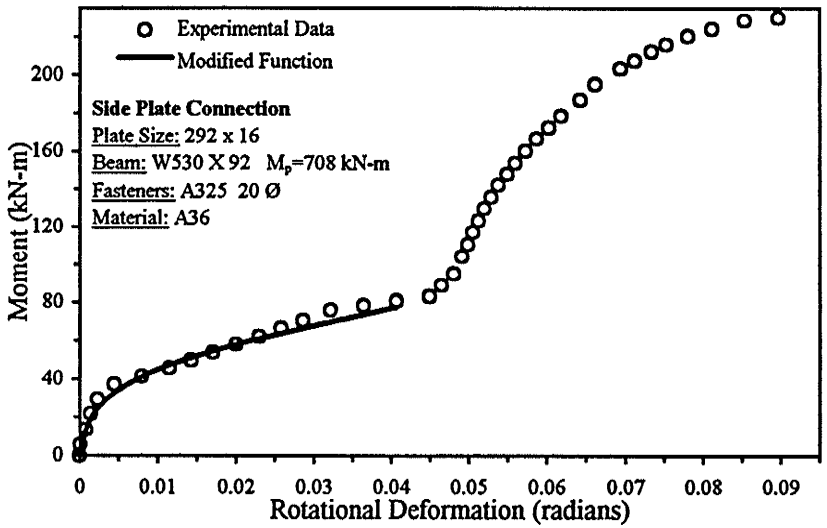


Figure A.39 (a) M-ϕ curve for Thompson: F-2-2 alt a

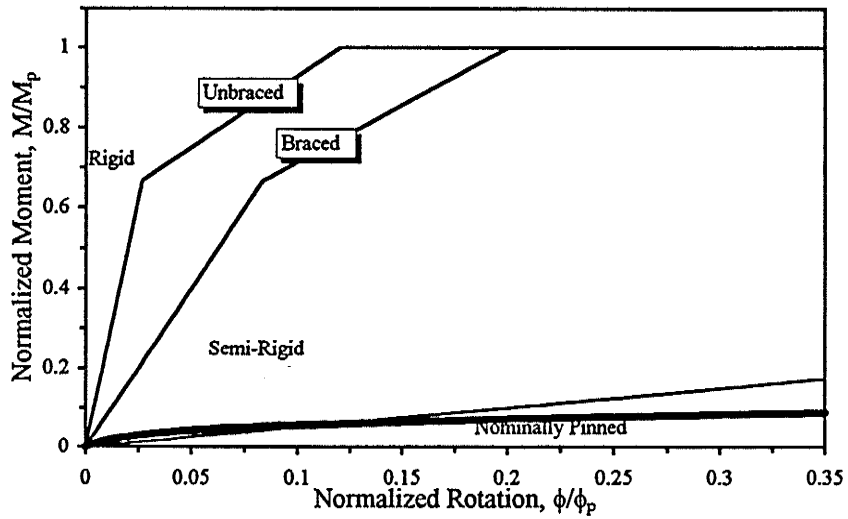


Figure A.39 (b) Eurocode3 Classification of Thompson: F-2-2 alt a

Table A.40 M-ϕ data for Thompson: F-2-2 alt b (1970)

Moment, M kN-m	Rotation, ϕ radians	Moment, M kN-m	Rotation, ϕ radians
0	0	142.171	0.0567
5.812	0.0003	148.067	0.0577
13.702	0.0011	153.963	0.0586
21.591	0.0019	160.275	0.0598
29.481	0.0031	166.587	0.0610
37.204	0.0051	172.649	0.0624
45.923	0.0082	178.711	0.0637
54.062	0.0117	187.015	0.0658
62.284	0.0152	195.319	0.0682
66.436	0.0176	203.458	0.0712
70.588	0.0199	207.610	0.0728
75.903	0.0233	212.095	0.0749
79.473	0.0258	215.914	0.0767
83.044	0.0282	220.233	0.0791
87.058	0.0312	224.219	0.0819
91.071	0.0343	228.704	0.0855
95.085	0.0373	230.032	0.0892
97.369	0.0408		
99.653	0.0444		
101.937	0.0479		
104.221	0.0514		
110.657	0.0524		
117.093	0.0534		
123.362	0.0542		
129.631	0.0549		
135.901	0.0558		

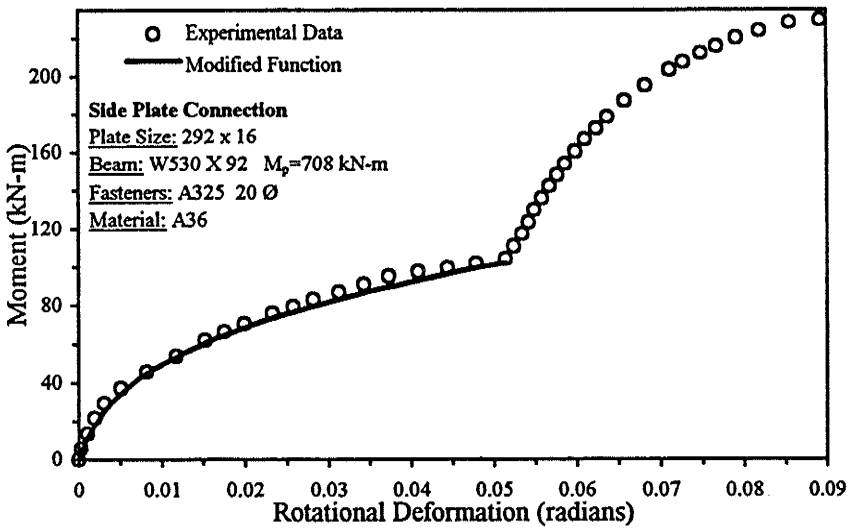


Figure A.40 (a) M-ϕ curve for Thompson: F-2-2 alt b

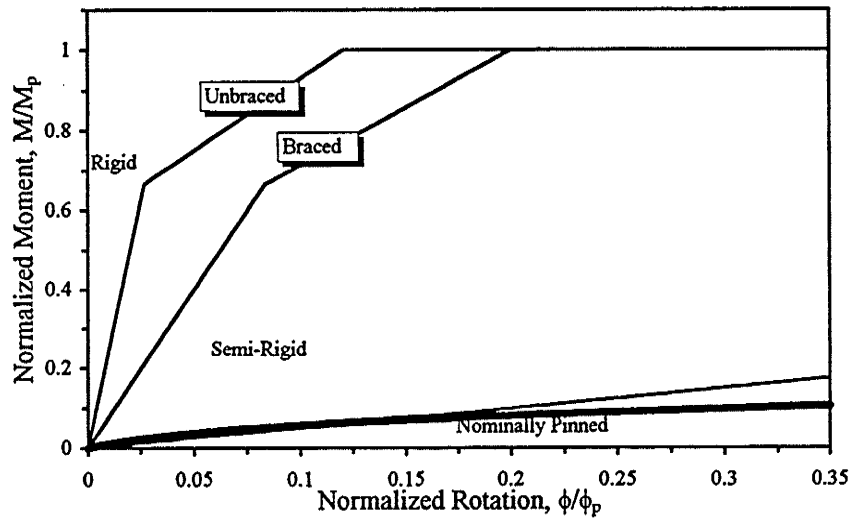


Figure A.40 (b) Eurocode3 Classification of Thompson: F-2-2 alt b

Table A.41 M-ϕ data for Thompson: F-2-3 alt a (1970)

Moment, M kN-m	Rotation, ϕ radians	Moment, M kN-m	Rotation, ϕ radians
0	0	164.323	0.0628
4.900	0.0002	170.448	0.0641
14.616	0.0010	176.282	0.0657
21.094	0.0031	182.115	0.0672
25.080	0.0059	188.178	0.0693
29.066	0.0087	194.240	0.0714
37.370	0.0135	203.707	0.0749
45.508	0.0179	207.445	0.0767
49.453	0.0205	211.846	0.0788
53.398	0.0230	216.413	0.0814
57.841	0.0256	220.399	0.0841
62.284	0.0282	224.432	0.0879
70.588	0.0324	225.654	0.0916
78.892	0.0368	226.876	0.0952
83.460	0.0409	224.219	0.0978
88.027	0.0450		
92.594	0.0491		
97.161	0.0532		
107.874	0.0542		
115.515	0.0550		
123.155	0.0558		
133.369	0.0574		
139.514	0.0584		
145.658	0.0593		
151.928	0.0604		
158.198	0.0615		

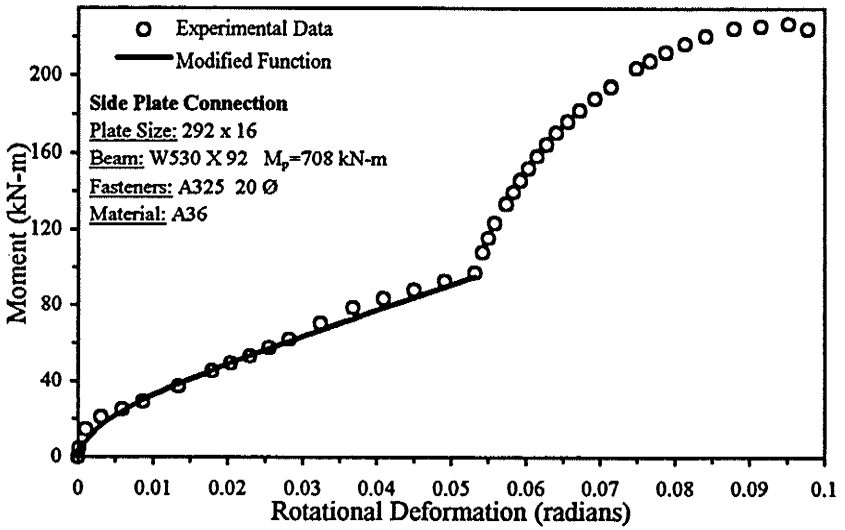


Figure A.41 (a) M-ϕ curve for Thompson: F-2-3 alt a

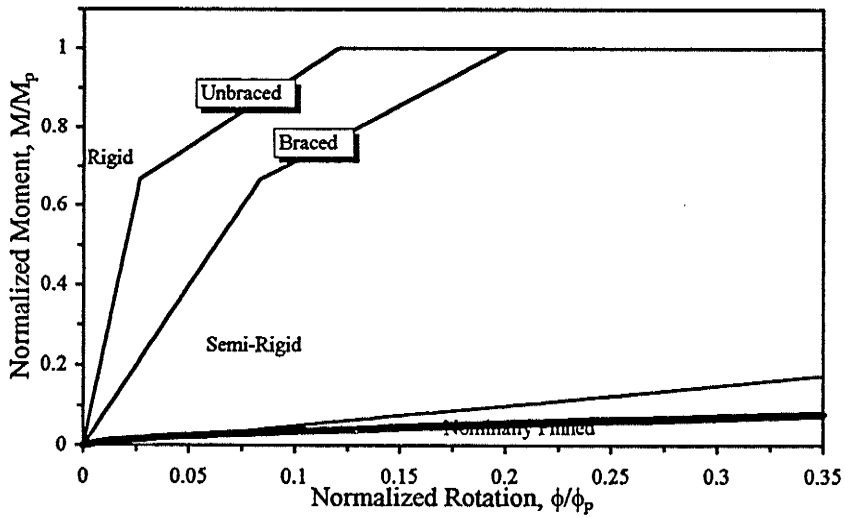


Figure A.41 (b) Eurocode3 Classification of Thompson: F-2-3 alt a

Table A.42 M-ϕ data for Thompson: F-2-3 alt b (1970)

Moment, M kN-m	Rotation, ϕ radians	Moment, M kN-m	Rotation, ϕ radians
0	0	203.043	0.0874
4.900	0.0002	211.846	0.0911
14.616	0.0011	216.122	0.0941
21.094	0.0019	220.399	0.0971
27.197	0.0073	222.558	0.1010
33.301	0.0127	224.717	0.1048
39.405	0.0180	226.876	0.1087
45.508	0.0234	224.219	0.1117
53.398	0.0278		
62.284	0.0330		
70.588	0.0376		
78.892	0.0426		
86.170	0.0472		
93.448	0.0518		
100.725	0.0564		
104.300	0.0617		
107.874	0.0669		
117.939	0.0684		
128.004	0.0700		
138.069	0.0715		
148.134	0.0731		
158.198	0.0746		
167.209	0.0769		
176.219	0.0792		
185.230	0.0814		
194.240	0.0837		

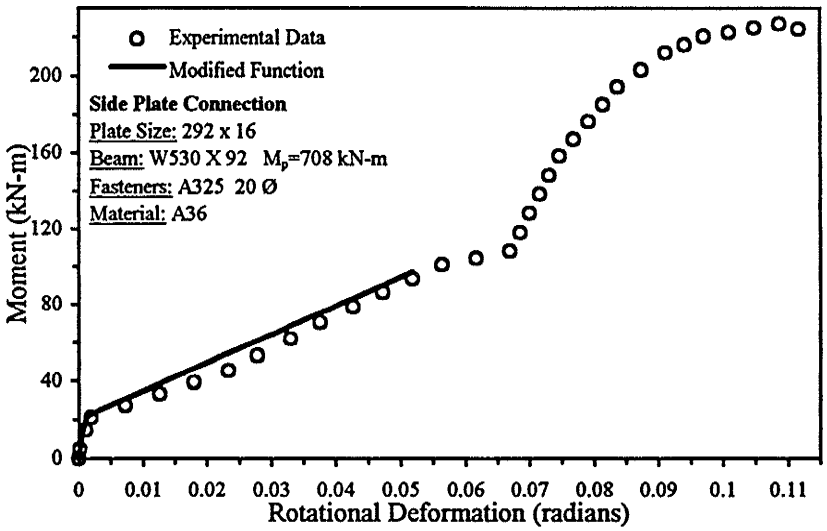


Figure A.42 (a) M-ϕ curve for Thompson: F-2-3 alt b

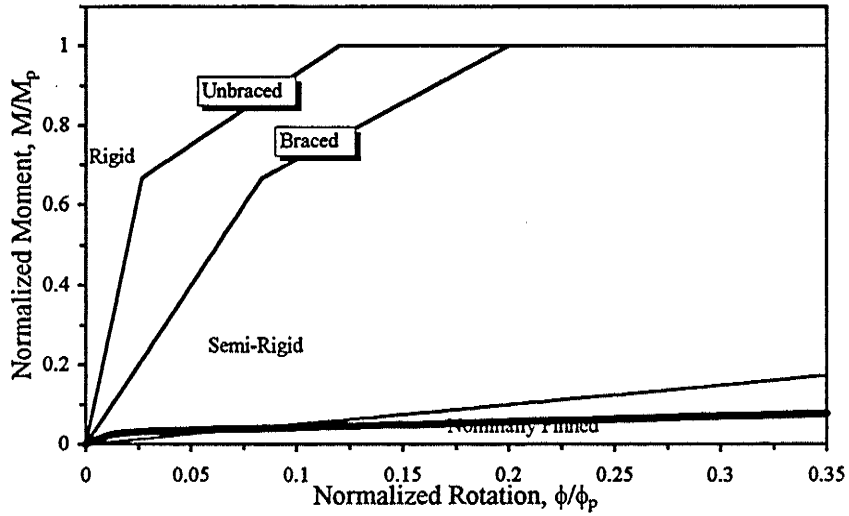


Figure A.42 (b) Eurocode3 Classification of Thompson: F-2-3 alt b

Table A.43 M-ϕ data for Richard: RGKL2 (1982)

Moment, M kN-m	Rotation, ϕ radians	Moment, M kN-m	Rotation, ϕ radians
0	0	5.181	0.0383
0.220	0.0003	5.304	0.0410
0.440	0.0005	5.426	0.0436
0.660	0.0008	5.555	0.0459
0.955	0.0011	5.684	0.0481
1.251	0.0014	5.812	0.0504
1.546	0.0018	5.909	0.0527
1.841	0.0021	6.006	0.0549
2.136	0.0024	6.103	0.0572
2.431	0.0027		
2.635	0.0032		
2.840	0.0037		
3.044	0.0042		
3.333	0.0067		
3.623	0.0091		
3.816	0.0117		
4.010	0.0143		
4.203	0.0169		
4.310	0.0189		
4.417	0.0209		
4.524	0.0229		
4.621	0.0254		
4.718	0.0279		
4.815	0.0304		
4.937	0.0330		
5.059	0.0357		

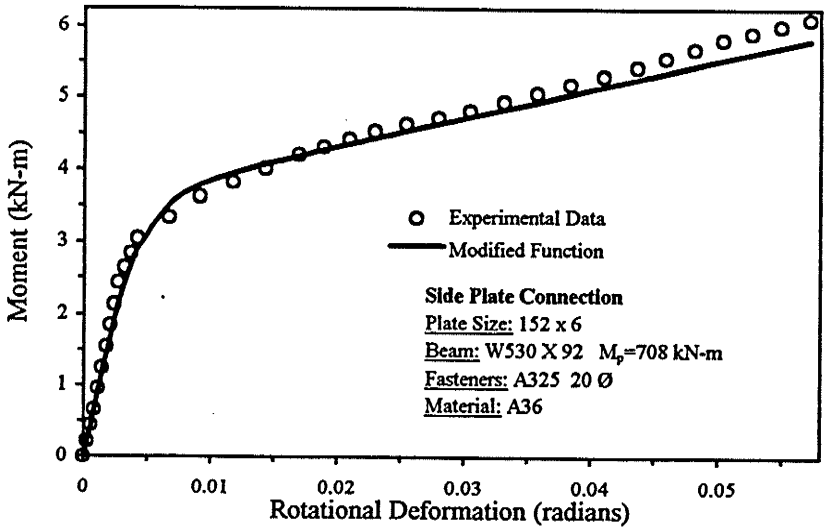


Figure A.43 (a) M-ϕ curve for Richard: RGKL2

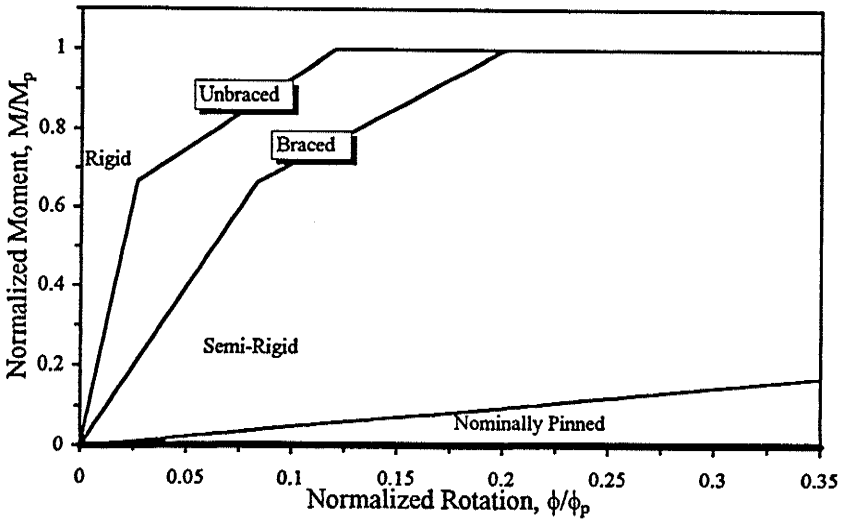


Figure A.43 (b) Eurocode3 Classification of Richard: RGKL2

Table A.44 M-ϕ data for Richard: RGKL3 (1982)

Moment, M kN-m	Rotation, ϕ radians	Moment, M kN-m	Rotation, ϕ radians
0	0	13.837	0.0304
0.739	0.0002	14.035	0.0331
1.428	0.0003	14.232	0.0357
2.118	0.0004	14.429	0.0384
2.758	0.0006	14.560	0.0410
3.398	0.0007	14.691	0.0436
4.038	0.0010	14.822	0.0462
4.678	0.0013	14.920	0.0487
5.367	0.0016	15.019	0.0513
6.056	0.0019	15.118	0.0538
6.746	0.0027	15.216	0.0563
7.435	0.0034	15.265	0.0583
8.076	0.0047	15.314	0.0602
8.717	0.0060		
9.306	0.0076		
9.701	0.0087		
10.095	0.0097		
10.784	0.0123		
11.473	0.0147		
11.818	0.0165		
12.163	0.0183		
12.507	0.0199		
12.852	0.0214		
13.049	0.0235		
13.246	0.0255		
13.542	0.0280		

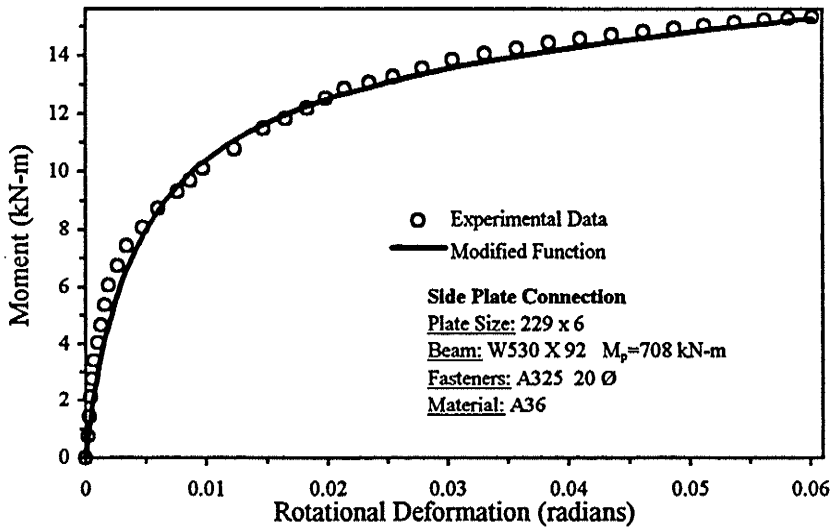


Figure A.44 (a) M-ϕ curve for Richard: RGKL3

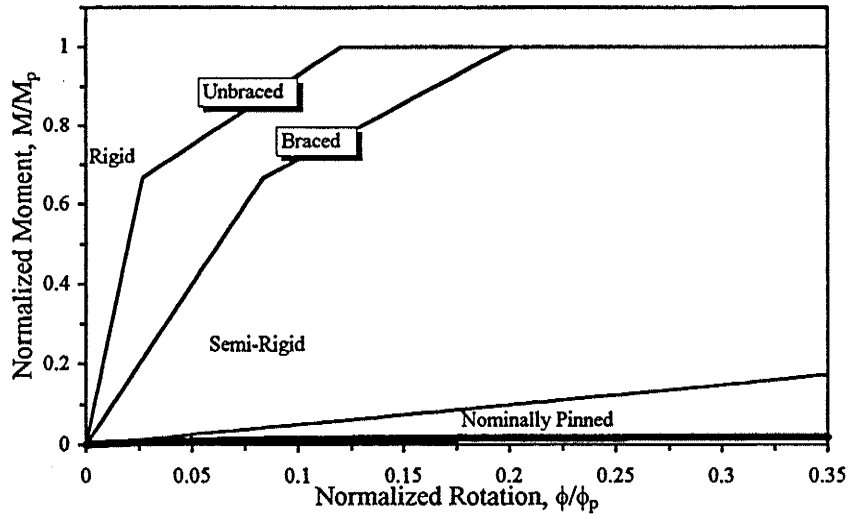


Figure A.44 (b) Eurocode3 Classification of Richard: RGKL3

Table A.45 M-ϕ data for Richard: RGKL5 (1982)

Moment, M kN-m	Rotation, ϕ radians	Moment, M kN-m	Rotation, ϕ radians
0	0	59.297	0.0196
3.185	0.0001	60.604	0.0219
6.371	0.0002	61.911	0.0242
9.310	0.0004	62.401	0.0264
12.251	0.0009	62.891	0.0286
14.212	0.0009	63.217	0.0302
16.662	0.0011	63.543	0.0318
19.112	0.0013	64.197	0.0342
21.562	0.0016	64.850	0.0366
24.013	0.0018	65.340	0.0389
26.953	0.0021	65.830	0.0412
29.893	0.0024	66.157	0.0441
32.507	0.0029	66.484	0.0471
35.121	0.0033	66.811	0.0500
37.081	0.0037	67.137	0.0524
39.041	0.0041	67.464	0.0548
41.491	0.0048	67.791	0.0572
43.942	0.0055	68.118	0.0596
46.229	0.0067		
48.515	0.0078		
51.456	0.0105		
52.763	0.0120		
54.070	0.0135		
55.540	0.0151		
57.010	0.0166		
58.153	0.0181		

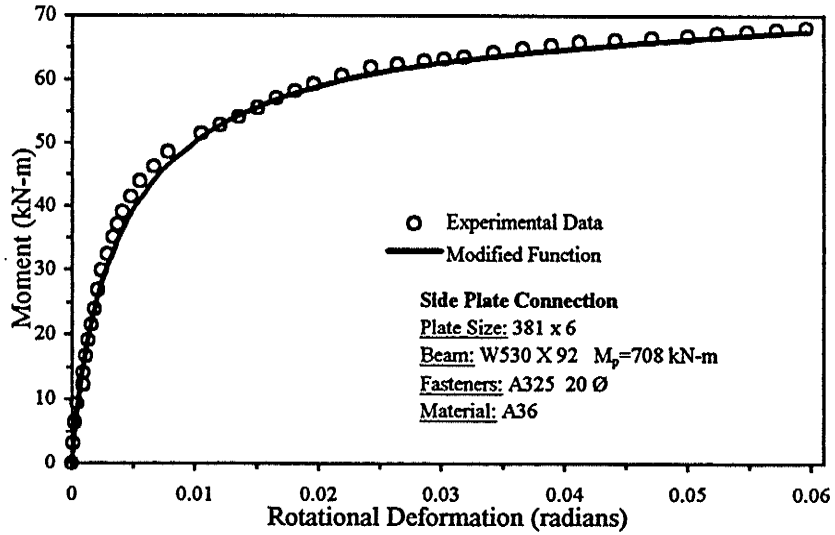


Figure A.45 (a) M-ϕ curve for Richard: RGKL5

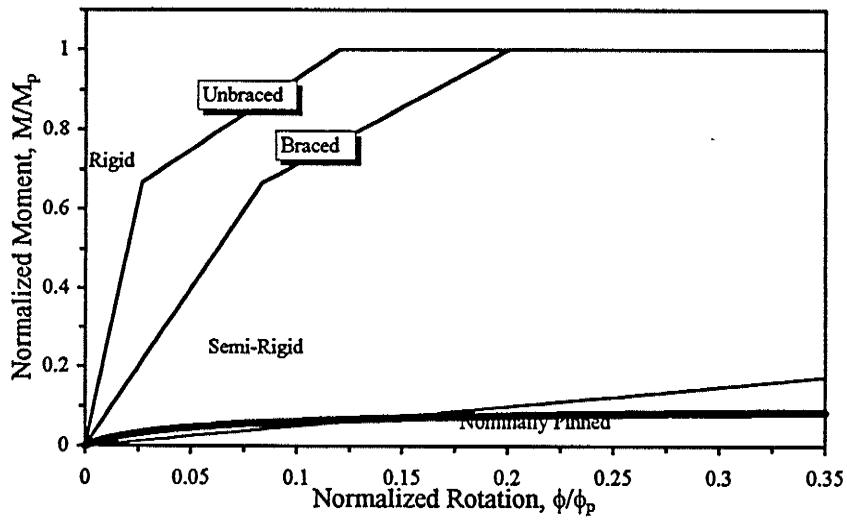


Figure A.45 (b) Eurocode3 Classification of Richard: RGKL5

Table A.46 M-ϕ data for Richard: RGKL7 (1982)

Moment, M kN-m	Rotation, ϕ radians	Moment, M kN-m	Rotation, ϕ radians
0	0	130.110	0.0238
6.054	0.0002	132.422	0.0255
12.108	0.0005	133.742	0.0276
18.163	0.0007	135.063	0.0297
24.106	0.0011	136.054	0.0315
30.050	0.0014	137.045	0.0332
35.994	0.0018	138.035	0.0348
42.379	0.0021	139.026	0.0364
48.763	0.0025	140.347	0.0390
55.148	0.0028	141.668	0.0417
60.872	0.0032	142.989	0.0443
66.596	0.0037	143.649	0.0471
72.319	0.0041	144.309	0.0498
77.273	0.0046	144.970	0.0526
82.226	0.0050	145.630	0.0552
86.850	0.0056	146.291	0.0578
91.473	0.0061	146.952	0.0604
96.427	0.0073		
101.380	0.0085		
105.342	0.0098		
109.305	0.0111		
114.588	0.0135		
117.891	0.0157		
120.863	0.0174		
123.835	0.0190		
127.798	0.0220		

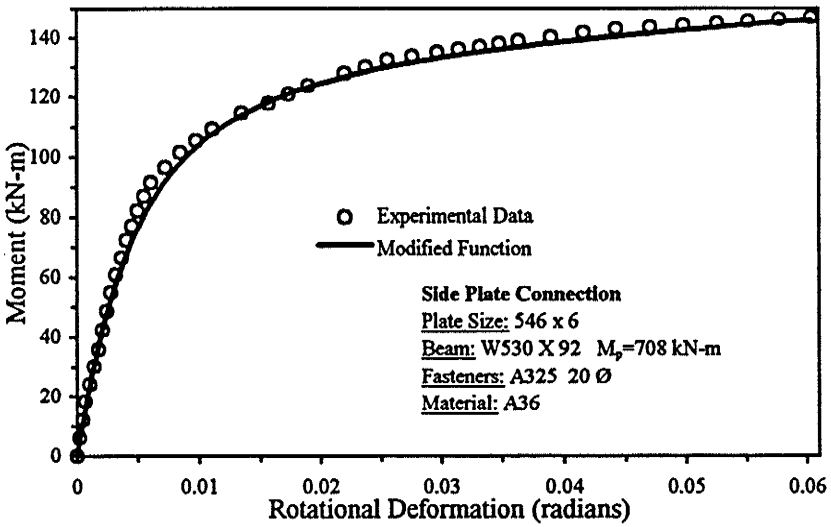


Figure A.46 (a) M-ϕ curve for Richard: RGKL7

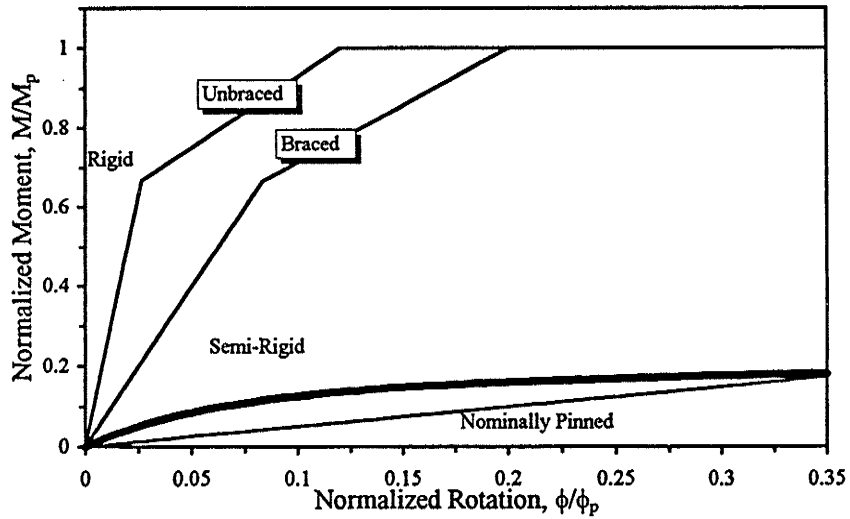


Figure A.46 (b) Eurocode3 Classification of Richard: RGKL7

Table A.47 M-ϕ data for Lewitt: FK-4AB-M (1966)

Moment, M kN-m	Rotation, ϕ radians	Moment, M kN-m	Rotation, ϕ radians
0	0	47.048	0.0491
2.157	0.0002	47.978	0.0524
4.486	0.0005	48.908	0.0557
6.816	0.0009	49.838	0.0590
8.918	0.0012	50.697	0.0620
11.248	0.0017	51.556	0.0650
13.635	0.0022	52.415	0.0681
15.910	0.0027	53.274	0.0711
18.184	0.0033	54.133	0.0741
20.460	0.0040		
22.679	0.0047		
24.959	0.0057		
27.239	0.0068		
29.582	0.0086		
31.926	0.0103		
34.113	0.0135		
36.301	0.0166		
37.809	0.0198		
39.316	0.0230		
40.824	0.0262		
41.696	0.0295		
42.569	0.0327		
43.442	0.0360		
44.314	0.0392		
45.187	0.0424		
46.117	0.0458		

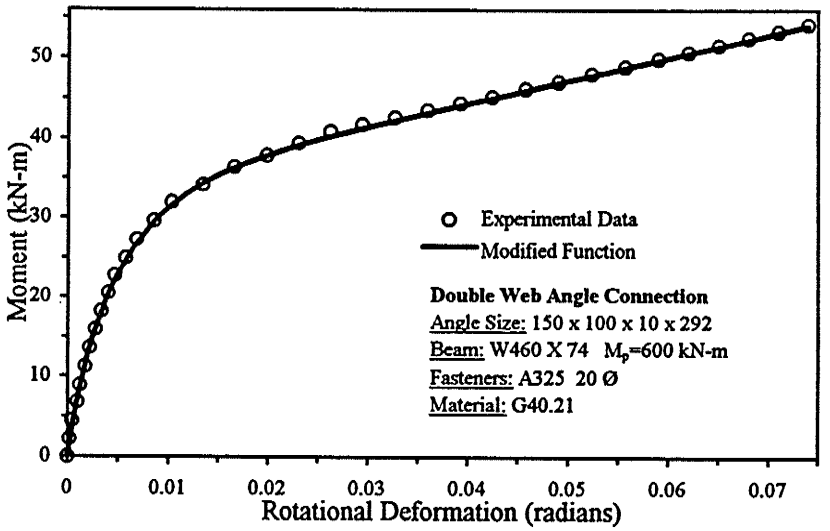


Figure A.47 (a) M-ϕ curve for Lewitt: FK-4AB-M

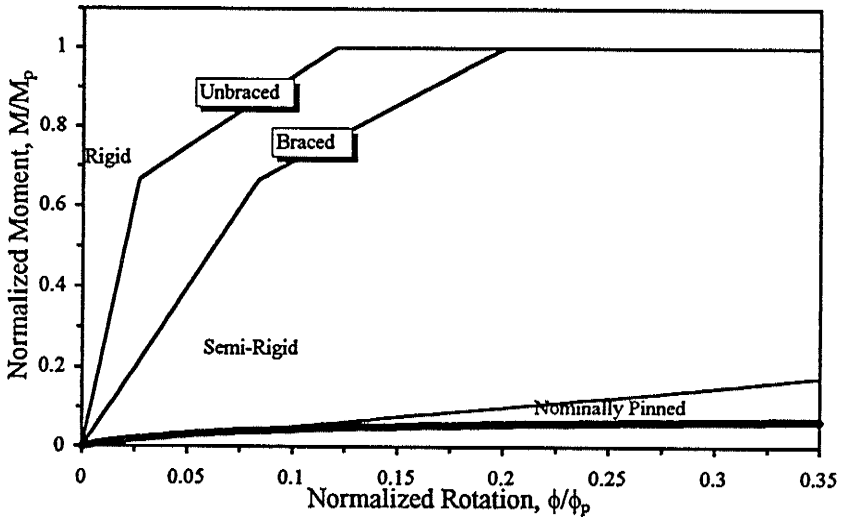


Figure A.47 (b) Eurocode3 Classification of Lewitt: FK-4AB-M

Table A.48 M-ϕ data for Bose: B1 (1981)

Moment, M kN-m	Rotation, ϕ radians	Moment, M kN-m	Rotation, ϕ radians
0	0	77.858	0.0066
3.117	0.0001	79.291	0.0069
6.234	0.0003	81.416	0.0073
9.350	0.0004	83.541	0.0076
12.810	0.0006	85.666	0.0080
16.269	0.0008	87.514	0.0083
19.728	0.0010	89.362	0.0087
22.913	0.0012	91.209	0.0090
26.099	0.0013		
29.284	0.0015		
32.674	0.0017		
36.064	0.0019		
39.454	0.0021		
43.700	0.0024		
47.946	0.0028		
51.773	0.0031		
55.600	0.0035		
57.768	0.0038		
59.935	0.0040		
62.339	0.0044		
64.742	0.0047		
67.146	0.0051		
69.761	0.0054		
72.376	0.0057		
74.991	0.0060		
76.424	0.0063		

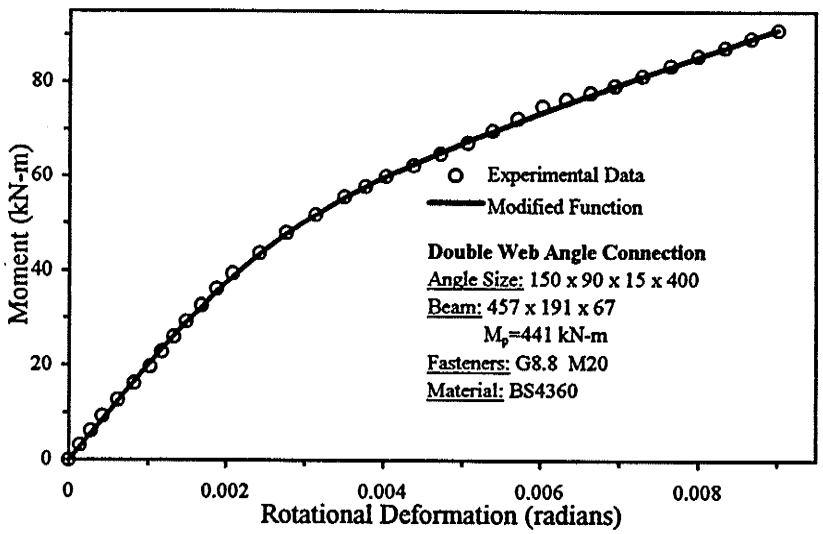


Figure A.48 (a) M-ϕ curve for Bose: B1

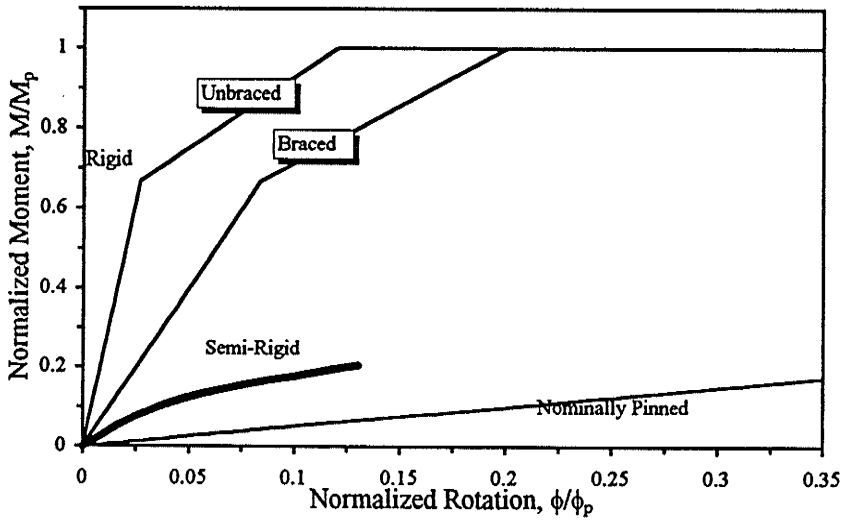


Figure A.48 (b) Eurocode3 Classification of Bose: B1

Table A.49 M-ϕ data for Thompson: A1-1 alt a (1970)

Moment, M kN-m	Rotation, ϕ radians	Moment, M kN-m	Rotation, ϕ radians
0	0	41.522	0.1002
2.768	0.0017	43.598	0.1014
5.536	0.0034	45.675	0.1026
8.304	0.0052	47.751	0.1030
11.073	0.0069	49.826	0.1034
13.841	0.0086	51.903	0.1038
16.609	0.0103	53.979	0.1041
18.435	0.0153	56.055	0.1051
19.826	0.0207	58.131	0.1060
21.217	0.0260	60.207	0.1073
22.608	0.0314	62.284	0.1086
23.999	0.0367	64.359	0.1118
25.266	0.0421	66.435	0.1149
26.533	0.0474		
27.799	0.0528		
29.066	0.0581		
29.481	0.0634		
29.896	0.0687		
30.312	0.0741		
30.727	0.0794		
31.142	0.0847		
32.180	0.0898		
33.218	0.0948		
35.294	0.0964		
37.370	0.0979		
39.446	0.0991		

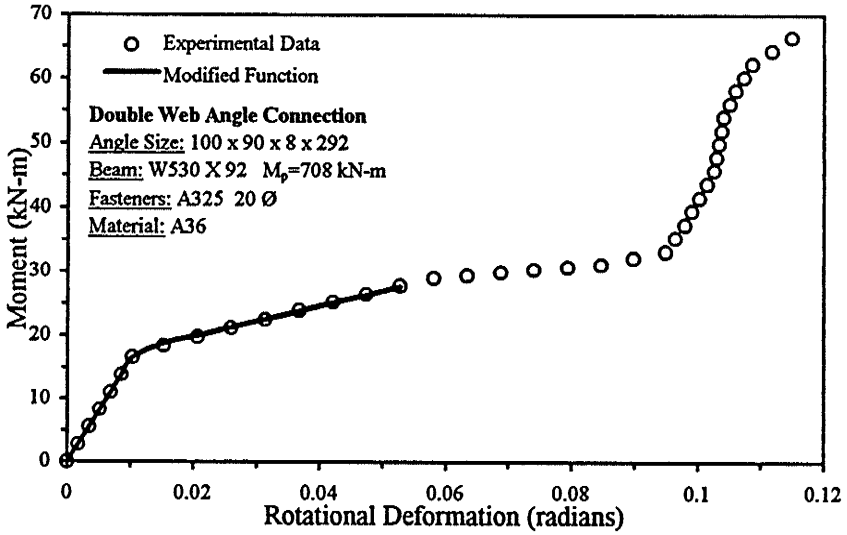


Figure A.49 (a) M-ϕ curve for Thompson: A1-1 alt a

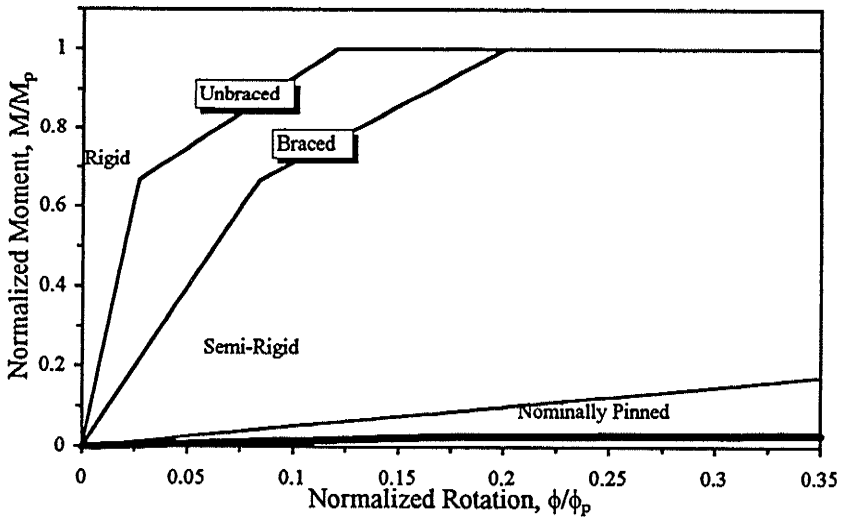


Figure A.49 (b) Eurocode3 Classification of Thompson: A1-1 alt a

Table A.50 M-ϕ data for Thompson: A1-1 alt b (1970)

Moment, M kN-m	Rotation, ϕ radians	Moment, M kN-m	Rotation, ϕ radians
0	0	39.446	0.1076
2.768	0.0019	41.522	0.1085
5.536	0.0039	43.598	0.1096
8.304	0.0058	45.675	0.1107
11.073	0.0077	47.751	0.1117
13.841	0.0097	49.826	0.1126
16.609	0.0116	51.903	0.1136
18.435	0.0177	53.979	0.1145
19.548	0.0229	56.055	0.1158
20.661	0.0281	58.131	0.1170
21.774	0.0332	60.207	0.1188
22.887	0.0384	62.284	0.1205
23.999	0.0436	64.359	0.1235
24.633	0.0496	66.435	0.1264
25.266	0.0555		
25.899	0.0615		
26.533	0.0675		
27.166	0.0734		
27.799	0.0794		
28.433	0.0853		
29.066	0.0913		
30.104	0.0969		
31.142	0.1025		
33.218	0.1048		
35.294	0.1057		
37.370	0.1066		

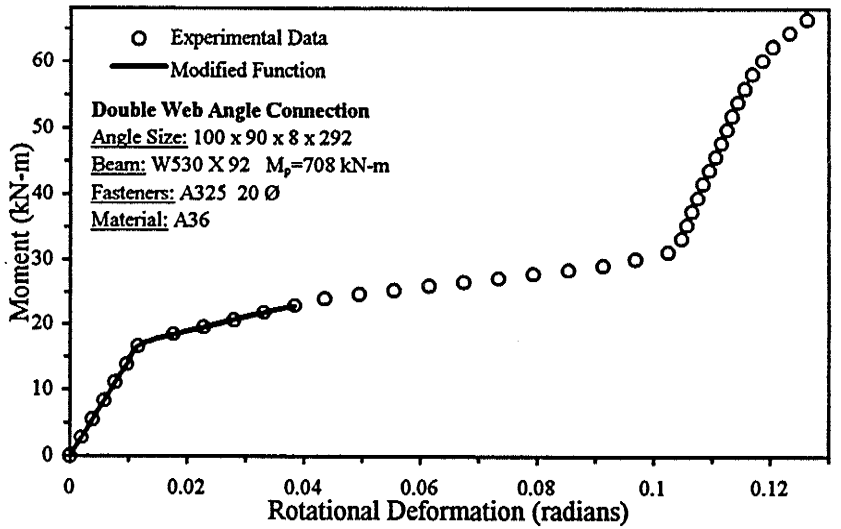


Figure A.50 (a) M-ϕ curve for Thompson: A1-1 alt b

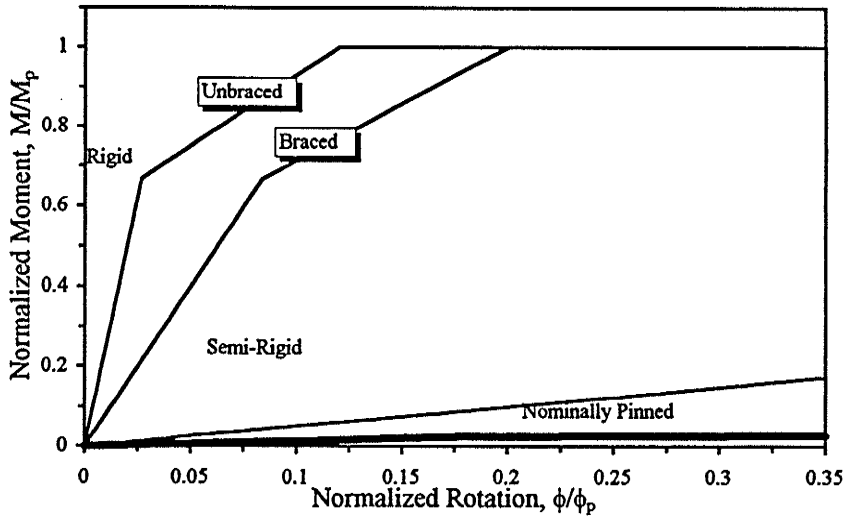


Figure A.50 (b) Eurocode3 Classification of Thompson: A1-1 alt b

Table A.51 M-ϕ data for Thompson: A1-2 alt a (1970)

Moment, M kN-m	Rotation, ϕ radians	Moment, M kN-m	Rotation, ϕ radians
0	0	35.293	0.0745
2.325	0.0006	36.332	0.0790
4.650	0.0011	37.370	0.0835
6.810	0.0017	39.446	0.0838
8.969	0.0022	41.522	0.0848
12.540	0.0033	43.847	0.0858
14.533	0.0042	46.110	0.0865
16.609	0.0060	48.373	0.0872
18.685	0.0083	50.594	0.0891
20.762	0.0118	52.816	0.0909
22.837	0.0145	56.387	0.0911
23.875	0.0175	58.297	0.0914
24.913	0.0204	60.207	0.0916
25.951	0.0237	62.283	0.0918
26.989	0.0270	64.359	0.0920
28.028	0.0310	66.435	0.0922
29.066	0.0350	68.511	0.0924
30.104	0.0387	70.587	0.0927
31.142	0.0424	72.664	0.0930
31.834	0.0460		
32.526	0.0496		
33.218	0.0532		
33.633	0.0575		
34.048	0.0617		
34.463	0.0660		
34.878	0.0702		

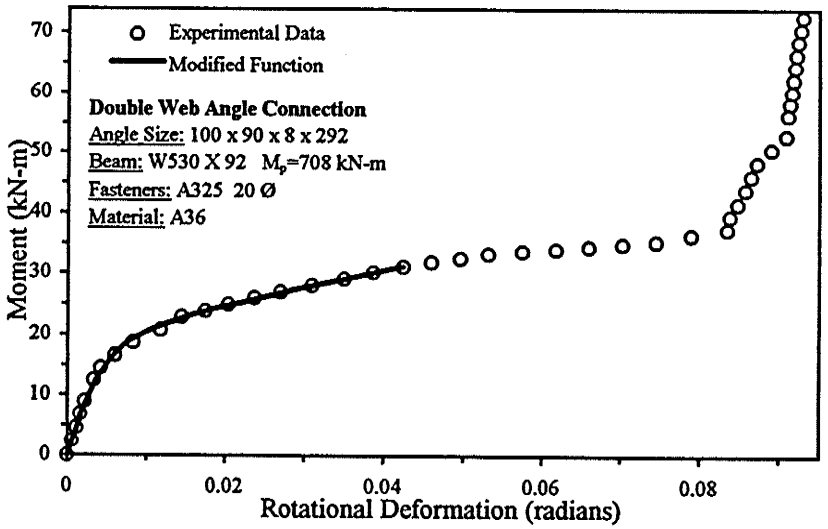


Figure A.51 (a) M-ϕ curve for Thompson: A1-2 alt a

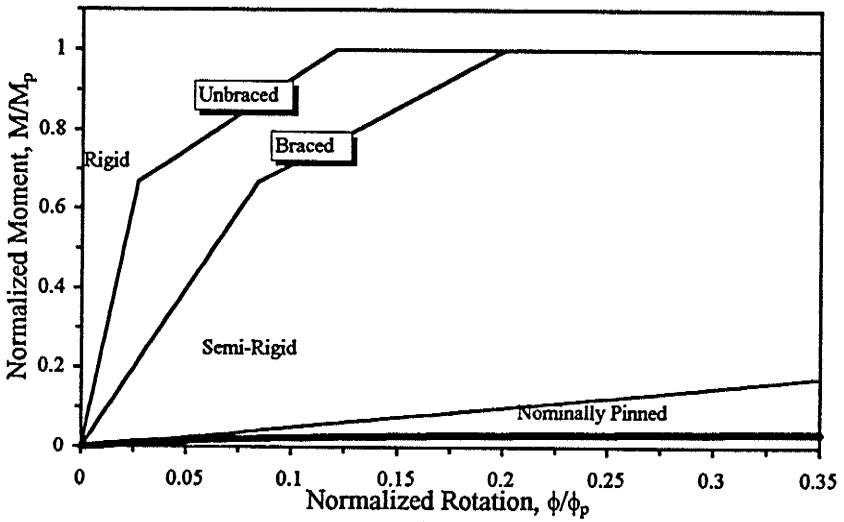


Figure A.51 (b) Eurocode3 Classification of Thompson: A1-2 alt a

Table A.52 M-ϕ data for Thompson: A1-2 alt b (1970)

Moment, M kN-m	Rotation, ϕ radians	Moment, M kN-m	Rotation, ϕ radians
0	0	36.540	0.0776
2.325	0.0006	36.955	0.0823
4.650	0.0012	37.370	0.0870
6.810	0.0017	38.408	0.0899
8.969	0.0022	39.446	0.0928
12.540	0.0035	41.522	0.0949
14.533	0.0047	43.847	0.0963
16.609	0.0066	46.110	0.0971
18.685	0.0088	48.373	0.0979
20.762	0.0118	50.594	0.0989
22.837	0.0142	52.816	0.0998
23.875	0.0175	56.387	0.0999
24.913	0.0207	58.297	0.1001
25.951	0.0244	60.207	0.1002
26.989	0.0280	62.283	0.1003
29.066	0.0328	64.359	0.1004
29.758	0.0363	66.435	0.1006
30.450	0.0397	68.511	0.1008
31.142	0.0432	70.587	0.1012
31.834	0.0469	72.664	0.1015
32.526	0.0507		
33.218	0.0544		
34.255	0.0590		
35.293	0.0635		
35.709	0.0682		
36.124	0.0729		

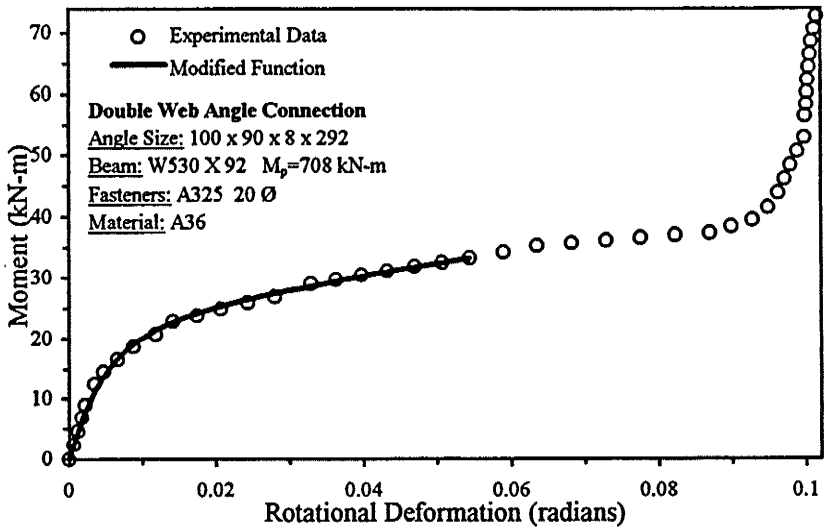


Figure A.52 (a) M-ϕ curve for Thompson: A1-2 alt b

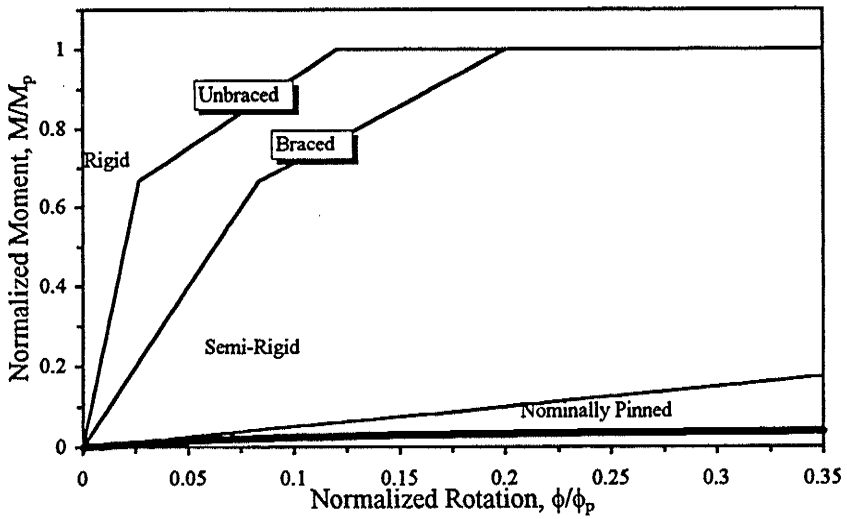


Figure A.52 (b) Eurocode3 Classification of Thompson: A1-2 alt b

Table A.53 M-ϕ data for Thompson: A1-3 alt a (1970)

Moment, M kN-m	Rotation, ϕ radians	Moment, M kN-m	Rotation, ϕ radians
0	0	37.038	0.0884
2.508	0.0005	37.370	0.0934
5.015	0.0009	38.782	0.0969
8.719	0.0016	40.193	0.1003
12.457	0.0028	43.348	0.1020
14.533	0.0040	45.923	0.1031
16.609	0.0059	48.498	0.1042
18.685	0.0084	52.234	0.1046
20.762	0.0127	54.269	0.1048
22.837	0.0174	56.304	0.1050
23.875	0.0207	58.505	0.1052
24.913	0.0240	60.705	0.1054
25.951	0.0283	62.615	0.1056
26.989	0.0326	64.525	0.1057
28.028	0.0367	66.518	0.1060
29.066	0.0407	68.511	0.1062
30.145	0.0450	71.833	0.1066
31.225	0.0493	75.569	0.1071
31.702	0.0540		
32.179	0.0587		
33.529	0.0629		
34.878	0.0670		
35.460	0.0702		
36.042	0.0733		
36.374	0.0783		
36.706	0.0834		

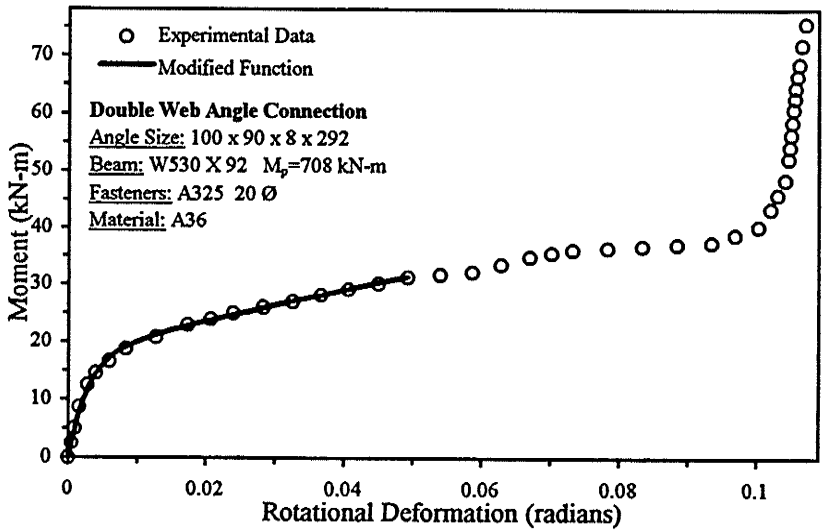


Figure A.53 (a) M-ϕ curve for Thompson: A1-3 alt a

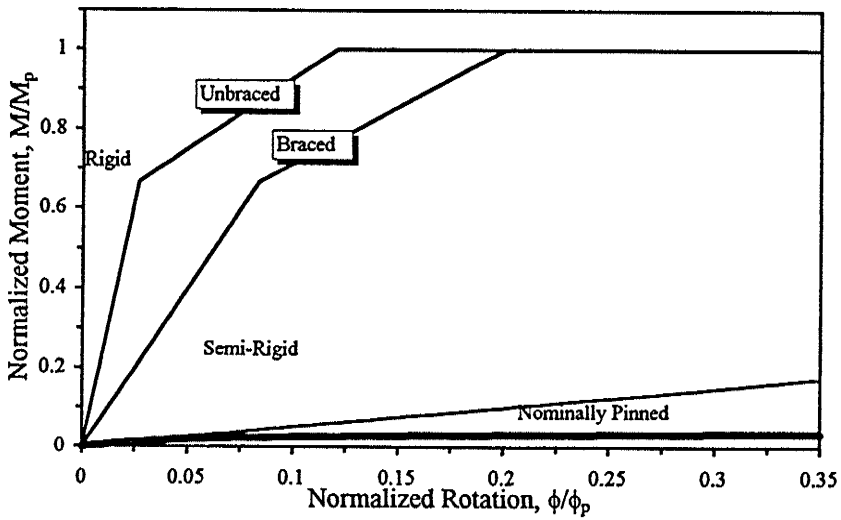


Figure A.53 (b) Eurocode3 Classification of Thompson: A1-3 alt a

Table A.54 M-ϕ data for Thompson: A1-3 alt b (1970)

Moment, M kN-m	Rotation, ϕ radians	Moment, M kN-m	Rotation, ϕ radians
0	0	37.370	0.0956
2.508	0.0004	40.193	0.1009
5.015	0.0008	43.348	0.1026
8.719	0.0017	45.923	0.1034
12.457	0.0031	48.498	0.1041
14.533	0.0044	52.234	0.1043
16.609	0.0064	54.269	0.1045
18.685	0.0094	56.304	0.1046
20.762	0.0146	58.505	0.1048
22.837	0.0197	60.705	0.1049
23.875	0.0232	62.615	0.1051
24.913	0.0267	64.525	0.1052
25.951	0.0311	66.518	0.1055
26.989	0.0355	68.511	0.1057
28.028	0.0397	71.833	0.1066
29.066	0.0438	75.569	0.1086
30.145	0.0484		
31.225	0.0529		
31.702	0.0573		
32.179	0.0616		
32.854	0.0669		
33.529	0.0722		
34.204	0.0774		
34.878	0.0827		
35.460	0.0877		
36.042	0.0926		

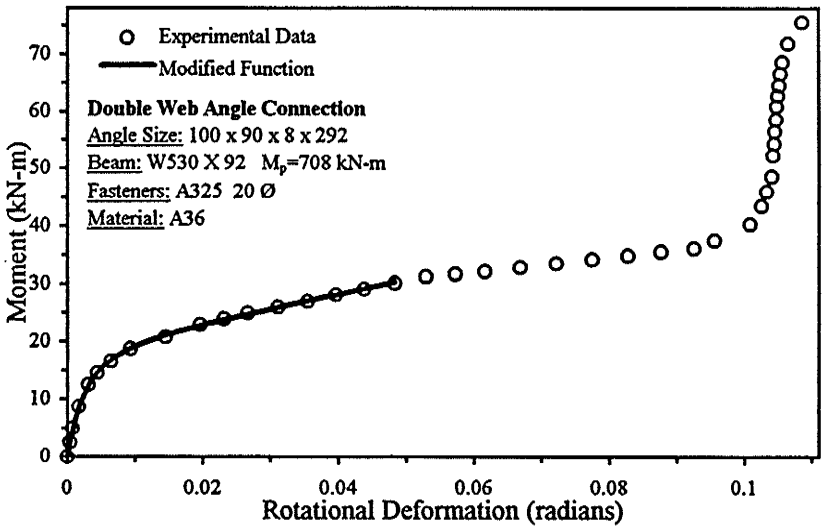


Figure A.54 (a) M-ϕ curve for Thompson: A1-3 alt b

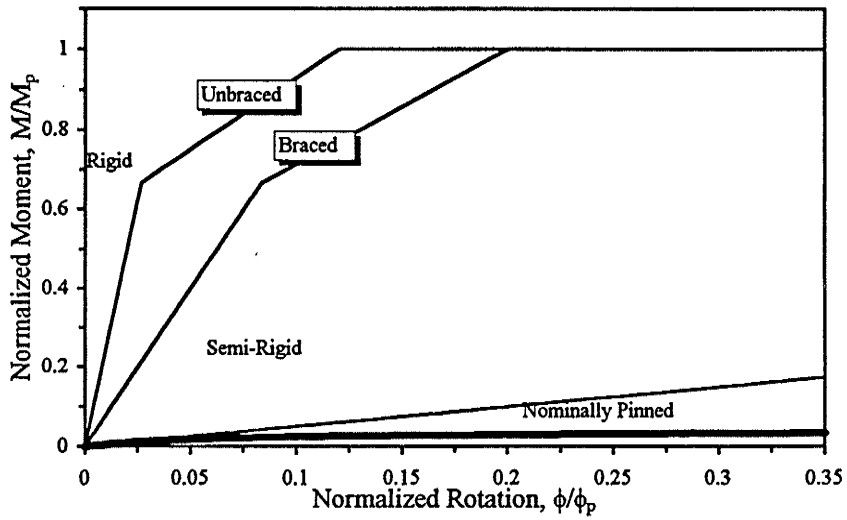


Figure A.54 (b) Eurocode3 Classification of Thompson: A1-3 alt b

Table A.55 M-ϕ data for Thompson: B1-1 alt a (1970)

Moment, M kN-m	Rotation, ϕ radians	Moment, M kN-m	Rotation, ϕ radians
0	0	58.131	0.0770
4.728	0.0004	60.788	0.0800
9.457	0.0008	66.435	0.0819
13.490	0.0015	70.795	0.0832
17.523	0.0021	75.072	0.0844
21.467	0.0030	79.058	0.0855
25.412	0.0038	83.044	0.0865
31.142	0.0055	87.196	0.0878
35.293	0.0078	91.348	0.0890
39.529	0.0104	95.501	0.0908
43.847	0.0146	99.653	0.0925
45.799	0.0172	103.805	0.0946
47.751	0.0198	107.957	0.0967
48.581	0.0242	112.109	0.0991
49.411	0.0286	116.262	0.1015
50.242	0.0331		
51.072	0.0375		
51.902	0.0419		
52.941	0.0459		
53.979	0.0499		
54.394	0.0541		
54.810	0.0583		
55.225	0.0624		
55.640	0.0666		
56.055	0.0708		
57.093	0.0739		

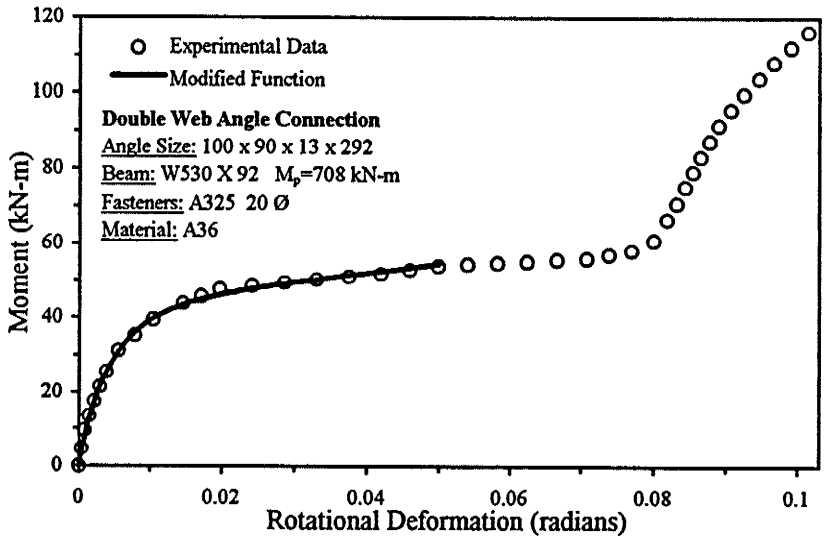


Figure A.55 (a) M-ϕ curve for Thompson: B1-1 alt a

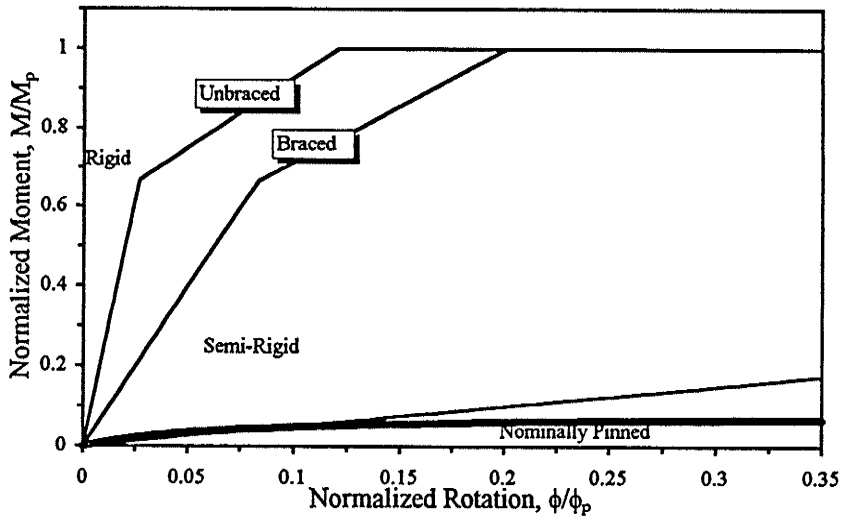


Figure A.55 (b) Eurocode3 Classification of Thompson: B1-1 alt a

Table A.56 M-ϕ data for Thompson: B1-1 alt b (1970)

Moment, M kN-m	Rotation, ϕ radians	Moment, M kN-m	Rotation, ϕ radians
0	0	66.435	0.0966
4.728	0.0004	70.795	0.1011
9.457	0.0007	74.878	0.1022
13.490	0.0011	78.961	0.1034
17.523	0.0014	83.044	0.1045
21.467	0.0023	87.196	0.1058
25.412	0.0031	91.348	0.1070
31.142	0.0047	95.501	0.1087
35.293	0.0069	99.653	0.1103
39.529	0.0094	103.805	0.1122
43.847	0.0137	107.957	0.1141
47.751	0.0193	112.109	0.1163
48.517	0.0240	116.262	0.1185
49.283	0.0286		
50.156	0.0339		
51.029	0.0392		
51.902	0.0445		
52.760	0.0485		
53.619	0.0525		
54.477	0.0565		
56.304	0.0623		
58.131	0.0681		
58.795	0.0738		
59.459	0.0796		
60.124	0.0853		
60.788	0.0910		
66.43518	0.0966		

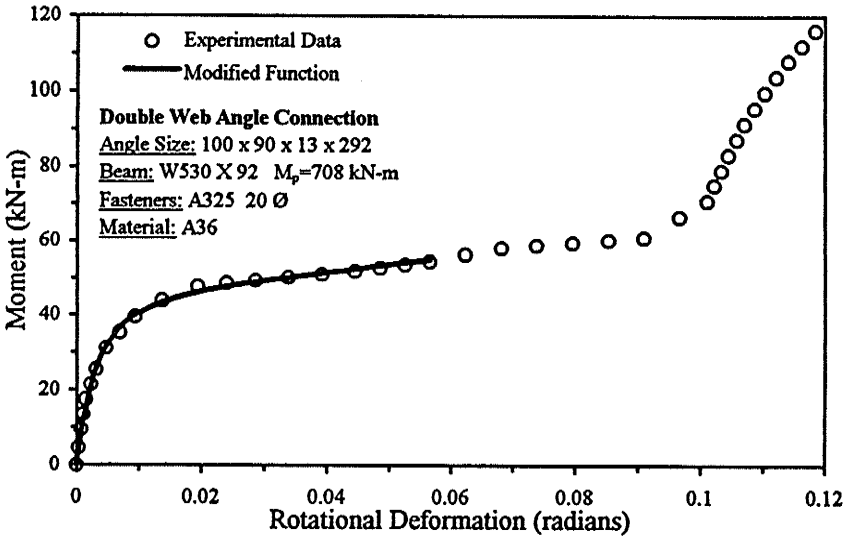


Figure A.56 (a) M-ϕ curve for Thompson: B1-1 alt b

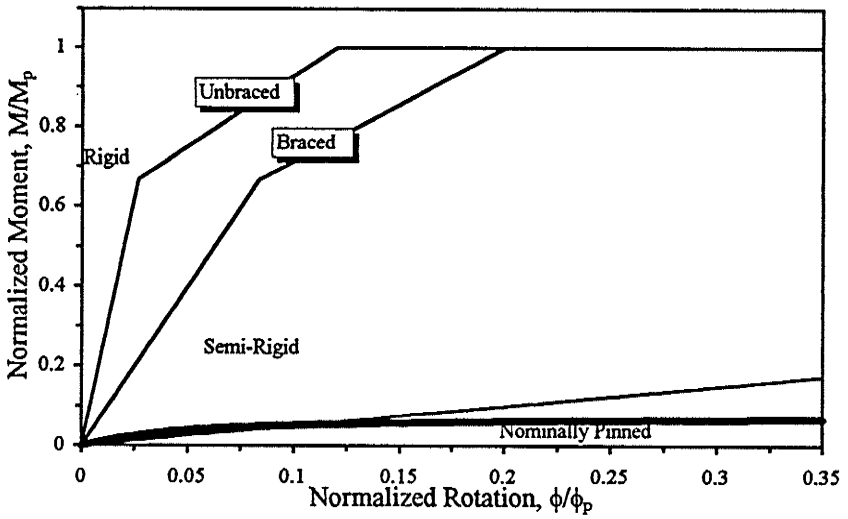


Figure A.56 (b) Eurocode3 Classification of Thompson: B1-1 alt b

Table A.57 M-ϕ data for Thompson: B1-2 alt a (1970)

Moment, M kN-m	Rotation, ϕ radians	Moment, M kN-m	Rotation, ϕ radians
0	0	75.030	0.0851
4.775	0.0004	79.141	0.0862
9.550	0.0007	83.293	0.0875
13.578	0.0013	87.445	0.0888
17.605	0.0018	91.514	0.0904
21.259	0.0026	95.584	0.0919
25.163	0.0035	99.695	0.0940
29.397	0.0050	103.806	0.0961
31.307	0.0093	107.958	0.0991
33.508	0.0138	112.110	0.1021
35.708	0.0182	116.262	0.1071
37.536	0.0238	120.414	0.1120
39.696	0.0278	123.183	0.1172
40.692	0.0326	125.951	0.1223
41.689	0.0374	128.719	0.1275
43.847	0.0443	130.103	0.1349
45.799	0.0495	131.487	0.1424
47.751	0.0546	132.870	0.1498
48.581	0.0599		
49.411	0.0652		
50.241	0.0705		
54.062	0.0774		
58.277	0.0795		
62.491	0.0815		
66.706	0.0828		
70.920	0.0840		

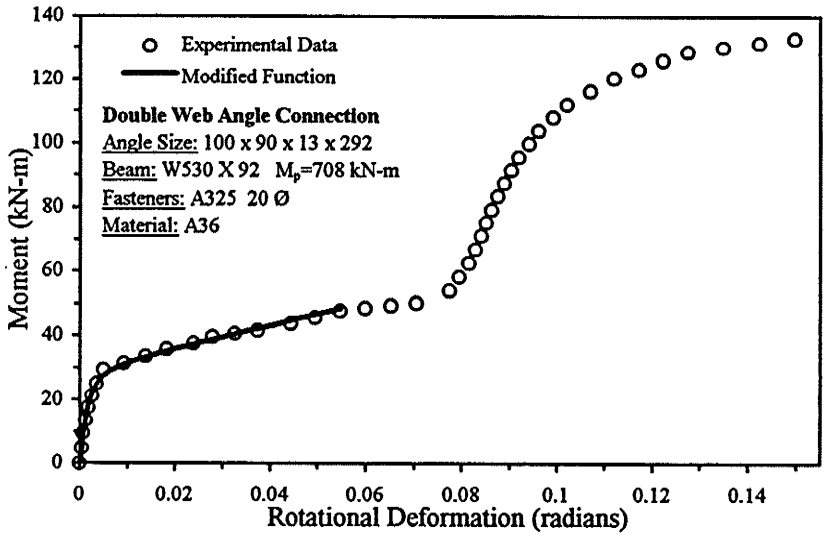


Figure A.57 (a) M-ϕ curve for Thompson: B1-2 alt a

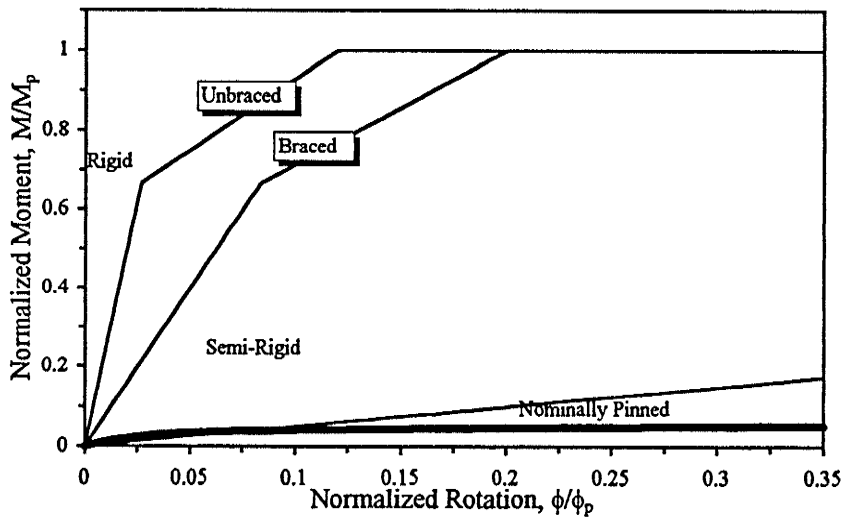


Figure A.57 (b) Eurocode3 Classification of Thompson: B1-2 alt a

Table A.58 M-ϕ data for Thompson: B1-2 alt b (1970)

Moment, M kN-m	Rotation, ϕ radians	Moment, M kN-m	Rotation, ϕ radians
0	0	54.427	0.2754
4.775	0.0004	56.404	0.2901
9.550	0.0007	58.380	0.3048
13.578	0.0012	62.491	0.3061
17.605	0.0016	66.706	0.3075
21.259	0.0024	70.920	0.3089
25.163	0.0032	75.030	0.3101
25.834	0.0062	79.141	0.3113
26.506	0.0092	83.293	0.3127
27.849	0.0151	87.445	0.3141
29.397	0.0270	91.514	0.3156
30.352	0.0380	95.584	0.3171
31.307	0.0490	99.695	0.3199
33.384	0.0666	103.806	0.3226
35.460	0.0842	107.958	0.3249
37.536	0.1018	112.110	0.3272
39.612	0.1194	116.262	0.3307
41.689	0.1370	120.414	0.3342
42.824	0.1527	124.567	0.3409
43.958	0.1684	128.719	0.3475
45.093	0.1842	132.870	0.3576
46.228	0.1999		
47.363	0.2156		
48.498	0.2313		
50.474	0.2460		
52.451	0.2607		

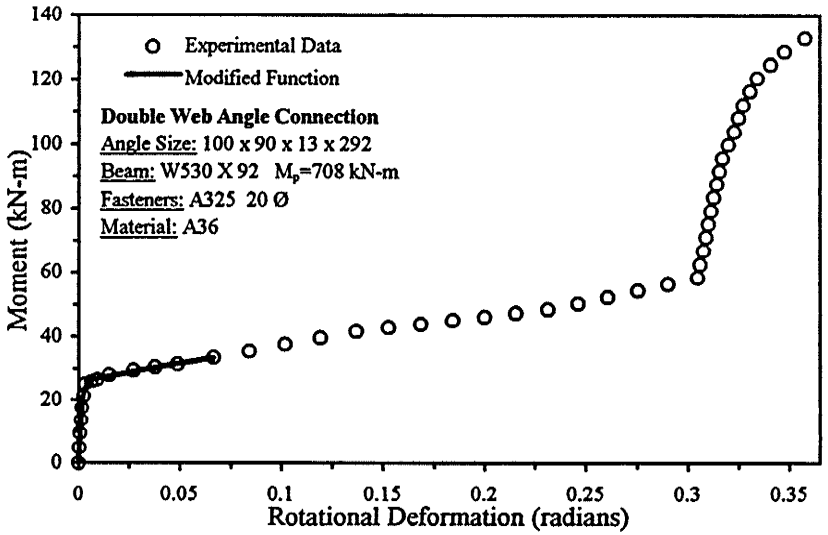


Figure A.58 (a) M-ϕ curve for Thompson: B1-2 alt b

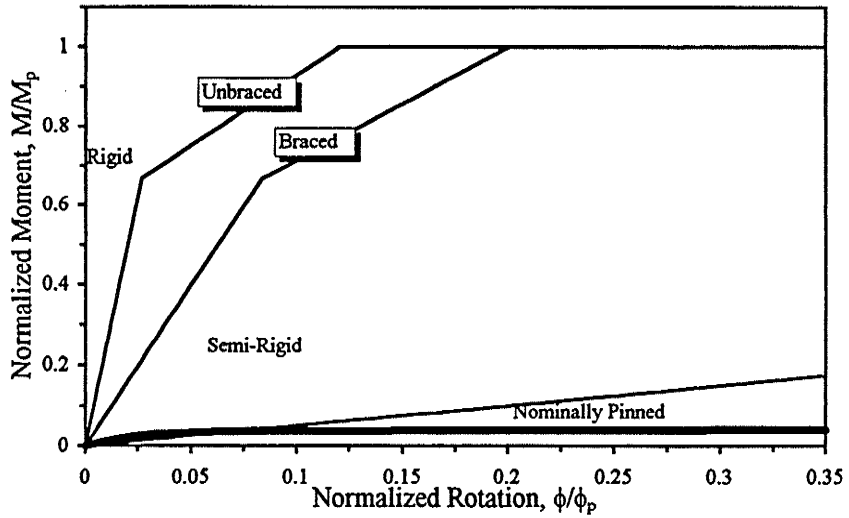


Figure A.58 (b) Eurocode3 Classification of Thompson: B1-2 alt b

Table A.59 M-ϕ data for Thompson: B1-3 alt a (1970)

Moment, M kN-m	Rotation, ϕ radians	Moment, M kN-m	Rotation, ϕ radians
0	0	49.401	0.0302
2.782	0.0002	49.951	0.0341
5.564	0.0004	52.234	0.0357
7.516	0.0006	53.107	0.0397
9.468	0.0007	53.979	0.0436
11.215	0.0009	55.017	0.0459
12.963	0.0010	56.055	0.0481
15.201	0.0013	56.263	0.0521
17.440	0.0015	56.470	0.0561
19.308	0.0018	56.678	0.0601
21.177	0.0021	56.886	0.0641
23.211	0.0026	57.093	0.0681
25.245	0.0030	57.301	0.0721
27.280	0.0036	58.796	0.0755
29.314	0.0041	60.291	0.0788
31.225	0.0048	62.449	0.0800
33.300	0.0057	64.650	0.0809
35.460	0.0065	66.850	0.0817
37.370	0.0075		
39.530	0.0093		
41.689	0.0110		
43.598	0.0129		
45.675	0.0151		
47.751	0.0183		
48.301	0.0223		
48.851	0.0262		

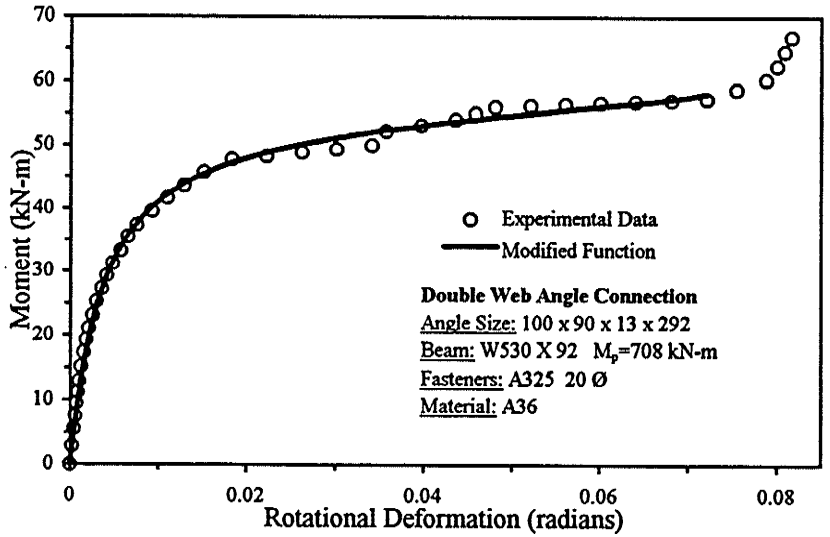


Figure A.59 (a) M-ϕ curve for Thompson: B1-3 alt a

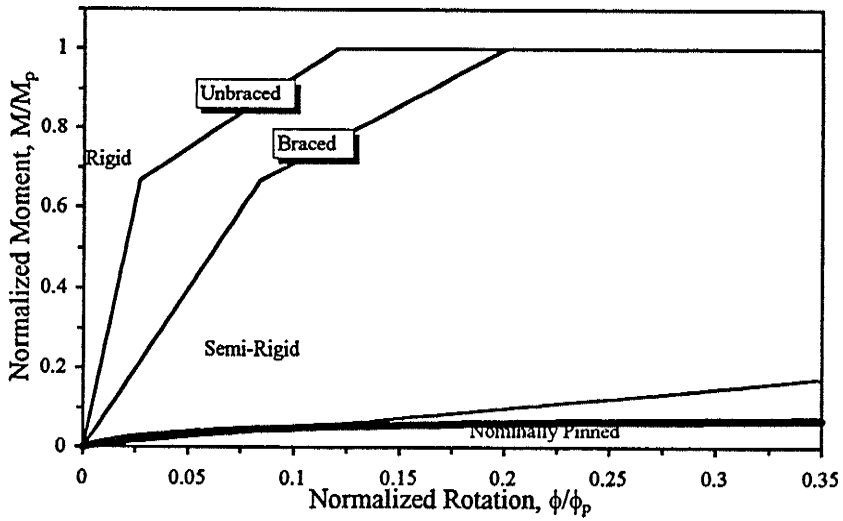


Figure A.59 (b) Eurocode3 Classification of Thompson: B1-3 alt a

Table A.60 M-ϕ data for Thompson: B1-3 alt b (1970)

Moment, M kN-m	Rotation, ϕ radians	Moment, M kN-m	Rotation, ϕ radians
0	0	49.951	0.0395
2.782	0.0002	52.234	0.0416
5.564	0.0004	53.979	0.0464
7.516	0.0006	54.325	0.0512
9.468	0.0008	54.671	0.0559
11.215	0.0011	55.017	0.0607
12.963	0.0014	55.363	0.0655
15.201	0.0018	55.709	0.0702
17.440	0.0022	56.055	0.0750
19.308	0.0027	56.159	0.0794
21.177	0.0031	56.262	0.0837
23.211	0.0039	56.366	0.0881
25.245	0.0046	56.470	0.0924
27.280	0.0057	56.885	0.0973
29.314	0.0067	57.301	0.1021
31.225	0.0079	58.796	0.1058
33.300	0.0091	60.291	0.1095
35.460	0.0103	62.449	0.1115
37.370	0.0115	64.650	0.1125
39.530	0.0135	66.850	0.1134
41.689	0.0154		
43.598	0.0174		
45.675	0.0197		
47.751	0.0226		
48.484	0.0282		
49.218	0.0339		

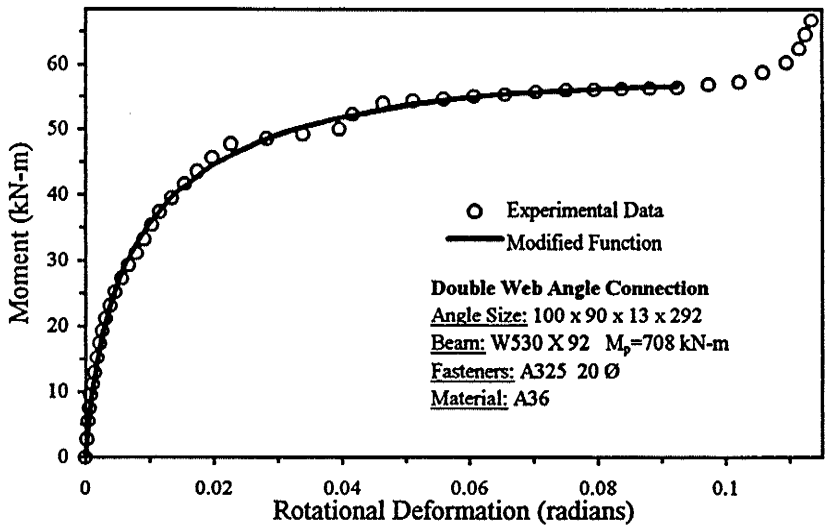


Figure A.60 (a) M-ϕ curve for Thompson: B1-3 alt b

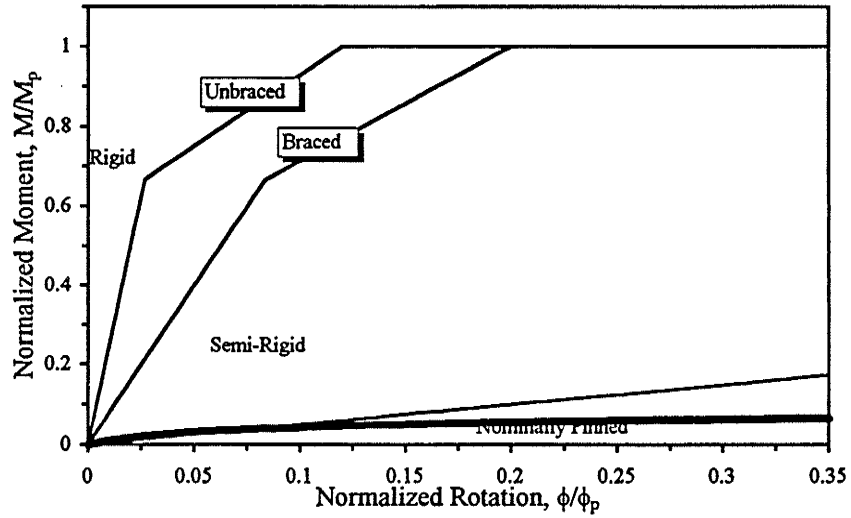


Figure A.60 (b) Eurocode3 Classification of Thompson: B1-3 alt b

Table A.61 M-ϕ data for Thompson: D1-1 alt a (1970)

Moment, M kN-m	Rotation, ϕ radians	Moment, M kN-m	Rotation, ϕ radians
0	0	38.366	0.0647
2.657	0.0003	40.027	0.0678
5.315	0.0006	41.689	0.0708
9.384	0.0011	46.339	0.0720
13.038	0.0017	50.491	0.0733
17.273	0.0026	54.643	0.0745
19.141	0.0031	58.795	0.0758
20.762	0.0036	62.823	0.0770
22.837	0.0044	66.850	0.0782
24.913	0.0057	70.878	0.0793
27.156	0.0071	74.905	0.0803
29.231	0.0087	79.057	0.0823
30.187	0.0127	83.209	0.0842
31.142	0.0167	87.279	0.0854
32.180	0.0192	91.348	0.0866
33.218	0.0216	95.501	0.0887
33.649	0.0257	99.653	0.0908
34.081	0.0298		
34.513	0.0339		
34.944	0.0380		
35.376	0.0421		
36.415	0.0454		
37.453	0.0486		
37.681	0.0526		
37.909	0.0567		
38.138	0.0607		

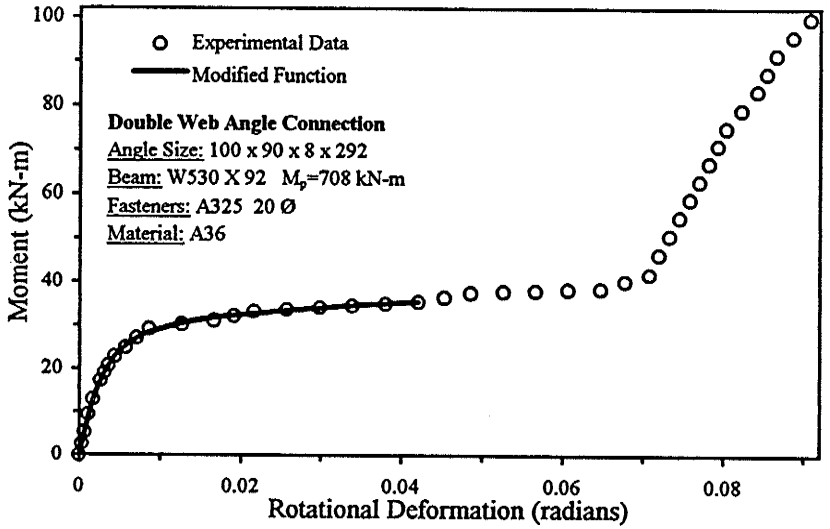


Figure A.61 (a) M-ϕ curve for Thompson: D1-1 alt a

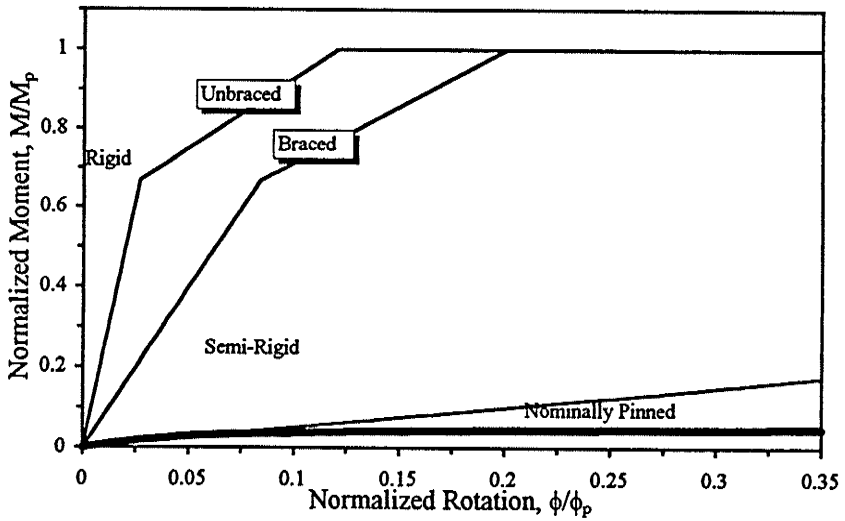


Figure A.61 (b) Eurocode3 Classification of Thompson: D1-1 alt a

Table A.62 M-ϕ data for Thompson: D1-1 alt b (1970)

Moment, M kN-m	Rotation, ϕ radians	Moment, M kN-m	Rotation, ϕ radians
0	0	41.896	0.0595
2.657	0.0003	42.104	0.0631
5.315	0.0006	42.311	0.0666
9.384	0.0013	42.519	0.0702
13.038	0.0021	44.429	0.0736
17.273	0.0032	46.339	0.0769
19.141	0.0037	50.656	0.0788
20.762	0.0043	54.726	0.0798
22.837	0.0052	58.795	0.0807
24.913	0.0067	62.823	0.0817
27.156	0.0080	66.850	0.0827
29.231	0.0095	70.878	0.0838
31.142	0.0119	74.905	0.0848
32.180	0.0150	79.057	0.0861
33.218	0.0180	83.209	0.0873
33.757	0.0223	87.279	0.0890
34.297	0.0266	91.348	0.0906
34.836	0.0308	95.501	0.0925
35.376	0.0351	99.653	0.0944
36.415	0.0381		
37.453	0.0410		
37.909	0.0436		
38.366	0.0461		
39.473	0.0494		
40.581	0.0526		
41.689	0.0559		

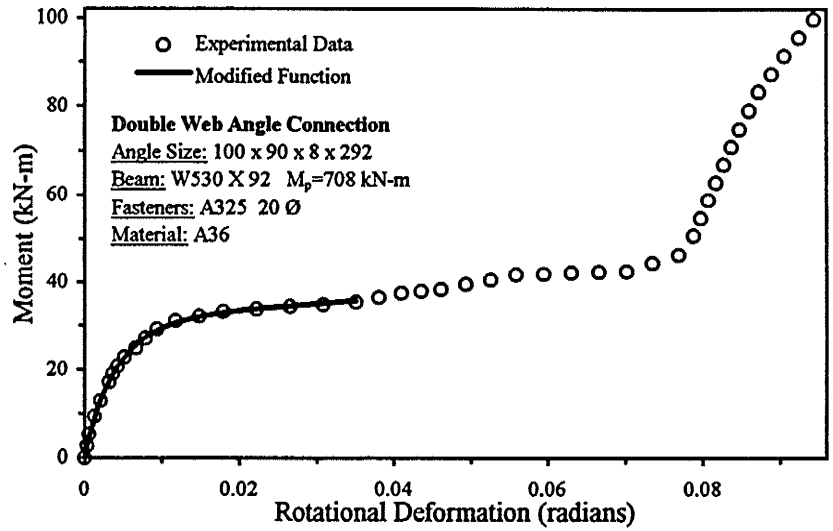


Figure A.62 (a) M-ϕ curve for Thompson: D1-1 alt b

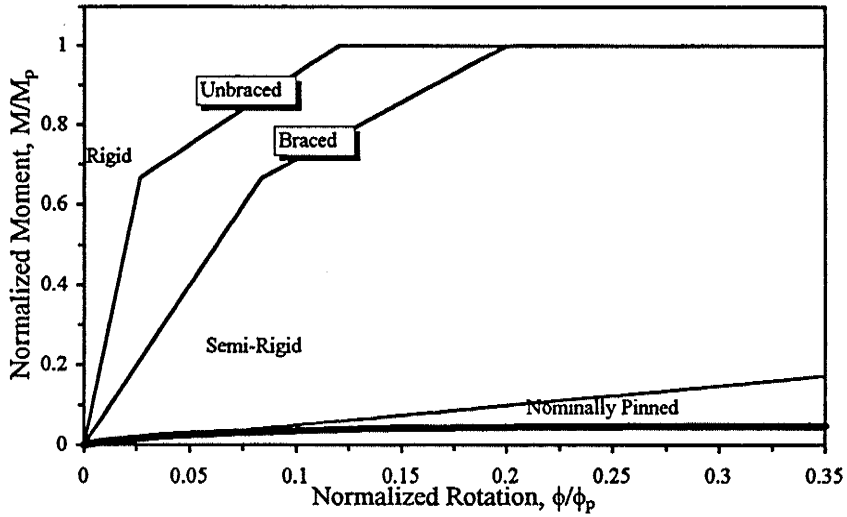


Figure A.62 (b) Eurocode3 Classification of Thompson: D1-1 alt b

Table A.63 M-ϕ data for Thompson: D1-2 alt a (1970)

Moment, M kN-m	Rotation, ϕ radians	Moment, M kN-m	Rotation, ϕ radians
0	0	54.310	0.0734
5.149	0.0006	58.587	0.0746
9.136	0.0011	62.864	0.0758
13.287	0.0018	66.850	0.0770
16.983	0.0027	70.836	0.0782
21.094	0.0039	74.968	0.0794
24.996	0.0054	79.100	0.0806
29.231	0.0084	83.148	0.0820
31.225	0.0109	87.197	0.0833
33.218	0.0134	91.340	0.0852
35.377	0.0167	95.482	0.0870
37.536	0.0199	99.644	0.0891
39.529	0.0241	103.806	0.0911
41.522	0.0282		
41.829	0.0324		
42.136	0.0366		
42.444	0.0407		
42.751	0.0449		
43.058	0.0491		
43.365	0.0533		
43.673	0.0575		
43.980	0.0616		
44.287	0.0658		
44.594	0.0700		
47.751	0.0711		
51.030	0.0723		

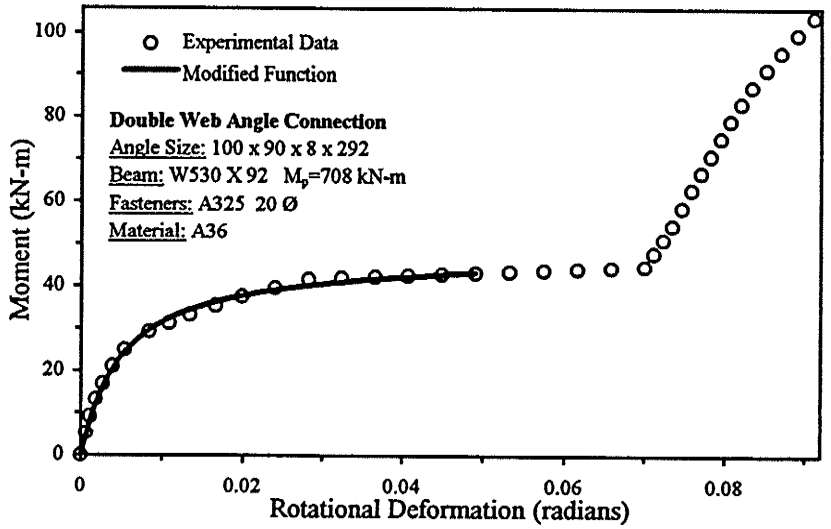


Figure A.63 (a) M-ϕ curve for Thompson: D1-2 alt a

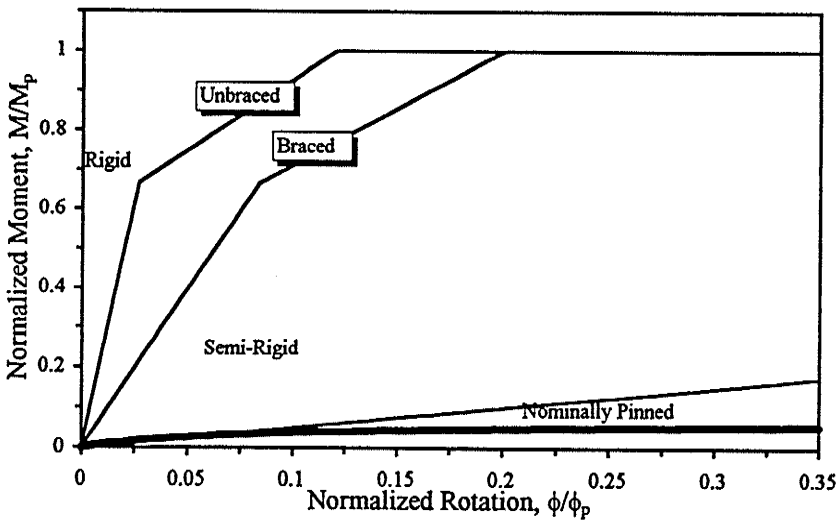


Figure A.63 (b) Eurocode3 Classification of Thompson: D1-2 alt a

Table A.64 M-ϕ data for Thompson: D1-2 alt b (1970)

Moment, M kN-m	Rotation, ϕ radians	Moment, M kN-m	Rotation, ϕ radians
0	0	54.310	0.0814
5.149	0.0006	58.587	0.0825
9.136	0.0011	62.864	0.0836
13.287	0.0019	66.850	0.0846
16.983	0.0027	70.836	0.0856
21.094	0.0039	74.968	0.0867
24.996	0.0053	79.100	0.0878
29.231	0.0079	83.148	0.0890
33.218	0.0117	87.197	0.0902
35.377	0.0142	91.340	0.0921
37.536	0.0167	95.482	0.0939
39.529	0.0198	99.644	0.0957
41.522	0.0229	103.806	0.0975
41.906	0.0274		
42.290	0.0318		
42.674	0.0363		
43.058	0.0408		
43.442	0.0452		
43.826	0.0497		
44.210	0.0541		
44.594	0.0586		
45.383	0.0634		
46.172	0.0683		
46.962	0.0731		
47.751	0.0779		
51.030	0.0797		

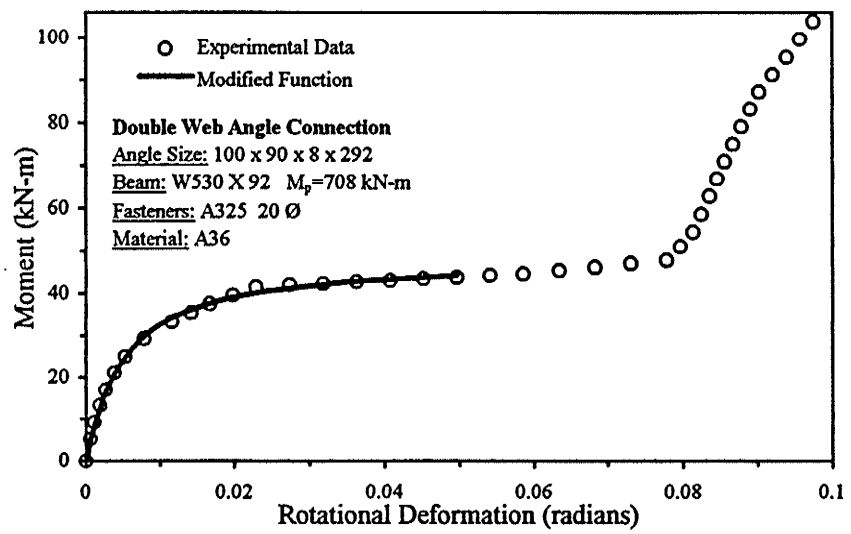


Figure A.64 (a) M-ϕ curve for Thompson: D1-2 alt b

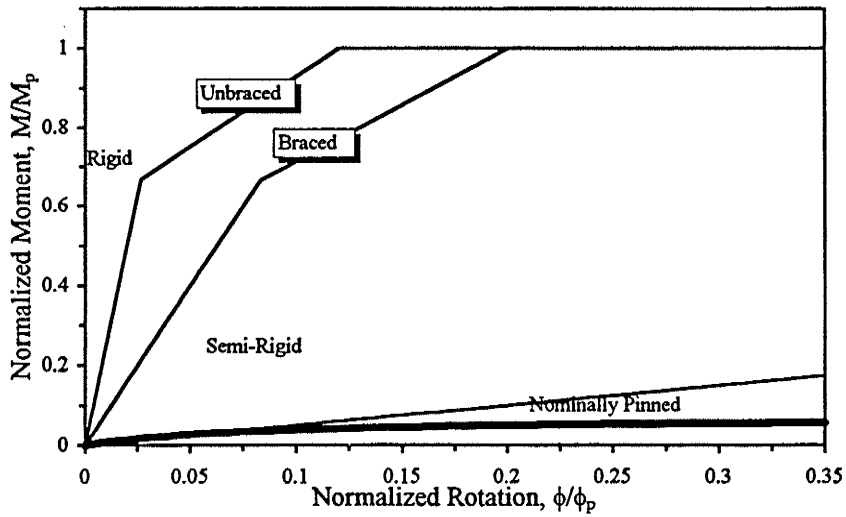


Figure A.64 (b) Eurocode3 Classification of Thompson: D1-2 alt b

Table A.65 M-ϕ data for Thompson: D1-3 alt a (1970)

Moment, M kN-m	Rotation, ϕ radians	Moment, M kN-m	Rotation, ϕ radians
0	0	50.367	0.0795
4.983	0.0005	54.644	0.0807
9.136	0.0011	58.624	0.0818
13.122	0.0018	62.605	0.0828
17.024	0.0028	66.721	0.0840
20.762	0.0041	70.836	0.0851
25.079	0.0066	74.988	0.0863
29.066	0.0095	79.141	0.0875
31.142	0.0125	83.169	0.0888
31.834	0.0166	87.197	0.0901
32.526	0.0207	91.349	0.0917
33.218	0.0248	95.501	0.0933
34.255	0.0277	99.653	0.0956
35.293	0.0305	103.806	0.0979
37.370	0.0343		
38.947	0.0390		
40.235	0.0418		
41.522	0.0446		
42.214	0.0484		
42.906	0.0523		
43.598	0.0561		
44.096	0.0605		
44.595	0.0649		
45.093	0.0694		
45.591	0.0738		
46.090	0.0782		

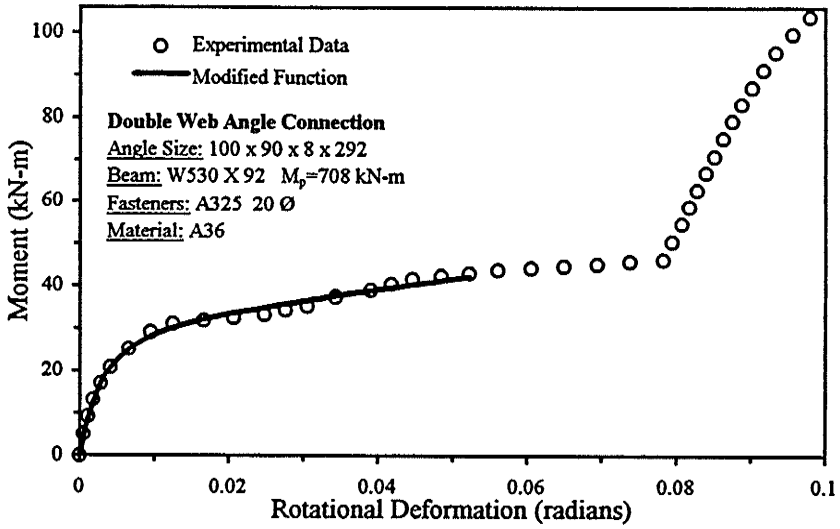


Figure A.65 (a) M-ϕ curve for Thompson: D1-3 alt a

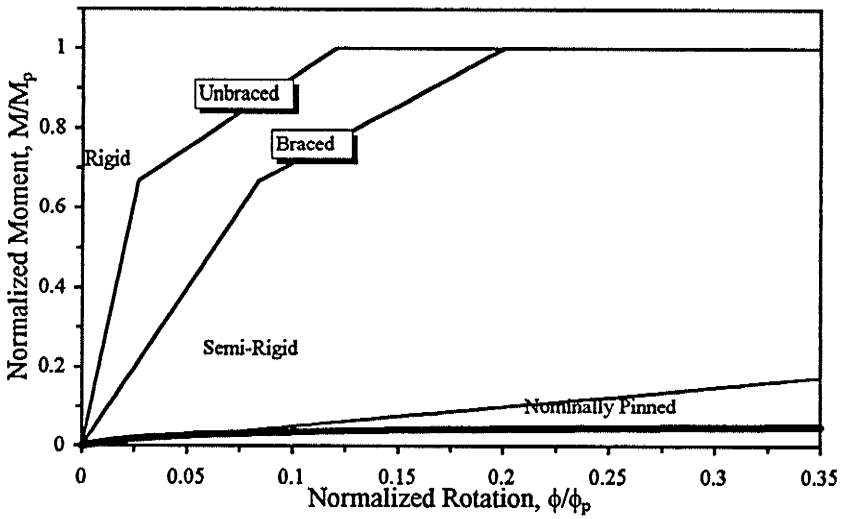


Figure A.65 (b) Eurocode3 Classification of Thompson: D1-3 alt a

Table A.66 M-ϕ data for Thompson: D1-3 alt b (1970)

Moment, M kN-m	Rotation, ϕ radians	Moment, M kN-m	Rotation, ϕ radians
0	0	54.644	0.0758
4.983	0.0006	58.624	0.0768
9.136	0.0013	62.605	0.0778
13.122	0.0020	66.721	0.0788
17.024	0.0029	70.836	0.0798
20.762	0.0042	74.988	0.0810
25.079	0.0071	79.141	0.0821
29.066	0.0104	83.169	0.0835
31.142	0.0140	87.197	0.0849
31.661	0.0186	91.349	0.0866
32.180	0.0231	95.501	0.0883
32.699	0.0277	99.653	0.0908
33.218	0.0322	103.806	0.0933
34.255	0.0353		
35.293	0.0384		
37.370	0.0425		
38.159	0.0459		
38.947	0.0492		
39.591	0.0534		
40.235	0.0576		
40.878	0.0618		
41.522	0.0660		
42.560	0.0686		
43.598	0.0712		
46.090	0.0734		
50.367	0.0746		

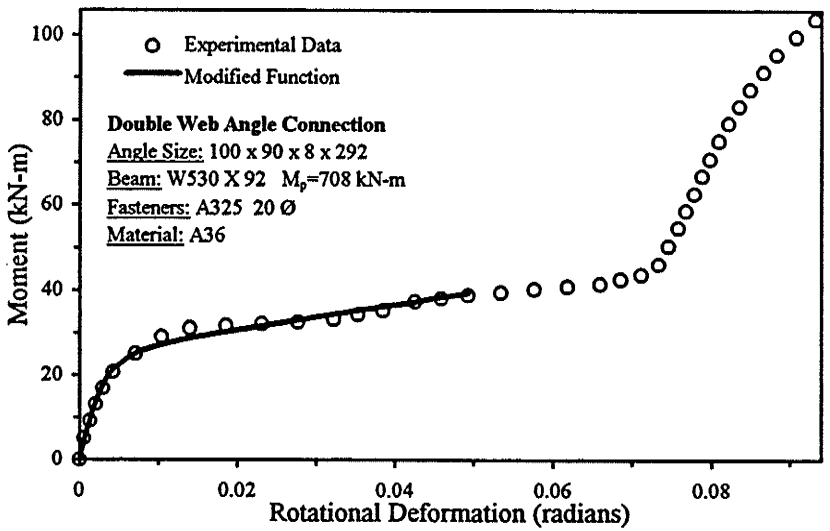


Figure A.66 (a) M-ϕ curve for Thompson: D1-3 alt b

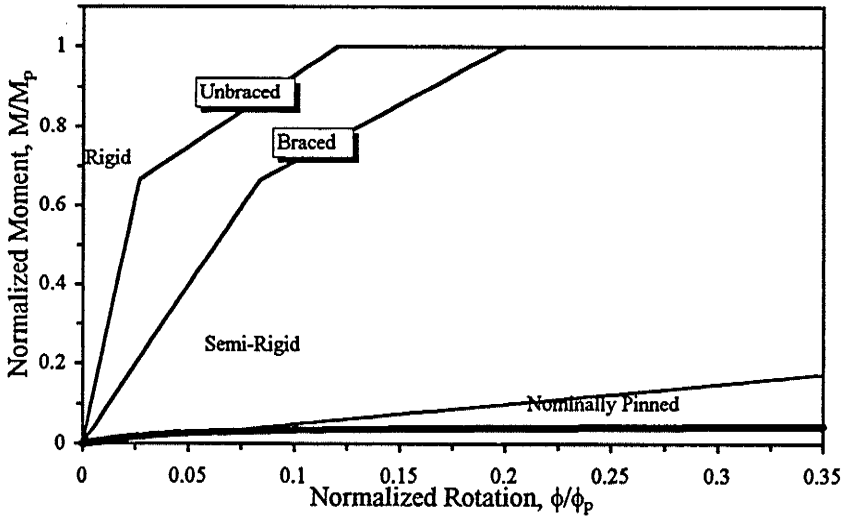


Figure A.66 (b) Eurocode3 Classification of Thompson: D1-3 alt b

Table A.67 M-ϕ data for Thompson: E1-1 alt a (1970)

Moment, M kN-m	Rotation, ϕ radians	Moment, M kN-m	Rotation, ϕ radians
0	0	58.131	0.0671
4.027	0.0002	58.131	0.0675
8.055	0.0004	61.120	0.0680
12.083	0.0007	68.117	0.0692
16.111	0.0010	75.114	0.0703
19.993	0.0014	80.594	0.0712
23.875	0.0017	86.075	0.0721
28.235	0.0022	91.556	0.0730
33.717	0.0030	98.719	0.0746
37.536	0.0038	105.881	0.0761
37.764	0.0053	112.109	0.0781
37.990	0.0068	118.337	0.0800
38.142	0.0108	125.313	0.0832
38.794	0.0136	129.092	0.0850
39.446	0.0164	132.870	0.0868
41.522	0.0202	137.023	0.0893
43.598	0.0239	141.175	0.0929
46.920	0.0288	143.251	0.0957
49.411	0.0335	145.328	0.0984
51.902	0.0381	147.403	0.1021
52.941	0.0415	149.479	0.1058
53.979	0.0448		
54.207	0.0494		
54.435	0.0540		
54.664	0.0585		
54.892	0.0631		

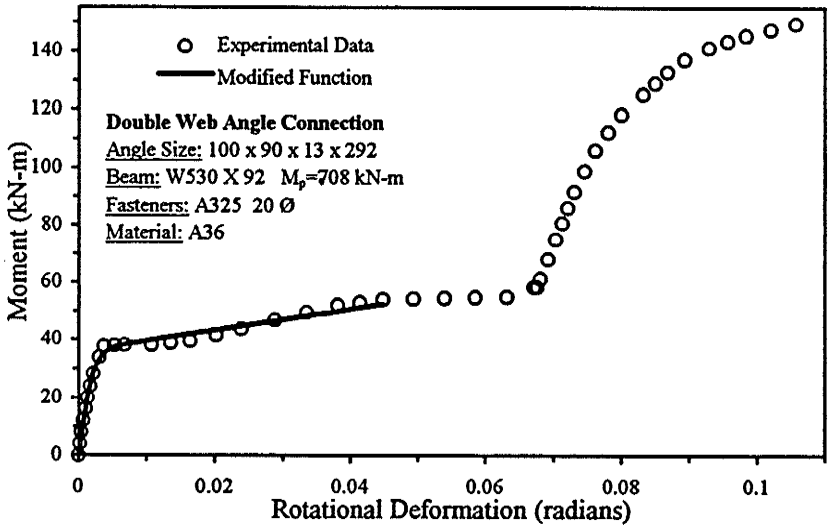


Figure A.67 (a) M-ϕ curve for Thompson: E1-1 alt a

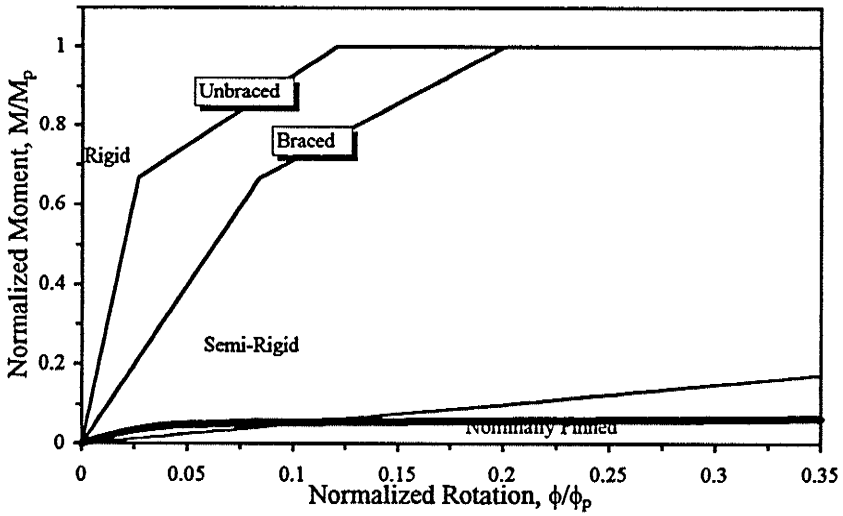


Figure A.67 (b) Eurocode3 Classification of Thompson: E1-1 alt a

Table A.68 M-ϕ data for Thompson: E1-1 alt b (1970)

Moment, M kN-m	Rotation, ϕ radians	Moment, M kN-m	Rotation, ϕ radians
0	0	60.522	0.0933
4.027	0.0002	61.120	0.0999
8.055	0.0004	68.117	0.1014
12.083	0.0007	75.114	0.1028
16.111	0.0010	80.594	0.1038
19.993	0.0014	86.075	0.1048
23.875	0.0017	91.556	0.1058
28.235	0.0023	98.719	0.1074
33.717	0.0031	105.881	0.1090
37.536	0.0038	112.109	0.1111
39.446	0.0043	118.337	0.1132
43.598	0.0057	125.313	0.1166
45.259	0.0123	129.092	0.1183
46.920	0.0189	132.870	0.1200
49.411	0.0234	137.023	0.1226
51.902	0.0278	141.175	0.1263
53.979	0.0345	145.328	0.1307
54.892	0.0403	149.479	0.1371
56.511	0.0451		
58.131	0.0499		
58.131	0.0556		
58.131	0.0614		
58.131	0.0671		
58.729	0.0737		
59.327	0.0802		
59.925	0.0868		

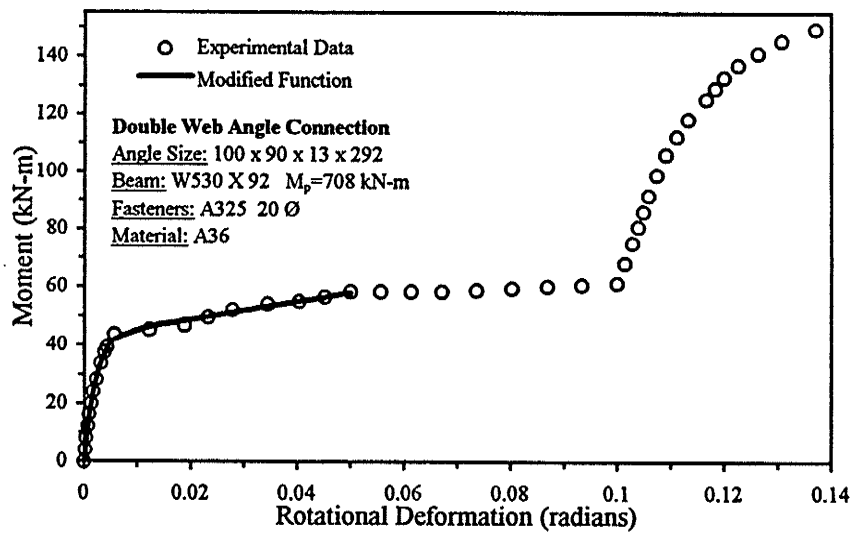


Figure A.68 (a) M-ϕ curve for Thompson: E1-1 alt b

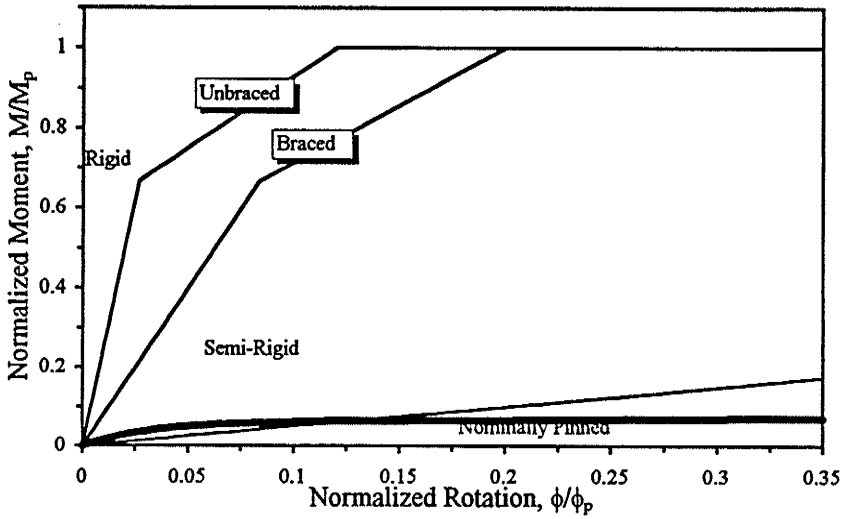


Figure A.68 (b) Eurocode3 Classification of Thompson: E1-1 alt b

Table A.69 M-ϕ data for Thompson: E1-2 alt a (1970)

Moment, M kN-m	Rotation, ϕ radians	Moment, M kN-m	Rotation, ϕ radians
0	0	75.239	0.0893
4.899	0.0003	83.335	0.0907
9.799	0.0006	91.431	0.0920
13.909	0.0009	95.542	0.0928
18.020	0.0011	99.653	0.0936
21.757	0.0014	107.126	0.0956
23.335	0.0056	111.694	0.0967
24.913	0.0098	116.262	0.0978
27.197	0.0138	120.414	0.0995
29.481	0.0178	124.566	0.1012
37.370	0.0191	128.718	0.1031
39.446	0.0256	132.870	0.1050
41.522	0.0306	137.023	0.1080
43.598	0.0340	141.175	0.1109
45.675	0.0392	145.328	0.1145
49.826	0.0457	148.971	0.1187
51.902	0.0528	152.615	0.1228
52.941	0.0579	157.276	0.1280
53.979	0.0629	161.936	0.1332
54.561	0.0686	166.088	0.1398
55.142	0.0742	164.012	0.1470
55.723	0.0799		
56.304	0.0855		
61.619	0.0867		
66.934	0.0879		
71.086	0.0886		

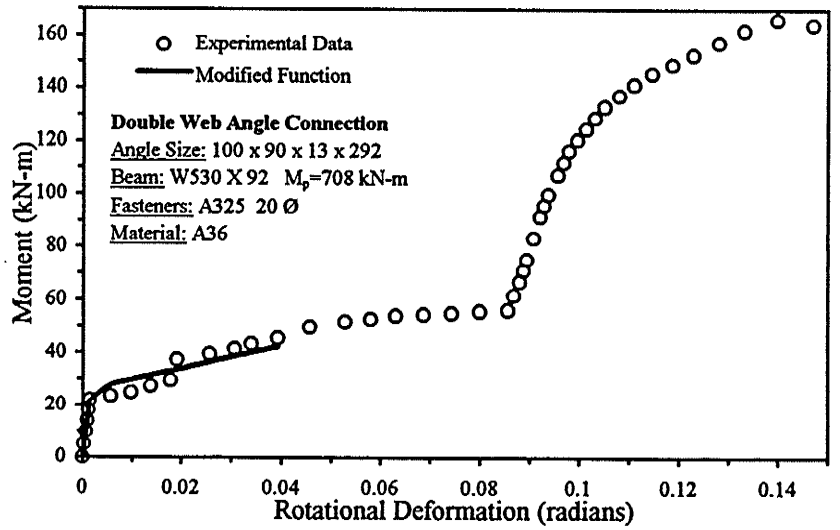


Figure A.69 (a) M-ϕ curve for Thompson: E1-2 alt a

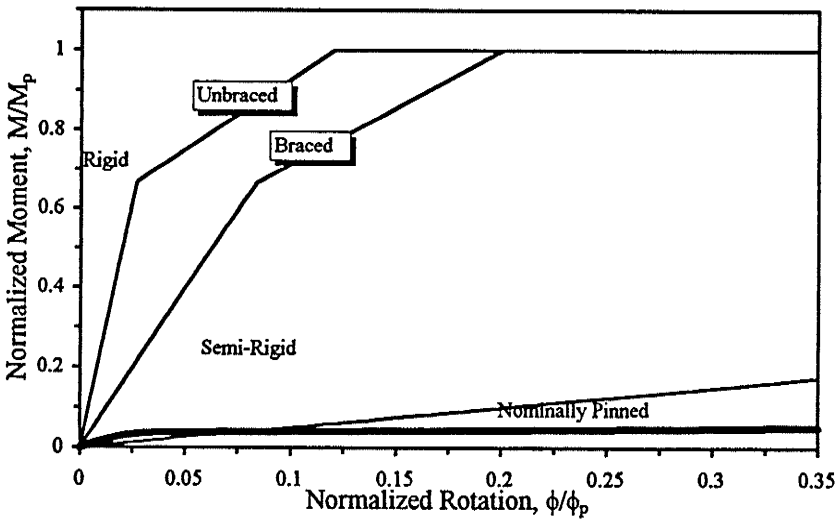


Figure A.69 (b) Eurocode3 Classification of Thompson: E1-2 alt a

Table A.70 M-ϕ data for Thompson: E1-2 alt b (1970)

Moment, M kN-m	Rotation, ϕ radians	Moment, M kN-m	Rotation, ϕ radians
0	0	83.708	0.0720
4.899	0.0004	91.431	0.0735
9.799	0.0007	95.542	0.0746
13.909	0.0010	99.653	0.0757
18.020	0.0013	105.189	0.0774
21.757	0.0018	110.725	0.0790
22.458	0.0038	116.262	0.0807
23.510	0.0068	121.798	0.0836
24.913	0.0108	127.334	0.0865
29.481	0.0168	132.870	0.0894
35.293	0.0233	137.023	0.0936
37.370	0.0288	141.175	0.0977
41.522	0.0351	145.328	0.1014
43.598	0.0393	148.971	0.1053
47.751	0.0457	152.615	0.1091
49.826	0.0491	157.276	0.1156
50.403	0.0551	161.936	0.1221
50.979	0.0610	166.088	0.1278
51.902	0.0630	165.050	0.1342
53.979	0.0653	164.012	0.1405
56.304	0.0665		
61.619	0.0680		
66.934	0.0694		
71.086	0.0700		
75.239	0.0705		
79.473	0.0713		

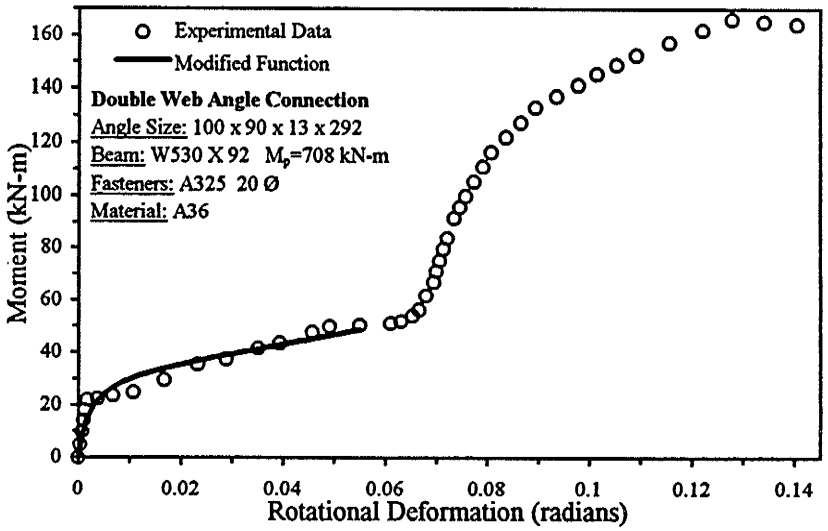


Figure A.70 (a) M-ϕ curve for Thompson: E1-2 alt b

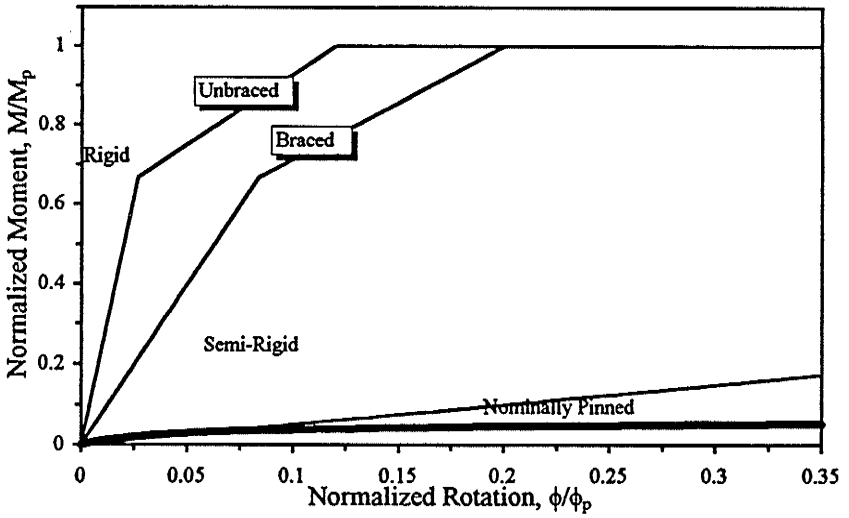


Figure A.70 (b) Eurocode3 Classification of Thompson: E1-2 alt b

Table A.71 M-ϕ data for Thompson: E1-3 alt a (1970)

Moment, M kN-m	Rotation, ϕ radians	Moment, M kN-m	Rotation, ϕ radians
0	0	79.349	0.0690
5.294	0.0003	83.626	0.0697
10.588	0.0005	87.903	0.0709
18.435	0.0010	92.179	0.0720
24.083	0.0016	100.068	0.0736
30.103	0.0022	107.957	0.0754
33.799	0.0027	112.109	0.0765
37.370	0.0034	116.262	0.0776
39.364	0.0052	120.414	0.0791
42.021	0.0055	124.566	0.0805
42.975	0.0109	128.718	0.0836
43.930	0.0162	132.870	0.0866
45.093	0.0209	137.023	0.0892
46.255	0.0255	141.175	0.0918
48.193	0.0300	145.327	0.0955
50.131	0.0344	149.479	0.0991
52.069	0.0389	152.247	0.1041
53.024	0.0425	155.015	0.1091
53.979	0.0460	157.784	0.1141
56.055	0.0507	163.841	0.1200
56.747	0.0556		
57.439	0.0604		
58.131	0.0653		
62.740	0.0662		
67.349	0.0670		
75.072	0.0683		

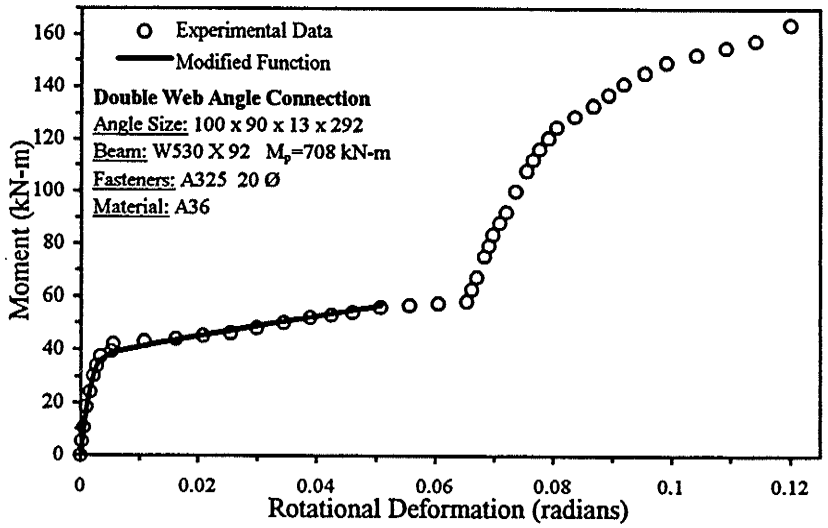


Figure A.71 (a) M-ϕ curve for Thompson: E1-3 alt a

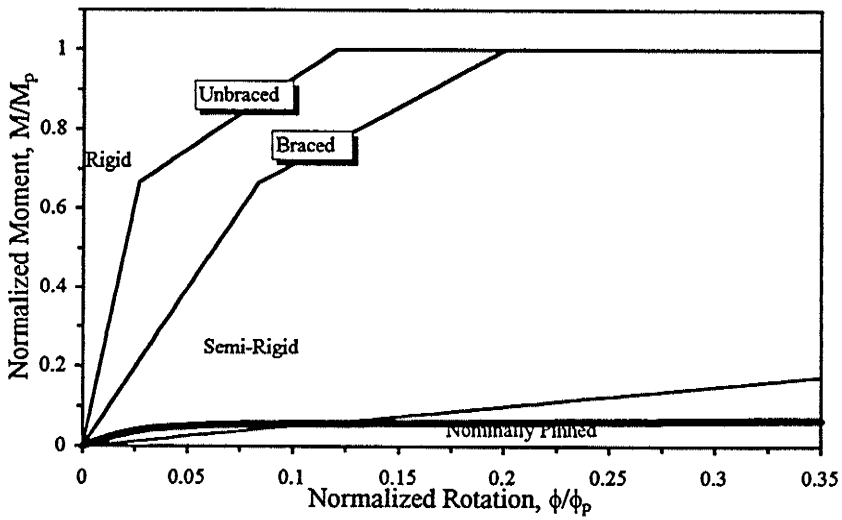


Figure A.71 (b) Eurocode3 Classification of Thompson: E1-3 alt a

Table A.72 M-ϕ data for Thompson: E1-3 alt b (1970)

Moment, M kN-m	Rotation, ϕ radians	Moment, M kN-m	Rotation, ϕ radians
0	0	83.626	0.0698
5.294	0.0003	87.903	0.0708
10.588	0.0005	92.179	0.0718
18.435	0.0011	100.068	0.0730
24.083	0.0017	107.957	0.0747
30.103	0.0026	112.109	0.0760
33.799	0.0033	116.262	0.0772
37.370	0.0042	120.414	0.0788
38.367	0.0076	124.566	0.0804
39.364	0.0109	128.718	0.0815
42.021	0.0158	132.870	0.0825
43.930	0.0205	137.023	0.0862
45.093	0.0235	141.175	0.0899
46.255	0.0265	145.327	0.0934
49.162	0.0321	149.479	0.0968
52.069	0.0376	153.631	0.1013
53.024	0.0425	157.784	0.1058
53.979	0.0473	160.812	0.1114
56.055	0.0514	163.841	0.1169
56.747	0.0562		
57.439	0.0610		
58.131	0.0658		
62.740	0.0667		
67.349	0.0675		
75.072	0.0689		
79.349	0.0694		

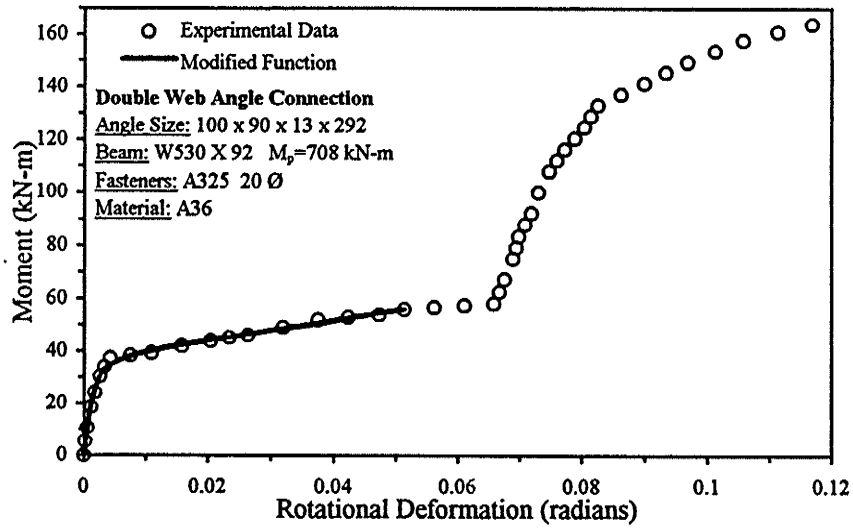


Figure A.72 (a) M-ϕ curve for Thompson: E1-3 alt b

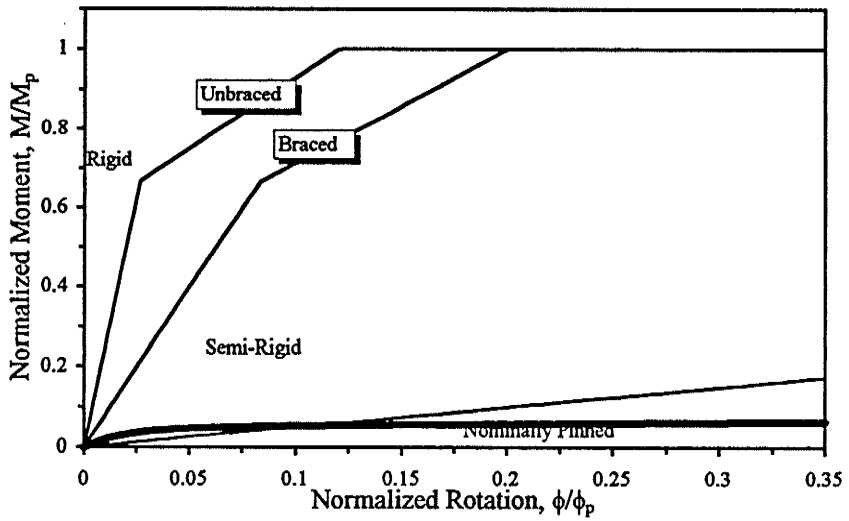


Figure A.72 (b) Eurocode3 Classification of Thompson: E1-3 alt b

Table A.72 M-ϕ data for Thompson: E1-3 alt b (1970)

Moment, M kN-m	Rotation, ϕ radians	Moment, M kN-m	Rotation, ϕ radians
0	0	83.626	0.0698
5.294	0.0003	87.903	0.0708
10.588	0.0005	92.179	0.0718
18.435	0.0011	100.068	0.0730
24.083	0.0017	107.957	0.0747
30.103	0.0026	112.109	0.0760
33.799	0.0033	116.262	0.0772
37.370	0.0042	120.414	0.0788
38.367	0.0076	124.566	0.0804
39.364	0.0109	128.718	0.0815
42.021	0.0158	132.870	0.0825
43.930	0.0205	137.023	0.0862
45.093	0.0235	141.175	0.0899
46.255	0.0265	145.327	0.0934
49.162	0.0321	149.479	0.0968
52.069	0.0376	153.631	0.1013
53.024	0.0425	157.784	0.1058
53.979	0.0473	160.812	0.1114
56.055	0.0514	163.841	0.1169
56.747	0.0562		
57.439	0.0610		
58.131	0.0658		
62.740	0.0667		
67.349	0.0675		
75.072	0.0689		
79.349	0.0694		

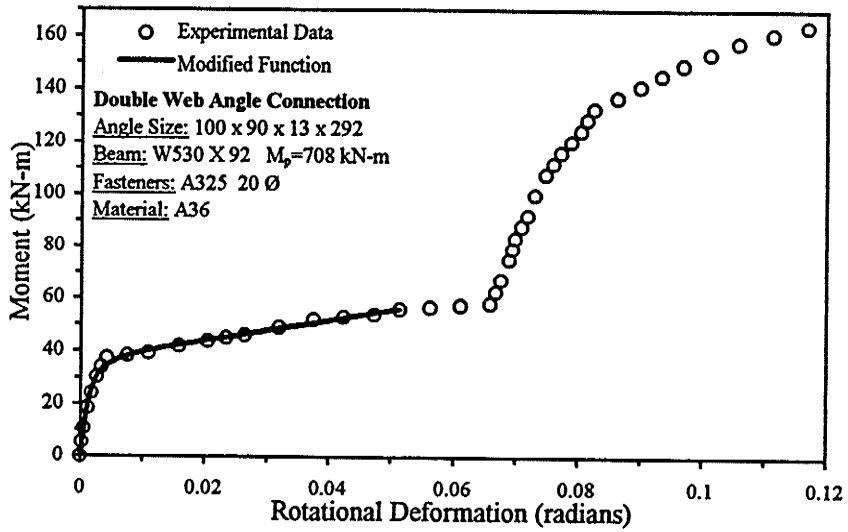


Figure A.72 (a) M-ϕ curve for Thompson: E1-3 alt b

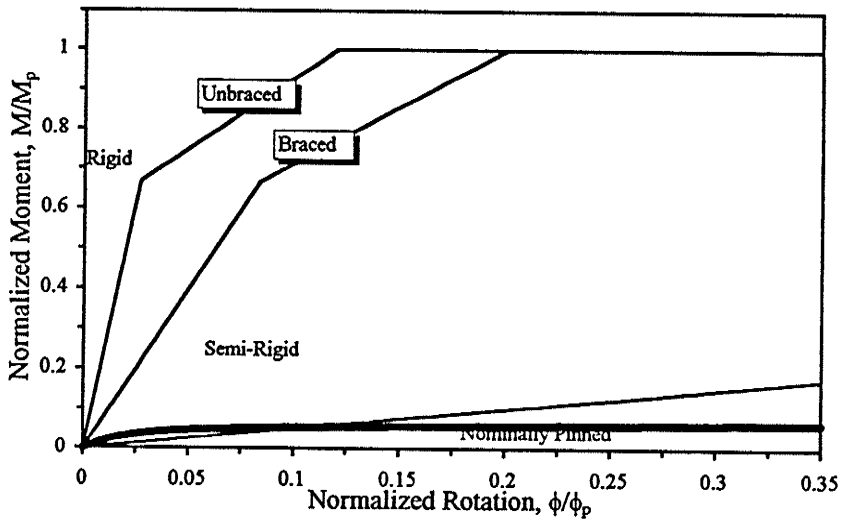


Figure A.72 (b) Eurocode3 Classification of Thompson: E1-3 alt b

Table A.73 M-ϕ data for Thompson: A2-1 alt a (1970)

Moment, M kN-m	Rotation, ϕ radians	Moment, M kN-m	Rotation, ϕ radians
0	0	78.892	0.1397
4.484	0.0011	82.878	0.1465
8.304	0.0037	86.863	0.1533
10.381	0.0088	91.182	0.1596
12.457	0.0139	95.501	0.1659
14.533	0.0206	99.653	0.1713
16.609	0.0272	103.806	0.1767
18.685	0.0334	107.958	0.1827
20.762	0.0396	112.110	0.1887
22.547	0.0472	116.262	0.1952
24.332	0.0548	120.414	0.2017
25.287	0.0622		
26.242	0.0696		
27.155	0.0770		
28.069	0.0844		
28.982	0.0918		
32.989	0.0939		
36.996	0.0960		
41.460	0.0976		
45.923	0.0992		
51.653	0.1028		
57.384	0.1064		
62.482	0.1133		
66.535	0.1204		
70.588	0.1274		
74.740	0.1336		

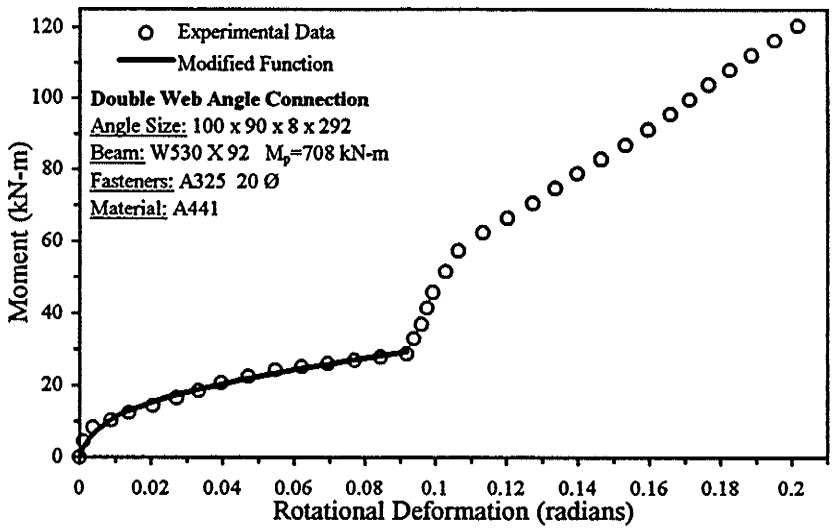


Figure A.73 (a) M-ϕ curve for Thompson: A2-1 alt a

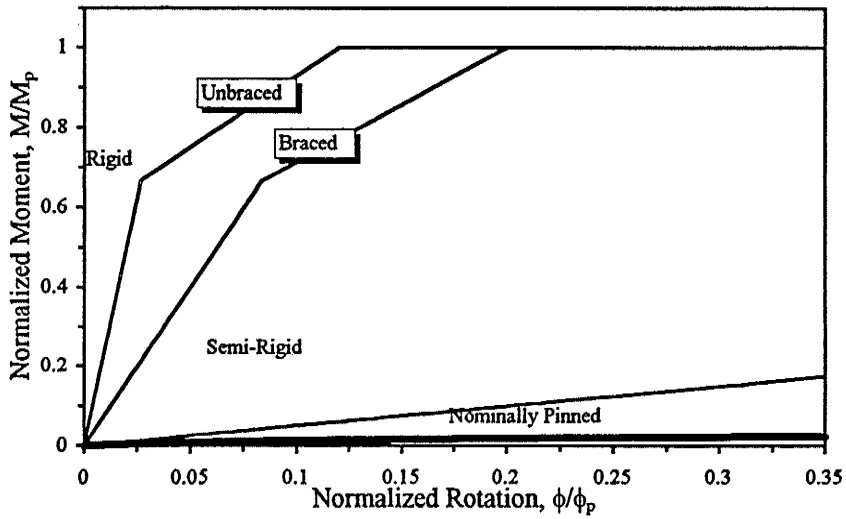


Figure A.73 (b) Eurocode3 Classification of Thompson: A2-1 alt a

Table A.74 M-ϕ data for Thompson: A2-1 alt b (1970)

Moment, M kN-m	Rotation, ϕ radians	Moment, M kN-m	Rotation, ϕ radians
0	0	86.863	0.1410
4.484	0.0015	91.182	0.1473
8.304	0.0034	95.501	0.1536
10.381	0.0105	99.653	0.1595
12.457	0.0176	103.806	0.1653
16.609	0.0234	107.958	0.1723
20.762	0.0330	112.110	0.1793
22.547	0.0413	116.262	0.1871
24.332	0.0495	120.414	0.1948
25.287	0.0547		
26.242	0.0599		
27.155	0.0679		
28.069	0.0759		
28.982	0.0839		
32.989	0.0861		
36.996	0.0882		
41.460	0.0895		
45.923	0.0908		
51.653	0.0932		
57.384	0.0955		
62.482	0.1020		
66.535	0.1090		
70.588	0.1159		
74.740	0.1225		
78.892	0.1290		
82.878	0.1350		

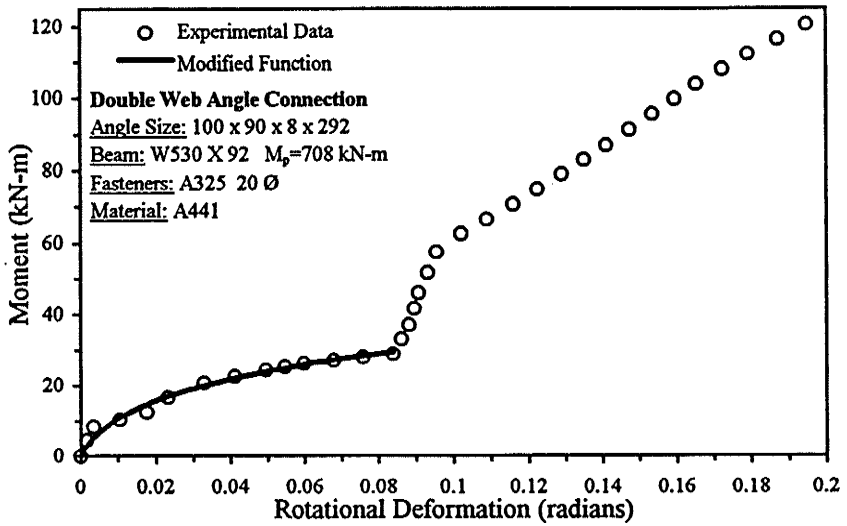


Figure A.74 (a) M-ϕ curve for Thompson: A2-1 alt b

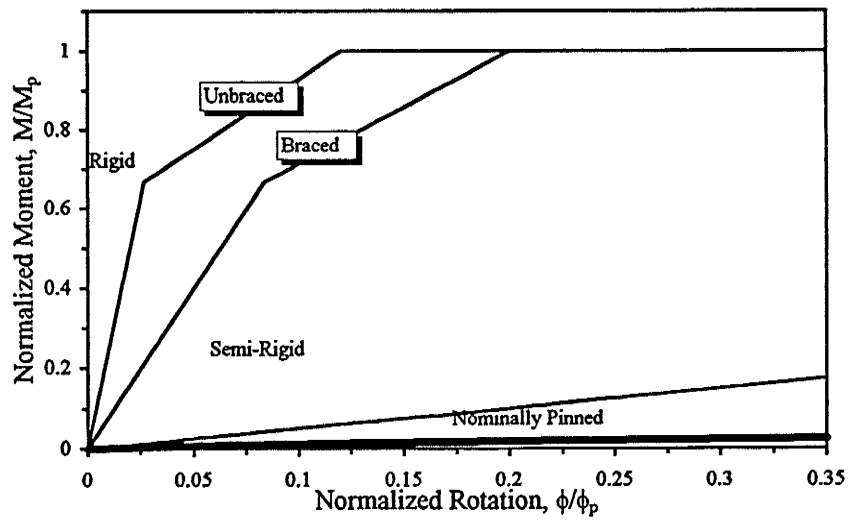


Figure A.74 (b) Eurocode3 Classification of Thompson: A2-1 alt b

Table A.75 M-ϕ data for Thompson: A2-2 alt a (1970)

Moment, M kN-m	Rotation, ϕ radians	Moment, M kN-m	Rotation, ϕ radians
0	0	91.224	0.1455
4.568	0.0007	95.501	0.1523
8.803	0.0017	99.404	0.1582
13.204	0.0032	103.307	0.1640
14.657	0.0096	107.500	0.1697
16.110	0.0160	111.694	0.1754
18.436	0.0218	116.095	0.1817
20.762	0.0275	120.497	0.1880
22.443	0.0369	124.608	0.1950
24.124	0.0462	128.719	0.2020
26.969	0.0553		
29.813	0.0644		
30.837	0.0741		
31.861	0.0838		
32.885	0.0935		
37.342	0.0953		
41.799	0.0970		
46.255	0.0988		
52.525	0.1009		
58.795	0.1029		
64.774	0.1060		
70.753	0.1091		
74.823	0.1174		
78.892	0.1257		
82.920	0.1322		
86.947	0.1386		

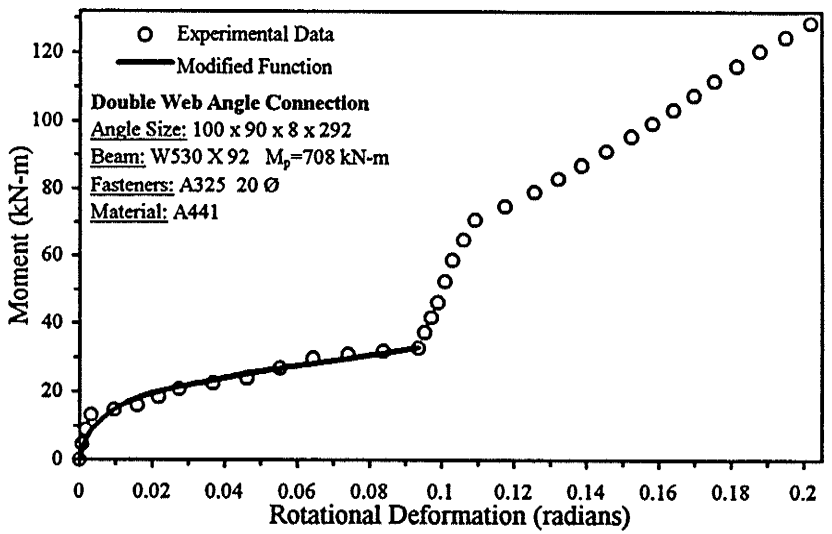


Figure A.75 (a) M-ϕ curve for Thompson: A2-2 alt a

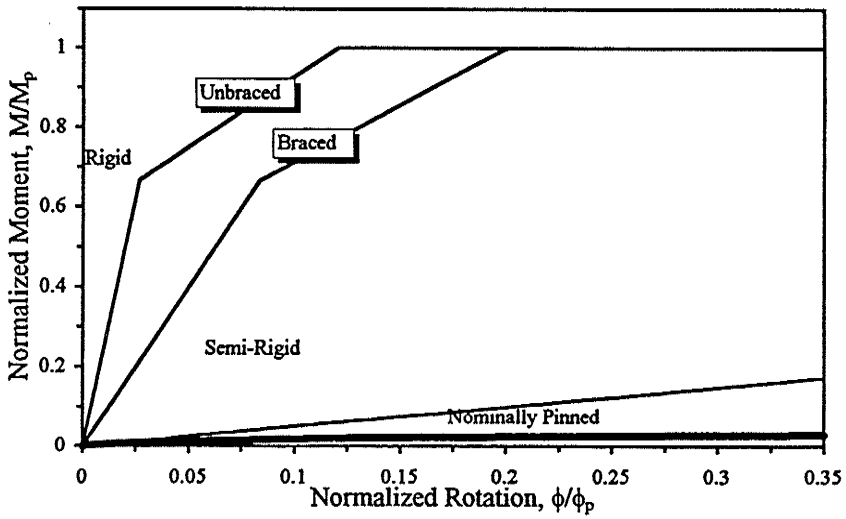


Figure A.75 (b) Eurocode3 Classification of Thompson: A2-2 alt a

Table A.76 M-ϕ data for Thompson: A2-2 alt b (1970)

Moment, M kN-m	Rotation, ϕ radians	Moment, M kN-m	Rotation, ϕ radians
0	0	95.501	0.1398
4.568	0.0010	99.404	0.1460
8.803	0.0022	103.307	0.1521
13.204	0.0036	107.500	0.1586
16.110	0.0082	111.694	0.1651
18.436	0.0134	116.095	0.1723
20.762	0.0185	120.497	0.1795
22.443	0.0267	124.608	0.1884
24.124	0.0348	128.719	0.1972
26.969	0.0426		
29.813	0.0503		
30.837	0.0575		
31.861	0.0646		
32.885	0.0718		
37.342	0.0742		
41.799	0.0765		
46.255	0.0789		
52.525	0.0812		
58.795	0.0834		
64.774	0.0882		
70.753	0.0930		
74.823	0.1021		
78.892	0.1112		
82.920	0.1181		
86.947	0.1250		
91.224	0.1324		

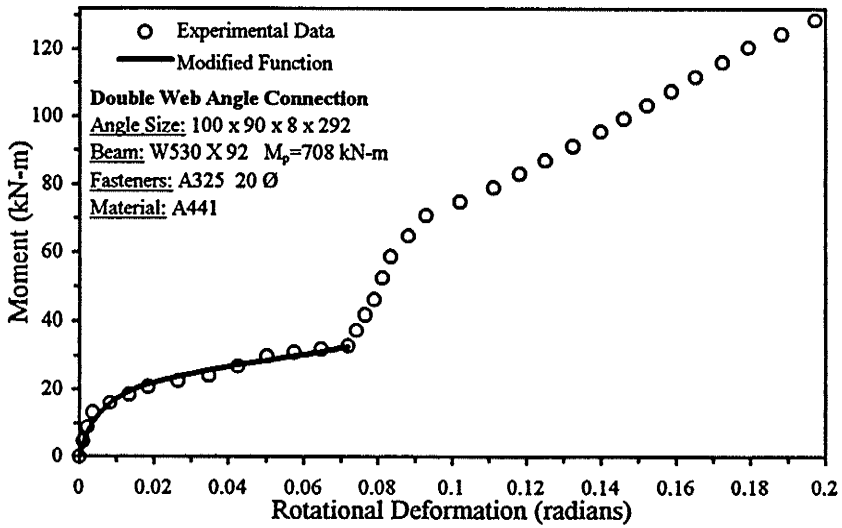


Figure A.76 (a) M-ϕ curve for Thompson: A2-2 alt b

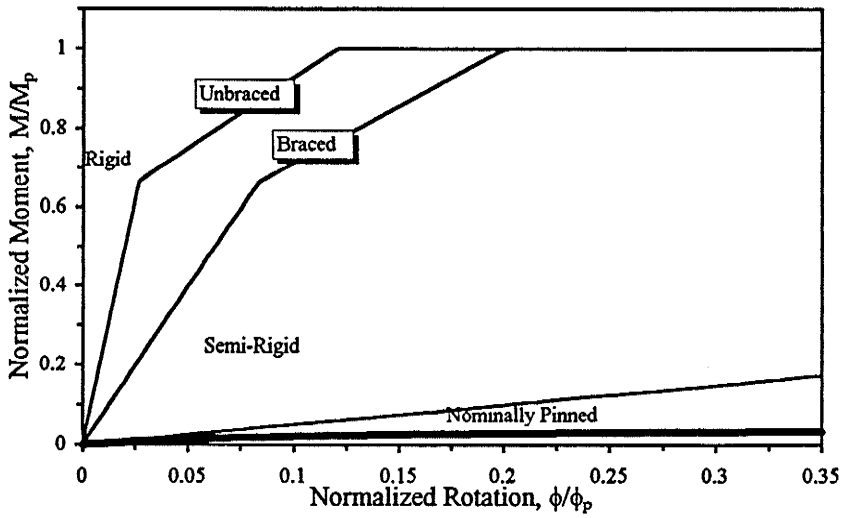


Figure A.76 (b) Eurocode3 Classification of Thompson: A2-2 alt b

Table A.77 M-ϕ data for Thompson: A2-3 alt a (1970)

Moment, M kN-m	Rotation, ϕ radians	Moment, M kN-m	Rotation, ϕ radians
0	0	78.808	0.1381
4.153	0.0018	83.003	0.1441
8.470	0.0042	87.197	0.1500
12.373	0.0090	91.432	0.1556
14.491	0.0166	95.667	0.1612
16.609	0.0241	99.736	0.1668
18.394	0.0324	103.806	0.1723
20.180	0.0406	107.958	0.1789
21.301	0.0457	112.110	0.1855
22.423	0.0507	115.847	0.1907
23.170	0.0580	119.583	0.1958
23.917	0.0653		
25.744	0.0743		
27.571	0.0834		
29.398	0.0924		
33.550	0.0939		
37.702	0.0955		
41.854	0.0970		
45.965	0.0986		
50.076	0.1001		
54.145	0.1028		
58.214	0.1054		
62.284	0.1081		
66.352	0.1164		
70.421	0.1247		
74.615	0.1314		

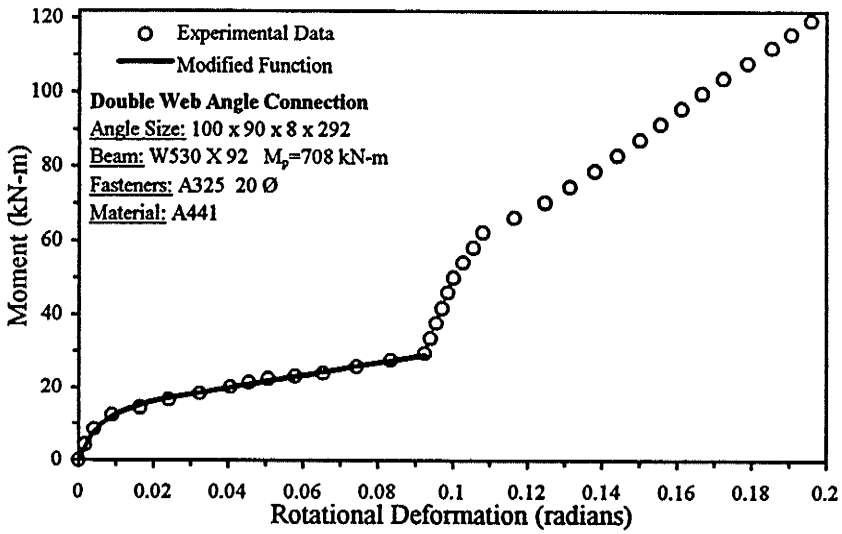


Figure A.77 (a) M-ϕ curve for Thompson: A2-3 alt a

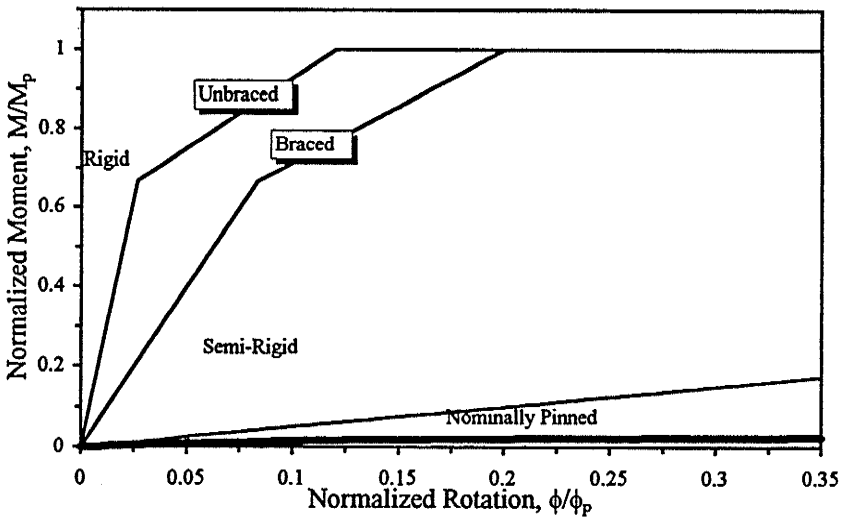


Figure A.77 (b) Eurocode3 Classification of Thompson: A2-3 alt a

Table A.78 M-ϕ data for Thompson: A2-3 alt b (1970)

Moment, M kN-m	Rotation, ϕ radians	Moment, M kN-m	Rotation, ϕ radians
0	0	83.003	0.1418
4.153	0.0021	87.197	0.1485
8.470	0.0049	91.432	0.1549
10.422	0.0124	95.667	0.1612
12.373	0.0198	99.736	0.1667
14.491	0.0256	103.806	0.1722
16.609	0.0313	107.958	0.1797
18.394	0.0385	112.110	0.1872
20.180	0.0457	114.601	0.1943
21.301	0.0517	117.092	0.2014
22.423	0.0576	119.583	0.2085
23.170	0.0672		
23.917	0.0767		
28.817	0.0797		
33.717	0.0827		
37.785	0.0843		
41.854	0.0858		
45.965	0.0879		
50.076	0.0899		
54.145	0.0948		
58.214	0.0996		
62.284	0.1045		
66.352	0.1126		
70.421	0.1206		
74.615	0.1278		
78.808	0.1350		

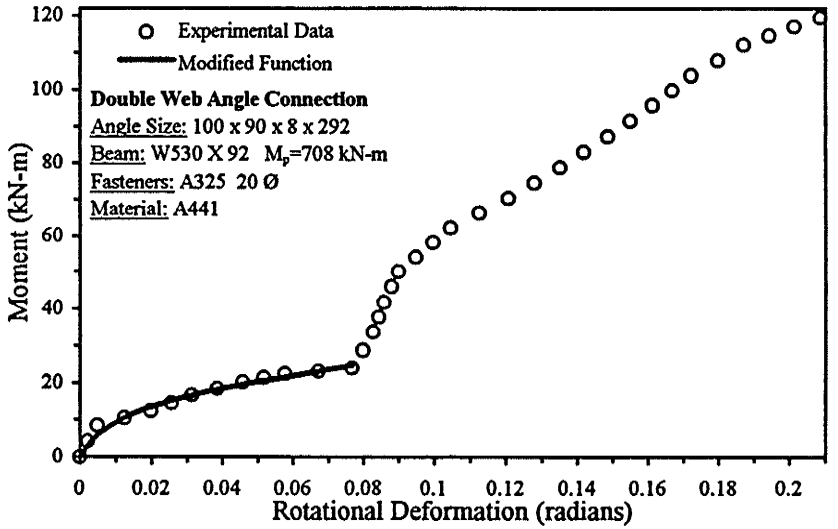


Figure A.78 (a) M-ϕ curve for Thompson: A2-3 alt b

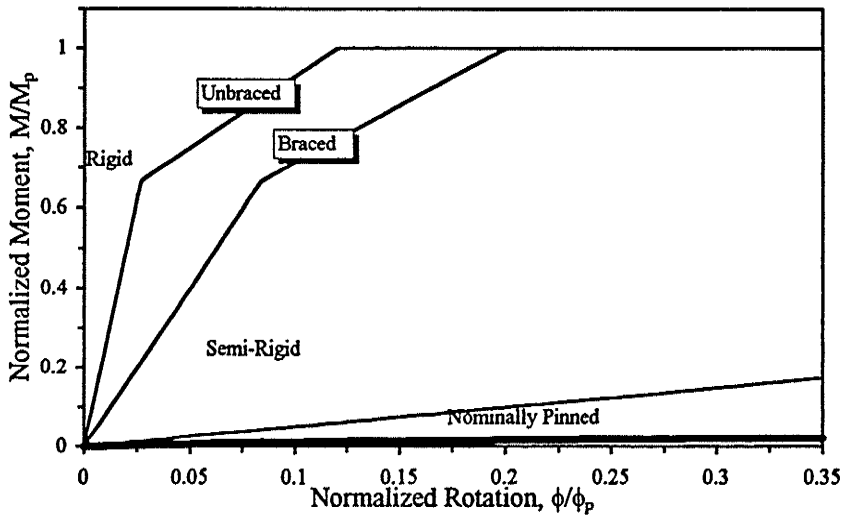


Figure A.78 (b) Eurocode3 Classification of Thompson: A2-3 alt b

Table A.79 M-ϕ data for Thompson: B2-1 alt a (1970)

Moment, M kN-m	Rotation, ϕ radians	Moment, M kN-m	Rotation, ϕ radians
0	0	101.895	0.1043
5.065	0.0007	107.957	0.1118
8.803	0.0018	111.860	0.1149
9.281	0.0036	115.763	0.1180
9.758	0.0055	120.164	0.1233
11.190	0.0110	124.566	0.1286
12.623	0.0166	128.677	0.1330
16.775	0.0201	132.788	0.1373
20.927	0.0236	136.899	0.1425
24.997	0.0278	141.009	0.1477
29.066	0.0320	145.162	0.1552
33.218	0.0390	149.314	0.1626
35.501	0.0455	153.631	0.1727
37.785	0.0520	157.949	0.1828
40.007	0.0615	156.413	0.1925
42.228	0.0710	154.877	0.2022
48.228	0.0730		
54.227	0.0750		
59.736	0.0767		
65.245	0.0784		
70.753	0.0801		
76.235	0.0825		
81.716	0.0849		
87.197	0.0873		
91.515	0.0920		
95.833	0.0967		

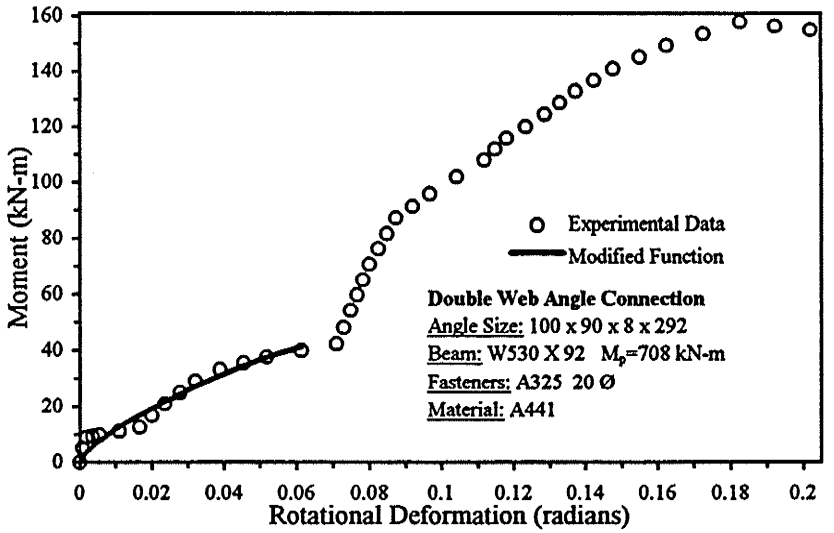


Figure A.79 (a) M-ϕ curve for Thompson: B2-1 alt a

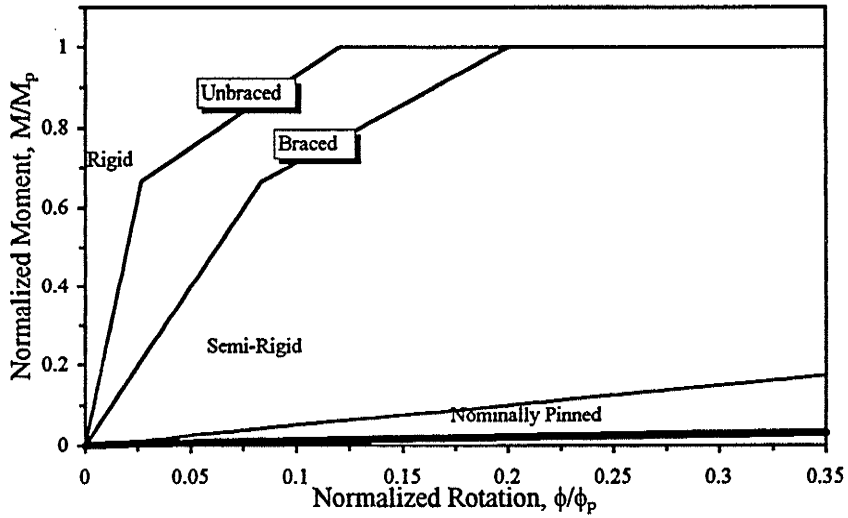


Figure A.79 (b) Eurocode3 Classification of Thompson: B2-1 alt a

Table A.80 M-ϕ data for Thompson: B2-1 alt b (1970)

Moment, M kN-m	Rotation, ϕ radians	Moment, M kN-m	Rotation, ϕ radians
0	0	95.833	0.1220
5.065	0.0008	101.895	0.1284
8.803	0.0014	107.957	0.1347
12.623	0.0025	111.860	0.1391
16.776	0.0133	115.763	0.1435
18.159	0.0207	120.164	0.1497
19.543	0.0282	124.566	0.1558
20.927	0.0356	128.677	0.1596
22.837	0.0415	132.788	0.1633
24.748	0.0473	136.899	0.1695
28.983	0.0535	141.009	0.1756
33.218	0.0596	145.162	0.1828
35.896	0.0663	149.314	0.1900
38.574	0.0729	152.192	0.1973
39.792	0.0812	155.071	0.2045
41.010	0.0894	157.949	0.2118
42.228	0.0977	154.877	0.2176
48.228	0.0995		
54.227	0.1013		
59.736	0.1028		
65.245	0.1043		
70.753	0.1058		
76.235	0.1082		
81.716	0.1105		
87.197	0.1129		
91.515	0.1175		

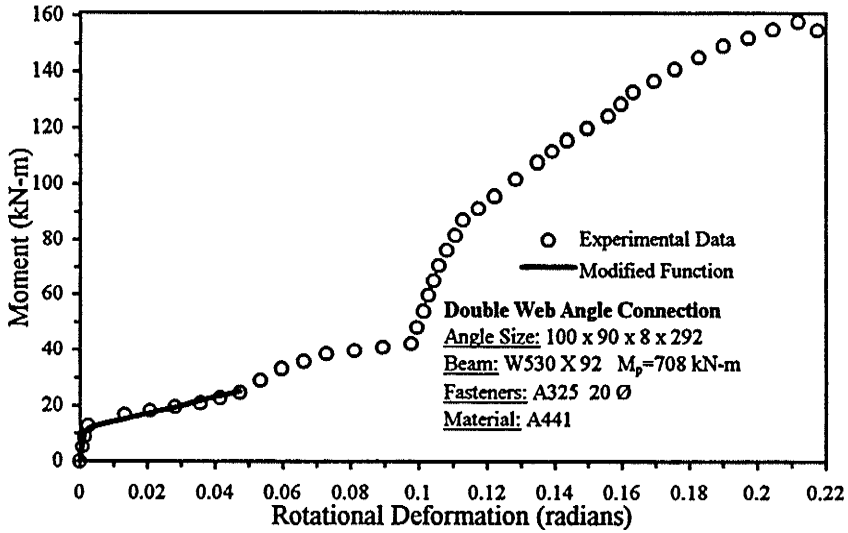


Figure A.80 (a) M-ϕ curve for Thompson: B2-1 alt b

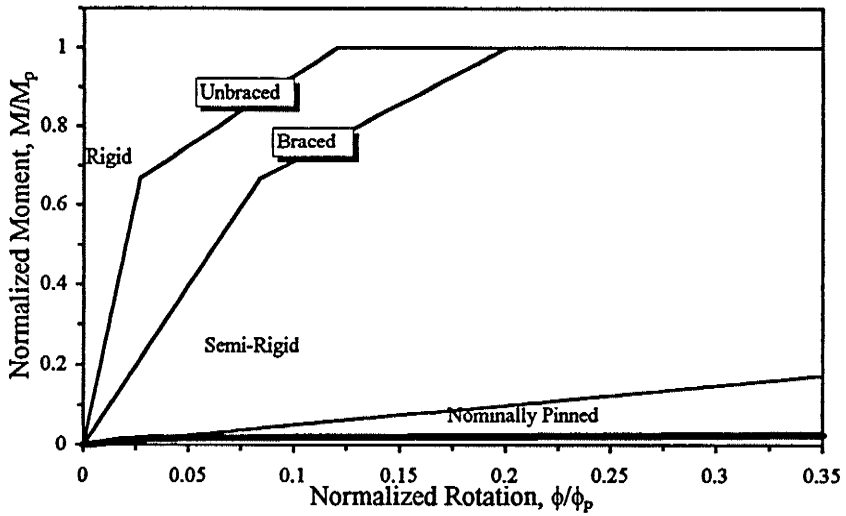


Figure A.80 (b) Eurocode3 Classification of Thompson: B2-1 alt b

Table A.81 M-ϕ data for Thompson: B2-2 alt a (1970)

Moment, M kN-m	Rotation, ϕ radians	Moment, M kN-m	Rotation, ϕ radians
0	0	99.985	0.1078
4.941	0.0006	104.221	0.1115
8.719	0.0013	108.456	0.1152
12.788	0.0023	112.400	0.1194
13.743	0.0094	116.344	0.1235
14.698	0.0166	120.455	0.1285
15.654	0.0237	124.566	0.1334
16.609	0.0308	128.677	0.1386
20.761	0.0382	132.788	0.1437
24.913	0.0455	137.189	0.1502
30.062	0.0530	141.590	0.1567
35.211	0.0604	145.659	0.1643
36.789	0.0690	149.729	0.1718
38.367	0.0776	153.154	0.1805
44.346	0.0794	156.580	0.1892
50.325	0.0812		
54.519	0.0823		
58.712	0.0834		
62.865	0.0846		
67.017	0.0858		
71.086	0.0873		
75.154	0.0887		
82.380	0.0936		
87.071	0.0969		
91.763	0.1002		
95.874	0.1040		

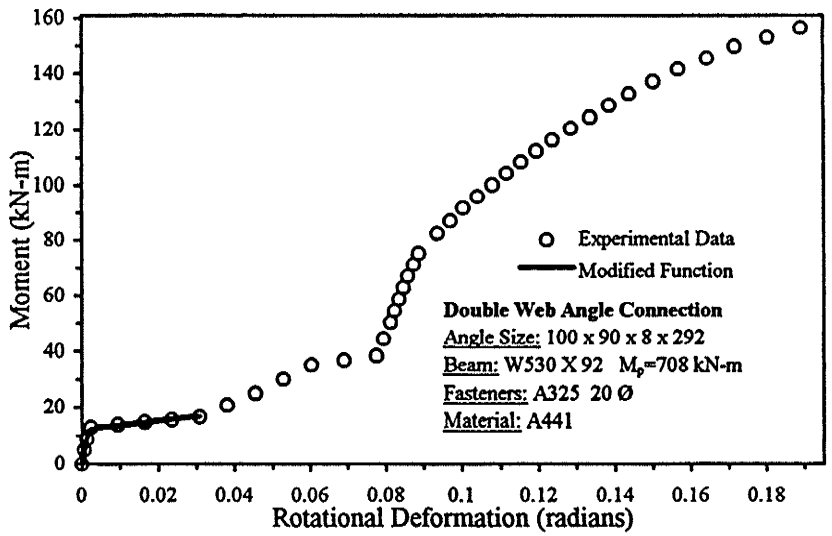


Figure A.81 (a) M-ϕ curve for Thompson: B2-2 alt a

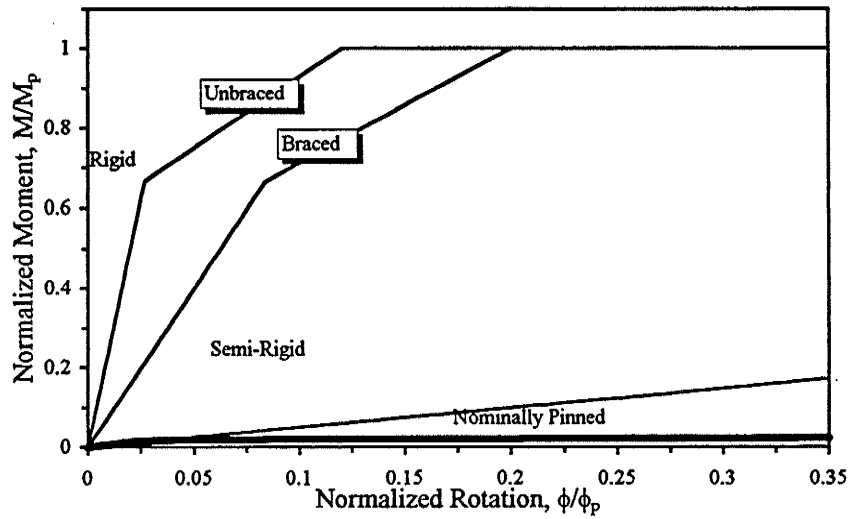


Figure A.81 (b) Eurocode3 Classification of Thompson: B2-2 alt a

Table A.82 M-ϕ data for Thompson: B2-2 alt b (1970)

Moment, M kN-m	Rotation, ϕ radians	Moment, M kN-m	Rotation, ϕ radians
0	0	91.763	0.1030
4.941	0.0015	95.874	0.1065
8.719	0.0022	99.985	0.1099
12.788	0.0031	104.221	0.1136
14.062	0.0097	108.456	0.1172
15.335	0.0164	112.400	0.1223
16.609	0.0230	116.344	0.1273
18.809	0.0282	122.532	0.1346
21.010	0.0334	128.719	0.1418
24.913	0.0429	135.154	0.1507
28.858	0.0494	141.590	0.1596
32.803	0.0559	145.659	0.1670
35.211	0.0616	149.729	0.1743
37.370	0.0694	152.012	0.1818
39.528	0.0771	154.296	0.1892
41.687	0.0849	156.580	0.1967
46.006	0.0861		
50.325	0.0873		
54.519	0.0884		
58.712	0.0895		
62.865	0.0906		
67.017	0.0917		
71.086	0.0930		
75.154	0.0943		
82.380	0.0978		
87.071	0.1004		

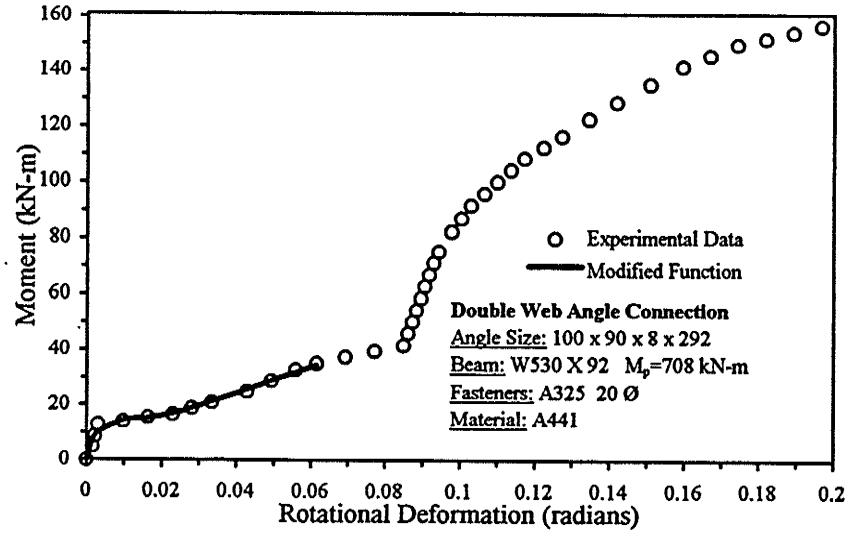


Figure A.82 (a) M-ϕ curve for Thompson: B2-2 alt b

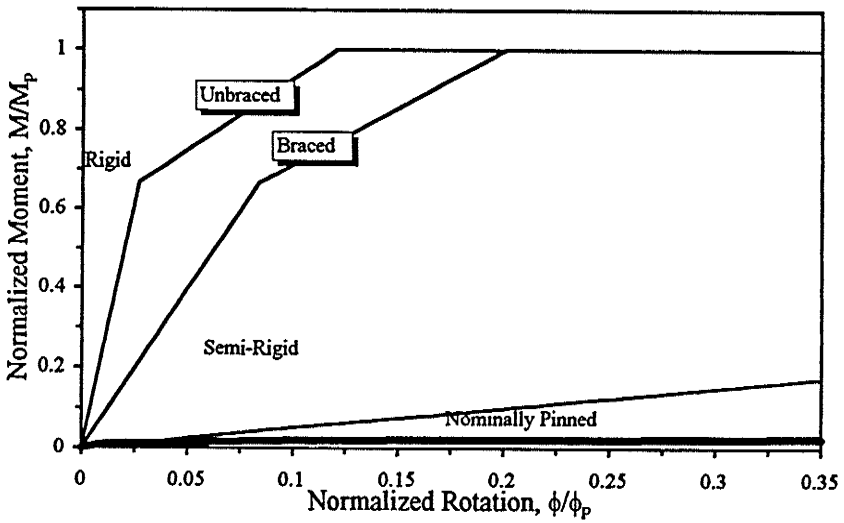


Figure A.82 (b) Eurocode3 Classification of Thompson: B2-2 alt b

Table A.83 M-ϕ data for Thompson: B2-3 alt a (1970)

Moment, M kN-m	Rotation, ϕ radians	Moment, M kN-m	Rotation, ϕ radians
0	0	99.653	0.1108
5.232	0.0004	103.929	0.1179
8.844	0.0010	108.206	0.1251
12.457	0.0023	112.483	0.1322
12.986	0.0046	118.566	0.1377
13.516	0.0069	124.649	0.1431
15.104	0.0137	128.718	0.1482
16.692	0.0206	132.788	0.1532
20.885	0.0272	139.058	0.1623
25.079	0.0338	145.328	0.1713
27.196	0.0398	149.521	0.1796
29.314	0.0458	153.715	0.1879
34.961	0.0536	153.244	0.1961
40.608	0.0614	152.773	0.2044
42.020	0.0702	152.302	0.2126
43.432	0.0790		
44.844	0.0878		
51.944	0.0901		
59.045	0.0923		
64.415	0.0938		
69.785	0.0954		
75.154	0.0969		
80.719	0.0989		
86.283	0.1010		
91.847	0.1030		
95.750	0.1069		

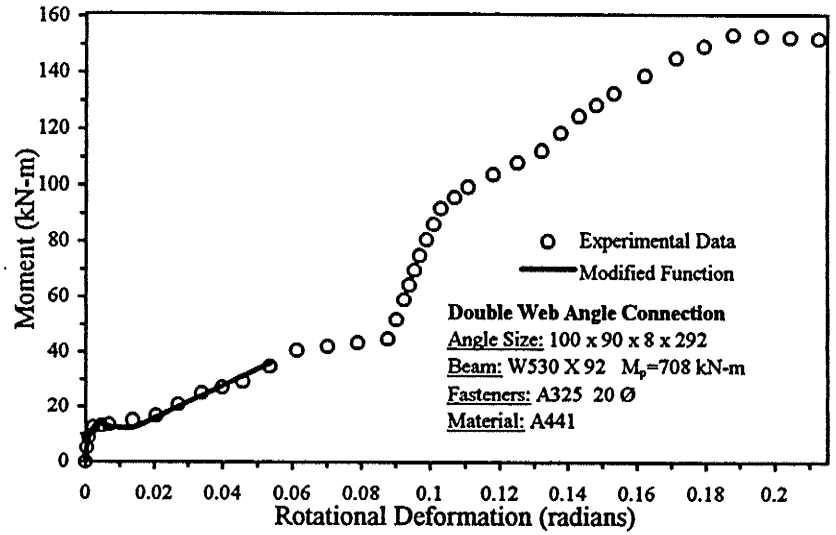


Figure A.83 (a) M-ϕ curve for Thompson: B2-3 alt a

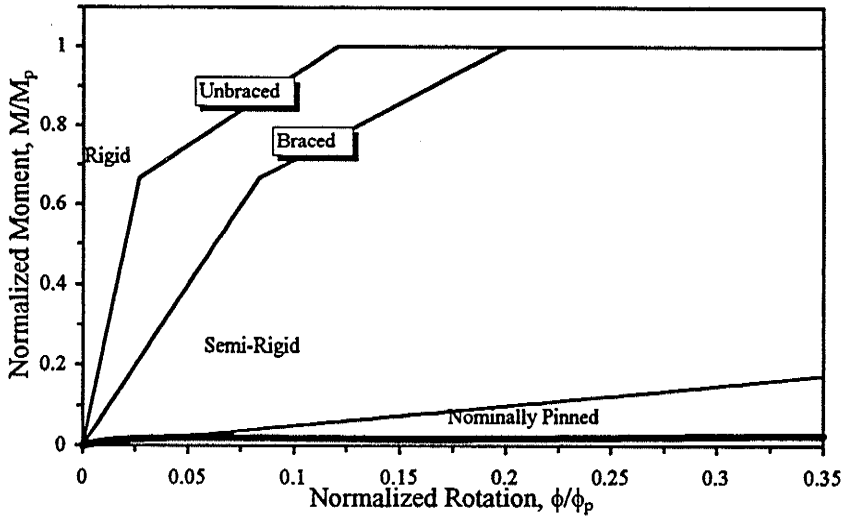


Figure A.83 (b) Eurocode3 Classification of Thompson: B2-3 alt a

Table A.84 M-ϕ data for Thompson: B2-3 alt b (1970)

Moment, M kN-m	Rotation, ϕ radians	Moment, M kN-m	Rotation, ϕ radians
0	0	99.653	0.1103
5.232	0.0008	103.805	0.1154
8.844	0.0015	107.957	0.1205
12.457	0.0022	113.521	0.1270
16.692	0.0054	119.085	0.1335
19.487	0.0125	124.649	0.1400
22.283	0.0197	130.836	0.1474
25.079	0.0268	137.023	0.1548
29.273	0.0332	141.175	0.1610
33.467	0.0396	145.328	0.1671
37.038	0.0455	149.521	0.1757
40.608	0.0513	153.715	0.1843
42.726	0.0589	153.008	0.1893
44.844	0.0665	152.302	0.1942
46.615	0.0738		
48.387	0.0812		
50.159	0.0885		
55.806	0.0901		
61.453	0.0918		
67.100	0.0934		
72.774	0.0951		
78.449	0.0968		
84.123	0.0985		
87.985	0.1003		
91.847	0.1020		
95.750	0.1062		

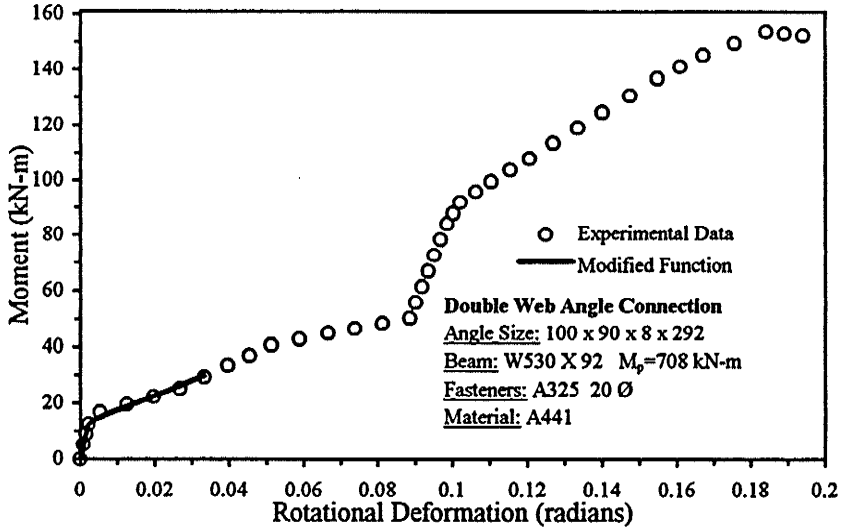


Figure A.84 (a) M-ϕ curve for Thompson: B2-3 alt b

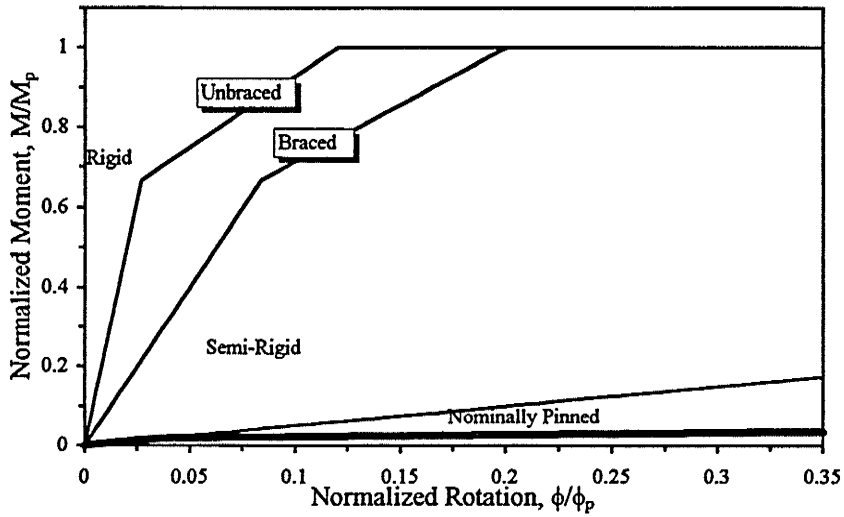


Figure A.84 (b) Eurocode3 Classification of Thompson: B2-3 alt b

Table A.85 M-ϕ data for Thompson: C2-1 alt a (1970)

Moment, M kN-m	Rotation, ϕ radians	Moment, M kN-m	Rotation, ϕ radians
0	0	101.687	0.1144
4.401	0.0003	107.957	0.1214
8.719	0.0009	112.109	0.1264
10.588	0.0037	116.262	0.1313
12.457	0.0064	122.490	0.1408
14.533	0.0115	128.719	0.1502
16.609	0.0166	132.995	0.1575
20.802	0.0261	137.271	0.1648
24.996	0.0355	141.299	0.1714
29.066	0.0417	145.328	0.1780
33.218	0.0505	147.431	0.1858
35.294	0.0557	149.534	0.1936
37.370	0.0609	151.638	0.2014
39.694	0.0675		
40.926	0.0746		
42.158	0.0816		
43.390	0.0887		
50.241	0.0905		
55.099	0.0917		
59.957	0.0929		
65.438	0.0945		
70.919	0.0961		
77.106	0.0982		
83.293	0.1003		
89.355	0.1038		
95.417	0.1073		

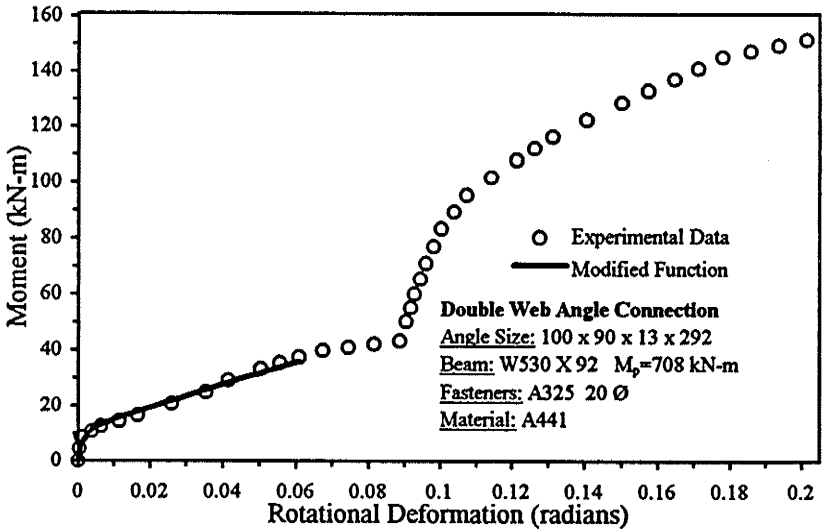


Figure A.85 (a) M-ϕ curve for Thompson: C2-1 alt a

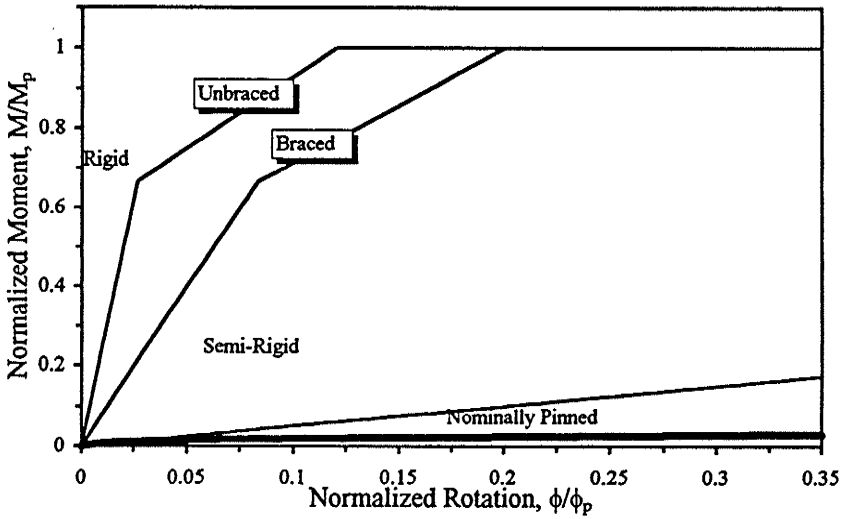


Figure A.85 (b) Eurocode3 Classification of Thompson: C2-1 alt a

Table A.86 M-ϕ data for Thompson: C2-1 alt b (1970)

Moment, M kN-m	Rotation, ϕ radians	Moment, M kN-m	Rotation, ϕ radians
0	0	116.262	0.1046
4.401	0.0005	120.414	0.1104
8.719	0.0012	124.566	0.1163
12.457	0.0020	128.719	0.1221
16.609	0.0062	132.995	0.1298
21.092	0.0105	137.271	0.1374
24.996	0.0148	141.299	0.1439
29.066	0.0200	145.328	0.1504
33.218	0.0262	148.483	0.1575
37.370	0.0338	151.638	0.1645
39.694	0.0400		
41.542	0.0454		
43.390	0.0507		
46.816	0.0589		
50.241	0.0670		
55.099	0.0682		
59.957	0.0693		
65.438	0.0707		
70.919	0.0720		
77.106	0.0739		
83.293	0.0757		
89.355	0.0787		
95.417	0.0816		
101.687	0.0882		
107.957	0.0947		
112.109	0.0997		

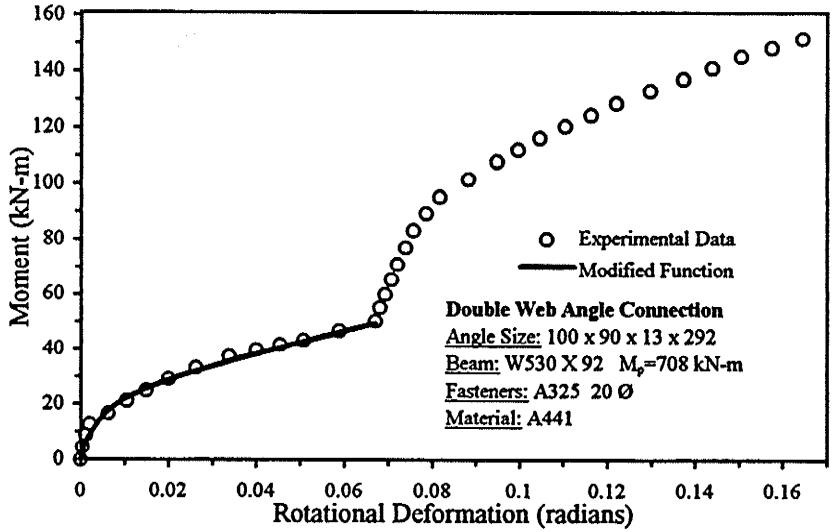


Figure A.86 (a) M-ϕ curve for Thompson: C2-1 alt b

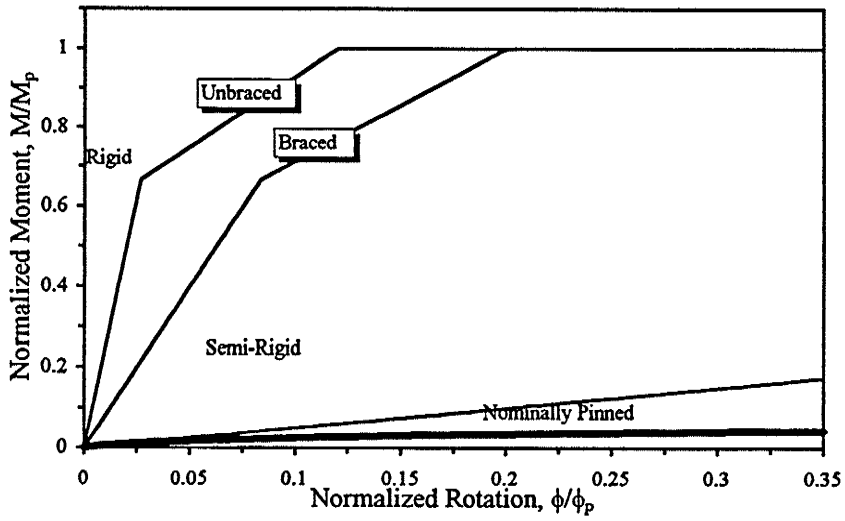


Figure A.86 (b) Eurocode3 Classification of Thompson: C2-1 alt b

Table A.87 M-ϕ data for Thompson: C2-2 alt a (1970)

Moment, M kN-m	Rotation, ϕ radians	Moment, M kN-m	Rotation, ϕ radians
0	0	89.521	0.0993
4.568	0.0001	95.168	0.1019
8.658	0.0006	101.562	0.1072
12.747	0.0011	107.957	0.1125
13.794	0.0030	112.109	0.1174
14.842	0.0049	116.262	0.1223
15.892	0.0068	120.414	0.1297
16.941	0.0087	124.566	0.1370
18.851	0.0136	128.593	0.1429
20.762	0.0184	132.621	0.1488
24.913	0.0249	137.355	0.1569
29.149	0.0304	142.089	0.1649
33.260	0.0380	144.621	0.1703
37.370	0.0455	147.154	0.1757
39.446	0.0525		
41.522	0.0594		
44.097	0.0658		
46.145	0.0729		
48.193	0.0800		
50.241	0.0871		
54.601	0.0883		
58.961	0.0894		
65.355	0.0911		
71.750	0.0928		
77.812	0.0948		
83.874	0.0967		

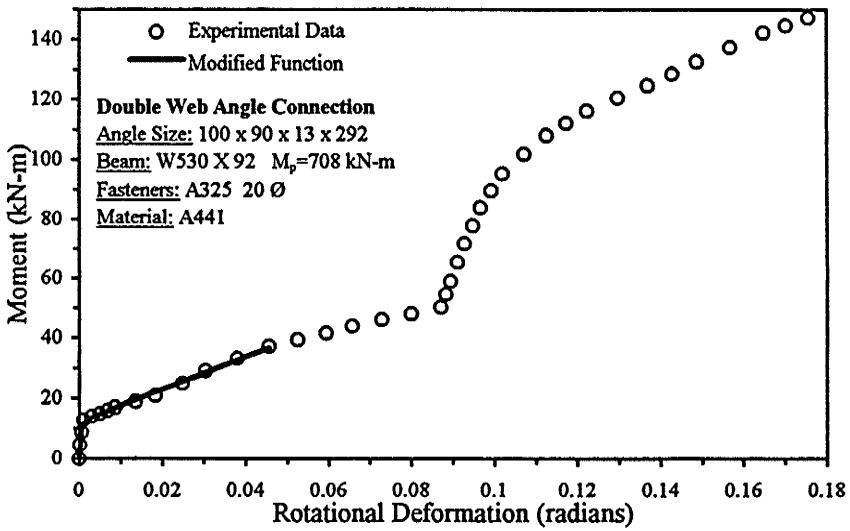


Figure A.87 (a) M-ϕ curve for Thompson: C2-2 alt a

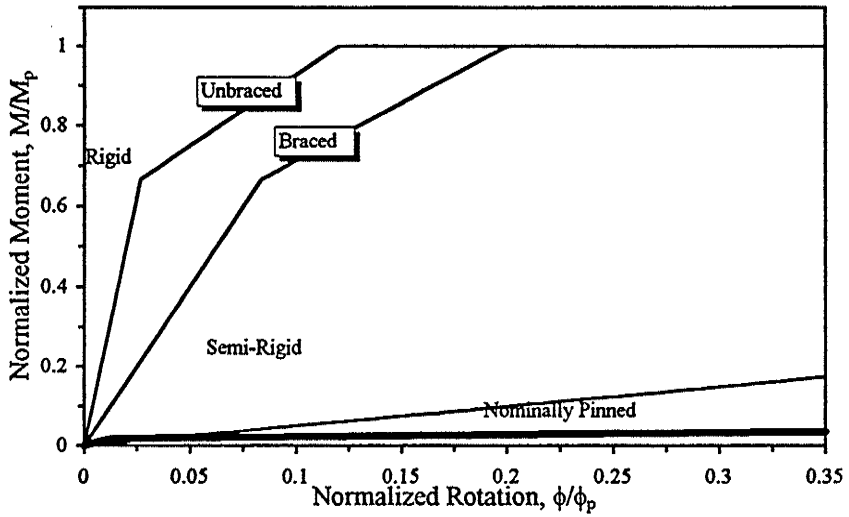


Figure A.87 (b) Eurocode3 Classification of Thompson: C2-2 alt a

Table A.88 M-ϕ data for Thompson: C2-2 alt b (1970)

Moment, M kN-m	Rotation, ϕ radians	Moment, M kN-m	Rotation, ϕ radians
0	0	116.262	0.1132
4.568	0.0005	120.414	0.1206
8.658	0.0011	124.566	0.1279
12.747	0.0017	128.593	0.1356
16.941	0.0030	132.621	0.1432
20.762	0.0075	137.355	0.1523
24.913	0.0125	142.089	0.1614
29.149	0.0184	143.777	0.1697
33.260	0.0263	145.465	0.1781
37.370	0.0341	147.154	0.1864
39.446	0.0413		
41.522	0.0484		
44.097	0.0565		
47.169	0.0655		
50.241	0.0744		
54.601	0.0758		
58.961	0.0771		
65.355	0.0790		
71.750	0.0808		
77.812	0.0830		
83.874	0.0852		
89.521	0.0879		
95.168	0.0906		
101.562	0.0956		
107.957	0.1006		
112.109	0.1069		

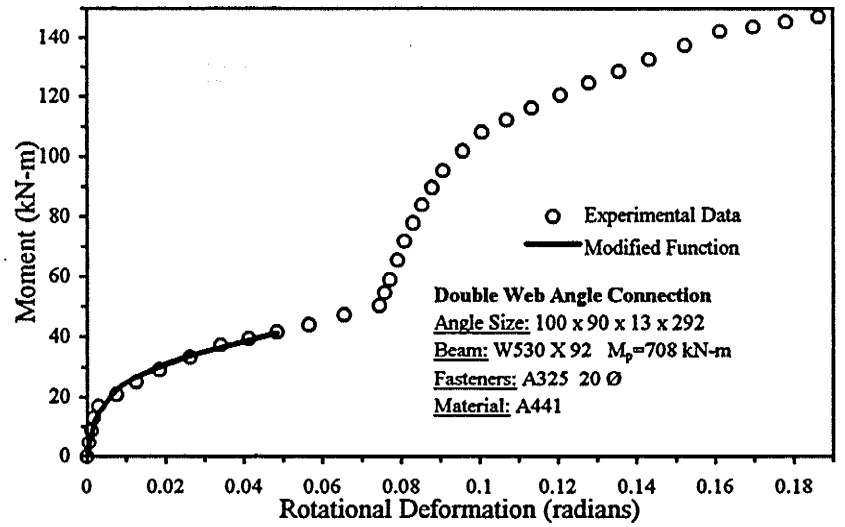


Figure A.88 (a) M-ϕ curve for Thompson: C2-2 alt b

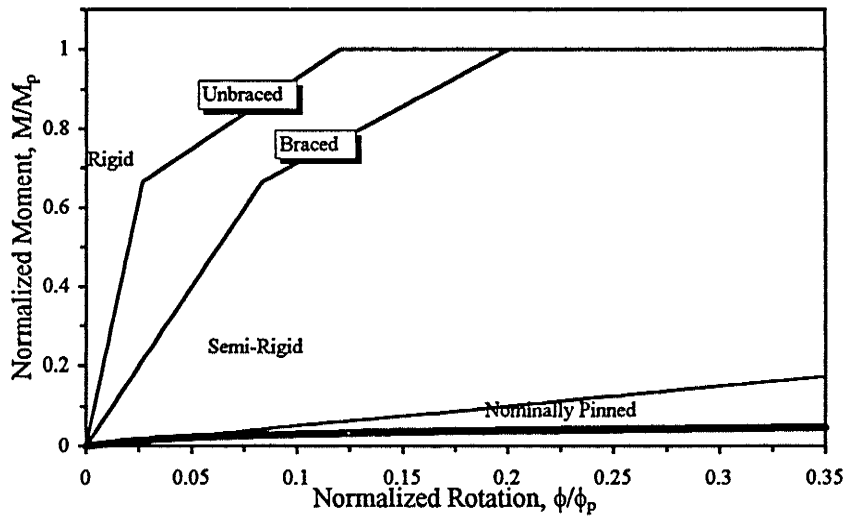


Figure A.88 (b) Eurocode3 Classification of Thompson: C2-2 alt b

Table A.89 M-ϕ data for Thompson: C2-3 alt a (1970)

Moment, M kN-m	Rotation, ϕ radians	Moment, M kN-m	Rotation, ϕ radians
0	0	97.743	0.1093
4.900	0.0004	103.806	0.1130
8.865	0.0013	108.165	0.1164
12.830	0.0021	112.525	0.1198
13.775	0.0045	116.552	0.1253
14.720	0.0070	120.580	0.1308
16.609	0.0118	124.649	0.1379
18.643	0.0205	128.719	0.1449
20.678	0.0291	132.871	0.1535
24.913	0.0336	137.023	0.1621
29.065	0.0387	141.258	0.1693
33.218	0.0437	145.493	0.1764
37.370	0.0514	148.317	0.1820
41.522	0.0591	151.140	0.1875
44.553	0.0656		
47.584	0.0720		
50.435	0.0798		
53.286	0.0875		
56.138	0.0953		
60.331	0.0965		
64.525	0.0977		
70.919	0.0995		
75.528	0.1007		
80.137	0.1018		
85.909	0.1037		
91.681	0.1055		

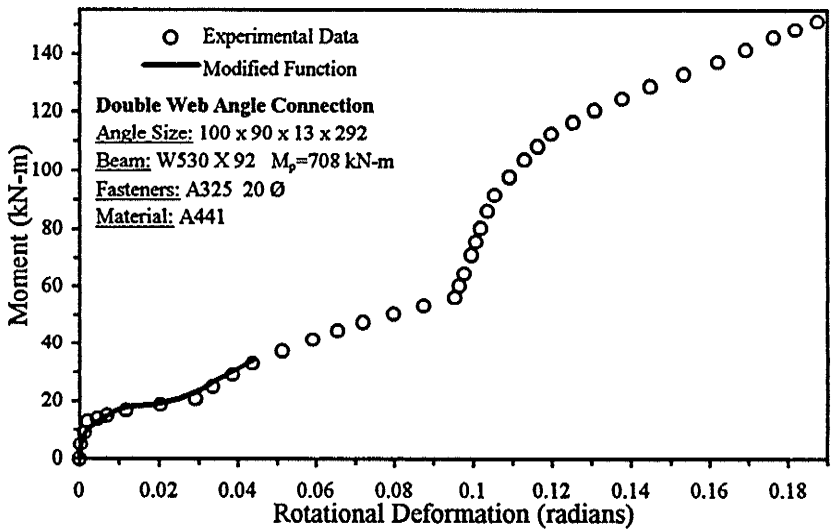


Figure A.89 (a) M-ϕ curve for Thompson: C2-3 alt a

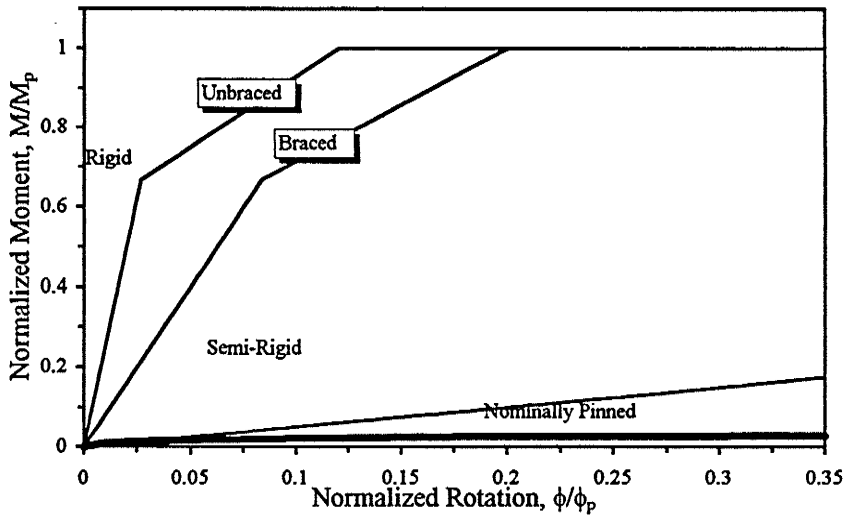


Figure A.89 (b) Eurocode3 Classification of Thompson: C2-3 alt a

Table A.90 M-ϕ data for Thompson: C2-3 alt b (1970)

Moment, M kN-m	Rotation, ϕ radians	Moment, M kN-m	Rotation, ϕ radians
0	0	112.525	0.0951
4.900	0.0005	116.552	0.1002
8.865	0.0012	120.580	0.1053
12.830	0.0018	124.649	0.1106
16.609	0.0039	128.719	0.1159
20.678	0.0081	132.871	0.1240
24.913	0.0133	137.023	0.1320
29.065	0.0187	139.847	0.1377
33.218	0.0240	142.670	0.1435
35.986	0.0295	145.493	0.1492
38.754	0.0351	148.317	0.1572
41.522	0.0406	151.140	0.1651
44.553	0.0463		
47.584	0.0520		
51.861	0.0581		
56.138	0.0641		
60.331	0.0671		
64.525	0.0700		
70.919	0.0715		
75.528	0.0727		
80.137	0.0738		
85.909	0.0757		
91.681	0.0775		
97.743	0.0812		
103.806	0.0848		
108.165	0.0900		

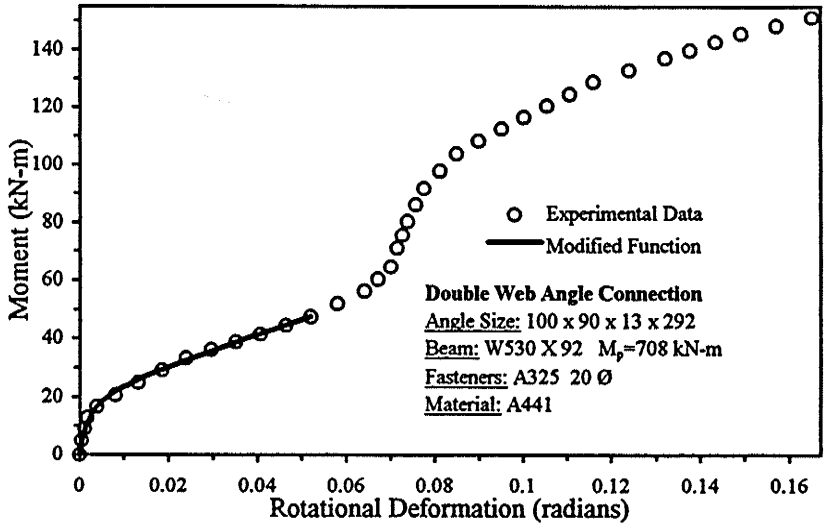


Figure A.90 (a) M-ϕ curve for Thompson: C2-3 alt b

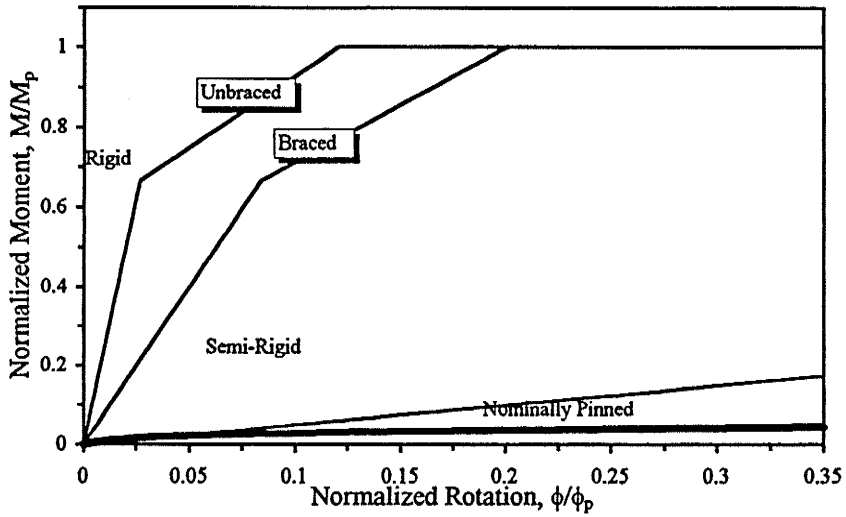


Figure A.90 (b) Eurocode3 Classification of Thompson: C2-3 alt b

Table A.91 M-ϕ data for Thompson: D2-1 alt a (1970)

Moment, M kN-m	Rotation, ϕ radians	Moment, M kN-m	Rotation, ϕ radians
0	0	96.331	0.0800
4.318	0.0003	102.352	0.0814
8.637	0.0006	108.372	0.0828
16.359	0.0030	114.435	0.0847
18.560	0.0062	120.497	0.0865
20.762	0.0093	126.684	0.0891
24.872	0.0138	132.870	0.0917
28.982	0.0182	136.566	0.0955
33.218	0.0231	140.261	0.0992
37.370	0.0289	144.109	0.1033
39.446	0.0322	147.957	0.1075
41.522	0.0355	151.804	0.1116
45.675	0.0406	157.784	0.1158
47.751	0.0443	161.936	0.1192
49.826	0.0479		
51.570	0.0520		
53.314	0.0561		
55.722	0.0606		
58.131	0.0651		
60.539	0.0695		
62.948	0.0740		
67.432	0.0746		
71.915	0.0752		
78.185	0.0765		
84.455	0.0777		
90.393	0.0789		

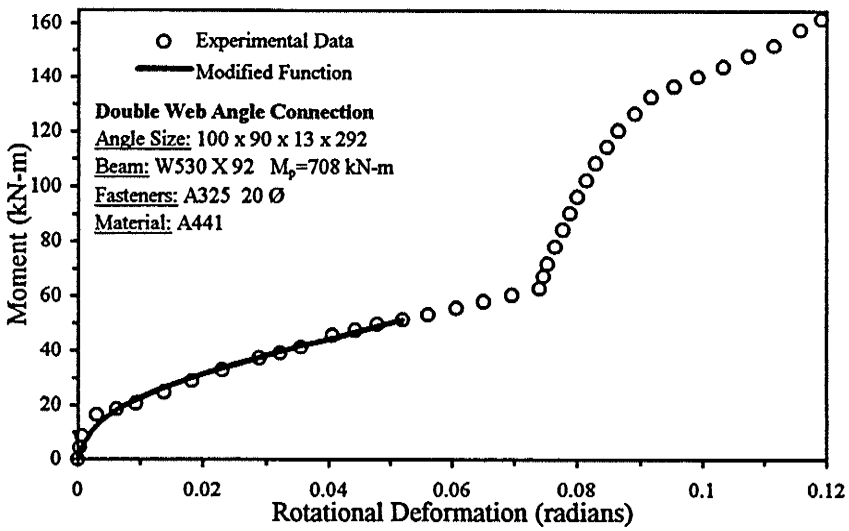


Figure A.91 (a) M-ϕ curve for Thompson: D2-1 alt a

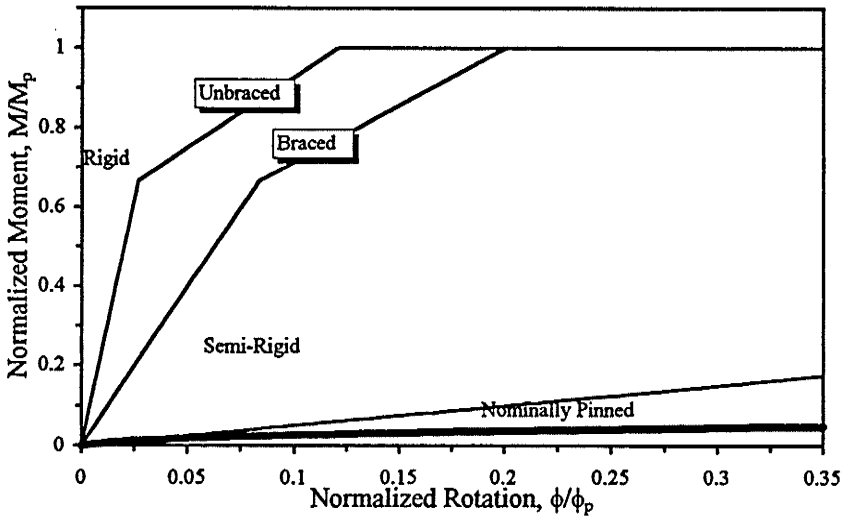


Figure A.91 (b) Eurocode3 Classification of Thompson: D2-1 alt a

Table A.92 M-ϕ data for Thompson: D2-1 alt b (1970)

Moment, M kN-m	Rotation, ϕ radians	Moment, M kN-m	Rotation, ϕ radians
0	0	108.372	0.0758
4.318	0.0004	114.435	0.0777
8.637	0.0008	120.497	0.0795
16.359	0.0057	126.684	0.0821
20.762	0.0092	132.870	0.0846
24.872	0.0144	136.566	0.0890
28.982	0.0196	140.261	0.0933
33.218	0.0230	144.109	0.0974
37.370	0.0272	147.957	0.1016
41.522	0.0326	151.804	0.1057
45.675	0.0380	154.794	0.1092
47.751	0.0413	157.784	0.1126
49.826	0.0446	159.860	0.1158
50.698	0.0501	161.936	0.1189
51.570	0.0555		
52.442	0.0610		
53.314	0.0664		
58.131	0.0671		
62.948	0.0677		
67.432	0.0684		
71.915	0.0691		
78.185	0.0701		
84.455	0.0710		
90.393	0.0721		
96.331	0.0732		
102.352	0.0745		

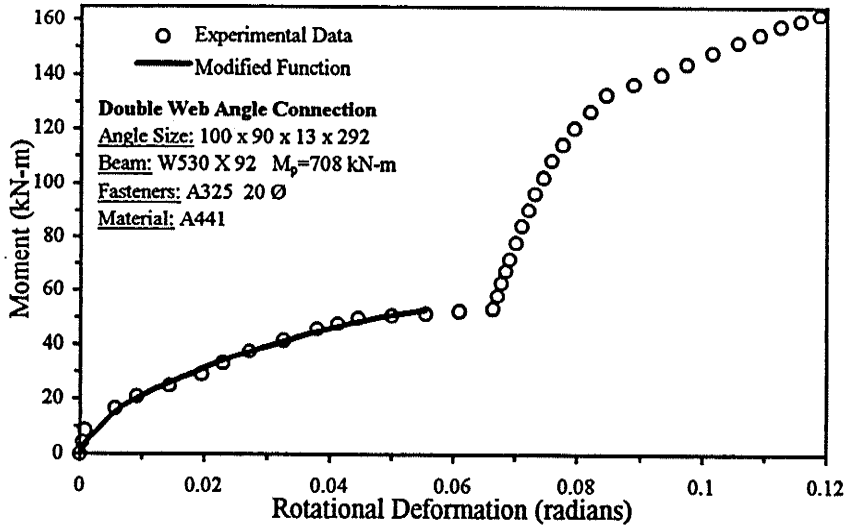


Figure A.92 (a) M-ϕ curve for Thompson: D2-1 alt b

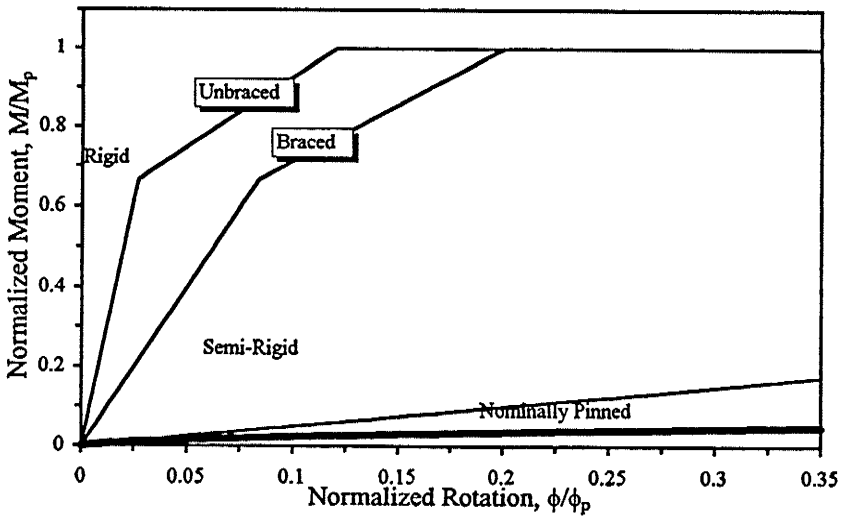


Figure A.92 (b) Eurocode3 Classification of Thompson: D2-1 alt b

Table A.93 M-ϕ data for Thompson: D2-2 alt a (1970)

Moment, M kN-m	Rotation, ϕ radians	Moment, M kN-m	Rotation, ϕ radians
0	0	114.559	0.0882
4.145	0.0003	120.580	0.0901
8.384	0.0009	124.773	0.0934
12.623	0.0015	128.967	0.0967
13.398	0.0079	132.995	0.1002
14.173	0.0142	137.023	0.1036
14.948	0.0206	141.217	0.1063
17.855	0.0267	145.410	0.1090
20.762	0.0327	149.521	0.1130
25.018	0.0362	153.632	0.1170
29.274	0.0396	156.870	0.1230
35.398	0.0455	160.109	0.1290
41.522	0.0514		
43.556	0.0574		
45.591	0.0633		
47.625	0.0693		
49.660	0.0752		
56.774	0.0764		
63.888	0.0775		
71.003	0.0787		
77.190	0.0798		
83.376	0.0808		
89.895	0.0821		
96.414	0.0834		
102.476	0.0849		
108.539	0.0863		

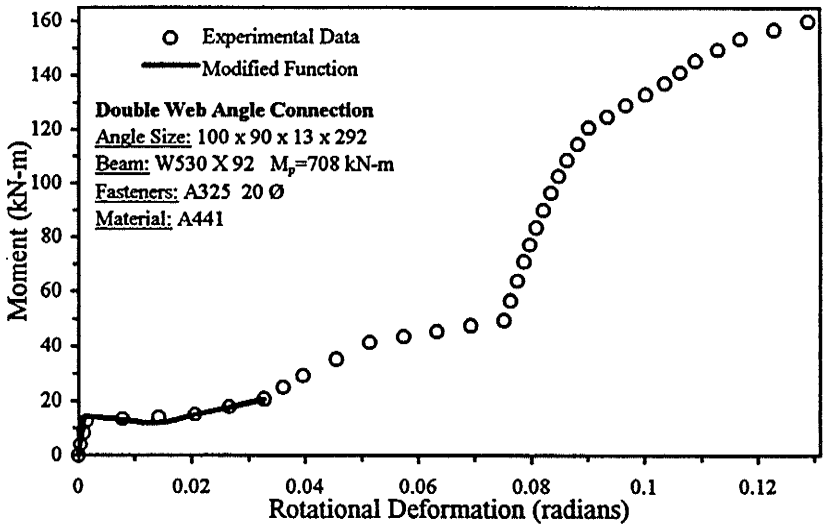


Figure A.93 (a) M-ϕ curve for Thompson: D2-2 alt a

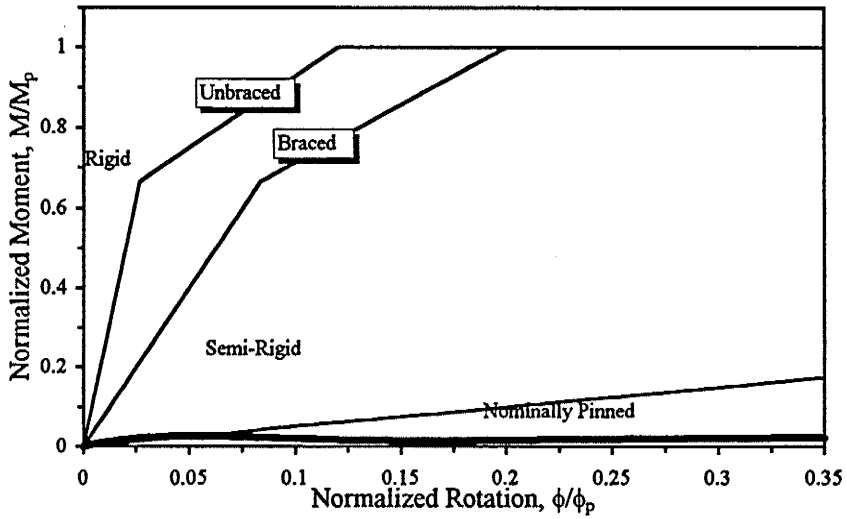


Figure A.93 (b) Eurocode3 Classification of Thompson: D2-2 alt a

Table A.94 M-ϕ data for Thompson: D2-2 alt b (1970)

Moment, M kN-m	Rotation, ϕ radians	Moment, M kN-m	Rotation, ϕ radians
0	0	102.248	0.0769
4.145	0.0002	108.539	0.0783
8.384	0.0006	114.559	0.0800
12.623	0.0010	120.580	0.0817
14.948	0.0016	124.773	0.0834
17.855	0.0056	128.967	0.0851
20.762	0.0096	132.995	0.0873
22.962	0.0127	137.023	0.0895
25.163	0.0158	141.217	0.0940
27.218	0.0199	145.410	0.0984
29.274	0.0240	149.521	0.1019
33.322	0.0284	153.632	0.1053
37.370	0.0328	156.870	0.1088
40.567	0.0373	160.109	0.1122
43.765	0.0418		
46.712	0.0466		
49.660	0.0513		
52.649	0.0569		
55.639	0.0625		
58.628	0.0681		
64.816	0.0693		
71.003	0.0704		
77.190	0.0716		
83.376	0.0727		
89.667	0.0741		
95.957	0.0755		

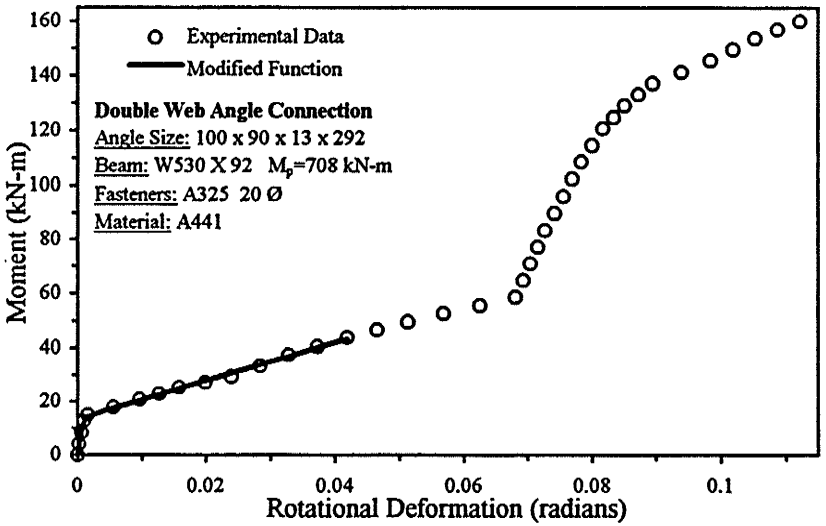


Figure A.94 (a) M-ϕ curve for Thompson: D2-2 alt b

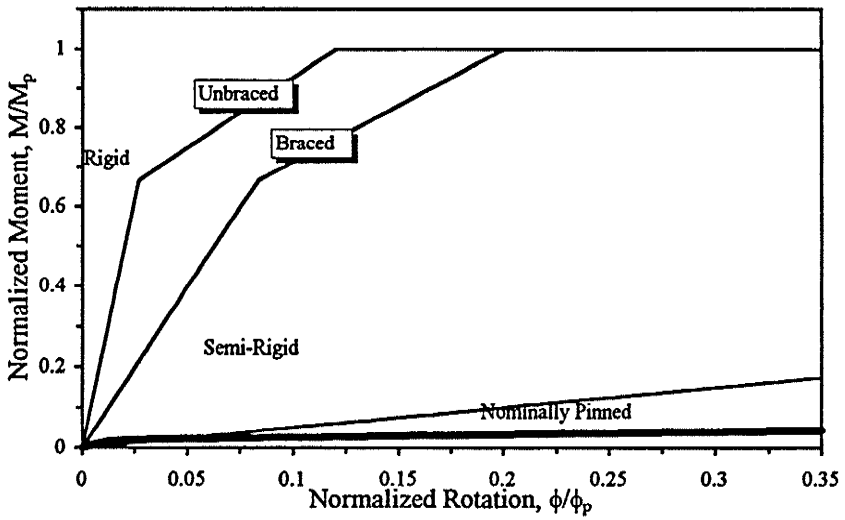


Figure A.94 (b) Eurocode3 Classification of Thompson: D2-2 alt b

Table A.95 M-ϕ data for Thompson: D2-3 alt a (1970)

Moment, M kN-m	Rotation, ϕ radians	Moment, M kN-m	Rotation, ϕ radians
0	0	99.902	0.0718
4.650	0.0002	106.089	0.0738
8.554	0.0020	112.275	0.0757
12.457	0.0038	118.421	0.0795
14.533	0.0083	124.566	0.0832
16.609	0.0128	128.718	0.0876
20.762	0.0163	132.871	0.0921
23.875	0.0197	137.023	0.0965
26.989	0.0230	141.175	0.1004
30.103	0.0270	145.328	0.1042
33.218	0.0309	149.480	0.1075
35.847	0.0359	153.632	0.1108
38.477	0.0409		
41.107	0.0459		
42.630	0.0510		
44.152	0.0560		
45.675	0.0611		
50.117	0.0618		
54.560	0.0625		
58.587	0.0631		
62.614	0.0637		
68.926	0.0650		
75.237	0.0662		
81.424	0.0675		
87.612	0.0688		
93.757	0.0703		

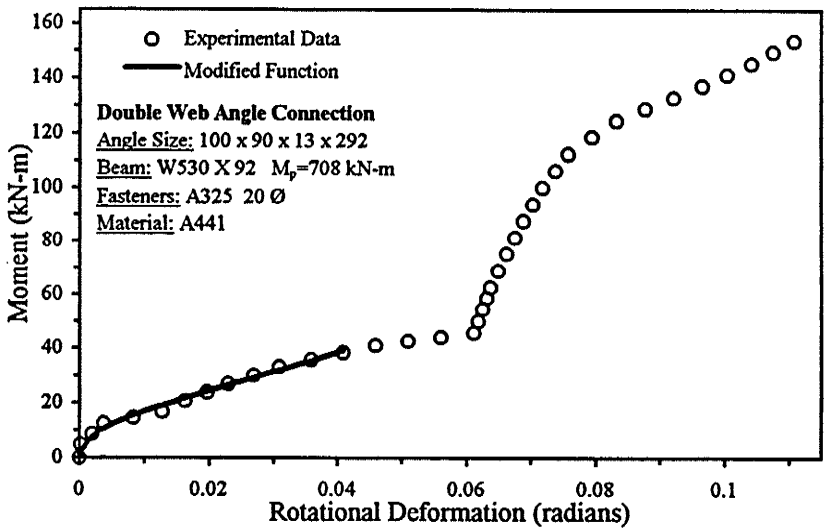


Figure A.95 (a) M-ϕ curve for Thompson: D2-3 alt a

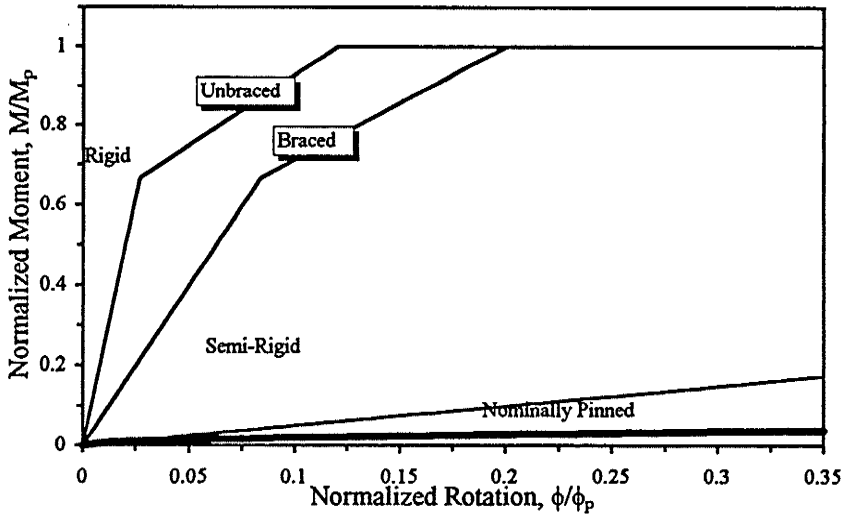


Figure A.95 (b) Eurocode3 Classification of Thompson: D2-3 alt a

Table A.96 M-ϕ data for Thompson: D2-3 alt b (1970)

Moment, M kN-m	Rotation, ϕ radians	Moment, M kN-m	Rotation, ϕ radians
0	0	106.089	0.0765
4.650	0.0003	112.275	0.0782
8.554	0.0007	118.421	0.0807
12.457	0.0010	124.566	0.0831
16.609	0.0015	130.795	0.0875
20.762	0.0032	137.023	0.0918
26.989	0.0084	139.791	0.0965
30.103	0.0118	142.560	0.1012
33.218	0.0152	145.328	0.1059
37.162	0.0204	149.480	0.1100
41.107	0.0255	153.632	0.1140
42.630	0.0297		
44.152	0.0338		
45.675	0.0380		
48.636	0.0421		
51.598	0.0461		
54.560	0.0502		
57.245	0.0558		
59.930	0.0613		
62.614	0.0669		
68.926	0.0685		
75.237	0.0701		
81.424	0.0712		
87.612	0.0722		
93.757	0.0735		
99.902	0.0748		

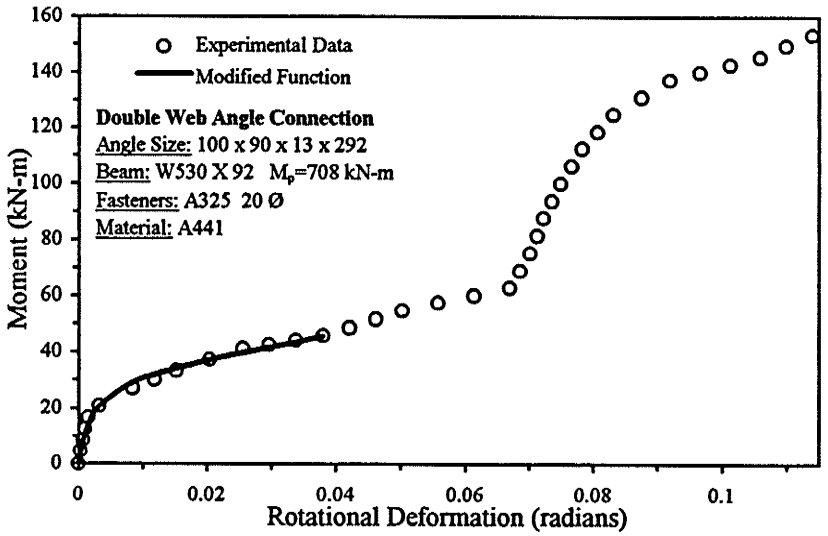


Figure A.96 (a) M-ϕ curve for Thompson: D2-3 alt b

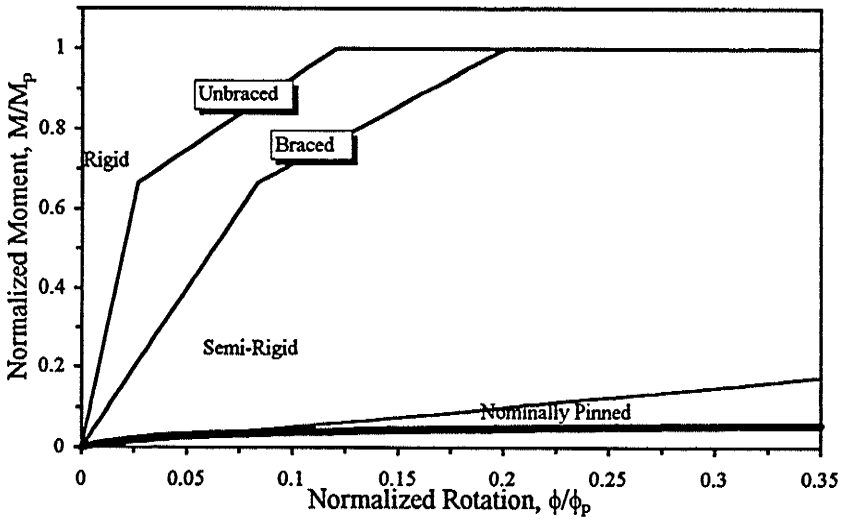


Figure A.96 (b) Eurocode3 Classification of Thompson: D2-3 alt b

Table A.97 M-ϕ data for Sommer: Test 21 (1969)

Moment, M kN-m	Rotation, ϕ radians	Moment, M kN-m	Rotation, ϕ radians
0	0	111.912	0.0598
7.626	0.0031	117.505	0.0603
13.332	0.0053	125.413	0.0622
18.643	0.0076	133.322	0.0640
24.066	0.0106	139.724	0.0667
29.602	0.0140	146.127	0.0694
32.502	0.0171	152.530	0.0721
35.402	0.0201	159.309	0.0755
38.302	0.0232	166.088	0.0789
40.223	0.0270		
42.144	0.0307		
44.064	0.0345		
45.985	0.0382		
46.889	0.0412		
47.793	0.0442		
48.697	0.0472		
50.109	0.0506		
51.521	0.0539		
57.001	0.0547		
62.480	0.0555		
70.615	0.0560		
77.507	0.0568		
84.400	0.0575		
91.706	0.0581		
99.013	0.0586		
106.319	0.0592		

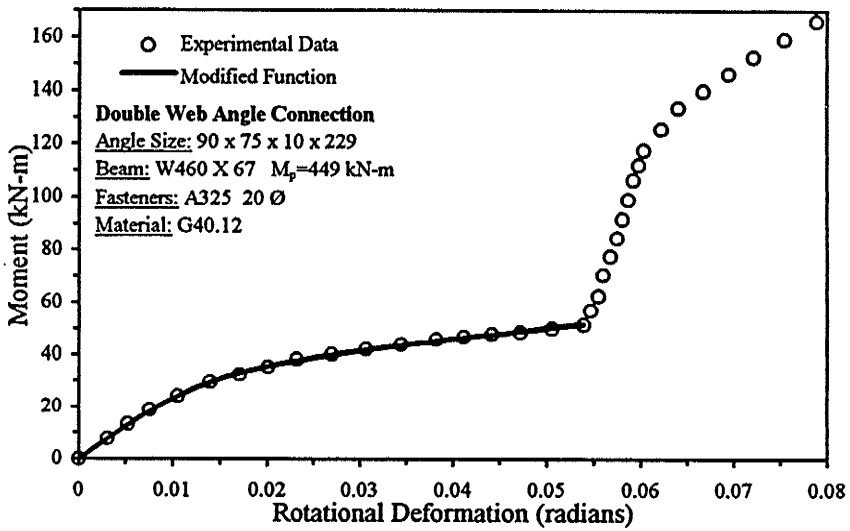


Figure A.97 (a) M-ϕ curve for Sommer: Test 21

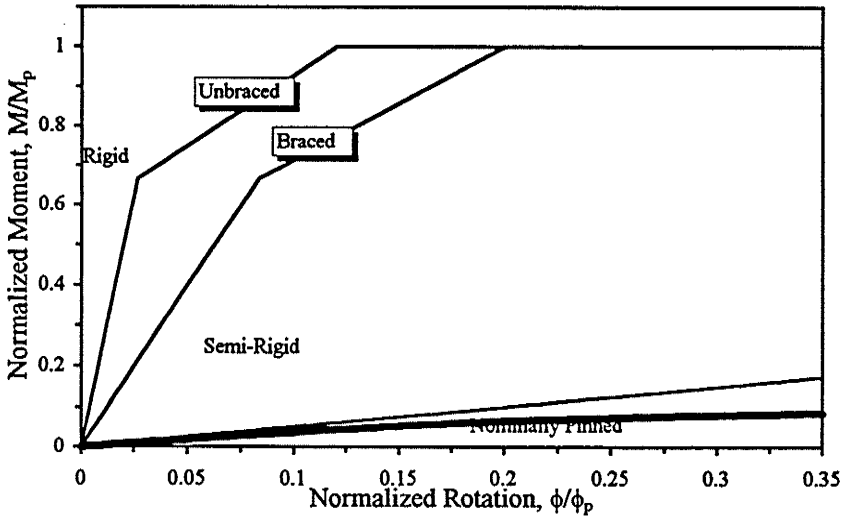


Figure A.97 (b) Eurocode3 Classification of Sommer: Test 21

Table A.98 M-ϕ data for Sommer: Test 22 (1969)

Moment, M kN-m	Rotation, ϕ radians	Moment, M kN-m	Rotation, ϕ radians
0	0	123.153	0.0780
6.214	0.0009	128.238	0.0790
12.428	0.0019	133.322	0.0799
18.643	0.0028	140.101	0.0813
26.834	0.0043	146.880	0.0827
35.025	0.0058	154.225	0.0844
43.273	0.0079	161.569	0.0861
51.521	0.0100	166.653	0.0879
57.001	0.0122	171.738	0.0896
62.480	0.0143	172.867	0.0931
67.941	0.0184	171.737	0.0957
73.403	0.0224	170.607	0.0982
78.864	0.0265		
81.632	0.0301		
84.400	0.0336		
87.111	0.0380		
89.823	0.0424		
91.650	0.0473		
93.476	0.0521		
95.303	0.0570		
97.129	0.0619		
98.956	0.0667		
100.782	0.0716		
104.059	0.0740		
111.743	0.0756		
117.448	0.0768		

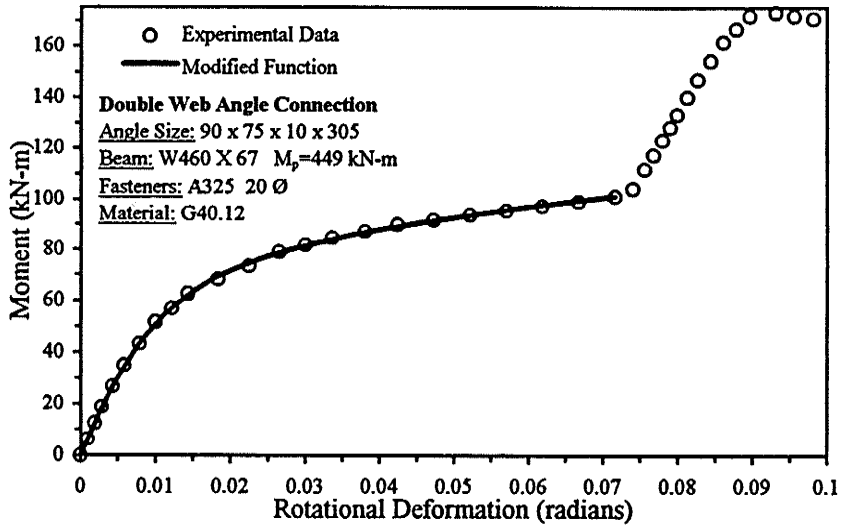


Figure A.98 (a) M-ϕ curve for Sommer: Test 22

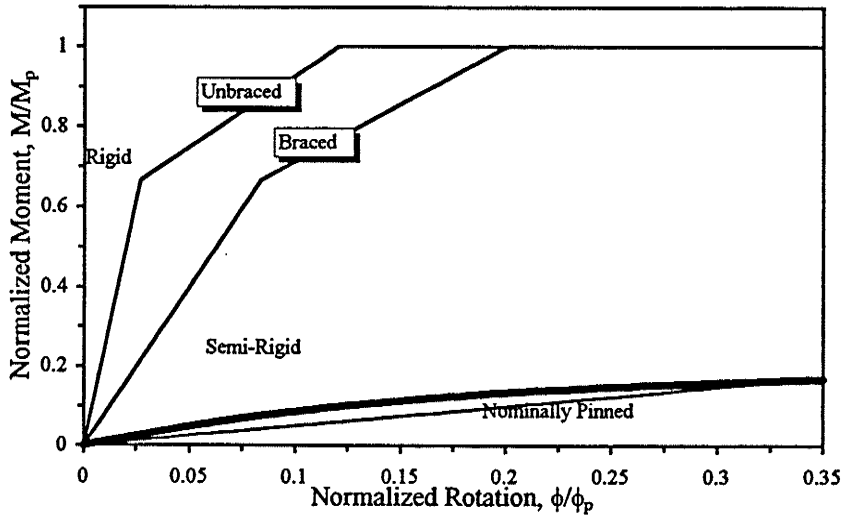


Figure A.98 (b) Eurocode3 Classification of Sommer: Test 22

Table A.99 M-ϕ data for Sommer: Test 23 (1969)

Moment, M kN-m	Rotation, ϕ radians	Moment, M kN-m	Rotation, ϕ radians
0	0	146.880	0.0699
8.565	0.0011	153.659	0.0704
16.835	0.0023	163.263	0.0710
24.970	0.0034	172.867	0.0716
33.218	0.0047	185.296	0.0727
41.465	0.0060	197.724	0.0738
49.657	0.0080	210.152	0.0749
57.849	0.0099	222.581	0.0760
63.328	0.0124	233.314	0.0791
68.808	0.0149	244.048	0.0821
73.553	0.0188	255.346	0.0861
78.299	0.0226	258.170	0.0885
83.044	0.0265	260.995	0.0909
86.349	0.0304		
89.654	0.0344		
92.958	0.0383		
96.263	0.0422		
99.003	0.0462		
101.743	0.0502		
104.483	0.0542		
107.222	0.0582		
110.103	0.0626		
112.985	0.0670		
123.153	0.0681		
131.627	0.0688		
140.101	0.0694		

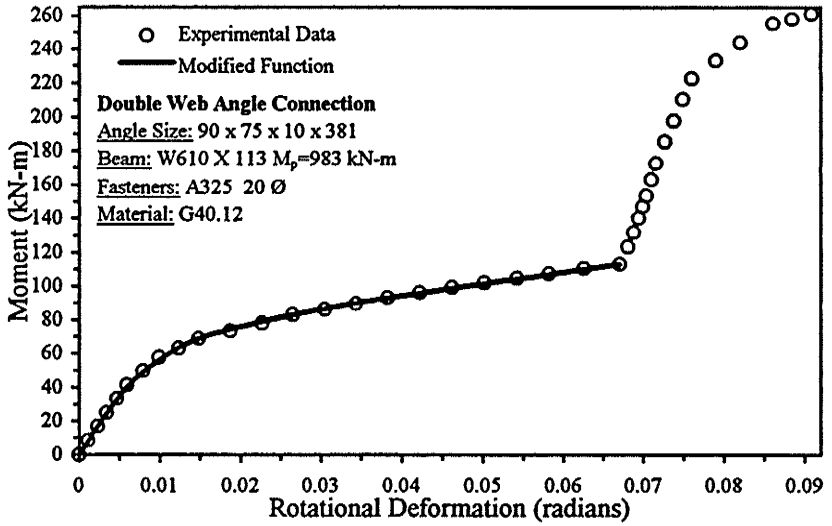


Figure A.99 (a) M-ϕ curve for Sommer: Test 23

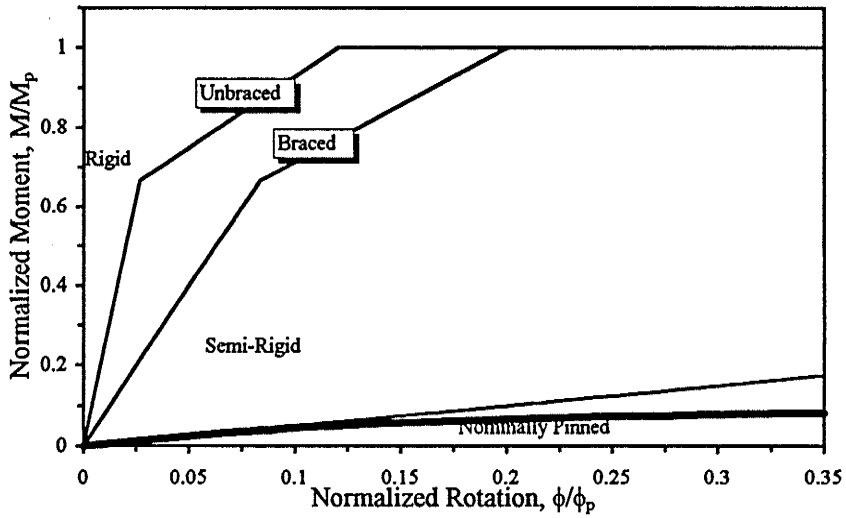


Figure A.99 (b) Eurocode3 Classification of Sommer: Test 23

Table A.100 M-ϕ data for Sommer: Test 24 (1969)

Moment, M kN-m	Rotation, ϕ radians	Moment, M kN-m	Rotation, ϕ radians
0	0	161.286	0.0621
8.654	0.0008	164.959	0.0653
15.682	0.0015	167.218	0.0675
22.710	0.0021	169.478	0.0697
29.263	0.0027	178.517	0.0733
35.817	0.0033	188.685	0.0748
44.064	0.0041	198.289	0.0760
52.312	0.0048	207.892	0.0772
62.141	0.0061	214.671	0.0787
71.971	0.0073	221.450	0.0801
81.236	0.0094	228.229	0.0837
90.501	0.0115		
98.749	0.0147		
106.997	0.0178		
112.251	0.0207		
117.505	0.0236		
123.154	0.0272		
128.803	0.0307		
131.628	0.0342		
134.453	0.0377		
138.407	0.0414		
142.361	0.0451		
146.315	0.0487		
150.270	0.0524		
153.942	0.0556		
157.614	0.0589		

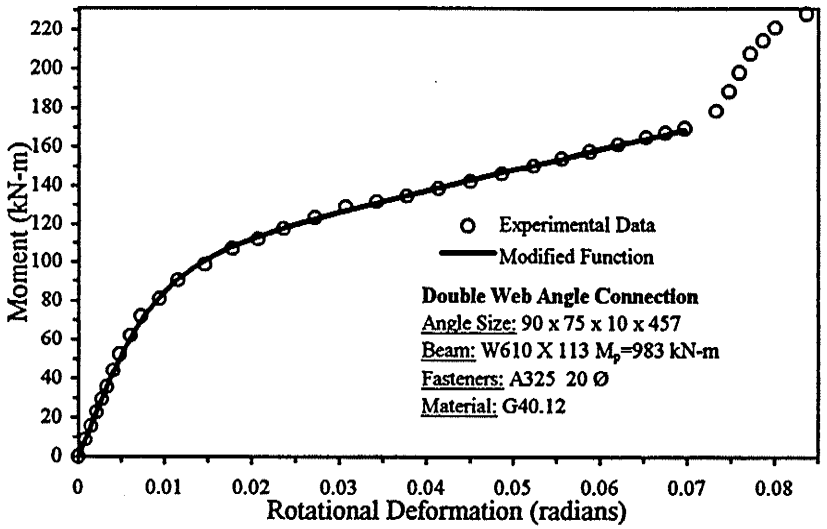


Figure A.100 (a) M-ϕ curve for Sommer: Test 24

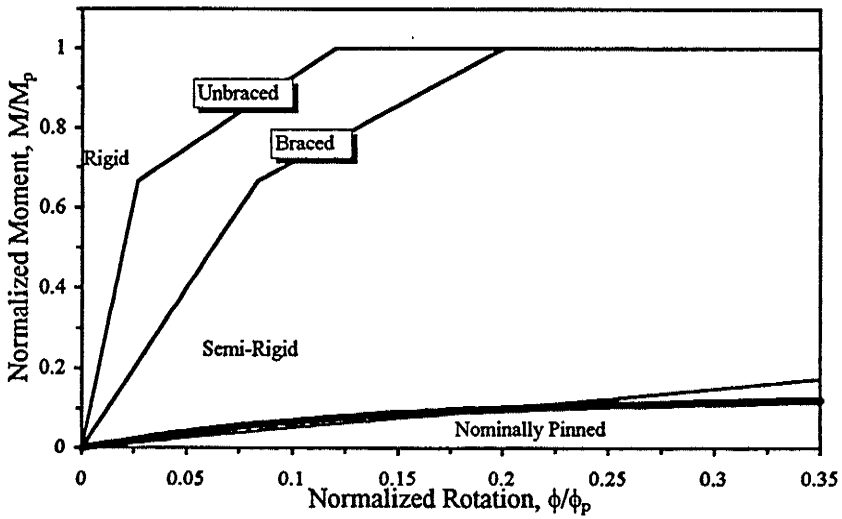


Figure A.100 (b) Eurocode3 Classification of Sommer: Test 24

Table A.101 M-ϕ data for Onuah: Test A01B (1988)

Moment, M kN-m	Rotation, ϕ radians	Moment, M kN-m	Rotation, ϕ radians
0	0	88.939	0.0361
5.865	0.0002	90.897	0.0381
9.773	0.0004	92.855	0.0401
14.663	0.0008	96.763	0.0452
20.529	0.0012	101.653	0.0503
25.412	0.0015	104.579	0.0551
30.302	0.0019	108.494	0.0600
35.186	0.0025	112.402	0.0651
40.076	0.0030	115.328	0.0701
45.943	0.0038	118.261	0.0751
50.826	0.0045	120.211	0.0790
52.784	0.0052		
55.711	0.0083		
58.644	0.0101		
62.551	0.0121		
65.484	0.0142		
68.417	0.0162		
73.300	0.0181		
75.257	0.0204		
76.233	0.0223		
78.190	0.0240		
79.165	0.0260		
82.098	0.0280		
83.081	0.0301		
84.056	0.0320		
86.989	0.0341		

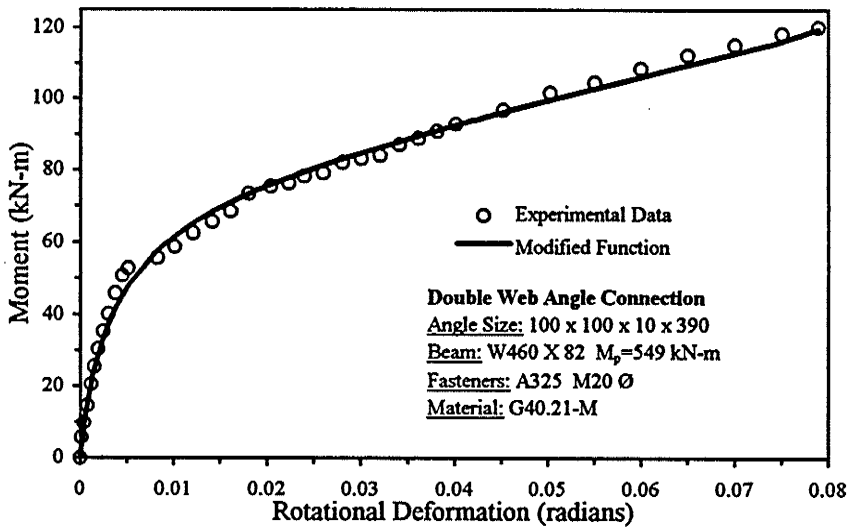


Figure A.101 (a) M-ϕ curve for Onuah: Test A01B

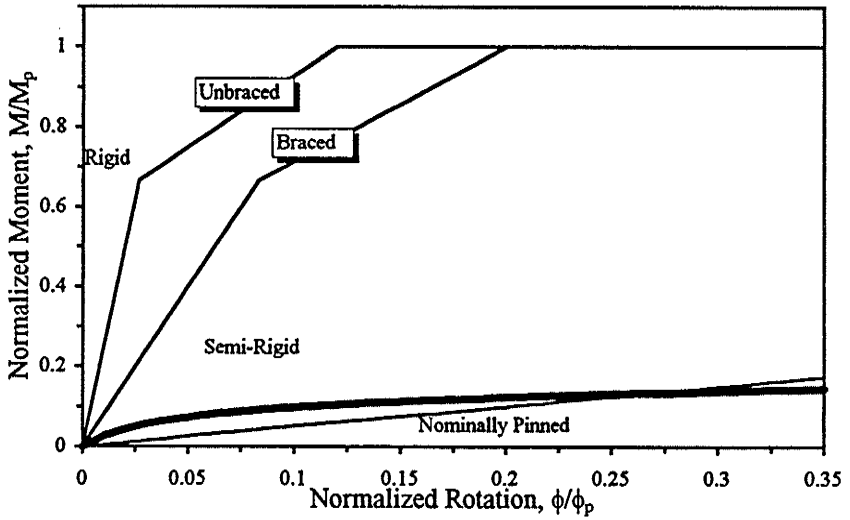


Figure A.101 (b) Eurocode3 Classification of Onuah: Test A01B

Table A.102 M-ϕ data for Onuah: Test A02 (1988)

Moment, M kN-m	Rotation, ϕ radians	Moment, M kN-m	Rotation, ϕ radians
0	0	81.120	0.0341
5.865	0.0006	82.095	0.0352
10.748	0.0012	84.053	0.0371
15.638	0.0020	85.027	0.0390
21.503	0.0024	86.010	0.0410
25.410	0.0032	86.985	0.0431
30.300	0.0037	88.935	0.0451
33.232	0.0041	89.917	0.0465
35.183	0.0046	90.893	0.0477
38.115	0.0048	91.868	0.0496
40.072	0.0053	92.850	0.0510
43.005	0.0060	93.825	0.0518
45.938	0.0066	94.800	0.0532
48.870	0.0073	95.783	0.0544
50.820	0.0079	96.757	0.0565
53.753	0.0091	97.733	0.0580
56.685	0.0101	98.715	0.0593
60.593	0.0120	99.690	0.0636
65.483	0.0151	100.665	0.0650
68.415	0.0181	102.623	0.0667
69.390	0.0219	103.598	0.0684
70.373	0.0250	104.572	0.0702
73.298	0.0270	105.555	0.0713
76.230	0.0291	106.530	0.0729
78.188	0.0311		
79.163	0.0330		

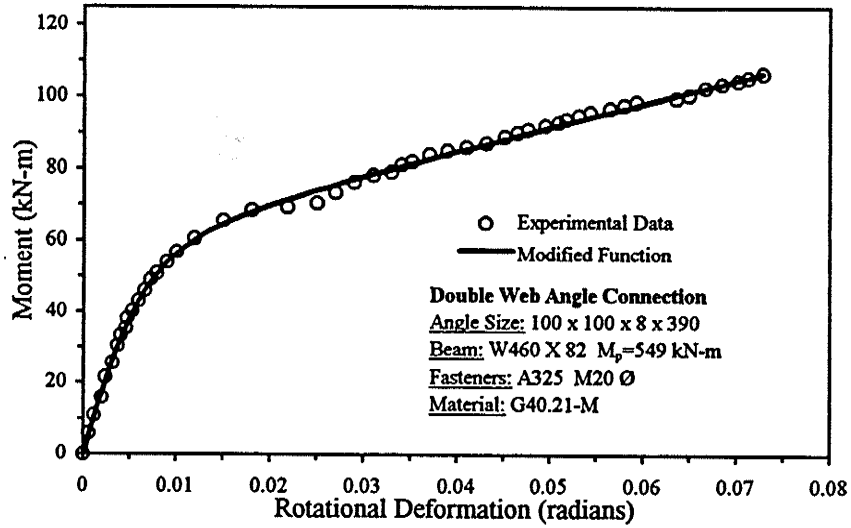


Figure A.102 (a) M-ϕ curve for Onuah: Test A02

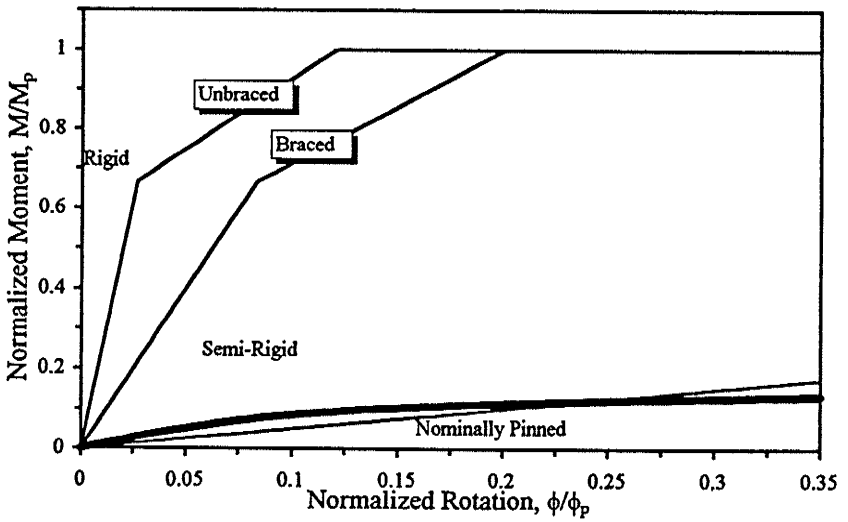


Figure A.102 (b) Eurocode3 Classification of Onuah: Test A02

Table A.103 M-ϕ data for Onuah: Test A03 (1988)

Moment, M kN-m	Rotation, ϕ radians	Moment, M kN-m	Rotation, ϕ radians
0	0	82.095	0.0161
4.890	0.0004	85.027	0.0170
9.773	0.0009	87.960	0.0181
14.662	0.0012	88.935	0.0191
18.570	0.0015	90.893	0.0201
22.478	0.0017	91.868	0.0211
25.410	0.0021	92.850	0.0220
30.300	0.0022	94.800	0.0231
35.183	0.0026	95.783	0.0241
41.048	0.0029	96.757	0.0250
45.938	0.0032	98.715	0.0261
50.820	0.0037	99.690	0.0272
55.710	0.0040	101.648	0.0280
60.593	0.0045	102.623	0.0290
62.550	0.0046	104.572	0.0301
65.483	0.0052	106.530	0.0321
67.440	0.0054	109.463	0.0341
68.415	0.0063	111.420	0.0361
69.390	0.0071	114.353	0.0380
70.373	0.0075	115.328	0.0400
71.348	0.0106	120.210	0.0451
72.323	0.0114	123.143	0.0502
74.280	0.0120	125.100	0.0532
77.213	0.0130	126.075	0.0549
79.163	0.0141		
79.163	0.0151		

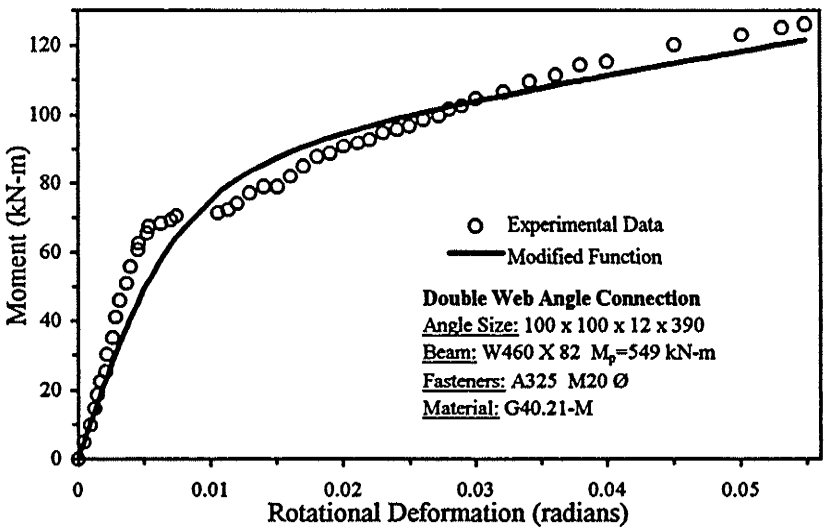


Figure A.103 (a) M-ϕ curve for Onuah: Test A03

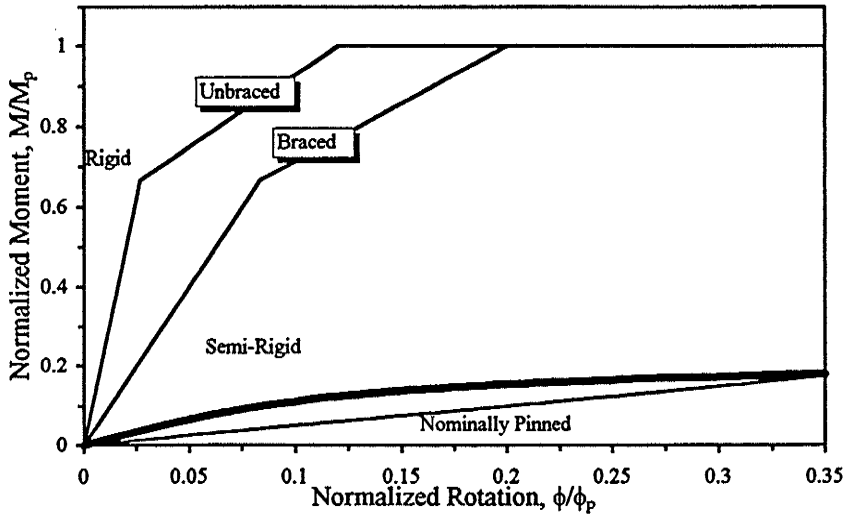


Figure A.103 (b) Eurocode3 Classification of Onuah: Test A03

Table A.104 M-ϕ data for Onuah: Test A04 (1988)

Moment, M kN-m	Rotation, ϕ radians	Moment, M kN-m	Rotation, ϕ radians
0	0	87.964	0.0393
53.753	0.0074	88.940	0.0407
55.711	0.0076	89.922	0.0424
56.686	0.0080	90.897	0.0440
57.661	0.0084	91.873	0.0453
58.643	0.0085	92.855	0.0475
59.618	0.0087	93.830	0.0487
60.594	0.0092	93.831	0.0500
61.576	0.0097	94.806	0.0509
63.526	0.0101	95.788	0.0520
63.526	0.0111	95.789	0.0541
65.484	0.0120	96.764	0.0548
66.459	0.0130	96.764	0.0581
69.392	0.0140	97.739	0.0582
70.374	0.0150	97.739	0.0601
72.324	0.0161	98.722	0.0611
73.299	0.0169	99.697	0.0634
74.282	0.0180	100.672	0.0657
76.232	0.0211	101.648	0.0679
78.190	0.0240	102.623	0.0695
80.148	0.0270	103.598	0.0711
82.098	0.0280		
83.081	0.0301		
85.031	0.0312		
86.014	0.0376		
86.989	0.0389		

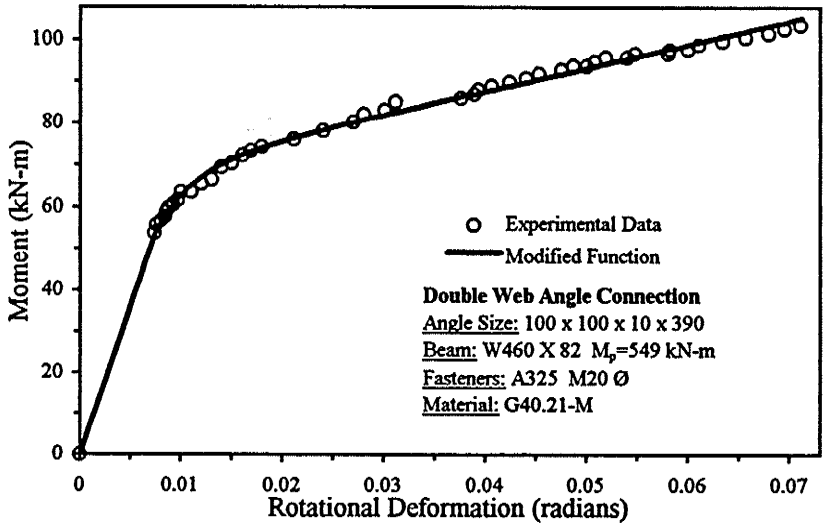


Figure A.104 (a) M-ϕ curve for Onuah: Test A04

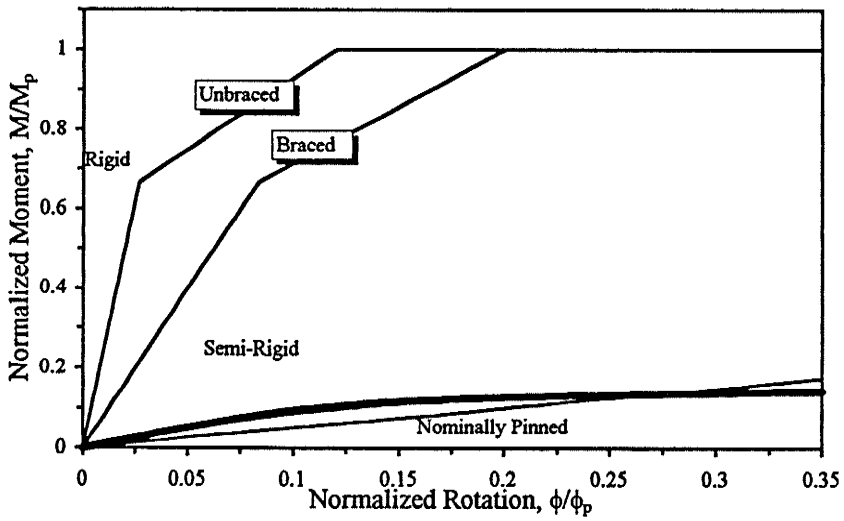


Figure A.104 (b) Eurocode3 Classification of Onuah: Test A04

Table A.105 M-ϕ data for Onuah: Test A07 (1988)

Moment, M kN-m	Rotation, ϕ radians	Moment, M kN-m	Rotation, ϕ radians
0	0	50.822	0.0140
4.890	0.0005	55.712	0.0161
9.773	0.0010	59.620	0.0180
14.664	0.0013	62.552	0.0201
19.546	0.0015	66.460	0.0221
22.479	0.0018	70.375	0.0240
24.437	0.0018	74.283	0.0261
27.370	0.0022	76.233	0.0282
28.346	0.0028	80.148	0.0301
29.321	0.0028	82.099	0.0321
30.304	0.0035	85.031	0.0340
31.280	0.0051	86.989	0.0361
32.257	0.0061	88.939	0.0380
33.239	0.0062	90.897	0.0401
34.208	0.0066	92.855	0.0420
35.183	0.0072	94.805	0.0441
36.166	0.0088	96.763	0.0461
37.141	0.0095	98.720	0.0481
38.116	0.0100	99.696	0.0501
39.099	0.0102	102.628	0.0520
40.074	0.0105	104.579	0.0541
41.049	0.0107	106.536	0.0560
42.024	0.0111	108.494	0.0581
44.956	0.0120	110.444	0.0601
47.889	0.0131	113.377	0.0621
48.872	0.0133	114.360	0.0629

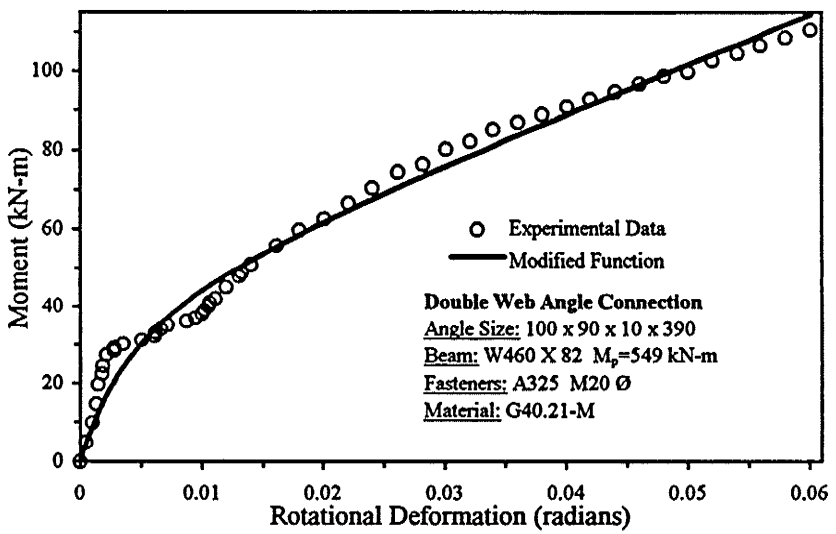


Figure A.105 (a) M-ϕ curve for Onuah: Test A07

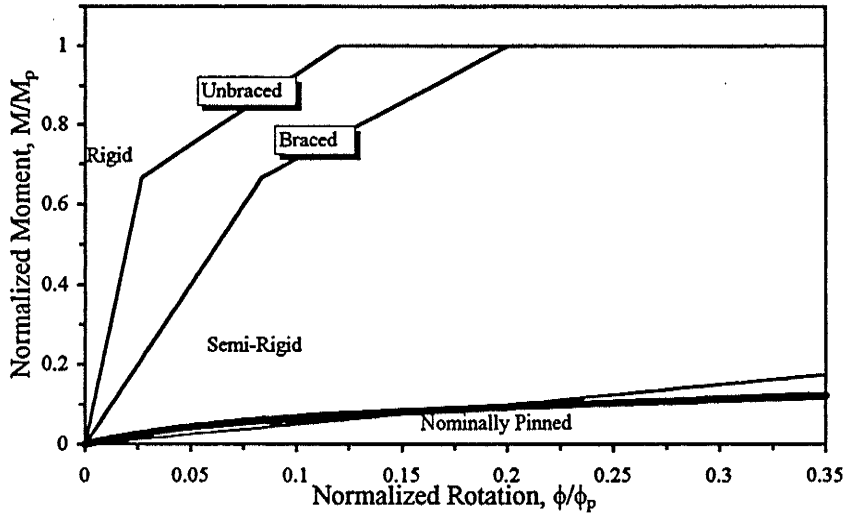


Figure A.105 (b) Eurocode3 Classification of Onuah: Test A07

Table A.106 M-ϕ data for Onuah: Test A08 (1988)

Moment, M kN-m	Rotation, ϕ radians	Moment, M kN-m	Rotation, ϕ radians
0	0	105.559	0.0351
5.865	0.0004	107.509	0.0371
9.773	0.0007	109.467	0.0390
15.638	0.0010	110.442	0.0412
19.546	0.0012	112.400	0.0431
25.412	0.0016	113.375	0.0450
30.302	0.0019	116.308	0.0471
34.210	0.0023	117.291	0.0492
37.143	0.0028	118.266	0.0511
42.026	0.0031	120.216	0.0531
43.009	0.0033	121.199	0.0551
45.943	0.0049	122.174	0.0571
49.846	0.0070	124.132	0.0591
57.661	0.0091	125.107	0.0611
61.576	0.0111	125.107	0.0631
66.459	0.0130	127.065	0.0652
69.392	0.0151	128.033	0.0670
74.282	0.0171	129.991	0.0691
79.165	0.0191	130.966	0.0711
84.055	0.0211	132.923	0.0730
88.938	0.0231	133.898	0.0752
91.870	0.0250	134.873	0.0772
94.803	0.0272	136.831	0.0792
97.736	0.0290	137.806	0.0810
100.669	0.0313	139.763	0.0831
102.626	0.0330	140.738	0.0843

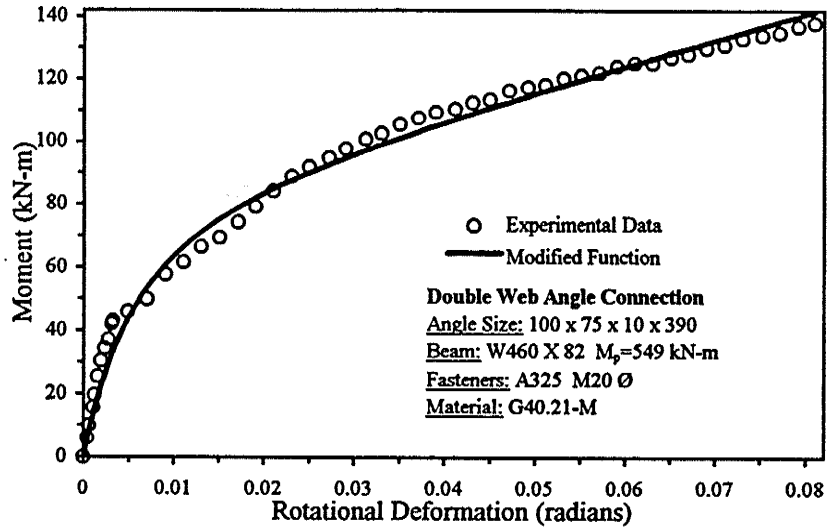


Figure A.106 (a) M-ϕ curve for Onuah: Test A08

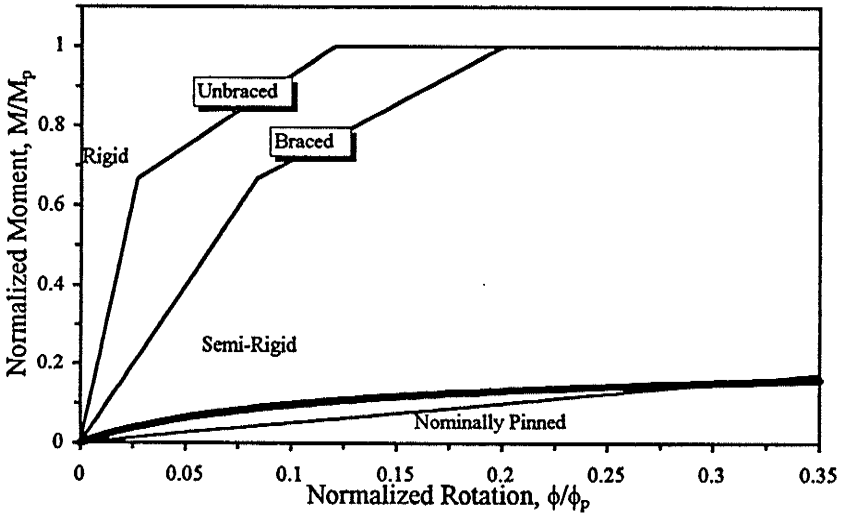


Figure A.106 (b) Eurocode3 Classification of Onuah: Test A08

Table A.107 M-ϕ data for Onuah: Test A10 (1988)

Moment, M kN-m	Rotation, ϕ radians	Moment, M kN-m	Rotation, ϕ radians
0	0	26.067	0.0482
2.606	0.0011	26.718	0.0502
5.216	0.0021	26.718	0.0522
7.822	0.0033	27.368	0.0541
10.427	0.0046	28.018	0.0561
12.383	0.0062	28.018	0.0582
13.034	0.0071	28.673	0.0602
14.339	0.0080	28.673	0.0623
14.990	0.0090	29.323	0.0643
16.291	0.0101	29.323	0.0662
18.246	0.0122	29.973	0.0683
18.896	0.0143	30.629	0.0703
19.546	0.0151	30.629	0.0722
20.201	0.0190	31.279	0.0741
20.851	0.0231	31.279	0.0760
20.851	0.0241	31.279	0.0782
20.851	0.0250	31.929	0.0800
22.156	0.0262	32.584	0.0821
22.807	0.0302	33.234	0.0841
23.457	0.0321	33.234	0.0860
23.457	0.0341	33.884	0.0880
24.112	0.0361	34.540	0.0900
24.762	0.0382	35.190	0.0921
25.412	0.0422		
25.412	0.0441		
26.067	0.0462		

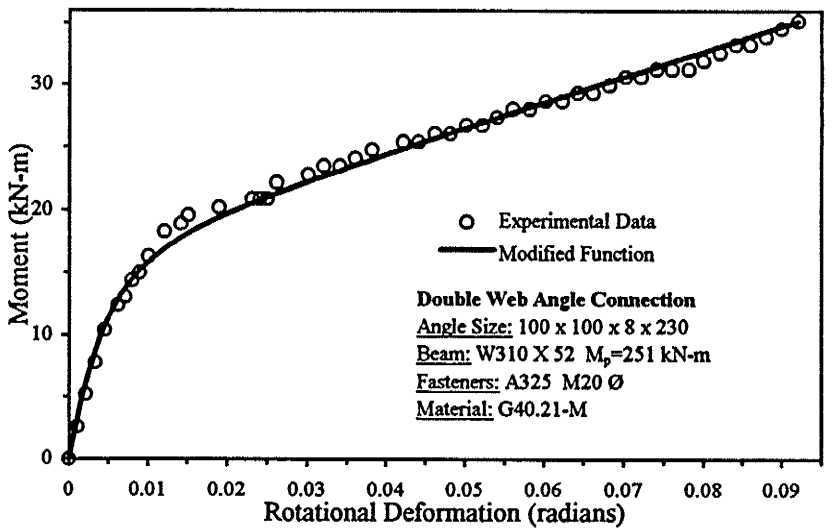


Figure A.107 (a) M-ϕ curve for Onuah: Test A10

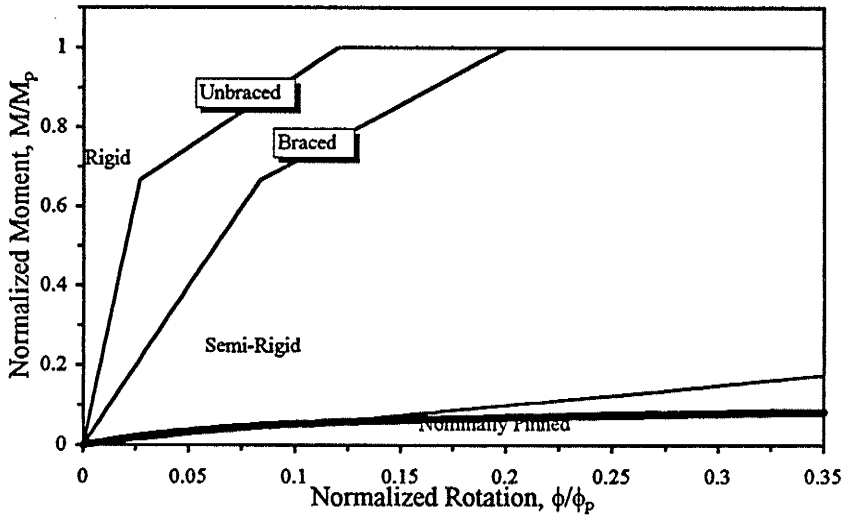


Figure A.107 (b) Eurocode3 Classification of Onuah: Test A10

Table A.108 M-ϕ data for Onuah: Test A11 (1988)

Moment, M kN-m	Rotation, ϕ radians	Moment, M kN-m	Rotation, ϕ radians
0	0	28.671	0.0250
2.605	0.0007	29.321	0.0262
4.561	0.0012	30.626	0.0280
7.821	0.0022	31.277	0.0302
10.426	0.0028	32.582	0.0321
12.382	0.0037	33.232	0.0342
14.337	0.0044	33.882	0.0372
15.642	0.0047	33.882	0.0401
15.643	0.0060	35.187	0.0427
16.293	0.0064	35.837	0.0451
16.295	0.0088	36.492	0.0474
17.595	0.0094	37.143	0.0501
18.246	0.0099	38.443	0.0525
19.546	0.0105	39.098	0.0551
22.156	0.0122	39.098	0.0575
23.456	0.0133	39.748	0.0600
23.456	0.0151	40.398	0.0626
24.111	0.0161	41.053	0.0633
24.761	0.0174		
24.761	0.0182		
25.411	0.0192		
26.066	0.0202		
26.716	0.0210		
27.366	0.0221		
27.366	0.0230		
28.671	0.0240		

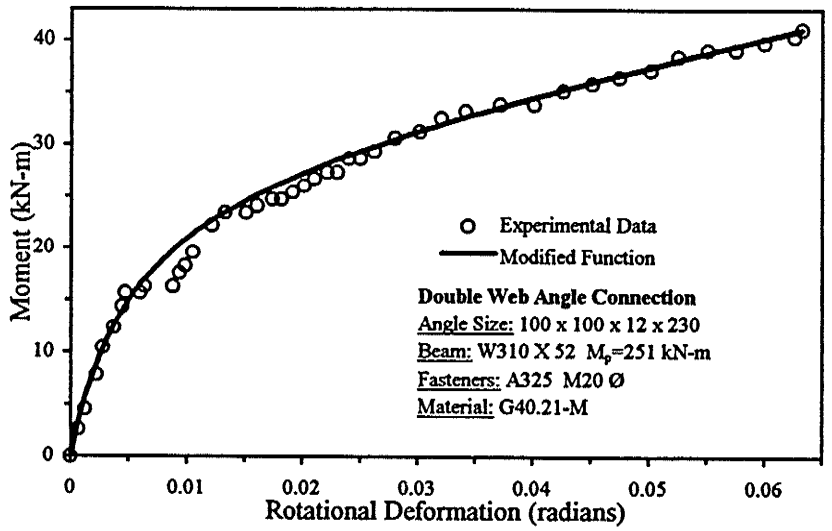


Figure A.108 (a) M-ϕ curve for Onuah: Test A11

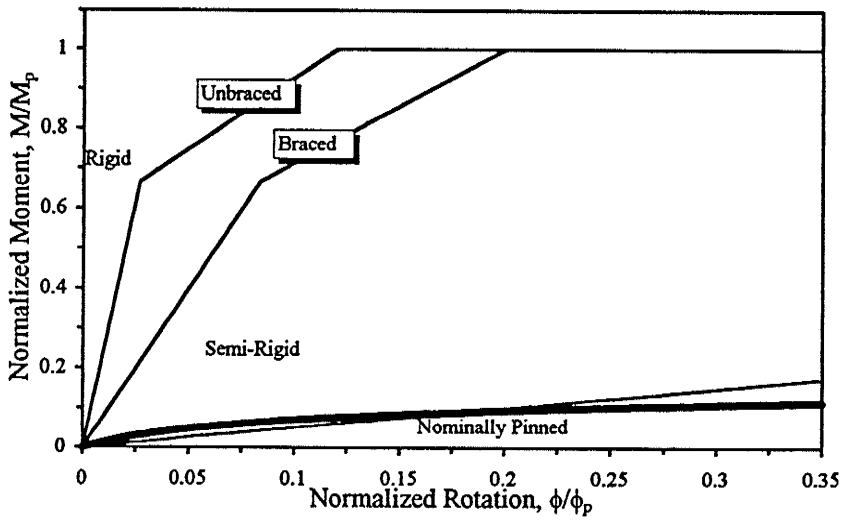


Figure A.108 (b) Eurocode3 Classification of Onuah: Test A11

Table A.109 M-ϕ data for Onuah: Test A13 (1988)

Moment, M kN-m	Rotation, ϕ radians
0	0
2.933	0.0004
4.892	0.0024
7.826	0.0032
8.802	0.0042
9.778	0.0050
10.753	0.0052
11.737	0.0064
12.706	0.0071
13.681	0.0086
14.664	0.0094
15.639	0.0117
16.614	0.0136
17.597	0.0162
18.572	0.0200
19.547	0.0221
20.530	0.0261
21.506	0.0338
22.482	0.0380
23.465	0.0442
24.441	0.0512
25.416	0.0558
26.392	0.0656
27.368	0.0773

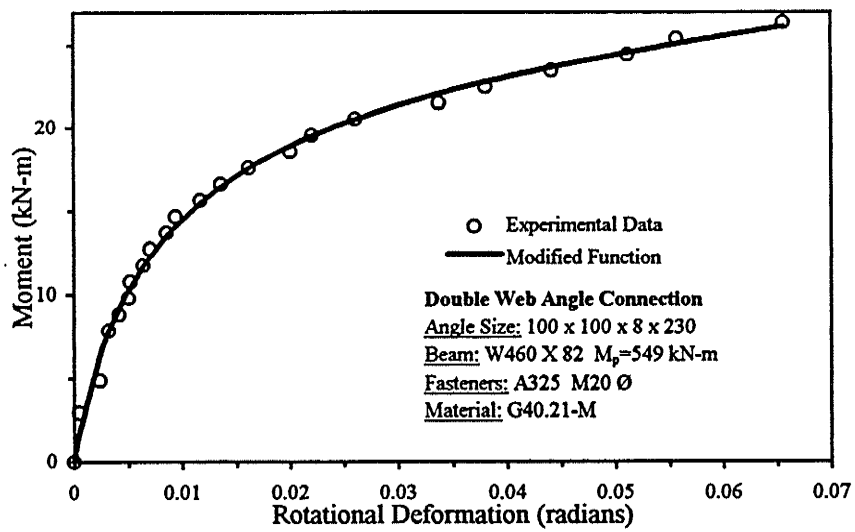


Figure A.109 (a) M-ϕ curve for Onuah: Test A13

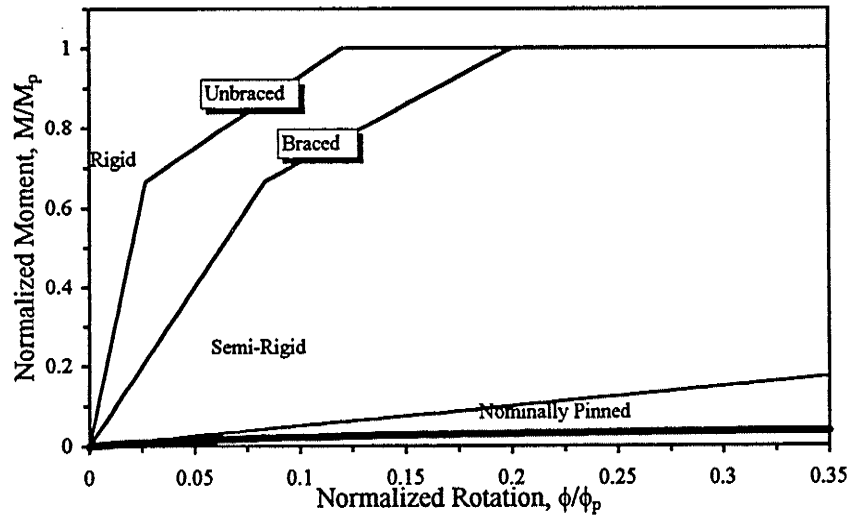


Figure A.109 (b) Eurocode3 Classification of Onuah: Test A13

Table A.110 M-ϕ data for Onuah: Test A14 (1988)

Moment, M kN-m	Rotation, ϕ radians	Moment, M kN-m	Rotation, ϕ radians
0	0	38.118	0.0190
2.934	0.0005	39.100	0.0215
4.892	0.0009	41.050	0.0223
5.867	0.0009	43.008	0.0233
7.825	0.0014	43.983	0.0251
9.775	0.0020	44.958	0.0272
11.732	0.0025	45.941	0.0311
14.666	0.0035	46.916	0.0330
17.599	0.0043	47.892	0.0412
19.549	0.0052	48.875	0.0430
20.531	0.0053	49.851	0.0472
21.506	0.0056	50.826	0.0481
22.482	0.0062	51.809	0.0490
23.465	0.0065	51.809	0.0501
24.440	0.0069	52.784	0.0520
26.390	0.0080	52.785	0.0541
28.349	0.0088	53.760	0.0561
29.324	0.0093	54.742	0.0621
30.307	0.0104	55.711	0.0641
31.276	0.0110	56.686	0.0661
32.251	0.0120	57.661	0.0686
34.208	0.0131	58.643	0.0711
35.184	0.0142	59.618	0.0720
36.167	0.0151		
36.168	0.0171		
37.143	0.0180		

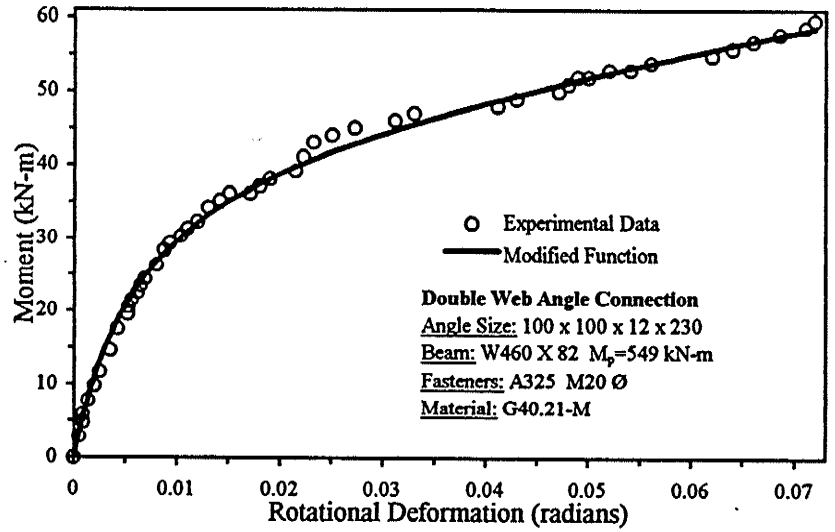


Figure A.110 (a) M-ϕ curve for Onuah: Test A14

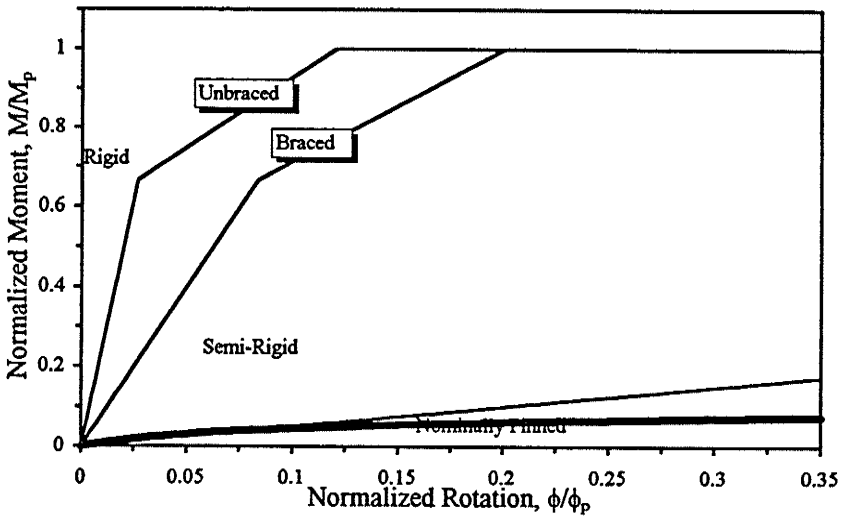


Figure A.110 (b) Eurocode3 Classification of Onuah: Test A14

Table A.111 M-ϕ data for Onuah: Test A15 (1988)

Moment, M kN-m	Rotation, ϕ radians	Moment, M kN-m	Rotation, ϕ radians
0	0	49.847	0.0208
2.933	0.0002	50.822	0.0215
5.865	0.0004	51.805	0.0221
7.823	0.0007	52.780	0.0240
10.748	0.0010	53.756	0.0271
13.681	0.0012	57.663	0.0280
15.639	0.0015	59.621	0.0300
18.571	0.0017	61.579	0.0320
21.505	0.0023	62.554	0.0351
23.462	0.0022	67.445	0.0421
25.413	0.0026	69.395	0.0440
27.371	0.0030	70.378	0.0461
30.304	0.0033	73.303	0.0500
32.254	0.0037	74.286	0.0521
34.212	0.0044	76.236	0.0540
36.170	0.0047	77.219	0.0561
38.121	0.0055	79.169	0.0580
36.166	0.0066	80.152	0.0601
37.141	0.0082	81.127	0.0621
38.116	0.0091	83.085	0.0651
40.074	0.0099	86.011	0.0701
41.049	0.0110	88.936	0.0741
43.007	0.0173	92.851	0.0782
44.957	0.0181	94.801	0.0797
46.915	0.0190		
47.890	0.0200		

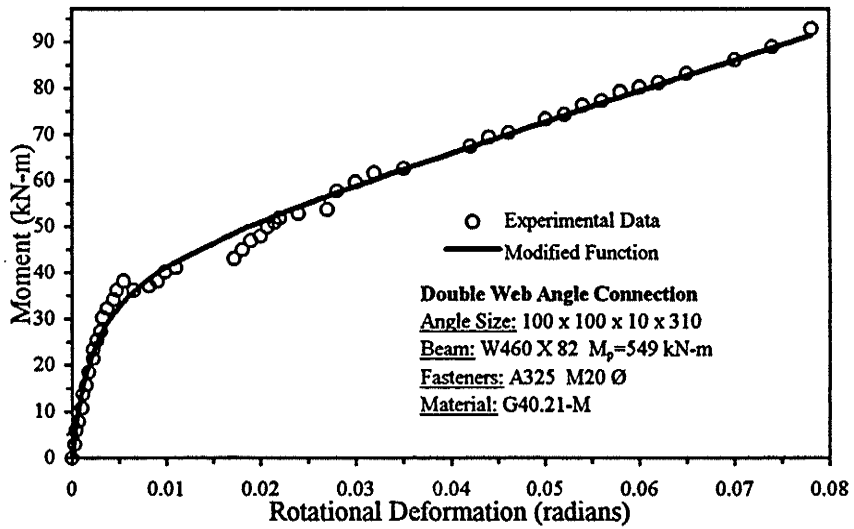


Figure A.111 (a) M-ϕ curve for Onuah: Test A15

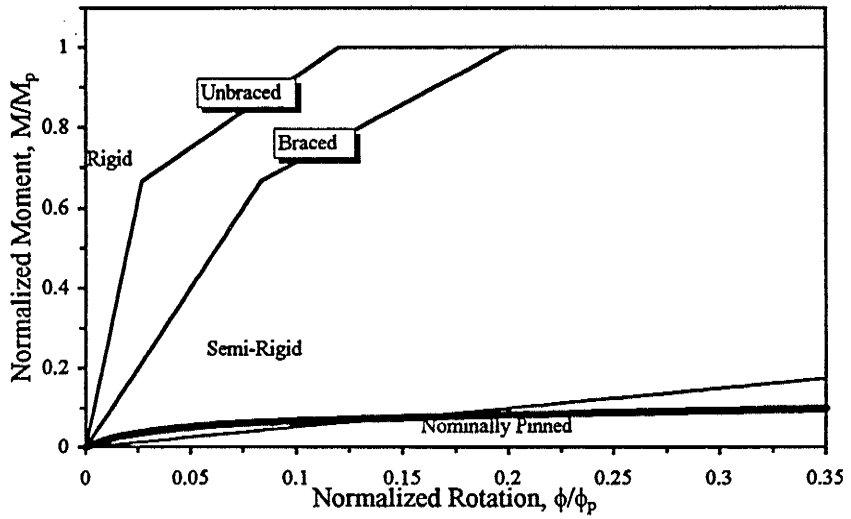


Figure A.111 (b) Eurocode3 Classification of Onuah: Test A15

Table A.112 M-ϕ data for Onuah: Test A16 (1988)

Moment, M kN-m	Rotation, ϕ radians	Moment, M kN-m	Rotation, ϕ radians
0	0	70.373	0.0170
3.910	0.0003	70.374	0.0181
6.520	0.0004	72.984	0.0190
9.121	0.0006	74.284	0.0210
14.331	0.0008	75.584	0.0221
18.242	0.0010	76.885	0.0230
22.152	0.0013	78.195	0.0241
28.673	0.0016	79.495	0.0250
35.184	0.0021	80.795	0.0261
39.095	0.0025	80.795	0.0271
43.006	0.0030	82.106	0.0290
44.317	0.0034	83.406	0.0300
46.918	0.0038	84.706	0.0321
48.228	0.0041	86.017	0.0340
50.821	0.0052	89.928	0.0403
49.521	0.0061	91.228	0.0421
52.131	0.0072	92.529	0.0440
53.432	0.0083	95.139	0.0460
56.032	0.0091	96.440	0.0481
58.642	0.0100	97.731	0.0501
61.252	0.0111	100.341	0.0551
63.852	0.0121	102.951	0.0575
65.163	0.0130	105.551	0.0625
65.163	0.0140	108.161	0.0651
66.463	0.0151	110.771	0.0672
67.763	0.0160		

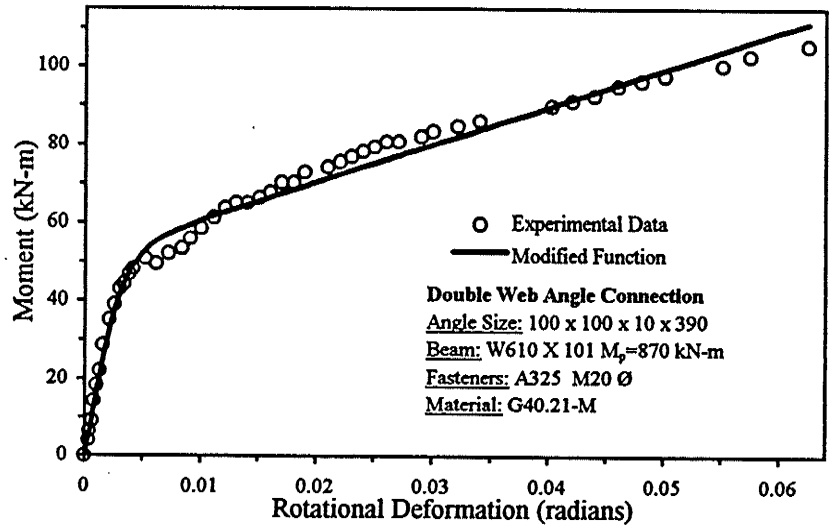


Figure A.112 (a) M-ϕ curve for Onuah: Test A16

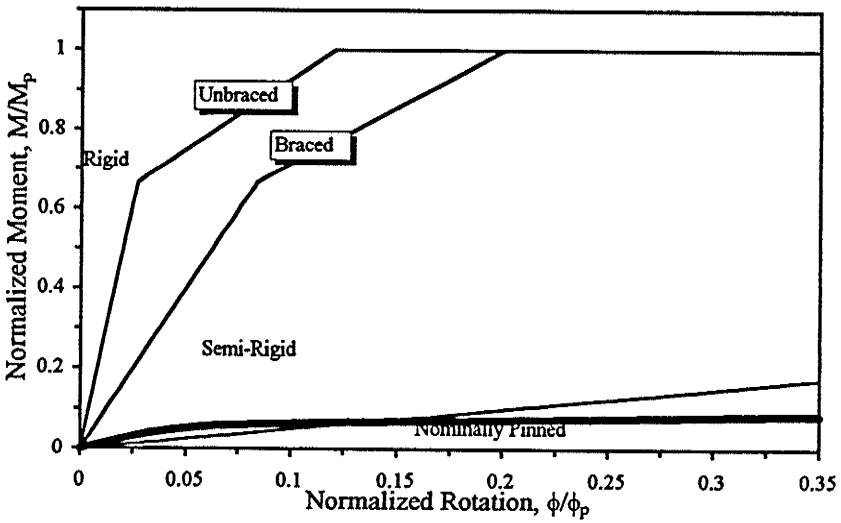


Figure A.112 (b) Eurocode3 Classification of Onuah: Test A16

Table A.113 M-ϕ data for Onuah: Test A18 (1988)

Moment, M kN-m	Rotation, ϕ radians	Moment, M kN-m	Rotation, ϕ radians
0	0	93.834	0.0201
5.210	0.0001	95.134	0.0210
10.430	0.0003	96.434	0.0220
16.941	0.0005	99.045	0.0231
22.151	0.0008	100.345	0.0240
27.372	0.0010	102.955	0.0251
31.282	0.0012	104.255	0.0260
35.183	0.0014	105.555	0.0270
39.093	0.0017	106.866	0.0280
43.004	0.0018	108.166	0.0291
46.914	0.0023	108.166	0.0291
49.525	0.0024	109.466	0.0301
52.136	0.0028	112.076	0.0311
56.036	0.0031	113.377	0.0320
59.948	0.0041	115.987	0.0332
63.851	0.0051	115.987	0.0340
66.462	0.0075	118.587	0.0351
69.072	0.0081	119.897	0.0360
71.672	0.0090	121.198	0.0371
74.282	0.0095	123.808	0.0381
76.882	0.0115	125.108	0.0390
78.193	0.0140	126.408	0.0401
82.103	0.0150	127.718	0.0411
86.013	0.0171		
88.614	0.0180		
91.224	0.0191		

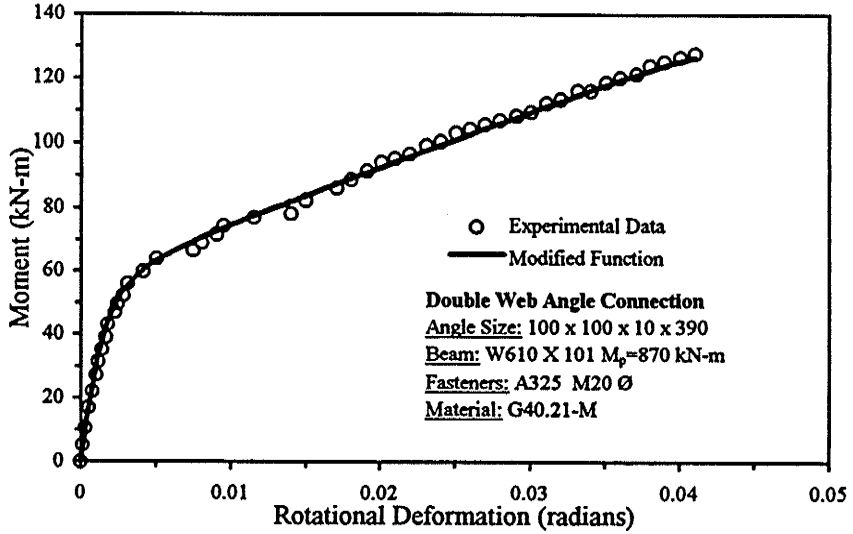


Figure A.113 (a) M-ϕ curve for Onuah: Test A18

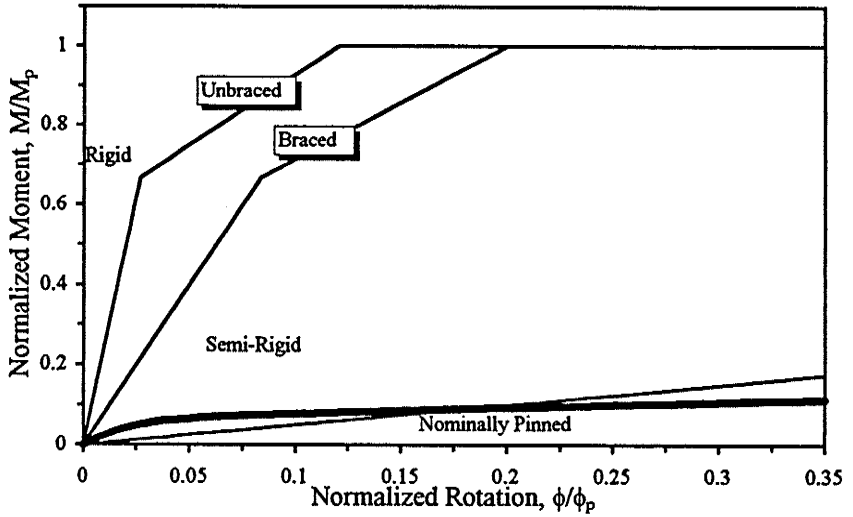


Figure A.113 (b) Eurocode3 Classification of Onuah: Test A18

Table A.114 M-ϕ data for Onuah: Test A19 (1988)

Moment, M kN-m	Rotation, ϕ radians	Moment, M kN-m	Rotation, ϕ radians
0	0	152.475	0.0241
2.610	0.0002	153.775	0.0250
6.520	0.0003	157.685	0.0261
9.121	0.0005	161.596	0.0281
13.031	0.0007	164.196	0.0291
16.942	0.0009	165.506	0.0301
20.852	0.0011	168.106	0.0310
24.763	0.0014	169.417	0.0320
31.283	0.0017	170.717	0.0330
36.494	0.0019	172.017	0.0340
41.704	0.0020	174.627	0.0350
46.915	0.0024	0.000	0.0000
50.825	0.0027	0.000	0.0000
56.036	0.0028	0.000	0.0000
61.256	0.0030	0.000	0.0000
65.167	0.0034	0.000	0.0000
71.678	0.0038	0.000	0.0000
75.588	0.0041	0.000	0.0000
84.701	0.0050	0.000	0.0000
97.732	0.0080	0.000	0.0000
113.372	0.0110	0.000	0.0000
123.803	0.0140	0.000	0.0000
130.314	0.0170	0.000	0.0000
136.834	0.0191		
142.044	0.0211		
148.565	0.0230		

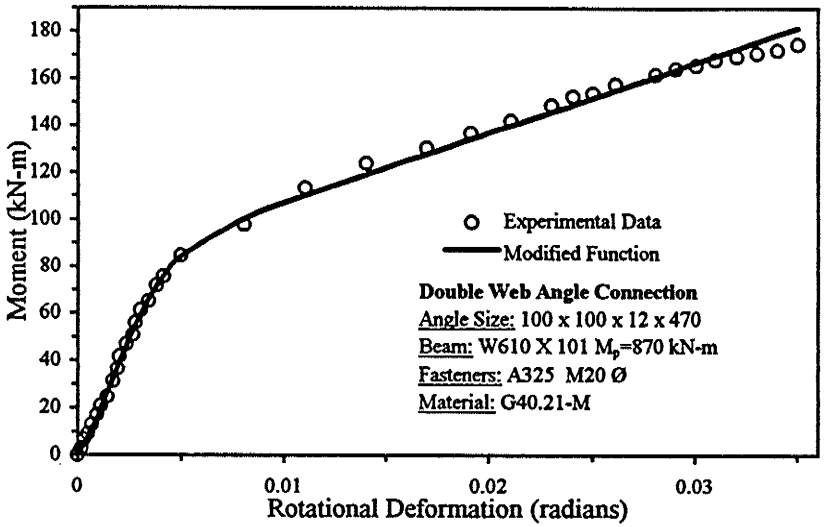


Figure A.114 (a) M-ϕ curve for Onuah: Test A19

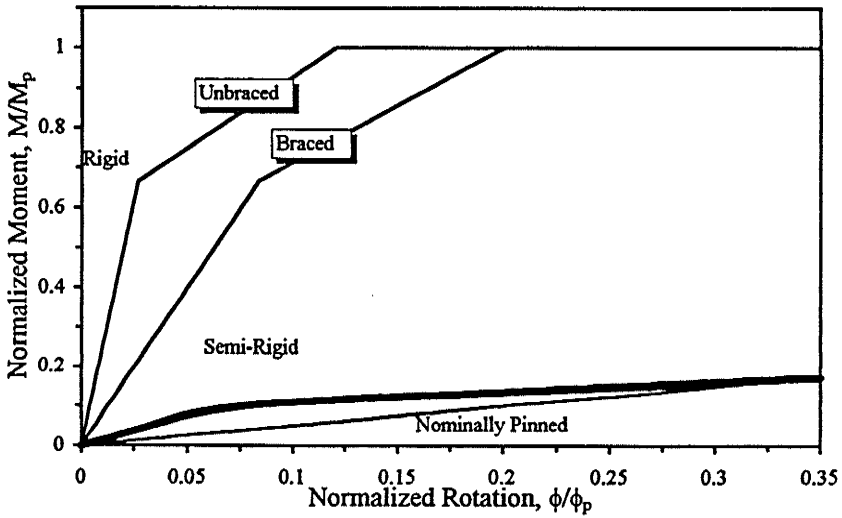


Figure A.114 (b) Eurocode3 Classification of Onuah: Test A19

Table A.115 M-ϕ data for Marley: A-1/4-1 (1982)

Moment, M kN-m	Rotation, ϕ radians	Moment, M kN-m	Rotation, ϕ radians
0	0	5.010	0.0234
0.200	0.0002	5.078	0.0253
0.400	0.0003	5.147	0.0271
0.651	0.0007	5.193	0.0284
0.902	0.0010	5.239	0.0297
1.152	0.0014	5.307	0.0314
1.403	0.0018	5.376	0.0331
1.620	0.0023	5.444	0.0347
1.837	0.0027	5.513	0.0362
2.077	0.0033	5.570	0.0379
2.317	0.0039	5.627	0.0395
2.556	0.0045	5.695	0.0414
2.796	0.0050	5.764	0.0433
3.081	0.0060	5.764	0.0433
3.367	0.0070		
3.560	0.0081		
3.754	0.0092		
3.960	0.0106		
4.063	0.0117		
4.165	0.0128		
4.268	0.0139		
4.371	0.0150		
4.554	0.0169		
4.782	0.0187		
4.839	0.0200		
4.896	0.0213		

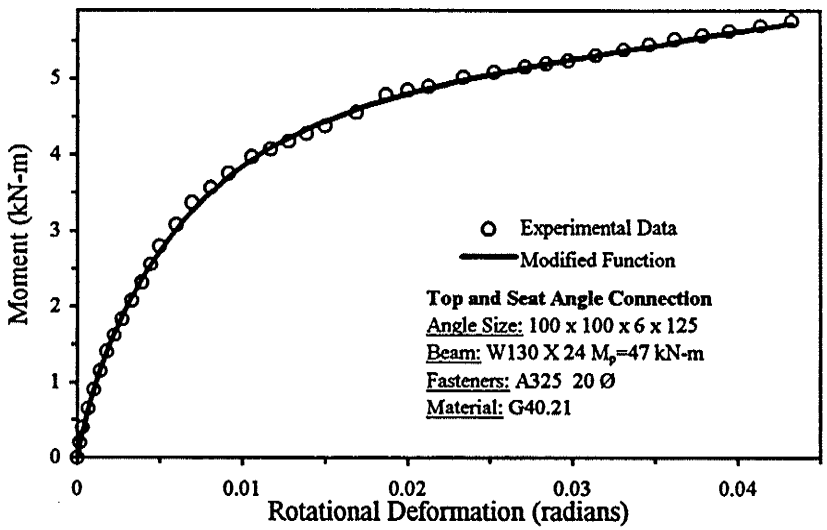


Figure A.115 (a) M-ϕ curve for Marley: A-1/4-1

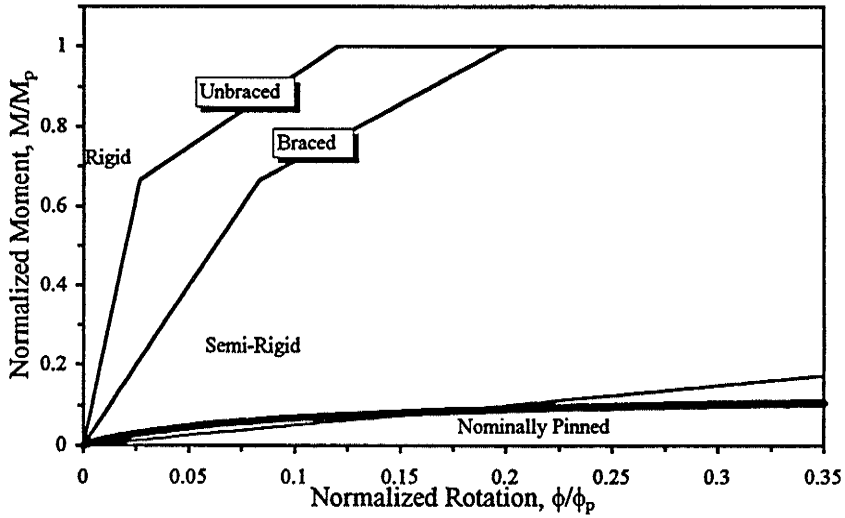


Figure A.115 (b) Eurocode3 Classification of Marley: A-1/4-1

Table A.116 M-ϕ data for Marley: A-1/4-2 (1982)

Moment, M kN-m	Rotation, ϕ radians	Moment, M kN-m	Rotation, ϕ radians
0	0	4.462	0.0158
0.179	0.0002	4.523	0.0166
0.358	0.0003	4.584	0.0173
0.537	0.0005	4.645	0.0181
0.753	0.0009	4.696	0.0189
0.969	0.0013	4.747	0.0198
1.145	0.0016	4.799	0.0206
1.320	0.0019	4.850	0.0214
1.495	0.0022		
1.663	0.0027		
1.830	0.0031		
1.997	0.0036		
2.237	0.0043		
2.477	0.0049		
2.671	0.0055		
2.865	0.0061		
3.104	0.0072		
3.343	0.0082		
3.473	0.0090		
3.603	0.0097		
3.733	0.0105		
3.858	0.0112		
3.983	0.0119		
4.109	0.0130		
4.234	0.0140		
4.348	0.0149		

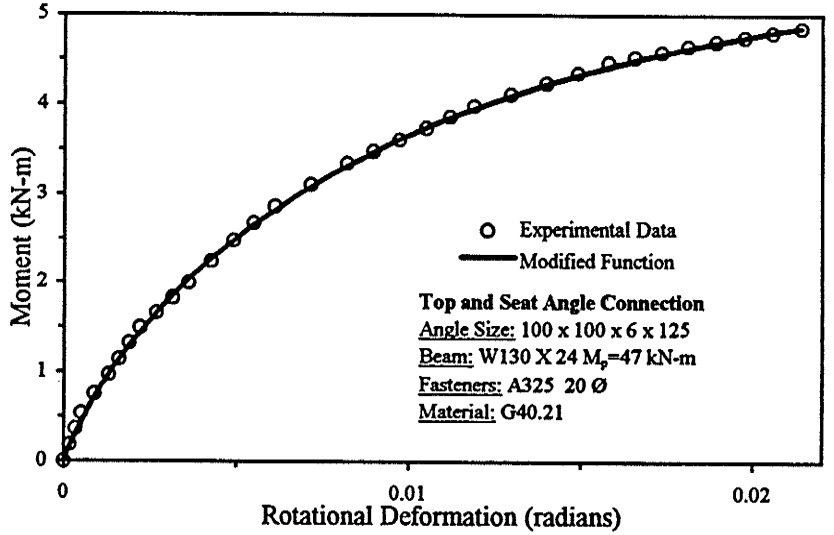


Figure A.116 (a) M-ϕ curve for Marley: A-1/4-2

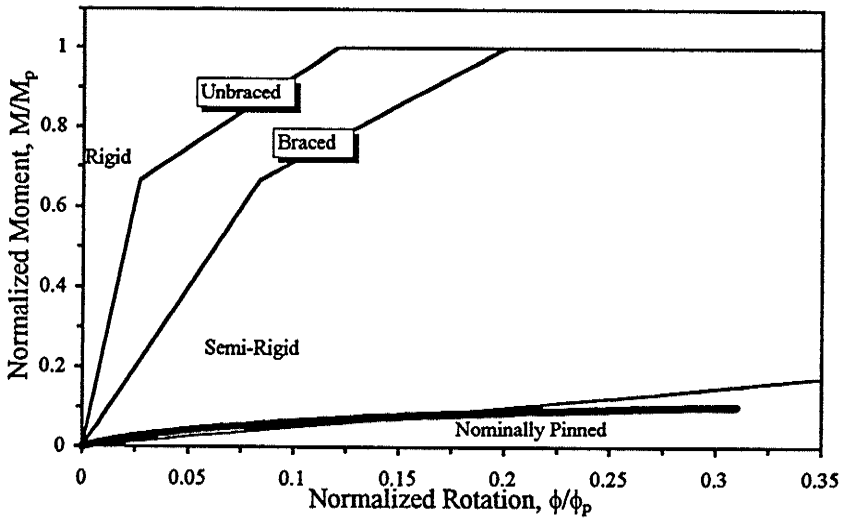


Figure A.116 (b) Eurocode3 Classification of Marley: A-1/4-2

Table A.117 M-ϕ data for Marley: B-1/4-1 (1982)

Moment, M kN-m	Rotation, ϕ radians	Moment, M kN-m	Rotation, ϕ radians
0	0	4.478	0.0091
0.221	0.0000	4.551	0.0098
0.443	0.0000	4.625	0.0104
0.664	0.0000	4.699	0.0110
0.910	0.0001	4.773	0.0116
1.157	0.0001	4.847	0.0122
1.403	0.0003	4.890	0.0129
1.649	0.0005	4.933	0.0136
1.870	0.0009	4.976	0.0142
2.091	0.0012	5.019	0.0149
2.263	0.0013	5.069	0.0157
2.435	0.0014	5.118	0.0165
2.595	0.0017	5.167	0.0173
2.755	0.0019		
2.952	0.0023		
3.150	0.0026		
3.297	0.0030		
3.444	0.0033		
3.559	0.0039		
3.673	0.0045		
3.788	0.0051		
3.912	0.0058		
4.035	0.0064		
4.183	0.0071		
4.330	0.0078		
4.404	0.0085		

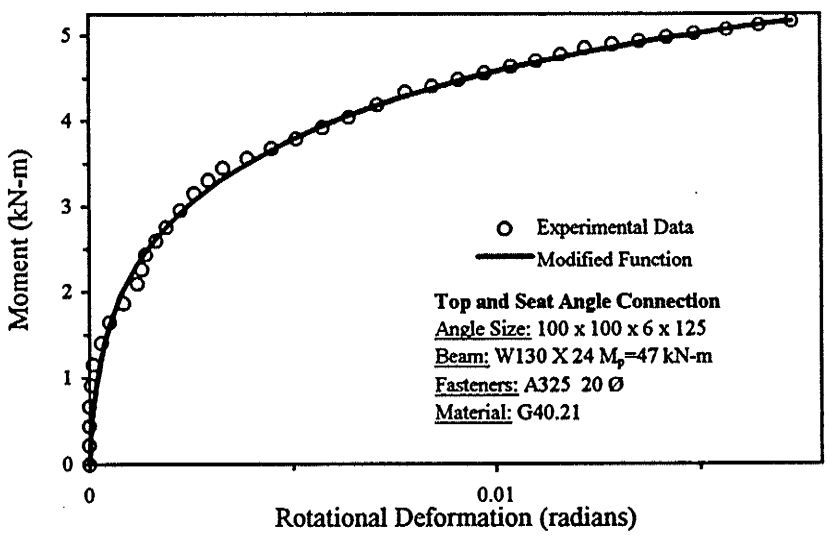


Figure A.117 (a) M-ϕ curve for Marley: B-1/4-1

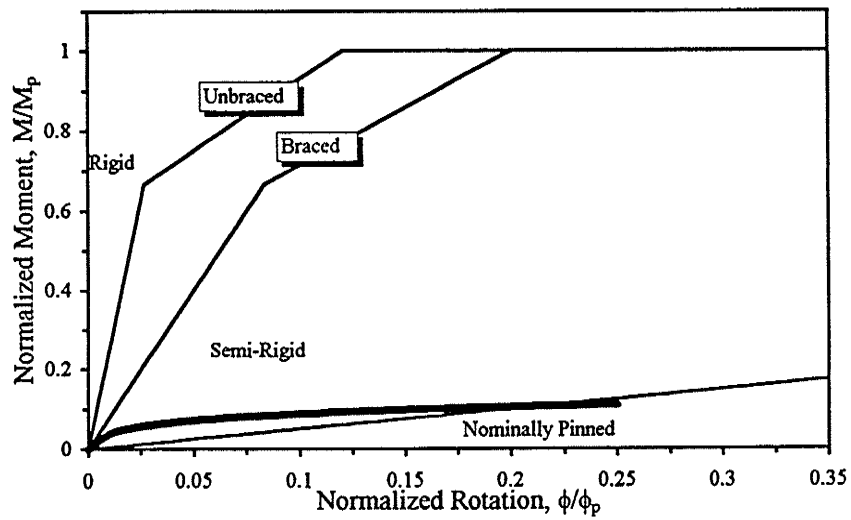


Figure A.117 (b) Eurocode3 Classification of Marley: B-1/4-1

Table A.118 M-ϕ data for Marley: B-1/4-2 (1982)

Moment, M kN-m	Rotation, ϕ radians	Moment, M kN-m	Rotation, ϕ radians
0	0	4.348	0.0230
0.197	0.0001	4.462	0.0245
0.394	0.0002	4.538	0.0256
0.591	0.0002	4.615	0.0267
0.788	0.0003	4.691	0.0278
1.008	0.0005	4.782	0.0291
1.229	0.0007	4.873	0.0303
1.449	0.0009	4.976	0.0313
1.678	0.0013	5.079	0.0323
1.906	0.0017		
2.134	0.0021		
2.339	0.0031		
2.545	0.0040		
2.727	0.0055		
2.910	0.0070		
3.047	0.0082		
3.183	0.0095		
3.320	0.0107		
3.469	0.0123		
3.617	0.0139		
3.739	0.0153		
3.861	0.0168		
3.983	0.0182		
4.067	0.0193		
4.151	0.0204		
4.234	0.0215		

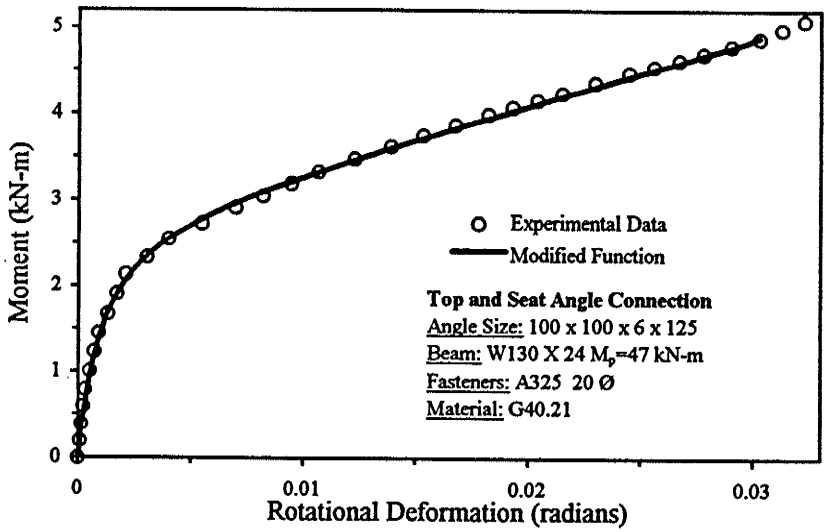


Figure A.118 (a) M-ϕ curve for Marley: B-1/4-2

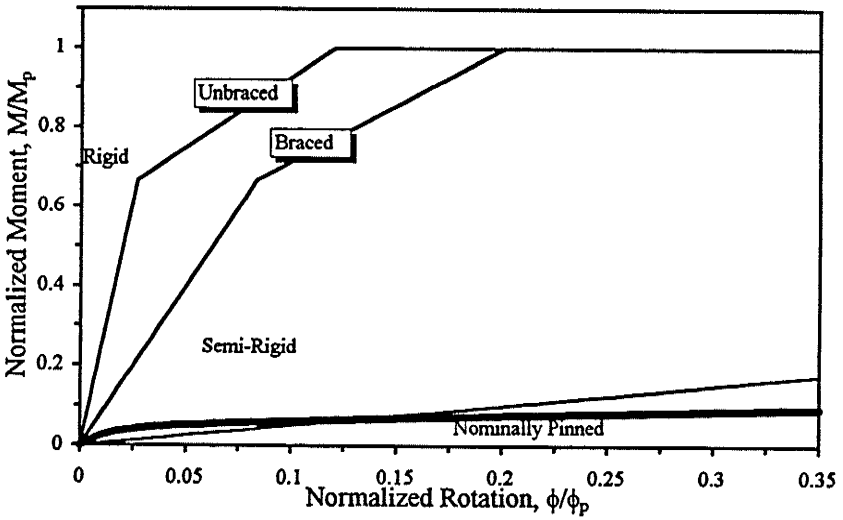


Figure A.118 (b) Eurocode3 Classification of Marley: B-1/4-2

Table A.119 M-ϕ data for Marley: C1-1/4-2 (1982)

Moment, M kN-m	Rotation, ϕ radians	Moment, M kN-m	Rotation, ϕ radians
0	0	4.884	0.0236
0.255	0.0001	5.033	0.0254
0.510	0.0002	5.124	0.0274
0.765	0.0003	5.216	0.0293
0.993	0.0006	5.284	0.0315
1.222	0.0008	5.353	0.0337
1.461	0.0011	5.433	0.0356
1.700	0.0014	5.513	0.0374
1.940	0.0017	5.547	0.0393
2.180	0.0019	5.581	0.0412
2.408	0.0024	5.627	0.0433
2.636	0.0029	5.673	0.0453
2.784	0.0033		
2.933	0.0036		
3.104	0.0045		
3.276	0.0054		
3.458	0.0067		
3.640	0.0080		
3.777	0.0098		
3.914	0.0115		
4.074	0.0133		
4.234	0.0150		
4.371	0.0168		
4.508	0.0185		
4.622	0.0201		
4.736	0.0217		

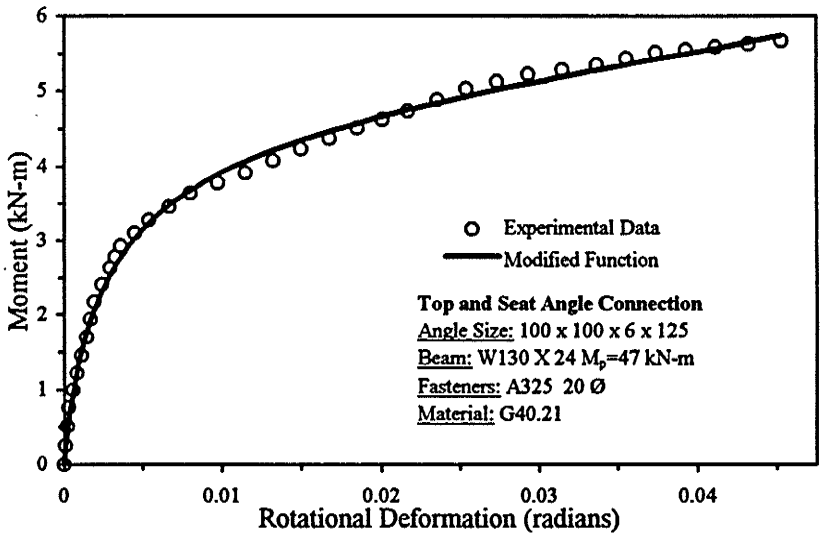


Figure A.119 (a) M-ϕ curve for Marley: C1-1/4-2

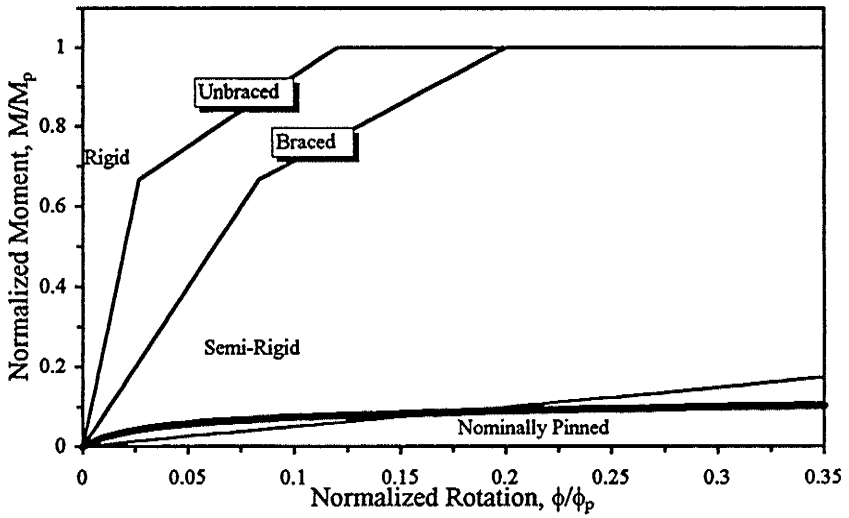


Figure A.119 (b) Eurocode3 Classification of Marley: C1-1/4-2

Table A.120 M-ϕ data for Marley: C2-1/4-1 (1982)

Moment, M kN-m	Rotation, ϕ radians	Moment, M kN-m	Rotation, ϕ radians
0	0	4.725	0.0241
0.225	0.0001	4.828	0.0258
0.449	0.0001	4.965	0.0274
0.674	0.0002	5.102	0.0290
0.917	0.0004	5.181	0.0304
1.160	0.0005	5.261	0.0318
1.403	0.0007	5.307	0.0331
1.601	0.0010	5.353	0.0343
1.799	0.0014	5.410	0.0364
1.997	0.0017	5.467	0.0384
2.271	0.0025	5.524	0.0400
2.545	0.0032	5.581	0.0415
2.727	0.0037	5.627	0.0433
2.910	0.0042	5.673	0.0450
3.093	0.0053	5.752	0.0473
3.276	0.0063	5.831	0.0495
3.458	0.0077		
3.640	0.0091		
3.755	0.0107		
3.870	0.0122		
3.995	0.0141		
4.120	0.0160		
4.246	0.0178		
4.371	0.0196		
4.497	0.0210		
4.622	0.0224		

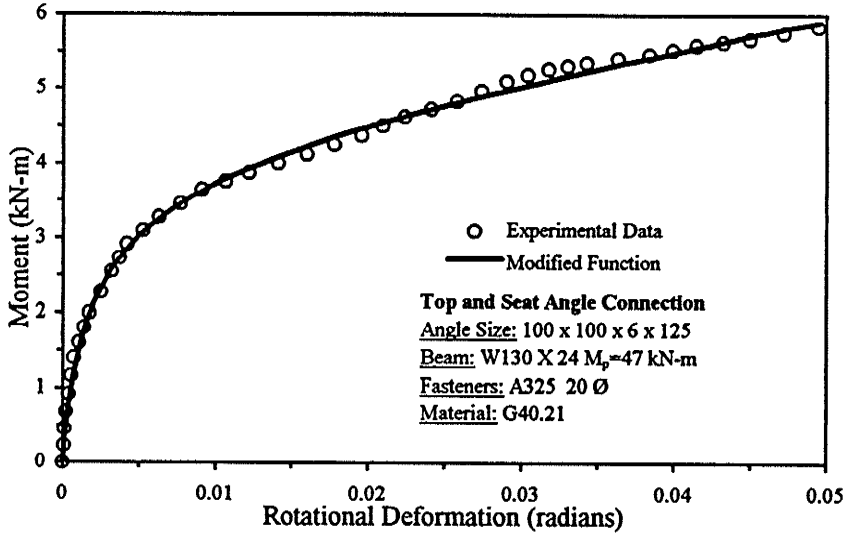


Figure A.120 (a) M-ϕ curve for Marley: C2-1/4-1

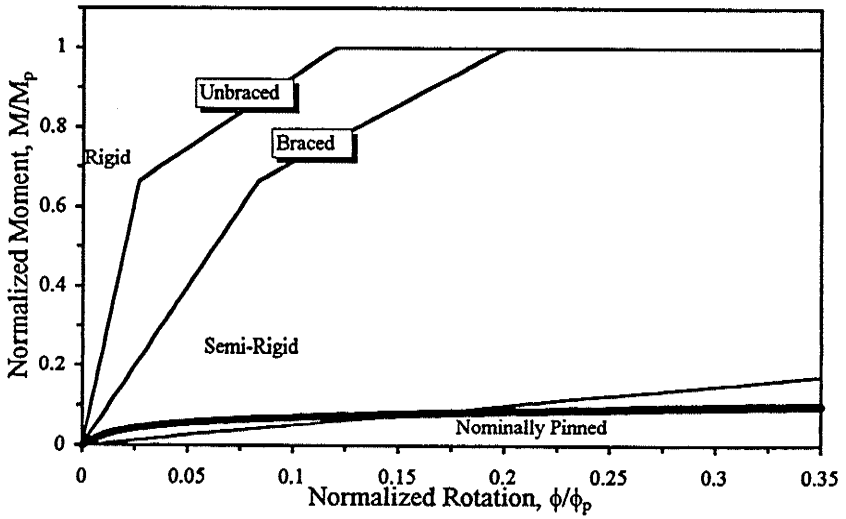


Figure A.120 (b) Eurocode3 Classification of Marley: C2-1/4-1

Table A.121 M-ϕ data for Marley: C2-1/4-2 (1982)

Moment, M kN-m	Rotation, ϕ radians	Moment, M kN-m	Rotation, ϕ radians
0	0	4.422	0.0225
0.239	0.0002	4.558	0.0242
0.477	0.0003	4.695	0.0256
0.716	0.0005	4.831	0.0269
0.954	0.0008	4.933	0.0285
1.193	0.0010	5.036	0.0300
1.432	0.0014	5.115	0.0313
1.670	0.0017	5.194	0.0326
1.898	0.0022	5.274	0.0341
2.126	0.0026	5.354	0.0355
2.308	0.0033	5.411	0.0370
2.489	0.0040	5.468	0.0384
2.649	0.0045	5.547	0.0401
2.808	0.0050	5.627	0.0417
2.967	0.0058	5.672	0.0432
3.125	0.0066	5.717	0.0446
3.284	0.0082	5.763	0.0459
3.444	0.0097	5.808	0.0472
3.558	0.0111	5.854	0.0492
3.672	0.0125		
3.762	0.0140		
3.853	0.0155		
3.967	0.0169		
4.081	0.0183		
4.183	0.0196		
4.286	0.0208		

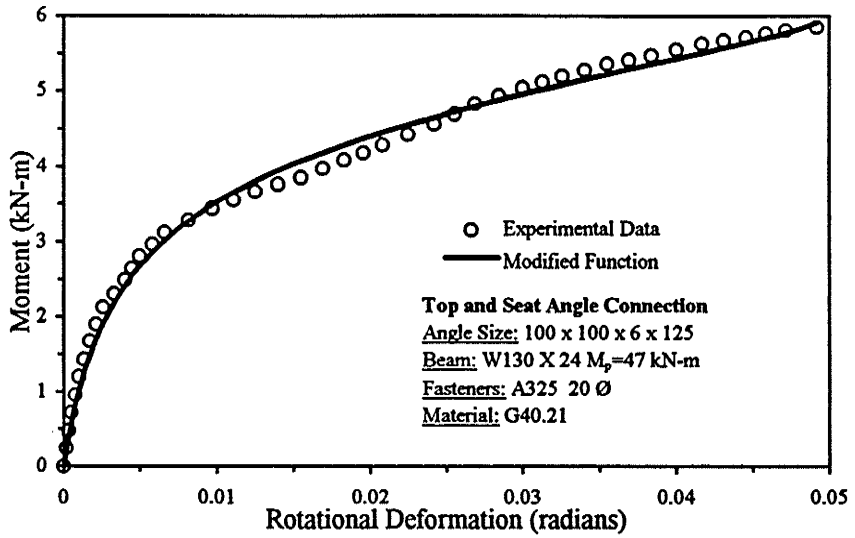


Figure A.121 (a) M-ϕ curve for Marley: C2-1/4-2

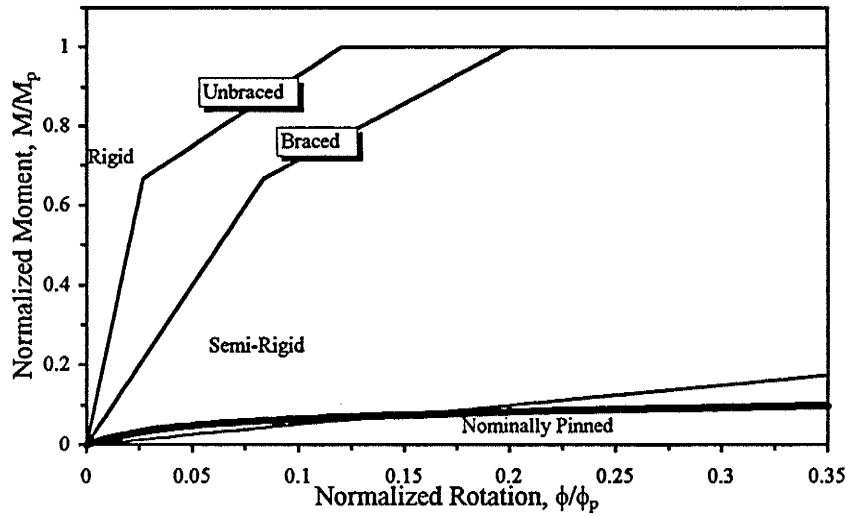


Figure A.121 (b) Eurocode3 Classification of Marley: C2-1/4-2

Table A.122 M-ϕ data for Marley: D1-1/4-1 (1982)

Moment, M kN-m	Rotation, ϕ radians	Moment, M kN-m	Rotation, ϕ radians
0	0	5.076	0.0270
0.269	0.0005	5.179	0.0287
0.538	0.0010	5.282	0.0304
0.729	0.0013	5.385	0.0321
0.921	0.0015	5.488	0.0337
1.112	0.0018	5.558	0.0353
1.318	0.0022	5.627	0.0369
1.524	0.0027		
1.730	0.0031		
2.005	0.0037		
2.280	0.0042		
2.556	0.0049		
2.831	0.0055		
3.037	0.0063		
3.243	0.0070		
3.461	0.0084		
3.678	0.0097		
3.861	0.0115		
4.044	0.0133		
4.205	0.0150		
4.366	0.0167		
4.503	0.0184		
4.641	0.0201		
4.756	0.0219		
4.870	0.0236		
4.973	0.0253		

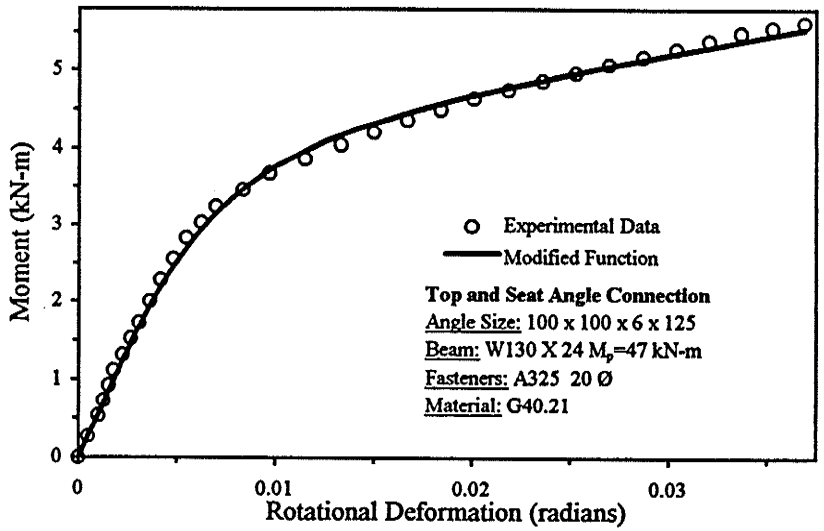


Figure A.122 (a) M-ϕ curve for Marley: D1-1/4-1

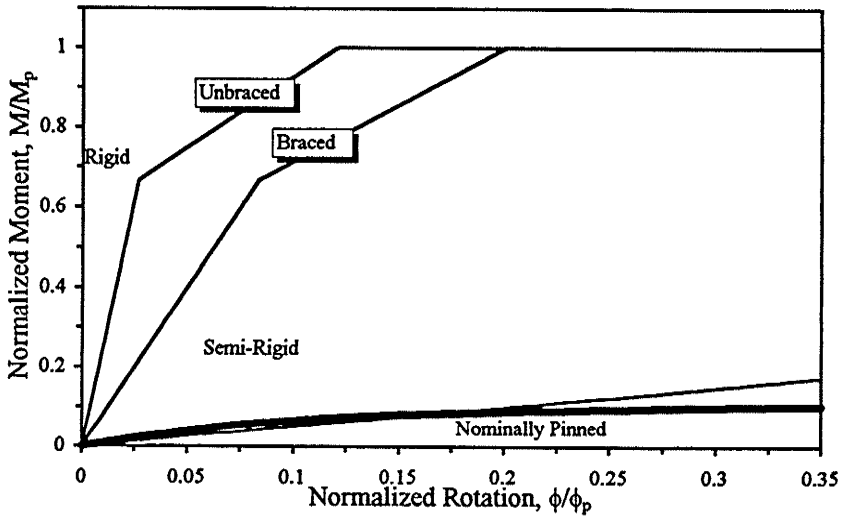


Figure A.122 (b) Eurocode3 Classification of Marley: D1-1/4-1

Table A.123 M-ϕ data for Marley: D1-1/4-2 (1982)

Moment, M kN-m	Rotation, ϕ radians	Moment, M kN-m	Rotation, ϕ radians
0	0	4.702	0.0272
0.186	0.0003	4.782	0.0285
0.372	0.0007	4.839	0.0301
0.559	0.0010	4.896	0.0317
0.832	0.0018	4.964	0.0335
1.106	0.0025	5.033	0.0352
1.346	0.0032	5.101	0.0370
1.586	0.0038	5.170	0.0388
1.849	0.0046	5.215	0.0404
2.111	0.0054	5.261	0.0420
2.316	0.0061	5.318	0.0435
2.522	0.0067	5.376	0.0449
2.670	0.0074	5.410	0.0469
2.819	0.0080	5.444	0.0488
2.990	0.0092	5.490	0.0501
3.162	0.0103		
3.390	0.0117		
3.617	0.0130		
3.777	0.0145		
3.937	0.0159		
4.086	0.0177		
4.234	0.0195		
4.337	0.0212		
4.439	0.0229		
4.530	0.0244		
4.622	0.0259		

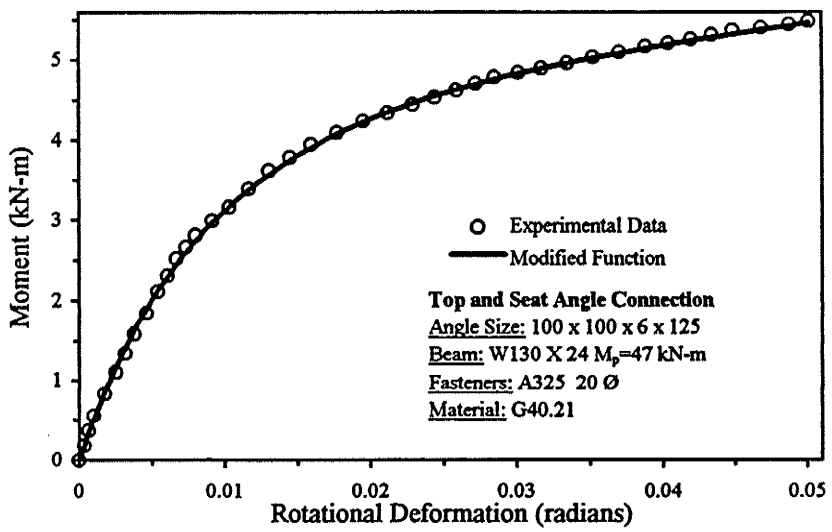


Figure A.123 (a) M-ϕ curve for Marley: D1-1/4-2

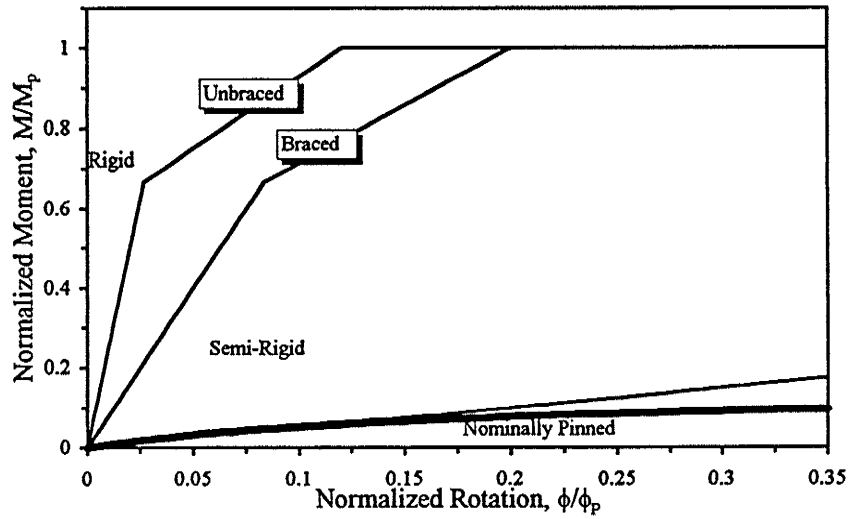


Figure A.123 (b) Eurocode3 Classification of Marley: D1-1/4-2

Table A.124 M-ϕ data for Marley: D2-1/4-1 (1982)

Moment, M kN-m	Rotation, ϕ radians	Moment, M kN-m	Rotation, ϕ radians
0	0	4.758	0.0244
0.206	0.0003	4.918	0.0257
0.411	0.0005	5.078	0.0269
0.617	0.0008	5.181	0.0284
0.808	0.0011	5.284	0.0298
0.998	0.0015	5.364	0.0309
1.189	0.0018	5.444	0.0320
1.464	0.0023	5.501	0.0333
1.738	0.0027	5.558	0.0346
2.013	0.0033	5.615	0.0358
2.287	0.0039	5.673	0.0370
2.447	0.0042		
2.607	0.0045		
2.836	0.0061		
3.064	0.0076		
3.270	0.0093		
3.476	0.0109		
3.636	0.0123		
3.796	0.0136		
3.796	0.0136		
3.918	0.0150		
4.040	0.0163		
4.162	0.0177		
4.311	0.0194		
4.459	0.0210		
4.608	0.0227		

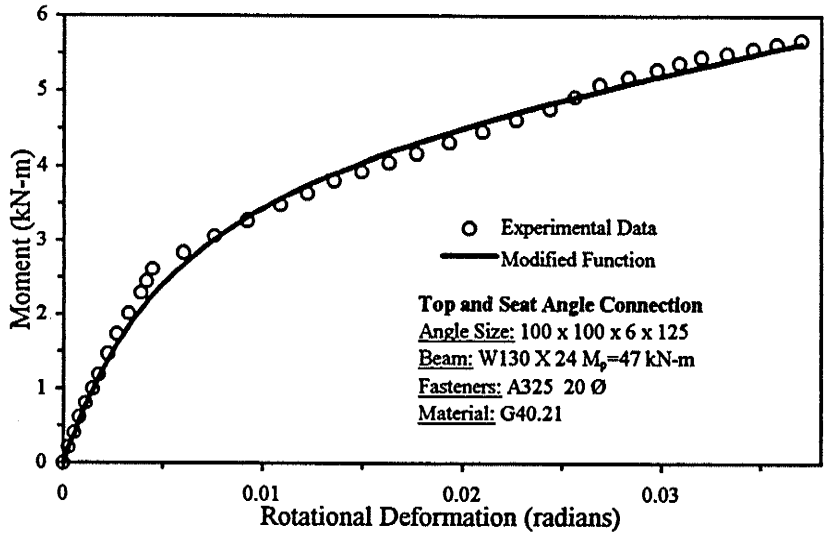


Figure A.124 (a) M-ϕ curve for Marley: D2-1/4-1

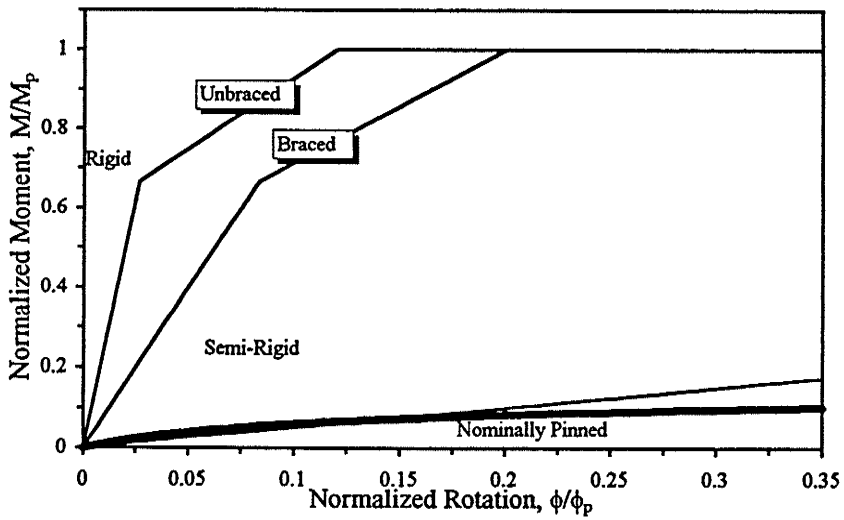


Figure A.124 (b) Eurocode3 Classification of Marley: D2-1/4-1

Table A.125 M-ϕ data for Marley: D2-1/4-2 (1982)

Moment, M kN-m	Rotation, ϕ radians	Moment, M kN-m	Rotation, ϕ radians
0	0	4.825	0.0231
0.263	0.0002	4.985	0.0241
0.526	0.0003	5.100	0.0254
0.778	0.0009	5.214	0.0266
1.029	0.0014	5.329	0.0282
1.269	0.0018	5.444	0.0297
1.509	0.0021	5.535	0.0310
1.692	0.0026	5.627	0.0322
1.875	0.0031		
2.081	0.0036		
2.287	0.0041		
2.493	0.0046		
2.699	0.0053		
2.904	0.0060		
3.076	0.0075		
3.247	0.0089		
3.385	0.0104		
3.522	0.0118		
3.625	0.0132		
3.729	0.0145		
3.842	0.0159		
3.956	0.0172		
4.128	0.0185		
4.299	0.0197		
4.482	0.0209		
4.665	0.0220		

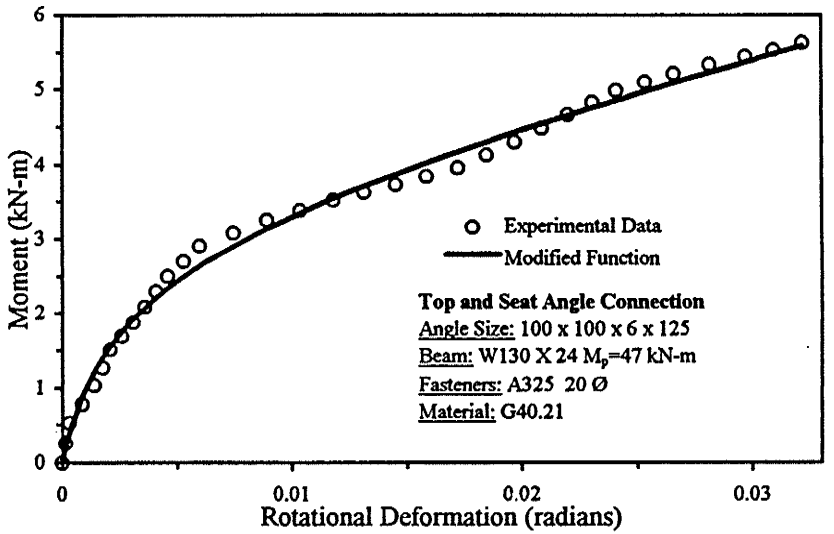


Figure A.125 (a) M-ϕ curve for Marley: D2-1/4-2

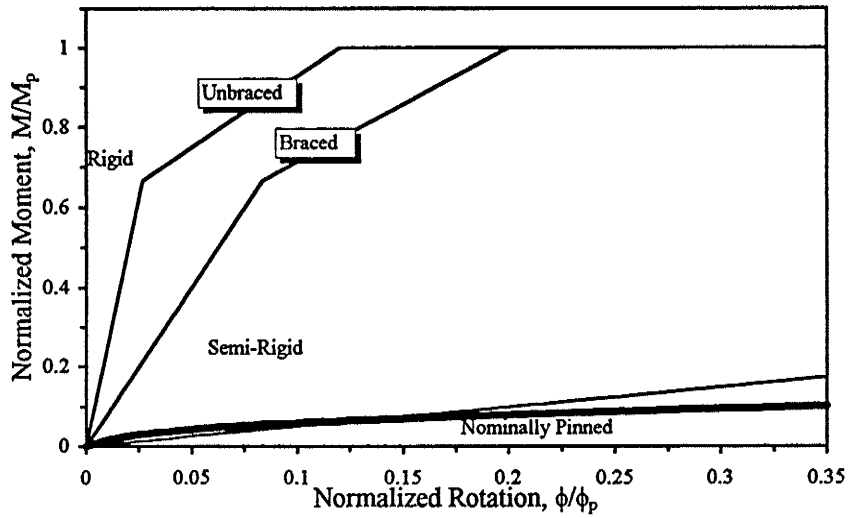


Figure A.125 (b) Eurocode3 Classification of Marley: D2-1/4-2

Table A.126 M-ϕ data for Marley: D3-1/4-1 (1982)

Moment, M kN-m	Rotation, ϕ radians	Moment, M kN-m	Rotation, ϕ radians
0	0	3.797	0.0182
0.163	0.0002	3.899	0.0193
0.325	0.0004	3.945	0.0204
0.488	0.0006	3.990	0.0216
0.632	0.0009	4.035	0.0227
0.776	0.0012	4.050	0.0237
0.921	0.0015	4.066	0.0247
1.102	0.0019	4.081	0.0257
1.284	0.0024	4.096	0.0269
1.466	0.0028	4.111	0.0280
1.670	0.0033	4.126	0.0292
1.875	0.0037		
2.080	0.0042		
2.232	0.0047		
2.384	0.0053		
2.535	0.0058		
2.672	0.0068		
2.808	0.0078		
2.929	0.0090		
3.050	0.0102		
3.171	0.0114		
3.270	0.0125		
3.368	0.0135		
3.467	0.0146		
3.581	0.0158		
3.695	0.0170		

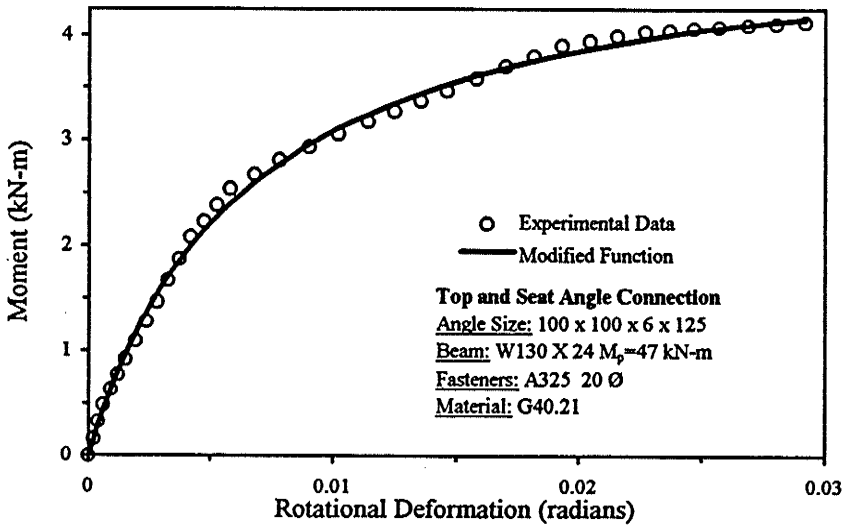


Figure A.126 (a) M-ϕ curve for Marley: D3-1/4-1

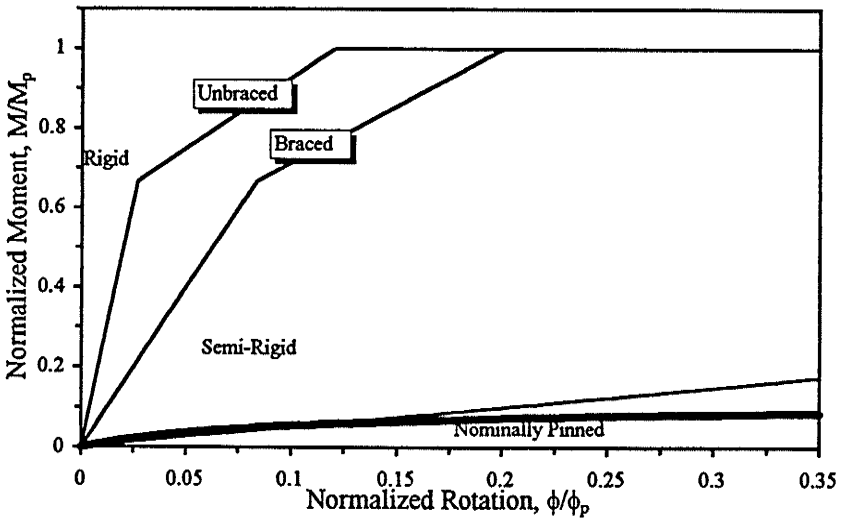


Figure A.126 (b) Eurocode3 Classification of Marley: D3-1/4-1

Table A.127 M-ϕ data for Marley: D3-1/4-2 (1982)

Moment, M kN-m	Rotation, ϕ radians	Moment, M kN-m	Rotation, ϕ radians
0	0	3.957	0.0283
0.168	0.0006	4.002	0.0303
0.335	0.0012	4.037	0.0326
0.503	0.0018	4.072	0.0348
0.678	0.0026	4.128	0.0368
0.854	0.0035	4.185	0.0387
1.029	0.0043	4.242	0.0405
1.181	0.0050	4.299	0.0422
1.334	0.0056	4.322	0.0438
1.486	0.0063	4.345	0.0453
1.669	0.0070	4.392	0.0477
1.852	0.0078	4.425	0.0491
2.035	0.0085	4.459	0.0504
2.196	0.0092		
2.356	0.0098		
2.516	0.0105		
2.710	0.0115		
2.904	0.0125		
3.087	0.0141		
3.270	0.0156		
3.373	0.0174		
3.476	0.0191		
3.579	0.0210		
3.682	0.0228		
3.797	0.0245		
3.912	0.0262		

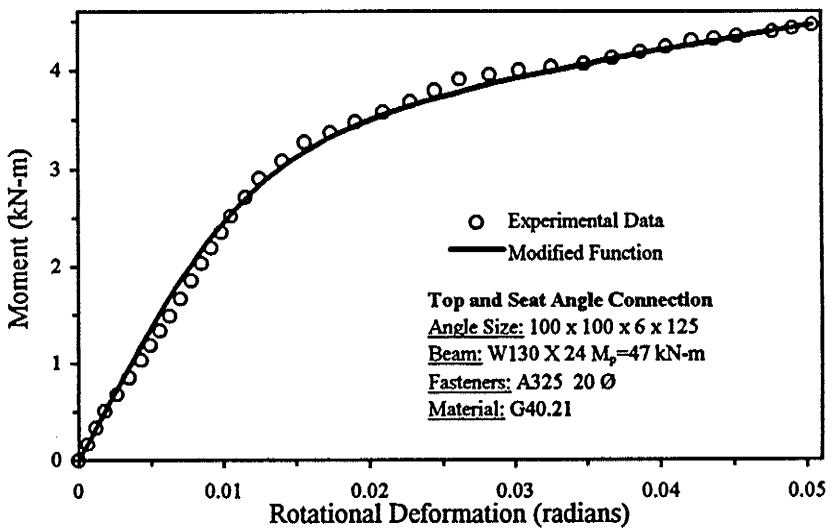


Figure A.127 (a) M-ϕ curve for Marley: D3-1/4-2

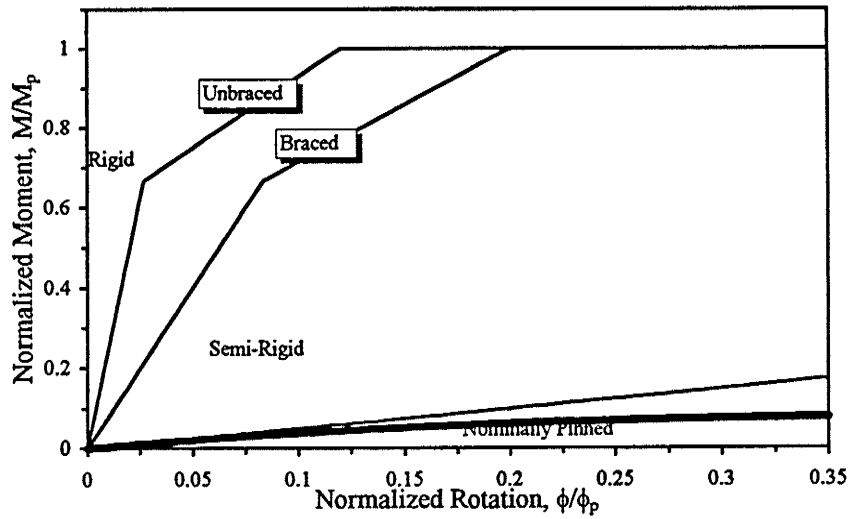


Figure A.127 (b) Eurocode3 Classification of Marley: D3-1/4-2

Table A.128 M-ϕ data for Marley: A-1/2-1 (1982)

Moment, M kN-m	Rotation, ϕ radians	Moment, M kN-m	Rotation, ϕ radians
0	0	18.332	0.0266
0.907	0.0005	18.605	0.0284
1.815	0.0009	18.816	0.0298
2.722	0.0014	19.028	0.0312
3.660	0.0019	19.239	0.0326
4.598	0.0023	19.466	0.0343
5.536	0.0028	19.693	0.0359
6.352	0.0033	19.920	0.0375
7.169	0.0039	20.146	0.0390
7.986	0.0044	20.282	0.0401
8.712	0.0051	20.419	0.0411
9.438	0.0058		
10.165	0.0065		
11.162	0.0077		
12.160	0.0088		
13.068	0.0102		
13.976	0.0116		
14.611	0.0131		
15.246	0.0145		
15.791	0.0159		
16.335	0.0172		
16.335	0.0172		
16.925	0.0190		
17.514	0.0207		
17.787	0.0227		
18.060	0.0247		

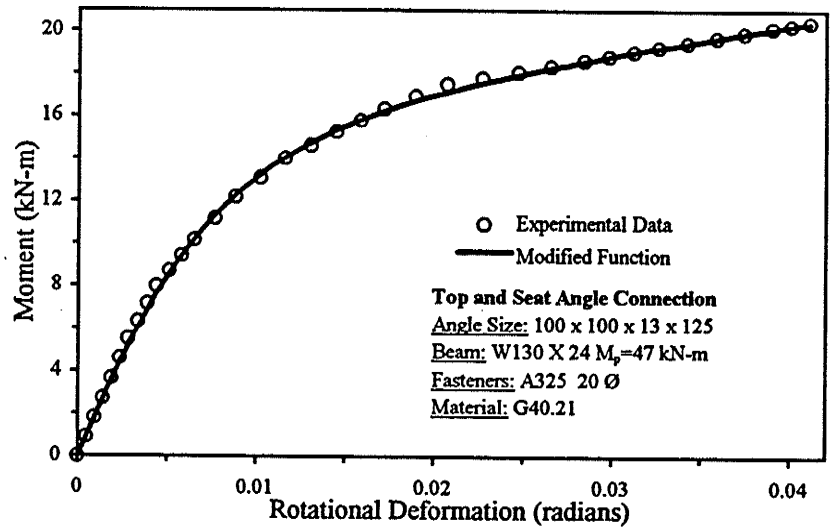


Figure A.128 (a) M-ϕ curve for Marley: A-1/2-1

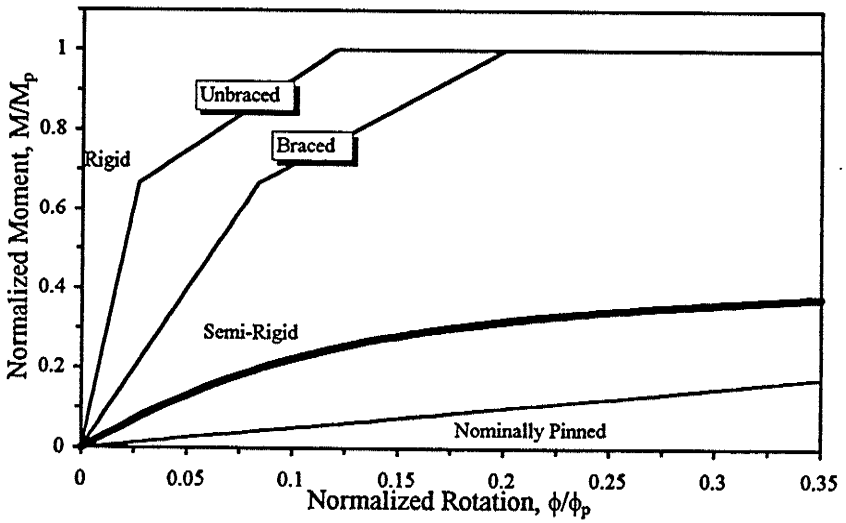


Figure A.128 (b) Eurocode3 Classification of Marley: A-1/2-1

Table A.129 M-ϕ data for Marley: B-1/2-1 (1982)

Moment, M kN-m	Rotation, ϕ radians	Moment, M kN-m	Rotation, ϕ radians
0	0	16.767	0.0206
0.693	0.0001	17.083	0.0222
1.386	0.0002	17.354	0.0237
2.078	0.0003	17.626	0.0251
2.078	0.0003	17.987	0.0268
3.028	0.0008	18.348	0.0284
3.977	0.0012	18.559	0.0298
4.610	0.0015	18.770	0.0312
5.243	0.0017	18.981	0.0326
6.147	0.0021	18.981	0.0324
7.050	0.0025	19.162	0.0338
7.818	0.0030	19.343	0.0352
8.586	0.0035	19.524	0.0366
9.445	0.0041	19.705	0.0382
10.304	0.0047	19.885	0.0397
10.982	0.0055	20.066	0.0413
11.660	0.0063		
12.474	0.0073		
13.287	0.0083		
13.875	0.0097		
14.463	0.0110		
14.884	0.0125		
15.306	0.0139		
15.728	0.0154		
16.089	0.0172		
16.450	0.0190		

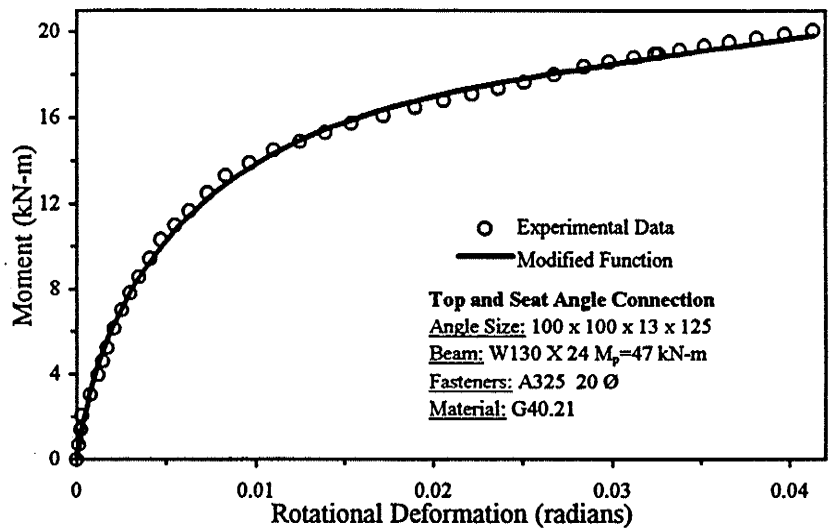


Figure A.129 (a) M-ϕ curve for Marley: B-1/2-1

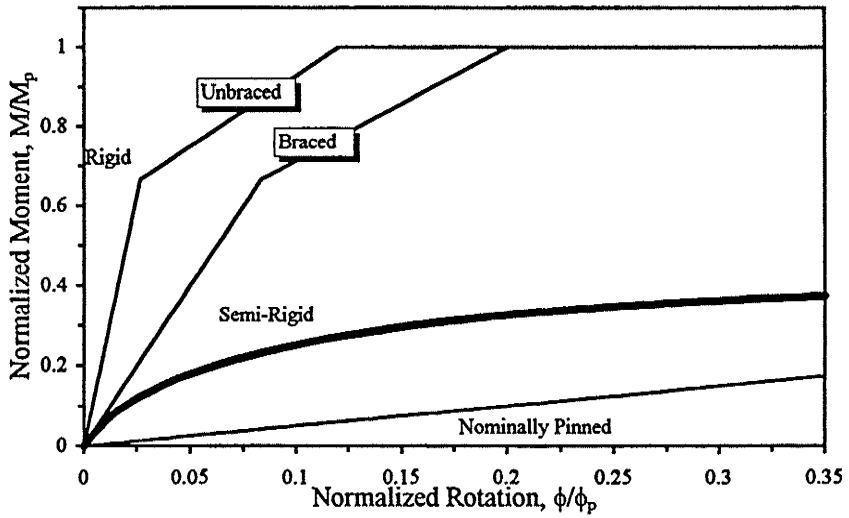


Figure A.129 (b) Eurocode3 Classification of Marley: B-1/2-1

Table A.130 M-ϕ data for Marley: B-1/2-2 (1982)

Moment, M kN-m	Rotation, ϕ radians	Moment, M kN-m	Rotation, ϕ radians
0	0	14.792	0.0131
0.771	0.0002	15.065	0.0140
1.543	0.0003	15.307	0.0147
2.329	0.0005	15.549	0.0155
3.116	0.0007	15.791	0.0162
3.902	0.0009	16.033	0.0170
4.477	0.0012	16.275	0.0177
5.052	0.0016	16.517	0.0185
5.627	0.0019	16.668	0.0193
6.202	0.0021	16.819	0.0202
6.776	0.0024	16.971	0.0210
7.351	0.0026		
8.123	0.0031		
8.894	0.0035		
9.484	0.0041		
10.074	0.0046		
10.664	0.0052		
11.253	0.0057		
11.889	0.0063		
12.524	0.0068		
12.932	0.0076		
13.340	0.0084		
13.643	0.0094		
13.946	0.0103		
14.248	0.0113		
14.520	0.0122		

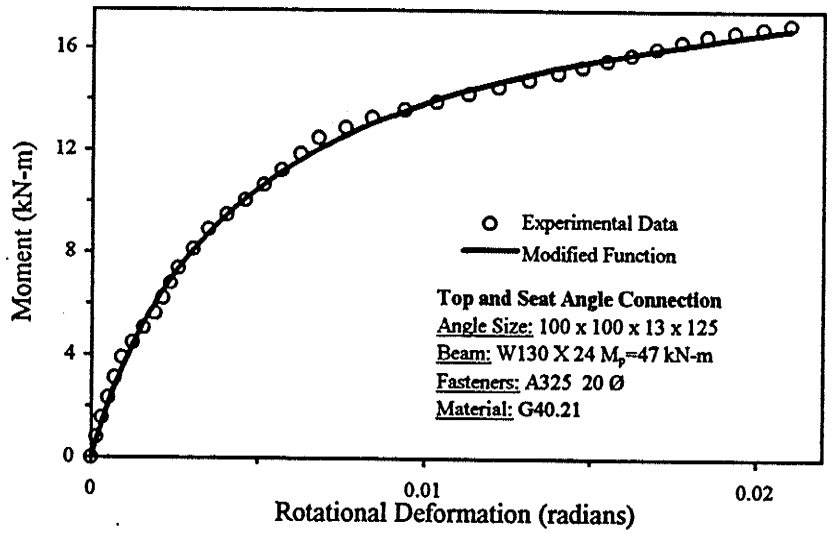


Figure A.130 (a) M-ϕ curve for Marley: B-1/2-2

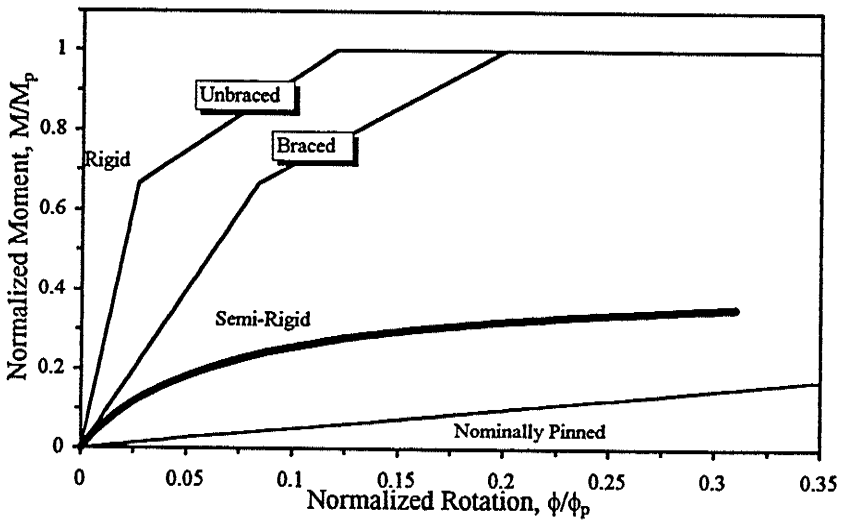


Figure A.130 (b) Eurocode3 Classification of Marley: B-1/2-2

Table A.131 M-ϕ data for Marley: C1-1/2-1 (1982)

Moment, M kN-m	Rotation, ϕ radians	Moment, M kN-m	Rotation, ϕ radians
0	0	18.785	0.0206
0.786	0.0002	19.027	0.0219
1.573	0.0004	19.269	0.0233
2.359	0.0006	19.512	0.0246
3.176	0.0008	19.693	0.0258
3.993	0.0009	19.875	0.0271
4.810	0.0011	20.057	0.0283
5.808	0.0016	20.268	0.0296
6.806	0.0020	20.480	0.0308
7.805	0.0027	20.691	0.0321
8.803	0.0033	20.843	0.0335
9.575	0.0042	20.994	0.0350
10.346	0.0051	21.145	0.0364
11.162	0.0061		
11.979	0.0071		
12.705	0.0080		
13.431	0.0088		
14.338	0.0097		
15.246	0.0106		
16.108	0.0117		
16.971	0.0128		
17.243	0.0140		
17.515	0.0153		
17.787	0.0165		
18.120	0.0179		
18.452	0.0192		

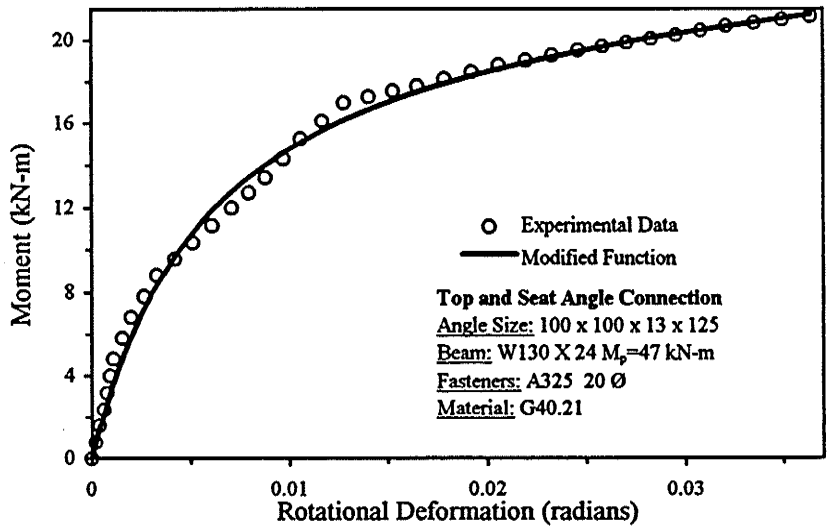


Figure A.131 (a) M-ϕ curve for Marley: C1-1/2-1

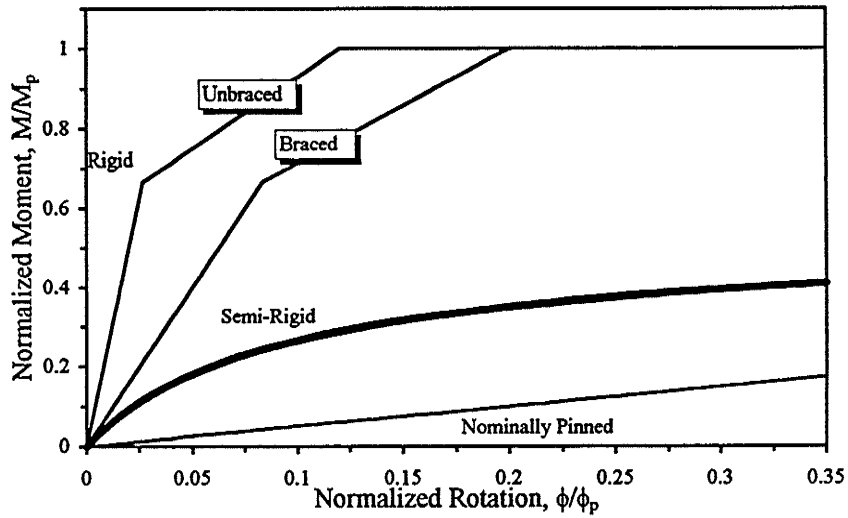


Figure A.131 (b) Eurocode3 Classification of Marley: C1-1/2-1

Table A.132 M-ϕ data for Marley: C1-1/2-2 (1982)

Moment, M kN-m	Rotation, ϕ radians	Moment, M kN-m	Rotation, ϕ radians
0	0	18.710	0.0234
0.994	0.0000	19.072	0.0250
1.989	0.0000	19.433	0.0266
3.028	0.0000	19.659	0.0283
4.067	0.0000	19.886	0.0299
4.881	0.0003	20.112	0.0315
5.694	0.0005	20.337	0.0330
6.508	0.0008	20.518	0.0346
7.547	0.0012	20.699	0.0362
8.586	0.0016	20.880	0.0373
9.400	0.0027	21.060	0.0384
10.213	0.0037		
10.847	0.0047		
11.480	0.0056		
12.112	0.0065		
12.745	0.0074		
13.694	0.0086		
14.643	0.0098		
15.185	0.0113		
15.728	0.0127		
16.270	0.0142		
16.812	0.0157		
17.264	0.0176		
17.716	0.0195		
18.048	0.0208		
18.379	0.0221		

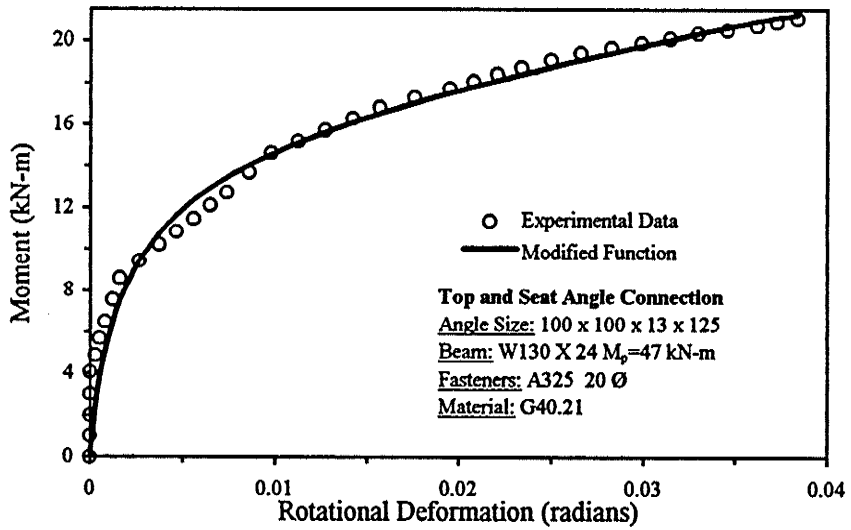


Figure A.132 (a) M-ϕ curve for Marley: C1-1/2-2

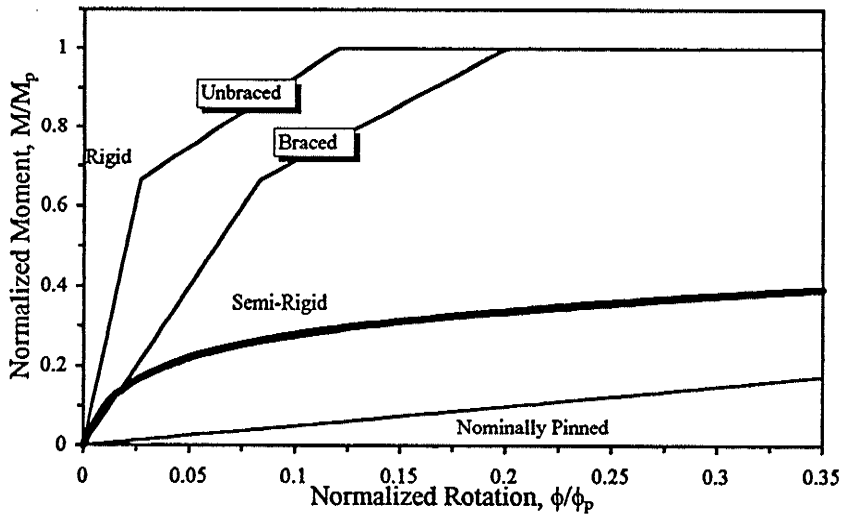


Figure A.132 (b) Eurocode3 Classification of Marley: C1-1/2-2

Table A.133 M-ϕ data for Marley: C2-1/2-1 (1982)

Moment, M kN-m	Rotation, ϕ radians	Moment, M kN-m	Rotation, ϕ radians
0	0	18.089	0.0238
0.817	0.0001	18.392	0.0251
1.634	0.0002	18.694	0.0265
2.420	0.0003	18.936	0.0278
3.207	0.0005	19.179	0.0291
3.993	0.0006	19.421	0.0304
4.946	0.0011	19.739	0.0322
5.899	0.0016	20.057	0.0339
6.655	0.0021	20.208	0.0352
7.411	0.0025	20.359	0.0366
8.167	0.0030	20.509	0.0379
9.014	0.0037		
9.861	0.0043		
10.708	0.0050		
11.707	0.0060		
12.705	0.0069		
13.341	0.0077		
13.976	0.0084		
14.520	0.0101		
15.065	0.0117		
15.609	0.0134		
16.153	0.0150		
16.517	0.0169		
16.880	0.0187		
17.333	0.0206		
17.787	0.0224		

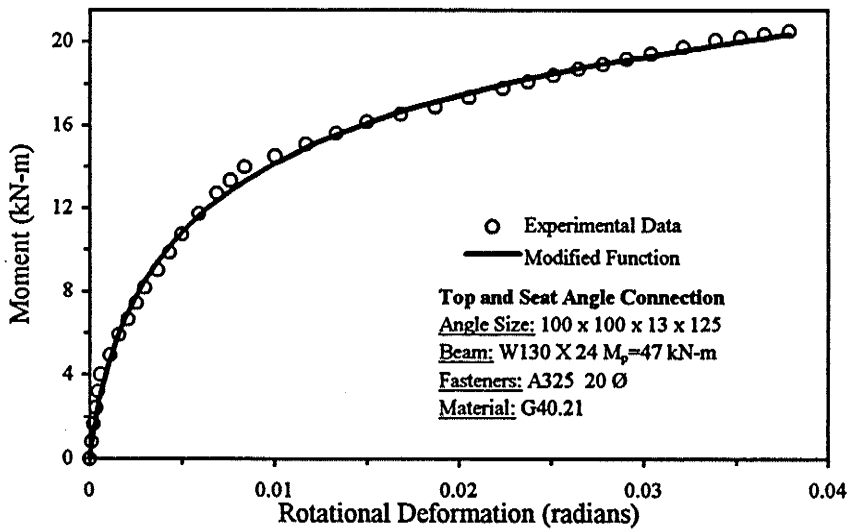


Figure A.133 (a) M-ϕ curve for Marley: C2-1/2-1

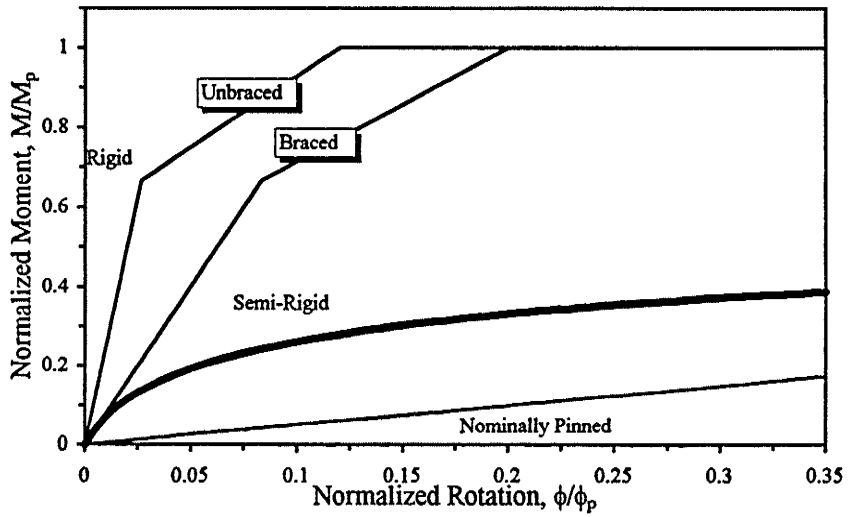


Figure A.133 (b) Eurocode3 Classification of Marley: C2-1/2-1

Table A.134 M-ϕ data for Marley: C2-1/2-2 (1982)

Moment, M kN-m	Rotation, ϕ radians	Moment, M kN-m	Rotation, ϕ radians
0	0	17.768	0.0250
1.002	0.0004	18.132	0.0266
2.004	0.0008	18.496	0.0281
2.961	0.0014	18.709	0.0295
3.918	0.0019	18.922	0.0310
4.875	0.0025	19.135	0.0324
5.831	0.0031	19.408	0.0341
6.652	0.0036	19.681	0.0358
7.472	0.0041	19.833	0.0373
8.201	0.0048	19.985	0.0388
8.929	0.0054	20.137	0.0403
9.613	0.0059		
10.296	0.0063		
11.025	0.0073		
11.754	0.0082		
12.392	0.0092		
13.029	0.0102		
13.758	0.0116		
14.487	0.0130		
14.897	0.0142		
15.307	0.0154		
15.717	0.0168		
16.127	0.0181		
16.583	0.0196		
17.039	0.0211		
17.403	0.0231		

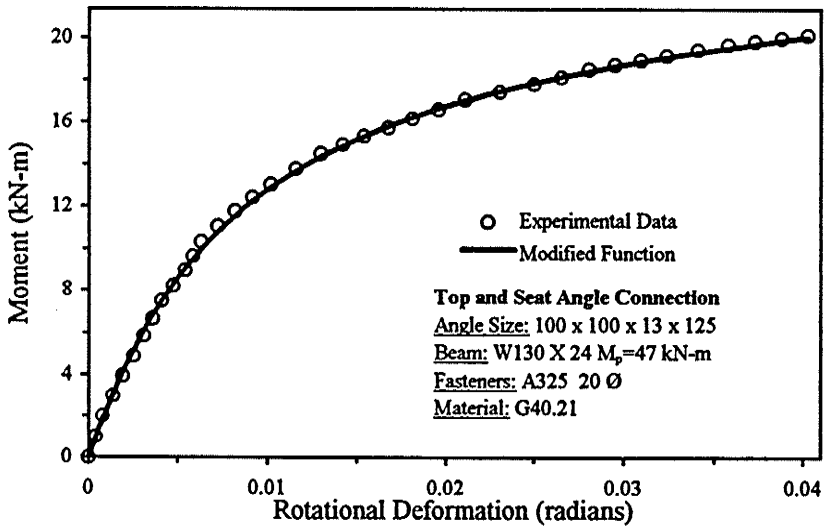


Figure A.134 (a) M-ϕ curve for Marley: C2-1/2-2

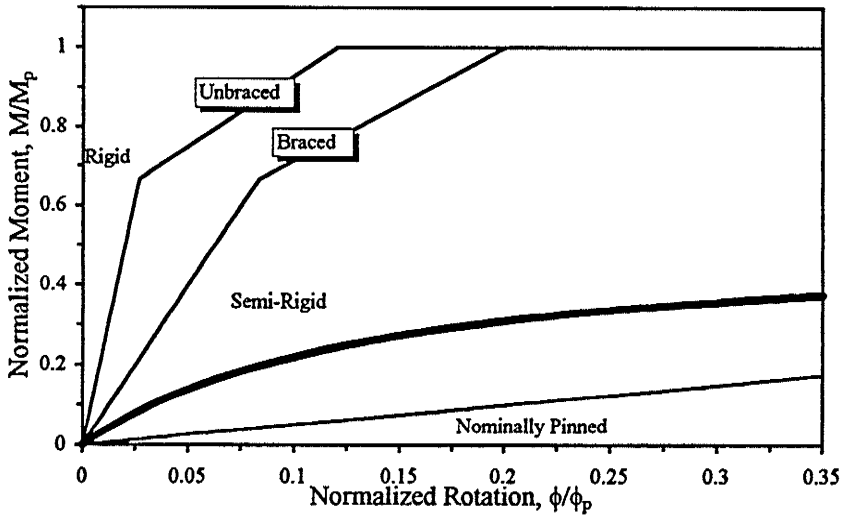


Figure A.134 (b) Eurocode3 Classification of Marley: C2-1/2-2

Table A.135 M-ϕ data for Marley: D1-1/2-1 (1982)

Moment, M kN-m	Rotation, ϕ radians	Moment, M kN-m	Rotation, ϕ radians
0	0	19.557	0.0234
0.908	0.0003	19.875	0.0252
1.815	0.0005	20.147	0.0269
2.662	0.0007	20.419	0.0285
3.509	0.0008	20.691	0.0299
4.356	0.0010	20.964	0.0312
5.445	0.0015	21.191	0.0328
6.534	0.0019	21.418	0.0343
7.487	0.0024	21.644	0.0358
8.440	0.0029	21.871	0.0373
9.302	0.0034	22.052	0.0389
10.165	0.0038	22.234	0.0405
11.072	0.0042		
11.979	0.0046		
12.705	0.0054		
13.431	0.0062		
14.202	0.0071		
14.974	0.0080		
15.563	0.0095		
16.153	0.0110		
16.653	0.0126		
17.152	0.0142		
17.697	0.0162		
18.241	0.0181		
18.740	0.0198		
19.239	0.0215		

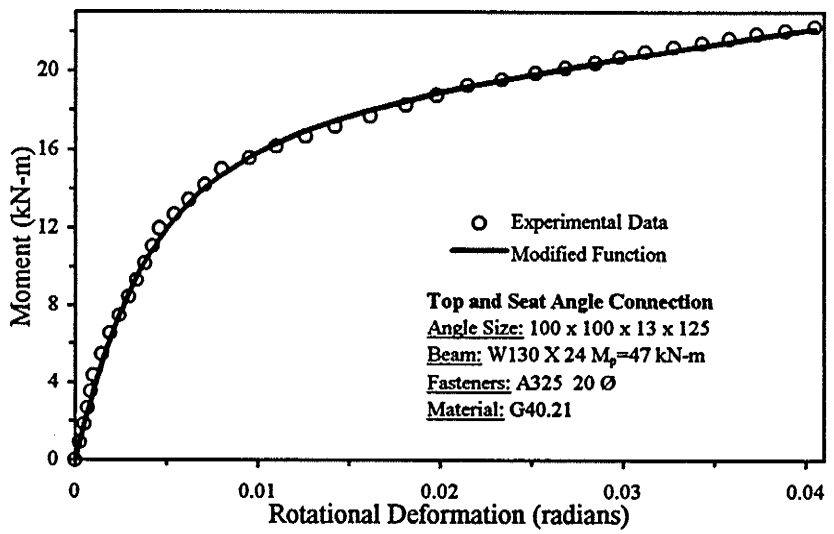


Figure A.135 (a) M-ϕ curve for Marley: D1-1/2-1

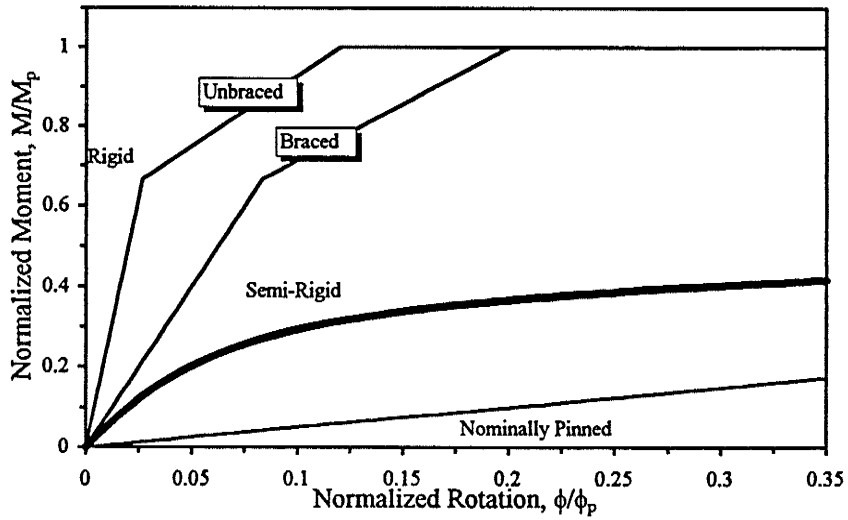


Figure A.135 (b) Eurocode3 Classification of Marley: D1-1/2-1

Table A.136 M-ϕ data for Marley: D1-1/2-2 (1982)

Moment, M kN-m	Rotation, ϕ radians	Moment, M kN-m	Rotation, ϕ radians
0	0	19.421	0.0212
0.877	0.0001	19.874	0.0233
1.754	0.0003	20.328	0.0253
2.632	0.0004	20.691	0.0273
3.221	0.0005	21.055	0.0293
3.811	0.0005	21.372	0.0309
4.810	0.0010	21.689	0.0324
5.808	0.0014	21.916	0.0340
6.625	0.0018	22.143	0.0355
7.442	0.0022	22.280	0.0366
8.349	0.0025	22.416	0.0376
9.256	0.0027	22.733	0.0397
10.073	0.0032	23.050	0.0417
10.890	0.0036		
11.798	0.0042		
12.705	0.0048		
13.749	0.0057		
14.792	0.0066		
15.473	0.0081		
16.153	0.0095		
16.653	0.0112		
17.152	0.0128		
17.606	0.0142		
18.060	0.0156		
18.513	0.0175		
18.967	0.0193		

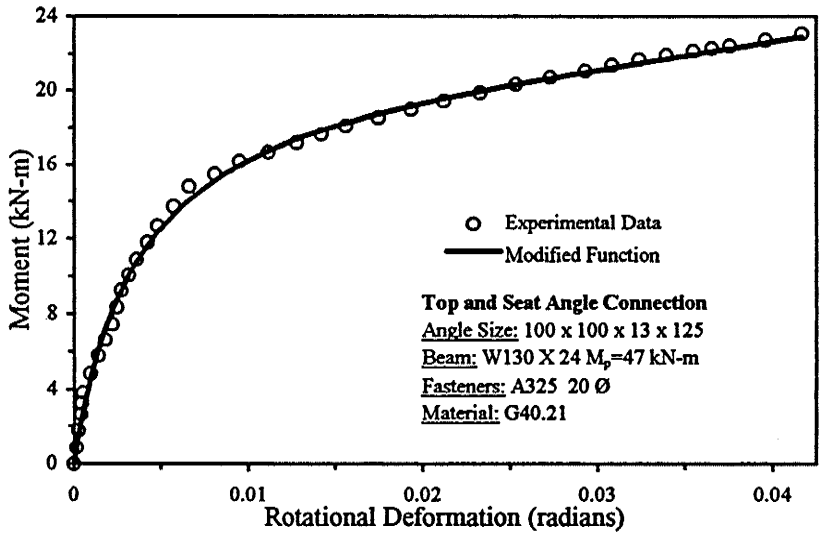


Figure A.136 (a) M-ϕ curve for Marley: D1-1/2-2

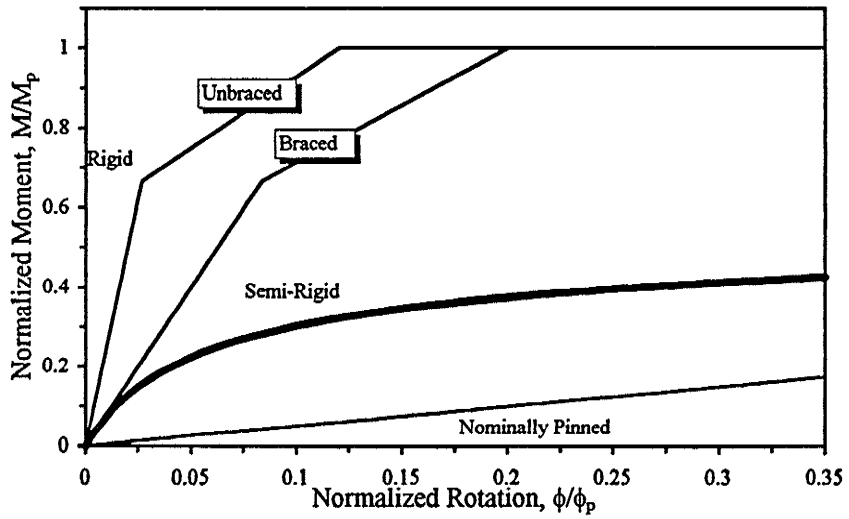


Figure A.136 (b) Eurocode3 Classification of Marley: D1-1/2-2

Table A.137 M-ϕ data for Marley: D2-1/2-1 (1982)

Moment, M kN-m	Rotation, ϕ radians	Moment, M kN-m	Rotation, ϕ radians
0	0	18.709	0.0228
1.098	0.0001	19.121	0.0246
2.195	0.0002	19.441	0.0262
3.247	0.0003	19.761	0.0278
4.299	0.0003	20.036	0.0292
5.062	0.0004	20.310	0.0306
5.824	0.0004	20.585	0.0326
6.587	0.0005	20.859	0.0345
7.502	0.0006	21.042	0.0364
8.417	0.0007	21.225	0.0382
9.378	0.0011	21.408	0.0399
10.338	0.0014	21.590	0.0415
11.024	0.0018	21.682	0.0433
11.710	0.0021	21.773	0.0451
12.396	0.0025	21.911	0.0468
13.082	0.0028	22.048	0.0484
13.814	0.0045		
14.272	0.0058		
14.730	0.0071		
15.370	0.0094		
15.873	0.0112		
16.376	0.0129		
16.925	0.0148		
17.474	0.0166		
17.885	0.0188		
18.297	0.0209		

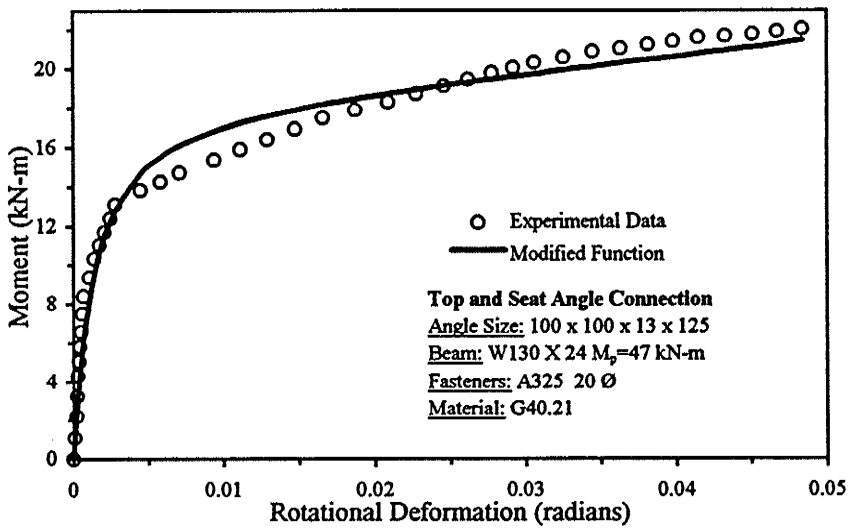


Figure A.137 (a) M-ϕ curve for Marley: D2-1/2-1

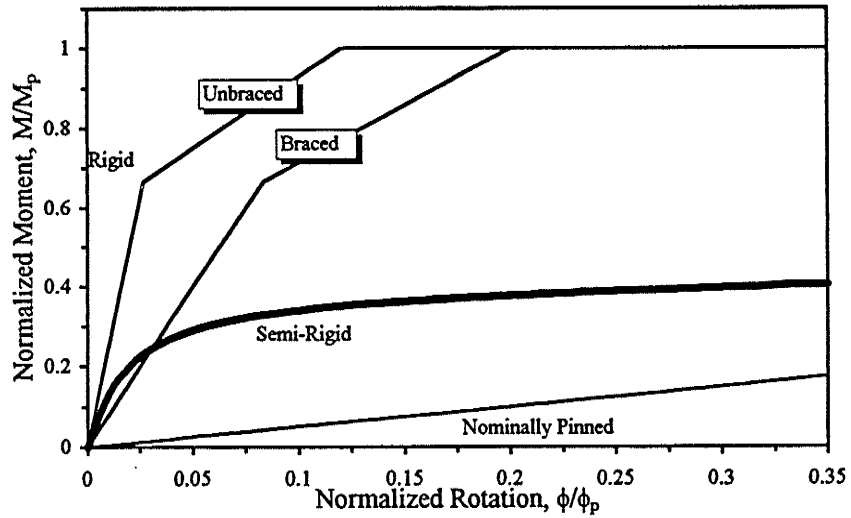


Figure A.137 (b) Eurocode3 Classification of Marley: D2-1/2-1

Table A.138 M-ϕ data for Marley: D2-1/2-2 (1982)

Moment, M kN-m	Rotation, ϕ radians	Moment, M kN-m	Rotation, ϕ radians
0	0	18.823	0.0171
0.803	0.0002	19.232	0.0181
1.606	0.0005	19.551	0.0196
2.409	0.0007	19.870	0.0211
3.364	0.0011	20.006	0.0230
4.320	0.0015	20.142	0.0248
5.047	0.0018	20.415	0.0267
5.774	0.0022	20.687	0.0285
6.501	0.0025	20.823	0.0298
7.502	0.0029	20.960	0.0311
8.502	0.0033	21.097	0.0330
9.321	0.0037	21.233	0.0348
10.139	0.0040	21.324	0.0361
10.912	0.0046	21.415	0.0374
11.684	0.0051		
12.321	0.0058		
12.958	0.0064		
13.685	0.0075		
14.412	0.0085		
15.413	0.0102		
15.959	0.0111		
16.504	0.0120		
16.914	0.0130		
17.323	0.0139		
17.868	0.0150		
18.413	0.0160		

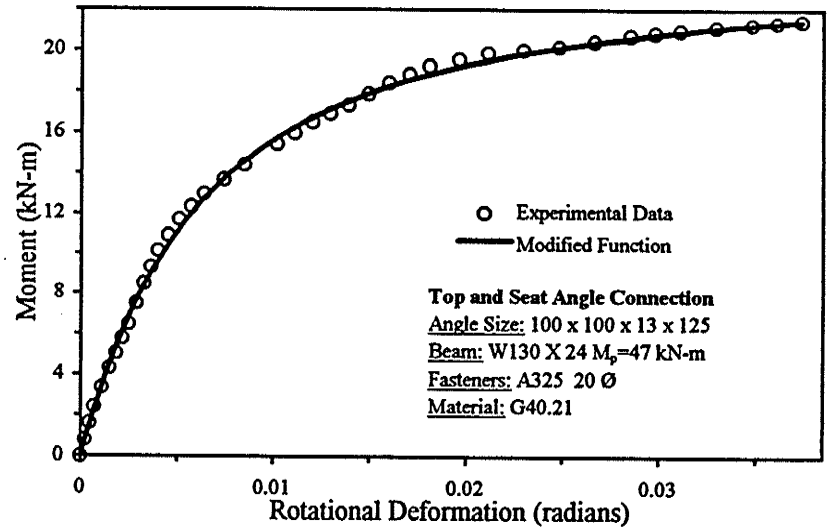


Figure A.138 (a) M-ϕ curve for Marley: D2-1/2-2

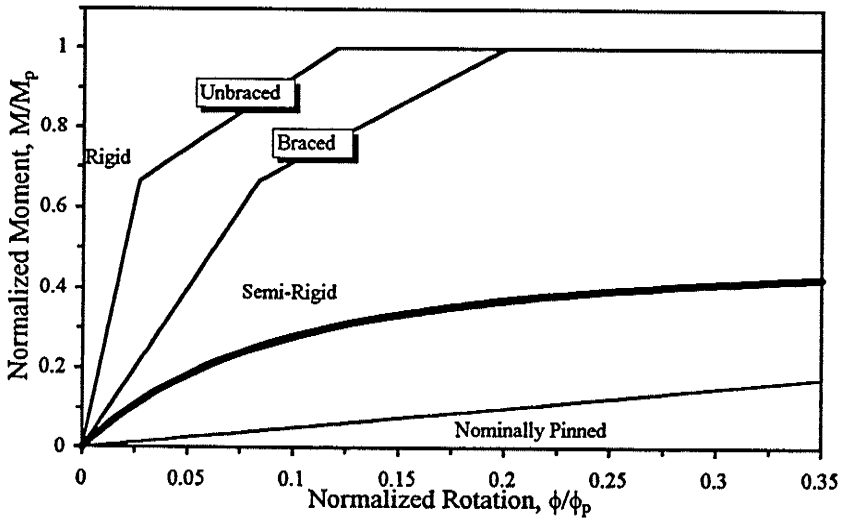


Figure A.138 (b) Eurocode3 Classification of Marley: D2-1/2-2

Table A.139 M-ϕ data for Marley: D3-1/2-1 (1982)

Moment, M kN-m	Rotation, ϕ radians	Moment, M kN-m	Rotation, ϕ radians
0	0	16.971	0.0167
0.862	0.0002	17.514	0.0189
1.725	0.0003	17.878	0.0207
2.632	0.0006	18.150	0.0219
3.539	0.0008	18.423	0.0230
4.356	0.0012	18.695	0.0247
5.172	0.0016	18.967	0.0263
5.762	0.0020	19.239	0.0277
6.352	0.0023	19.512	0.0290
7.033	0.0026	19.739	0.0304
7.713	0.0029	19.966	0.0318
8.576	0.0034	20.192	0.0333
9.438	0.0038	20.419	0.0347
10.209	0.0042	20.555	0.0361
10.981	0.0046	20.691	0.0375
11.661	0.0053	20.918	0.0388
12.342	0.0060	21.145	0.0401
13.023	0.0066	21.326	0.0421
13.703	0.0072	21.507	0.0440
14.248	0.0081		
14.792	0.0090		
15.155	0.0102		
15.519	0.0113		
15.927	0.0126		
16.335	0.0139		
16.653	0.0153		

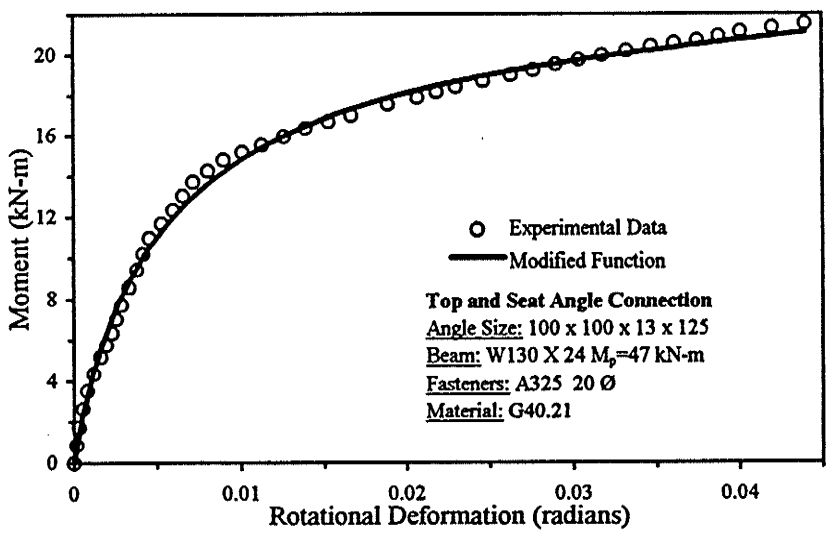


Figure A.139 (a) M-ϕ curve for Marley: D3-1/2-1

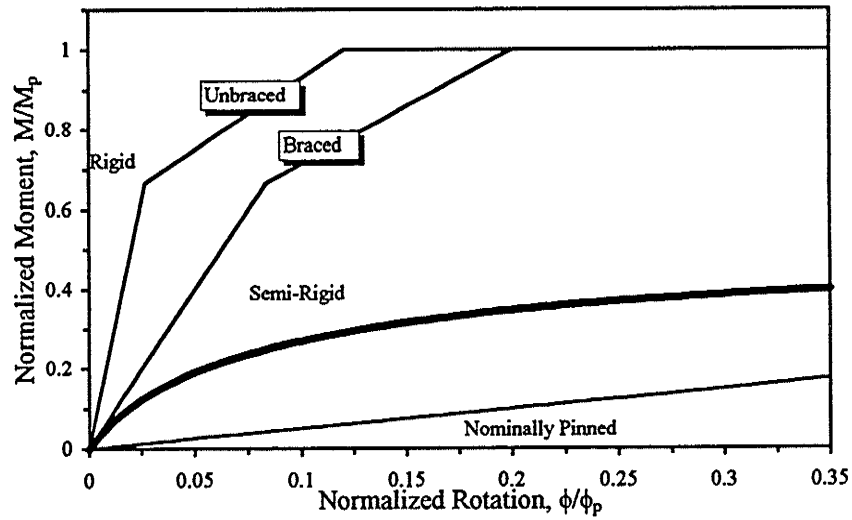


Figure A.139 (b) Eurocode3 Classification of Marley: D3-1/2-1

Table A.140 M-ϕ data for Marley: D3-1/2-2 (1982)

Moment, M kN-m	Rotation, ϕ radians	Moment, M kN-m	Rotation, ϕ radians
0	0	17.969	0.0207
0.908	0.0003	18.332	0.0220
1.815	0.0006	18.649	0.0234
2.632	0.0009	18.967	0.0248
3.449	0.0011	19.330	0.0262
4.220	0.0015	19.693	0.0275
4.991	0.0018	20.011	0.0291
5.944	0.0023	20.328	0.0307
6.897	0.0027	20.509	0.0323
6.897	0.0027	20.691	0.0338
7.669	0.0032	20.873	0.0351
8.440	0.0036	21.055	0.0364
9.166	0.0042	21.236	0.0381
9.892	0.0047	21.418	0.0397
10.617	0.0053	21.508	0.0412
11.389	0.0060	21.598	0.0427
12.160	0.0066		
13.069	0.0082		
13.477	0.0093		
13.885	0.0104		
14.656	0.0117		
15.428	0.0130		
15.927	0.0145		
16.426	0.0160		
17.016	0.0177		
17.605	0.0193		

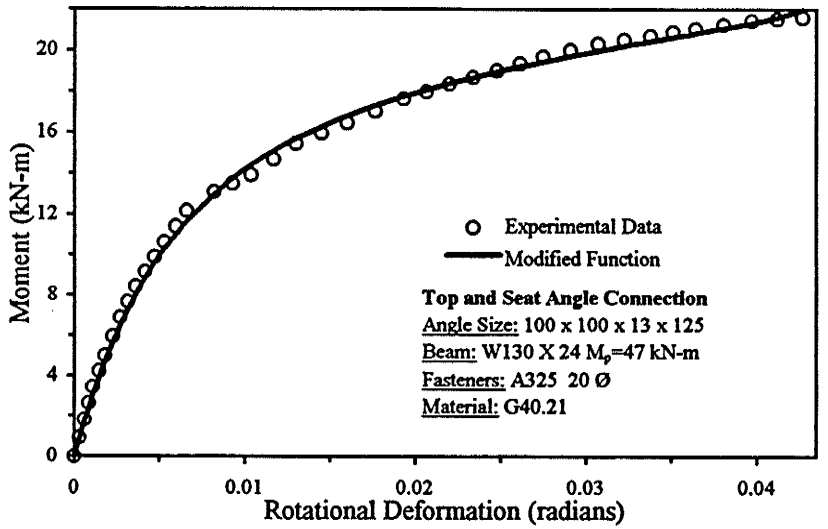


Figure A.140 (a) M-ϕ curve for Marley: D3-1/2-2

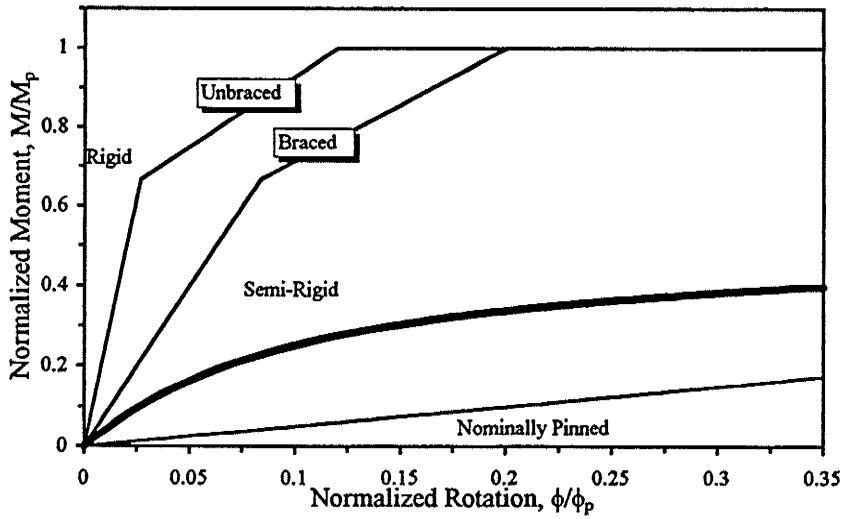


Figure A.140 (b) Eurocode3 Classification of Marley: D3-1/2-2

Table A.141 M-ϕ data for Maxwell: A1 (1981)

Moment, M kN-m	Rotation, ϕ radians	Moment, M kN-m	Rotation, ϕ radians
0	0	55.366	0.0074
2.505	0.0001	56.504	0.0077
5.010	0.0002	57.783	0.0081
7.516	0.0002	59.062	0.0084
10.021	0.0003	60.341	0.0088
12.900	0.0005	61.620	0.0093
15.778	0.0006	62.899	0.0097
18.657	0.0008		
21.536	0.0009		
23.810	0.0011		
26.084	0.0014		
28.358	0.0016		
31.130	0.0021		
33.902	0.0025		
35.821	0.0029		
37.739	0.0033		
39.658	0.0037		
41.578	0.0040		
42.999	0.0043		
44.420	0.0047		
45.842	0.0050		
47.548	0.0054		
49.254	0.0058		
51.173	0.0063		
53.091	0.0067		
54.229	0.0070		

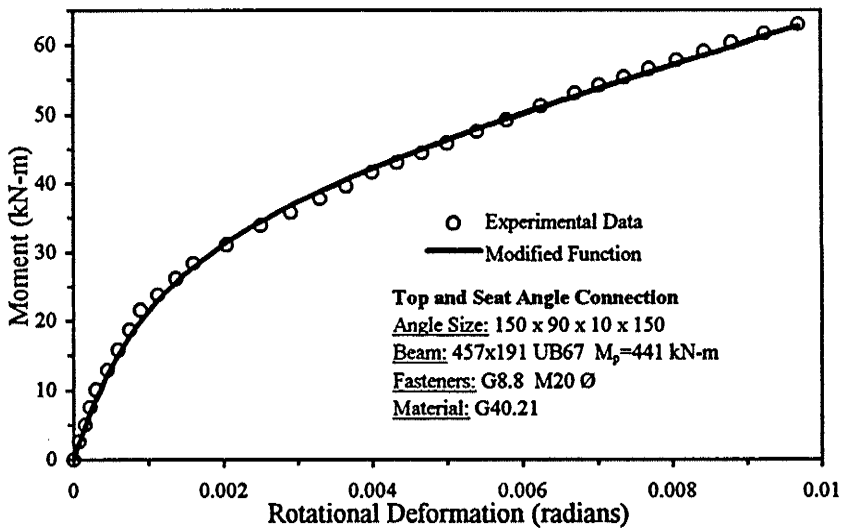


Figure A.141 (a) M-ϕ curve for Maxwell: A1

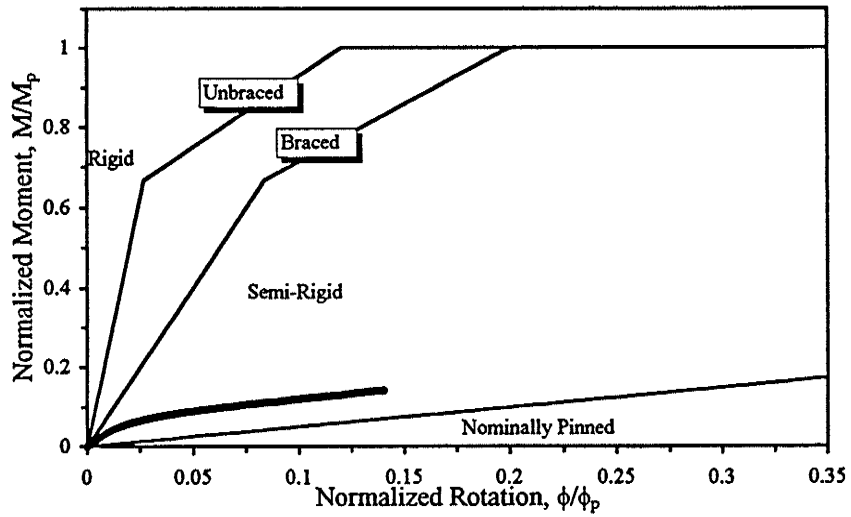


Figure A.141 (b) Eurocode3 Classification of Maxwell: A1

Table A.142 M-ϕ data for Maxwell: A2 (1981)

Moment, M kN-m	Rotation, ϕ radians	Moment, M kN-m	Rotation, ϕ radians
0	0	80.485	0.0074
3.277	0.0001	82.052	0.0078
6.553	0.0003	83.334	0.0081
9.830	0.0004	84.616	0.0085
13.391	0.0006	85.898	0.0088
16.951	0.0008	86.753	0.0091
20.512	0.0010	87.607	0.0095
24.786	0.0013	88.462	0.0098
29.059	0.0015		
33.333	0.0018		
37.179	0.0021		
41.026	0.0024		
44.872	0.0027		
48.148	0.0030		
51.424	0.0033		
54.701	0.0036		
57.550	0.0039		
60.399	0.0043		
63.248	0.0046		
65.954	0.0050		
68.661	0.0053		
71.368	0.0057		
73.362	0.0060		
75.356	0.0064		
77.351	0.0067		
78.918	0.0071		

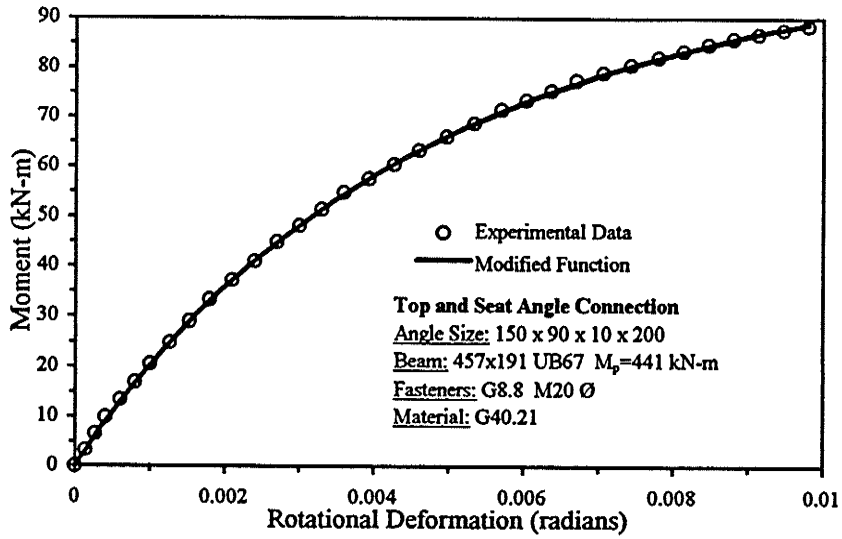


Figure A.142 (a) M-ϕ curve for Maxwell: A2

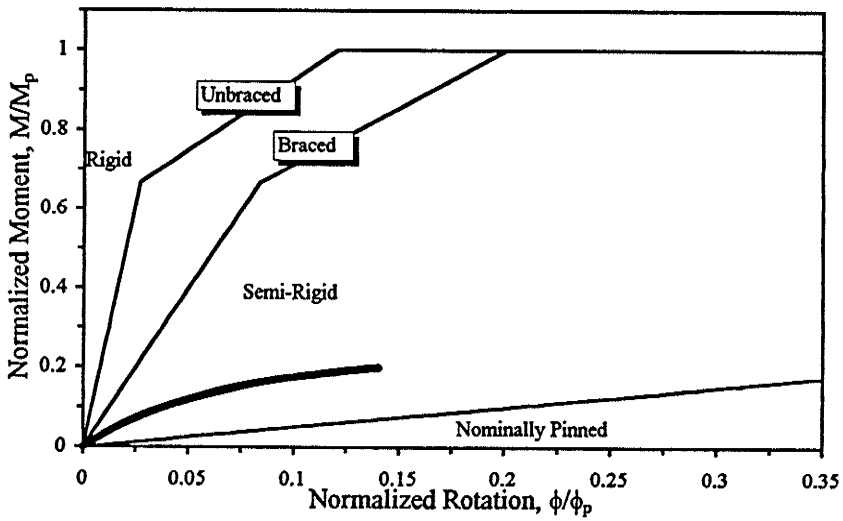


Figure A.142 (b) Eurocode3 Classification of Maxwell: A2

Table A.143 M-ϕ data for Maxwell: A3 (1981)

Moment, M kN-m	Rotation, ϕ radians	Moment, M kN-m	Rotation, ϕ radians
0	0	77.110	0.0086
3.326	0.0002	78.112	0.0089
6.652	0.0004	78.756	0.0093
9.978	0.0005	79.400	0.0097
13.305	0.0007		
17.167	0.0010		
21.030	0.0012		
24.177	0.0015		
27.325	0.0017		
30.472	0.0020		
34.335	0.0023		
38.198	0.0026		
41.845	0.0030		
45.493	0.0034		
49.356	0.0038		
53.219	0.0042		
57.081	0.0047		
60.944	0.0051		
63.090	0.0054		
65.236	0.0058		
67.382	0.0061		
69.742	0.0066		
72.103	0.0070		
73.605	0.0075		
75.107	0.0079		
76.109	0.0082		

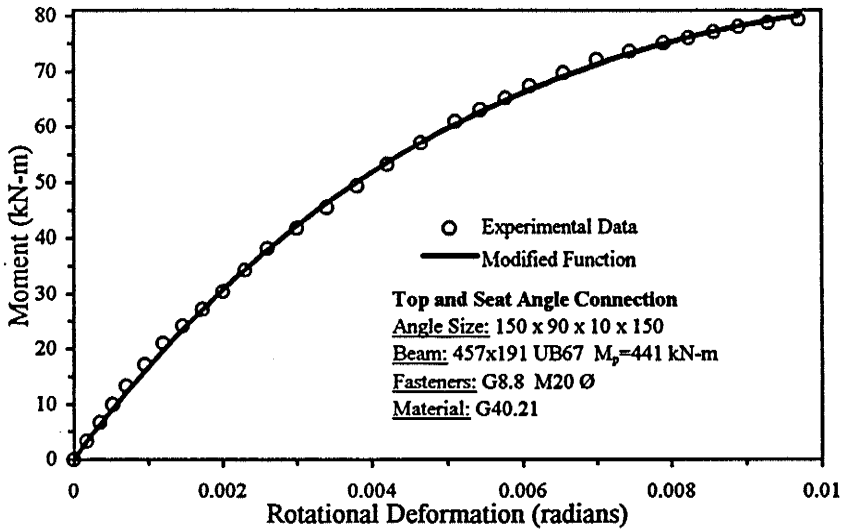


Figure A.143 (a) M-ϕ curve for Maxwell: A3

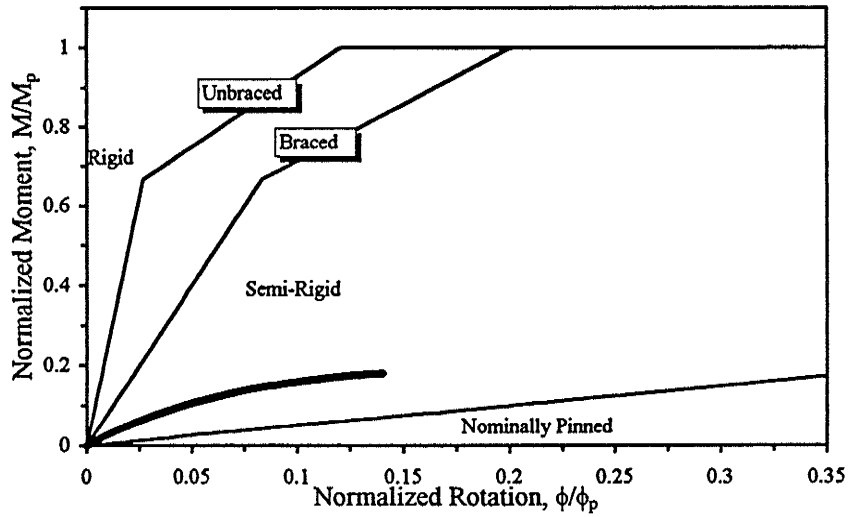


Figure A.143 (b) Eurocode3 Classification of Maxwell: A3

Table A.144 M-ϕ data for Maxwell: A4 (1981)

Moment, M kN-m	Rotation, ϕ radians	Moment, M kN-m	Rotation, ϕ radians
0	0	95.015	0.0081
4.843	0.0002	96.867	0.0085
9.687	0.0004	98.719	0.0088
14.530	0.0006	100.428	0.0093
19.373	0.0009	102.137	0.0097
24.216	0.0012		
29.059	0.0015		
33.333	0.0018		
37.606	0.0020		
41.880	0.0023		
45.299	0.0026		
48.718	0.0028		
52.137	0.0031		
56.624	0.0035		
61.111	0.0039		
66.026	0.0044		
70.941	0.0048		
73.932	0.0051		
76.923	0.0055		
79.915	0.0058		
82.194	0.0061		
84.473	0.0065		
86.752	0.0068		
88.889	0.0071		
91.026	0.0075		
93.162	0.0078		

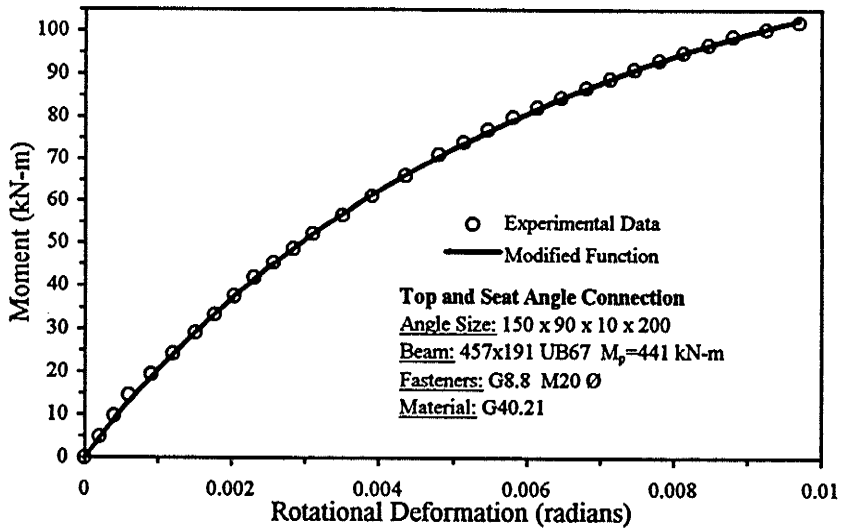


Figure A.144 (a) M-ϕ curve for Maxwell: A4

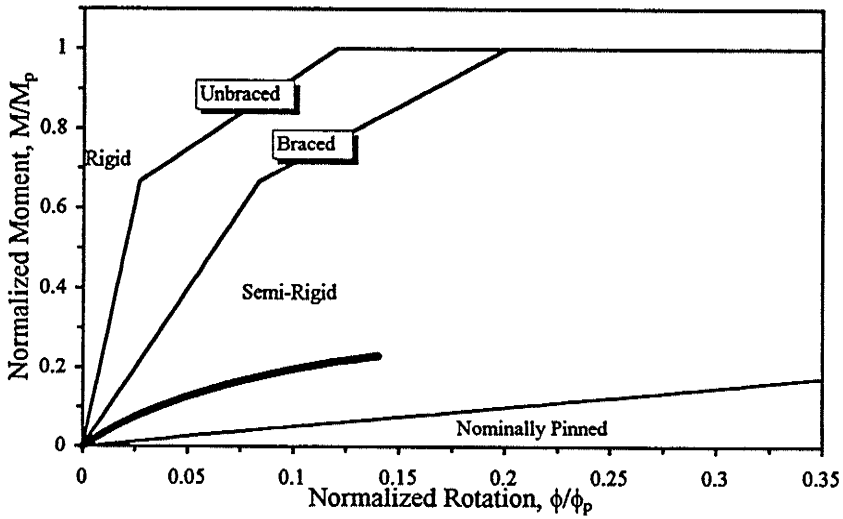


Figure A.144 (b) Eurocode3 Classification of Maxwell: A4

Table A.145 M-ϕ data for Maxwell: B1 (1981)

Moment, M kN-m	Rotation, ϕ radians	Moment, M kN-m	Rotation, ϕ radians
0	0	86.164	0.0092
4.123	0.0002	87.841	0.0095
8.246	0.0004	89.518	0.0098
12.369	0.0006		
16.562	0.0009		
20.754	0.0011		
24.947	0.0014		
28.721	0.0017		
32.494	0.0020		
36.268	0.0023		
39.902	0.0026		
43.536	0.0030		
47.170	0.0033		
51.363	0.0038		
55.556	0.0042		
59.120	0.0047		
62.684	0.0051		
65.618	0.0056		
68.553	0.0060		
71.279	0.0065		
74.005	0.0069		
76.310	0.0073		
78.616	0.0077		
80.922	0.0081		
83.228	0.0084		
84.696	0.0088		

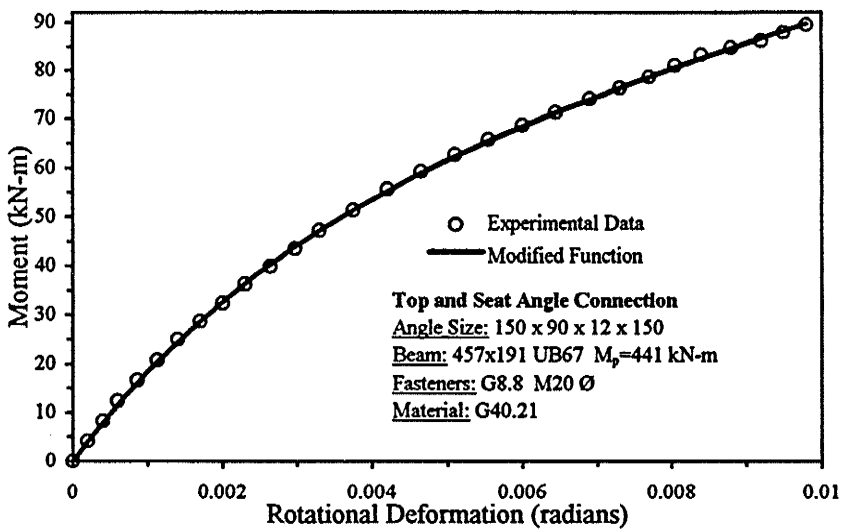


Figure A.145 (a) M-ϕ curve for Maxwell: B1

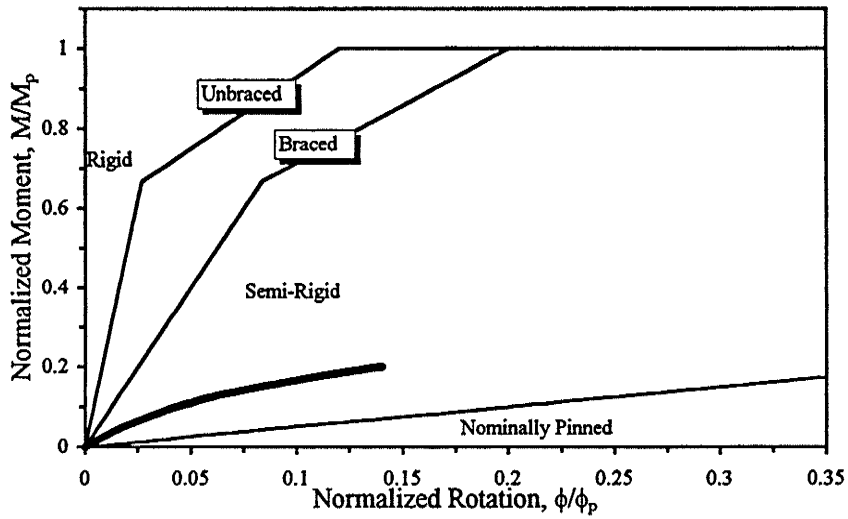


Figure A.145 (b) Eurocode3 Classification of Maxwell: B1

Table A.146 M-ϕ data for Maxwell: B2 (1981)

Moment, M kN-m	Rotation, ϕ radians	Moment, M kN-m	Rotation, ϕ radians
0	0	91.195	0.0083
3.878	0.0003	92.872	0.0087
7.757	0.0005	94.549	0.0090
11.530	0.0007	96.227	0.0093
15.304	0.0009	97.904	0.0097
19.078	0.0011	99.581	0.0100
23.900	0.0014		
28.722	0.0017		
33.543	0.0021		
38.364	0.0024		
41.719	0.0027		
45.073	0.0029		
48.637	0.0033		
52.202	0.0036		
55.975	0.0039		
59.748	0.0042		
63.103	0.0046		
66.457	0.0049		
70.021	0.0053		
73.584	0.0057		
76.100	0.0061		
78.616	0.0065		
81.761	0.0069		
84.906	0.0073		
87.212	0.0077		
89.518	0.0080		

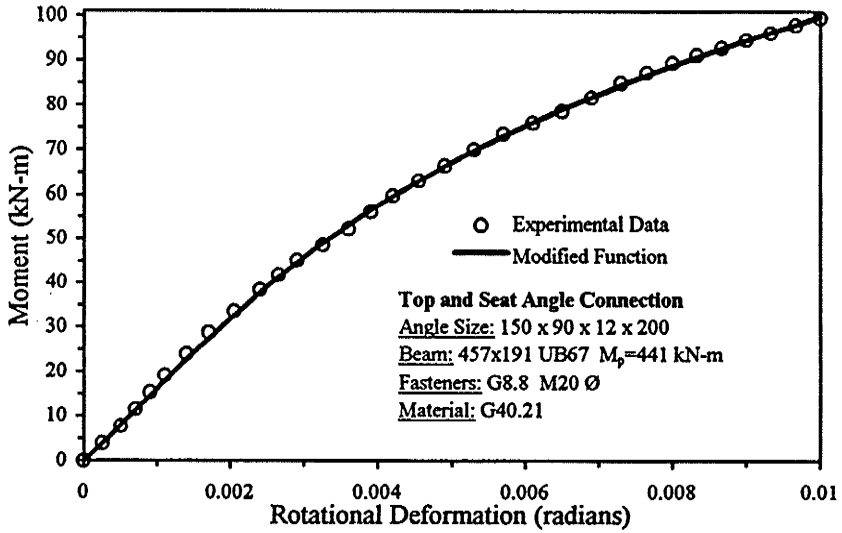


Figure A.146 (a) M-ϕ curve for Maxwell: B2

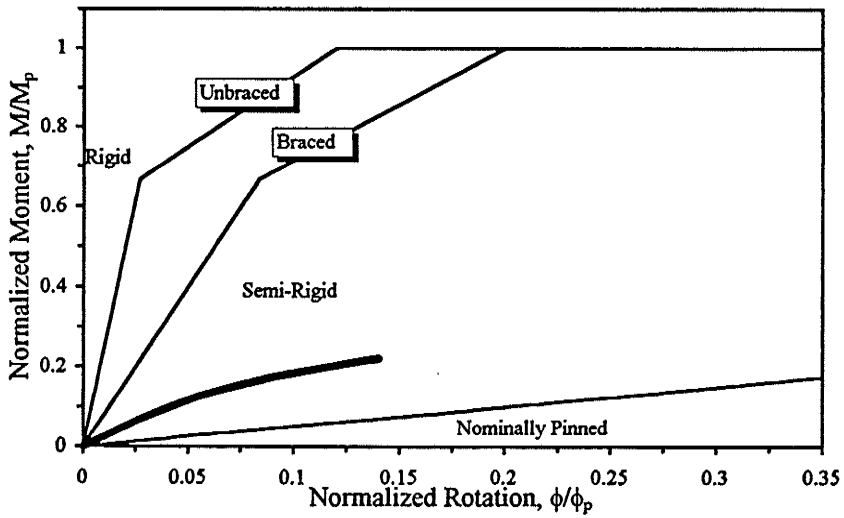


Figure A.146 (b) Eurocode3 Classification of Maxwell: B2

Table A.147 M-ϕ data for Maxwell: B3 (1981)

Moment, M kN-m	Rotation, ϕ radians	Moment, M kN-m	Rotation, ϕ radians
0	0	92.017	0.0083
4.622	0.0003	94.118	0.0087
8.964	0.0005	95.379	0.0091
13.306	0.0008	96.639	0.0094
17.647	0.0010	97.900	0.0098
22.129	0.0013		
26.611	0.0015		
31.093	0.0018		
35.295	0.0021		
39.496	0.0023		
43.698	0.0026		
47.339	0.0028		
50.981	0.0031		
54.622	0.0033		
58.613	0.0037		
62.605	0.0040		
66.386	0.0044		
70.168	0.0047		
73.109	0.0051		
76.051	0.0054		
78.782	0.0058		
81.513	0.0062		
83.614	0.0066		
85.715	0.0069		
87.816	0.0074		
89.917	0.0078		

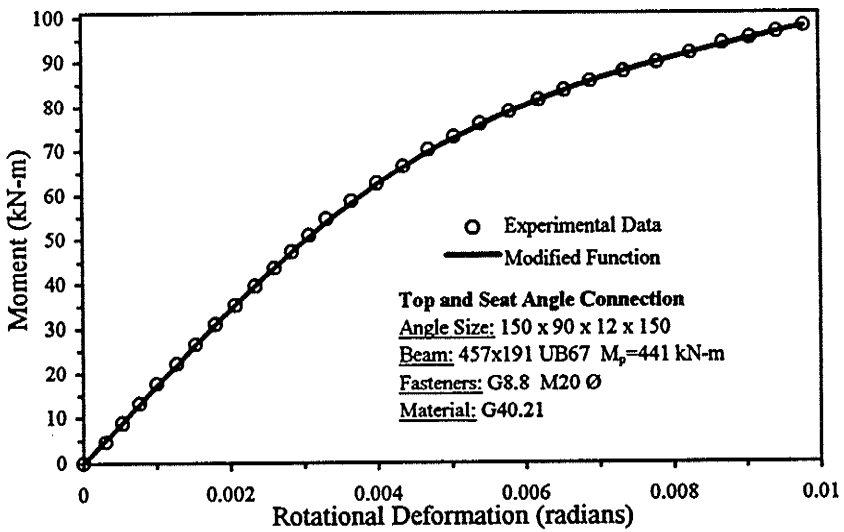


Figure A.147 (a) M-ϕ curve for Maxwell: B3

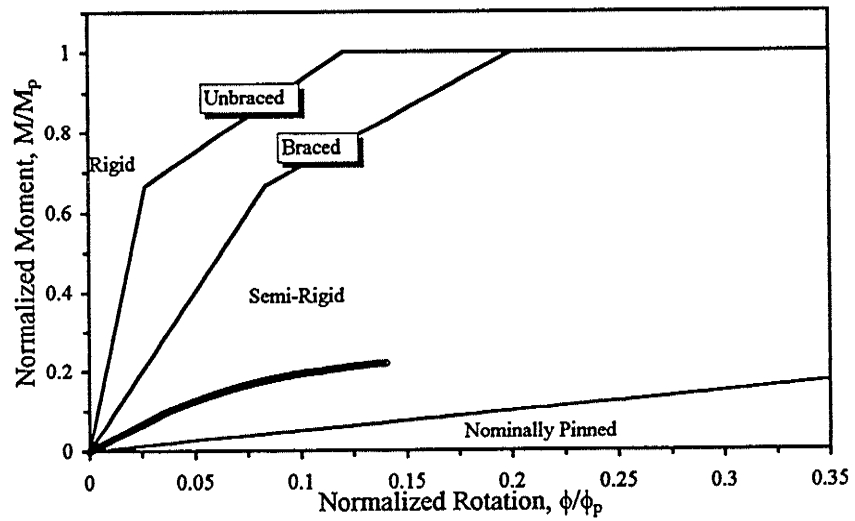


Figure A.147 (b) Eurocode3 Classification of Maxwell: B3

Table A.148 M-ϕ data for Maxwell: B4 (1981)

Moment, M kN-m	Rotation, ϕ radians	Moment, M kN-m	Rotation, ϕ radians
0	0	102.376	0.0084
4.961	0.0003	104.193	0.0087
9.923	0.0005	105.730	0.0090
14.884	0.0008	107.268	0.0094
18.798	0.0011	108.805	0.0097
22.711	0.0013		
26.624	0.0016		
30.398	0.0018		
34.172	0.0020		
38.924	0.0023		
43.675	0.0026		
48.427	0.0029		
53.459	0.0033		
58.490	0.0036		
63.312	0.0039		
68.134	0.0042		
72.536	0.0046		
76.939	0.0050		
81.342	0.0054		
85.745	0.0058		
88.889	0.0063		
92.033	0.0067		
94.269	0.0070		
96.505	0.0074		
98.742	0.0077		
100.559	0.0080		

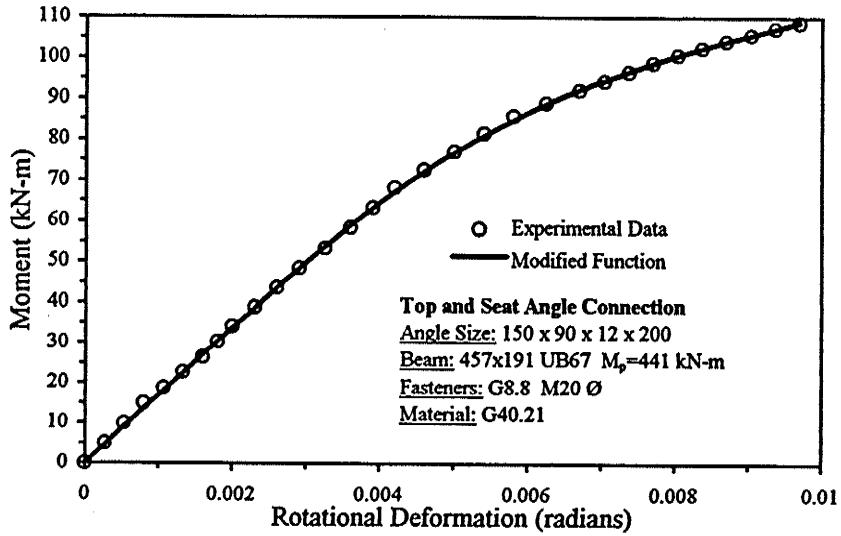


Figure A.148 (a) M-ϕ curve for Maxwell: B4

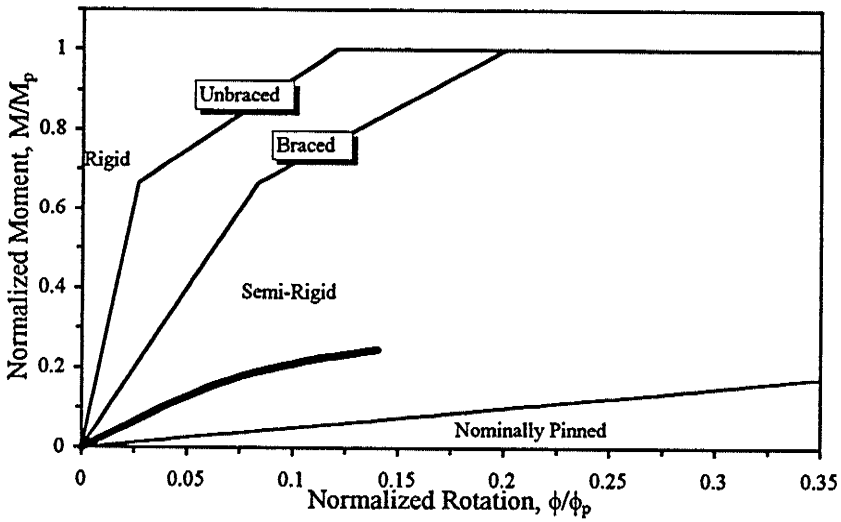


Figure A.148 (b) Eurocode3 Classification of Maxwell: B4

Table A.149 M-ϕ data for Maxwell: C1 (1981)

Moment, M kN-m	Rotation, ϕ radians	Moment, M kN-m	Rotation, ϕ radians
0	0	104.711	0.0081
3.962	0.0003	107.709	0.0085
7.923	0.0005	110.707	0.0089
12.206	0.0008	113.063	0.0094
16.489	0.0010	115.418	0.0098
20.771	0.0013		
24.768	0.0016		
28.765	0.0018		
32.762	0.0021		
37.616	0.0024		
42.470	0.0028		
47.324	0.0031		
51.892	0.0034		
56.460	0.0037		
61.028	0.0040		
64.882	0.0043		
68.736	0.0046		
72.591	0.0049		
76.874	0.0052		
81.157	0.0056		
85.440	0.0059		
88.580	0.0062		
91.721	0.0066		
94.861	0.0069		
98.287	0.0073		
101.714	0.0077		

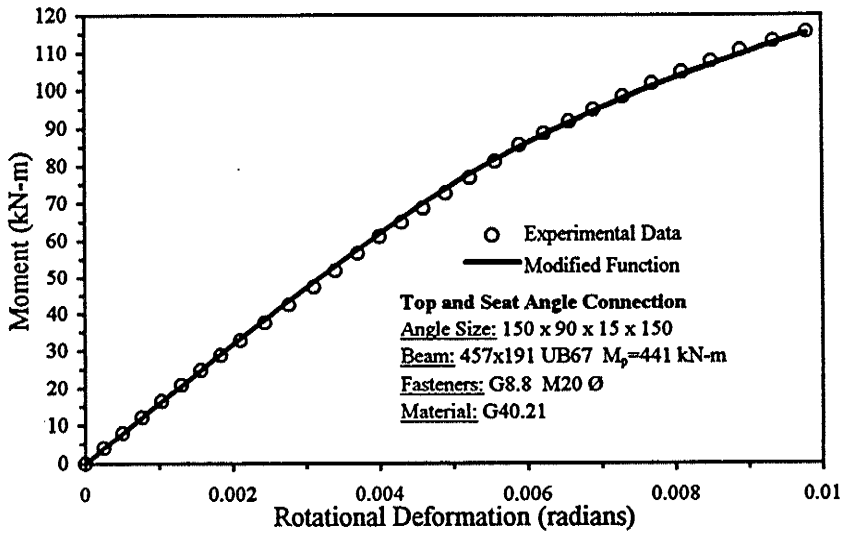


Figure A.149 (a) M-ϕ curve for Maxwell: C1

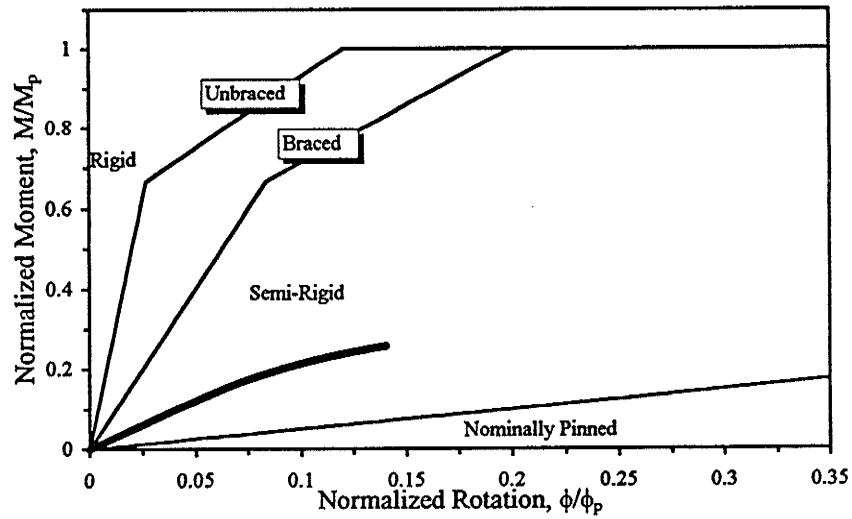


Figure A.149 (b) Eurocode3 Classification of Maxwell: C1

Table A.150 M-ϕ data for Maxwell: C2 (1981)

Moment, M kN-m	Rotation, ϕ radians	Moment, M kN-m	Rotation, ϕ radians
0	0	117.521	0.0082
2.991	0.0002	117.521	0.0085
7.692	0.0005	117.521	0.0088
12.393	0.0007	117.735	0.0091
17.094	0.0010	117.948	0.0094
22.863	0.0013	117.948	0.0097
28.632	0.0016	117.948	0.0099
33.761	0.0019		
38.889	0.0022		
44.017	0.0025		
49.146	0.0027		
54.915	0.0031		
60.684	0.0035		
66.239	0.0038		
71.795	0.0041		
76.710	0.0045		
81.624	0.0048		
85.898	0.0051		
90.172	0.0054		
94.659	0.0058		
99.146	0.0061		
103.633	0.0065		
108.120	0.0068		
112.607	0.0073		
117.094	0.0077		
117.308	0.0080		

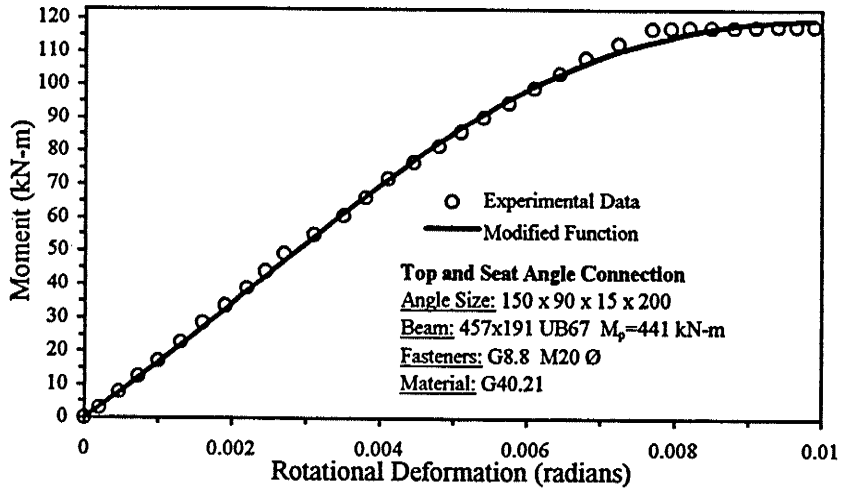


Figure A.150 (a) M-ϕ curve for Maxwell: C2

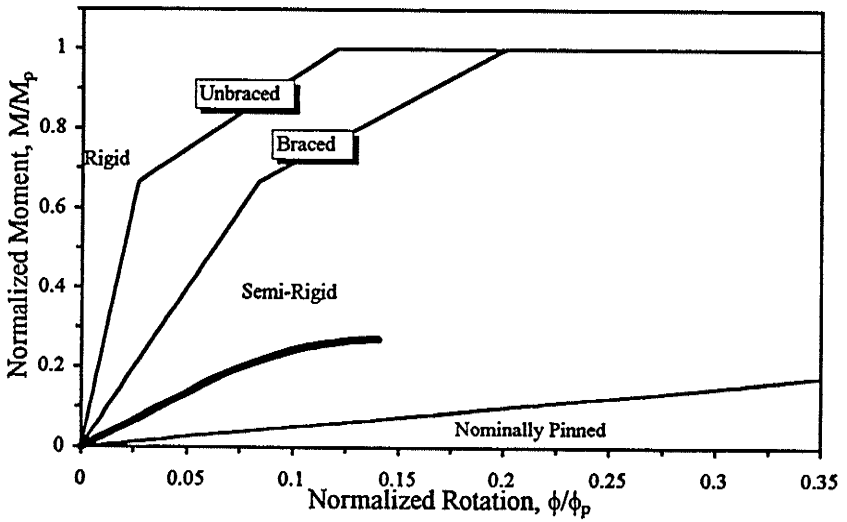


Figure A.150 (b) Eurocode3 Classification of Maxwell: C2

Table A.151 M-ϕ data for Maxwell: C3 (1981)

Moment, M kN-m	Rotation, ϕ radians	Moment, M kN-m	Rotation, ϕ radians
0	0	106.609	0.0081
4.478	0.0002	108.955	0.0084
8.956	0.0004	111.087	0.0089
13.433	0.0006	113.219	0.0093
17.271	0.0008		
21.109	0.0010		
24.947	0.0012		
30.490	0.0015		
36.034	0.0017		
41.365	0.0020		
46.696	0.0023		
52.026	0.0026		
57.357	0.0029		
61.834	0.0033		
66.312	0.0036		
70.007	0.0039		
73.703	0.0043		
77.398	0.0046		
80.384	0.0049		
83.369	0.0052		
87.633	0.0057		
91.897	0.0061		
95.096	0.0065		
98.294	0.0069		
101.279	0.0073		
104.264	0.0077		

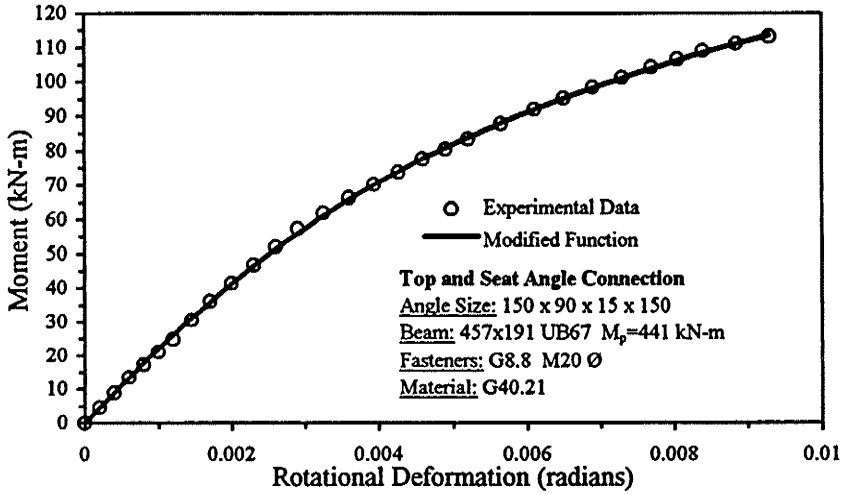


Figure A.151 (a) M-ϕ curve for Maxwell: C3

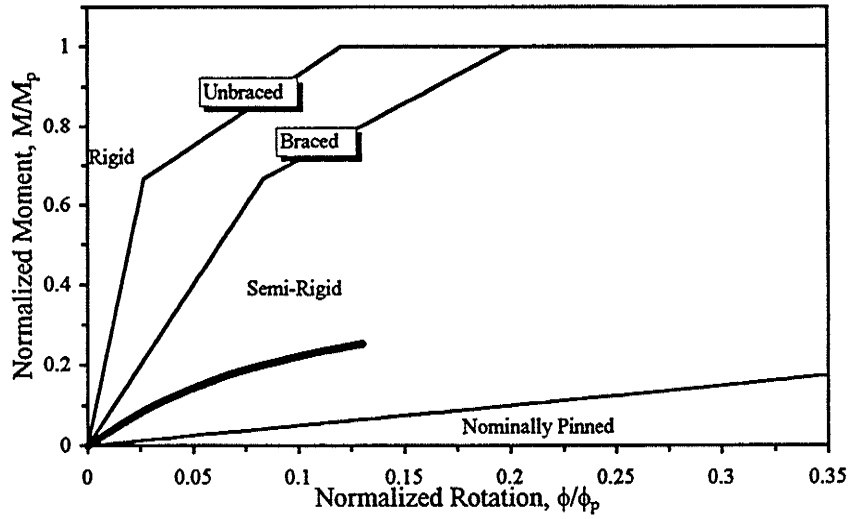


Figure A.151 (b) Eurocode3 Classification of Maxwell: C3

Table A.152 M-ϕ data for Maxwell: C4 (1981)

Moment, M kN-m	Rotation, ϕ radians	Moment, M kN-m	Rotation, ϕ radians
0	0	110.022	0.0062
4.318	0.0002	114.926	0.0066
8.635	0.0004	114.500	0.0069
12.953	0.0005	114.073	0.0071
17.270	0.0007	114.286	0.0074
21.108	0.0009	114.499	0.0077
24.946	0.0010	114.713	0.0081
28.784	0.0012	114.926	0.0084
32.764	0.0014		
36.745	0.0015		
40.725	0.0017		
44.563	0.0019		
48.401	0.0021		
52.238	0.0023		
56.077	0.0025		
59.915	0.0028		
63.753	0.0030		
67.591	0.0032		
71.429	0.0035		
75.267	0.0037		
80.597	0.0041		
85.928	0.0044		
90.832	0.0048		
95.736	0.0051		
100.427	0.0055		
105.118	0.0058		

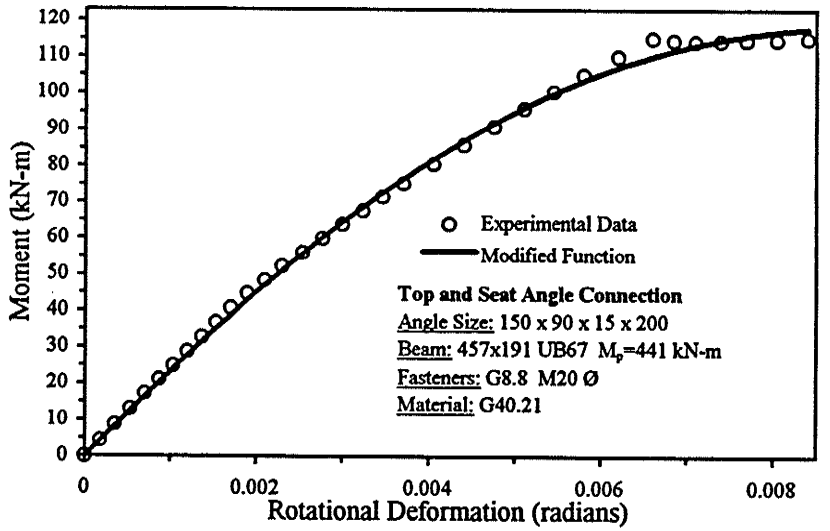


Figure A.152 (a) M-ϕ curve for Maxwell: C4

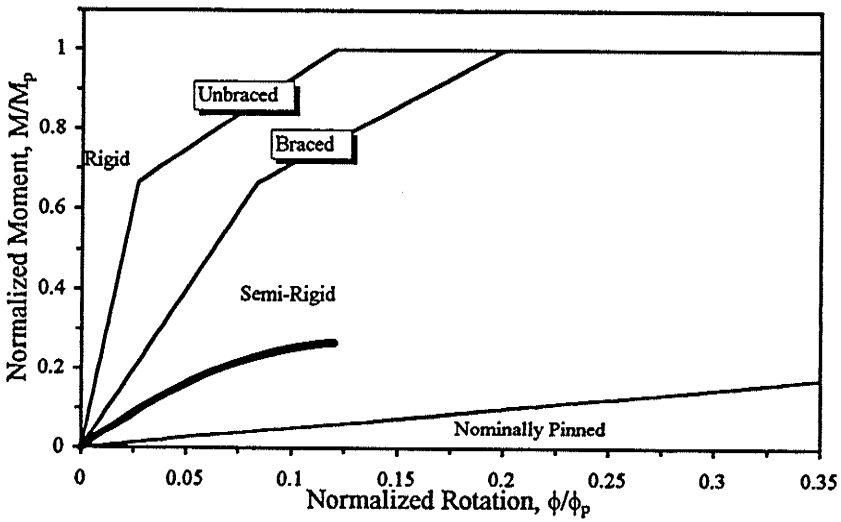


Figure A.152 (b) Eurocode3 Classification of Maxwell: C4

Table A.153 M-ϕ data for Azizinamini: 8S1 (1985)

Moment, M kN-m	Rotation, ϕ radians	Moment, M kN-m	Rotation, ϕ radians
0	0	34.581	0.0185
1.962	0.0002	35.346	0.0201
3.175	0.0004	36.111	0.0216
4.389	0.0005	36.842	0.0231
5.686	0.0008	37.574	0.0247
6.983	0.0010	38.056	0.0259
8.945	0.0013	38.538	0.0272
10.341	0.0015	39.054	0.0284
11.738	0.0017	39.569	0.0297
13.500	0.0021	39.968	0.0310
14.863	0.0024	40.367	0.0324
16.227	0.0028	40.816	0.0337
17.390	0.0031	41.265	0.0350
18.554	0.0034	41.581	0.0360
19.668	0.0038	41.897	0.0371
20.782	0.0043	42.262	0.0382
22.810	0.0051	42.628	0.0394
24.706	0.0064	42.861	0.0404
26.568	0.0079		
28.164	0.0096		
29.860	0.0113		
30.741	0.0126		
31.622	0.0140		
32.403	0.0151		
33.185	0.0162		
33.883	0.0174		

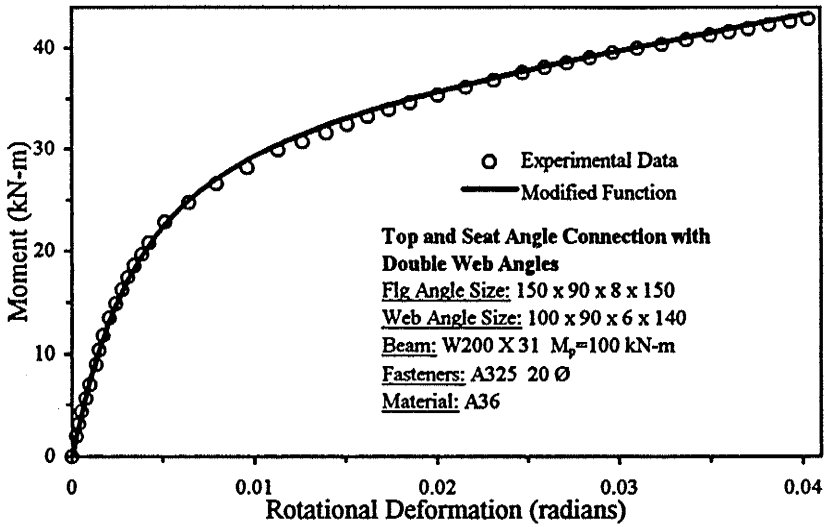


Figure A.153 (a) M-ϕ curve for Azizinamini: 8S1

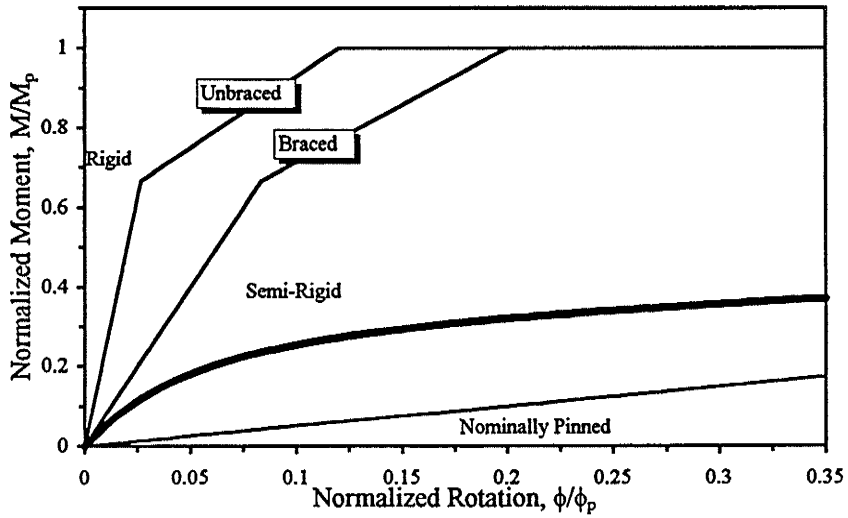


Figure A.153 (b) Eurocode3 Classification of Azizinamini: 8S1

Table A.154 M-ϕ data for Azizinamini: 8S2 (1985)

Moment, M kN-m	Rotation, ϕ radians	Moment, M kN-m	Rotation, ϕ radians
0	0	38.349	0.0082
1.485	0.0001	39.491	0.0092
2.970	0.0001	40.301	0.0102
4.455	0.0002	41.111	0.0112
5.668	0.0002	41.671	0.0121
6.882	0.0003	42.232	0.0131
8.444	0.0004	42.774	0.0144
10.006	0.0005	43.316	0.0157
11.768	0.0007	43.511	0.0168
13.529	0.0008	43.706	0.0178
15.047	0.0010	43.335	0.0188
16.565	0.0012	43.614	0.0196
18.082	0.0013	43.893	0.0204
19.611	0.0015	43.987	0.0214
21.140	0.0016	43.617	0.0223
22.669	0.0018	43.580	0.0232
24.081	0.0020	43.542	0.0241
25.493	0.0022	43.724	0.0255
27.320	0.0027	43.905	0.0269
28.564	0.0031	44.087	0.0283
29.809	0.0035		
31.901	0.0042		
33.277	0.0050		
34.653	0.0057		
35.930	0.0064		
37.207	0.0072		

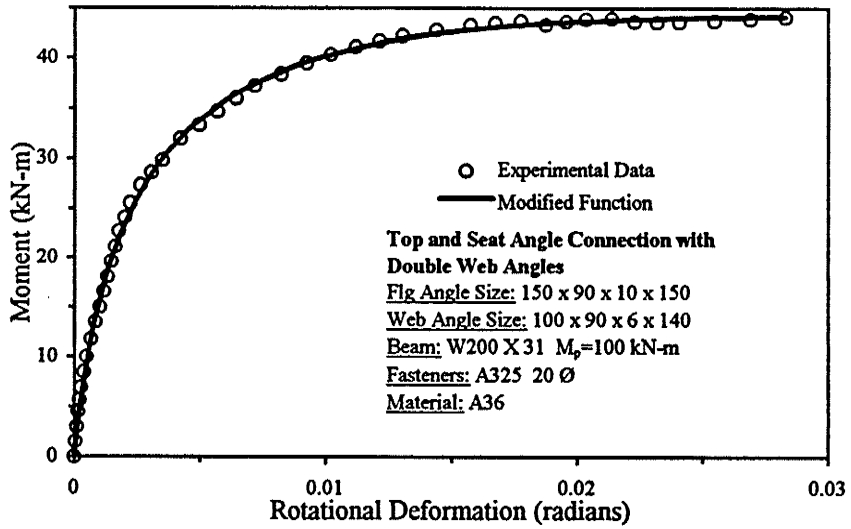


Figure A.154 (a) M-ϕ curve for Azizinamini: 8S2

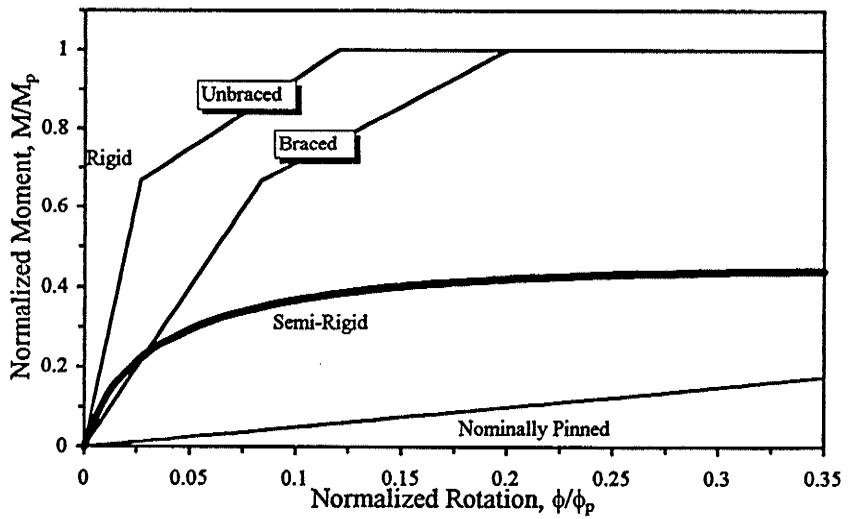


Figure A.154 (b) Eurocode3 Classification of Azizinamini: 8S2

Table A.155 M-ϕ data for Azizinamini: 8S3 (1985)

Moment, M kN-m	Rotation, ϕ radians	Moment, M kN-m	Rotation, ϕ radians
0	0	43.675	0.0165
2.226	0.0002	44.364	0.0178
4.452	0.0004	45.053	0.0192
6.695	0.0005	45.776	0.0205
8.938	0.0007	46.498	0.0218
11.181	0.0010	47.089	0.0233
13.425	0.0012	47.680	0.0249
15.768	0.0016	48.252	0.0262
18.112	0.0020	48.825	0.0275
19.674	0.0022	49.347	0.0286
21.237	0.0024	49.869	0.0297
23.032	0.0028	50.377	0.0314
24.828	0.0031	50.885	0.0330
27.089	0.0036	51.359	0.0343
29.551	0.0043	51.832	0.0357
31.682	0.0051	52.507	0.0375
33.064	0.0057	53.183	0.0392
34.446	0.0064		
36.246	0.0074		
37.748	0.0086		
39.385	0.0102		
40.238	0.0112		
41.092	0.0123		
41.746	0.0133		
42.400	0.0143		
43.038	0.0154		

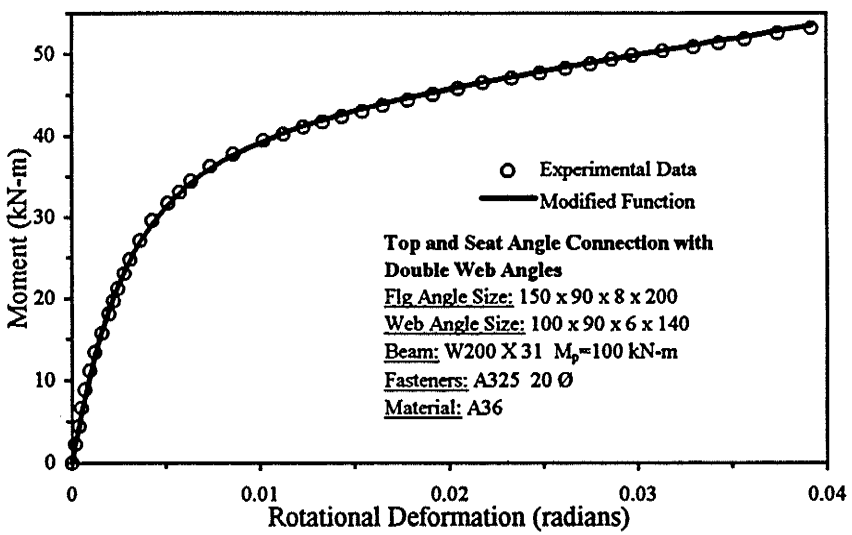


Figure A.155 (a) M-ϕ curve for Azizinamini: 8S3

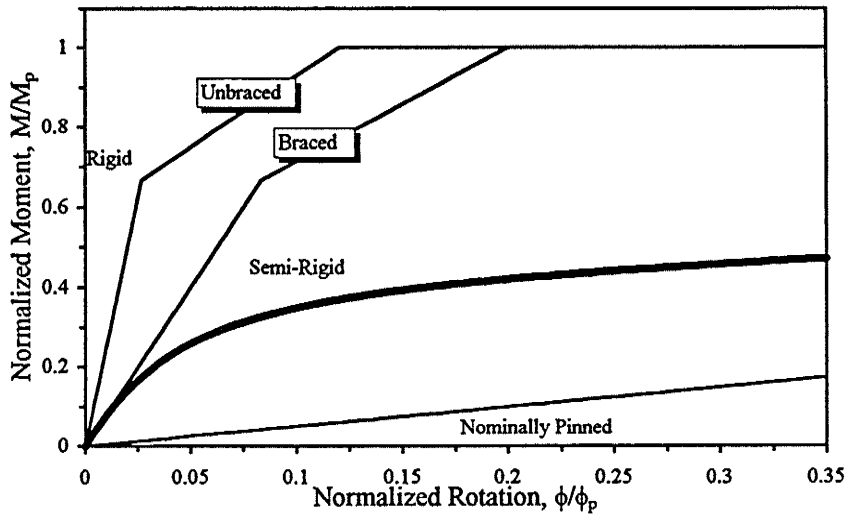


Figure A.155 (b) Eurocode3 Classification of Azizinamini: 8S3

Table A.156 M-ϕ data for Azizinamini: 8S4 (1985)

Moment, M kN-m	Rotation, ϕ radians	Moment, M kN-m	Rotation, ϕ radians
0	0	18.613	0.0248
0.774	0.0004	18.993	0.0262
1.549	0.0008	19.207	0.0276
2.323	0.0012	19.421	0.0290
3.075	0.0017	19.786	0.0295
3.827	0.0022	20.066	0.0310
4.579	0.0026	20.346	0.0324
5.583	0.0033	20.488	0.0340
6.587	0.0040	20.630	0.0357
7.590	0.0047	20.771	0.0373
8.594	0.0054	21.051	0.0389
9.622	0.0062	21.331	0.0406
10.651	0.0071		
11.679	0.0080		
12.458	0.0089		
13.237	0.0098		
14.099	0.0114		
14.960	0.0130		
15.490	0.0142		
16.020	0.0153		
16.367	0.0164		
16.714	0.0176		
17.094	0.0191		
17.473	0.0206		
17.854	0.0219		
18.234	0.0233		

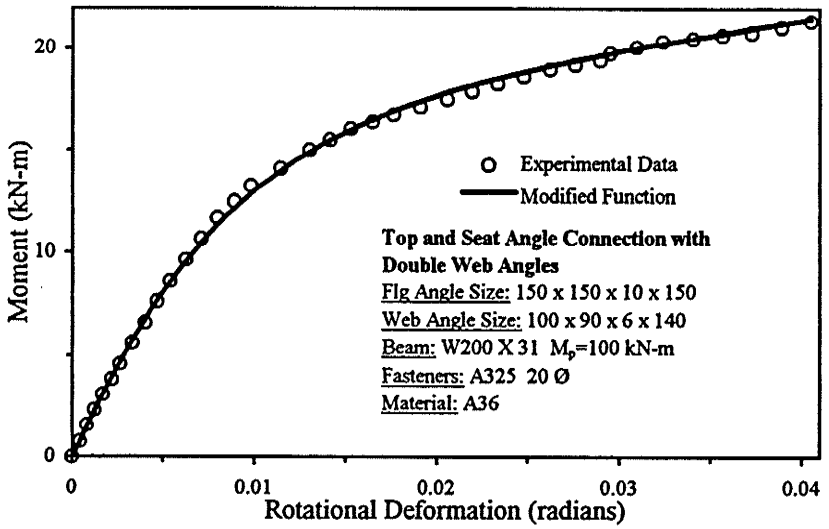


Figure A.156 (a) M-ϕ curve for Azizinamini: 8S4

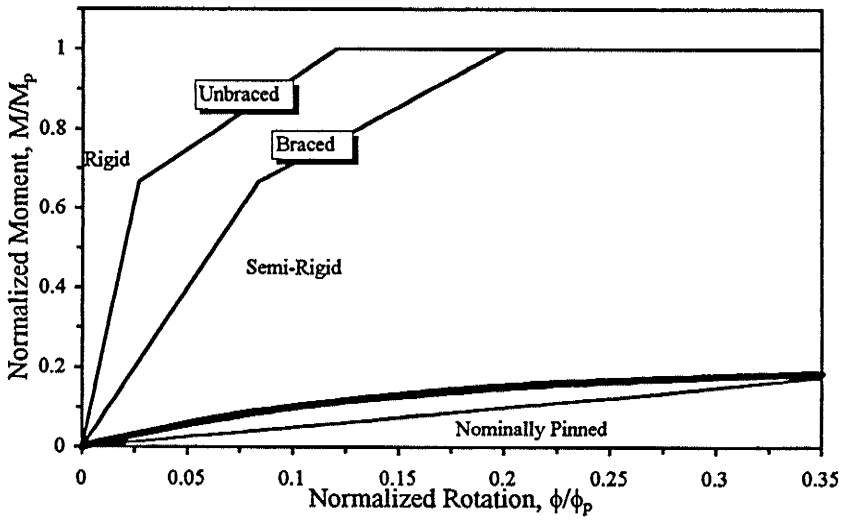


Figure A.156 (b) Eurocode3 Classification of Azizinamini: 8S4

Table A.157 M-ϕ data for Azizinamini: 8S5 (1985)

Moment, M kN-m	Rotation, ϕ radians	Moment, M kN-m	Rotation, ϕ radians
0	0	36.362	0.0192
1.641	0.0002	36.926	0.0206
3.282	0.0003	37.408	0.0222
4.923	0.0005	37.889	0.0239
6.920	0.0007	38.370	0.0255
8.917	0.0009	38.802	0.0270
10.495	0.0012	39.235	0.0284
12.073	0.0015	39.667	0.0299
13.651	0.0018	40.376	0.0318
15.096	0.0021	41.086	0.0338
16.542	0.0024	41.358	0.0355
17.987	0.0027	41.630	0.0372
20.026	0.0033	42.062	0.0386
22.065	0.0040	42.494	0.0400
23.640	0.0046		
25.215	0.0053		
26.997	0.0062		
28.778	0.0072		
30.335	0.0085		
31.893	0.0098		
32.814	0.0108		
33.735	0.0119		
34.234	0.0133		
34.733	0.0148		
35.232	0.0163		
35.797	0.0177		

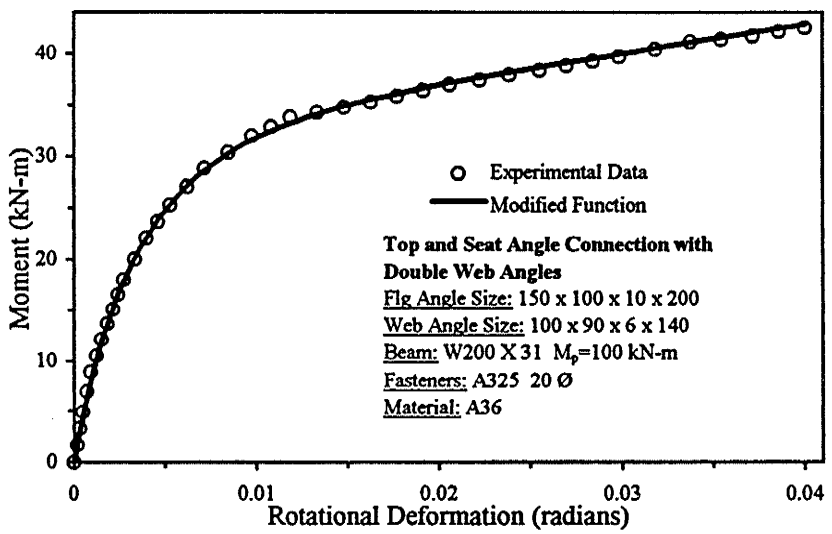


Figure A.157 (a) M-ϕ curve for Azizinamini: 8S5

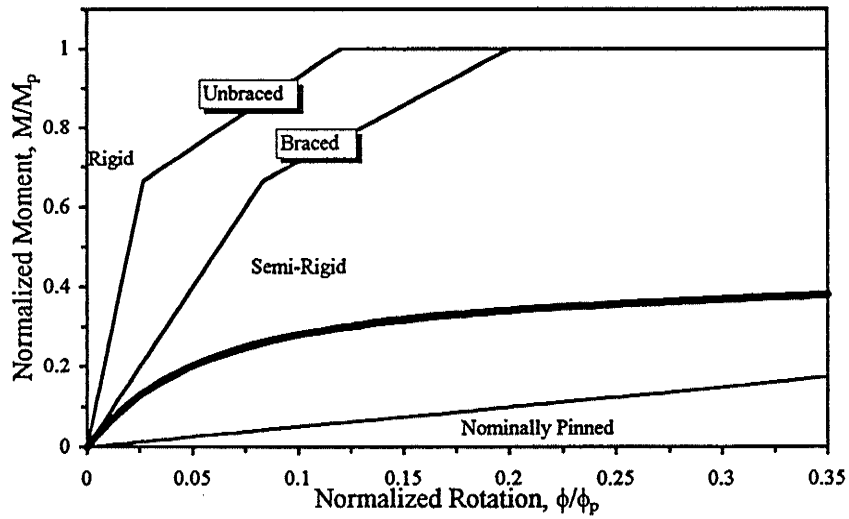


Figure A.157 (b) Eurocode3 Classification of Azizinamini: 8S5

Table A.158 M-ϕ data for Azizinamini: 8S6 (1985)

Moment, M kN-m	Rotation, ϕ radians	Moment, M kN-m	Rotation, ϕ radians
0	0	28.297	0.0244
1.297	0.0002	28.928	0.0262
2.595	0.0004	29.476	0.0281
3.576	0.0006	30.023	0.0300
4.558	0.0008	30.471	0.0317
5.922	0.0012	30.919	0.0333
7.285	0.0016	31.284	0.0349
8.250	0.0018	31.649	0.0365
9.215	0.0021	32.080	0.0385
10.656	0.0026	32.512	0.0405
12.098	0.0031		
13.539	0.0036		
14.803	0.0042		
16.067	0.0048		
16.981	0.0054		
17.896	0.0060		
19.259	0.0073		
20.622	0.0085		
21.620	0.0100		
22.617	0.0114		
23.514	0.0134		
24.411	0.0153		
25.274	0.0172		
26.138	0.0192		
26.902	0.0209		
27.666	0.0227		

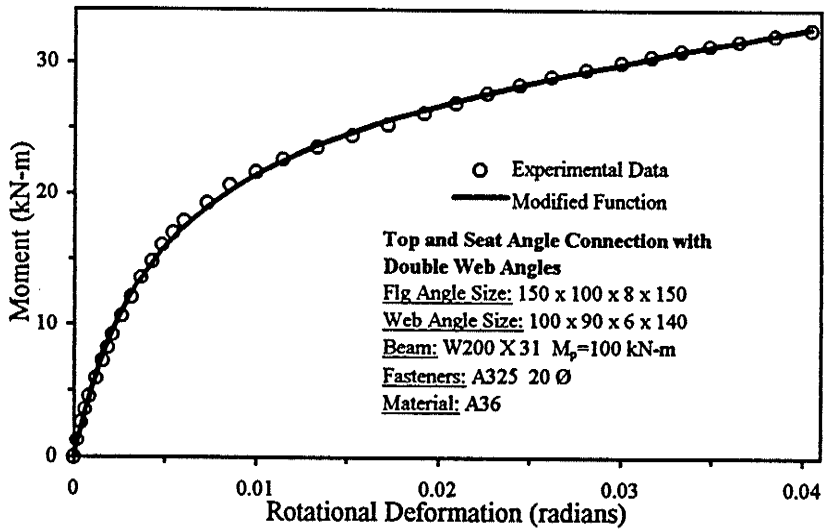


Figure A.158 (a) M-ϕ curve for Azizinamini: 8S6

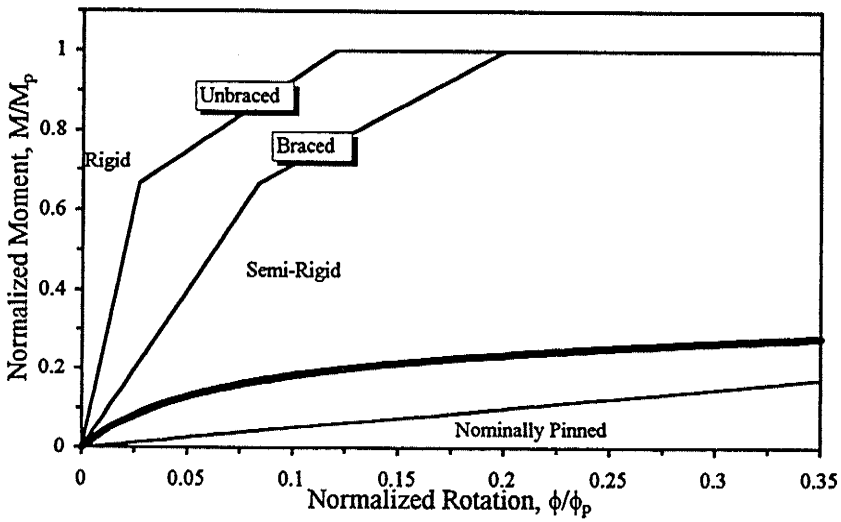


Figure A.158 (b) Eurocode3 Classification of Azizinamini: 8S6

Table A.159 M-ϕ data for Azizinamini: 8S7 (1985)

Moment, M kN-m	Rotation, ϕ radians	Moment, M kN-m	Rotation, ϕ radians
0	0	40.568	0.0226
1.312	0.0003	41.297	0.0246
2.623	0.0005	41.827	0.0261
4.516	0.0008	42.357	0.0277
6.757	0.0013	42.904	0.0294
8.999	0.0017	43.451	0.0310
10.571	0.0021	44.015	0.0327
12.142	0.0024	44.578	0.0343
13.714	0.0028	44.976	0.0356
15.955	0.0033	45.373	0.0368
18.197	0.0039	45.937	0.0385
19.813	0.0043	46.500	0.0402
21.429	0.0048		
23.044	0.0053		
25.037	0.0060		
27.029	0.0067		
29.054	0.0077		
31.112	0.0089		
32.871	0.0101		
34.099	0.0114		
35.062	0.0126		
36.024	0.0139		
37.069	0.0155		
38.114	0.0172		
38.976	0.0189		
39.838	0.0206		

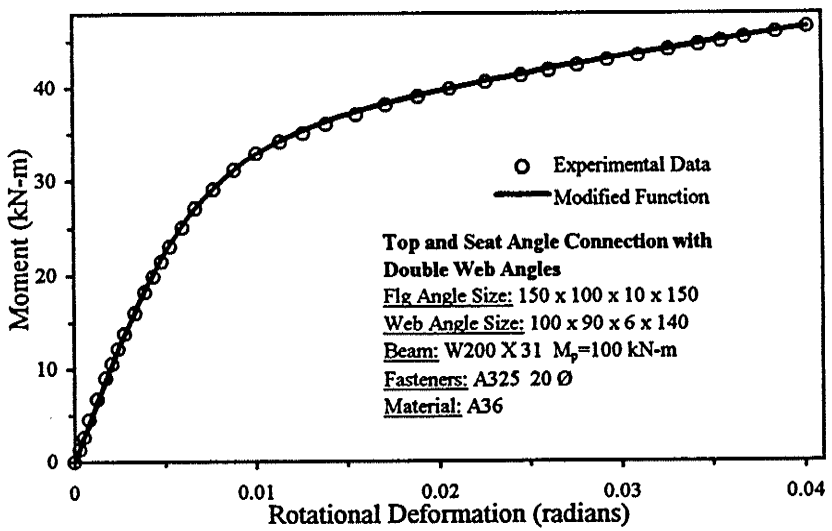


Figure A.159 (a) M-ϕ curve for Azizinamini: 8S7

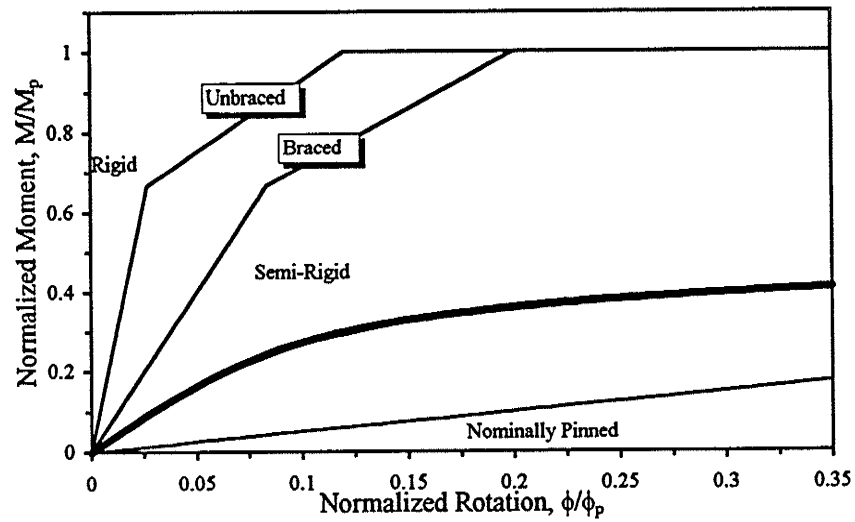


Figure A.159 (b) Eurocode3 Classification of Azizinamini: 8S7

Table A.160 M-ϕ data for Azizinamini: 8S8 (1985)

Moment, M kN-m	Rotation, ϕ radians	Moment, M kN-m	Rotation, ϕ radians
0	0	42.446	0.0230
1.656	0.0002	42.980	0.0244
3.312	0.0005	43.621	0.0258
4.914	0.0007	44.120	0.0274
6.516	0.0010	45.188	0.0293
7.941	0.0012	45.687	0.0306
9.365	0.0014	46.221	0.0317
10.807	0.0016	46.755	0.0328
12.250	0.0019	47.129	0.0338
13.656	0.0022	47.503	0.0348
15.063	0.0024	47.966	0.0362
17.199	0.0029	48.713	0.0378
19.122	0.0035	49.497	0.0395
21.294	0.0042		
23.466	0.0051		
25.710	0.0059		
27.882	0.0071		
29.912	0.0085		
32.369	0.0101		
34.292	0.0118		
36.286	0.0137		
37.675	0.0156		
38.956	0.0172		
39.669	0.0183		
40.381	0.0194		
41.520	0.0212		

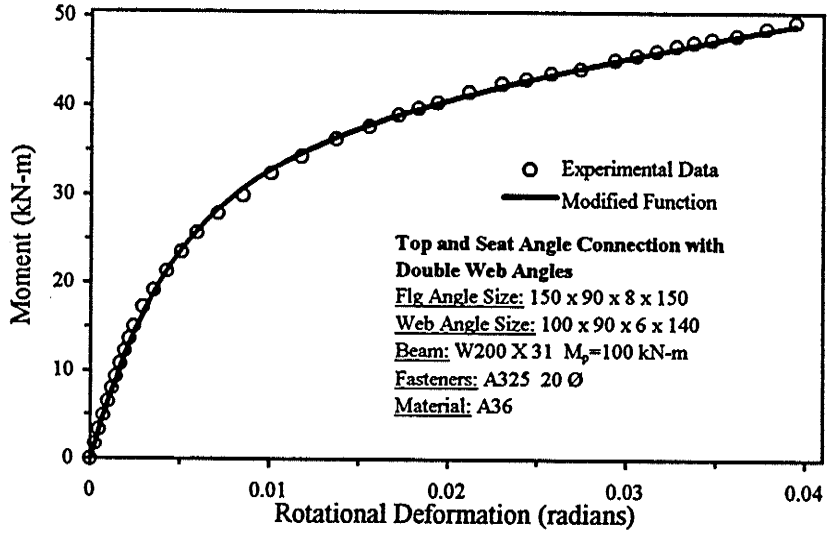


Figure A.160 (a) M-ϕ curve for Azizinamini: 8S8

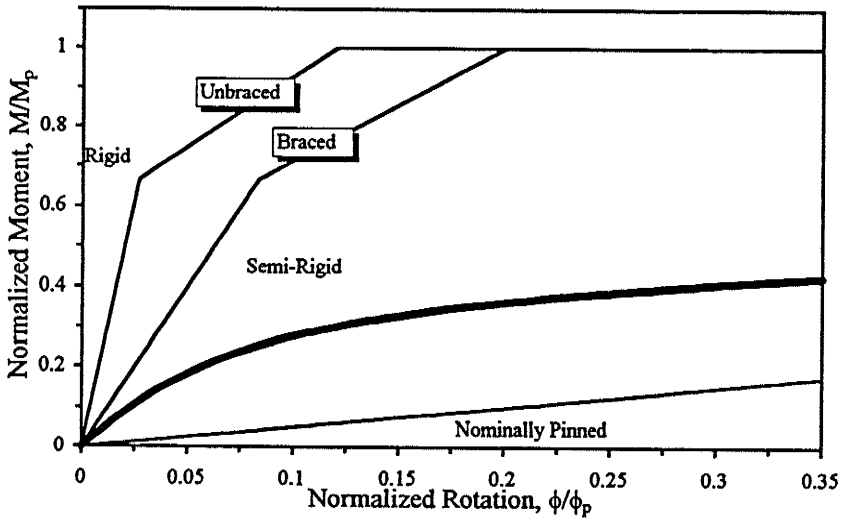


Figure A.160 (b) Eurocode3 Classification of Azizinamini: 8S8

Table A.161 M-ϕ data for Azizinamini: 8S9 (1985)

Moment, M kN-m	Rotation, ϕ radians	Moment, M kN-m	Rotation, ϕ radians
0	0	43.791	0.0177
1.882	0.0001	44.387	0.0188
3.765	0.0003	44.983	0.0199
5.399	0.0004	45.776	0.0211
7.033	0.0006	46.569	0.0224
8.437	0.0008	47.254	0.0236
9.840	0.0009	47.940	0.0248
11.315	0.0011	48.737	0.0265
12.789	0.0012	49.535	0.0282
14.673	0.0015	50.026	0.0294
16.557	0.0018	50.517	0.0306
18.121	0.0021	51.005	0.0316
19.686	0.0024	51.494	0.0327
22.284	0.0031	51.842	0.0338
24.188	0.0037	52.190	0.0349
26.093	0.0043	52.537	0.0359
28.766	0.0054	52.883	0.0369
31.439	0.0066	53.573	0.0385
33.867	0.0081		
36.438	0.0098		
38.513	0.0114		
39.552	0.0125		
40.591	0.0135		
41.489	0.0146		
42.387	0.0157		
43.089	0.0167		

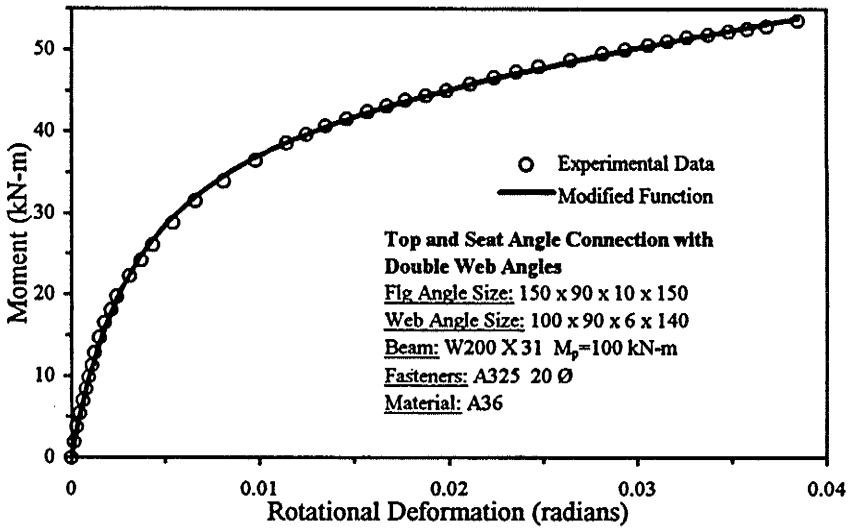


Figure A.161 (a) M-ϕ curve for Azizinamini: 8S9

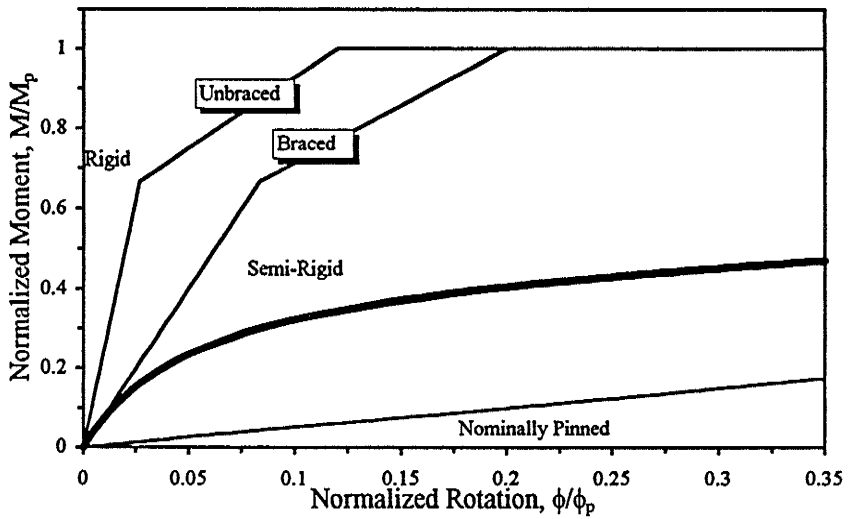


Figure A.161 (b) Eurocode3 Classification of Azizinamini: 8S9

Table A.162 M-ϕ data for Azizinamini: 8S10 (1985)

Moment, M kN-m	Rotation, ϕ radians	Moment, M kN-m	Rotation, ϕ radians
0	0	60.550	0.0128
3.110	0.0001	61.882	0.0137
6.220	0.0001	63.214	0.0146
9.330	0.0002	64.321	0.0157
12.820	0.0002	65.428	0.0168
16.310	0.0003	66.108	0.0179
19.408	0.0005	66.788	0.0190
22.507	0.0006	67.468	0.0202
25.095	0.0008	68.148	0.0213
27.683	0.0009	70.644	0.0225
30.271	0.0010	71.288	0.0234
33.761	0.0013	71.932	0.0244
37.252	0.0016	72.576	0.0253
40.209	0.0020	72.970	0.0261
43.166	0.0025	73.364	0.0269
45.304	0.0031		
47.442	0.0037		
49.332	0.0044		
51.221	0.0051		
49.727	0.0057		
51.511	0.0067		
53.295	0.0078		
54.864	0.0087		
56.434	0.0097		
57.826	0.0108		
59.218	0.0119		

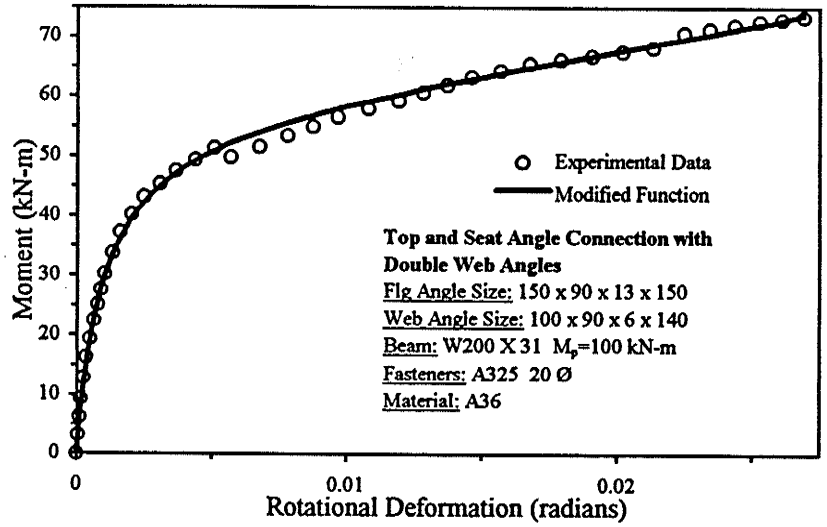


Figure A.162 (a) M-ϕ curve for Azizinamini: 8S10

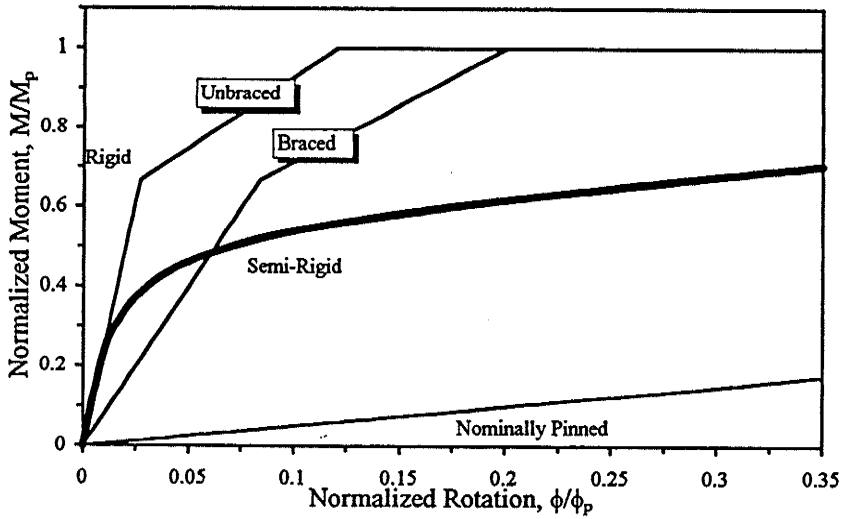


Figure A.162 (b) Eurocode3 Classification of Azizinamini: 8S10

Table A.163 M-ϕ data for Azizinamini: 14S1 (1985)

Moment, M kN-m	Rotation, ϕ radians	Moment, M kN-m	Rotation, ϕ radians
0	0	66.066	0.0107
2.909	0.0001	67.415	0.0118
5.819	0.0002	68.431	0.0129
8.728	0.0003	69.447	0.0141
10.891	0.0005	70.218	0.0154
14.009	0.0006	70.989	0.0167
17.126	0.0007	71.929	0.0182
19.982	0.0009	72.862	0.0194
22.837	0.0010	73.796	0.0205
25.692	0.0012	74.815	0.0218
28.439	0.0015	75.833	0.0230
30.894	0.0018	76.938	0.0244
33.349	0.0020	78.042	0.0258
36.427	0.0023	78.978	0.0271
39.505	0.0025	79.913	0.0283
41.921	0.0029	81.060	0.0298
44.336	0.0032	82.207	0.0313
46.959	0.0036		
49.582	0.0039		
53.086	0.0048		
55.381	0.0054		
57.676	0.0060		
59.769	0.0069		
61.861	0.0078		
63.289	0.0087		
64.717	0.0096		

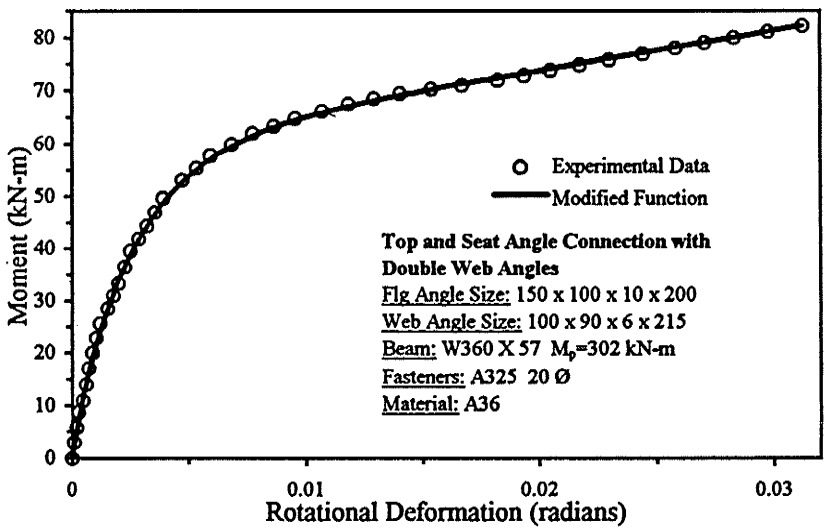


Figure A.163 (a) M-ϕ curve for Azizinamini: 14S1

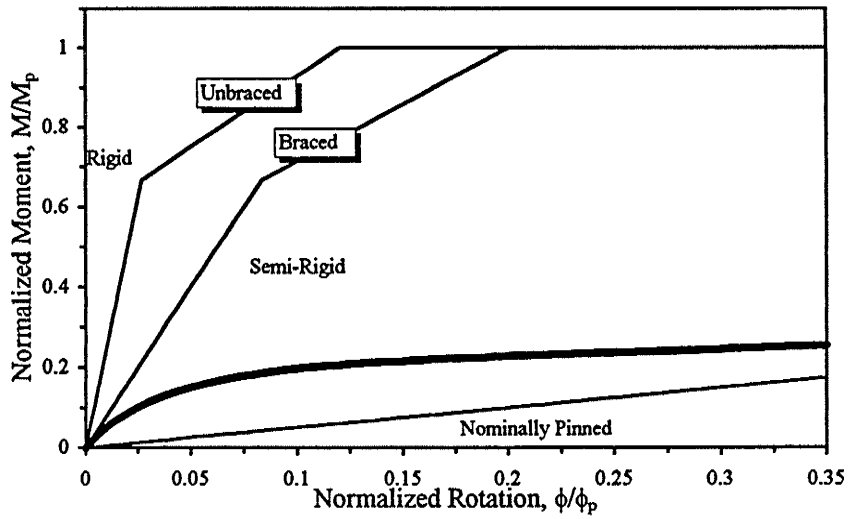


Figure A.163 (b) Eurocode3 Classification of Azizinamini: 14S1

Table A.164 M-ϕ data for Azizinamini: 14S2 (1985)

Moment, M kN-m	Rotation, ϕ radians	Moment, M kN-m	Rotation, ϕ radians
0	0	96.014	0.0130
5.568	0.0001	97.447	0.0142
11.136	0.0002	98.879	0.0154
16.665	0.0005	100.481	0.0167
22.194	0.0007	102.083	0.0181
27.764	0.0010	103.932	0.0193
33.335	0.0012	104.023	0.0197
37.271	0.0014	102.871	0.0204
41.207	0.0016	104.108	0.0215
45.143	0.0018	105.345	0.0225
50.800	0.0023	106.582	0.0236
56.457	0.0027	107.818	0.0246
59.577	0.0030	109.054	0.0257
62.697	0.0033	110.291	0.0267
67.276	0.0038	111.751	0.0278
70.274	0.0043	113.210	0.0290
73.272	0.0047	114.670	0.0301
76.438	0.0052		
79.605	0.0058		
85.194	0.0071		
87.701	0.0080		
90.209	0.0088		
92.305	0.0099		
94.400	0.0110		
95.744	0.0118		
97.088	0.0127		

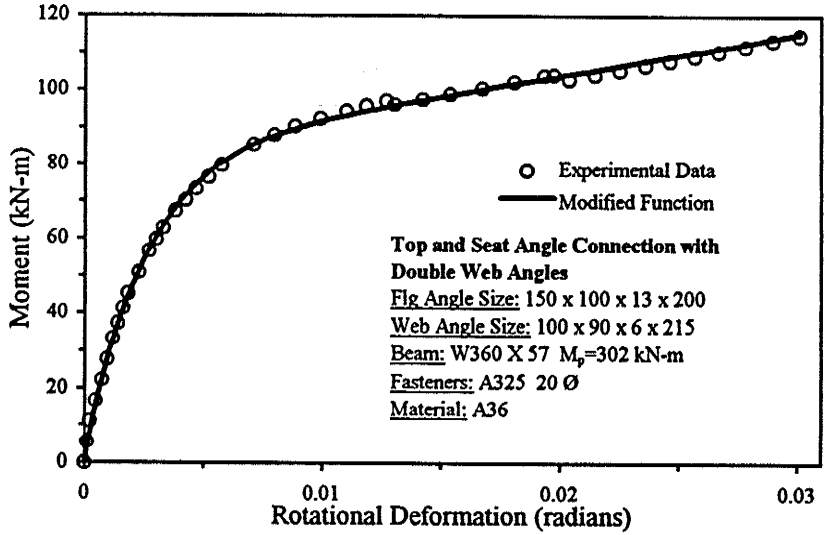


Figure A.164 (a) M-ϕ curve for Azizinamini: 14S2

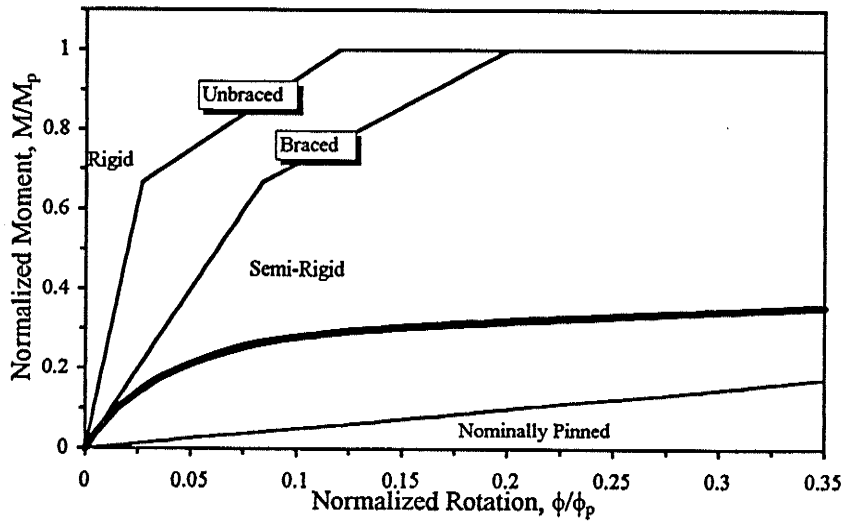


Figure A.164 (b) Eurocode3 Classification of Azizinamini: 14S2

Table A.165 M-ϕ data for Azizinamini: 14S3 (1985)

Moment, M kN-m	Rotation, ϕ radians	Moment, M kN-m	Rotation, ϕ radians
0	0	65.567	0.0152
2.926	0.0002	66.987	0.0166
5.852	0.0004	68.342	0.0181
8.779	0.0006	69.698	0.0196
11.817	0.0009	70.671	0.0208
14.855	0.0012	71.644	0.0220
17.893	0.0014	72.618	0.0231
21.065	0.0018	73.840	0.0246
24.237	0.0021	75.063	0.0261
27.409	0.0024	76.184	0.0275
30.426	0.0027	77.305	0.0289
33.444	0.0031	78.390	0.0301
36.461	0.0034	79.475	0.0314
38.857	0.0037		
40.324	0.0040		
42.989	0.0045		
45.654	0.0050		
47.957	0.0056		
50.259	0.0062		
52.366	0.0070		
54.473	0.0078		
57.953	0.0093		
59.567	0.0103		
61.180	0.0114		
62.663	0.0126		
64.147	0.0138		

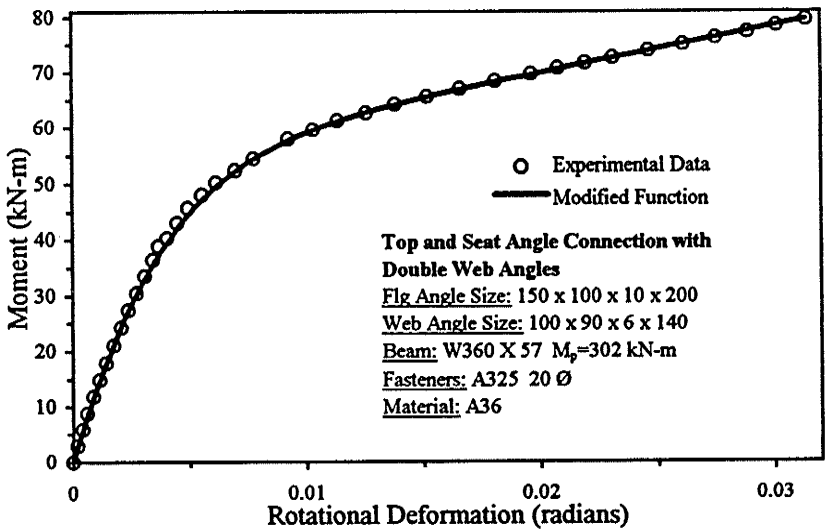


Figure A.165 (a) M-ϕ curve for Azizinamini: 14S3

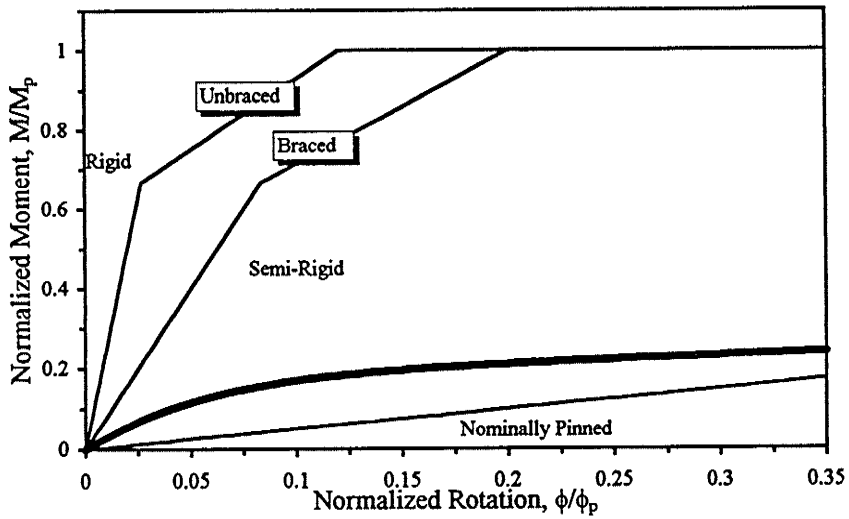


Figure A.165 (b) Eurocode3 Classification of Azizinamini: 14S3

Table A.166 M-ϕ data for Azizinamini: 14S4 (1985)

Moment, M kN-m	Rotation, ϕ radians	Moment, M kN-m	Rotation, ϕ radians
0	0	86.193	0.0169
4.456	0.0002	87.274	0.0180
8.911	0.0004	88.355	0.0192
13.434	0.0005	89.436	0.0203
17.956	0.0007	90.651	0.0215
22.445	0.0009	91.866	0.0228
26.935	0.0011	93.082	0.0240
31.459	0.0015	94.207	0.0252
35.983	0.0018	95.333	0.0264
40.475	0.0022	96.458	0.0275
44.967	0.0025	97.449	0.0286
49.627	0.0031	98.440	0.0297
54.288	0.0036	99.431	0.0307
58.286	0.0043		
62.285	0.0050		
65.251	0.0056		
68.217	0.0062		
70.821	0.0069		
73.425	0.0077		
76.969	0.0091		
78.445	0.0100		
79.922	0.0110		
81.337	0.0122		
82.752	0.0135		
83.899	0.0146		
85.046	0.0158		

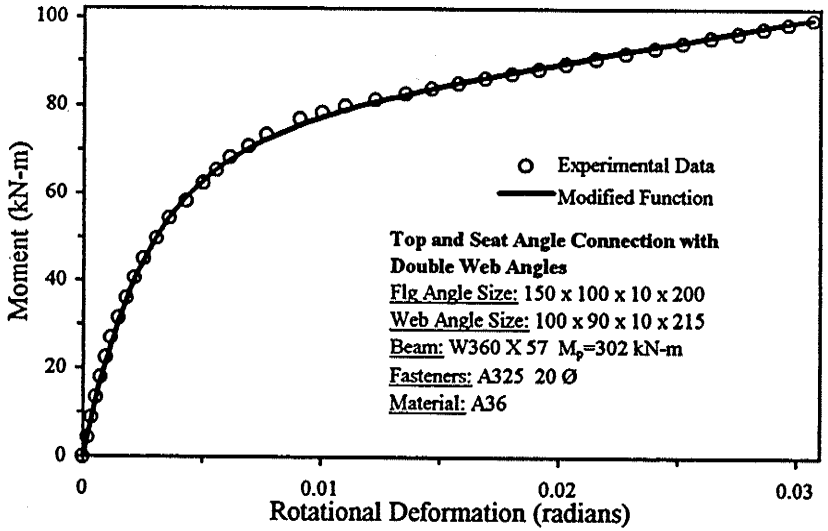


Figure A.166 (a) M-ϕ curve for Azizinamini: 14S4

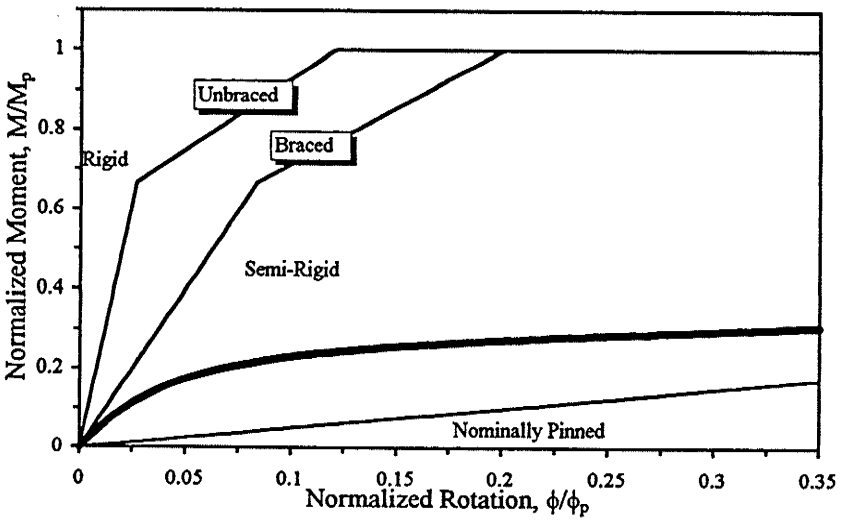


Figure A.166 (b) Eurocode3 Classification of Azizinamini: 14S4

Table A.167 M-ϕ data for Azizinamini: 14S5 (1985)

Moment, M kN-m	Rotation, ϕ radians	Moment, M kN-m	Rotation, ϕ radians
0	0	93.667	0.0140
5.520	0.0001	93.853	0.0150
11.040	0.0002	95.553	0.0162
14.736	0.0003	97.252	0.0173
18.432	0.0005	99.400	0.0187
23.329	0.0007	101.011	0.0200
28.227	0.0010	102.623	0.0212
32.235	0.0012	104.099	0.0222
36.243	0.0014	105.575	0.0232
40.162	0.0017	107.808	0.0241
44.081	0.0020	109.285	0.0252
48.445	0.0023	110.762	0.0264
52.809	0.0025	112.105	0.0273
56.061	0.0029	113.447	0.0283
59.313	0.0032	115.011	0.0291
64.747	0.0037	116.576	0.0300
70.005	0.0045	117.831	0.0312
74.283	0.0051		
78.117	0.0059		
81.862	0.0067		
85.966	0.0079		
89.002	0.0092		
89.899	0.0101		
90.795	0.0109		
91.870	0.0118		
92.945	0.0127		

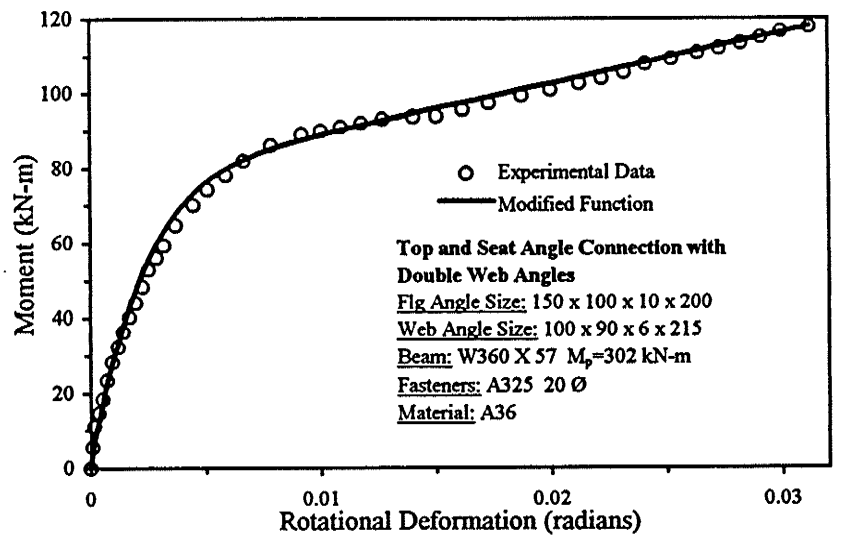


Figure A.167 (a) M-ϕ curve for Azizinamini: 14S5

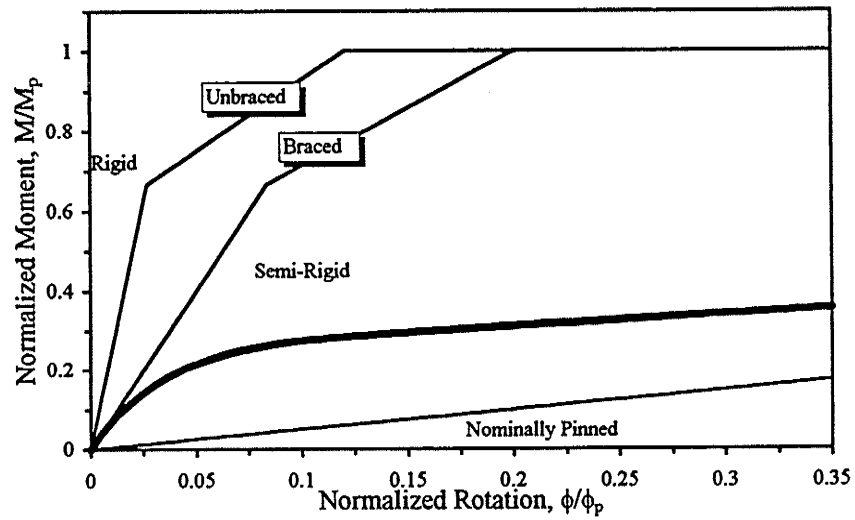


Figure A.167 (b) Eurocode3 Classification of Azizinamini: 14S5

Table A.168 M-ϕ data for Azizinamini: 14S6 (1985)

Moment, M kN-m	Rotation, ϕ radians	Moment, M kN-m	Rotation, ϕ radians
0	0	102.181	0.0130
4.455	0.0002	104.166	0.0141
8.910	0.0003	105.611	0.0149
13.723	0.0005	107.056	0.0156
18.535	0.0007	108.501	0.0165
23.347	0.0009	109.947	0.0173
28.159	0.0011	111.310	0.0183
32.973	0.0013	112.672	0.0194
37.787	0.0016	114.030	0.0203
42.424	0.0019	115.388	0.0211
47.062	0.0022	116.484	0.0222
51.434	0.0026	117.579	0.0232
55.805	0.0029	118.764	0.0243
60.178	0.0034	119.950	0.0254
64.550	0.0038	121.406	0.0266
68.479	0.0042	122.862	0.0278
72.409	0.0047	123.963	0.0291
75.983	0.0052	125.063	0.0303
79.558	0.0058		
85.112	0.0071		
87.892	0.0079		
90.673	0.0087		
93.097	0.0095		
95.521	0.0103		
97.858	0.0111		
100.195	0.0120		

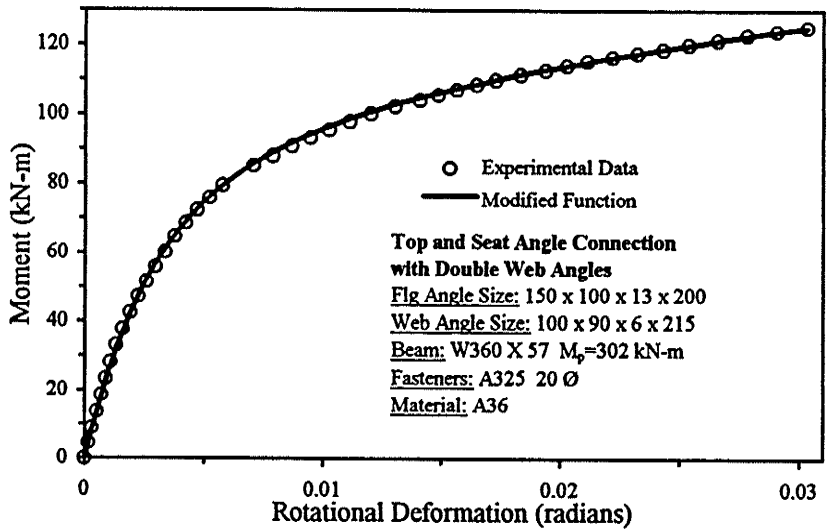


Figure A.168 (a) M-ϕ curve for Azizinamini: 14S6

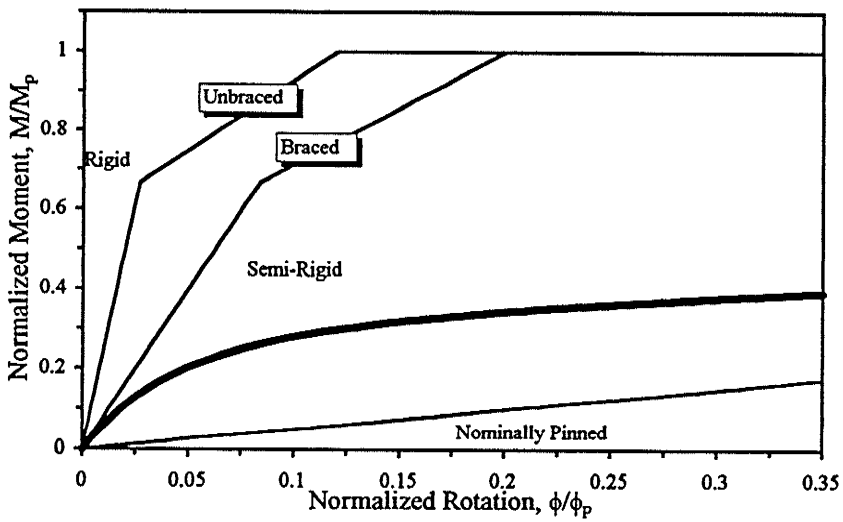


Figure A.168 (b) Eurocode3 Classification of Azizinamini: 14S6

Table A.169 M-ϕ data for Azizinamini: 14S8 (1985)

Moment, M kN-m	Rotation, ϕ radians	Moment, M kN-m	Rotation, ϕ radians
0	0	148.064	0.0096
6.531	0.0001	152.015	0.0108
13.063	0.0002	155.077	0.0120
19.594	0.0003	158.139	0.0131
26.363	0.0004	159.065	0.0143
33.132	0.0005	161.590	0.0154
39.902	0.0007	164.115	0.0165
46.672	0.0008	166.204	0.0179
52.285	0.0009	168.293	0.0193
57.897	0.0011	170.043	0.0203
64.223	0.0013	171.794	0.0213
70.549	0.0014	173.545	0.0223
75.450	0.0016	175.357	0.0234
80.352	0.0018	177.170	0.0245
86.414	0.0021	178.982	0.0255
92.476	0.0024	180.624	0.0269
98.272	0.0027	182.266	0.0282
104.068	0.0030	183.529	0.0287
109.244	0.0034		
114.421	0.0039		
119.781	0.0045		
125.141	0.0051		
130.237	0.0059		
135.332	0.0066		
139.723	0.0075		
144.113	0.0085		

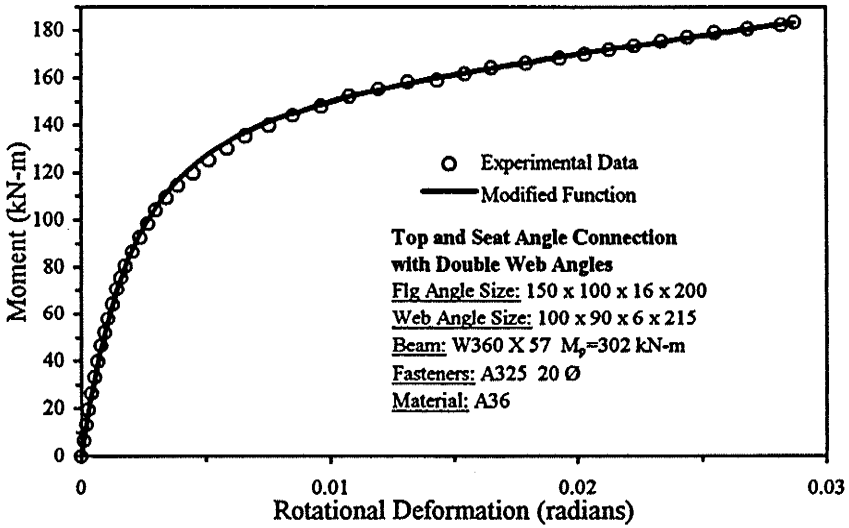


Figure A.169 (a) M-ϕ curve for Azizinamini: 14S8

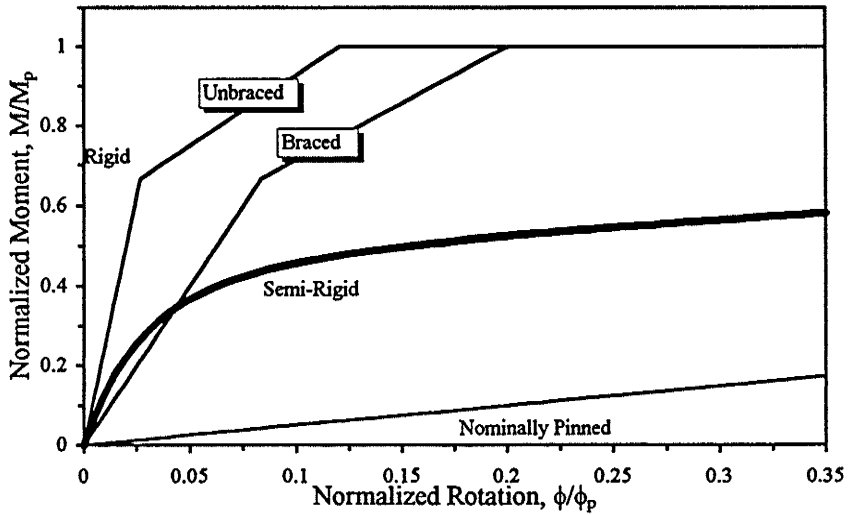


Figure A.169 (b) Eurocode3 Classification of Azizinamini: 14S8

Table A.170 M-ϕ data for Azizinamini: 14S9 (1985)

Moment, M kN-m	Rotation, ϕ radians	Moment, M kN-m	Rotation, ϕ radians
0	0	104.244	0.0129
4.274	0.0002	105.694	0.0139
8.549	0.0003	107.144	0.0149
11.932	0.0004	108.684	0.0160
15.315	0.0005	110.224	0.0170
21.194	0.0008	111.233	0.0182
27.251	0.0011	112.241	0.0193
31.883	0.0013	112.443	0.0203
36.515	0.0015	112.645	0.0212
40.345	0.0017	113.472	0.0222
44.175	0.0019	114.299	0.0232
47.829	0.0021	115.930	0.0243
51.483	0.0024	116.577	0.0253
55.494	0.0027	117.224	0.0262
59.505	0.0029	118.313	0.0271
62.893	0.0032	119.402	0.0279
66.281	0.0035	120.493	0.0288
70.921	0.0041	121.584	0.0297
75.561	0.0046		
79.580	0.0052		
83.599	0.0058		
87.716	0.0067		
91.833	0.0077		
96.852	0.0091		
99.914	0.0106		
102.079	0.0117		

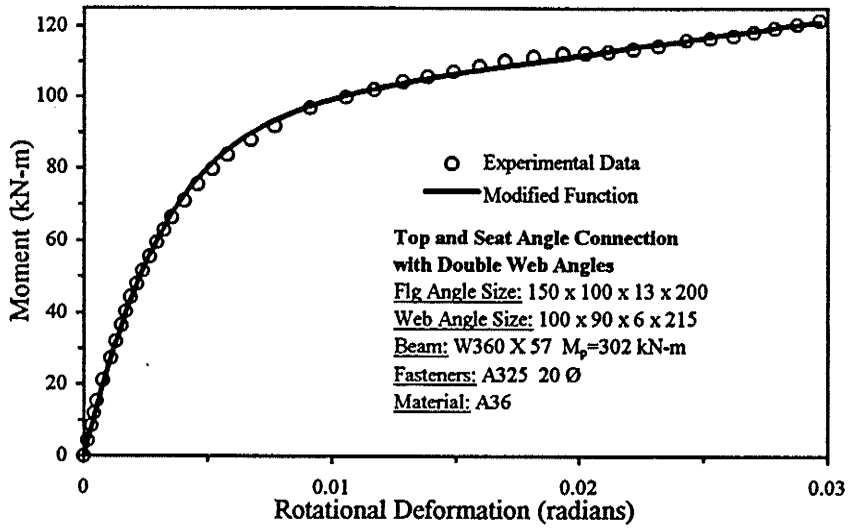


Figure A.170 (a) M-ϕ curve for Azizinamini: 14S9

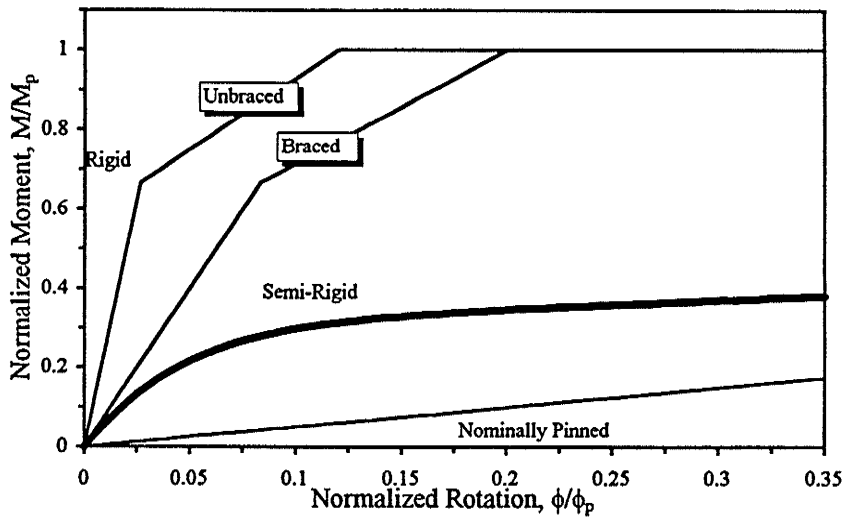


Figure A.170 (b) Eurocode3 Classification of Azizinamini: 14S9

Table A.171 M-ϕ data for Azizinamini: 14WS1 (1985)

Moment, M kN-m	Rotation, ϕ radians	Moment, M kN-m	Rotation, ϕ radians
0	0	90.799	0.0148
4.295	0.0000	92.596	0.0160
8.590	0.0000	94.392	0.0171
12.885	0.0000	95.920	0.0181
16.043	0.0003	97.449	0.0192
19.202	0.0005	99.517	0.0206
23.561	0.0008	100.600	0.0216
28.454	0.0012	101.682	0.0225
33.439	0.0017	103.029	0.0233
38.246	0.0022	104.376	0.0242
41.316	0.0025	106.267	0.0256
44.386	0.0027	106.726	0.0265
47.192	0.0031	107.185	0.0273
49.998	0.0035	108.276	0.0288
55.252	0.0042	109.136	0.0297
59.975	0.0050	109.996	0.0307
65.233	0.0059		
69.692	0.0068		
74.599	0.0080		
77.146	0.0088		
79.692	0.0097		
81.705	0.0105		
83.718	0.0113		
85.509	0.0121		
87.300	0.0129		
89.049	0.0138		

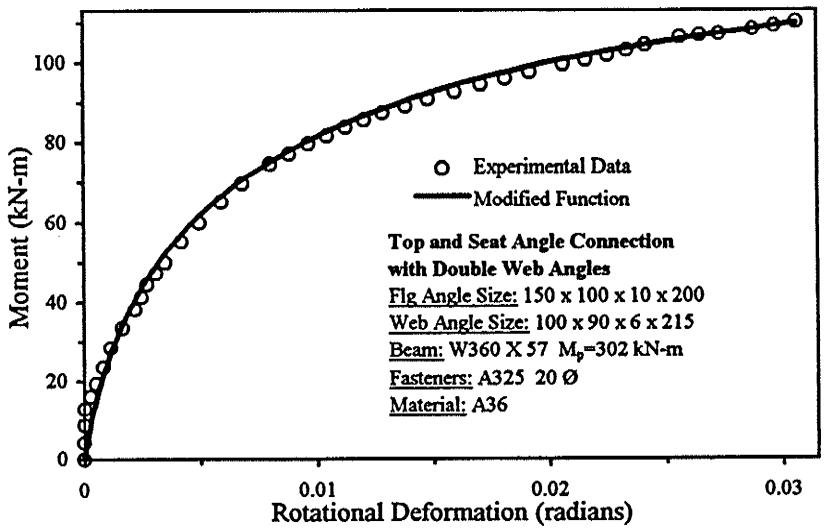


Figure A.171 (a) M-ϕ curve for Azizinamini: 14WS1

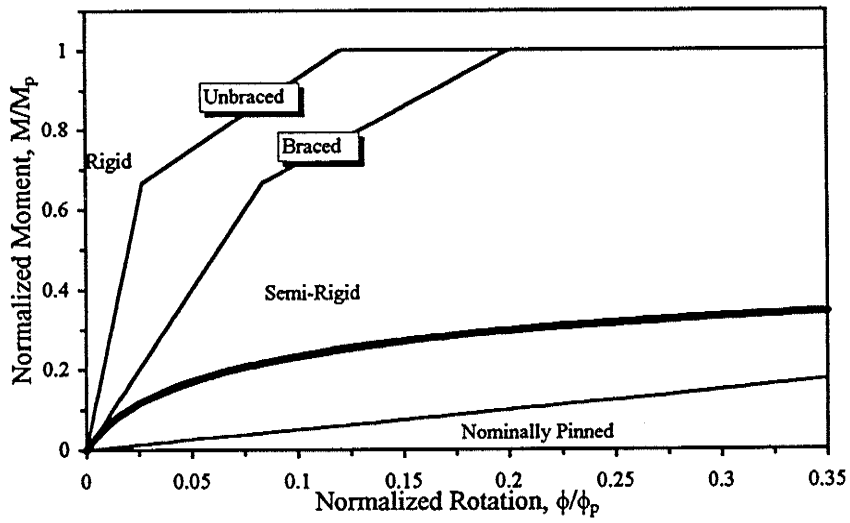


Figure A.171 (b) Eurocode3 Classification of Azizinamini: 14WS1

Table A.172 M-ϕ data for Azizinamini: 14WS2 (1985)

Moment, M kN-m	Rotation, ϕ radians	Moment, M kN-m	Rotation, ϕ radians
0	0	120.582	0.0122
6.439	0.0000	123.486	0.0133
12.878	0.0001	125.189	0.0142
16.565	0.0002	126.891	0.0151
20.252	0.0003	128.325	0.0159
24.605	0.0004	129.759	0.0166
28.958	0.0005	130.620	0.0176
33.045	0.0006	131.480	0.0186
37.132	0.0007	132.960	0.0195
42.331	0.0010	134.441	0.0204
47.531	0.0012	135.432	0.0212
52.729	0.0014	136.424	0.0221
57.928	0.0017	137.725	0.0229
62.329	0.0019	139.027	0.0237
66.729	0.0022	140.106	0.0245
72.510	0.0027	141.185	0.0253
77.091	0.0032	141.913	0.0263
81.672	0.0036	142.640	0.0273
88.788	0.0043	143.461	0.0285
95.552	0.0052		
100.631	0.0062		
106.248	0.0075		
109.461	0.0084		
112.673	0.0093		
115.176	0.0103		
117.678	0.0112		

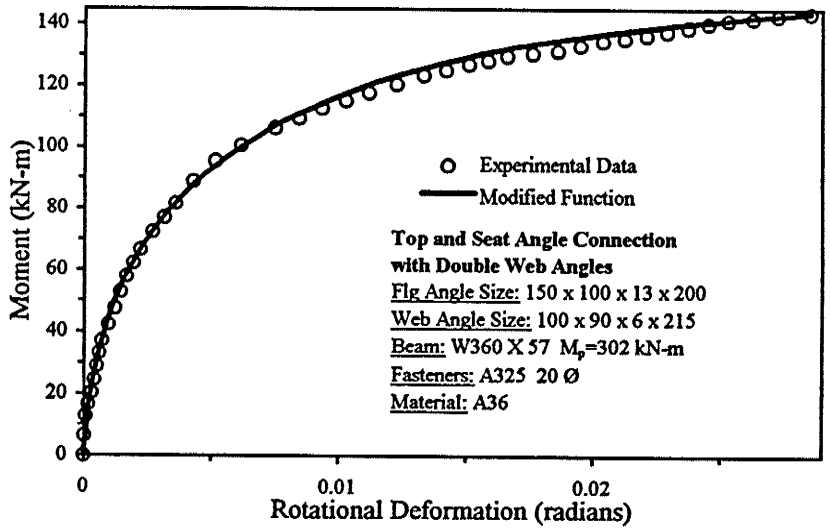


Figure A.172 (a) M-ϕ curve for Azizinamini: 14WS2

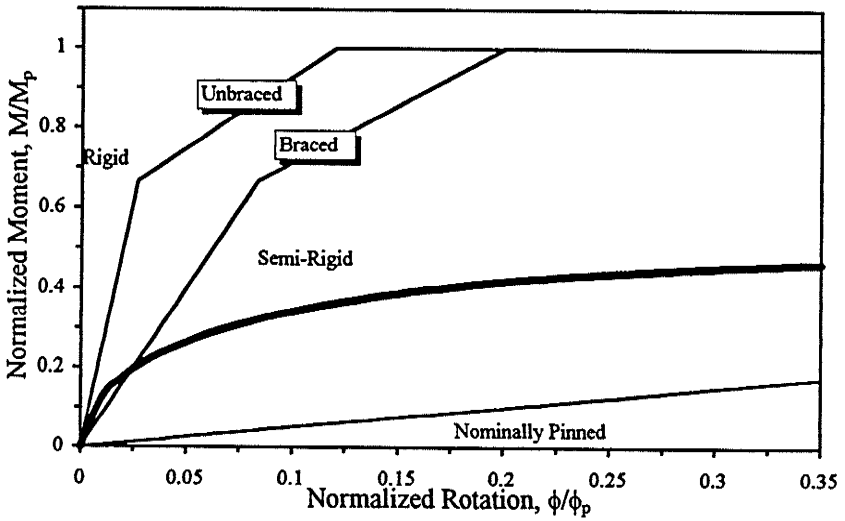


Figure A.172 (b) Eurocode3 Classification of Azizinamini: 14WS2

Table A.173 M-ϕ data for Sommer: Test 5 (1969)

Moment, M kN-m	Rotation, ϕ radians	Moment, M kN-m	Rotation, ϕ radians
0	0	93.664	0.0633
2.102	0.0002	96.376	0.0647
4.836	0.0004	99.087	0.0661
7.559	0.0008	105.641	0.0688
12.993	0.0011	111.177	0.0710
18.416	0.0014	115.470	0.0729
23.896	0.0021	119.764	0.0748
29.377	0.0027	123.719	0.0769
33.444	0.0036	127.674	0.0790
37.511	0.0045	132.758	0.0830
43.782	0.0087	137.842	0.0869
50.053	0.0128	140.666	0.0900
54.177	0.0170	143.490	0.0930
58.300	0.0212	145.185	0.0961
61.388	0.0252	146.880	0.0991
64.476	0.0292		
67.565	0.0332		
70.804	0.0369		
74.043	0.0405		
77.282	0.0442		
79.466	0.0476		
81.650	0.0509		
83.834	0.0543		
86.660	0.0576		
89.372	0.0601		
90.952	0.0616		

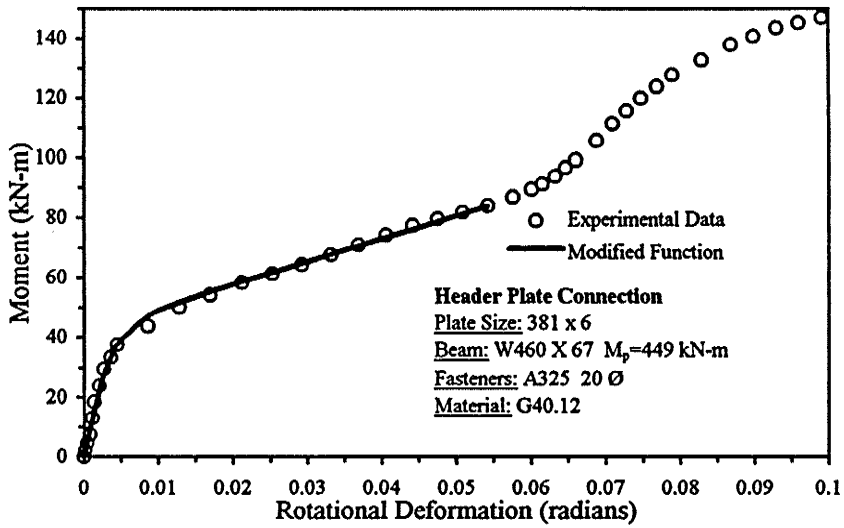


Figure A.172 (a) M-ϕ curve for Sommer: Test 5

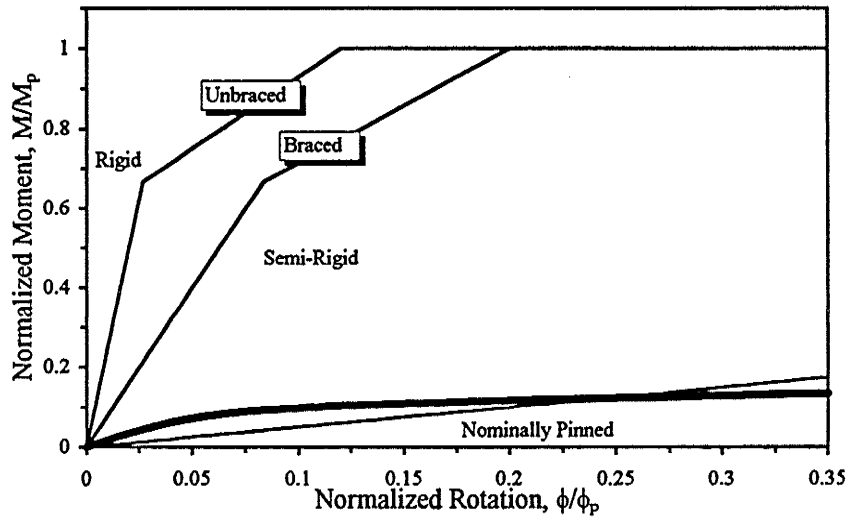


Figure A.172 (b) Eurocode3 Classification of Sommer: Test 5

Table A.174 M-ϕ data for Sommer: Test 6 (1969)

Moment, M kN-m	Rotation, ϕ radians	Moment, M kN-m	Rotation, ϕ radians
0	0	92.309	0.0282
2.960	0.0025	97.845	0.0290
4.598	0.0045	102.195	0.0302
6.237	0.0065	106.544	0.0313
7.869	0.0084	112.025	0.0331
9.502	0.0102	117.505	0.0349
11.682	0.0125	122.589	0.0368
13.863	0.0147	127.674	0.0387
16.043	0.0170	129.933	0.0407
17.851	0.0191	132.192	0.0426
19.659	0.0213	137.277	0.0444
21.467	0.0234	142.361	0.0461
23.839	0.0237	145.751	0.0481
27.116	0.0242	149.140	0.0502
31.974	0.0248	152.530	0.0522
35.703	0.0250	154.225	0.0542
41.126	0.0252	155.919	0.0561
46.776	0.0254	151.400	0.0567
51.577	0.0256	146.203	0.0570
56.379	0.0257	141.006	0.0573
60.785	0.0259	135.808	0.0577
65.192	0.0260	130.611	0.0580
70.615	0.0262	125.413	0.0583
76.038	0.0264		
81.405	0.0269		
86.772	0.0274		

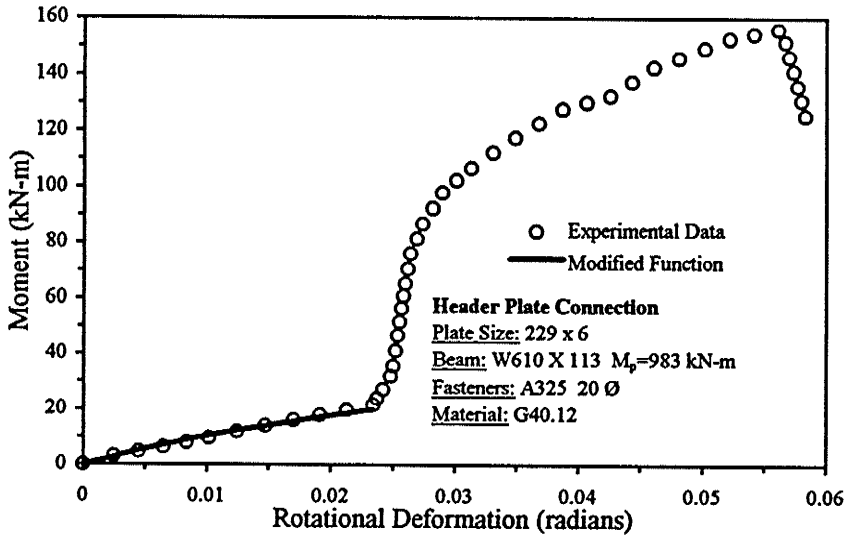


Figure A.174 (a) M-ϕ curve for Sommer: Test 6

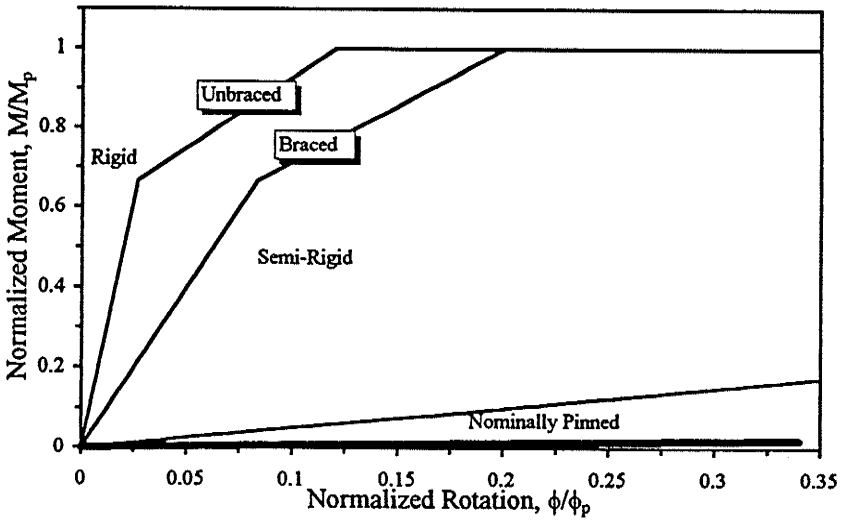


Figure A.174 (b) Eurocode3 Classification of Sommer: Test 6

Table A.175 M-ϕ data for Sommer: Test 7 (1969)

Moment, M kN-m	Rotation, ϕ radians	Moment, M kN-m	Rotation, ϕ radians
0	0	96.112	0.0256
2.972	0.0004	101.611	0.0258
6.260	0.0016	107.110	0.0261
9.548	0.0028	112.307	0.0266
12.852	0.0035	117.505	0.0271
16.157	0.0041	123.154	0.0283
19.998	0.0054	128.803	0.0296
23.839	0.0067	134.453	0.0308
26.579	0.0089	140.102	0.0325
29.320	0.0111	145.751	0.0342
32.060	0.0133	150.835	0.0359
34.800	0.0155	155.919	0.0376
36.438	0.0173	161.568	0.0393
38.075	0.0191	167.217	0.0409
40.787	0.0205	172.867	0.0432
43.499	0.0215	178.517	0.0455
47.905	0.0231	180.212	0.0478
53.442	0.0235	181.906	0.0501
57.227	0.0237	181.341	0.0519
61.012	0.0239	180.776	0.0537
64.854	0.0241	174.561	0.0542
68.695	0.0243	168.347	0.0548
74.175	0.0246	162.133	0.0553
79.654	0.0248	155.919	0.0558
85.134	0.0251		
90.614	0.0253		

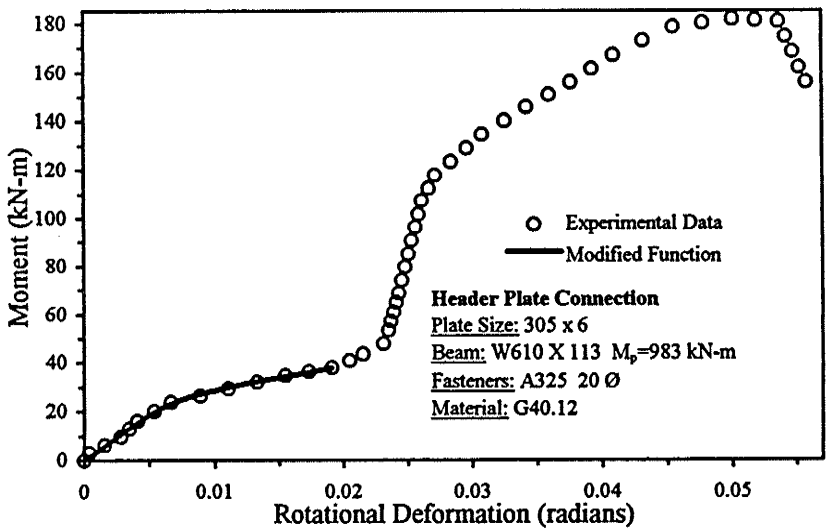


Figure A.175 (a) M-ϕ curve for Sommer: Test 7

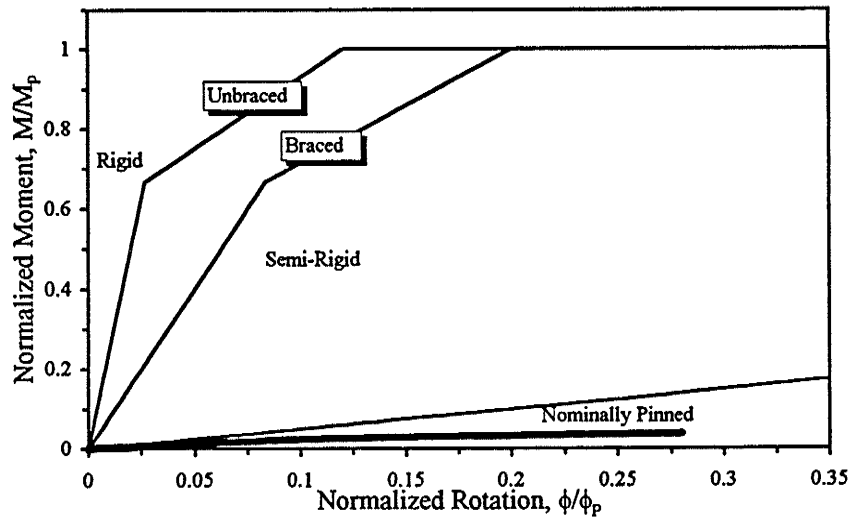


Figure A.175 (b) Eurocode3 Classification of Sommer: Test 7

Table A.176 M-ϕ data for Sommer: Test 8 (1969)

Moment, M kN-m	Rotation, ϕ radians	Moment, M kN-m	Rotation, ϕ radians
0	0	73.892	0.0271
2.983	0.0003	76.660	0.0275
5.050	0.0005	79.428	0.0279
8.429	0.0008	83.524	0.0282
11.976	0.0011	87.620	0.0285
15.704	0.0016	91.716	0.0287
19.433	0.0021	95.812	0.0290
22.202	0.0025	99.389	0.0292
24.970	0.0029	102.967	0.0295
27.625	0.0033	106.544	0.0297
30.280	0.0037	110.330	0.0301
32.991	0.0044	114.115	0.0305
35.703	0.0050	117.881	0.0307
38.414	0.0059	121.647	0.0309
41.126	0.0067	125.413	0.0311
43.838	0.0076	129.933	0.0315
46.549	0.0084	134.452	0.0319
50.617	0.0104	138.972	0.0323
54.684	0.0123	143.491	0.0328
57.792	0.0144	148.010	0.0332
60.899	0.0165	152.530	0.0337
62.933	0.0185	155.355	0.0353
65.588	0.0209	158.179	0.0368
68.242	0.0232	160.439	0.0392
69.429	0.0246		
70.615	0.0259		

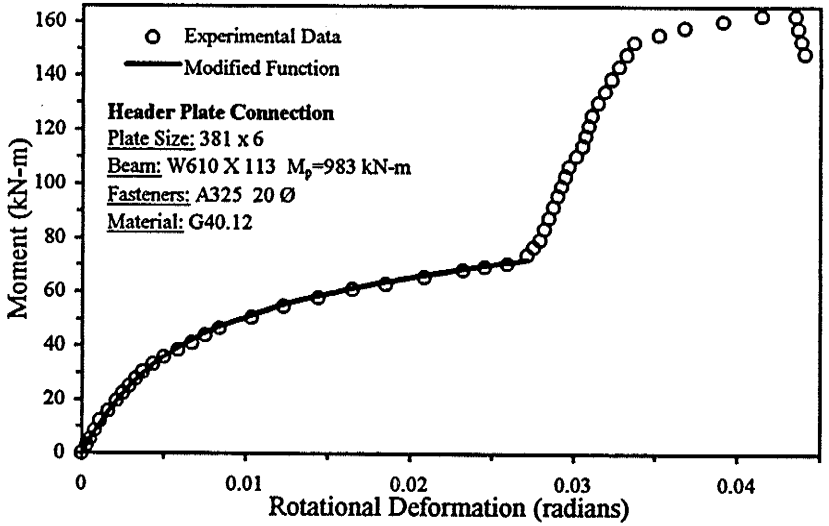


Figure A.176 (a) M-ϕ curve for Sommer: Test 8

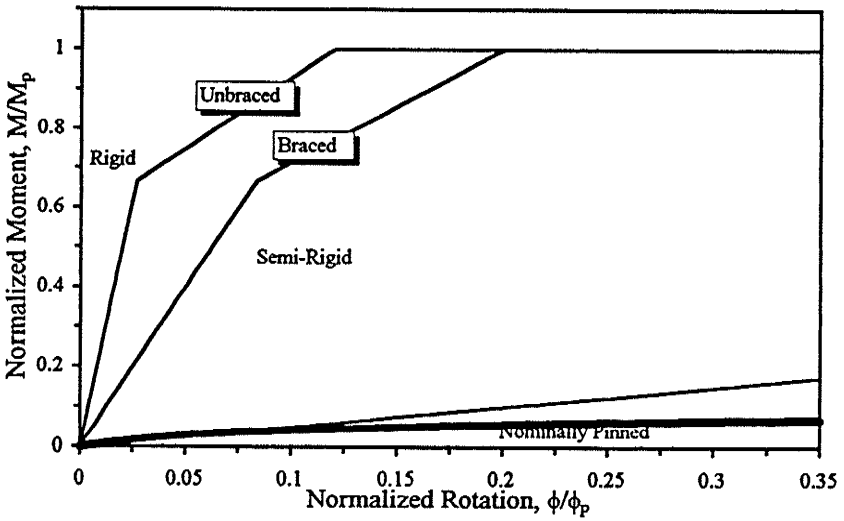


Figure A.176 (b) Eurocode3 Classification of Sommer: Test 8

Table A.177 M-ϕ data for Sommer: Test 9 (1969)

Moment, M kN-m	Rotation, ϕ radians	Moment, M kN-m	Rotation, ϕ radians
0	0	105.980	0.0239
3.006	0.0002	107.845	0.0252
6.294	0.0004	109.709	0.0265
10.779	0.0006	113.041	0.0283
15.140	0.0009	116.374	0.0301
20.676	0.0012	118.634	0.0317
24.461	0.0015	120.894	0.0333
28.246	0.0017	124.849	0.0343
32.144	0.0021	128.803	0.0353
36.042	0.0024	134.452	0.0361
40.336	0.0029	140.101	0.0369
44.630	0.0034	145.751	0.0381
48.471	0.0039	151.400	0.0393
52.312	0.0044	157.614	0.0407
56.210	0.0050	163.828	0.0420
60.108	0.0056	158.743	0.0435
64.458	0.0064	153.659	0.0450
68.808	0.0072	147.727	0.0454
74.401	0.0088	141.796	0.0459
79.993	0.0103	135.864	0.0463
85.190	0.0122	129.932	0.0467
88.844	0.0139		
92.497	0.0155		
96.151	0.0172		
99.427	0.0194		
102.704	0.0217		

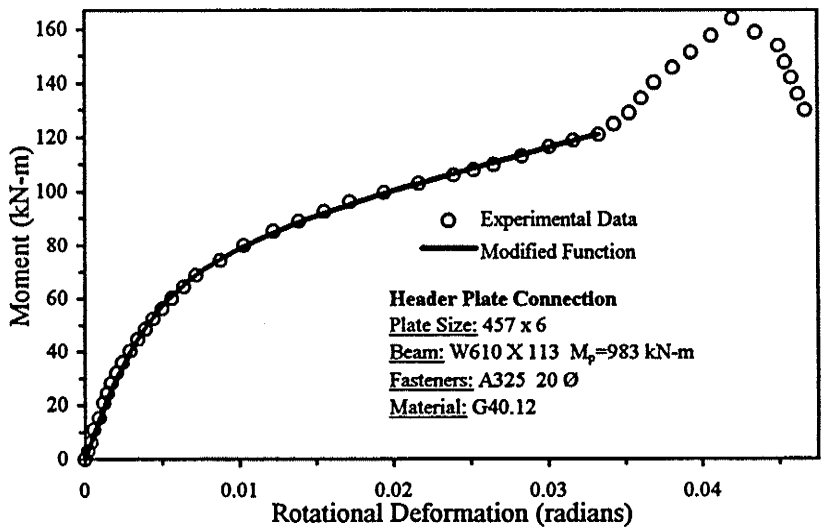


Figure A.177 (a) M-ϕ curve for Sommer: Test 9

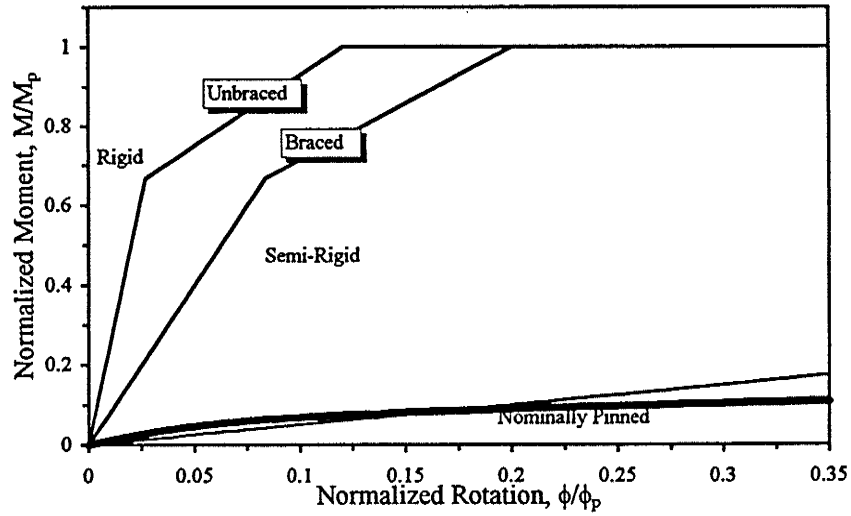


Figure A.177 (b) Eurocode3 Classification of Sommer: Test 9

Table A.178 M-ϕ data for Sommer: Test 10 (1969)

Moment, M kN-m	Rotation, ϕ radians	Moment, M kN-m	Rotation, ϕ radians
0	0	96.414	0.0316
2.746	0.0006	102.816	0.0320
7.118	0.0016	108.466	0.0325
9.853	0.0022	114.115	0.0329
12.541	0.0029	119.200	0.0339
18.077	0.0047	124.284	0.0349
20.789	0.0057	129.932	0.0367
23.500	0.0070	135.582	0.0394
26.212	0.0086	138.407	0.0411
28.924	0.0106	141.232	0.0427
30.336	0.0121	144.056	0.0446
31.749	0.0136	146.880	0.0464
33.105	0.0159	147.106	0.0491
34.461	0.0182	147.332	0.0517
35.817	0.0210	147.559	0.0544
37.173	0.0238	147.785	0.0570
40.448	0.0251	148.011	0.0597
43.160	0.0269		
48.132	0.0282		
52.199	0.0286		
56.267	0.0289		
63.102	0.0294		
69.938	0.0298		
76.774	0.0303		
83.609	0.0307		
90.012	0.0311		

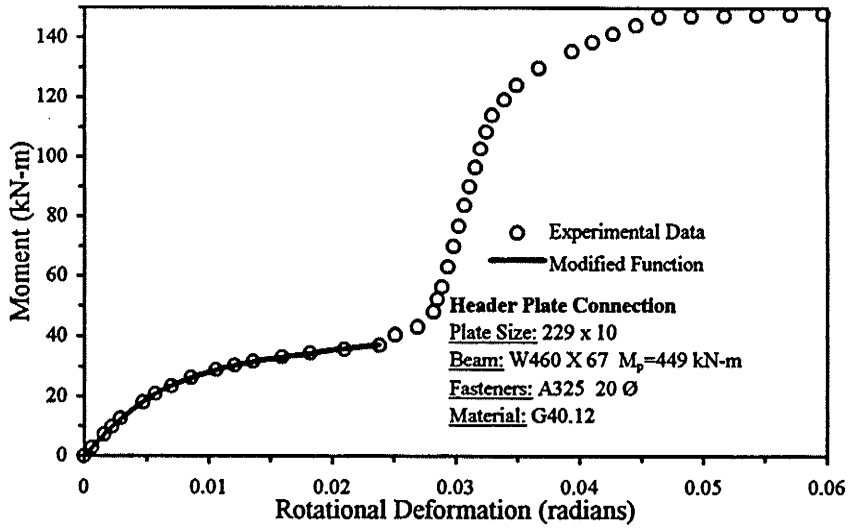


Figure A.178 (a) M-ϕ curve for Sommer: Test 10

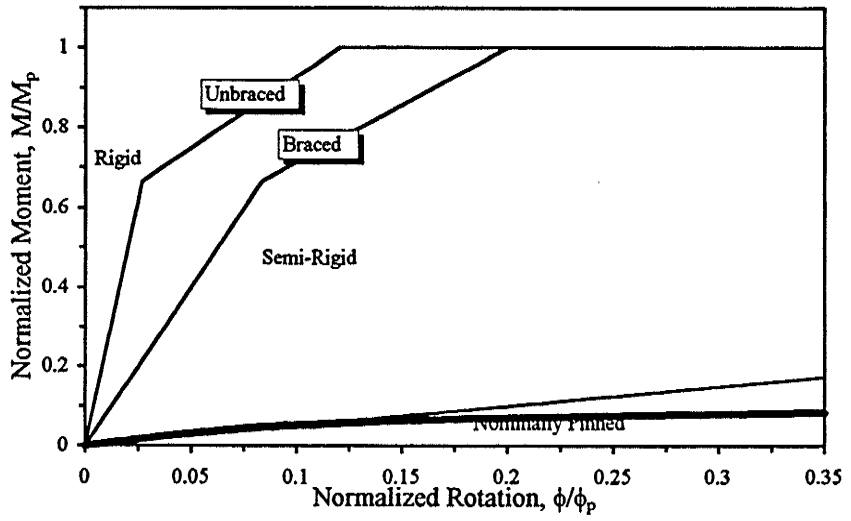


Figure A.178 (b) Eurocode3 Classification of Sommer: Test 10

Table A.179 M-ϕ data for Sommer: Test 11 (1969)

Moment, M kN-m	Rotation, ϕ radians	Moment, M kN-m	Rotation, ϕ radians
0	0	87.450	0.0474
2.135	0.0001	92.874	0.0481
7.819	0.0005	99.314	0.0492
9.186	0.0006	104.850	0.0499
16.609	0.0012	111.404	0.0506
21.920	0.0017	118.973	0.0512
26.269	0.0022	126.543	0.0518
30.618	0.0027	132.569	0.0532
36.042	0.0036	138.595	0.0545
43.725	0.0052	144.621	0.0559
48.132	0.0068	151.777	0.0576
51.408	0.0089	158.932	0.0592
54.684	0.0110	166.088	0.0609
57.961	0.0139	169.478	0.0638
60.334	0.0169	173.244	0.0669
62.707	0.0198	177.010	0.0700
64.684	0.0226	180.776	0.0731
66.662	0.0253	172.867	0.0765
68.092	0.0279		
69.523	0.0305		
70.954	0.0331		
72.837	0.0363		
74.721	0.0396		
76.604	0.0428		
78.129	0.0449		
79.654	0.0469		

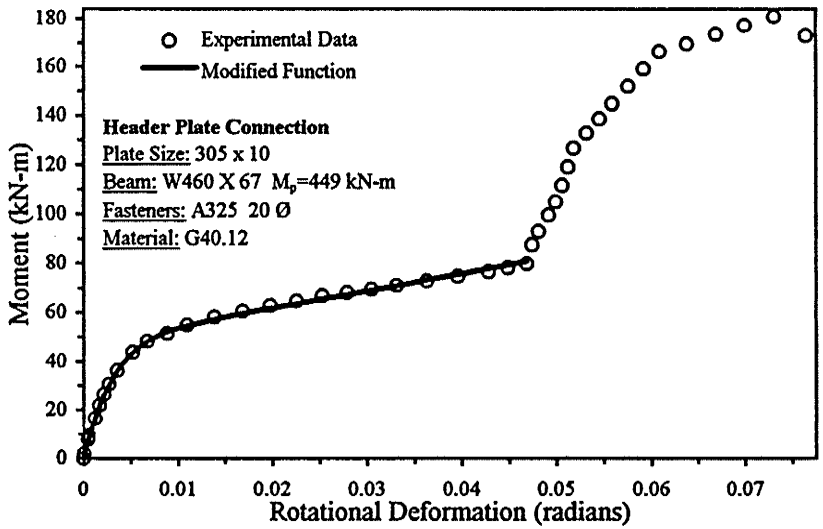


Figure A.179 (a) M-ϕ curve for Sommer: Test 11

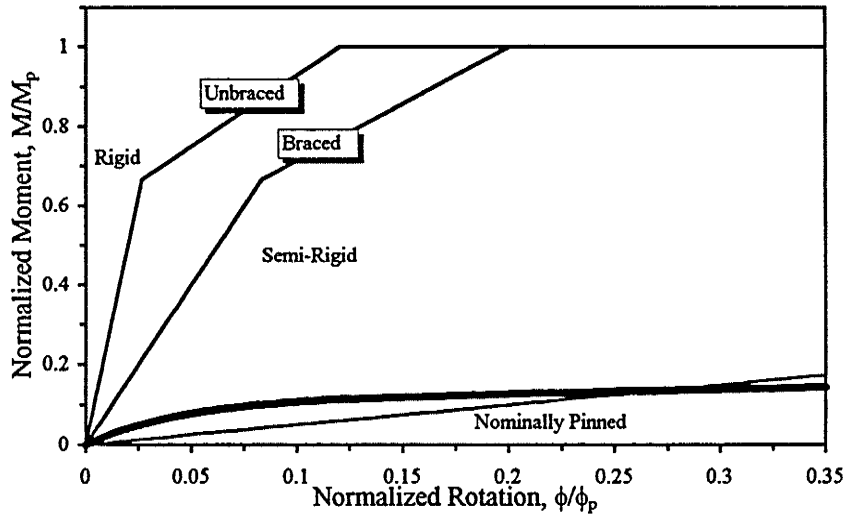


Figure A.179 (b) Eurocode3 Classification of Sommer: Test 11

Table A.180 M-ϕ data for Sommer: Test 12 (1969)

Moment, M kN-m	Rotation, ϕ radians	Moment, M kN-m	Rotation, ϕ radians
0	0	94.154	0.0157
2.135	0.0002	98.071	0.0179
5.141	0.0003	100.726	0.0204
7.870	0.0005	103.381	0.0229
10.598	0.0006	106.037	0.0254
13.208	0.0008	108.692	0.0279
15.818	0.0009	110.048	0.0299
18.530	0.0011	111.404	0.0320
21.242	0.0013	112.759	0.0340
25.648	0.0017	114.115	0.0360
30.054	0.0021	115.810	0.0387
34.122	0.0025	117.505	0.0413
38.189	0.0028	116.375	0.0435
41.748	0.0032	115.245	0.0458
45.307	0.0036	114.115	0.0480
49.036	0.0040	110.019	0.0495
52.764	0.0045	105.923	0.0509
56.493	0.0049	101.828	0.0524
61.163	0.0056	97.732	0.0538
65.833	0.0064		
70.503	0.0071		
73.892	0.0078		
77.282	0.0085		
81.801	0.0100		
86.321	0.0114		
90.238	0.0136		

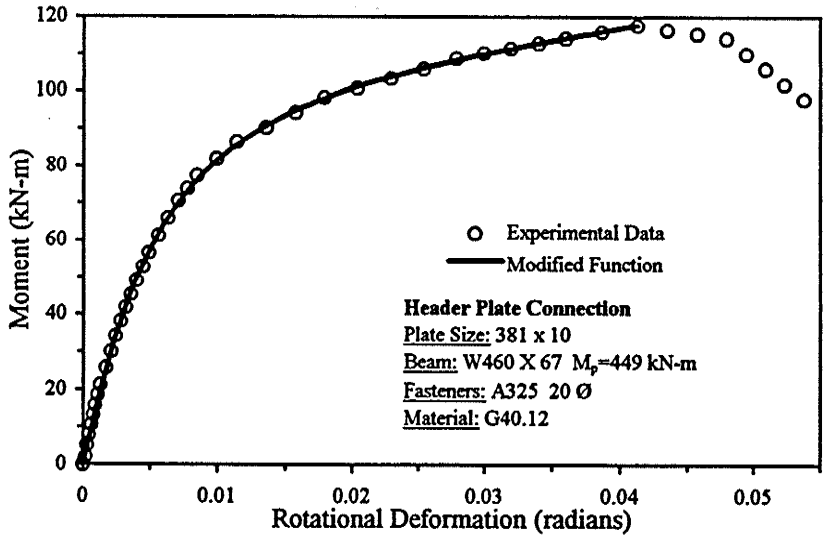


Figure A.180 (a) M-ϕ curve for Sommer: Test 12

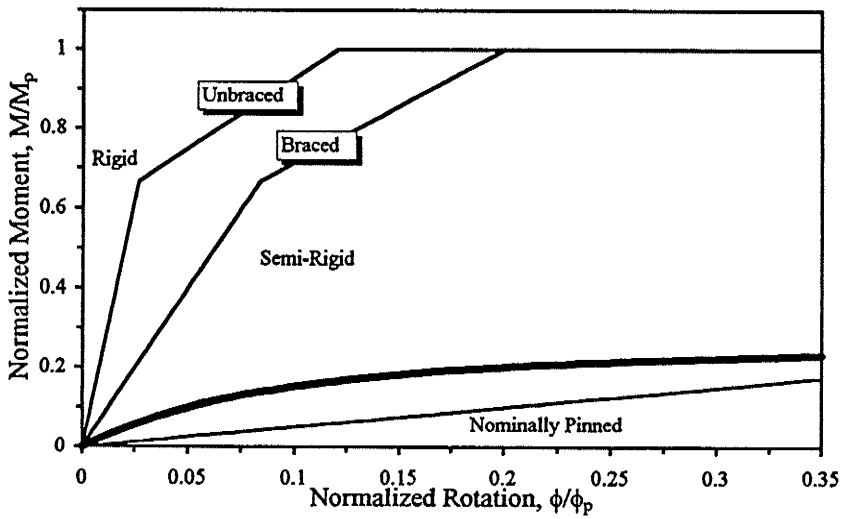


Figure A.180 (b) Eurocode3 Classification of Sommer: Test 12

Table A.181 M-ϕ data for Sommer: Test 13 (1969)

Moment, M kN-m	Rotation, ϕ radians	Moment, M kN-m	Rotation, ϕ radians
0	0	166.088	0.0303
4.192	0.0014	172.867	0.0306
8.383	0.0028	179.646	0.0309
13.785	0.0048	186.425	0.0314
19.208	0.0073	193.204	0.0318
24.631	0.0096	199.983	0.0328
28.247	0.0118	206.763	0.0338
31.862	0.0139	213.542	0.0352
35.478	0.0161	220.321	0.0365
38.613	0.0189	227.100	0.0386
41.748	0.0217	233.879	0.0407
44.884	0.0244	240.658	0.0435
48.019	0.0272	247.437	0.0462
54.459	0.0275	250.073	0.0485
63.950	0.0277	252.709	0.0509
73.441	0.0278	255.346	0.0532
84.287	0.0282	255.346	0.0556
95.134	0.0284		
103.269	0.0286		
111.404	0.0287		
122.024	0.0291		
130.498	0.0293		
138.972	0.0294		
145.751	0.0296		
152.530	0.0298		
159.309	0.0301		

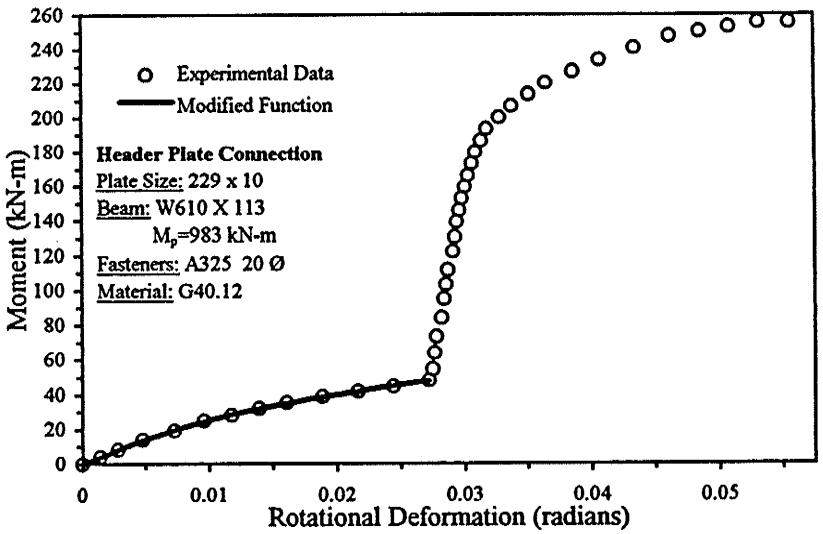


Figure A.181 (a) M-ϕ curve for Sommer: Test 13

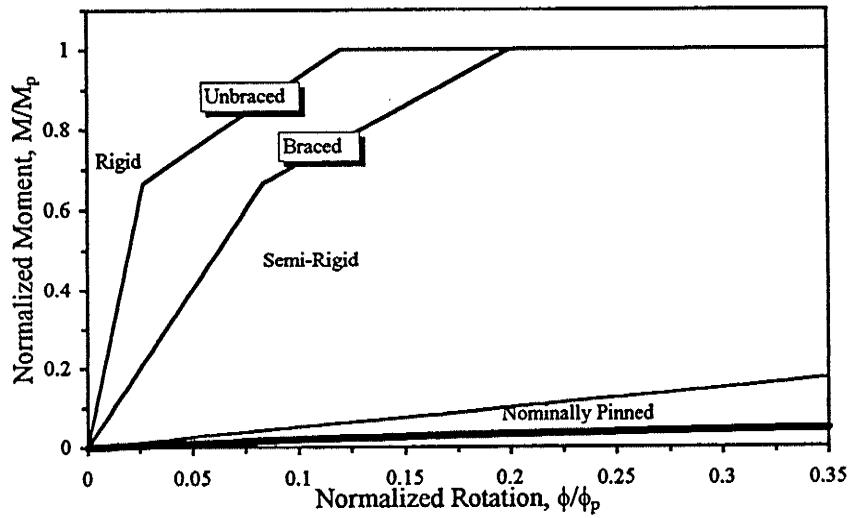


Figure A.181 (b) Eurocode3 Classification of Sommer: Test 13

Table A.182 M-ϕ data for Sommer: Test 14 (1969)

Moment, M kN-m	Rotation, ϕ radians	Moment, M kN-m	Rotation, ϕ radians
0	0	209.023	0.0360
13.897	0.0023	218.061	0.0364
22.145	0.0038	227.100	0.0368
30.393	0.0049	235.574	0.0372
44.064	0.0070	244.048	0.0375
50.900	0.0087	254.781	0.0387
57.735	0.0104	265.514	0.0398
61.388	0.0123	276.813	0.0421
65.042	0.0143	288.112	0.0444
68.695	0.0162	294.609	0.0471
70.887	0.0185	301.105	0.0499
73.079	0.0209	307.602	0.0526
75.271	0.0232	314.099	0.0553
77.463	0.0256		
79.654	0.0279		
81.067	0.0296		
82.479	0.0312		
92.874	0.0320		
103.833	0.0325		
118.013	0.0330		
132.192	0.0335		
142.926	0.0339		
153.659	0.0342		
167.217	0.0347		
180.776	0.0351		
194.334	0.0356		

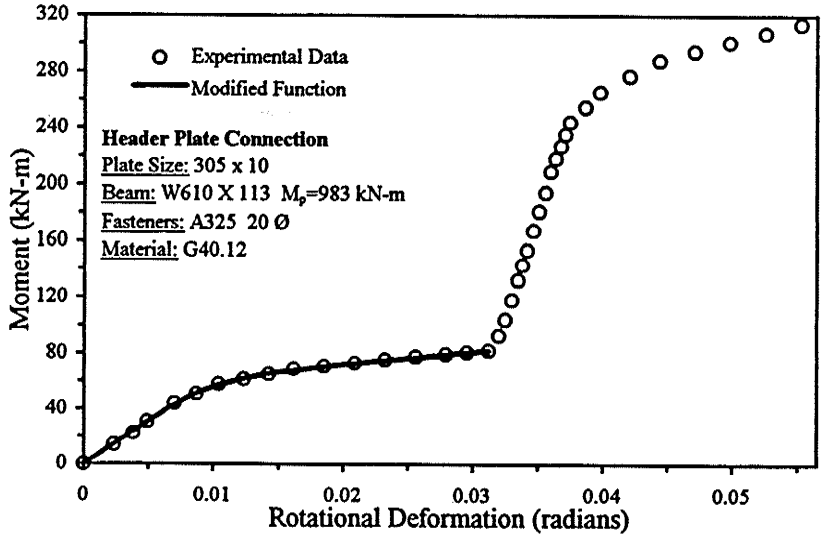


Figure A.182 (a) M-ϕ curve for Sommer: Test 14

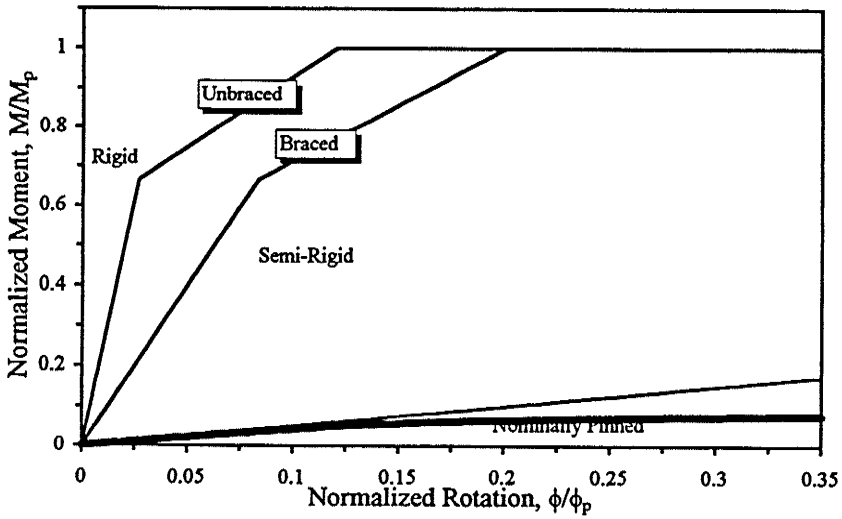


Figure A.182 (b) Eurocode3 Classification of Sommer: Test 14

Table A.183 M-ϕ data for Sommer: Test 15 (1969)

Moment, M kN-m	Rotation, ϕ radians	Moment, M kN-m	Rotation, ϕ radians
0	0	177.763	0.0472
8.519	0.0006	188.685	0.0481
14.010	0.0014	199.983	0.0498
24.856	0.0027	211.281	0.0515
35.817	0.0038	220.321	0.0540
44.008	0.0050	229.360	0.0564
52.199	0.0061	238.963	0.0596
60.390	0.0092	248.567	0.0628
68.581	0.0122	255.346	0.0658
71.881	0.0154	262.125	0.0688
75.180	0.0186	265.514	0.0720
78.479	0.0219	268.904	0.0752
81.778	0.0251		
85.078	0.0283		
87.375	0.0317		
89.672	0.0351		
91.969	0.0385		
95.924	0.0408		
101.460	0.0413		
108.917	0.0420		
116.374	0.0427		
125.413	0.0434		
134.453	0.0441		
145.186	0.0447		
155.919	0.0453		
166.841	0.0462		

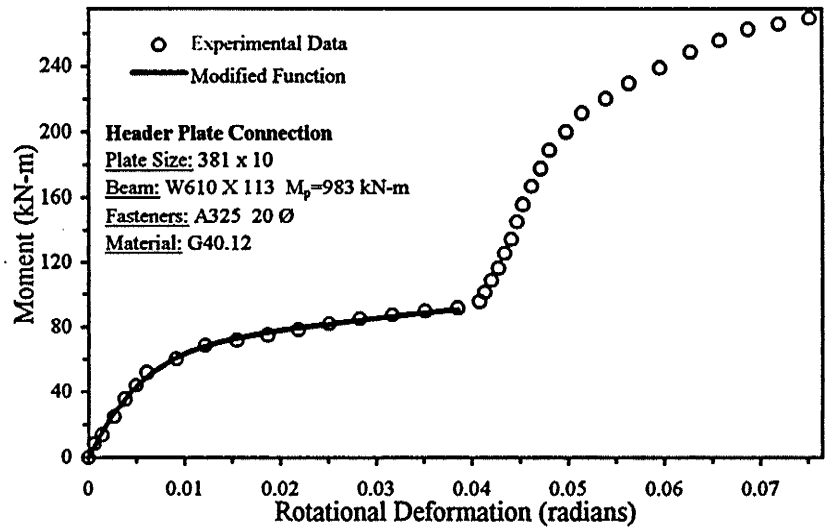


Figure A.183 (a) M-ϕ curve for Sommer: Test 15

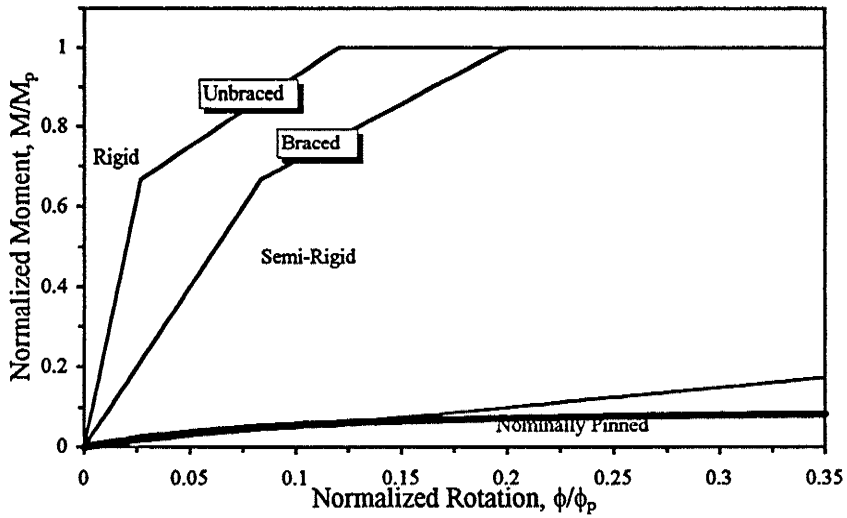


Figure A.183 (b) Eurocode3 Classification of Sommer: Test 15

Table A.184 M-ϕ data for Sommer: Test 16 (1969)

Moment, M kN-m	Rotation, ϕ radians	Moment, M kN-m	Rotation, ϕ radians
0	0	185.860	0.0572
12.428	0.0006	194.334	0.0582
24.856	0.0011	202.808	0.0592
35.817	0.0018	211.281	0.0601
44.008	0.0024	219.191	0.0612
52.199	0.0029	227.100	0.0623
65.870	0.0043	235.574	0.0635
79.542	0.0057	244.048	0.0646
87.733	0.0074	254.781	0.0665
95.924	0.0090	265.514	0.0684
103.118	0.0124	276.248	0.0712
110.311	0.0159	286.982	0.0739
117.505	0.0193	293.196	0.0778
121.742	0.0226	299.410	0.0816
125.979	0.0259		
130.216	0.0292		
134.453	0.0325		
137.842	0.0361		
141.232	0.0397		
144.621	0.0433		
147.634	0.0460		
150.647	0.0488		
153.659	0.0515		
159.309	0.0533		
167.217	0.0547		
177.386	0.0562		

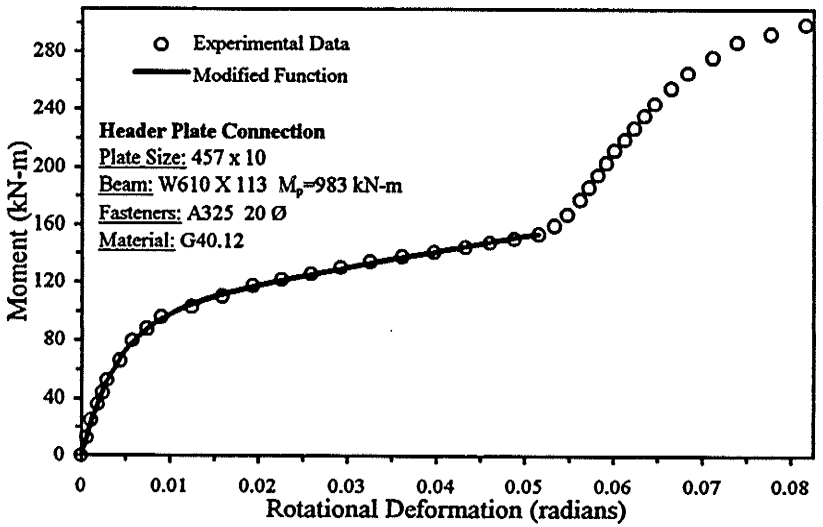


Figure A.184 (a) M-ϕ curve for Sommer: Test 16

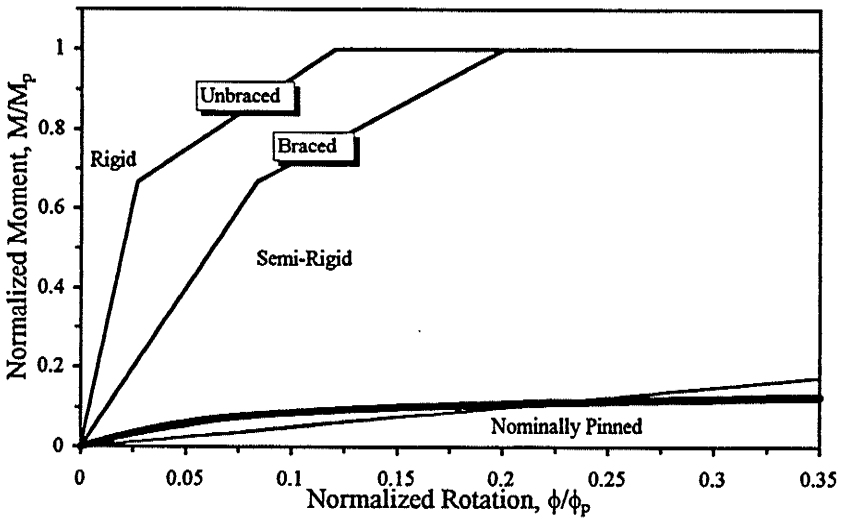


Figure A.184 (b) Eurocode3 Classification of Sommer: Test 16

Table A.185 M-ϕ data for Sommer: Test 17 (1969)

Moment, M kN-m	Rotation, ϕ radians	Moment, M kN-m	Rotation, ϕ radians
0	0	77.875	0.0332
4.203	0.0020	81.971	0.0346
8.406	0.0041	86.066	0.0359
11.152	0.0052	90.162	0.0373
13.897	0.0062	93.815	0.0391
16.609	0.0091	97.468	0.0410
19.320	0.0120	101.121	0.0428
20.752	0.0143	104.737	0.0447
22.183	0.0166	108.352	0.0466
23.614	0.0189	111.968	0.0485
25.252	0.0216	114.171	0.0505
26.890	0.0242	116.374	0.0524
29.150	0.0256	119.764	0.0552
33.444	0.0271	121.458	0.0568
36.212	0.0277	123.153	0.0583
38.980	0.0282	118.747	0.0587
41.691	0.0286	114.340	0.0590
44.403	0.0290	109.934	0.0594
48.188	0.0294	105.528	0.0598
51.973	0.0297	101.121	0.0601
55.626	0.0300	96.715	0.0605
59.280	0.0304		
62.933	0.0307		
66.549	0.0311		
70.164	0.0314		
73.780	0.0318		

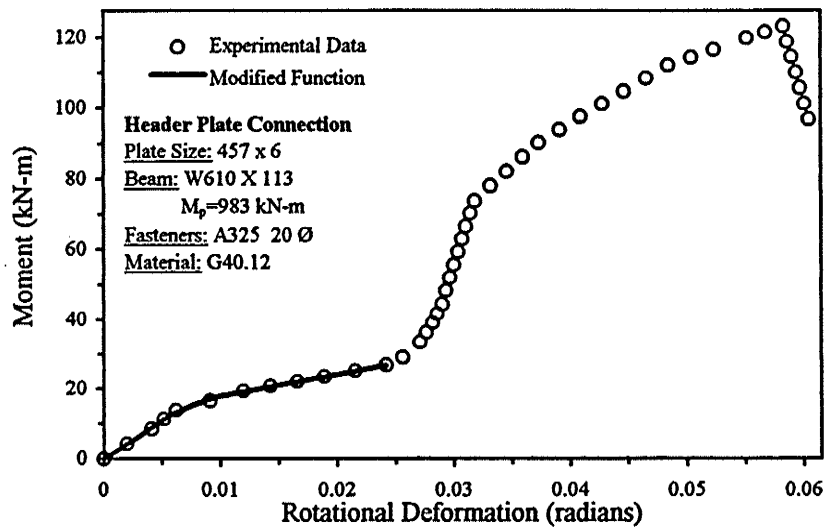


Figure A.185 (a) M-ϕ curve for Sommer: Test 17

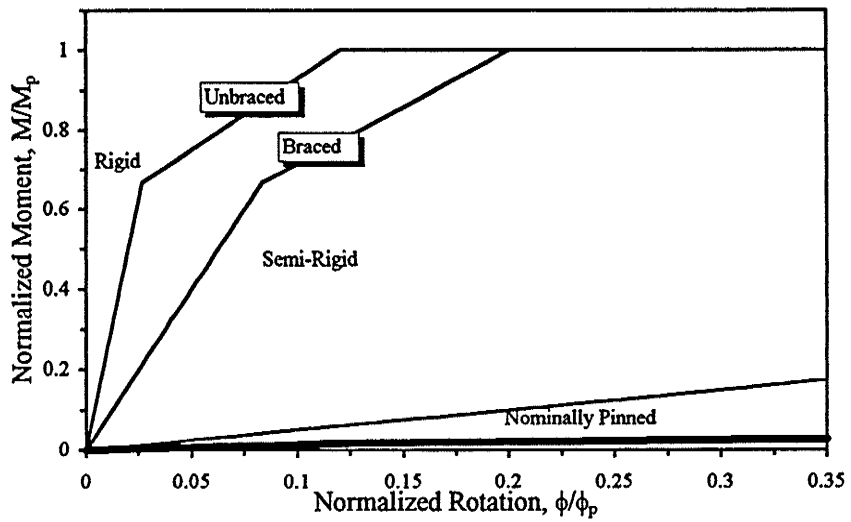


Figure A.185 (b) Eurocode3 Classification of Sommer: Test 17

Table A.186 M-ϕ data for Sommer: Test 18 (1969)

Moment, M kN-m	Rotation, ϕ radians	Moment, M kN-m	Rotation, ϕ radians
0	0	152.530	0.0583
8.406	0.0028	159.309	0.0608
13.897	0.0046	166.088	0.0632
19.320	0.0067	172.867	0.0653
26.890	0.0115	179.646	0.0674
31.296	0.0159	186.425	0.0706
35.703	0.0203	193.204	0.0738
38.414	0.0237	194.899	0.0777
41.126	0.0271	196.594	0.0816
44.403	0.0296	198.289	0.0854
48.697	0.0305	199.983	0.0893
51.973	0.0311	195.465	0.0940
57.453	0.0319	190.380	0.0979
62.933	0.0326	185.296	0.1017
68.356	0.0334		
73.780	0.0341		
79.259	0.0348		
84.739	0.0355		
92.930	0.0381		
101.121	0.0407		
109.313	0.0437		
117.505	0.0466		
125.413	0.0504		
132.192	0.0524		
138.972	0.0543		
145.751	0.0563		

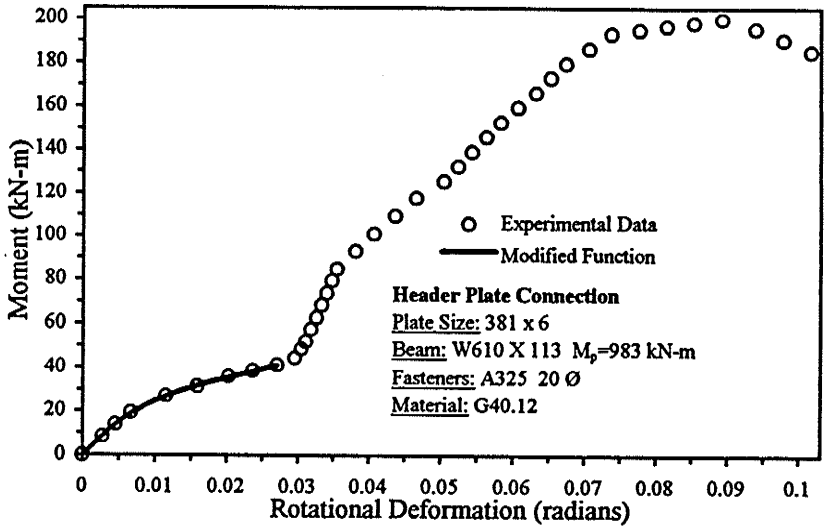


Figure A.186 (a) M-ϕ curve for Sommer: Test 18

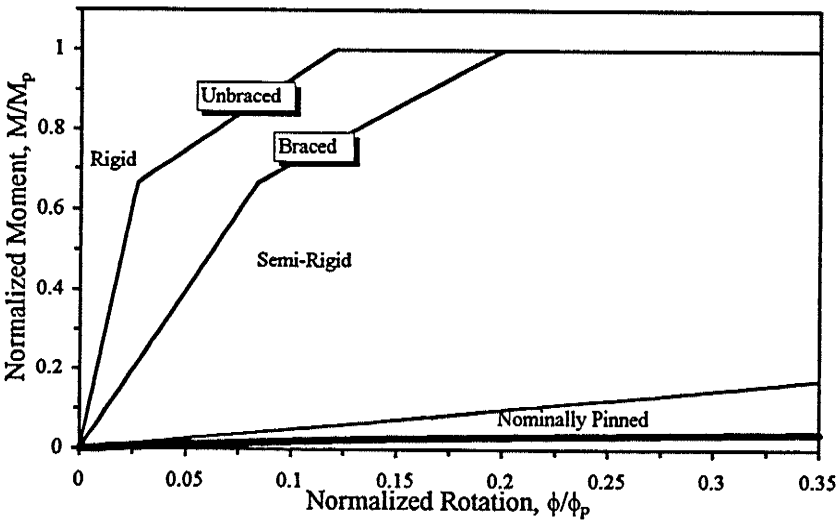


Figure A.186 (b) Eurocode3 Classification of Sommer: Test 18

Table A.187 M-ϕ data for Sommer: Test 19 (1969)

Moment, M kN-m	Rotation, ϕ radians	Moment, M kN-m	Rotation, ϕ radians
0	0	171.172	0.0511
14.010	0.0022	180.776	0.0515
22.202	0.0039	190.379	0.0519
30.393	0.0055	199.983	0.0522
41.353	0.0093	211.282	0.0528
49.601	0.0120	222.581	0.0534
57.849	0.0147	236.139	0.0550
60.589	0.0182	245.742	0.0567
63.328	0.0217	255.346	0.0584
66.068	0.0252	262.502	0.0614
68.808	0.0287	269.658	0.0644
71.520	0.0319	276.814	0.0674
74.231	0.0351	279.073	0.0713
75.587	0.0376	281.333	0.0752
76.943	0.0401	282.463	0.0783
78.355	0.0429	283.593	0.0814
79.767	0.0457		
84.965	0.0469		
87.902	0.0474		
96.151	0.0479		
104.398	0.0483		
112.646	0.0487		
126.373	0.0493		
140.101	0.0499		
150.835	0.0503		
161.569	0.0507		

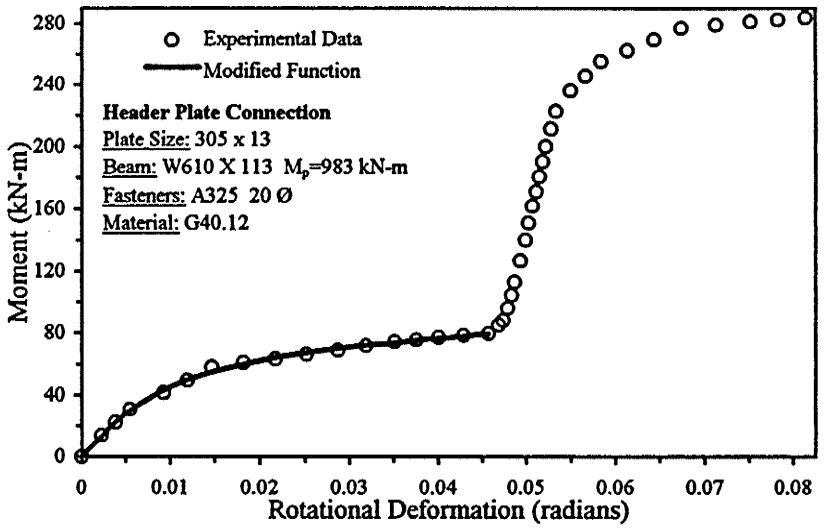


Figure A.187 (a) M-ϕ curve for Sommer: Test 19

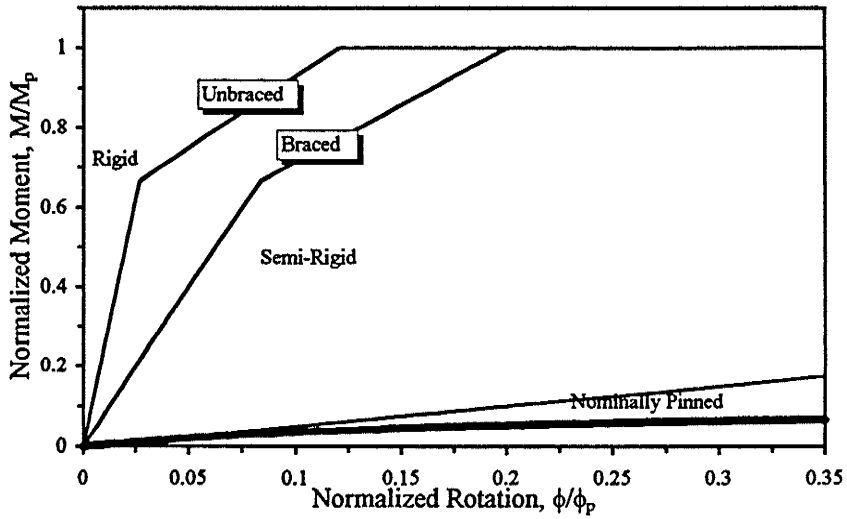


Figure A.187 (b) Eurocode3 Classification of Sommer: Test 19

Table A.188 M-ϕ data for Sommer: Test 20 (1969)

Moment, M kN-m	Rotation, ϕ radians	Moment, M kN-m	Rotation, ϕ radians
0	0	144.621	0.0496
6.949	0.0005	155.919	0.0503
13.897	0.0009	166.653	0.0509
24.856	0.0015	177.386	0.0514
35.703	0.0024	188.120	0.0521
43.895	0.0031	198.854	0.0528
52.087	0.0038	209.776	0.0536
60.278	0.0050	220.697	0.0544
68.469	0.0061	231.619	0.0552
76.604	0.0081	238.963	0.0563
84.739	0.0101	246.308	0.0574
90.200	0.0131	248.850	0.0601
95.660	0.0162	251.392	0.0628
101.121	0.0192	253.934	0.0655
103.861	0.0220	256.476	0.0682
106.601	0.0248		
109.341	0.0276		
112.082	0.0304		
114.793	0.0338		
117.505	0.0372		
119.011	0.0397		
120.517	0.0422		
122.024	0.0447		
124.284	0.0475		
127.674	0.0484		
133.322	0.0489		

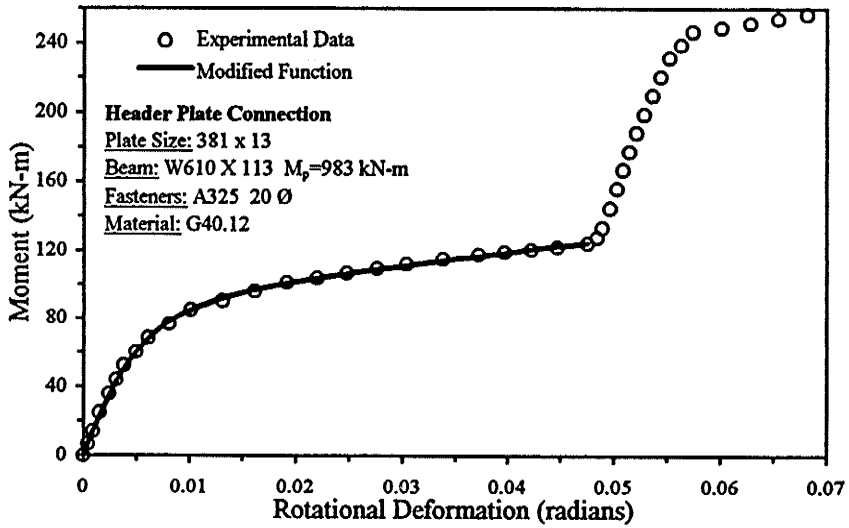


Figure A.188 (a) M-ϕ curve for Sommer: Test 20

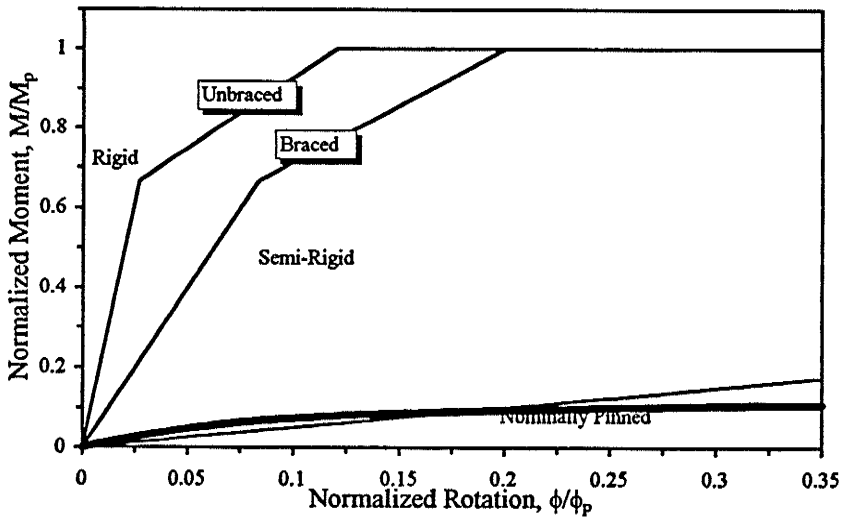


Figure A.188 (b) Eurocode3 Classification of Sommer: Test 20

Table A.189 M-ϕ data for Sommer: Test 25 (1969)

Moment, M kN-m	Rotation, ϕ radians	Moment, M kN-m	Rotation, ϕ radians
0	0	71.256	0.0540
3.232	0.0009	74.834	0.0550
6.463	0.0017	78.411	0.0560
8.757	0.0025	82.065	0.0588
11.050	0.0032	85.718	0.0617
14.790	0.0046	89.372	0.0645
18.530	0.0060	90.539	0.0670
21.242	0.0075	91.706	0.0695
23.953	0.0089	92.874	0.0720
26.665	0.0122	88.957	0.0726
29.377	0.0156	85.040	0.0733
32.088	0.0189	81.123	0.0739
34.800	0.0222		
36.608	0.0258		
38.415	0.0295		
40.223	0.0331		
41.692	0.0360		
43.161	0.0390		
44.630	0.0419		
47.341	0.0453		
50.053	0.0486		
53.329	0.0493		
56.605	0.0500		
60.296	0.0510		
63.987	0.0520		
67.678	0.0530		

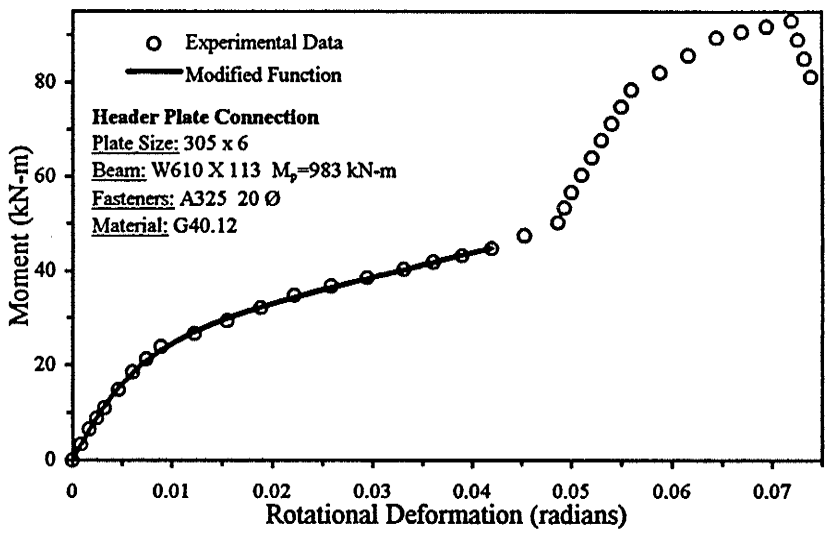


Figure A.189 (a) M-ϕ curve for Sommer: Test 25

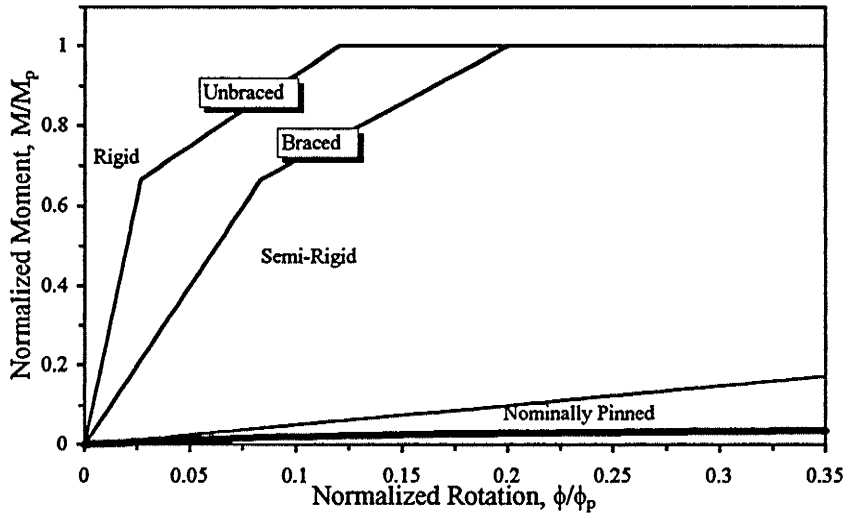


Figure A.189 (b) Eurocode3 Classification of Sommer: Test 25

Table A.190 M-ϕ data for Sommer: Test 26 (1969)

Moment, M kN-m	Rotation, ϕ radians	Moment, M kN-m	Rotation, ϕ radians
0	0	54.854	0.0314
1.915	0.0006	57.396	0.0333
3.830	0.0012	59.938	0.0351
5.745	0.0019	62.480	0.0369
7.660	0.0025	65.022	0.0388
10.327	0.0048	67.565	0.0406
12.993	0.0071	69.147	0.0427
14.077	0.0099	70.729	0.0447
15.162	0.0127	72.198	0.0477
16.247	0.0156	73.667	0.0508
17.331	0.0184	75.135	0.0538
18.416	0.0212	74.684	0.0564
21.242	0.0239	74.232	0.0589
23.237	0.0247	73.780	0.0615
25.233	0.0254	71.313	0.0617
27.229	0.0262	68.846	0.0618
29.941	0.0266	66.379	0.0620
32.652	0.0270	63.912	0.0622
35.176	0.0273	61.445	0.0623
37.699	0.0276	58.978	0.0625
40.223	0.0279		
42.641	0.0282		
45.059	0.0286		
47.476	0.0289		
49.894	0.0293		
52.312	0.0296		

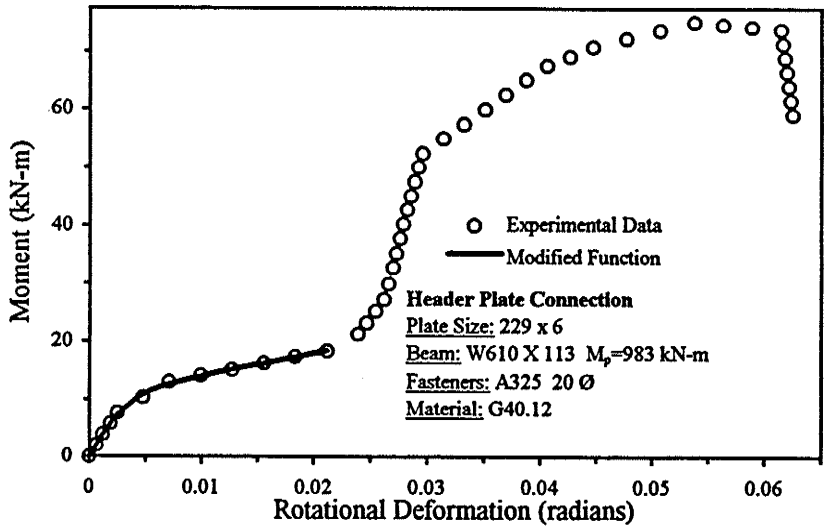


Figure A.190 (a) M-ϕ curve for Sommer: Test 26

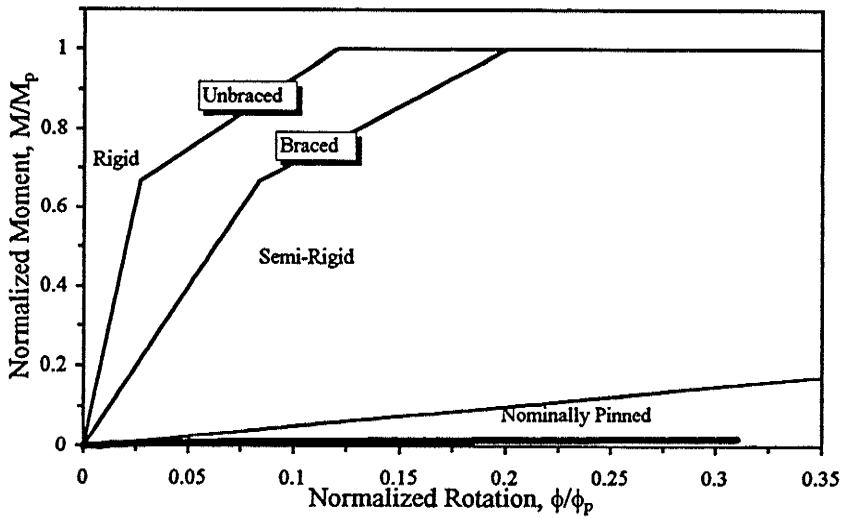


Figure A.190 (b) Eurocode3 Classification of Sommer: Test 26

Table A.191 M-ϕ data for Sommer: Test 27 (1969)

Moment, M kN-m	Rotation, ϕ radians	Moment, M kN-m	Rotation, ϕ radians
0	0	32.879	0.0488
1.167	0.0006	34.234	0.0503
2.335	0.0013	35.138	0.0542
3.502	0.0019	36.042	0.0580
4.670	0.0026	36.946	0.0619
5.838	0.0032	37.511	0.0659
7.006	0.0039	38.075	0.0699
8.361	0.0051	38.641	0.0747
9.717	0.0063	39.206	0.0794
11.073	0.0075	39.460	0.0832
12.429	0.0087	39.715	0.0871
13.898	0.0116	39.969	0.0909
15.366	0.0146	40.223	0.0947
16.835	0.0175	38.867	0.0961
17.551	0.0215	37.511	0.0974
18.266	0.0254	36.156	0.0988
18.981	0.0294	34.800	0.1001
20.450	0.0316	33.444	0.1015
21.919	0.0338		
23.388	0.0360		
24.744	0.0381		
26.100	0.0401		
27.455	0.0422		
28.811	0.0442		
30.167	0.0457		
31.523	0.0473		

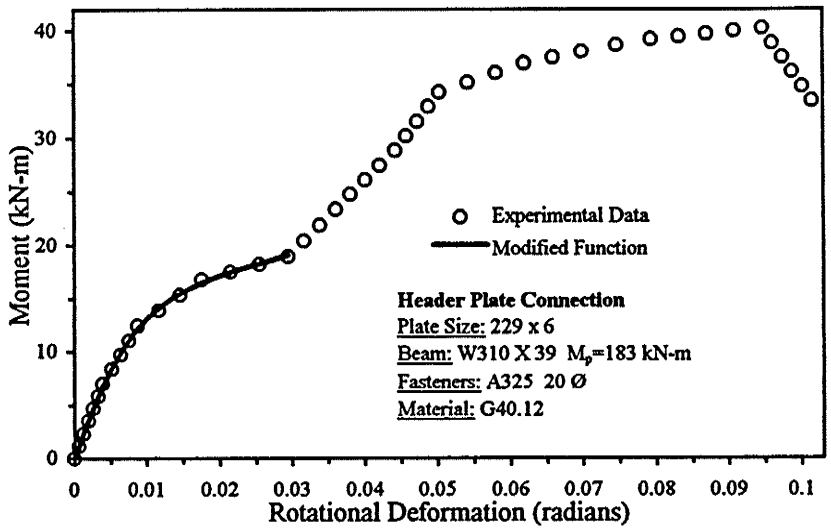


Figure A.191 (a) M-ϕ curve for Sommer: Test 27

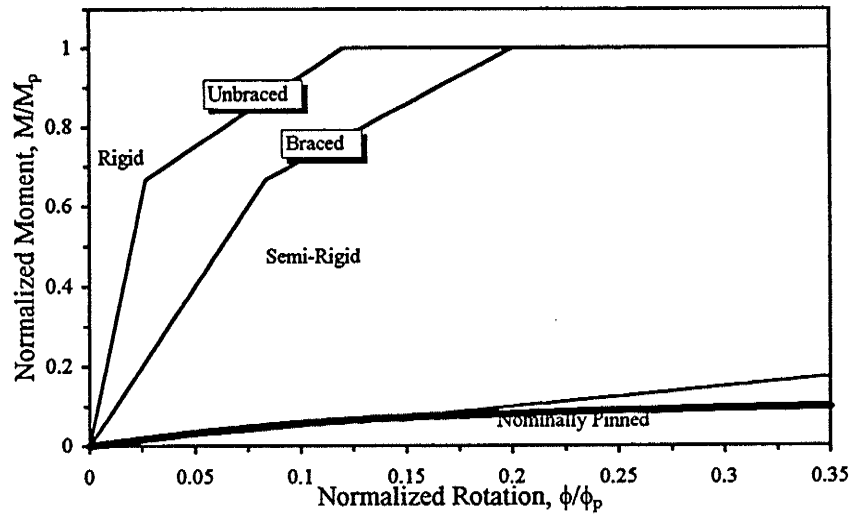


Figure A.191 (b) Eurocode3 Classification of Sommer: Test 27

Table A.192 M-ϕ data for Sommer: Test 28 (1969)

Moment, M kN-m	Rotation, ϕ radians	Moment, M kN-m	Rotation, ϕ radians
0	0	38.603	0.0928
1.548	0.0025	39.695	0.0973
2.774	0.0076	40.787	0.1018
4.000	0.0127	41.889	0.1065
5.225	0.0178	42.990	0.1113
6.451	0.0229	44.092	0.1160
7.107	0.0271	45.194	0.1207
7.762	0.0312	45.194	0.1250
8.633	0.0370		
10.022	0.0386		
11.412	0.0402		
13.558	0.0415		
15.704	0.0427		
17.512	0.0437		
19.320	0.0448		
21.128	0.0458		
22.973	0.0488		
24.819	0.0519		
26.665	0.0549		
28.303	0.0588		
29.941	0.0626		
31.579	0.0682		
33.218	0.0737		
35.364	0.0777		
36.438	0.0830		
37.511	0.0883		

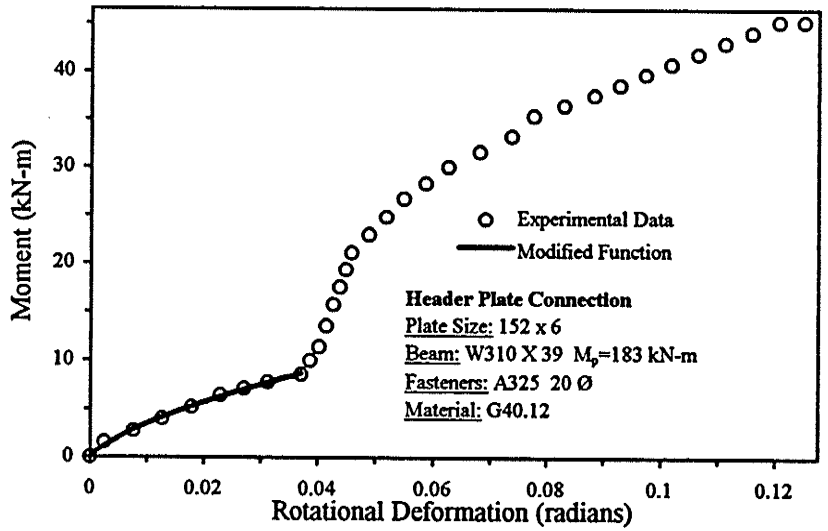


Figure A.192 (a) M-ϕ curve for Sommer: Test 28

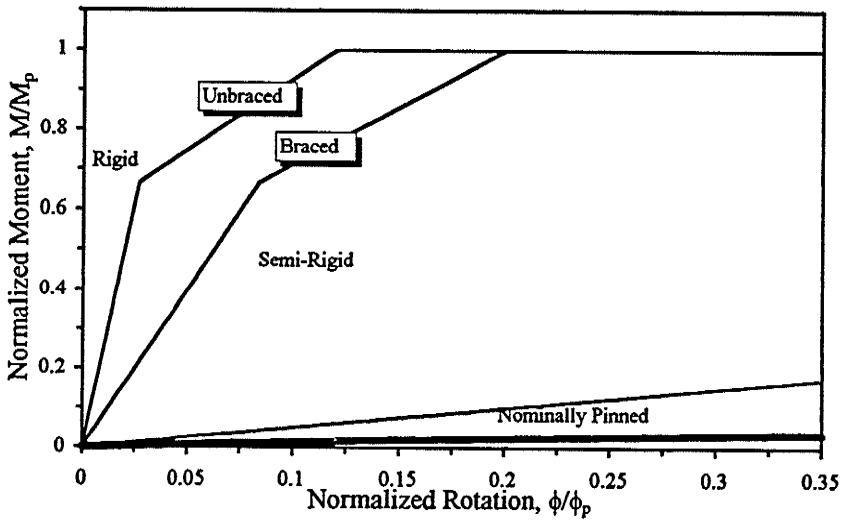


Figure A.192 (b) Eurocode3 Classification of Sommer: Test 28

Table A.193 M-ϕ data for Ostrander: Test 1 (1970)

Moment, M kN-m	Rotation, ϕ radians	Moment, M kN-m	Rotation, ϕ radians
0	0	56.775	0.0316
2.712	0.0003	57.397	0.0340
5.311	0.0006	58.018	0.0365
7.965	0.0009	58.639	0.0389
10.620	0.0011	59.185	0.0416
13.276	0.0014	59.732	0.0443
15.931	0.0017	60.278	0.0470
18.586	0.0021	60.824	0.0496
21.242	0.0024	61.370	0.0523
23.896	0.0030	61.916	0.0550
26.551	0.0035		
29.206	0.0043		
31.862	0.0051		
34.517	0.0061		
37.173	0.0070		
39.827	0.0084		
42.482	0.0097		
45.137	0.0117		
47.793	0.0136		
49.412	0.0158		
51.031	0.0179		
52.651	0.0201		
53.526	0.0224		
54.402	0.0246		
55.278	0.0269		
56.154	0.0291		

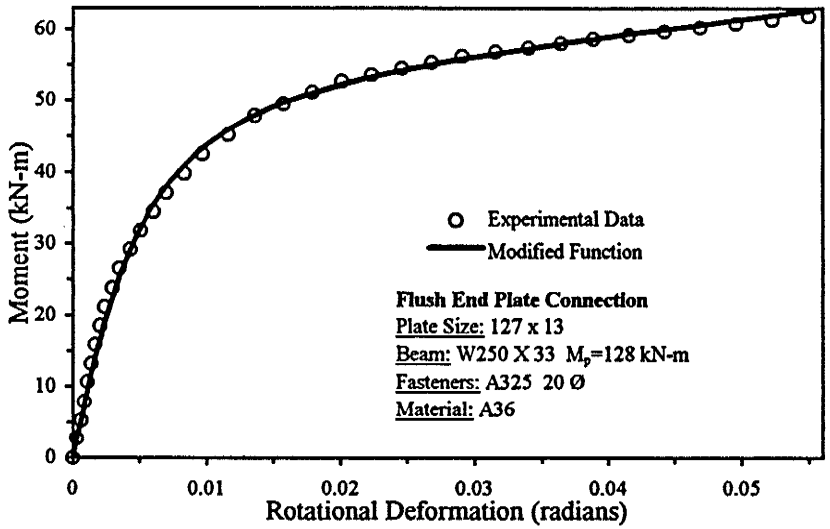


Figure A.193 (a) M-ϕ curve for Ostrander: Test 1

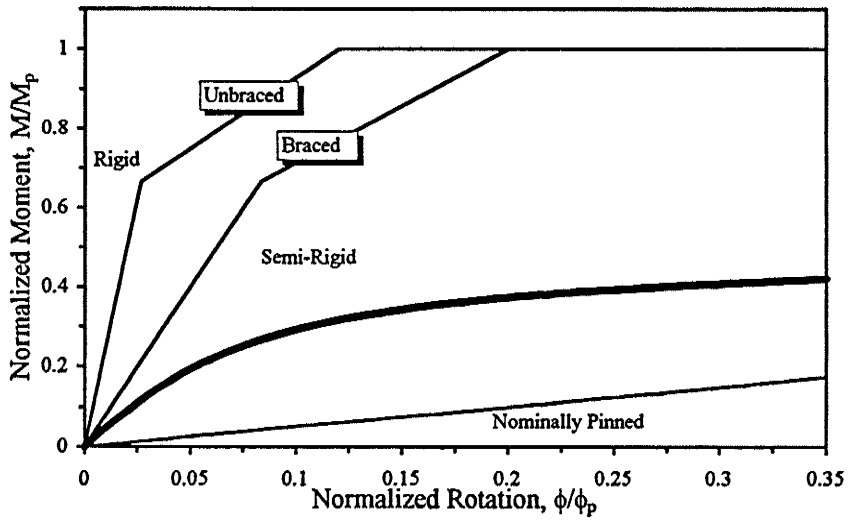


Figure A.193 (b) Eurocode3 Classification of Ostrander: Test 1

Table A.194 M-ϕ data for Ostrander: Test 3 (1970)

Moment, M kN-m	Rotation, ϕ radians	Moment, M kN-m	Rotation, ϕ radians
0	0	52.087	0.0375
2.655	0.0003	52.557	0.0400
5.311	0.0005	53.028	0.0425
7.965	0.0009	53.499	0.0450
10.620	0.0012	53.969	0.0475
13.276	0.0016	54.440	0.0500
15.931	0.0020	54.911	0.0525
18.586	0.0025		
21.242	0.0030		
23.896	0.0037		
26.551	0.0044		
29.206	0.0054		
31.862	0.0063		
34.517	0.0078		
37.173	0.0093		
39.827	0.0118		
42.482	0.0142		
43.810	0.0165		
45.137	0.0188		
46.465	0.0210		
47.793	0.0233		
48.508	0.0257		
49.224	0.0280		
49.940	0.0304		
50.655	0.0328		
51.371	0.0351		

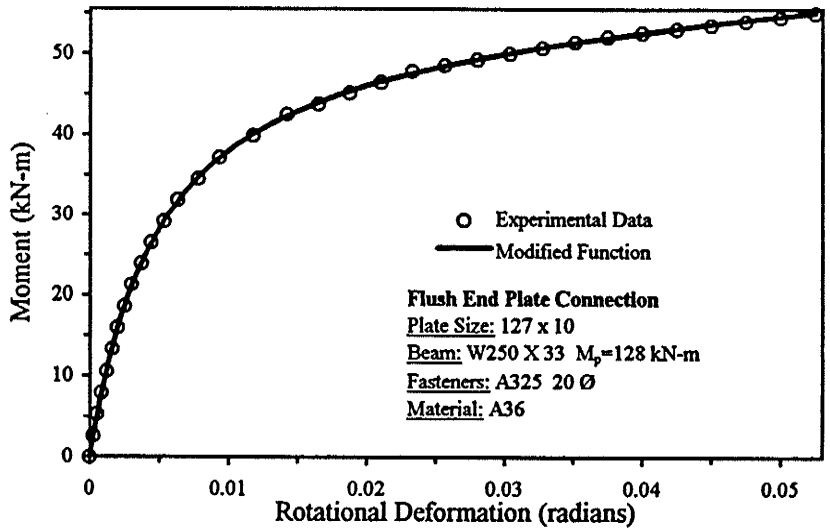


Figure A.194 (a) M-ϕ curve for Ostrander: Test 3

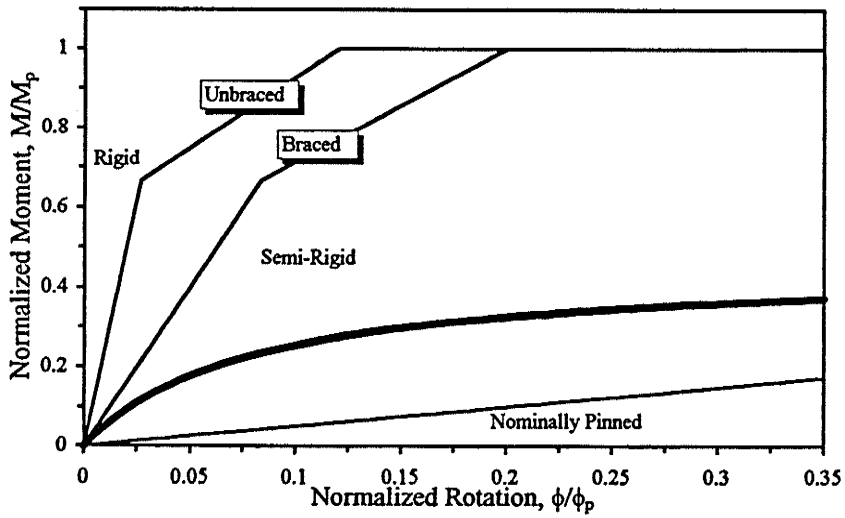


Figure A.194 (b) Eurocode3 Classification of Ostrander: Test 3

Table A.195 M-ϕ data for Ostrander: Test 4 (1970)

Moment, M kN-m	Rotation, ϕ radians	Moment, M kN-m	Rotation, ϕ radians
0	0	26.961	0.0243
1.328	0.0003	27.370	0.0260
2.655	0.0005	27.780	0.0277
3.983	0.0008	28.190	0.0294
5.311	0.0010	28.599	0.0311
6.638	0.0013	29.009	0.0328
7.965	0.0016	29.418	0.0345
9.293	0.0018	29.828	0.0362
10.620	0.0021		
11.948	0.0026		
13.276	0.0030		
14.603	0.0035		
15.931	0.0039		
17.259	0.0053		
18.586	0.0066		
19.914	0.0080		
21.242	0.0093		
21.920	0.0108		
22.597	0.0123		
23.275	0.0137		
23.953	0.0152		
24.473	0.0167		
24.992	0.0182		
25.512	0.0196		
26.031	0.0211		
26.551	0.0226		

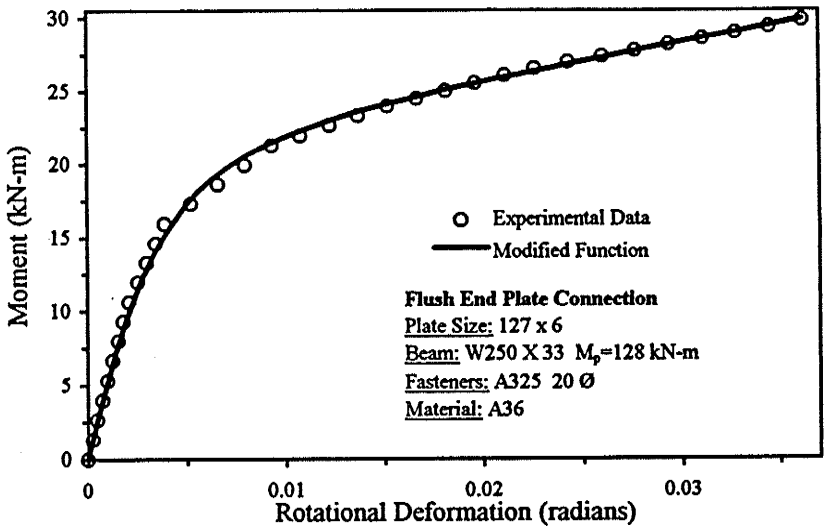


Figure A.195 (a) M-ϕ curve for Ostrander: Test 4

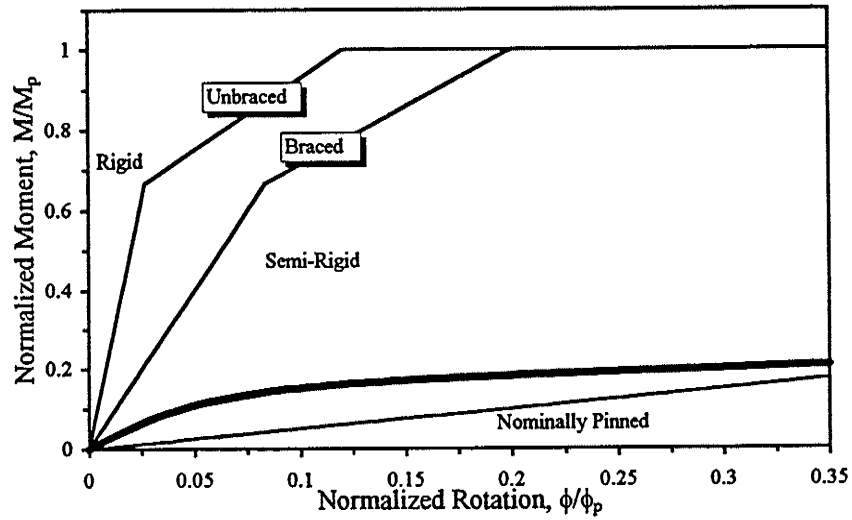


Figure A.195 (b) Eurocode3 Classification of Ostrander: Test 4

Table A.196 M-ϕ data for Ostrander: Test 9 (1970)

Moment, M kN-m	Rotation, ϕ radians	Moment, M kN-m	Rotation, ϕ radians
0	0	60.842	0.0288
2.655	0.0002	61.539	0.0314
5.311	0.0003	62.236	0.0339
7.965	0.0004	62.933	0.0365
10.620	0.0005	63.540	0.0393
13.276	0.0007	64.148	0.0422
15.931	0.0009	64.755	0.0450
18.586	0.0011	65.362	0.0478
21.242	0.0013	65.969	0.0506
23.896	0.0016	66.577	0.0535
26.551	0.0018	67.184	0.0563
29.206	0.0021	67.791	0.0591
31.862	0.0024		
34.517	0.0030		
37.173	0.0035		
39.827	0.0044		
42.482	0.0052		
44.798	0.0064		
47.115	0.0076		
49.883	0.0100		
52.651	0.0124		
54.684	0.0153		
56.718	0.0182		
58.752	0.0211		
59.449	0.0237		
60.146	0.0262		

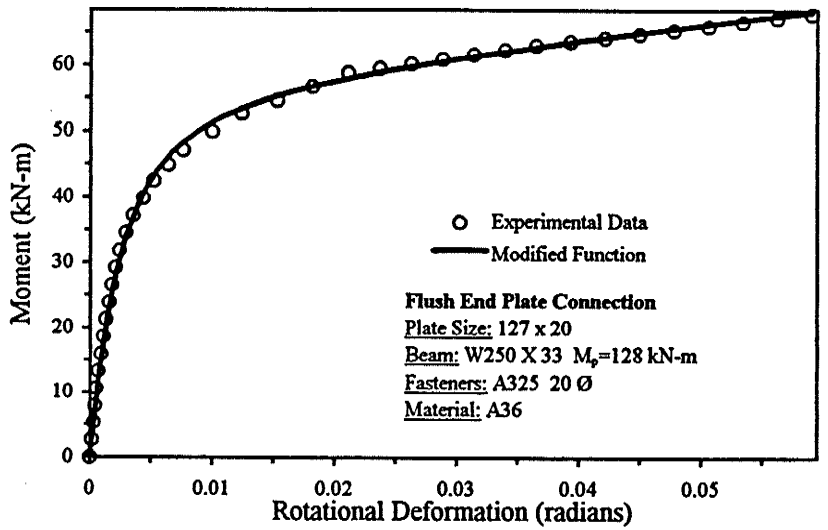


Figure A.196 (a) M-ϕ curve for Ostrander: Test 9

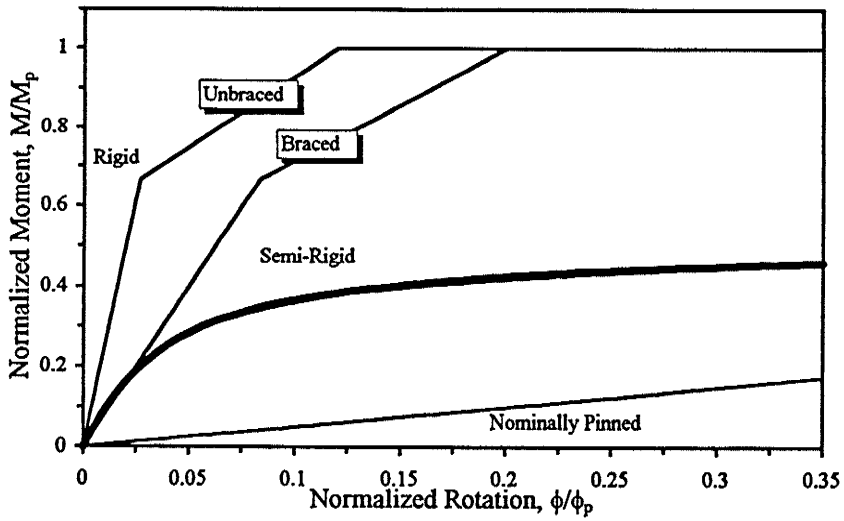


Figure A.196 (b) Eurocode3 Classification of Ostrander: Test 9

Table A.197 M-ϕ data for Ostrander: Test 11 (1970)

Moment, M kN-m	Rotation, ϕ radians	Moment, M kN-m	Rotation, ϕ radians
0	0	62.141	0.0279
2.655	0.0002	63.094	0.0303
5.311	0.0004	64.046	0.0327
7.965	0.0006	64.998	0.0351
10.620	0.0008	65.951	0.0374
13.276	0.0011	66.903	0.0398
15.931	0.0013	67.856	0.0422
18.586	0.0017	68.808	0.0446
21.242	0.0020	69.655	0.0468
23.896	0.0024	70.503	0.0490
26.551	0.0027	71.350	0.0512
29.206	0.0031	72.197	0.0534
31.862	0.0035		
34.517	0.0040		
37.173	0.0045		
39.827	0.0053		
42.482	0.0061		
44.855	0.0074		
47.227	0.0086		
50.052	0.0107		
52.877	0.0128		
54.534	0.0153		
56.192	0.0179		
57.849	0.0204		
59.280	0.0229		
60.710	0.0254		

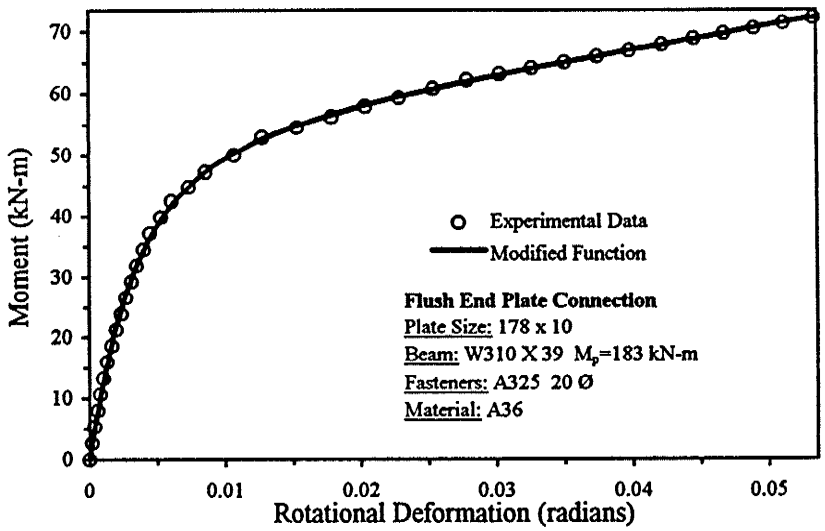


Figure A.197 (a) M-ϕ curve for Ostrander: Test 11

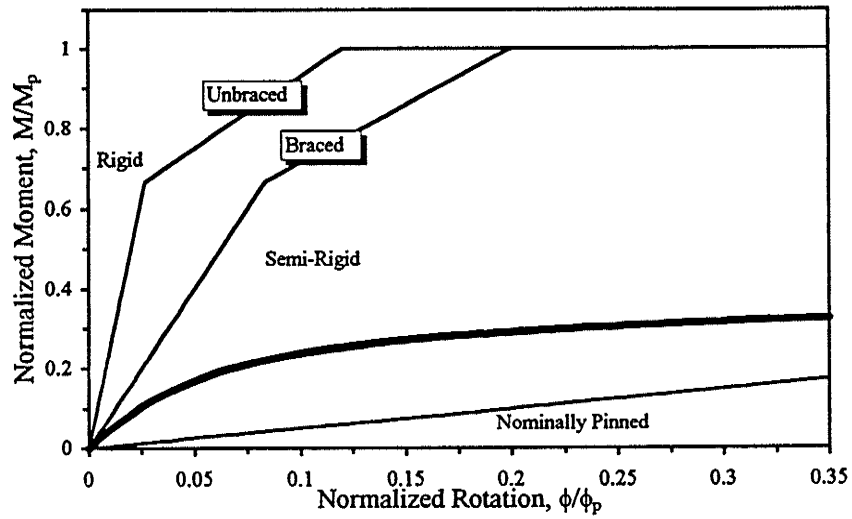


Figure A.197 (b) Eurocode3 Classification of Ostrander: Test 11

Table A.198 M-ϕ data for Ostrander: Test 12 (1970)

Moment, M kN-m	Rotation, ϕ radians	Moment, M kN-m	Rotation, ϕ radians
0	0	79.089	0.0223
3.540	0.0002	80.784	0.0249
7.080	0.0003	82.479	0.0275
10.620	0.0005	84.173	0.0301
14.161	0.0007	84.833	0.0325
17.701	0.0009	85.492	0.0349
21.242	0.0011	86.151	0.0374
24.782	0.0013	86.810	0.0398
28.322	0.0015	87.469	0.0422
31.862	0.0017	88.128	0.0446
35.402	0.0020	89.145	0.0471
38.942	0.0022	90.162	0.0497
42.482	0.0025	91.179	0.0522
46.022	0.0030		
49.563	0.0035		
53.103	0.0040		
55.758	0.0048		
58.413	0.0056		
61.124	0.0069		
63.836	0.0081		
66.435	0.0096		
69.034	0.0111		
71.576	0.0134		
74.119	0.0157		
75.775	0.0179		
77.432	0.0201		

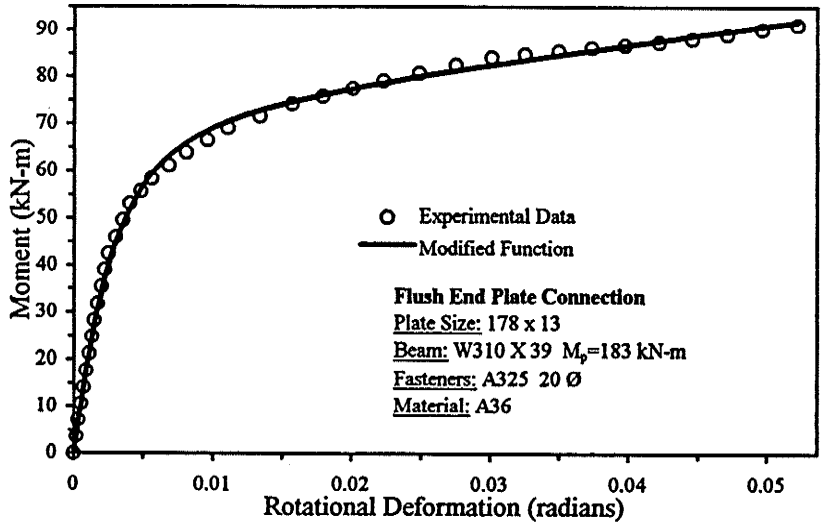


Figure A.198 (a) M-ϕ curve for Ostrander: Test 12

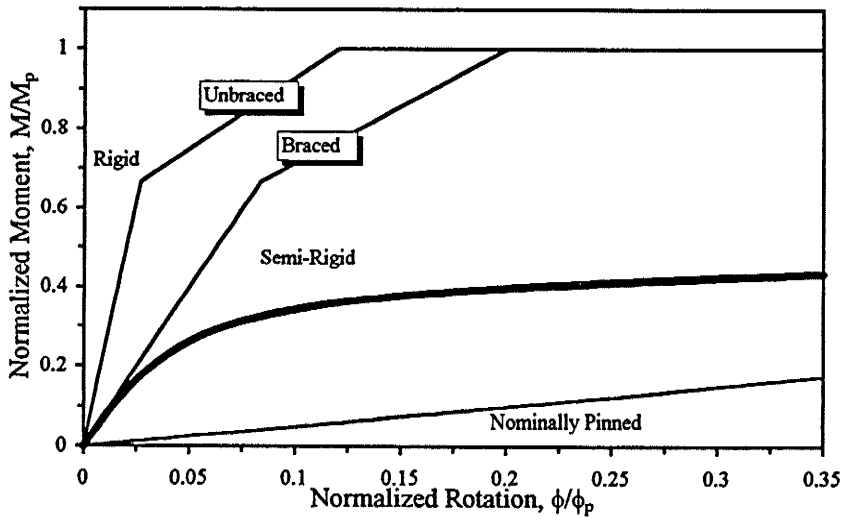


Figure A.198 (b) Eurocode3 Classification of Ostrander: Test 12

Table A.199 M-ϕ data for Ostrander: Test 13 (1970)

Moment, M kN-m	Rotation, ϕ radians	Moment, M kN-m	Rotation, ϕ radians
0	0	86.170	0.0191
3.540	0.0003	87.714	0.0205
7.080	0.0005	89.258	0.0218
10.620	0.0008	90.557	0.0236
14.161	0.0011	91.857	0.0254
17.701	0.0015	93.156	0.0272
21.242	0.0018	94.456	0.0290
24.782	0.0021	95.586	0.0309
28.322	0.0025	96.715	0.0328
31.862	0.0028	97.845	0.0346
35.402	0.0032	98.975	0.0365
38.942	0.0037	100.104	0.0384
42.482	0.0041		
46.022	0.0046		
49.563	0.0052		
53.103	0.0057		
56.643	0.0065		
60.183	0.0072		
63.724	0.0080		
66.379	0.0088		
69.034	0.0096		
74.005	0.0114		
76.830	0.0127		
79.654	0.0140		
82.140	0.0159		
84.626	0.0178		

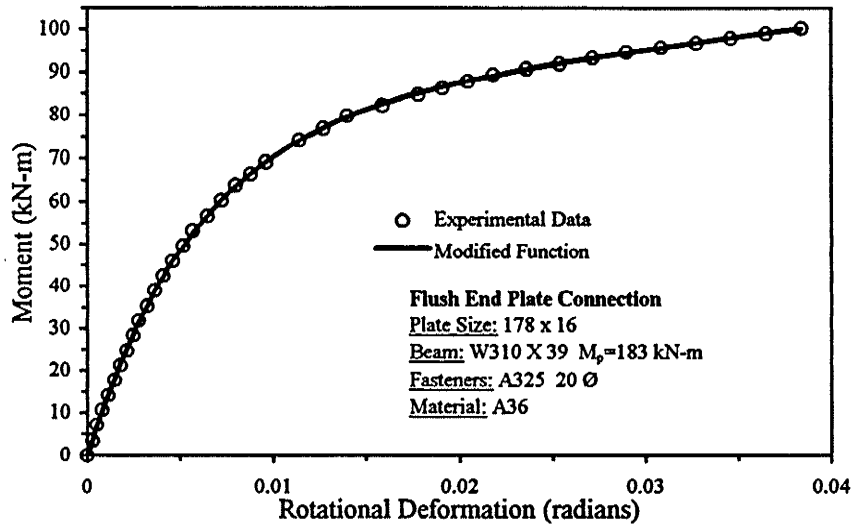


Figure A.199 (a) M-ϕ curve for Ostrander: Test 13

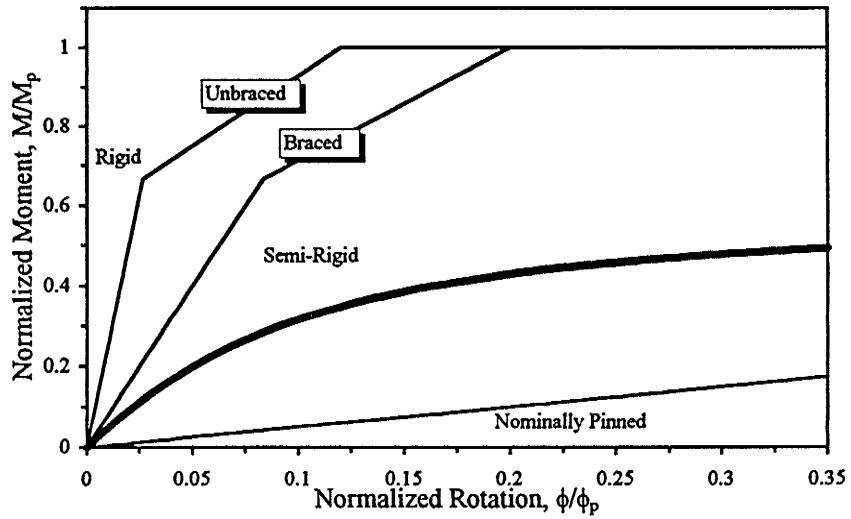


Figure A.199 (b) Eurocode3 Classification of Ostrander: Test 13

Table A.200 M-ϕ data for Ostrander: Test 17 (1970)

Moment, M kN-m	Rotation, ϕ radians	Moment, M kN-m	Rotation, ϕ radians
0	0	59.034	0.0372
2.655	0.0002	60.023	0.0402
5.310	0.0004	61.012	0.0433
7.965	0.0006	61.667	0.0469
10.620	0.0008	62.323	0.0505
13.276	0.0011	62.978	0.0541
15.931	0.0014	63.634	0.0577
18.586	0.0017	64.289	0.0613
21.242	0.0020	64.543	0.0646
23.897	0.0025	64.797	0.0680
26.552	0.0030	65.052	0.0713
29.207	0.0034	65.306	0.0746
31.862	0.0039		
34.517	0.0050		
37.172	0.0062		
39.827	0.0073		
42.482	0.0084		
45.137	0.0106		
47.793	0.0128		
50.165	0.0162		
52.538	0.0196		
53.668	0.0225		
54.797	0.0253		
55.927	0.0282		
57.057	0.0310		
58.046	0.0341		

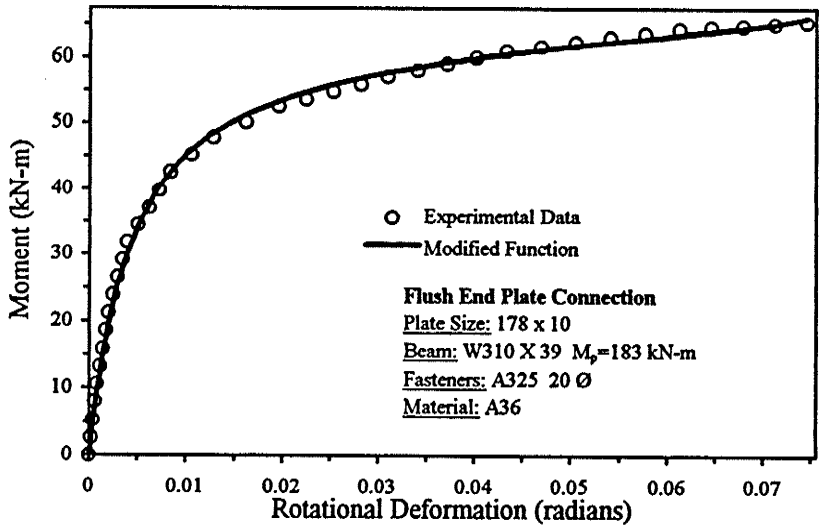


Figure A.200 (a) M-ϕ curve for Ostrander: Test 17

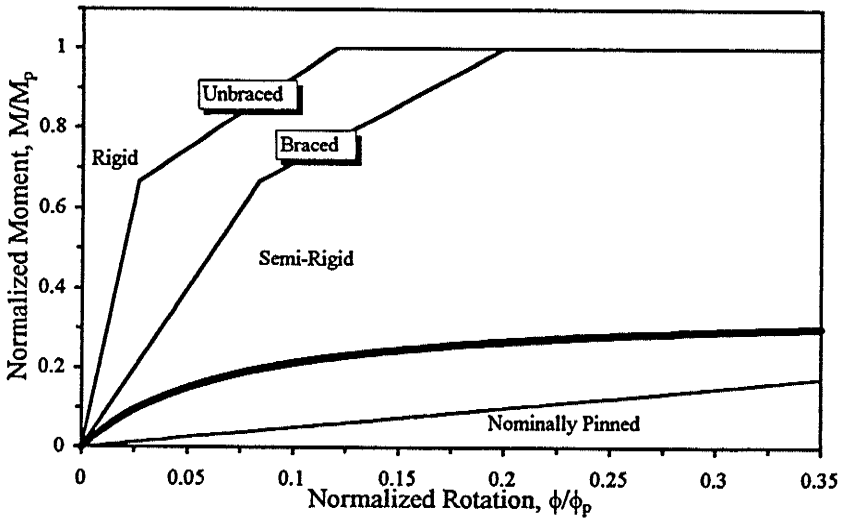


Figure A.200 (b) Eurocode3 Classification of Ostrander: Test 17

Table A.201 M-ϕ data for Ostrander: Test 18 (1970)

Moment, M kN-m	Rotation, ϕ radians	Moment, M kN-m	Rotation, ϕ radians
0	0	74.096	0.0515
3.540	0.0004	74.638	0.0554
7.080	0.0009	75.180	0.0594
10.620	0.0013	75.723	0.0633
14.161	0.0018	76.265	0.0672
17.701	0.0023	75.898	0.0702
21.242	0.0028	75.531	0.0732
24.782	0.0034	75.164	0.0762
28.322	0.0041	74.797	0.0792
31.862	0.0047		
35.402	0.0058		
38.942	0.0069		
42.482	0.0080		
45.834	0.0098		
49.186	0.0115		
52.538	0.0133		
55.419	0.0157		
58.300	0.0181		
61.012	0.0220		
63.724	0.0258		
65.305	0.0293		
66.887	0.0327		
68.469	0.0362		
70.164	0.0400		
71.858	0.0438		
73.553	0.0476		

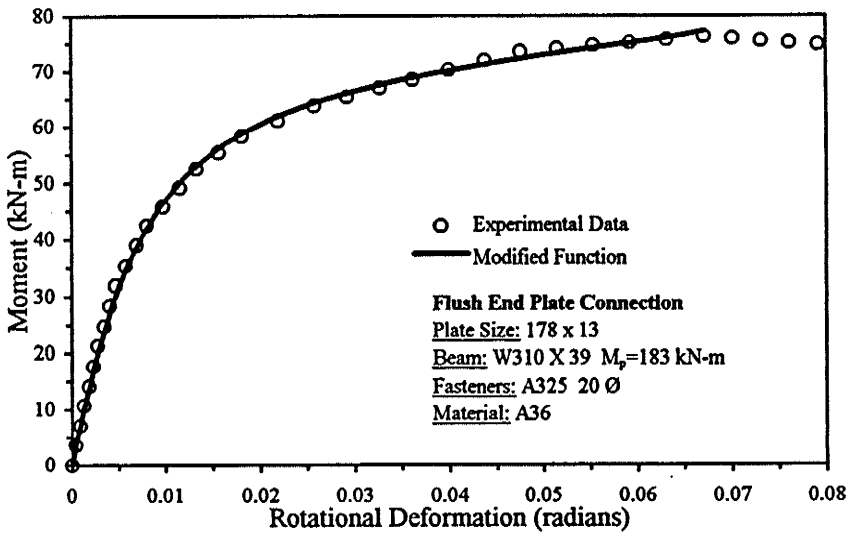


Figure A.201 (a) M-ϕ curve for Ostrander: Test 18

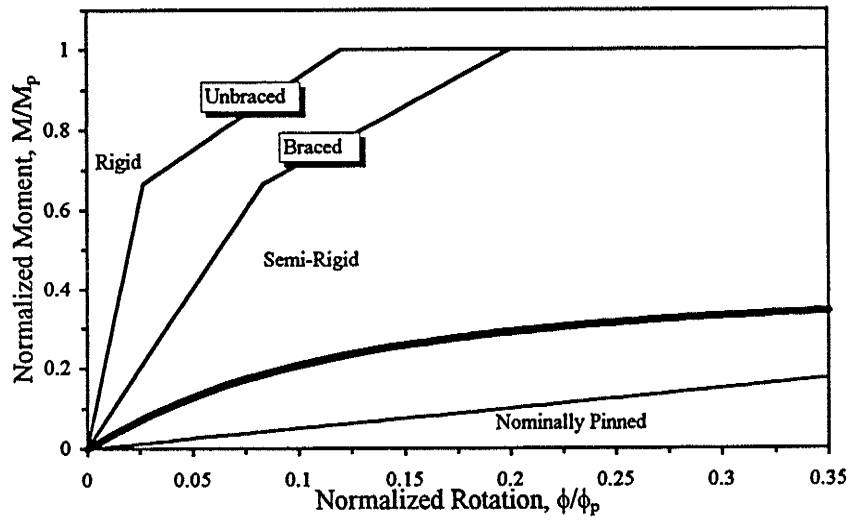


Figure A.201 (b) Eurocode3 Classification of Ostrander: Test 18

Table A.202 M-ϕ data for Ostrander: Test 19 (1970)

Moment, M kN-m	Rotation, ϕ radians	Moment, M kN-m	Rotation, ϕ radians
0	0	64.175	0.0231
2.655	0.0002	64.853	0.0251
5.311	0.0004	65.531	0.0270
7.965	0.0007	66.209	0.0290
10.620	0.0009	66.887	0.0309
13.276	0.0012	67.546	0.0331
15.931	0.0014	68.205	0.0353
18.586	0.0017	68.864	0.0375
21.242	0.0020	69.523	0.0397
23.896	0.0024	70.182	0.0419
26.551	0.0027	70.842	0.0441
29.206	0.0032		
31.862	0.0036		
34.517	0.0042		
37.173	0.0047		
39.827	0.0054		
42.482	0.0061		
44.968	0.0071		
47.454	0.0081		
50.279	0.0095		
53.103	0.0109		
55.758	0.0128		
58.413	0.0147		
60.108	0.0169		
61.802	0.0190		
63.497	0.0212		

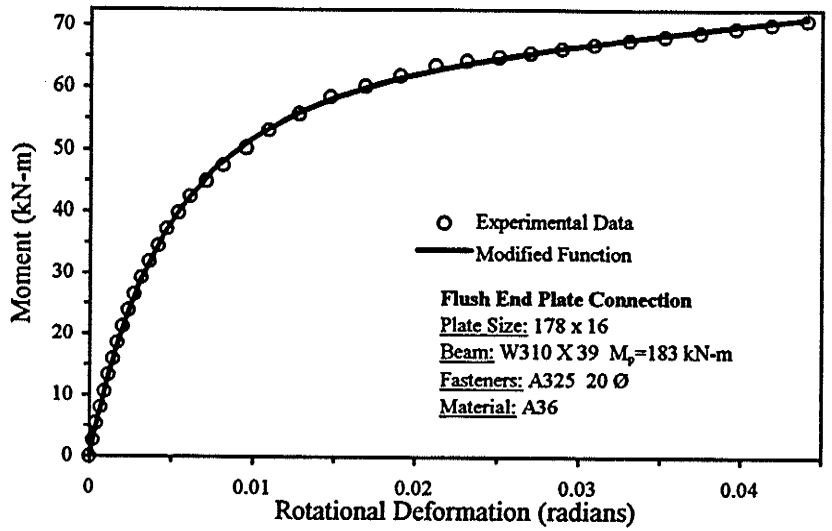


Figure A.202 (a) M-ϕ curve for Ostrander: Test 19

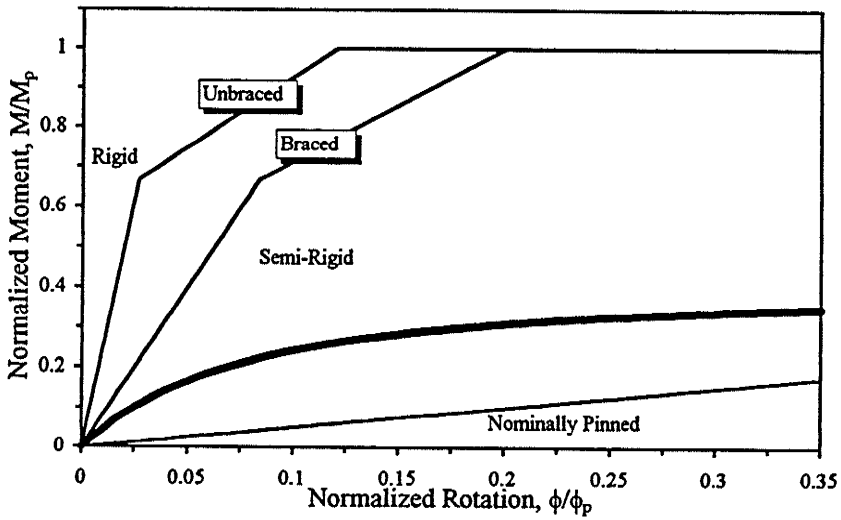


Figure A.202 (b) Eurocode3 Classification of Ostrander: Test 19

Table A.203 M-ϕ data for Ostrander: Test 23 (1970)

Moment, M kN-m	Rotation, ϕ radians	Moment, M kN-m	Rotation, ϕ radians
0	0	81.462	0.0093
3.540	0.0002	83.552	0.0103
7.080	0.0003	85.642	0.0113
10.620	0.0005	87.733	0.0122
14.161	0.0007	89.823	0.0132
17.701	0.0008	91.094	0.0142
21.242	0.0010	92.365	0.0152
24.782	0.0013	93.636	0.0161
28.322	0.0015	94.907	0.0171
31.862	0.0018	95.906	0.0182
35.402	0.0021	96.904	0.0193
38.942	0.0023	97.902	0.0205
42.482	0.0026	98.900	0.0216
45.137	0.0028	99.898	0.0227
47.793	0.0030	100.896	0.0238
50.448	0.0033		
53.103	0.0035		
55.758	0.0038		
58.413	0.0041		
61.068	0.0045		
63.724	0.0048		
66.266	0.0053		
68.808	0.0057		
71.689	0.0064		
74.570	0.0070		
78.016	0.0082		

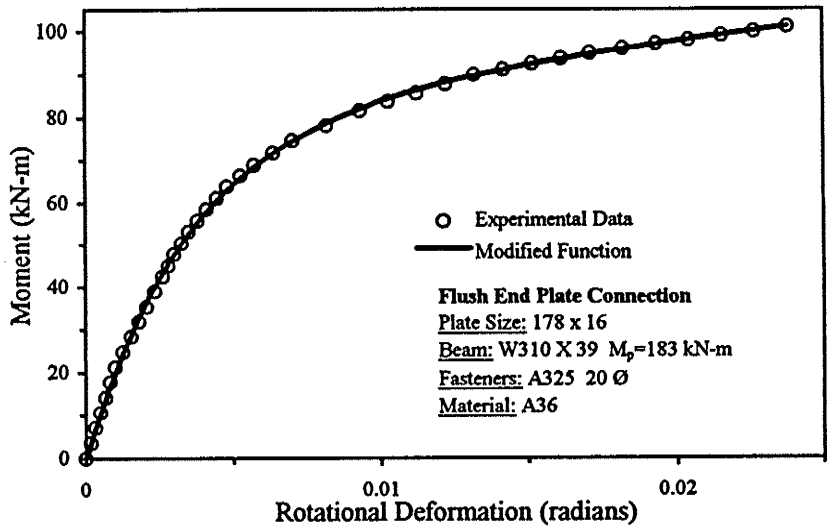


Figure A.203 (a) M-ϕ curve for Ostrander: Test 23

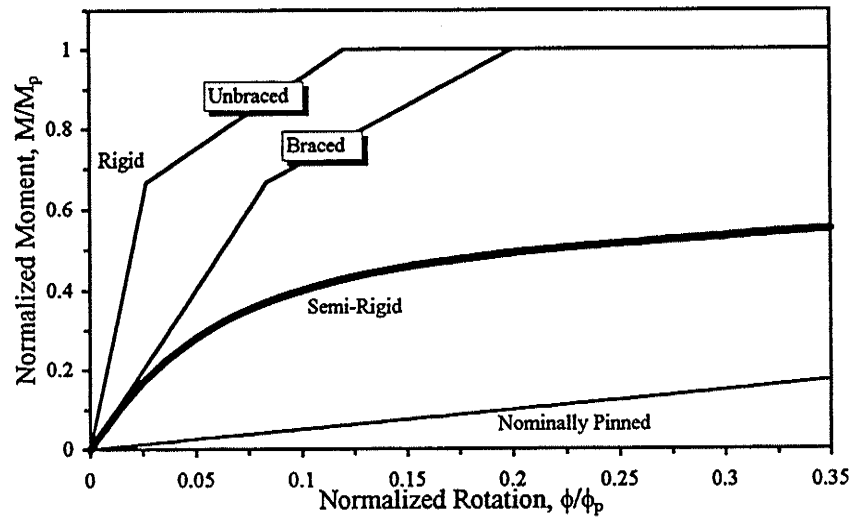


Figure A.203 (b) Eurocode3 Classification of Ostrander: Test 23

Table A.204 M-ϕ data for Ostrander: Test 2 (1970)

Moment, M kN-m	Rotation, ϕ radians	Moment, M kN-m	Rotation, ϕ radians
0	0	62.503	0.0235
2.712	0.0002	63.497	0.0256
5.311	0.0005	64.198	0.0278
7.965	0.0008	64.898	0.0300
10.620	0.0010	65.599	0.0323
13.276	0.0013	66.300	0.0345
15.931	0.0016	67.001	0.0367
18.586	0.0019	67.565	0.0390
21.242	0.0022	68.130	0.0413
23.896	0.0025	68.695	0.0436
26.551	0.0028	69.260	0.0458
29.206	0.0033	69.825	0.0481
31.862	0.0037	70.390	0.0504
34.517	0.0043		
37.173	0.0048		
39.827	0.0055		
42.482	0.0062		
45.137	0.0073		
47.793	0.0083		
50.222	0.0097		
52.651	0.0111		
55.589	0.0132		
58.527	0.0152		
59.521	0.0173		
60.515	0.0194		
61.509	0.0214		

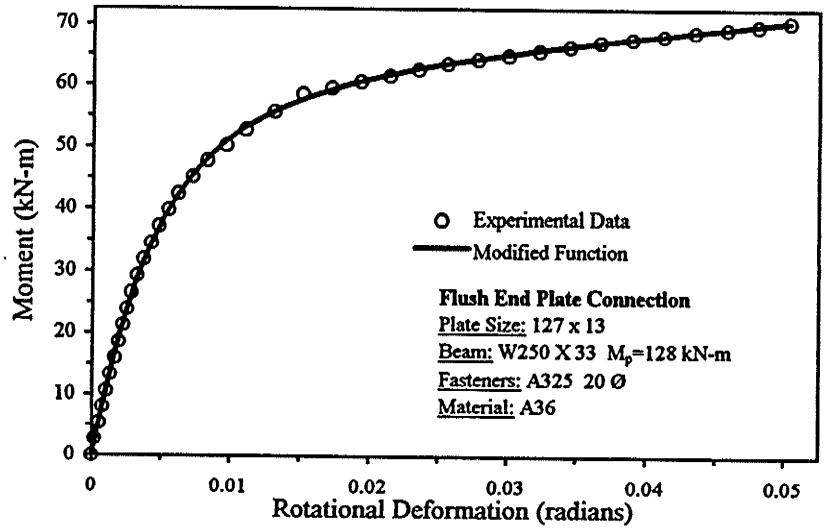


Figure A.204 (a) M-ϕ curve for Ostrander: Test 2

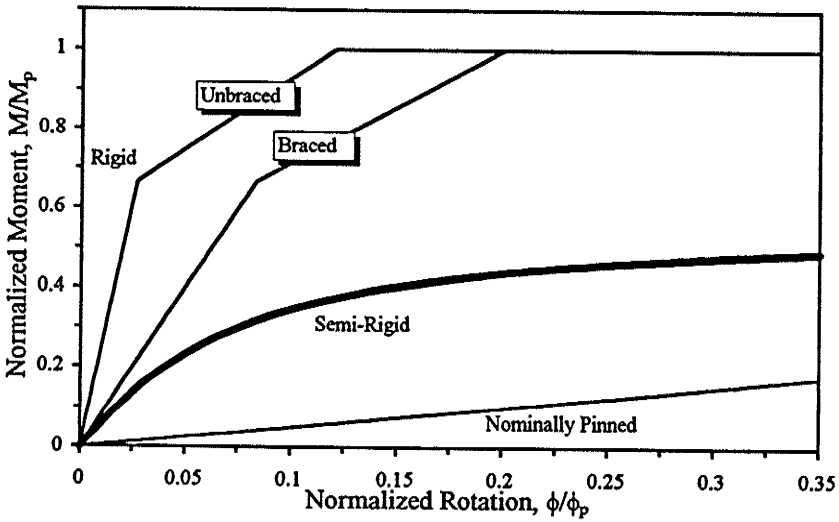


Figure A.204 (b) Eurocode3 Classification of Ostrander: Test 2

Table A.205 M-ϕ data for Ostrander: Test 5 (1970)

Moment, M kN-m	Rotation, ϕ radians	Moment, M kN-m	Rotation, ϕ radians
0	0	64.430	0.0366
2.655	0.0003	65.475	0.0414
5.311	0.0005	66.520	0.0462
7.965	0.0008	67.565	0.0510
10.620	0.0010	68.304	0.0556
13.276	0.0013	69.044	0.0603
15.931	0.0015	69.783	0.0649
18.586	0.0018	70.523	0.0695
21.242	0.0020	71.262	0.0742
23.896	0.0024	72.002	0.0788
26.551	0.0027	72.741	0.0835
29.206	0.0032	73.481	0.0881
31.862	0.0036	74.220	0.0927
34.517	0.0042	74.960	0.0974
37.173	0.0048	75.699	0.1020
39.827	0.0056		
42.482	0.0064		
45.137	0.0077		
47.793	0.0090		
50.448	0.0110		
53.103	0.0129		
55.758	0.0161		
58.413	0.0193		
60.070	0.0235		
61.727	0.0276		
63.385	0.0318		

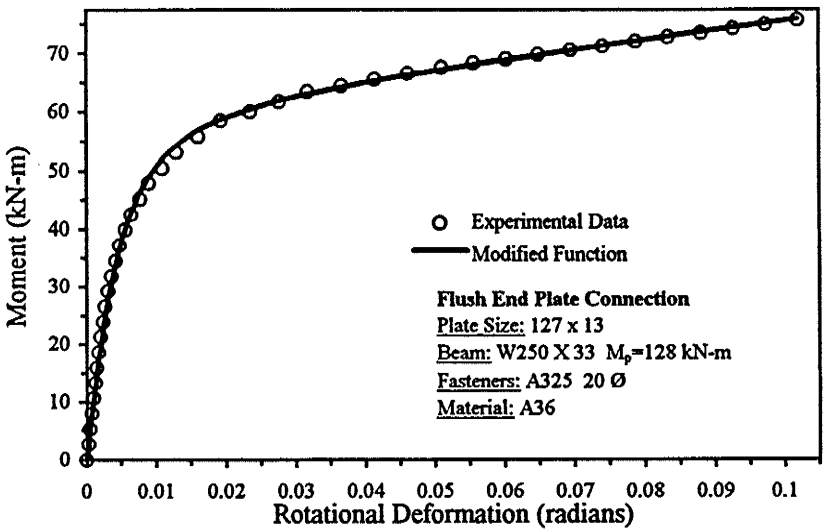


Figure A.205 (a) M-ϕ curve for Ostrander: Test 5

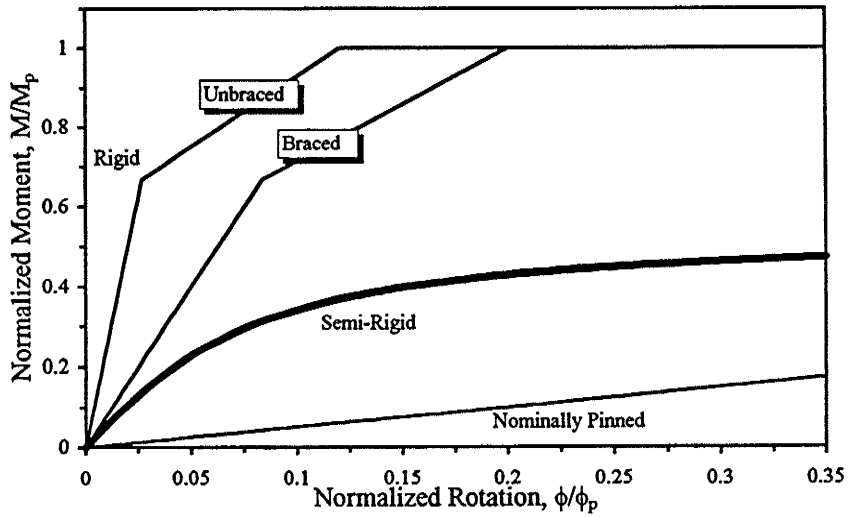


Figure A.205 (b) Eurocode3 Classification of Ostrander: Test 5

Table A.206 M-ϕ data for Ostrander: Test 6 (1970)

Moment, M kN-m	Rotation, ϕ radians	Moment, M kN-m	Rotation, ϕ radians
0	0	56.221	0.0437
2.655	0.0002	56.854	0.0469
5.311	0.0003	57.486	0.0502
7.965	0.0005	58.119	0.0534
10.620	0.0007	58.752	0.0566
13.276	0.0009	59.136	0.0600
15.931	0.0011	59.520	0.0633
18.586	0.0016	59.904	0.0667
21.242	0.0020	60.289	0.0700
23.896	0.0026	60.673	0.0734
26.551	0.0031		
29.206	0.0039		
31.862	0.0047		
34.517	0.0061		
37.173	0.0074		
39.827	0.0097		
42.482	0.0119		
45.137	0.0154		
47.793	0.0188		
49.111	0.0221		
50.429	0.0253		
51.748	0.0286		
52.708	0.0316		
53.668	0.0346		
54.628	0.0375		
55.589	0.0405		

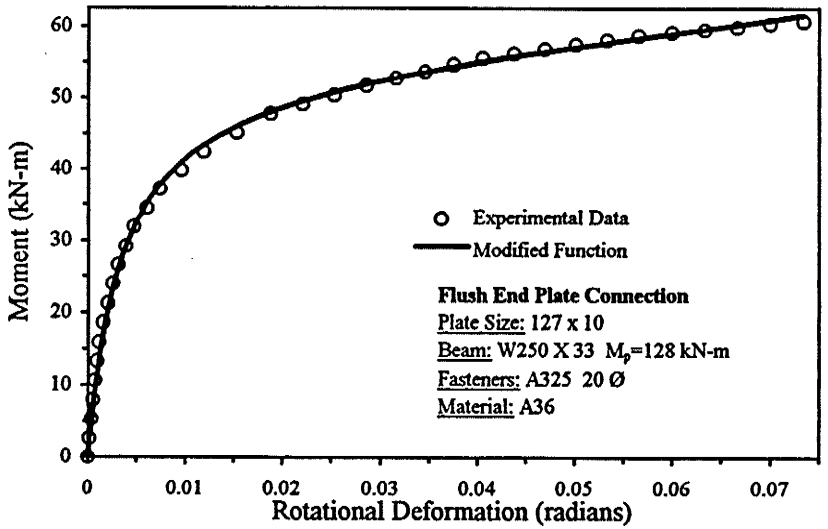


Figure A.206 (a) M-ϕ curve for Ostrander: Test 6

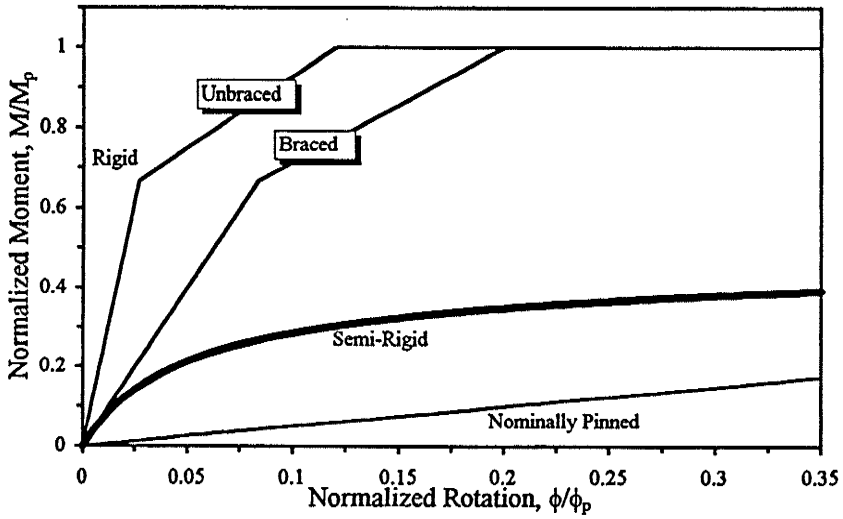


Figure A.206 (b) Eurocode3 Classification of Ostrander: Test 6

Table A.207 M-ϕ data for Ostrander: Test 7 (1970)

Moment, M kN-m	Rotation, ϕ radians	Moment, M kN-m	Rotation, ϕ radians
0	0	29.828	0.0280
1.328	0.0002	30.506	0.0302
2.655	0.0005	31.184	0.0324
3.983	0.0007	31.862	0.0346
5.311	0.0009	32.404	0.0367
6.638	0.0012	32.946	0.0389
7.965	0.0015	33.489	0.0410
9.293	0.0017	34.031	0.0432
10.620	0.0020	34.573	0.0453
11.948	0.0024	34.799	0.0470
13.276	0.0028	35.025	0.0488
14.603	0.0032	35.251	0.0505
15.931	0.0036		
17.259	0.0046		
18.586	0.0056		
19.914	0.0066		
21.242	0.0076		
22.597	0.0097		
23.953	0.0117		
24.819	0.0136		
25.685	0.0155		
26.551	0.0174		
27.201	0.0195		
27.851	0.0216		
28.500	0.0237		
29.150	0.0258		

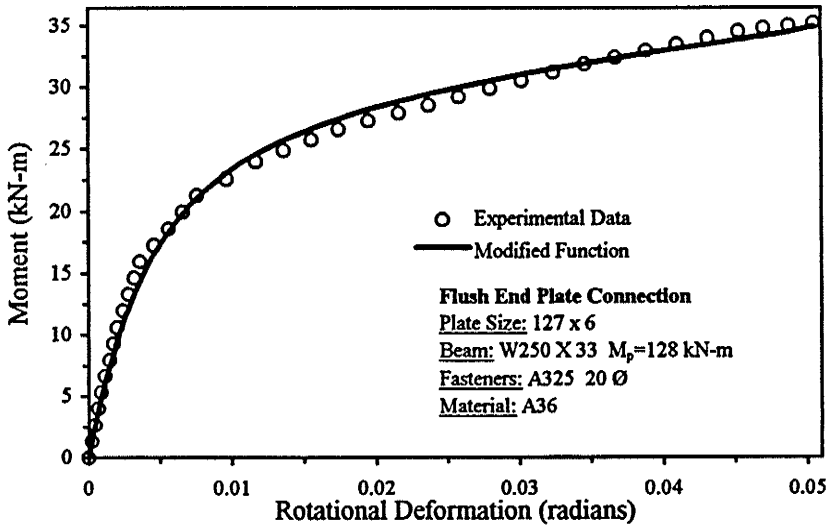


Figure A.207 (a) M-ϕ curve for Ostrander: Test 7

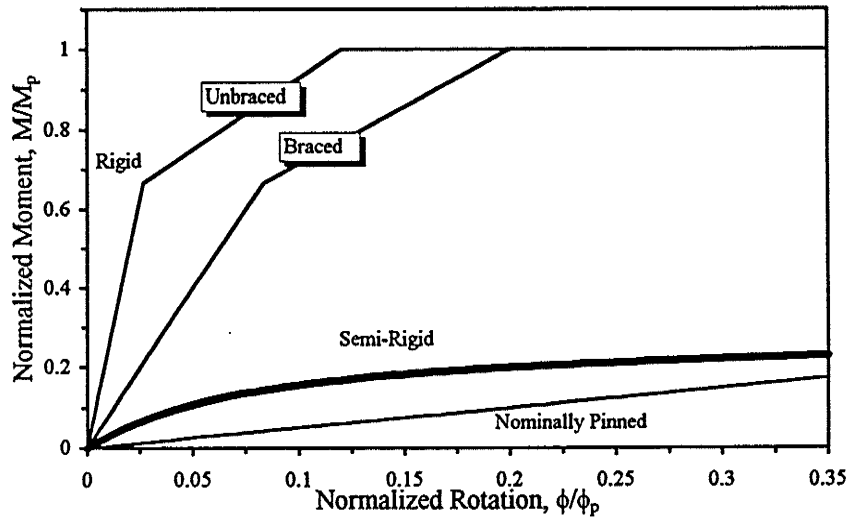


Figure A.207 (b) Eurocode3 Classification of Ostrander: Test 7

Table A.208 M-ϕ data for Ostrander: Test 8 (1970)

Moment, M kN-m	Rotation, ϕ radians	Moment, M kN-m	Rotation, ϕ radians
0	0	29.828	0.0283
1.328	0.0001	30.506	0.0305
2.655	0.0003	31.184	0.0327
3.983	0.0004	31.862	0.0349
5.311	0.0005	32.291	0.0368
6.638	0.0008	32.720	0.0387
7.965	0.0011	33.150	0.0406
9.293	0.0013	33.579	0.0425
10.620	0.0016	34.008	0.0444
11.948	0.0020		
13.276	0.0024		
14.603	0.0027		
15.931	0.0031		
17.259	0.0041		
18.586	0.0051		
19.914	0.0061		
21.242	0.0071		
22.597	0.0092		
23.953	0.0112		
24.819	0.0133		
25.685	0.0153		
26.551	0.0174		
27.201	0.0196		
27.851	0.0218		
28.500	0.0239		
29.150	0.0261		

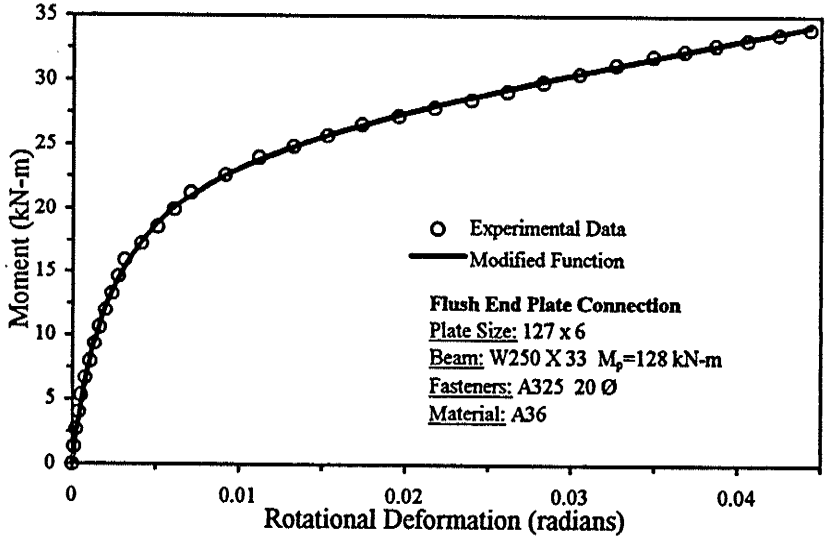


Figure A.208 (a) M-ϕ curve for Ostrander: Test 8

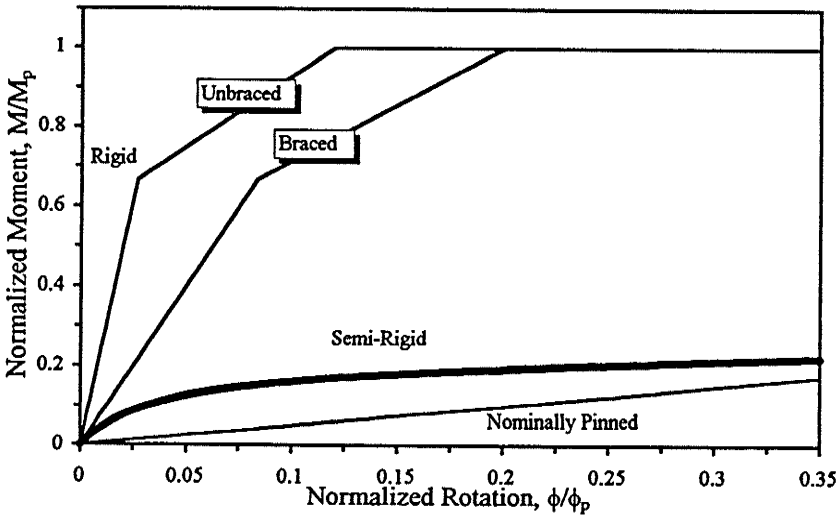


Figure A.208 (b) Eurocode3 Classification of Ostrander: Test 8

Table A.209 M-ϕ data for Ostrander: Test 10 (1970)

Moment, M kN-m	Rotation, ϕ radians	Moment, M kN-m	Rotation, ϕ radians
0	0	68.469	0.0146
2.655	0.0001	70.164	0.0168
5.311	0.0001	71.858	0.0190
7.965	0.0003	73.553	0.0212
10.620	0.0004	74.401	0.0233
13.276	0.0006	75.248	0.0254
15.931	0.0007	76.095	0.0275
18.586	0.0009	76.943	0.0295
21.242	0.0010	77.790	0.0316
23.896	0.0012	78.638	0.0337
26.551	0.0013	79.396	0.0358
29.206	0.0015	80.155	0.0379
31.862	0.0017	80.914	0.0400
34.517	0.0020	81.672	0.0420
37.173	0.0023	82.431	0.0441
39.827	0.0026	83.190	0.0462
42.482	0.0029	83.948	0.0483
45.137	0.0034		
47.793	0.0038		
50.448	0.0045		
53.103	0.0052		
55.758	0.0062		
58.413	0.0072		
60.899	0.0086		
63.385	0.0099		
65.927	0.0123		

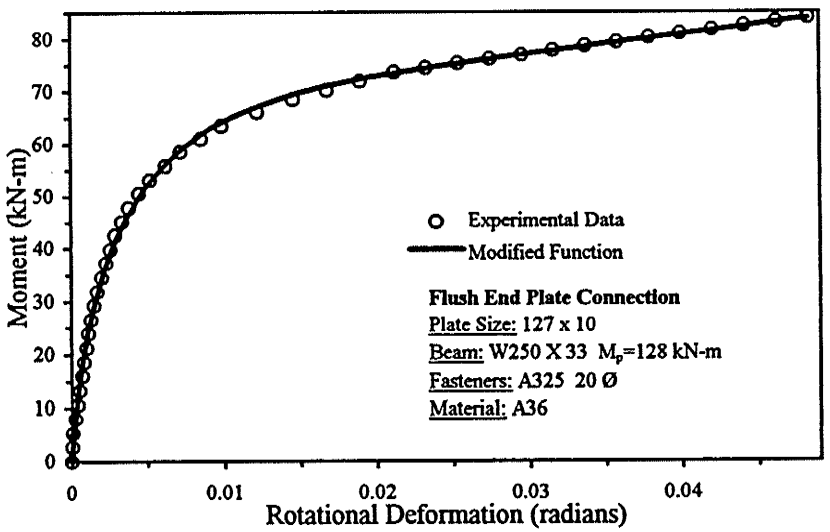


Figure A.209 (a) M-ϕ curve for Ostrander: Test 10

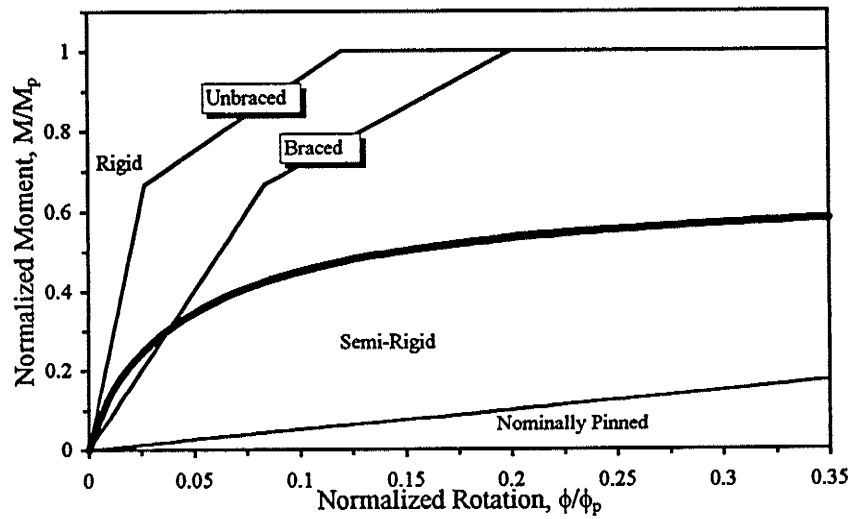


Figure A.209 (b) Eurocode3 Classification of Ostrander: Test 10

Table A.210 M-ϕ data for Ostrander: Test 14 (1970)

Moment, M kN-m	Rotation, ϕ radians	Moment, M kN-m	Rotation, ϕ radians
0	0	71.237	0.0323
2.655	0.0001	72.509	0.0345
5.311	0.0002	73.780	0.0368
8.851	0.0009	75.107	0.0393
12.391	0.0015	76.434	0.0418
15.931	0.0022	77.762	0.0442
19.471	0.0028	79.089	0.0467
23.011	0.0034	79.616	0.0488
26.551	0.0040	80.144	0.0509
30.092	0.0047	80.671	0.0530
33.632	0.0053		
37.173	0.0060		
40.713	0.0069		
44.253	0.0078		
47.793	0.0087		
50.448	0.0099		
53.103	0.0111		
55.758	0.0129		
58.413	0.0146		
60.785	0.0169		
63.158	0.0191		
64.514	0.0215		
65.870	0.0239		
67.283	0.0258		
68.695	0.0277		
69.966	0.0300		

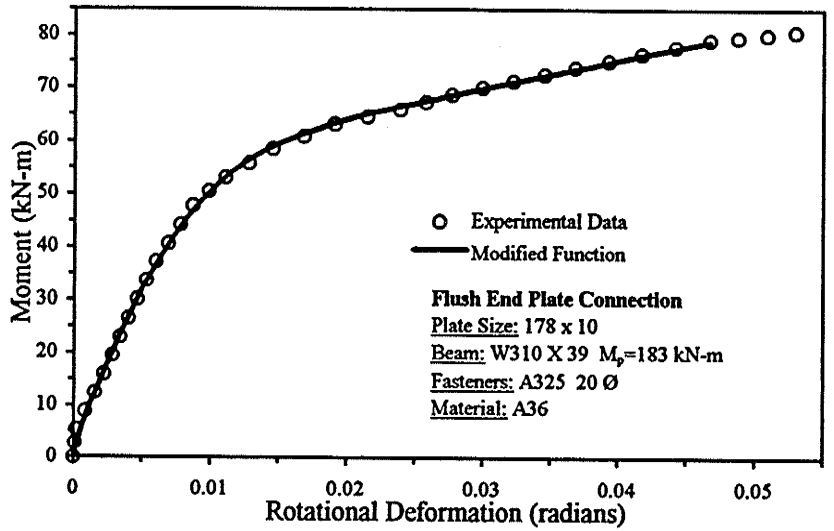


Figure A.210 (a) M-ϕ curve for Ostrander: Test 14

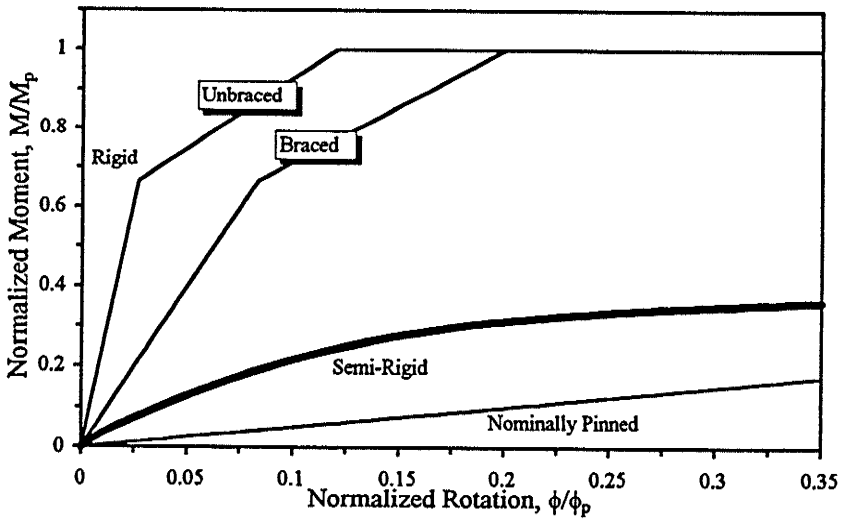


Figure A.210 (b) Eurocode3 Classification of Ostrander: Test 14

Table A.211 M-ϕ data for Ostrander: Test 15 (1970)

Moment, M kN-m	Rotation, ϕ radians	Moment, M kN-m	Rotation, ϕ radians
0	0	81.198	0.0117
3.540	0.0001	82.969	0.0127
7.080	0.0003	84.739	0.0136
10.620	0.0004	86.010	0.0146
14.161	0.0006	87.281	0.0156
17.701	0.0008	88.552	0.0165
21.242	0.0010	89.823	0.0175
24.782	0.0011	90.953	0.0185
28.322	0.0013	92.083	0.0194
31.862	0.0014	92.959	0.0206
35.402	0.0018	93.834	0.0218
38.942	0.0021	94.710	0.0230
42.482	0.0025	95.585	0.0242
46.022	0.0029		
49.563	0.0034		
53.103	0.0038		
55.758	0.0042		
58.413	0.0046		
61.068	0.0051		
63.724	0.0055		
66.379	0.0062		
69.034	0.0068		
71.689	0.0077		
74.344	0.0086		
76.886	0.0097		
79.428	0.0108		

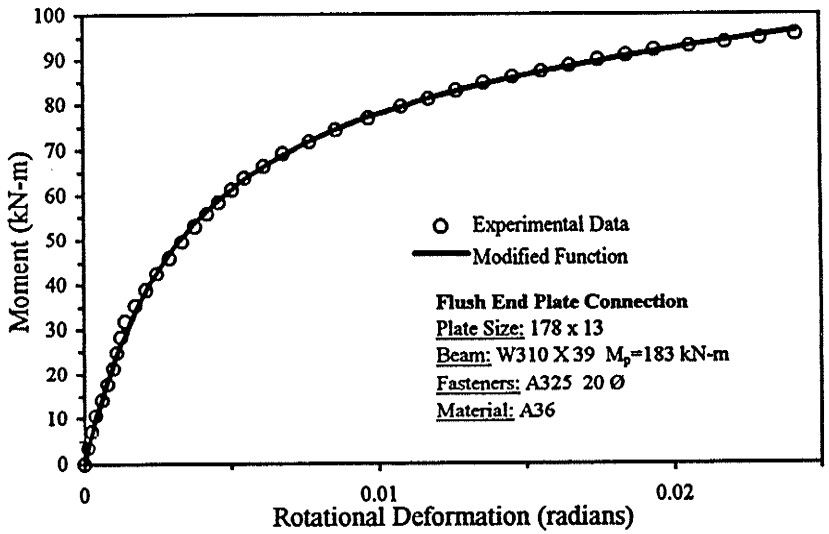


Figure A.211 (a) M-ϕ curve for Ostrander: Test 15

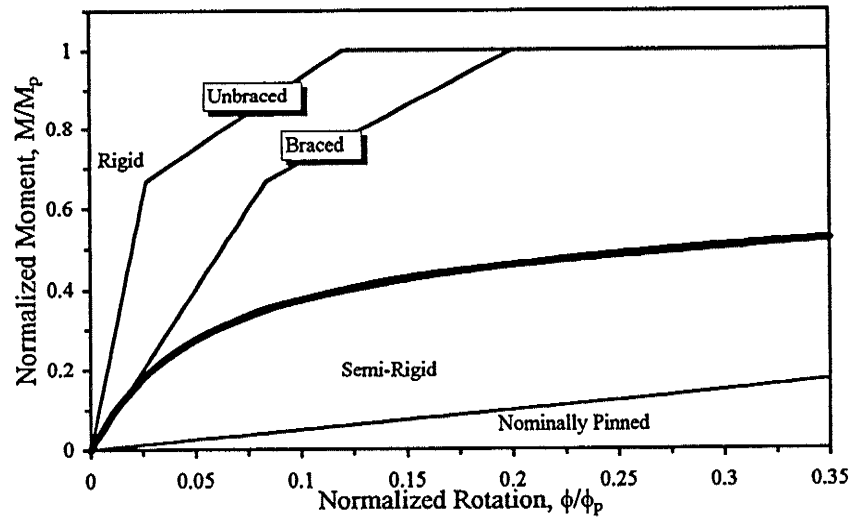


Figure A.211 (b) Eurocode3 Classification of Ostrander: Test 15

Table A.212 M-ϕ data for Ostrander: Test 16 (1970)

Moment, M kN-m	Rotation, ϕ radians	Moment, M kN-m	Rotation, ϕ radians
0	0	103.833	0.0171
5.310	0.0002	105.415	0.0185
10.620	0.0003	106.364	0.0197
15.931	0.0005	107.313	0.0209
21.242	0.0006	108.262	0.0222
26.552	0.0008	109.211	0.0234
31.862	0.0009	110.160	0.0246
37.172	0.0011	110.866	0.0259
42.482	0.0012	111.572	0.0271
47.793	0.0016	112.279	0.0284
53.103	0.0019	112.985	0.0296
58.413	0.0023		
63.724	0.0028		
69.034	0.0034		
74.344	0.0041		
79.315	0.0051		
82.140	0.0058		
84.965	0.0065		
87.338	0.0074		
89.711	0.0082		
92.309	0.0095		
94.907	0.0107		
96.828	0.0119		
98.749	0.0131		
100.670	0.0143		
102.251	0.0157		

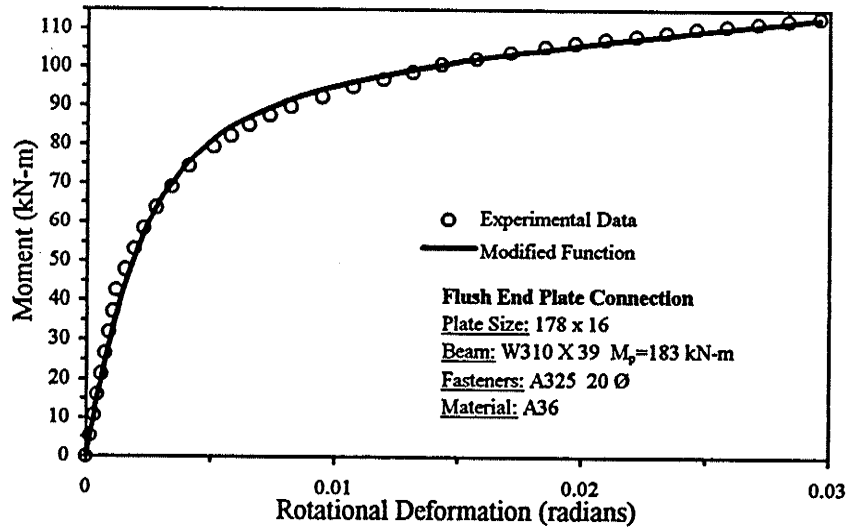


Figure A.212 (a) M-ϕ curve for Ostrander: Test 16

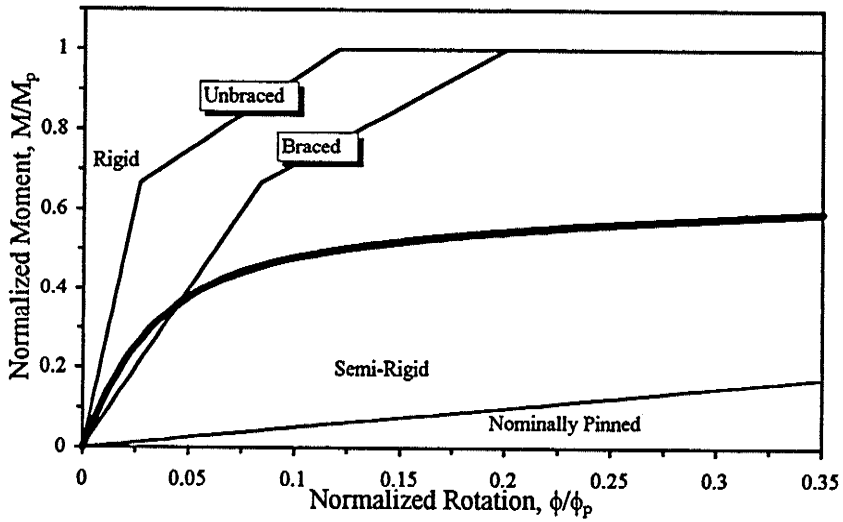


Figure A.212 (b) Eurocode3 Classification of Ostrander: Test 16

Table A.213 M-ϕ data for Ostrander: Test 20 (1970)

Moment, M kN-m	Rotation, ϕ radians	Moment, M kN-m	Rotation, ϕ radians
0	0	64.995	0.0446
3.540	0.0004	65.757	0.0473
7.080	0.0007	66.492	0.0503
10.620	0.0011	67.226	0.0532
14.161	0.0014	67.961	0.0562
17.701	0.0018	68.695	0.0591
21.242	0.0021	69.524	0.0626
24.782	0.0026	70.352	0.0660
28.322	0.0032	71.181	0.0695
31.862	0.0037		
35.402	0.0048		
38.942	0.0059		
42.482	0.0070		
45.137	0.0086		
47.793	0.0102		
50.448	0.0129		
53.103	0.0155		
54.610	0.0184		
56.116	0.0213		
57.622	0.0242		
58.893	0.0273		
60.165	0.0303		
61.436	0.0334		
62.707	0.0364		
63.469	0.0391		
64.232	0.0419		

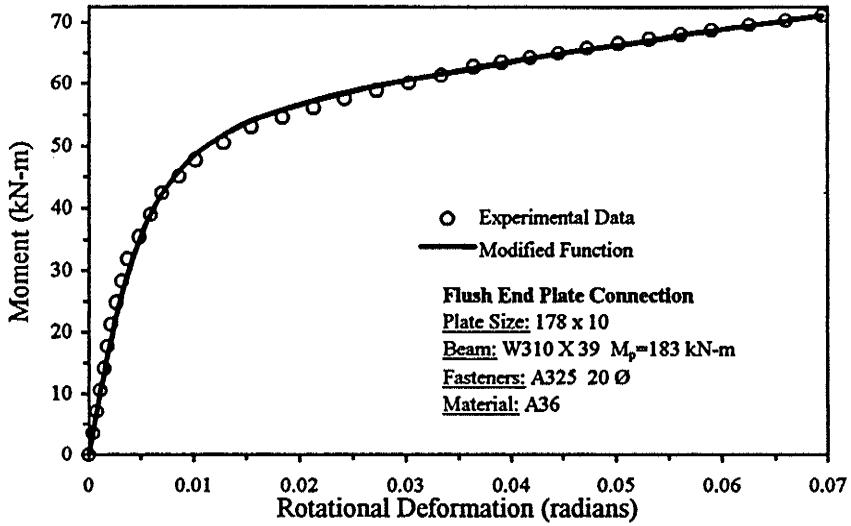


Figure A.213 (a) M-ϕ curve for Ostrander: Test 20

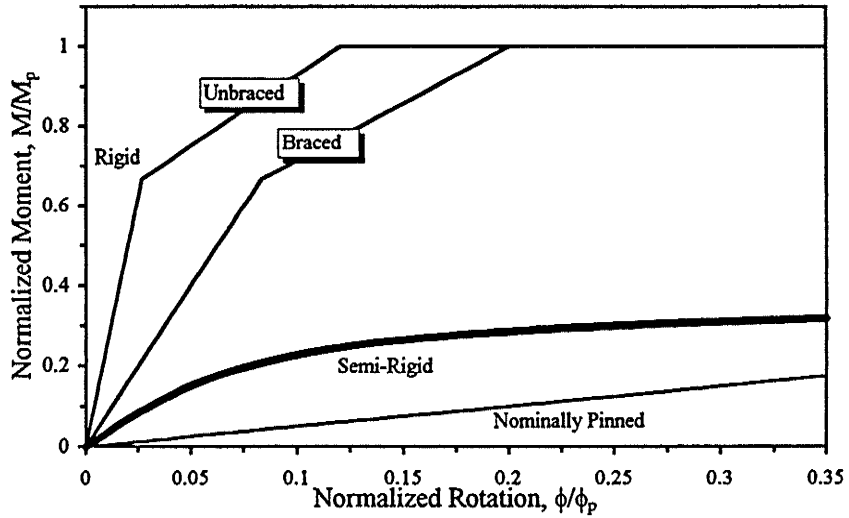


Figure A.213 (b) Eurocode3 Classification of Ostrander: Test 20

Table A.214 M-ϕ data for Ostrander: Test 21 (1970)

Moment, M kN-m	Rotation, ϕ radians	Moment, M kN-m	Rotation, ϕ radians
0	0	78.864	0.0328
3.540	0.0003	79.881	0.0350
7.080	0.0007	80.898	0.0373
10.620	0.0010	81.915	0.0395
14.161	0.0014	83.383	0.0426
17.701	0.0017	84.287	0.0446
21.242	0.0021	85.190	0.0465
24.782	0.0026	86.358	0.0496
28.322	0.0032	87.526	0.0527
31.862	0.0037	88.694	0.0558
35.402	0.0044	89.343	0.0584
38.942	0.0050	89.993	0.0609
42.482	0.0057	90.642	0.0635
46.022	0.0068	91.291	0.0660
49.563	0.0080		
53.103	0.0091		
55.532	0.0103		
57.961	0.0115		
60.899	0.0133		
63.836	0.0150		
66.378	0.0175		
68.920	0.0200		
71.463	0.0228		
74.005	0.0256		
75.624	0.0280		
77.244	0.0304		

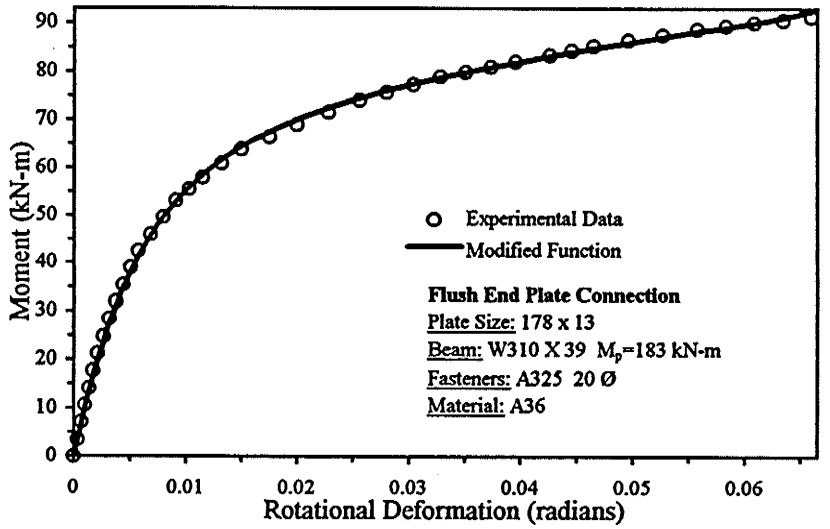


Figure A.214 (a) M-ϕ curve for Ostrander: Test 21

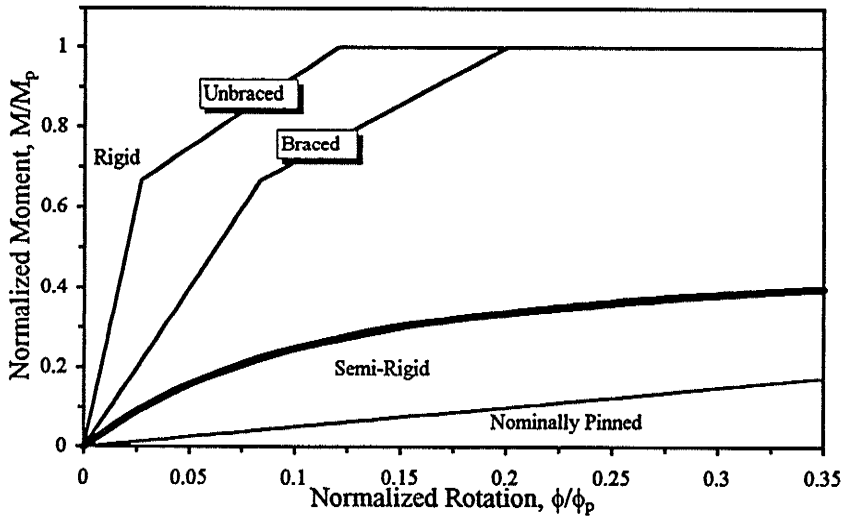


Figure A.214 (b) Eurocode3 Classification of Ostrander: Test 21

Table A.215 M-ϕ data for Ostrander: Test 22 (1970)

Moment, M kN-m	Rotation, ϕ radians	Moment, M kN-m	Rotation, ϕ radians
0	0	74.864	0.0227
3.540	0.0002	76.197	0.0246
7.080	0.0003	77.531	0.0266
10.620	0.0005	78.864	0.0286
14.161	0.0006	79.994	0.0305
17.701	0.0008	81.123	0.0324
21.242	0.0009	82.253	0.0343
24.782	0.0011	83.383	0.0362
28.322	0.0014	84.061	0.0380
31.862	0.0016	84.739	0.0397
35.402	0.0020	85.417	0.0415
38.942	0.0024		
42.482	0.0028		
46.022	0.0036		
49.563	0.0045		
53.103	0.0053		
55.419	0.0063		
57.735	0.0072		
60.729	0.0087		
63.724	0.0101		
65.983	0.0118		
68.242	0.0135		
69.561	0.0152		
70.879	0.0170		
72.197	0.0187		
73.531	0.0207		

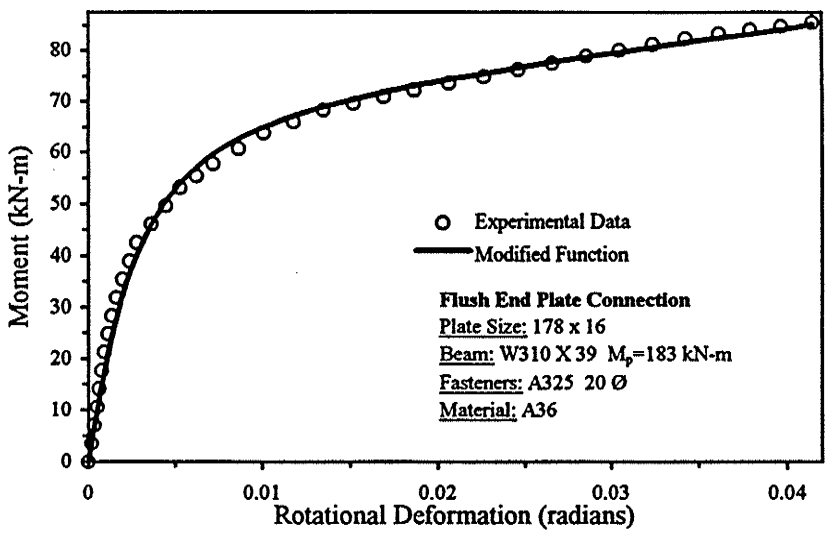


Figure A.215 (a) M-ϕ curve for Ostrander: Test 22

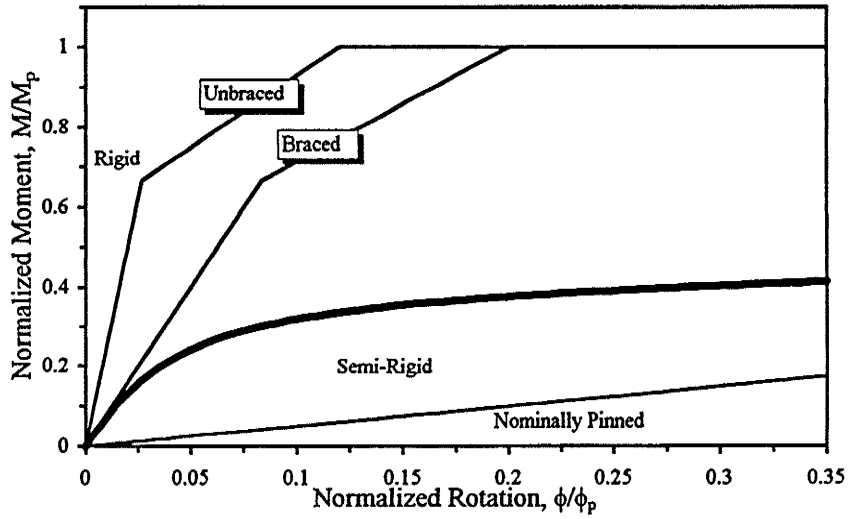


Figure A.215 (b) Eurocode3 Classification of Ostrander: Test 22

Table A.216 M-ϕ data for Ostrander: Test 24 (1970)

Moment, M kN-m	Rotation, ϕ radians	Moment, M kN-m	Rotation, ϕ radians
0	0	104.850	0.0131
5.310	0.0002	106.205	0.0139
10.620	0.0003	107.561	0.0146
15.931	0.0004	107.976	0.0153
21.242	0.0005	108.390	0.0160
26.552	0.0007	108.805	0.0167
31.862	0.0008	109.652	0.0175
37.172	0.0010	110.499	0.0182
42.482	0.0012	109.200	0.0191
47.793	0.0015	107.900	0.0199
53.103	0.0017		
58.413	0.0021		
63.724	0.0024		
69.034	0.0029		
74.344	0.0034		
79.372	0.0043		
84.400	0.0052		
87.111	0.0058		
89.823	0.0064		
92.309	0.0073		
94.795	0.0081		
96.716	0.0088		
98.636	0.0096		
100.557	0.0103		
101.988	0.0112		
103.419	0.0122		

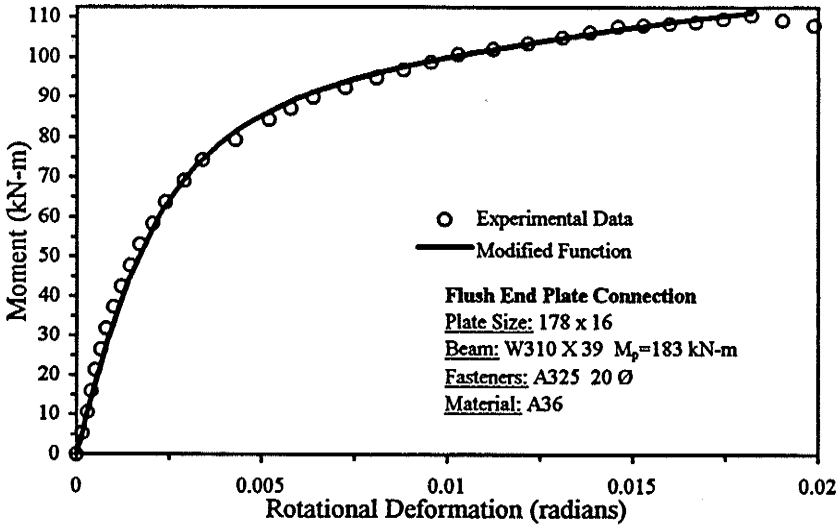


Figure A.216 (a) M-ϕ curve for Ostrander: Test 24

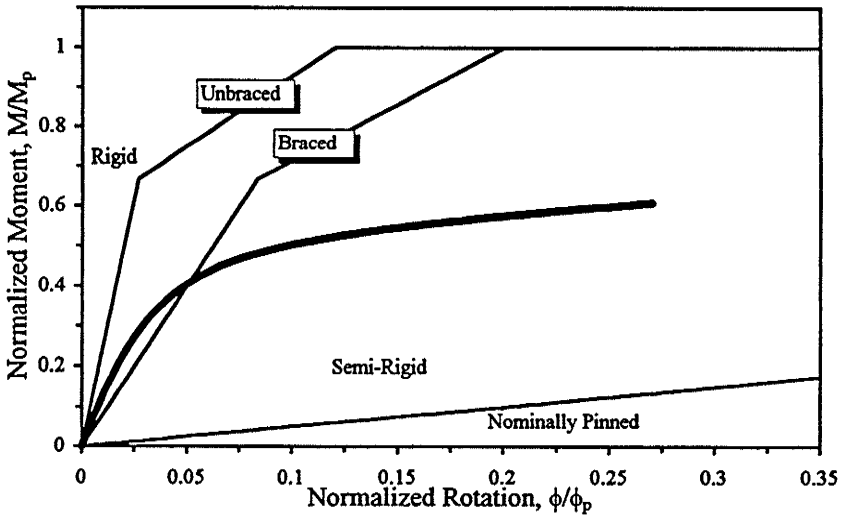


Figure A.216 (b) Eurocode3 Classification of Ostrander: Test 24

Table A.217 M-ϕ data for Ioannides: Test 1 (1978)

Moment, M kN-m	Rotation, ϕ radians	Moment, M kN-m	Rotation, ϕ radians
0	0	94.900	0.0157
4.707	0.0002	97.110	0.0169
9.413	0.0004	98.647	0.0179
14.120	0.0006	100.183	0.0189
18.663	0.0008	101.719	0.0199
23.206	0.0010	103.255	0.0210
27.749	0.0012	104.546	0.0220
31.525	0.0014	105.838	0.0231
35.301	0.0015	107.129	0.0242
39.078	0.0017	108.420	0.0252
43.593	0.0018		
48.108	0.0020		
52.545	0.0024		
56.242	0.0027		
59.939	0.0030		
64.544	0.0036		
69.323	0.0048		
72.952	0.0059		
76.583	0.0070		
78.978	0.0079		
81.373	0.0087		
83.442	0.0097		
85.511	0.0107		
87.995	0.0119		
90.479	0.0132		
92.689	0.0144		

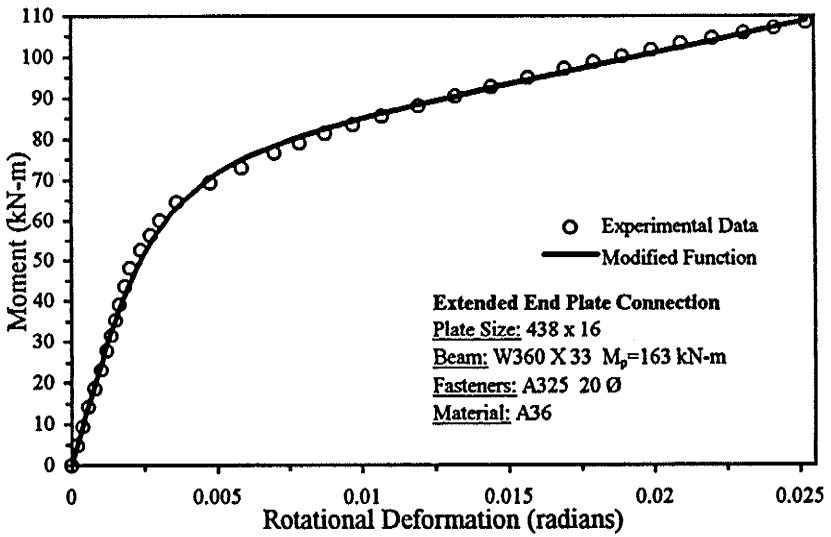


Figure A.217 (a) M-ϕ curve for Ioannides: Test 1

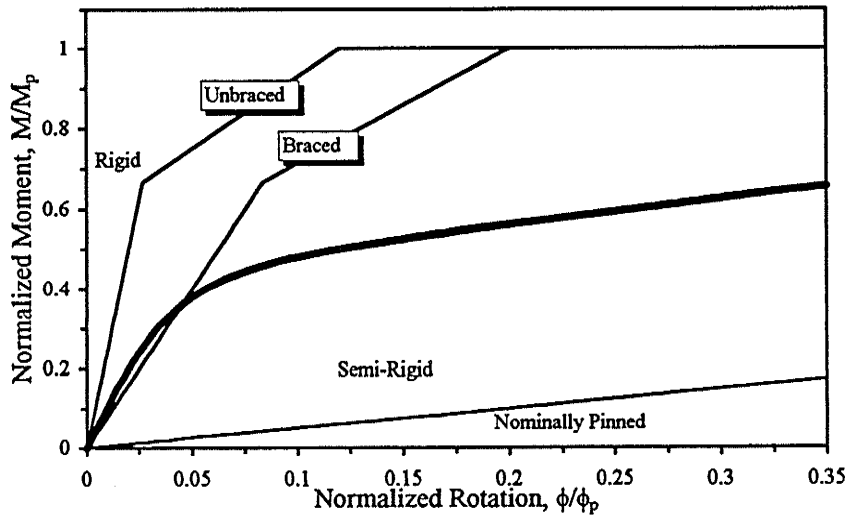


Figure A.217 (b) Eurocode3 Classification of Ioannides: Test 1

Table A.218 M-ϕ data for Ioannides: Test 2 (1978)

Moment, M kN-m	Rotation, ϕ radians	Moment, M kN-m	Rotation, ϕ radians
0	0	223.912	0.0127
12.627	0.0000	227.407	0.0135
25.254	0.0000	230.903	0.0144
37.881	0.0001	234.399	0.0153
50.508	0.0001	238.015	0.0160
63.135	0.0001	241.630	0.0168
74.241	0.0002	245.246	0.0176
85.347	0.0004	248.311	0.0184
95.146	0.0005	251.376	0.0192
104.946	0.0007	254.441	0.0200
114.735	0.0009	258.403	0.0211
125.501	0.0011	262.365	0.0222
135.924	0.0015		
146.339	0.0020		
158.368	0.0026		
169.715	0.0035		
178.764	0.0044		
183.920	0.0051		
189.076	0.0058		
193.567	0.0065		
198.059	0.0072		
202.691	0.0082		
207.324	0.0091		
211.625	0.0101		
215.926	0.0111		
219.919	0.0119		

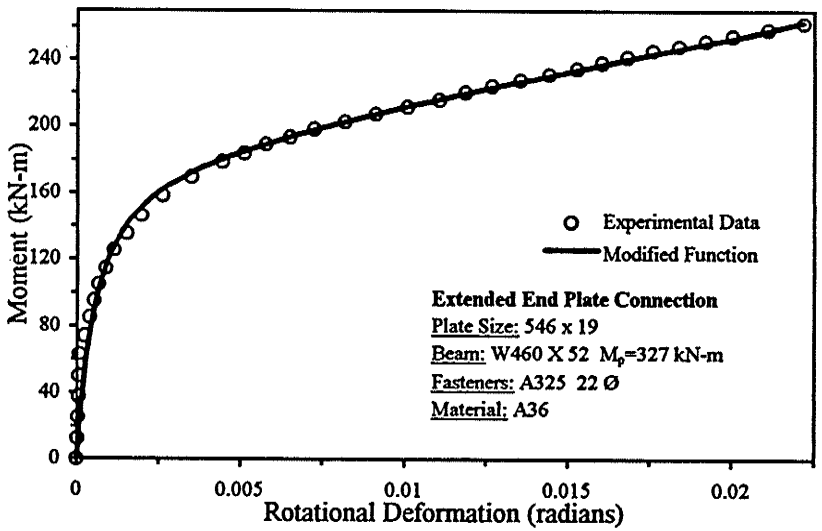


Figure A.218 (a) M-ϕ curve for Ioannides: Test 2

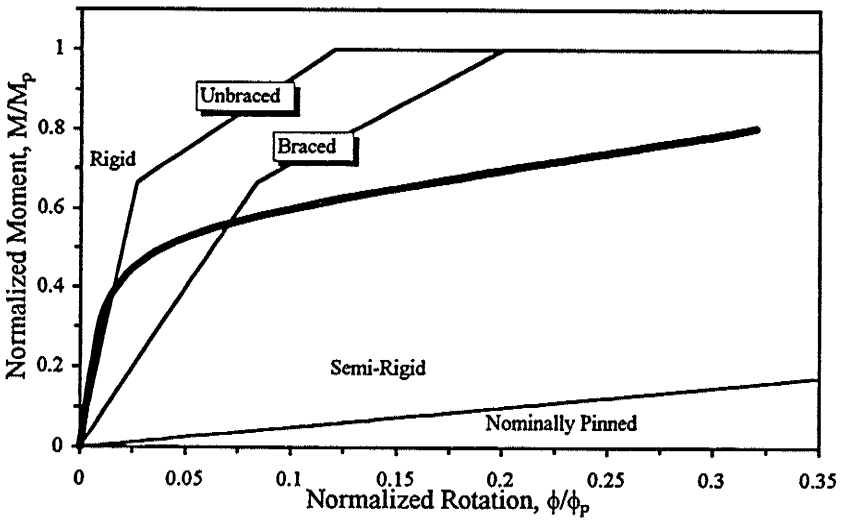


Figure A.218 (b) Eurocode3 Classification of Ioannides: Test 2

Table A.219 M-ϕ data for Ioannides: Test 3 (1978)

Moment, M kN-m	Rotation, ϕ radians	Moment, M kN-m	Rotation, ϕ radians
0	0	259.152	0.0051
11.056	0.0000	266.042	0.0055
22.112	0.0000	272.467	0.0061
33.168	0.0001	278.892	0.0067
42.842	0.0001	283.938	0.0072
52.516	0.0001	288.983	0.0076
62.420	0.0002	292.413	0.0082
72.324	0.0002	295.844	0.0088
81.766	0.0002	298.581	0.0093
91.208	0.0003	301.319	0.0099
100.878	0.0004	303.600	0.0104
110.549	0.0005	305.880	0.0109
121.139	0.0006	307.244	0.0114
131.729	0.0008	308.607	0.0118
143.928	0.0010		
156.127	0.0012		
169.017	0.0015		
181.906	0.0017		
192.256	0.0021		
202.605	0.0024		
210.425	0.0027		
218.245	0.0030		
226.751	0.0034		
235.256	0.0037		
243.759	0.0042		
252.263	0.0046		

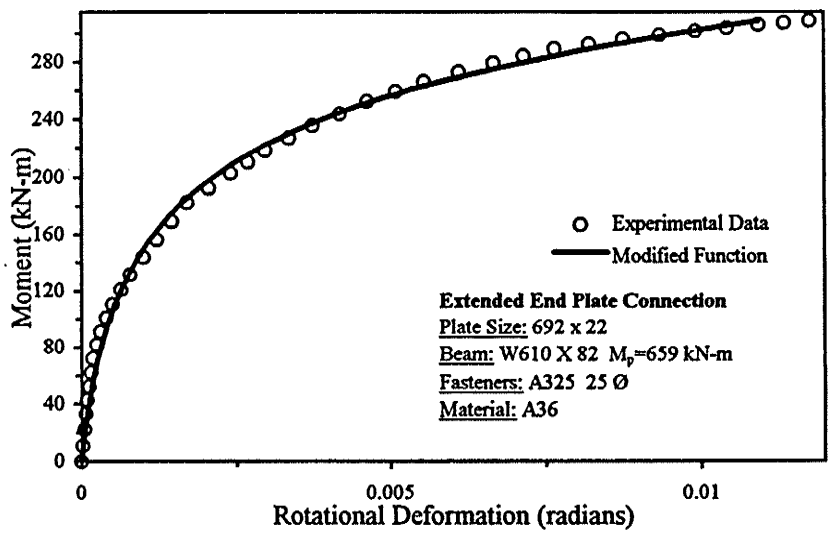


Figure A.219 (a) M-ϕ curve for Ioannides: Test 3

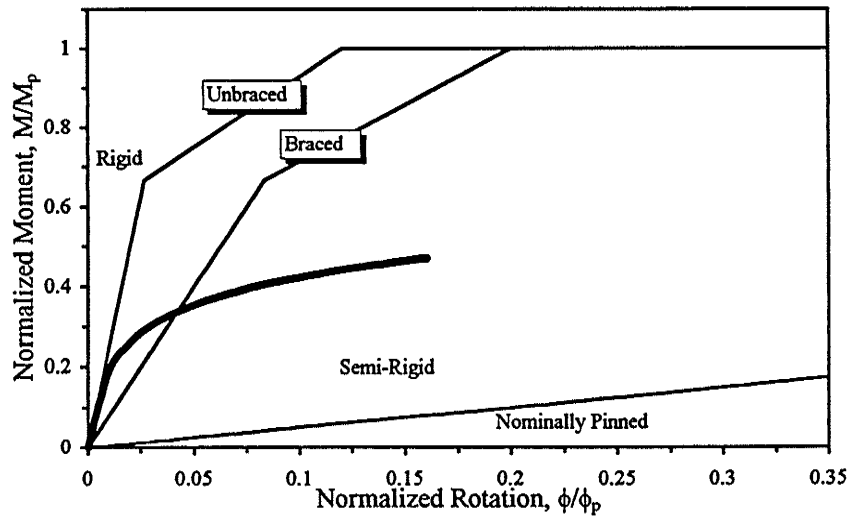


Figure A.219 (b) Eurocode3 Classification of Ioannides: Test 3

Table A.220 M-ϕ data for Ioannides: Test 4 (1978)

Moment, M kN-m	Rotation, ϕ radians	Moment, M kN-m	Rotation, ϕ radians
0	0	128.599	0.0246
6.094	0.0001	131.430	0.0267
12.842	0.0002	134.261	0.0287
19.590	0.0002	137.091	0.0308
26.338	0.0003	139.922	0.0329
30.452	0.0003	142.753	0.0349
34.566	0.0003	145.584	0.0370
41.649	0.0004	148.415	0.0390
48.406	0.0007	149.882	0.0405
55.670	0.0012	151.349	0.0420
60.047	0.0016		
64.424	0.0019		
68.812	0.0025		
73.200	0.0031		
77.773	0.0041		
82.346	0.0052		
87.683	0.0067		
93.021	0.0083		
97.703	0.0099		
102.385	0.0115		
106.498	0.0133		
110.612	0.0151		
114.648	0.0170		
118.684	0.0188		
122.226	0.0207		
125.768	0.0226		

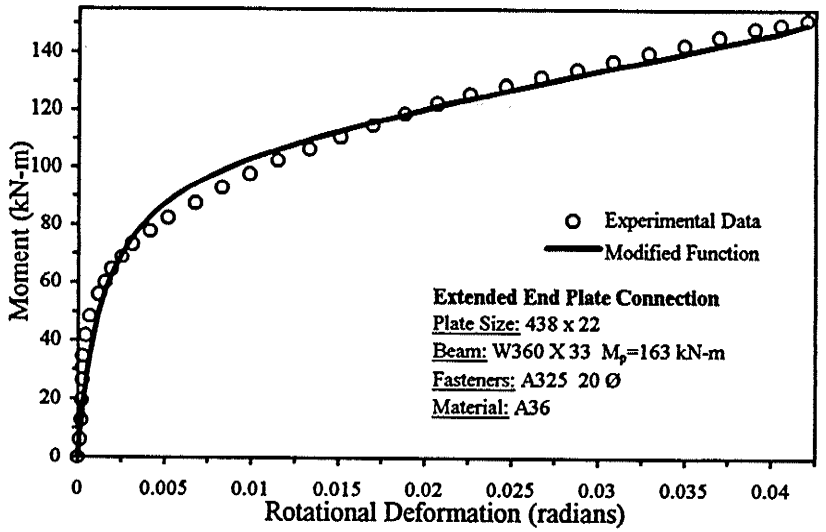


Figure A.220 (a) M-ϕ curve for Ioannides: Test 4

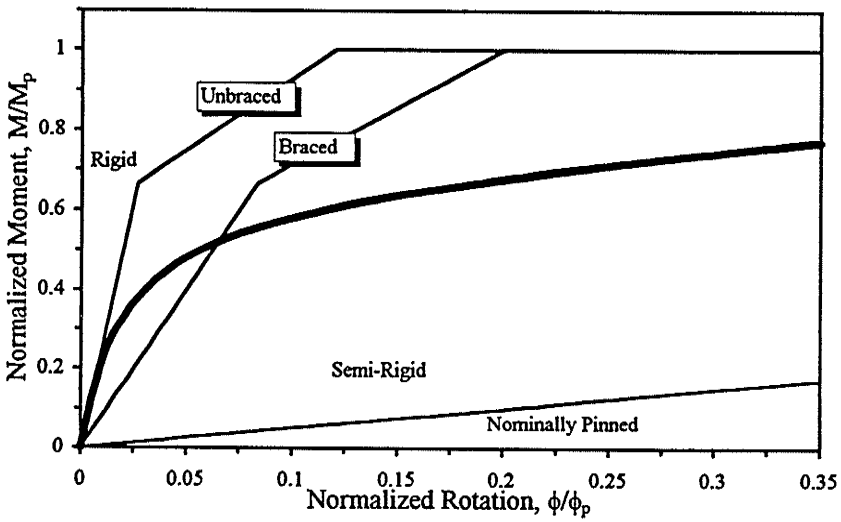


Figure A.220 (b) Eurocode3 Classification of Ioannides: Test 4

Table A.221 M-ϕ data for Ioannides: Test 5 (1978)

Moment, M kN-m	Rotation, ϕ radians	Moment, M kN-m	Rotation, ϕ radians
0	0	247.462	0.0205
11.063	0.0001	253.978	0.0221
22.126	0.0003	258.847	0.0238
33.189	0.0004	263.716	0.0255
45.016	0.0007	268.743	0.0273
56.843	0.0009	273.771	0.0292
69.488	0.0012	277.117	0.0305
82.132	0.0016	280.464	0.0319
92.802	0.0020	283.810	0.0333
103.472	0.0024	287.528	0.0350
114.796	0.0029	291.246	0.0367
126.121	0.0034	293.505	0.0379
136.782	0.0040	295.764	0.0390
147.443	0.0047		
157.768	0.0055		
168.093	0.0063		
176.937	0.0072		
185.781	0.0081		
193.134	0.0093		
200.487	0.0105		
208.490	0.0119		
216.493	0.0133		
223.506	0.0148		
230.519	0.0163		
235.733	0.0176		
240.946	0.0188		

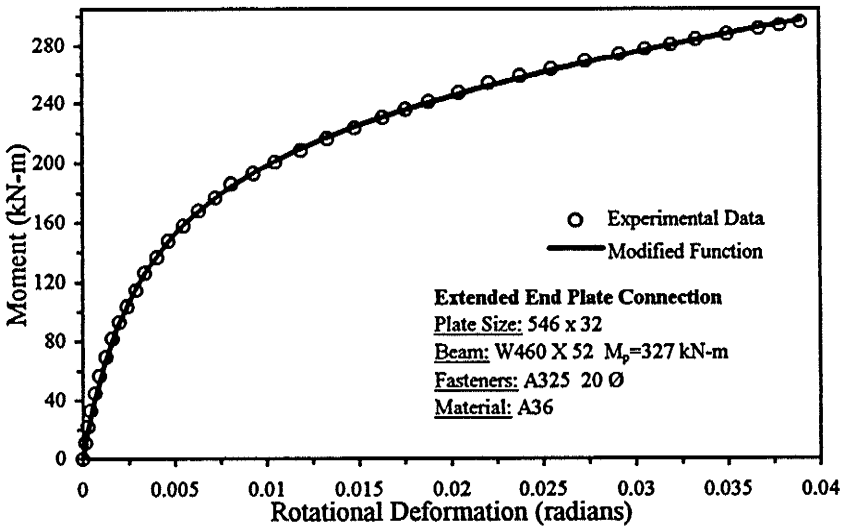


Figure A.221 (a) M-ϕ curve for Ioannides: Test 5

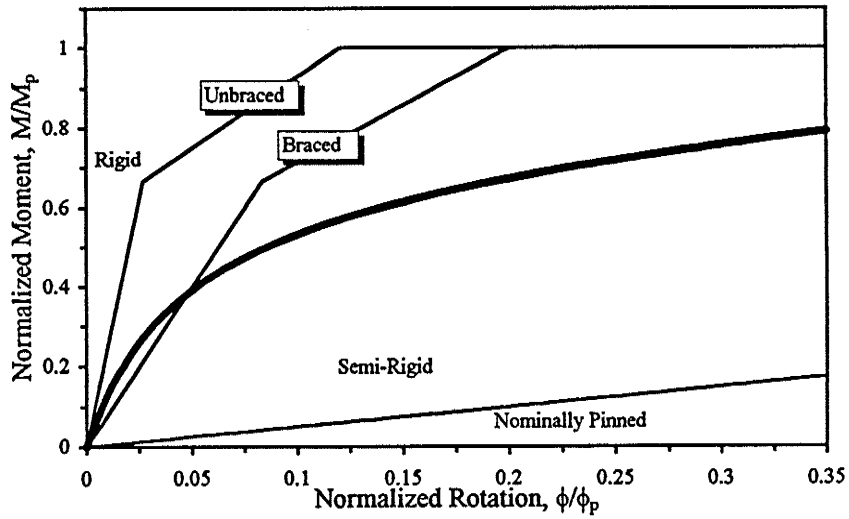


Figure A.221 (b) Eurocode3 Classification of Ioannides: Test 5

Table A.222 M-ϕ data for Dews: Test 1 (1979)

Moment, M kN-m	Rotation, ϕ radians	Moment, M kN-m	Rotation, ϕ radians
0	0	107.539	0.0416
4.314	0.0007	109.774	0.0444
8.628	0.0014	111.650	0.0471
12.489	0.0021	113.526	0.0497
16.351	0.0028	115.403	0.0524
22.251	0.0037	117.129	0.0550
28.151	0.0046	118.855	0.0576
33.677	0.0055	120.582	0.0603
39.202	0.0065	122.170	0.0632
43.966	0.0072	123.758	0.0661
48.730	0.0079	125.346	0.0690
53.878	0.0088	126.720	0.0716
59.026	0.0097	128.095	0.0742
63.095	0.0099	129.470	0.0768
68.408	0.0112		
71.762	0.0122		
74.833	0.0137		
79.321	0.0165		
84.276	0.0196		
89.090	0.0230		
91.749	0.0252		
94.407	0.0275		
97.248	0.0304		
100.090	0.0333		
102.697	0.0361		
105.305	0.0388		

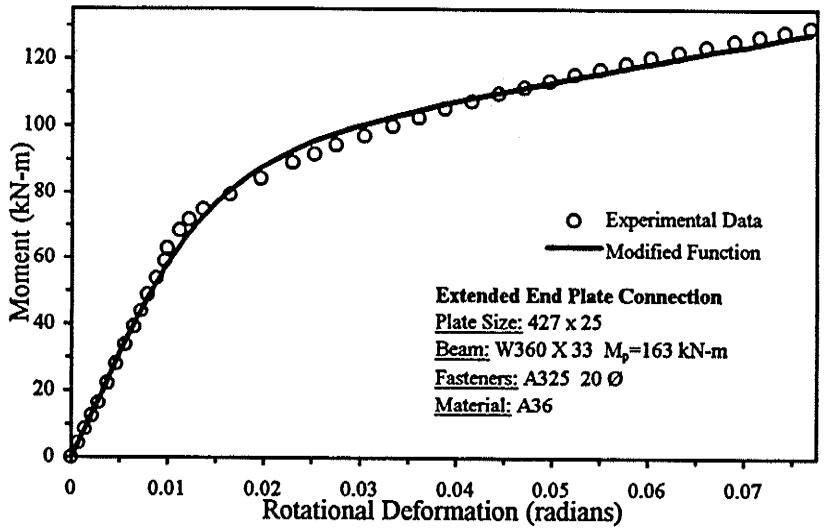


Figure A.222 (a) M-ϕ curve for Dews: Test 1

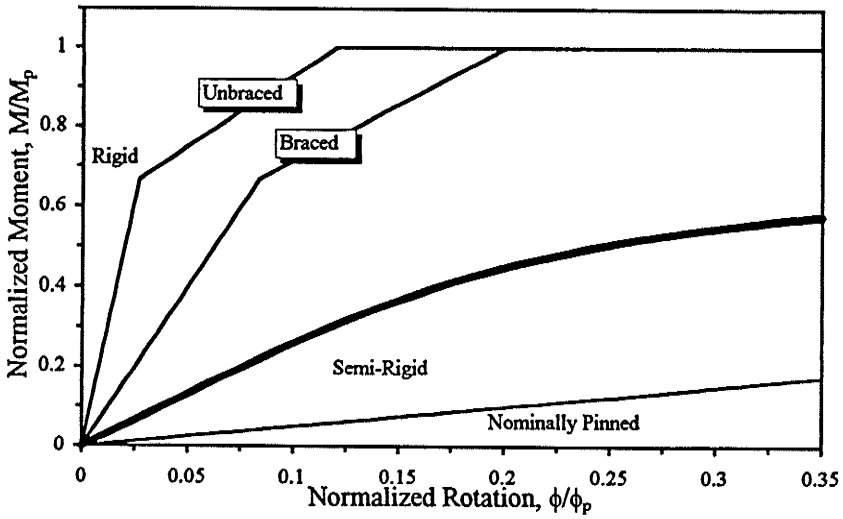


Figure A.222 (b) Eurocode3 Classification of Dews: Test 1

Table A.223 M-ϕ data for Dews: Test 2 (1979)

Moment, M kN-m	Rotation, ϕ radians	Moment, M kN-m	Rotation, ϕ radians
0	0	99.613	0.0308
4.558	0.0005	102.064	0.0332
9.116	0.0009	104.514	0.0356
13.675	0.0014	106.964	0.0381
18.432	0.0018	109.414	0.0405
23.190	0.0022	112.620	0.0432
27.947	0.0027	115.827	0.0460
34.185	0.0034	119.033	0.0487
40.422	0.0041	122.239	0.0514
44.931	0.0045	125.100	0.0544
49.439	0.0050	127.962	0.0574
53.947	0.0054	130.823	0.0603
58.605	0.0059		
63.262	0.0063		
68.373	0.0069		
72.145	0.0080		
75.323	0.0094		
77.230	0.0110		
79.138	0.0125		
81.882	0.0147		
84.627	0.0169		
86.869	0.0189		
89.111	0.0210		
91.353	0.0230		
94.106	0.0256		
96.860	0.0282		

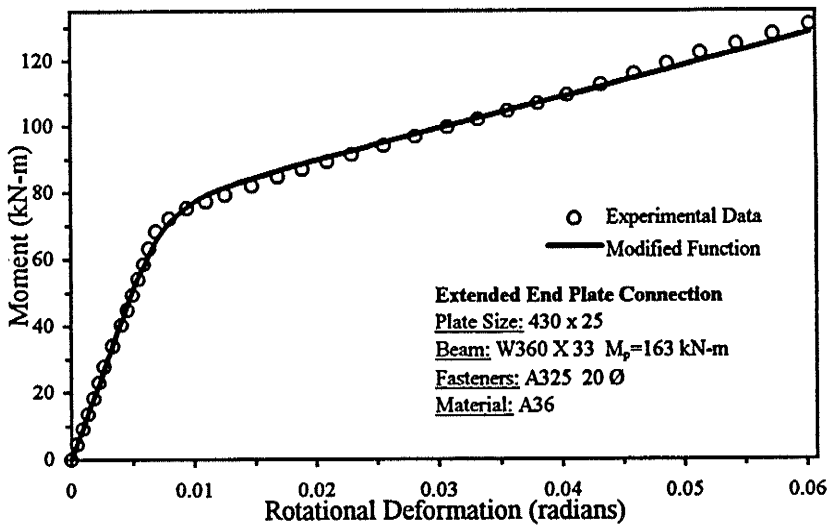


Figure A.223 (a) M-ϕ curve for Dews: Test 2

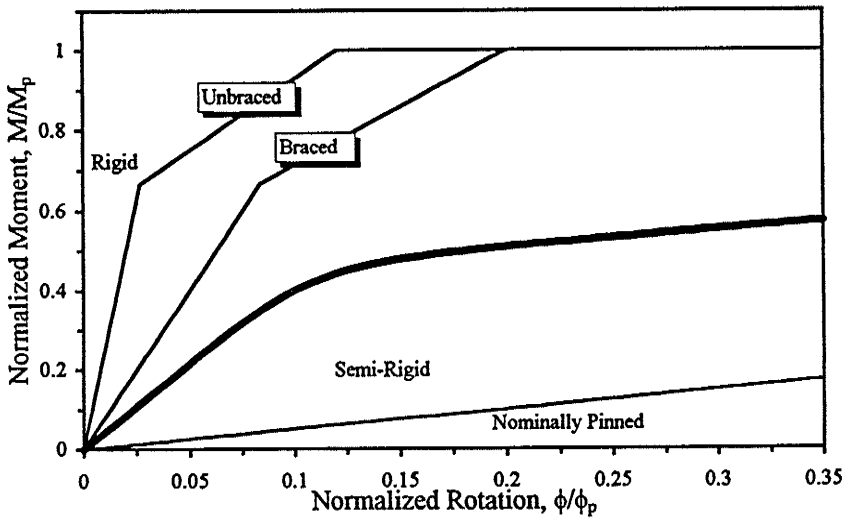


Figure A.223 (b) Eurocode3 Classification of Dews: Test 2

Table A.224 M-ϕ data for Sherbourne: Test A1 (1961)

Moment, M kN-m	Rotation, ϕ radians	Moment, M kN-m	Rotation, ϕ radians
0	0	306.472	0.0077
15.818	0.0002	308.449	0.0082
31.635	0.0003	312.403	0.0089
47.454	0.0004	316.358	0.0095
63.272	0.0005	318.994	0.0101
79.090	0.0007	321.631	0.0106
94.907	0.0008	324.267	0.0112
108.748	0.0010	325.256	0.0118
122.589	0.0012	326.244	0.0124
138.407	0.0013	327.233	0.0129
154.225	0.0014	328.221	0.0135
170.042	0.0017		
185.860	0.0019		
201.678	0.0021		
217.497	0.0023		
231.337	0.0028		
245.177	0.0032		
255.064	0.0037		
264.950	0.0041		
270.882	0.0045		
276.814	0.0049		
280.768	0.0053		
284.722	0.0057		
288.676	0.0062		
292.631	0.0066		
304.494	0.0071		

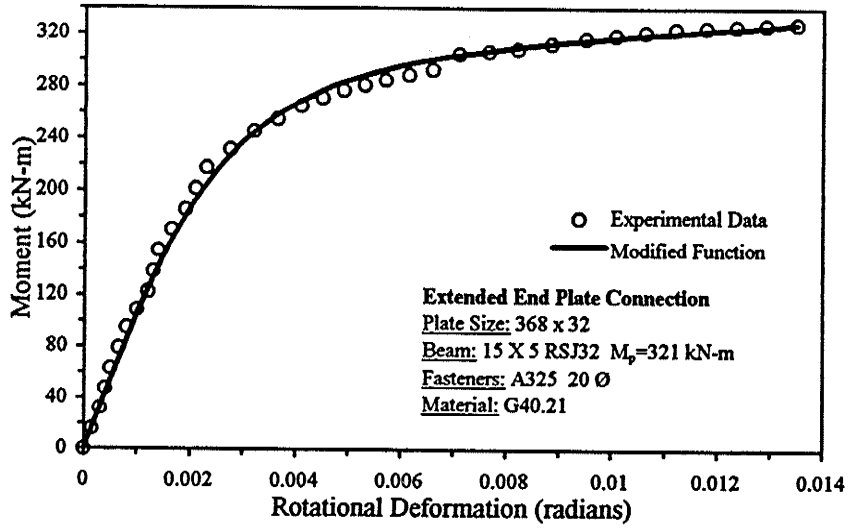


Figure A.224 (a) M-ϕ curve for Sherbourne: Test A1

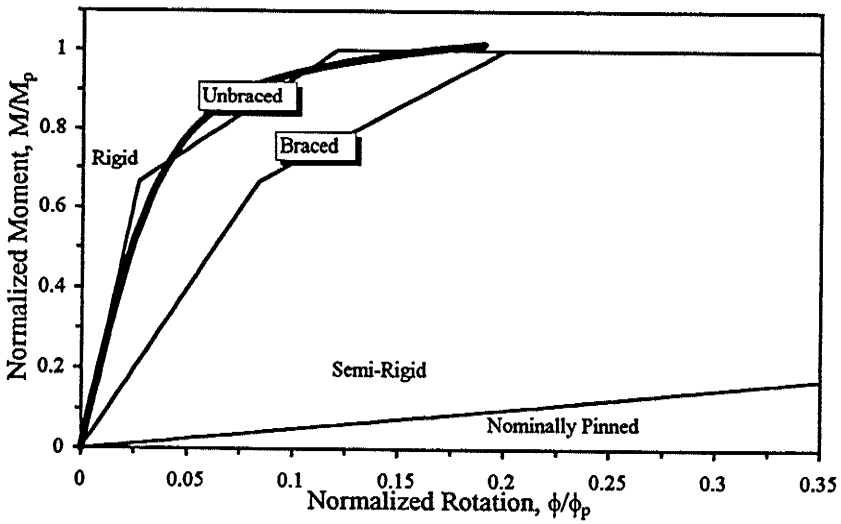


Figure A.224 (b) Eurocode3 Classification of Sherbourne: Test A1

Table A.225 M-ϕ data for Bailey: Test A1-L (1970)

Moment, M kN-m	Rotation, ϕ radians	Moment, M kN-m	Rotation, ϕ radians
0	0	192.690	0.0100
4.074	0.0003	204.195	0.0112
8.148	0.0006	212.823	0.0125
12.223	0.0009	220.492	0.0135
16.297	0.0012	227.203	0.0149
21.410	0.0014	232.954	0.0166
26.523	0.0016	238.707	0.0181
31.635	0.0018	241.103	0.0191
39.305	0.0022	243.500	0.0200
46.974	0.0025	246.376	0.0216
54.644	0.0029	247.813	0.0225
62.313	0.0032	249.251	0.0234
72.379	0.0037	250.210	0.0243
82.445	0.0041	251.170	0.0252
90.114	0.0045	252.128	0.0265
97.783	0.0048	253.087	0.0279
105.932	0.0052	253.087	0.0296
114.080	0.0056	253.566	0.0307
123.667	0.0061	254.045	0.0318
133.254	0.0065	255.004	0.0334
139.965	0.0069	255.963	0.0348
146.675	0.0072	255.004	0.0353
153.865	0.0077		
161.055	0.0081		
172.559	0.0088		
183.105	0.0092		

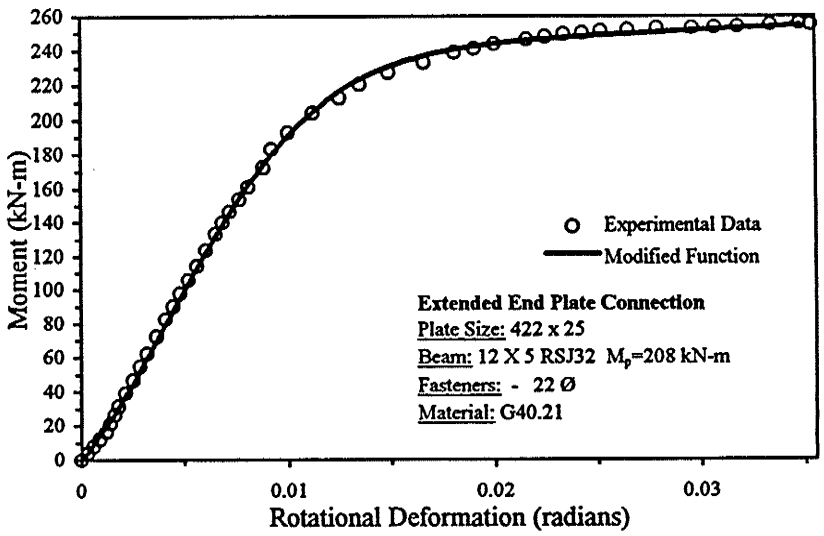


Figure A.225 (a) M-ϕ curve for Bailey: Test A1-L

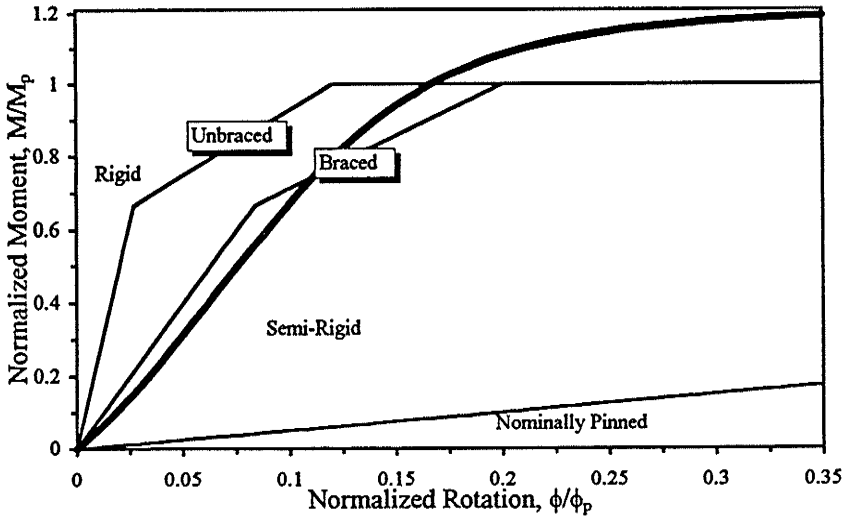


Figure A.225 (b) Eurocode3 Classification of Bailey: Test A1-L

Table A.226 M-ϕ data for Bailey: Test A1-R (1970)

Moment, M kN-m	Rotation, ϕ radians	Moment, M kN-m	Rotation, ϕ radians
0	0	222.641	0.0114
9.039	0.0002	229.300	0.0127
18.077	0.0004	233.106	0.0137
29.495	0.0008	235.485	0.0145
36.631	0.0010	237.864	0.0153
43.767	0.0012	241.669	0.0166
51.855	0.0015	245.475	0.0180
59.942	0.0017	247.377	0.0194
72.310	0.0022	249.281	0.0209
79.446	0.0024	250.708	0.0218
86.583	0.0025	252.135	0.0227
97.048	0.0027	253.087	0.0241
109.417	0.0032	254.037	0.0254
116.077	0.0034	254.037	0.0265
122.737	0.0036	254.989	0.0277
129.873	0.0038	255.941	0.0288
137.010	0.0040	255.941	0.0296
144.621	0.0042	255.941	0.0306
152.233	0.0044	255.941	0.0314
160.795	0.0048		
172.214	0.0053		
182.679	0.0059		
195.048	0.0068		
203.610	0.0078		
212.174	0.0090		
217.883	0.0102		

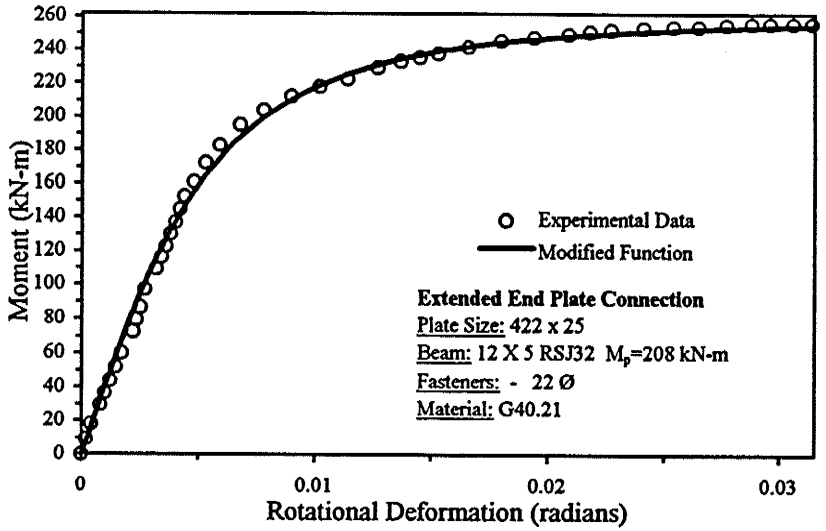


Figure A.226 (a) M-ϕ curve for Bailey: Test A1-R

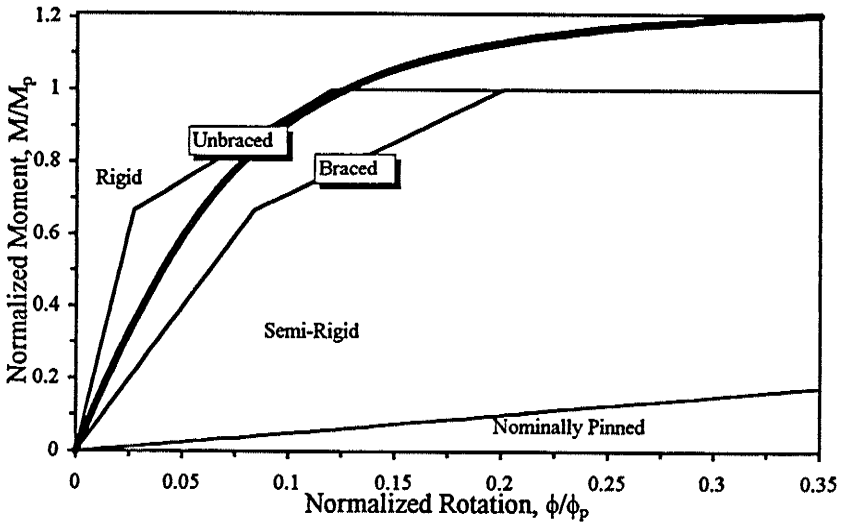


Figure A.226 (b) Eurocode3 Classification of Bailey: Test A1-R

Table A.227 M-ϕ data for Bailey: Test A2-L (1970)

Moment, M kN-m	Rotation, ϕ radians	Moment, M kN-m	Rotation, ϕ radians
0	0	94.250	0.0054
1.010	0.0001	98.077	0.0057
2.020	0.0002	101.905	0.0060
3.030	0.0003	107.645	0.0069
4.039	0.0004	111.473	0.0073
5.049	0.0005	115.300	0.0077
6.059	0.0006	120.085	0.0089
9.089	0.0009	123.912	0.0098
13.189	0.0011	126.783	0.0110
17.291	0.0013	128.696	0.0123
23.442	0.0016	130.131	0.0131
27.270	0.0018	131.566	0.0139
31.097	0.0020	133.002	0.0147
36.838	0.0022	134.438	0.0154
42.580	0.0024	135.873	0.0161
47.364	0.0026	137.308	0.0168
52.149	0.0027	137.308	0.0176
55.976	0.0030	137.308	0.0183
59.803	0.0033	137.787	0.0192
64.587	0.0037	138.265	0.0200
69.372	0.0040	138.265	0.0208
73.199	0.0042	138.265	0.0215
77.027	0.0044	140.178	0.0225
81.811	0.0046	140.178	0.0233
86.595	0.0048	140.178	0.0241
90.422	0.0051	141.135	0.0253
		140.178	0.0261

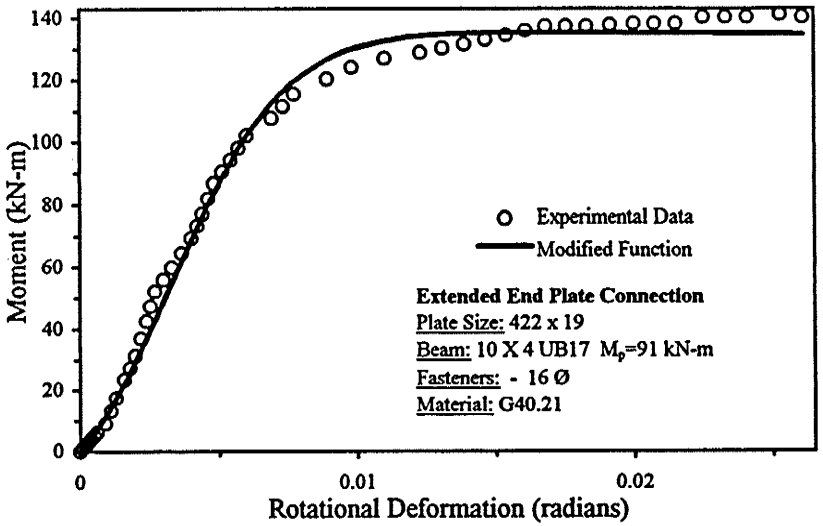


Figure A.227 (a) M-ϕ curve for Bailey: Test A2-L

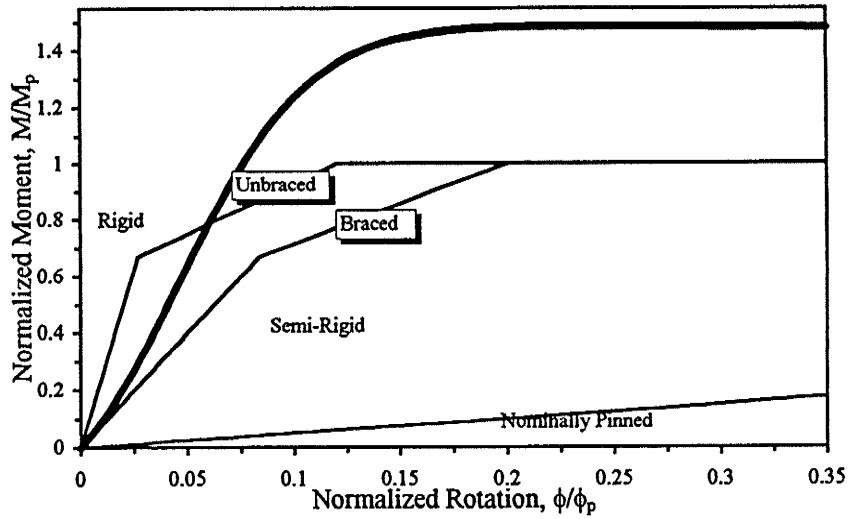


Figure A.227 (b) Eurocode3 Classification of Bailey: Test A2-L

Table A.228 M-ϕ data for Bailey: Test A2-R (1970)

Moment, M kN-m	Rotation, ϕ radians	Moment, M kN-m	Rotation, ϕ radians
0	0	115.300	0.0092
4.625	0.0003	120.085	0.0106
9.249	0.0006	122.955	0.0119
13.874	0.0009	123.912	0.0127
19.615	0.0013	124.868	0.0134
25.357	0.0016	125.826	0.0142
30.619	0.0018	126.783	0.0149
35.882	0.0019	128.696	0.0162
40.666	0.0021	129.174	0.0172
45.450	0.0023	129.653	0.0182
51.191	0.0024	129.653	0.0190
56.932	0.0024	129.653	0.0197
60.281	0.0027	130.132	0.0207
63.630	0.0029	130.610	0.0216
67.457	0.0032	130.610	0.0224
71.285	0.0034	130.610	0.0232
74.634	0.0036	131.088	0.0240
77.983	0.0038	131.566	0.0248
82.289	0.0041	131.088	0.0257
86.595	0.0044	130.610	0.0265
92.335	0.0052	131.567	0.0276
95.684	0.0057	132.523	0.0286
99.033	0.0062		
102.383	0.0067		
105.732	0.0071		
110.516	0.0080		

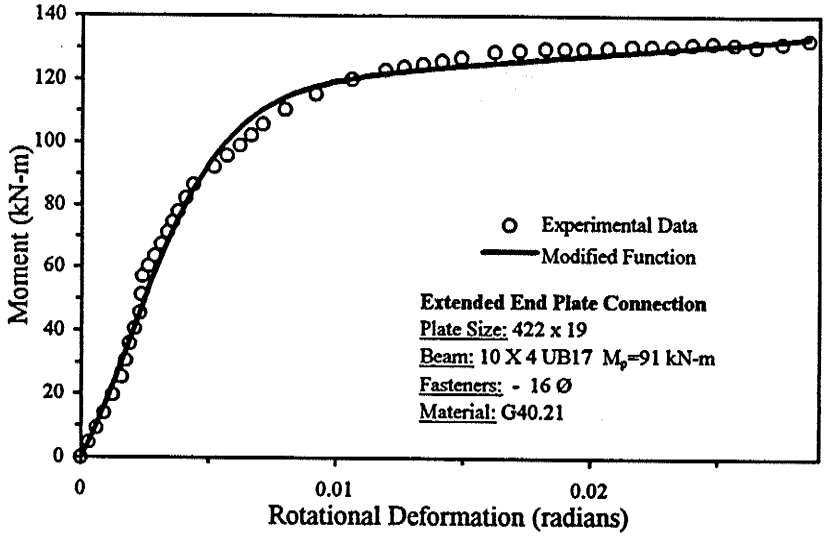


Figure A.228 (a) M-ϕ curve for Bailey: Test A2-R

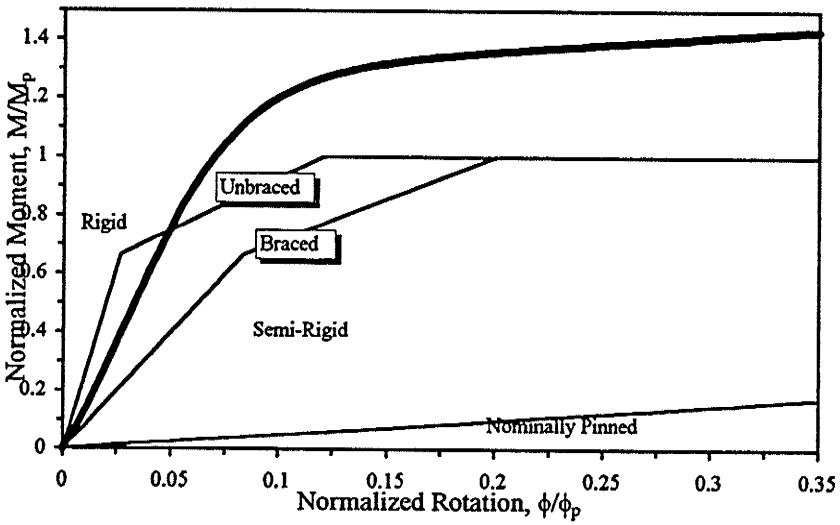


Figure A.228 (b) Eurocode3 Classification of Bailey: Test A2-R

Table A.229 M-ϕ data for Bailey: Test A3-L (1970)

Moment, M kN-m	Rotation, ϕ radians	Moment, M kN-m	Rotation, ϕ radians
0	0	131.105	0.0081
2.209	0.0002	134.947	0.0087
4.419	0.0004	138.790	0.0093
6.627	0.0006	141.671	0.0102
8.836	0.0008	144.552	0.0110
11.046	0.0010	146.953	0.0116
17.769	0.0014	149.354	0.0122
24.493	0.0017	150.795	0.0130
30.736	0.0020	152.236	0.0137
36.979	0.0023	153.196	0.0146
42.261	0.0026	154.157	0.0154
47.543	0.0028	155.117	0.0162
51.866	0.0031	156.078	0.0170
56.188	0.0034	156.398	0.0178
61.631	0.0036	156.718	0.0186
67.073	0.0039	157.038	0.0194
72.516	0.0041	156.558	0.0202
78.759	0.0045	156.078	0.0210
85.002	0.0048		
90.285	0.0051		
95.568	0.0054		
101.811	0.0059		
108.053	0.0063		
114.297	0.0067		
120.541	0.0070		
125.823	0.0076		

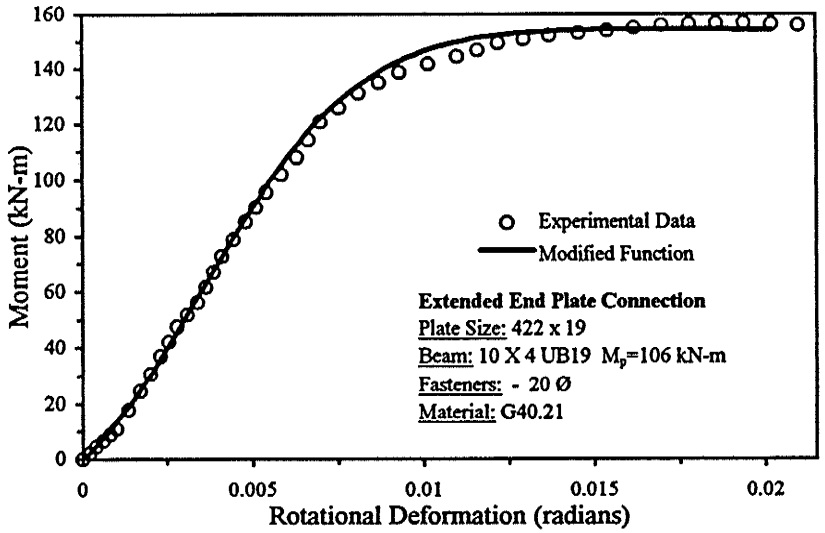


Figure A.229 (a) M-ϕ curve for Bailey: Test A3-L

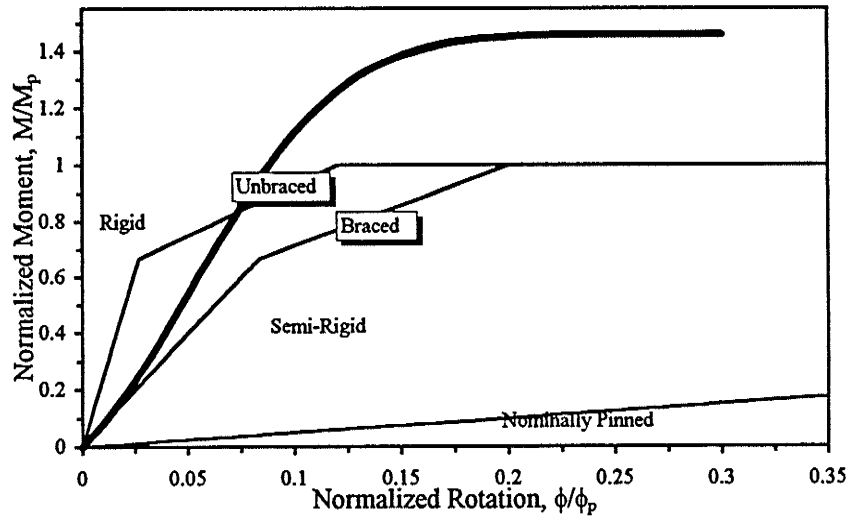


Figure A.229 (b) Eurocode3 Classification of Bailey: Test A3-L

Table A.230 M-ϕ data for Bailey: Test A3-R (1970)

Moment, M kN-m	Rotation, ϕ radians	Moment, M kN-m	Rotation, ϕ radians
0	0	133.480	0.0073
5.581	0.0002	141.135	0.0084
11.163	0.0005	143.527	0.0091
16.744	0.0007	145.919	0.0097
22.486	0.0010	150.703	0.0108
28.227	0.0013	152.139	0.0115
33.968	0.0016	153.574	0.0121
39.709	0.0019	154.531	0.0130
45.450	0.0022	155.488	0.0138
51.192	0.0024	156.445	0.0146
56.933	0.0026	157.401	0.0153
62.674	0.0027	158.836	0.0160
67.458	0.0030	160.271	0.0166
72.242	0.0032	160.750	0.0176
72.242	0.0032	161.229	0.0185
77.505	0.0035	160.750	0.0195
82.767	0.0038	160.271	0.0205
88.030	0.0041	161.229	0.0214
93.293	0.0043	162.186	0.0222
98.555	0.0045	161.867	0.0230
103.818	0.0047	161.548	0.0239
108.602	0.0050	161.229	0.0247
113.386	0.0053		
119.606	0.0057		
125.826	0.0061		
133.480	0.0073		

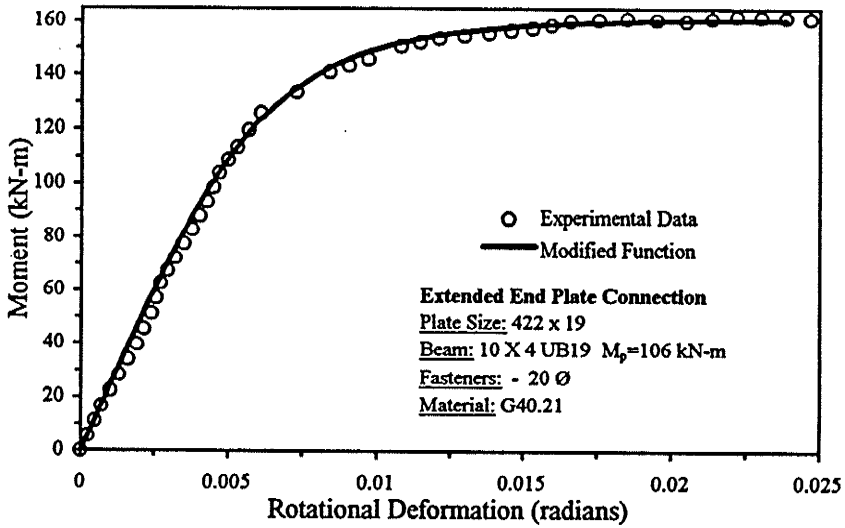


Figure A.230 (a) M-ϕ curve for Bailey: Test A3-R

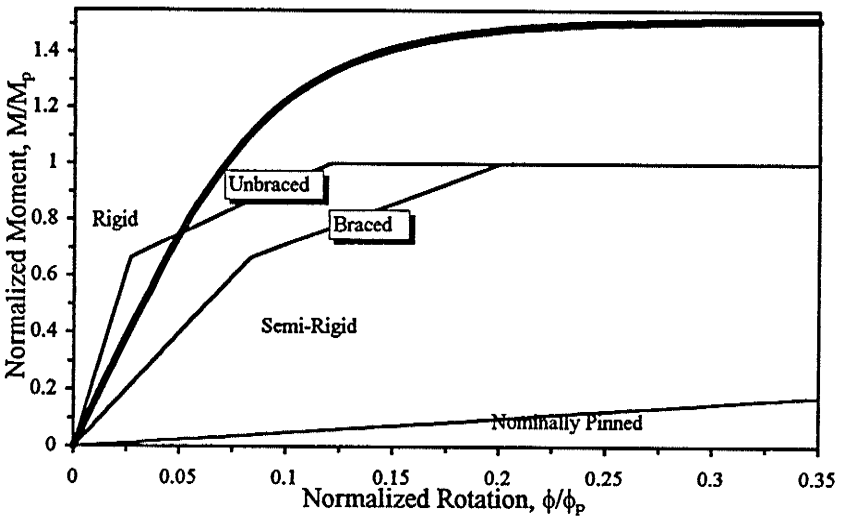


Figure A.230 (b) Eurocode3 Classification of Bailey: Test A3-R

Table A.231 M-ϕ data for Surtees: Test C1 (1970)

Moment, M kN-m	Rotation, ϕ radians	Moment, M kN-m	Rotation, ϕ radians
0	0	133.987	0.0091
5.491	0.0001	136.916	0.0096
10.982	0.0002	138.869	0.0100
16.840	0.0004	140.821	0.0104
22.697	0.0006	142.773	0.0108
28.555	0.0008	144.970	0.0113
34.900	0.0010	147.166	0.0118
41.245	0.0012		
47.591	0.0014		
52.960	0.0016		
58.330	0.0019		
63.699	0.0021		
71.021	0.0025		
78.342	0.0029		
85.663	0.0035		
92.985	0.0040		
97.866	0.0045		
102.748	0.0050		
107.629	0.0055		
112.510	0.0059		
117.391	0.0064		
122.272	0.0068		
124.224	0.0072		
126.177	0.0076		
128.129	0.0080		
131.058	0.0085		

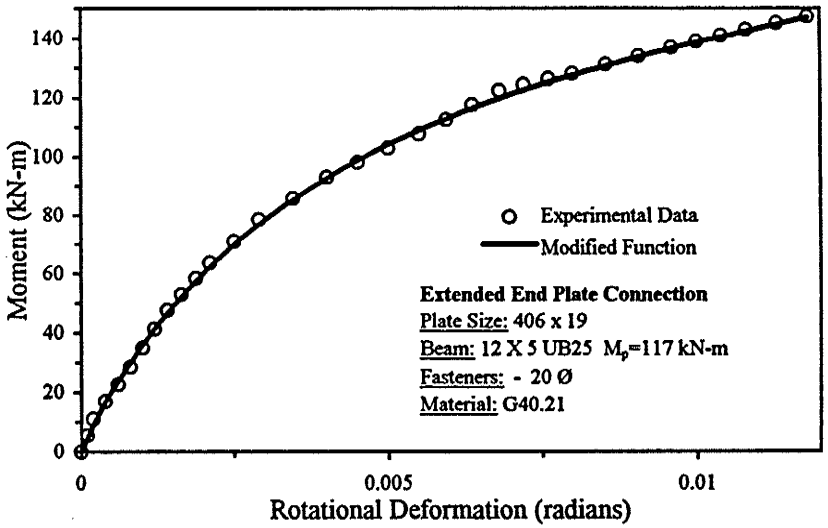


Figure A.231 (a) M-ϕ curve for Surtees: Test C1

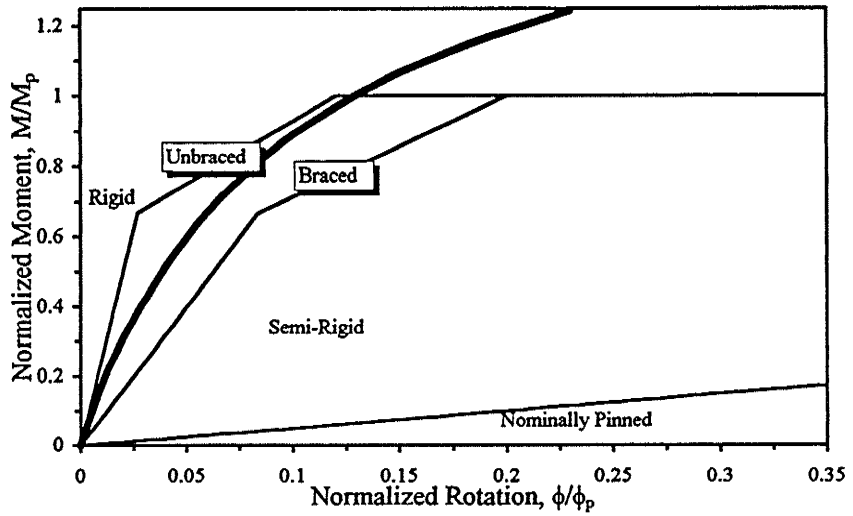


Figure A.231 (b) Eurocode3 Classification of Surtees: Test C1

Table A.232 M-ϕ data for Surtees: Test C2 (1970)

Moment, M kN-m	Rotation, ϕ radians	Moment, M kN-m	Rotation, ϕ radians
0	0	345.519	0.0110
13.571	0.0002	349.920	0.0121
27.142	0.0004	355.788	0.0134
38.146	0.0007	358.723	0.0148
49.150	0.0010	364.591	0.0163
61.621	0.0013	368.993	0.0174
74.091	0.0015	370.460	0.0188
88.030	0.0018	371.927	0.0200
101.969	0.0021	373.394	0.0214
115.173	0.0024	376.328	0.0225
128.377	0.0027	377.795	0.0238
143.783	0.0031	379.262	0.0249
159.188	0.0034	380.731	0.0262
171.659	0.0037	385.132	0.0275
184.130	0.0040	383.665	0.0285
196.601	0.0043	385.132	0.0299
209.072	0.0046	388.066	0.0315
222.276	0.0049	389.533	0.0330
235.480	0.0052	392.468	0.0344
247.951	0.0056	395.402	0.0355
260.422	0.0059	398.336	0.0370
279.496	0.0065	401.270	0.0388
295.634	0.0071	402.737	0.0399
308.838	0.0078		
324.978	0.0090		
338.182	0.0101		

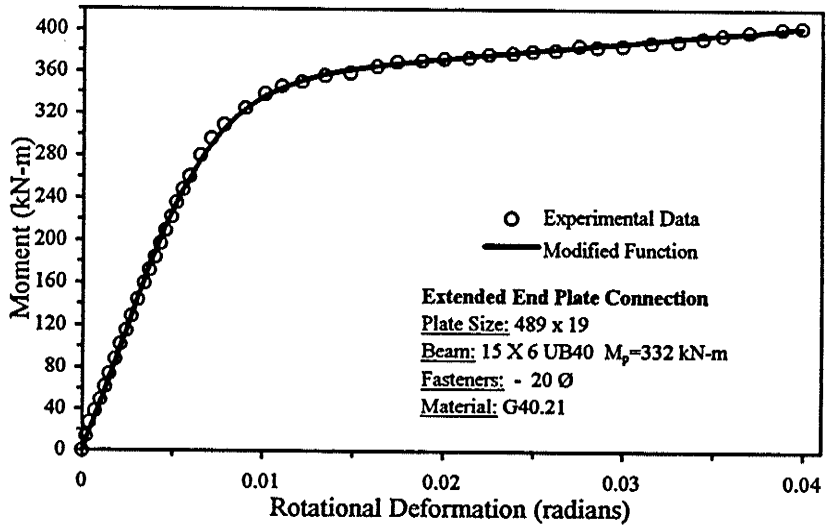


Figure A.232 (a) M-ϕ curve for Surtees: Test C2

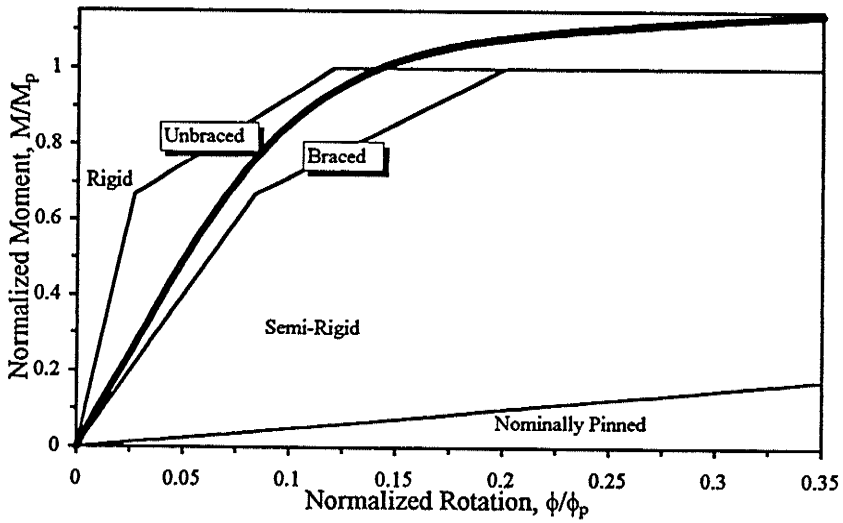


Figure A.232 (b) Eurocode3 Classification of Surtees: Test C2

Table A.233 M-ϕ data for Surtees: Test C3 (1970)

Moment, M kN-m	Rotation, ϕ radians	Moment, M kN-m	Rotation, ϕ radians
0	0	355.788	0.0076
11.371	0.0002	367.525	0.0089
22.741	0.0003	376.328	0.0099
41.081	0.0005	382.198	0.0112
59.420	0.0006	385.132	0.0122
73.358	0.0008	388.066	0.0132
87.296	0.0009	391.001	0.0143
101.234	0.0011	392.468	0.0154
115.173	0.0013	393.935	0.0166
127.644	0.0015	398.336	0.0179
140.115	0.0016	398.336	0.0188
157.721	0.0018	396.869	0.0202
175.327	0.0020	396.869	0.0219
189.998	0.0022	396.869	0.0232
204.669	0.0024	393.935	0.0245
217.141	0.0027	393.935	0.0259
229.612	0.0029	396.869	0.0275
242.817	0.0032	396.869	0.0288
256.021	0.0035	393.935	0.0299
269.959	0.0039	394.668	0.0313
283.897	0.0043	395.402	0.0326
294.167	0.0046	394.668	0.0337
304.437	0.0049	393.935	0.0347
322.044	0.0058	393.935	0.0365
332.314	0.0063	392.468	0.0384
342.583	0.0067	392.468	0.0400

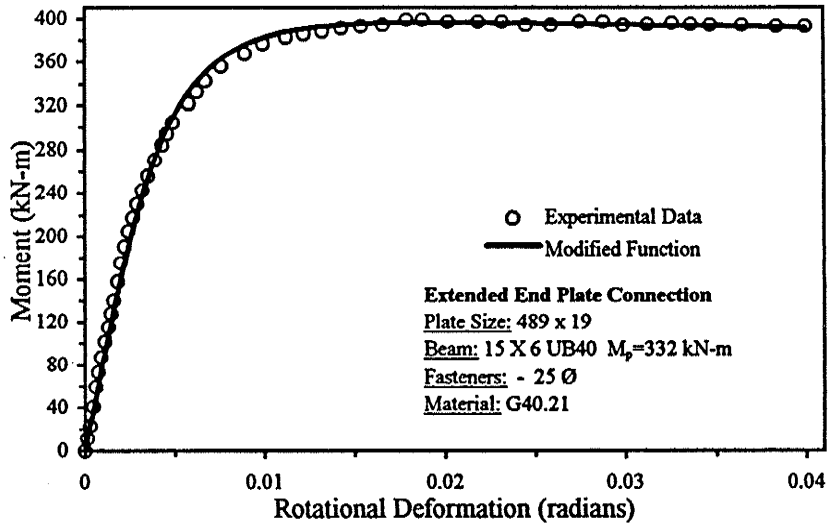


Figure A.233 (a) M-ϕ curve for Surtees: Test C3

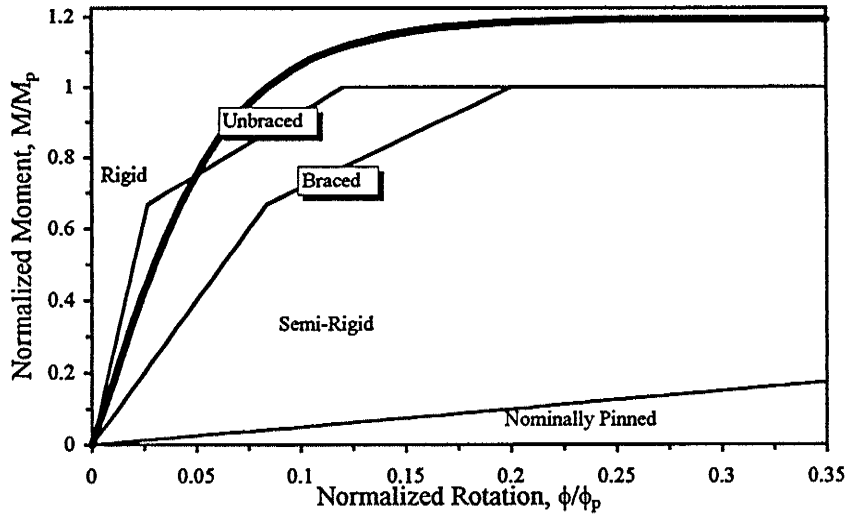


Figure A.233 (b) Eurocode3 Classification of Surtees: Test C3

Table A.234 M-ϕ data for Surtees: Test C4 (1970)

Moment, M kN-m	Rotation, ϕ radians	Moment, M kN-m	Rotation, ϕ radians
0	0	378.531	0.0131
14.277	0.0004	382.192	0.0144
28.555	0.0008	385.853	0.0156
46.127	0.0013	390.246	0.0168
63.699	0.0017	394.639	0.0179
76.878	0.0021	394.639	0.0191
90.056	0.0024	394.639	0.0203
106.164	0.0028	396.103	0.0214
122.272	0.0032	397.567	0.0225
139.112	0.0037	401.228	0.0245
155.952	0.0041	404.890	0.0264
169.131	0.0045	405.622	0.0277
182.310	0.0048	406.354	0.0289
198.418	0.0052	408.551	0.0301
214.526	0.0056	410.747	0.0312
229.901	0.0060	412.943	0.0326
245.276	0.0063	415.140	0.0339
261.384	0.0067	418.068	0.0354
277.492	0.0071	420.997	0.0368
291.403	0.0074	423.926	0.0384
305.314	0.0077	426.854	0.0400
318.494	0.0082		
331.673	0.0086		
347.780	0.0092		
360.959	0.0100		
372.674	0.0113		

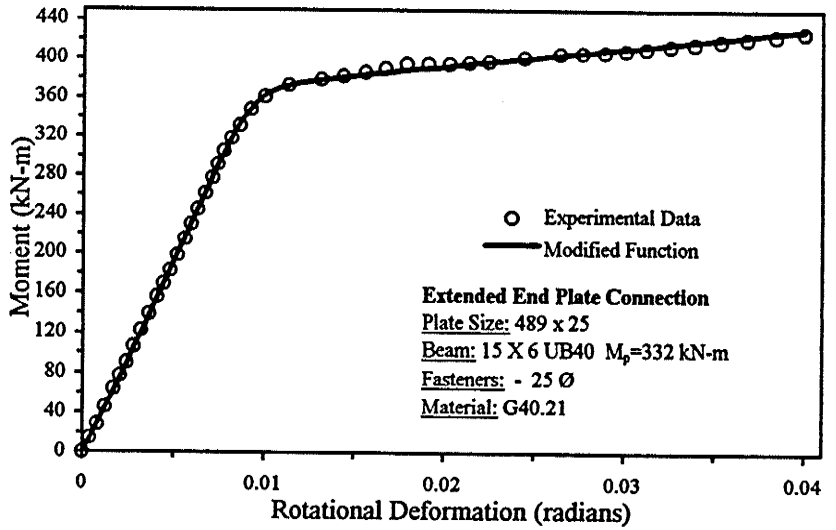


Figure A.234 (a) M-ϕ curve for Surtees: Test C4

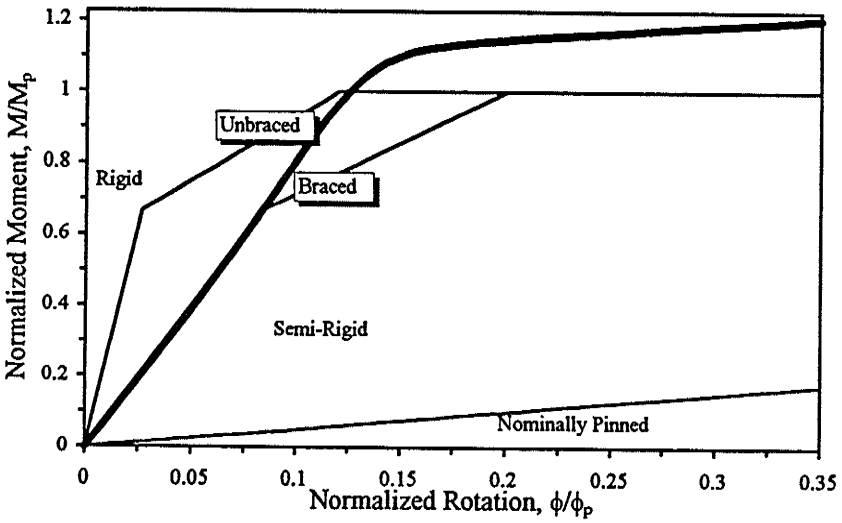


Figure A.234 (b) Eurocode3 Classification of Surtees: Test C4

Table A.235 M-ϕ data for Surtees: Test C5 (1970)

Moment, M kN-m	Rotation, ϕ radians	Moment, M kN-m	Rotation, ϕ radians
0	0	376.342	0.0142
18.634	0.0003	385.110	0.0157
37.269	0.0005	389.495	0.0170
50.422	0.0008	393.879	0.0183
63.576	0.0010	399.726	0.0193
86.961	0.0015	404.110	0.0212
108.883	0.0019	409.957	0.0226
129.344	0.0022	412.880	0.0239
143.960	0.0025	417.263	0.0255
158.575	0.0028	426.033	0.0268
174.652	0.0031	428.956	0.0283
190.729	0.0034	434.802	0.0297
204.613	0.0037	439.187	0.0308
218.497	0.0040	443.571	0.0318
233.843	0.0044	446.495	0.0331
249.189	0.0047	455.263	0.0350
261.612	0.0050	458.186	0.0363
274.034	0.0052	462.571	0.0377
293.035	0.0058	466.955	0.0389
310.572	0.0064	469.878	0.0400
323.726	0.0072		
338.342	0.0082		
348.572	0.0091		
357.341	0.0104		
364.649	0.0115		
370.495	0.0129		

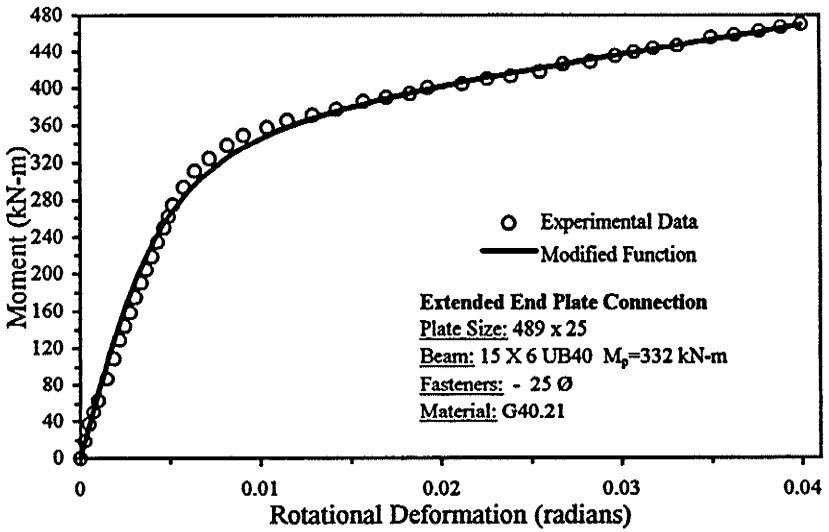


Figure A.235 (a) M-ϕ curve for Surtees: Test C5

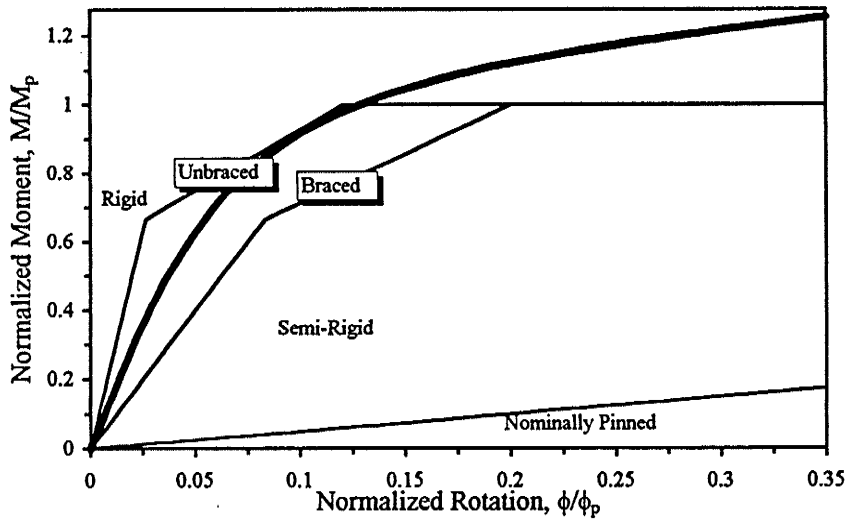


Figure A.235 (b) Eurocode3 Classification of Surtees: Test C5

Table A.236 M-ϕ data for Packer: Test J1 (1977)

Moment, M kN-m	Rotation, ϕ radians	Moment, M kN-m	Rotation, ϕ radians
0	0	96.774	0.0490
4.597	0.0003	98.709	0.0524
9.194	0.0006	99.677	0.0543
13.791	0.0009	101.613	0.0587
18.388	0.0012	102.581	0.0611
23.227	0.0017	102.581	0.0645
26.775	0.0019	104.516	0.0669
30.323	0.0020	104.516	0.0698
33.871	0.0022	105.484	0.0736
38.710	0.0029	106.452	0.0780
43.549	0.0036	106.452	0.0814
48.387	0.0041	106.452	0.0843
52.259	0.0055	107.419	0.0872
56.130	0.0070	106.452	0.0910
60.000	0.0089	106.452	0.0939
63.871	0.0114	104.516	0.0968
67.742	0.0138	103.548	0.0997
72.581	0.0167	101.613	0.1021
77.420	0.0200	99.677	0.1041
81.291	0.0244	98.709	0.1055
83.226	0.0273		
85.162	0.0302		
88.065	0.0340		
90.967	0.0379		
92.903	0.0413		
94.838	0.0452		

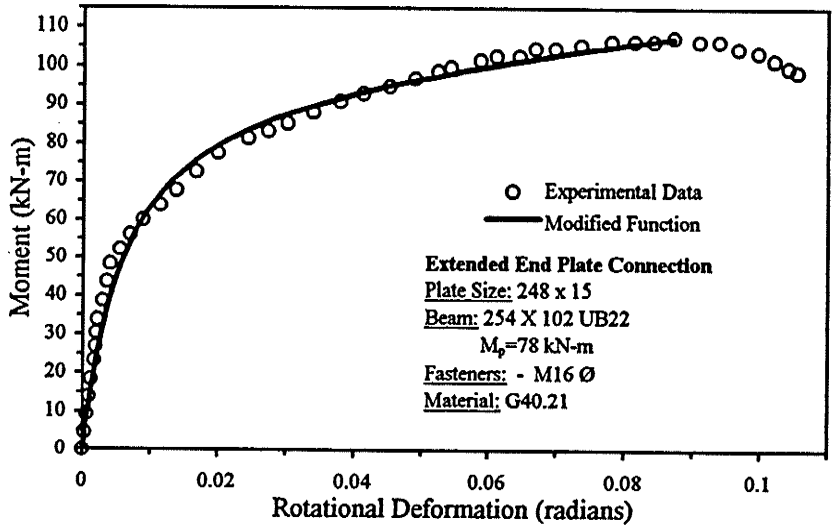


Figure A.236 (a) M-ϕ curve for Packer: Test J1

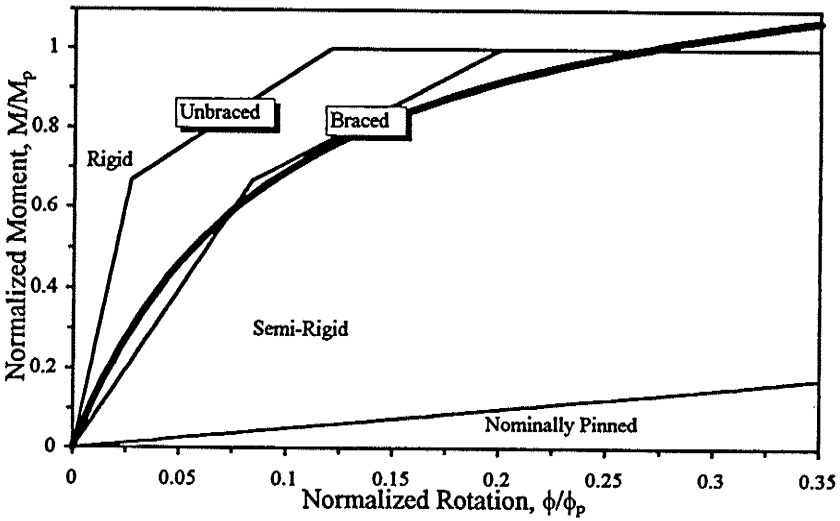


Figure A.236 (b) Eurocode3 Classification of Packer: Test J1

Table A.237 M-ϕ data for Packer: Test J2 (1977)

Moment, M kN-m	Rotation, ϕ radians	Moment, M kN-m	Rotation, ϕ radians
0	0	68.438	0.0376
3.750	0.0005	68.438	0.0424
6.563	0.0010	71.250	0.0477
9.375	0.0014	72.188	0.0516
11.719	0.0017	73.125	0.0559
14.063	0.0019	74.063	0.0578
16.406	0.0024	75.000	0.0617
18.750	0.0029	75.000	0.0660
22.500	0.0034	76.875	0.0708
24.375	0.0043	77.813	0.0757
27.187	0.0048	78.750	0.0790
30.000	0.0058	79.688	0.0829
33.750	0.0068	79.688	0.0872
37.501	0.0082	80.625	0.0916
38.437	0.0096	81.562	0.0954
40.781	0.0106	82.500	0.0993
43.125	0.0116	83.437	0.1041
46.875	0.0140	85.312	0.1080
49.688	0.0159	86.250	0.1108
51.562	0.0183	87.187	0.1157
54.375	0.0212	89.062	0.1195
56.719	0.0229	89.062	0.1234
59.062	0.0246	90.001	0.1263
62.812	0.0284	89.062	0.1287
64.688	0.0308		
66.563	0.0347		

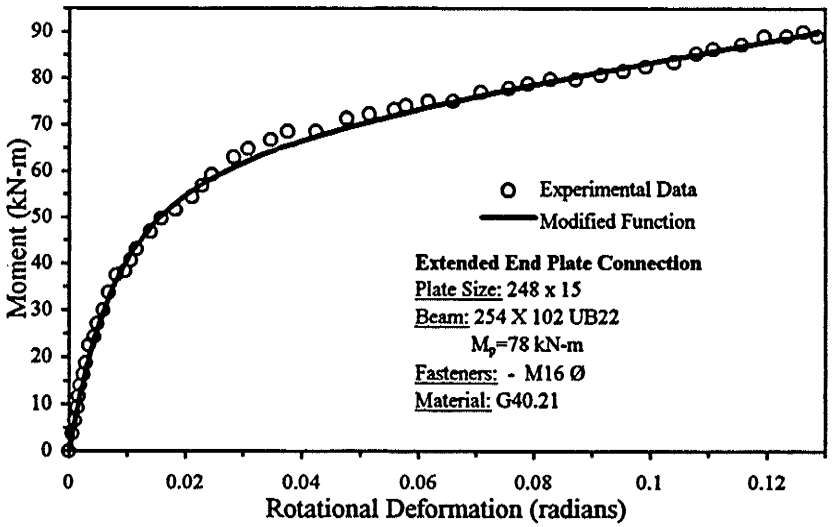


Figure A.237 (a) M-ϕ curve for Packer: Test J2

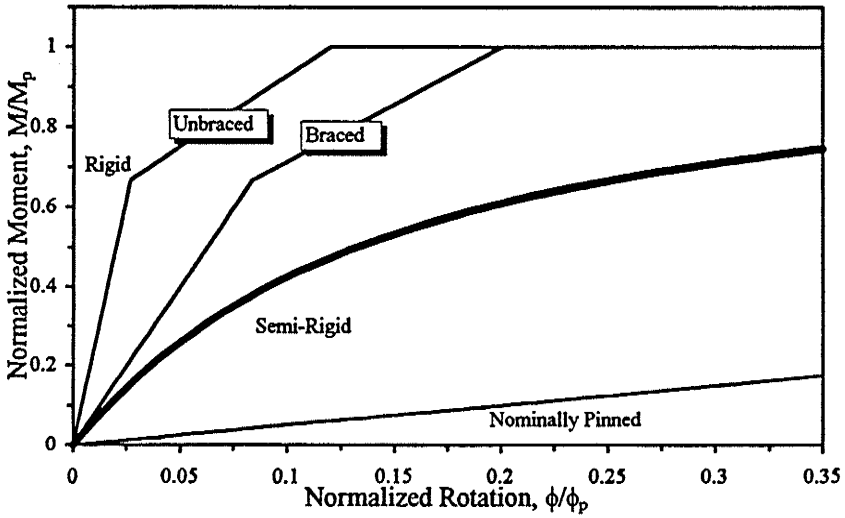


Figure A.237 (b) Eurocode3 Classification of Packer: Test J2

Table A.238 M-ϕ data for Packer: Test J3 (1977)

Moment, M kN-m	Rotation, ϕ radians	Moment, M kN-m	Rotation, ϕ radians
0	0	68.438	0.0376
3.750	0.0005	68.438	0.0424
6.563	0.0010	71.250	0.0477
9.375	0.0014	72.188	0.0516
11.719	0.0017	73.125	0.0559
14.063	0.0019	74.063	0.0578
16.406	0.0024	75.000	0.0617
18.750	0.0029	75.000	0.0660
22.500	0.0034	76.875	0.0708
24.375	0.0043	77.813	0.0757
27.187	0.0048	78.750	0.0790
30.000	0.0058	79.688	0.0829
33.750	0.0068	79.688	0.0872
37.501	0.0082	80.625	0.0916
38.437	0.0096	81.562	0.0954
40.781	0.0106	82.500	0.0993
43.125	0.0116	83.437	0.1041
46.875	0.0140	85.312	0.1080
49.688	0.0159	86.250	0.1108
51.562	0.0183	87.187	0.1157
54.375	0.0212	89.062	0.1195
56.719	0.0229	89.062	0.1234
59.062	0.0246	90.001	0.1263
62.812	0.0284	89.062	0.1287
64.688	0.0308		
66.563	0.0347		

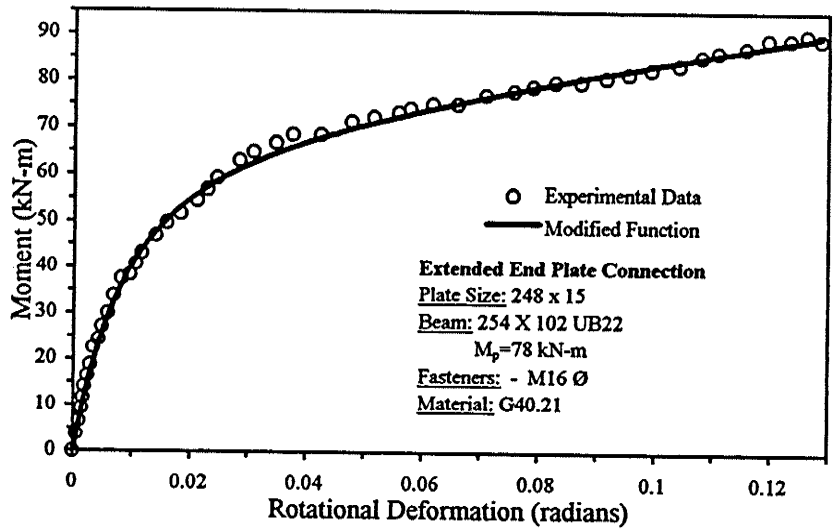


Figure A.238 (a) M-ϕ curve for Packer: Test J3

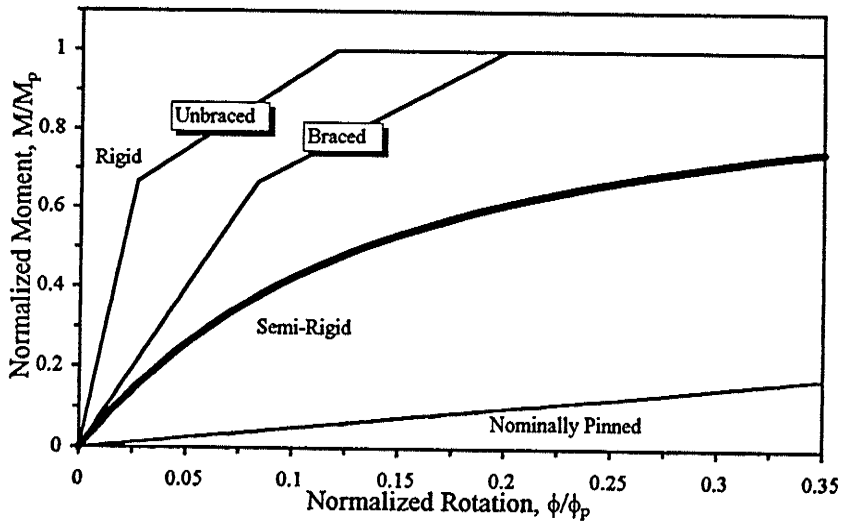


Figure A.238 (b) Eurocode3 Classification of Packer: Test J3

Table A.239 M-ϕ data for Grundy: T1 (1980)

Moment, M kN-m	Rotation, ϕ radians	Moment, M kN-m	Rotation, ϕ radians
0	0	850.279	0.0034
36.440	0.0001	871.102	0.0036
72.881	0.0002	888.455	0.0038
107.586	0.0003	905.808	0.0040
142.292	0.0004	909.279	0.0042
176.997	0.0005	912.749	0.0044
211.702	0.0006	926.631	0.0046
246.407	0.0007	940.513	0.0047
281.113	0.0008		
315.818	0.0009		
350.523	0.0010		
388.699	0.0011		
426.875	0.0012		
454.639	0.0013		
482.403	0.0014		
517.109	0.0016		
551.815	0.0017		
586.520	0.0019		
621.225	0.0020		
655.930	0.0022		
690.636	0.0023		
725.341	0.0025		
760.046	0.0027		
783.183	0.0029		
806.320	0.0030		
829.457	0.0032		

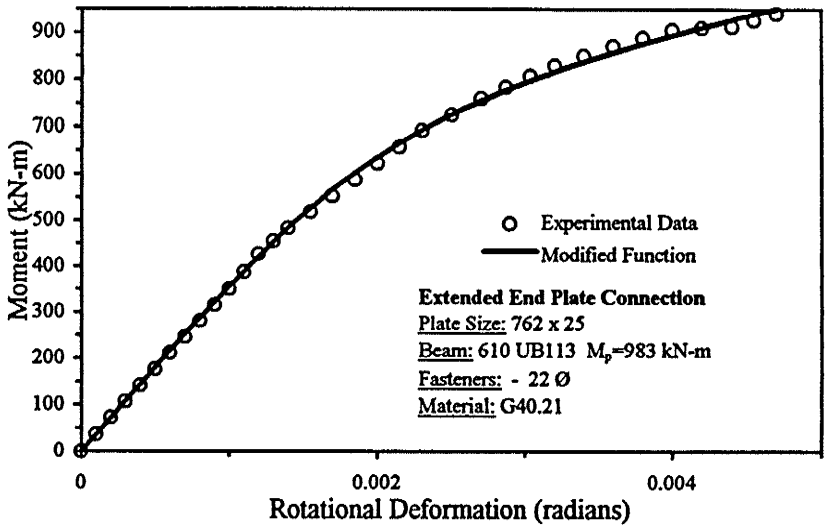


Figure A.239 (a) M-ϕ curve for Grundy: T1

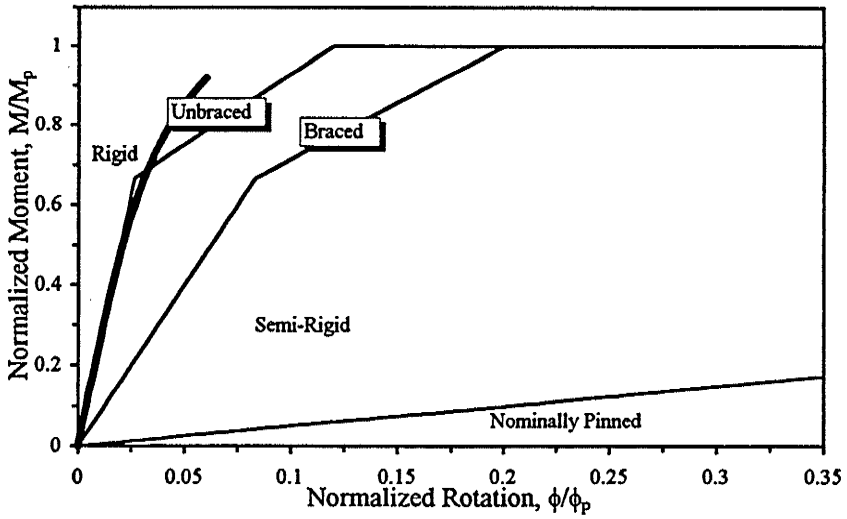


Figure A.239 (b) Eurocode3 Classification of Grundy: T1

Table A.240 M-ϕ data for Grundy: T2 (1980)

Moment, M kN-m	Rotation, ϕ radians	Moment, M kN-m	Rotation, ϕ radians
0	0	891.498	0.0034
34.824	0.0001	905.427	0.0036
69.648	0.0002	919.357	0.0039
104.473	0.0003	933.287	0.0041
139.297	0.0004	940.252	0.0043
188.050	0.0005	947.217	0.0044
236.804	0.0007	954.181	0.0046
285.557	0.0008	961.146	0.0047
320.382	0.0009	968.111	0.0050
355.206	0.0010	975.076	0.0052
390.030	0.0011	978.558	0.0054
424.854	0.0011	982.041	0.0055
463.161	0.0012	978.558	0.0057
501.468	0.0013	975.076	0.0059
539.774	0.0014		
578.081	0.0015		
609.423	0.0016		
640.765	0.0017		
672.106	0.0018		
703.448	0.0019		
734.790	0.0021		
766.132	0.0023		
797.473	0.0026		
828.814	0.0028		
853.191	0.0030		
877.568	0.0032		

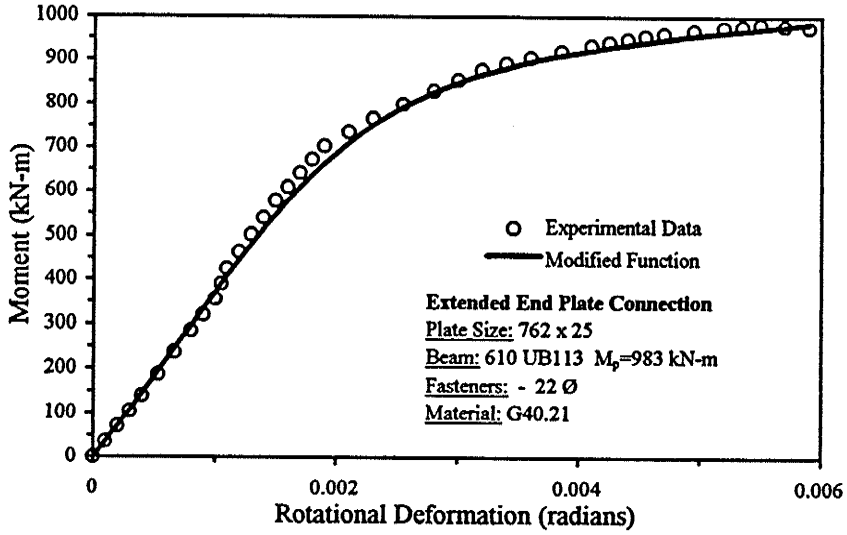


Figure A.240 (a) M-ϕ curve for Grundy: T2

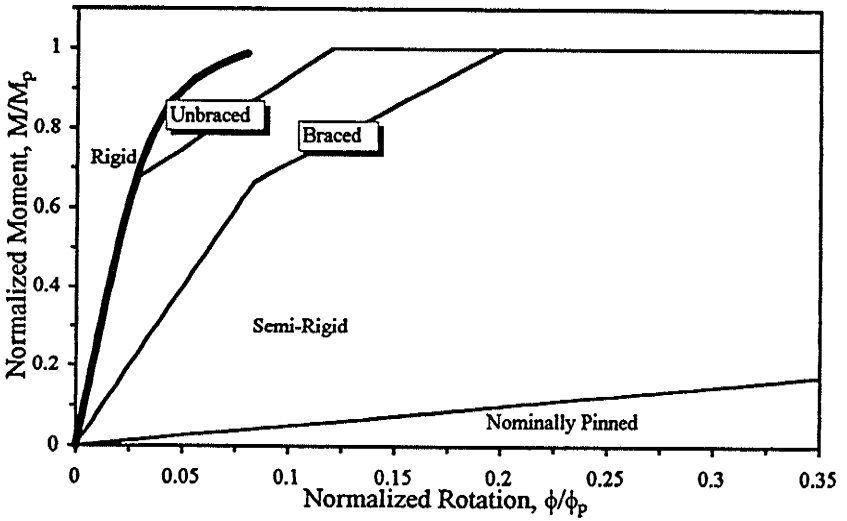


Figure A.240 (b) Eurocode3 Classification of Grundy: T2

Table A.241 M-ϕ data for Sherbourne: Test A2 (1961)

Moment, M kN-m	Rotation, ϕ radians	Moment, M kN-m	Rotation, ϕ radians
0	0	488.947	0.0070
22.857	0.0001	496.897	0.0081
45.715	0.0001	512.798	0.0092
68.572	0.0002	520.749	0.0100
91.430	0.0002	528.699	0.0107
107.330	0.0002	536.649	0.0117
123.230	0.0002	544.599	0.0127
143.106	0.0004	548.574	0.0136
162.982	0.0005	552.550	0.0144
182.858	0.0007	556.525	0.0151
200.747	0.0008	560.500	0.0157
218.635	0.0009	564.475	0.0164
234.536	0.0011	568.451	0.0171
250.436	0.0013	572.426	0.0179
278.263	0.0013	576.401	0.0186
294.163	0.0014	580.376	0.0195
310.064	0.0015	584.352	0.0203
337.891	0.0022	584.352	0.0201
353.791	0.0024	588.327	0.0210
369.691	0.0026	592.302	0.0218
385.592	0.0030	592.302	0.0216
401.494	0.0033	592.302	0.0224
421.369	0.0038	592.302	0.0231
437.270	0.0045	592.302	0.0238
457.146	0.0053	592.302	0.0244
473.047	0.0063		

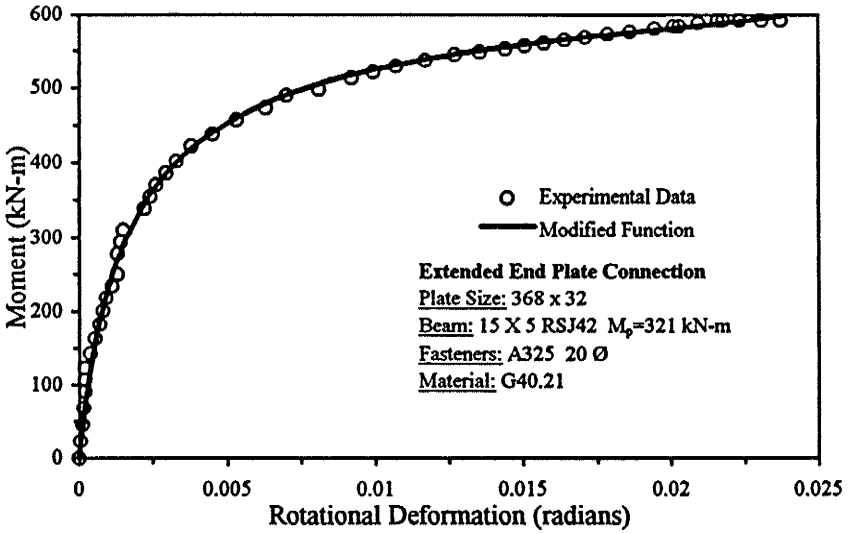


Figure A.241 (a) M-ϕ curve for Sherbourne: Test A2

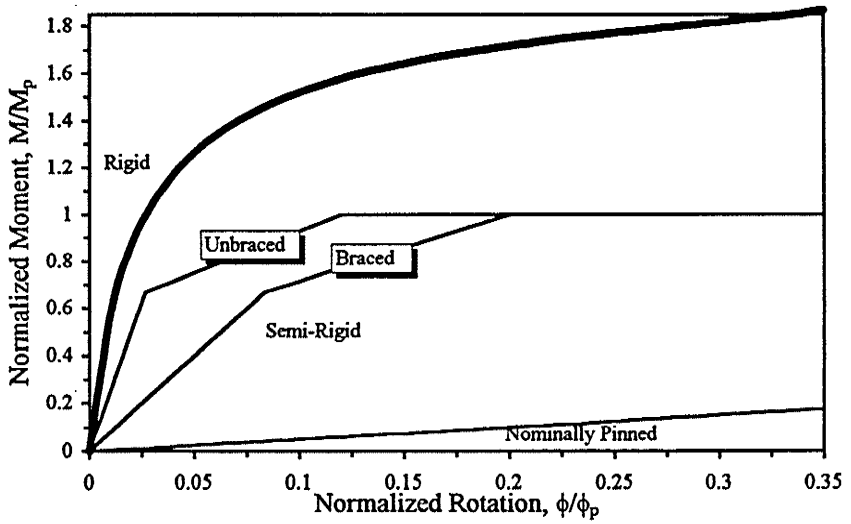


Figure A.241 (b) Eurocode3 Classification of Sherbourne: Test A2

Table A.242 M-ϕ data for Sherbourne: Test A3 (1961)

Moment, M kN-m	Rotation, ϕ radians	Moment, M kN-m	Rotation, ϕ radians
0	0	578.484	0.0146
32.138	0.0002	586.518	0.0157
60.258	0.0002	594.553	0.0167
88.379	0.0005	602.586	0.0179
120.517	0.0007	608.612	0.0189
152.656	0.0007	614.638	0.0198
176.758	0.0007	620.664	0.0210
194.836	0.0008	626.690	0.0221
212.914	0.0009	630.707	0.0235
245.052	0.0007	634.724	0.0249
273.172	0.0009	638.742	0.0259
301.293	0.0011	642.759	0.0268
333.431	0.0018	646.776	0.0278
361.552	0.0020	650.794	0.0287
379.630	0.0022	652.802	0.0296
397.707	0.0024	654.811	0.0304
429.845	0.0033	660.837	0.0316
461.983	0.0048	666.863	0.0327
474.035	0.0053		
486.087	0.0066		
506.172	0.0073		
522.242	0.0085		
528.267	0.0095		
534.293	0.0104		
550.363	0.0115		
562.414	0.0130		

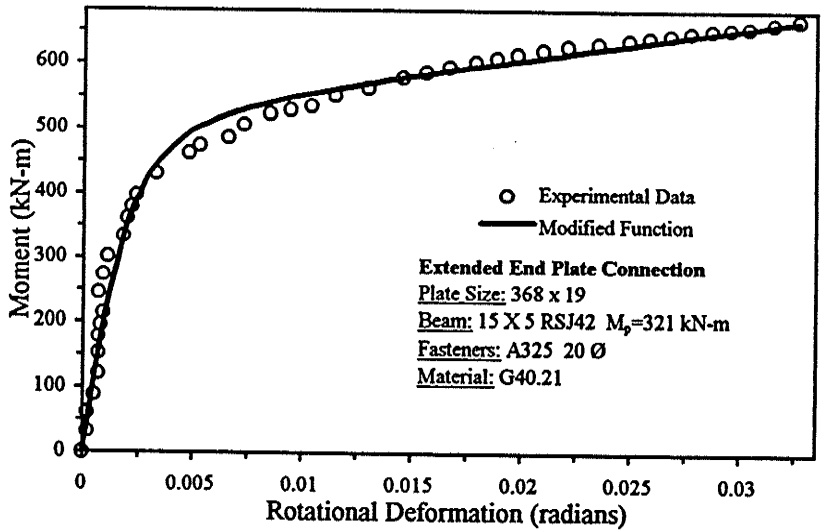


Figure A.242 (a) M-ϕ curve for Sherbourne: Test A3

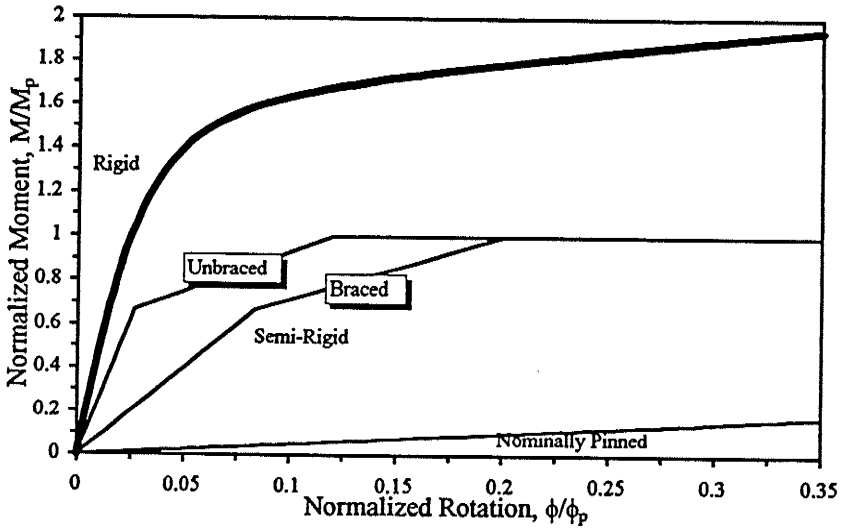


Figure A.242 (b) Eurocode3 Classification of Sherbourne: Test A3

Table A.243 M-ϕ data for Sherbourne: Test B1 (1961)

Moment, M kN-m	Rotation, ϕ radians	Moment, M kN-m	Rotation, ϕ radians
0	0	488.807	0.0134
29.814	0.0001	496.618	0.0148
59.628	0.0002	512.798	0.0177
85.466	0.0004	520.749	0.0194
111.305	0.0005	528.699	0.0211
131.181	0.0006	528.699	0.0211
151.057	0.0007	540.624	0.0236
168.945	0.0008	548.574	0.0255
186.833	0.0009	552.243	0.0274
206.709	0.0010	557.748	0.0292
226.585	0.0010	561.112	0.0308
244.473	0.0011	564.475	0.0324
262.362	0.0012	576.401	0.0353
278.262	0.0013	576.401	0.0373
294.163	0.0014	580.376	0.0389
321.990	0.0019	584.352	0.0405
337.891	0.0022	586.339	0.0421
365.716	0.0028	588.327	0.0437
381.617	0.0036	596.277	0.0465
397.518	0.0044	596.277	0.0494
413.554	0.0055	600.253	0.0517
429.590	0.0065	604.227	0.0547
441.685	0.0077	612.177	0.0577
458.175	0.0093	612.177	0.0606
469.586	0.0107	616.152	0.0616
480.996	0.0120		

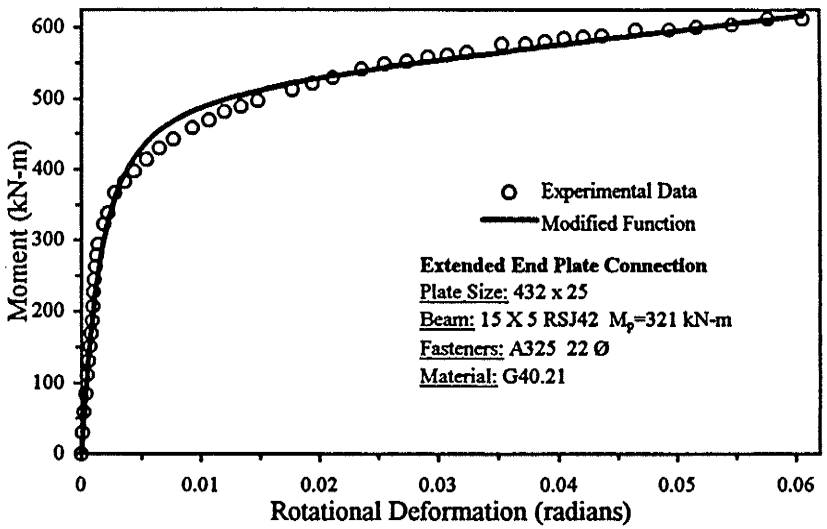


Figure A.243 (a) M-ϕ curve for Sherbourne: Test B1

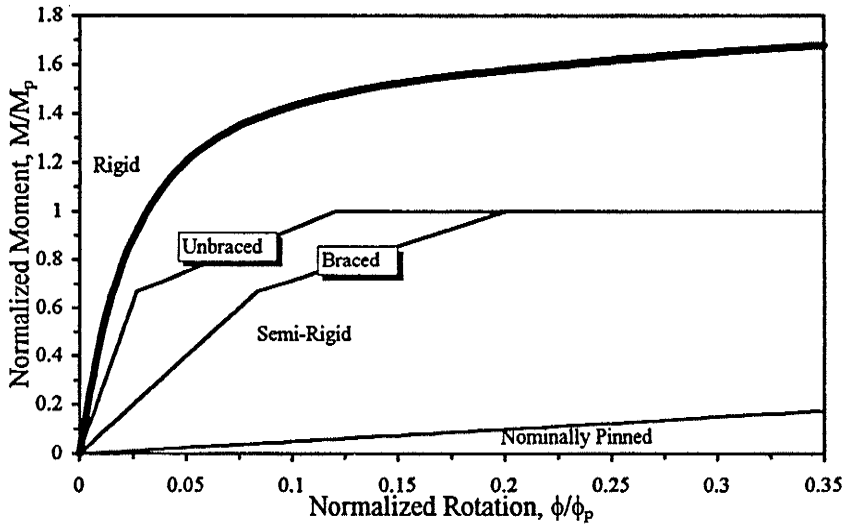


Figure A.243 (b) Eurocode3 Classification of Sherbourne: Test B1

Table A.244 M-ϕ data for Sherbourne: Test B2 (1961)

Moment, M kN-m	Rotation, ϕ radians	Moment, M kN-m	Rotation, ϕ radians
0	0	520.749	0.0126
22.526	0.0000	532.675	0.0142
45.052	0.0001	536.648	0.0157
67.578	0.0001	542.611	0.0169
88.779	0.0002	548.574	0.0180
109.980	0.0002	552.550	0.0194
131.181	0.0003	556.525	0.0208
151.057	0.0006	560.500	0.0218
175.902	0.0006	564.475	0.0227
200.747	0.0006	568.451	0.0244
225.592	0.0005	568.451	0.0254
250.436	0.0005	568.451	0.0264
266.337	0.0006	572.426	0.0281
282.238	0.0007	576.401	0.0298
310.064	0.0010	580.376	0.0313
337.891	0.0014	584.352	0.0330
365.716	0.0021	584.352	0.0343
383.605	0.0028	584.352	0.0355
401.494	0.0034		
425.344	0.0043		
445.220	0.0052		
465.096	0.0064		
477.021	0.0076		
492.922	0.0090		
500.872	0.0100		
508.823	0.0109		

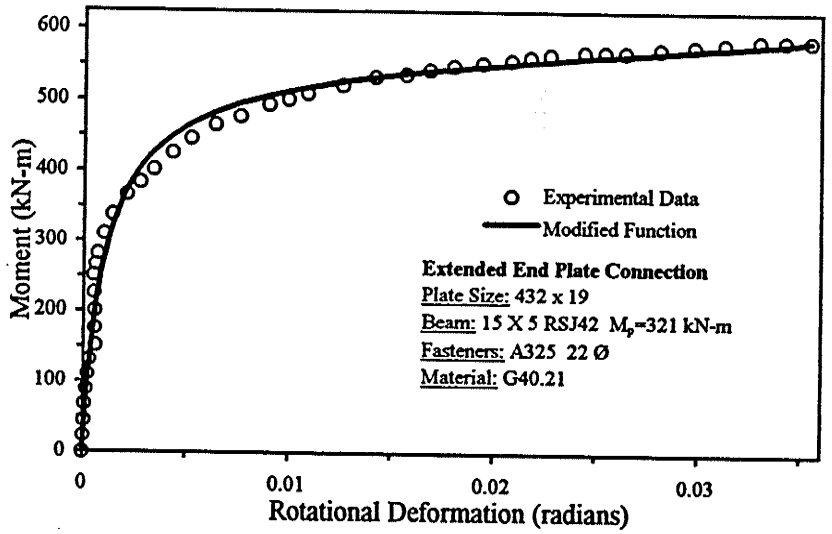


Figure A.244 (a) M-ϕ curve for Sherbourne: Test B2

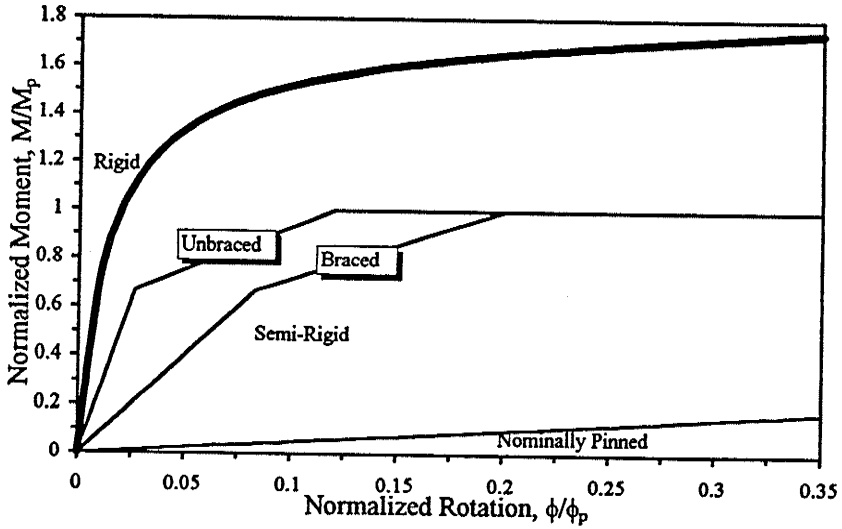


Figure A.244 (b) Eurocode3 Classification of Sherbourne: Test B2

Table A.245 M-ϕ data for Johnson: Test 5 (1960)

Moment, M kN-m	Rotation, ϕ radians	Moment, M kN-m	Rotation, ϕ radians
0	0	113.268	0.0073
4.782	0.0002	114.980	0.0078
9.564	0.0003	116.479	0.0084
14.346	0.0005	117.978	0.0090
19.057	0.0007	118.406	0.0095
23.767	0.0008	118.835	0.0099
28.478	0.0010	120.548	0.0105
33.188	0.0012	122.261	0.0110
37.899	0.0013	122.690	0.0117
42.609	0.0015	123.118	0.0123
47.606	0.0017	123.974	0.0128
52.602	0.0019	124.831	0.0132
57.598	0.0021	125.687	0.0137
62.451	0.0023		
67.305	0.0026		
72.158	0.0028		
76.583	0.0031		
81.008	0.0035		
85.433	0.0038		
89.501	0.0041		
93.569	0.0044		
97.423	0.0049		
101.277	0.0053		
104.489	0.0058		
107.701	0.0062		
110.484	0.0068		

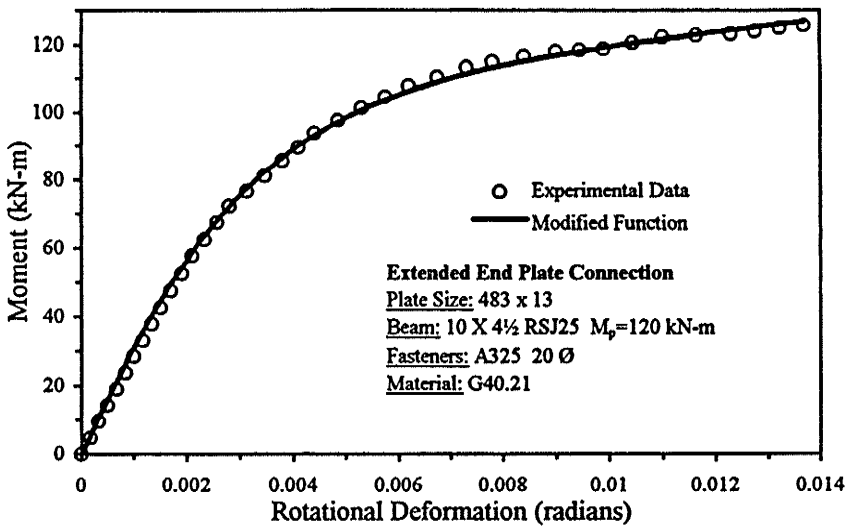


Figure A.245 (a) M-ϕ curve for Johnson: Test 5

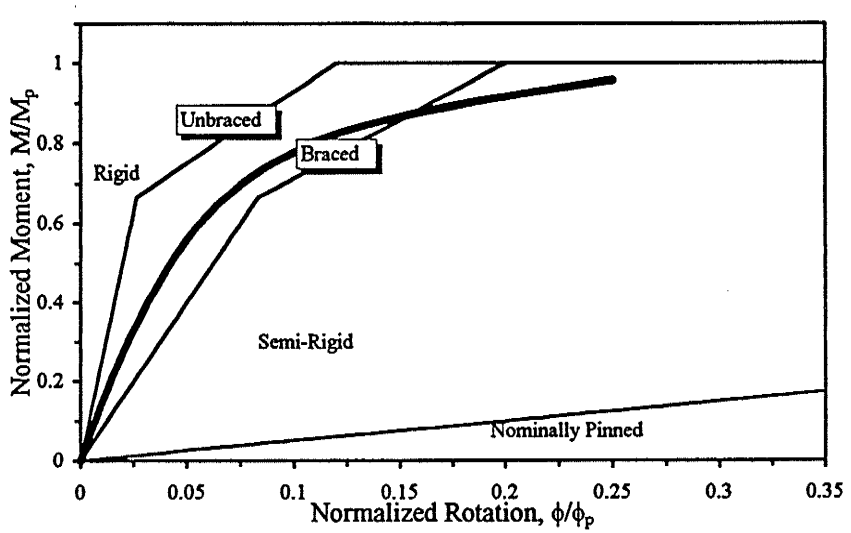


Figure A.245 (b) Eurocode3 Classification of Johnson: Test 5

Table A.246 M-ϕ data for Bailey: B4-L (1970)

Moment, M kN-m	Rotation, ϕ radians	Moment, M kN-m	Rotation, ϕ radians
0	0	216.726	0.0108
7.894	0.0003	224.381	0.0128
15.789	0.0005	231.079	0.0148
15.789	0.0004	234.907	0.0167
23.921	0.0006	240.647	0.0188
32.054	0.0008	242.562	0.0204
42.102	0.0010	246.389	0.0223
52.149	0.0012	248.302	0.0239
59.325	0.0015	250.215	0.0258
66.502	0.0018	252.130	0.0279
73.678	0.0021	255.000	0.0297
80.854	0.0024	255.957	0.0311
88.031	0.0025	257.870	0.0327
95.207	0.0026	258.827	0.0346
104.296	0.0029	259.785	0.0363
113.386	0.0032	260.742	0.0383
121.041	0.0033	261.698	0.0403
128.696	0.0034	261.698	0.0424
137.786	0.0037		
146.876	0.0040		
159.316	0.0042		
166.971	0.0049		
179.409	0.0055		
189.934	0.0066		
198.546	0.0077		
206.201	0.0092		

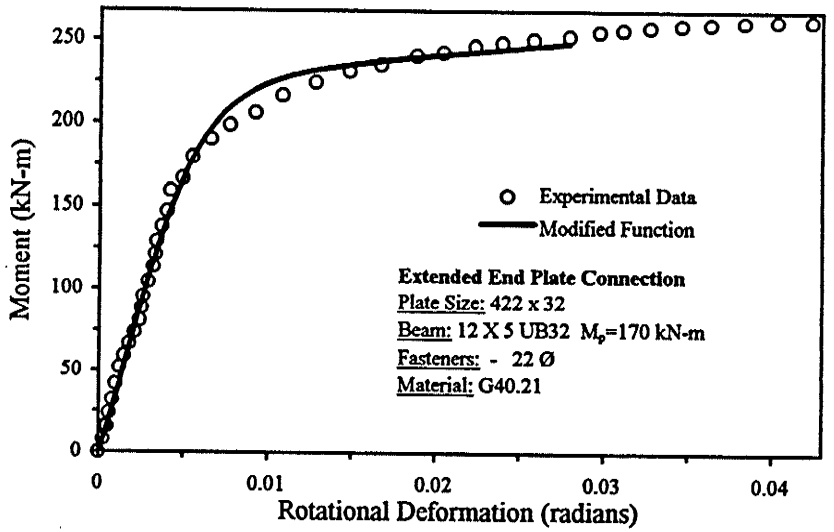


Figure A.246 (a) M-ϕ curve for Bailey: B4-L

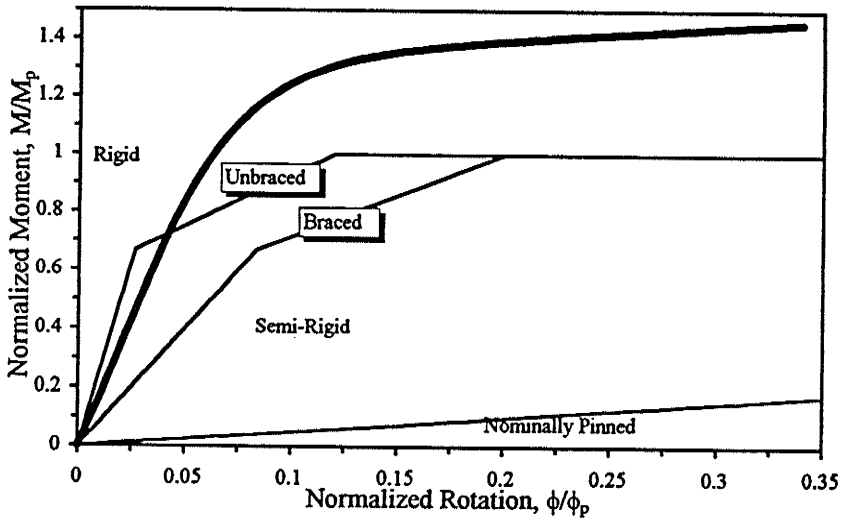


Figure A.246 (b) Eurocode3 Classification of Bailey: B4-L

Table A.247 M-ϕ data for Bailey: B4-R (1970)

Moment, M kN-m	Rotation, ϕ radians	Moment, M kN-m	Rotation, ϕ radians
0	0	222.525	0.0132
11.938	0.0003	226.345	0.0146
23.876	0.0006	229.211	0.0162
31.517	0.0007	233.030	0.0180
39.157	0.0007	236.851	0.0198
47.275	0.0010	239.716	0.0218
55.392	0.0012	242.581	0.0236
64.465	0.0014	246.401	0.0256
73.538	0.0015	248.312	0.0275
80.701	0.0017	251.177	0.0298
87.864	0.0018	253.087	0.0315
95.504	0.0021	254.041	0.0332
103.144	0.0023	255.952	0.0353
109.830	0.0024	256.906	0.0370
116.515	0.0024	257.862	0.0390
124.633	0.0026	257.862	0.0409
132.751	0.0028	258.817	0.0427
145.166	0.0032	259.771	0.0442
156.627	0.0035	260.727	0.0457
164.267	0.0041	260.727	0.0475
174.773	0.0052	260.727	0.0488
187.189	0.0066		
196.739	0.0077		
206.289	0.0090		
212.019	0.0104		
219.660	0.0119		

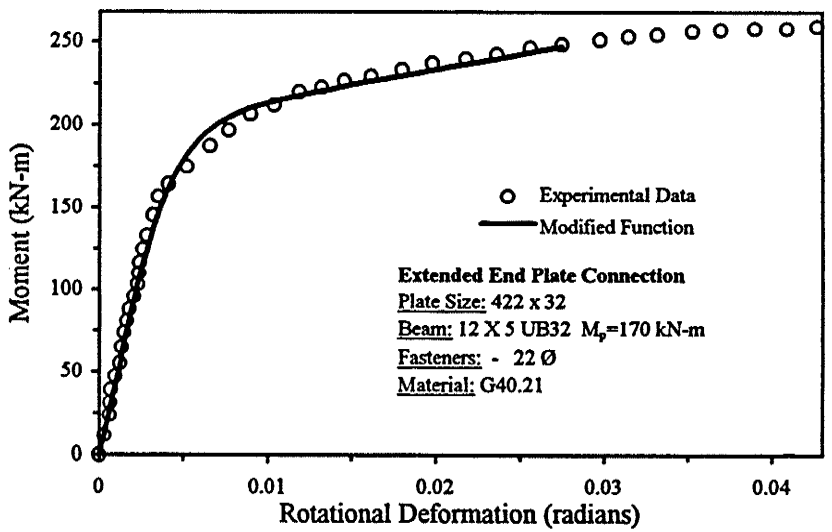


Figure A.247 (a) M-ϕ curve for Bailey: B4-R

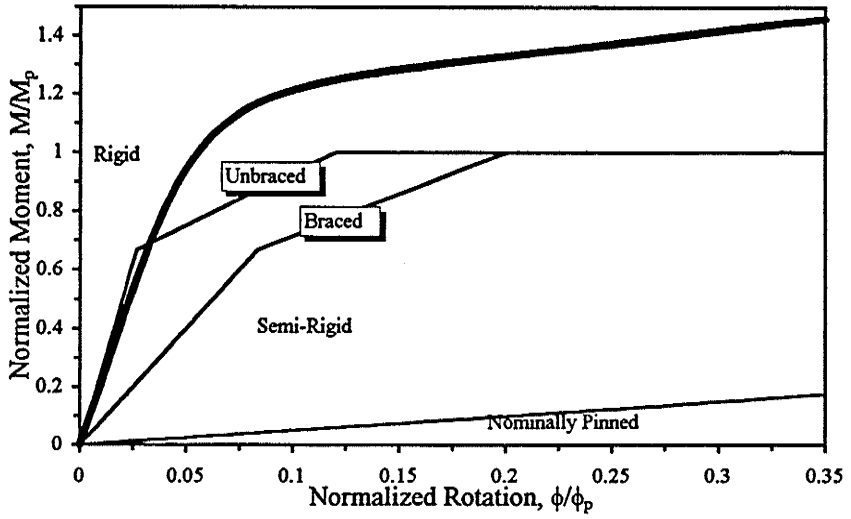


Figure A.247 (b) Eurocode3 Classification of Bailey: B4-R

Table A.248 M-ϕ data for Bailey: B5-L (1970)

Moment, M kN-m	Rotation, ϕ radians	Moment, M kN-m	Rotation, ϕ radians
0	0	206.112	0.0138
8.628	0.0004	209.946	0.0155
17.256	0.0007	213.782	0.0176
26.363	0.0010	217.616	0.0196
35.471	0.0012	219.533	0.0209
43.140	0.0015	221.450	0.0221
50.809	0.0017	223.367	0.0241
60.396	0.0020	223.847	0.0252
69.982	0.0023	224.327	0.0263
78.130	0.0026	225.286	0.0282
86.279	0.0029	225.286	0.0301
94.428	0.0031	225.286	0.0312
102.577	0.0033	225.286	0.0323
112.164	0.0036	227.203	0.0342
121.750	0.0039	227.203	0.0356
128.940	0.0042	227.203	0.0369
136.130	0.0045	227.203	0.0386
141.882	0.0049	227.203	0.0405
147.634	0.0052	228.161	0.0422
155.303	0.0059	229.120	0.0435
162.972	0.0066		
168.724	0.0072		
174.476	0.0078		
185.022	0.0093		
193.649	0.0108		
201.319	0.0122		

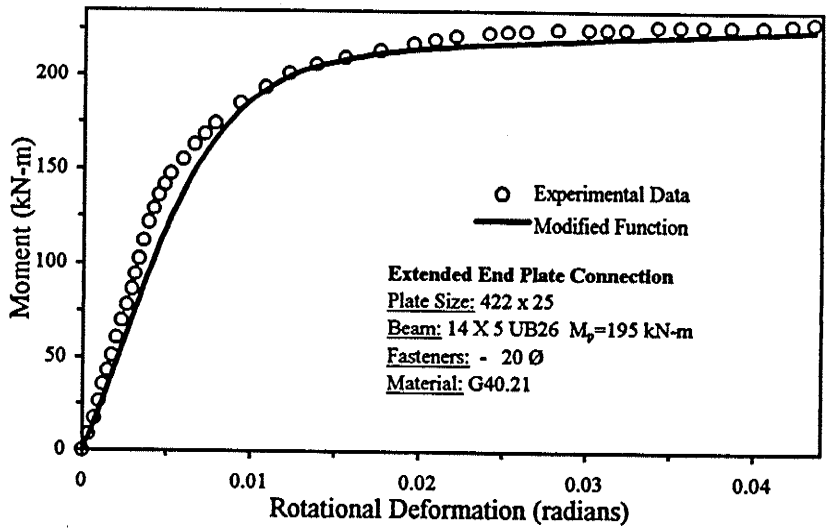


Figure A.248 (a) M-ϕ curve for Bailey: B5-L

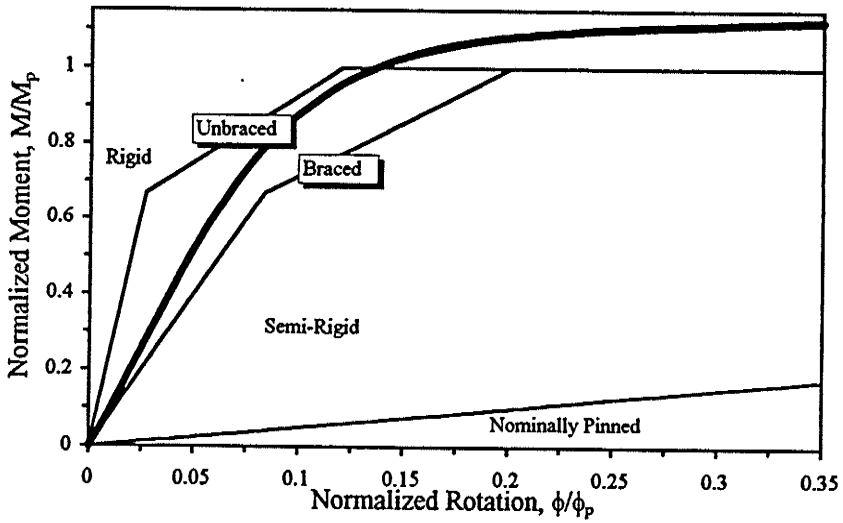


Figure A.248 (b) Eurocode3 Classification of Bailey: B5-L

Table A.249 M-ϕ data for Bailey: B5-R (1970)

Moment, M kN-m	Rotation, ϕ radians	Moment, M kN-m	Rotation, ϕ radians
0	0	197.379	0.0082
8.164	0.0001	202.181	0.0093
16.329	0.0003	206.022	0.0106
24.493	0.0004	208.905	0.0121
31.696	0.0006	213.707	0.0133
38.900	0.0008	216.588	0.0149
47.544	0.0010	217.548	0.0165
56.188	0.0012	220.431	0.0178
65.793	0.0014	222.350	0.0199
75.397	0.0016	223.312	0.0218
81.160	0.0017	224.272	0.0236
86.923	0.0018	225.233	0.0254
94.607	0.0021	225.233	0.0273
102.291	0.0023	225.233	0.0292
109.975	0.0023	226.193	0.0311
117.659	0.0022	226.193	0.0330
127.264	0.0025	226.193	0.0344
136.869	0.0028	226.193	0.0360
143.112	0.0030	227.154	0.0380
149.354	0.0032	227.154	0.0392
156.078	0.0035	228.114	0.0407
162.801	0.0038	227.154	0.0427
169.525	0.0045	227.154	0.0443
177.208	0.0055	228.114	0.0461
185.853	0.0064		
192.577	0.0073		

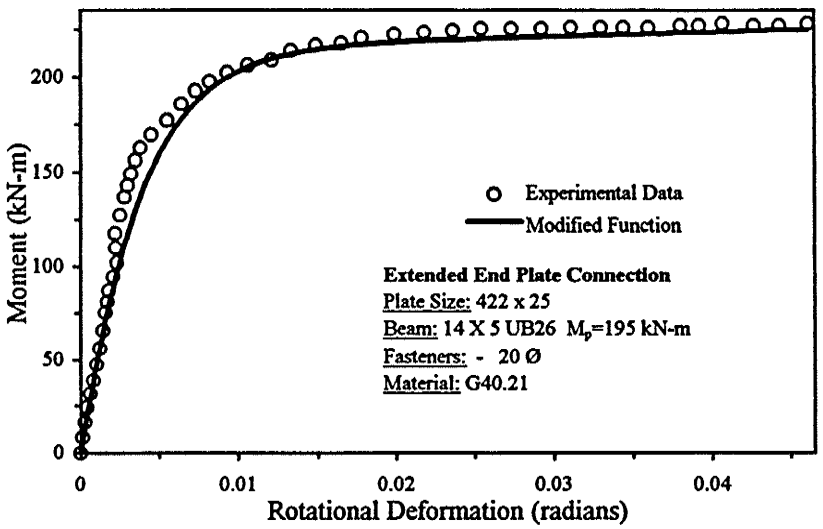


Figure A.249 (a) M-ϕ curve for Bailey: B5-R

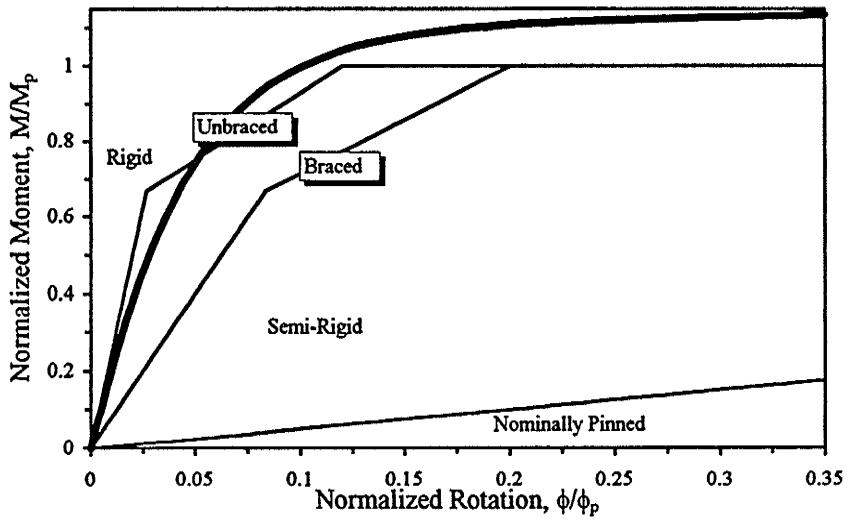


Figure A.249 (b) Eurocode3 Classification of Bailey: B5-R

Table A.250 M-ϕ data for Bailey: B6-L (1970)

Moment, M kN-m	Rotation, ϕ radians	Moment, M kN-m	Rotation, ϕ radians
0	0	358.940	0.0150
17.321	0.0007	363.761	0.0161
34.643	0.0013	373.378	0.0179
54.852	0.0018	377.226	0.0196
75.061	0.0022	381.072	0.0211
89.496	0.0025	388.766	0.0227
103.930	0.0028	392.613	0.0245
117.402	0.0032	394.537	0.0263
130.873	0.0035	397.422	0.0275
145.308	0.0038	400.307	0.0287
159.743	0.0041	402.256	0.0306
173.215	0.0045	403.217	0.0318
186.687	0.0048	404.179	0.0330
198.235	0.0051	409.950	0.0351
209.783	0.0053	410.911	0.0363
220.369	0.0057	411.872	0.0374
230.954	0.0060	417.643	0.0394
247.310	0.0067	423.413	0.0414
263.665	0.0074	423.413	0.0433
275.219	0.0078	423.413	0.0451
286.772	0.0082		
304.083	0.0095		
314.675	0.0103		
325.267	0.0110		
338.731	0.0123		
354.118	0.0138		

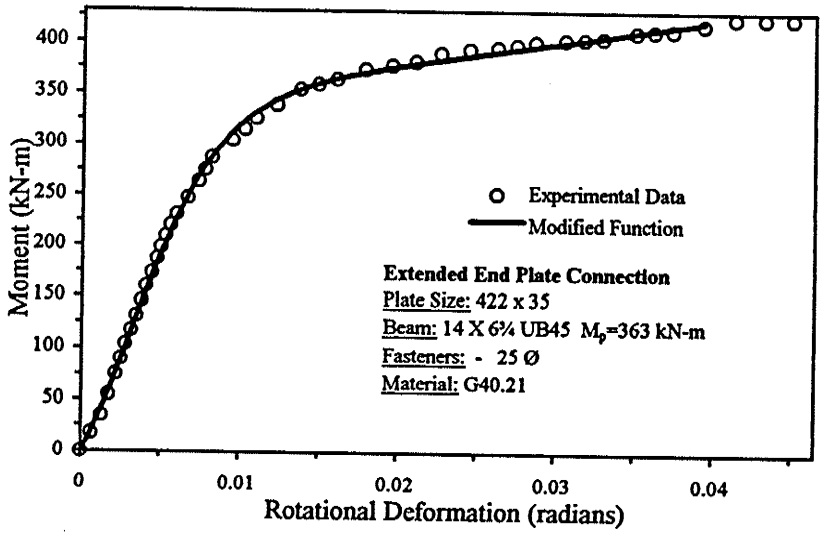


Figure A.250 (a) M-ϕ curve for Bailey: B6-L

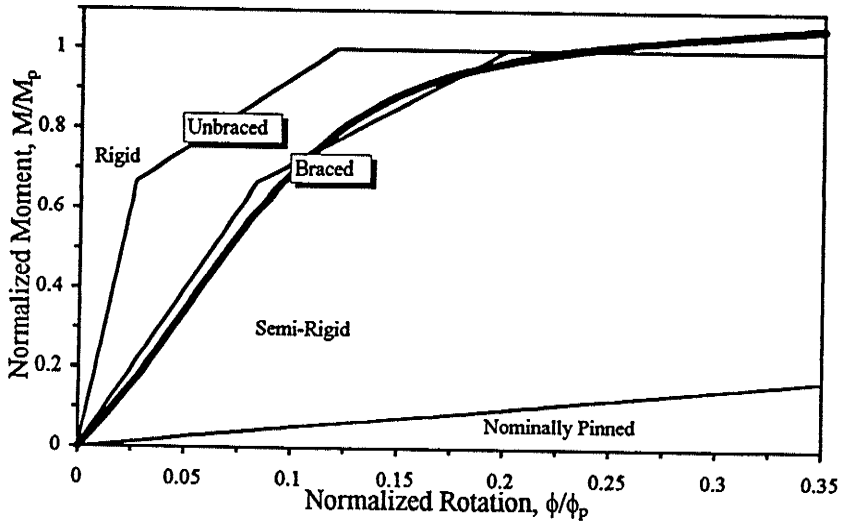


Figure A.250 (b) Eurocode3 Classification of Bailey: B6-L

Table A.251 M-ϕ data for Bailey: B6-R (1970)

Moment, M kN-m	Rotation, ϕ radians	Moment, M kN-m	Rotation, ϕ radians
0	0	381.554	0.0162
14.699	0.0003	389.222	0.0178
29.399	0.0007	398.813	0.0200
44.098	0.0010	400.711	0.0221
64.230	0.0012	404.559	0.0241
84.362	0.0014	410.304	0.0257
97.782	0.0018	410.304	0.0279
111.203	0.0022	414.150	0.0302
129.418	0.0026	416.048	0.0320
147.633	0.0030	419.896	0.0341
166.807	0.0034	420.857	0.0353
185.981	0.0037	421.819	0.0365
198.443	0.0041	421.819	0.0382
210.905	0.0044	425.641	0.0398
223.368	0.0047	423.717	0.0410
235.831	0.0049	421.819	0.0428
252.128	0.0054	423.717	0.0442
268.424	0.0059	423.717	0.0457
281.850	0.0066	425.641	0.0465
295.276	0.0072		
306.779	0.0079		
318.281	0.0086		
335.542	0.0097		
354.700	0.0111		
366.216	0.0126		
377.706	0.0144		

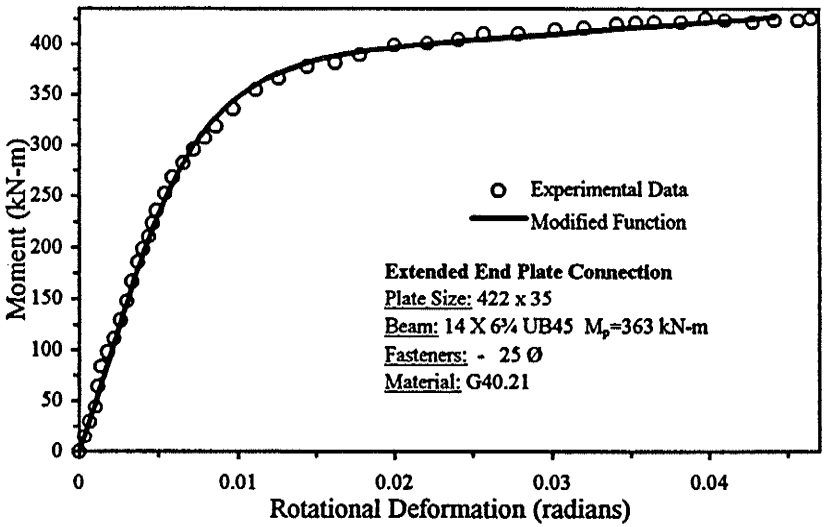


Figure A.251 (a) M-ϕ curve for Bailey: B6-R

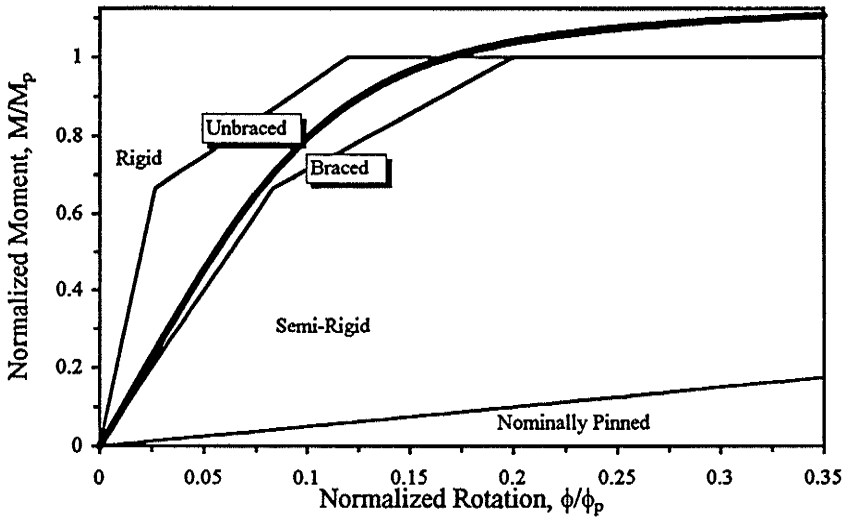


Figure A.251 (b) Eurocode3 Classification of Bailey: B6-R

Table A.252 M-ϕ data for Bailey: B7-L (1970)

Moment, M kN-m	Rotation, ϕ radians	Moment, M kN-m	Rotation, ϕ radians
0	0	262.125	0.0168
12.655	0.0005	267.548	0.0189
25.309	0.0010	269.357	0.0211
36.758	0.0014	272.971	0.0235
48.207	0.0017	276.587	0.0257
59.656	0.0021	277.491	0.0270
72.311	0.0026	278.395	0.0282
84.965	0.0030	280.203	0.0305
95.812	0.0034	283.818	0.0329
106.658	0.0037	283.818	0.0348
118.409	0.0039	282.914	0.0363
130.159	0.0041	282.011	0.0377
141.005	0.0044	285.627	0.0397
151.852	0.0046	285.627	0.0415
161.795	0.0051	289.241	0.0434
171.738	0.0056	287.434	0.0454
181.680	0.0061	287.434	0.0469
191.622	0.0065	289.241	0.0483
201.565	0.0072		
211.508	0.0079		
218.739	0.0087		
225.970	0.0094		
235.009	0.0104		
244.048	0.0114		
254.894	0.0135		
260.317	0.0152		

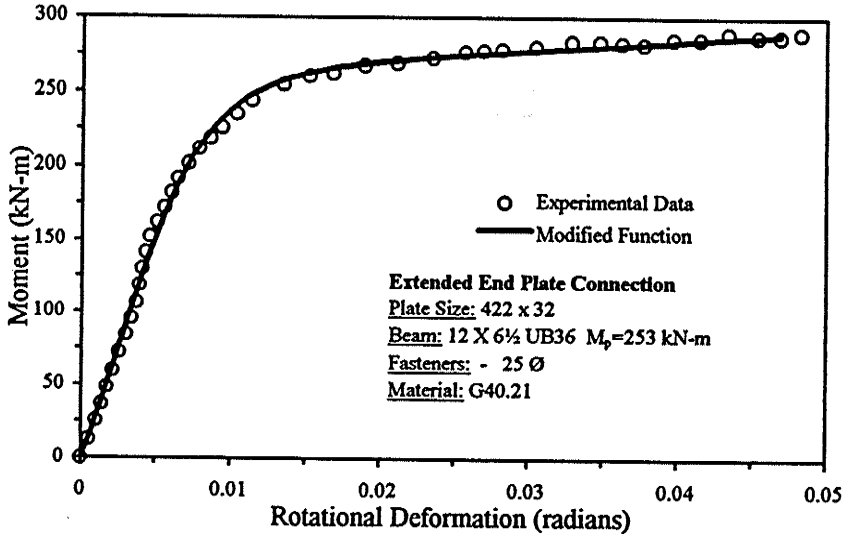


Figure A.252 (a) M-ϕ curve for Bailey: B7-L

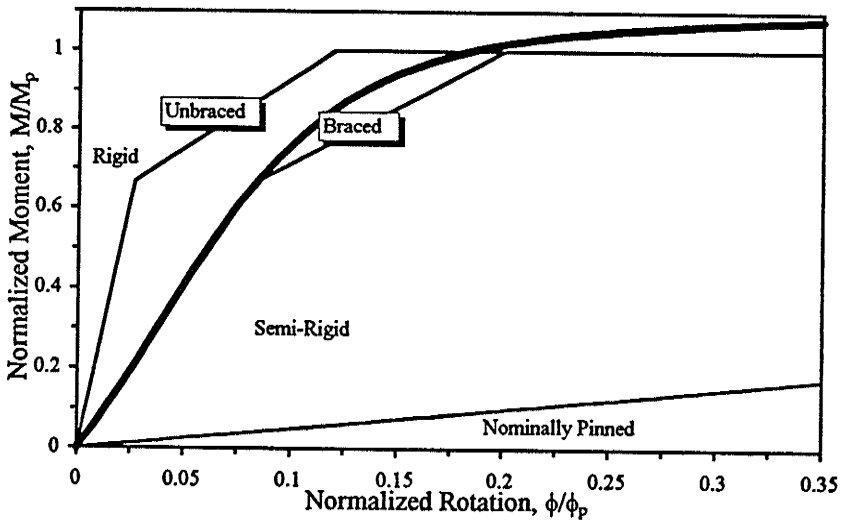


Figure A.252 (b) Eurocode3 Classification of Bailey: B7-L

Table A.253 M-ϕ data for Bailey: B7-R (1970)

Moment, M kN-m	Rotation, ϕ radians	Moment, M kN-m	Rotation, ϕ radians
0	0	274.857	0.0153
10.281	0.0003	279.392	0.0163
20.561	0.0007	283.021	0.0175
30.842	0.0010	286.650	0.0186
44.449	0.0014	287.557	0.0199
58.056	0.0018	288.464	0.0211
70.756	0.0021	291.185	0.0223
83.455	0.0024	293.907	0.0234
94.341	0.0026	295.721	0.0250
105.227	0.0028	295.721	0.0261
116.112	0.0031	295.721	0.0272
126.997	0.0035	295.721	0.0282
137.883	0.0038	295.721	0.0291
148.768	0.0042	296.628	0.0304
159.654	0.0045	297.535	0.0317
170.539	0.0049	299.350	0.0334
181.424	0.0055	299.350	0.0346
192.310	0.0060	299.350	0.0358
205.009	0.0067	299.350	0.0371
217.708	0.0074		
232.222	0.0087		
246.736	0.0100		
254.900	0.0111		
263.064	0.0122		
266.693	0.0133		
270.322	0.0143		

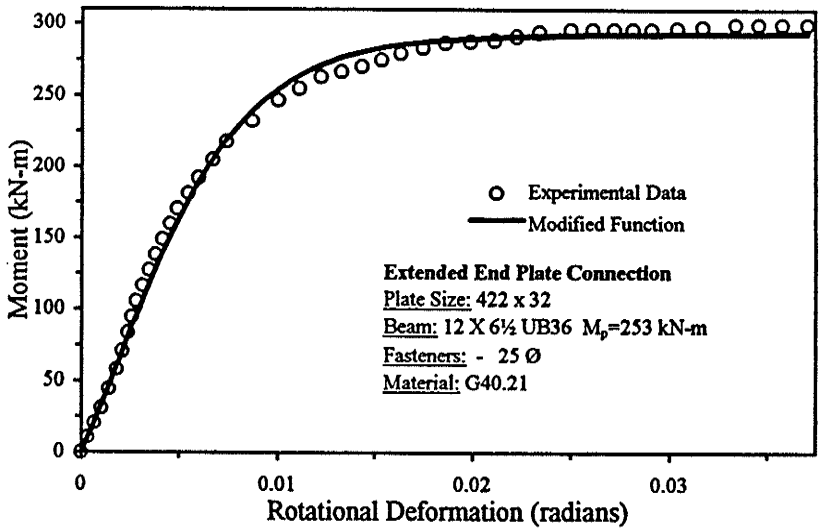


Figure A.253 (a) M-ϕ curve for Bailey: B7-R

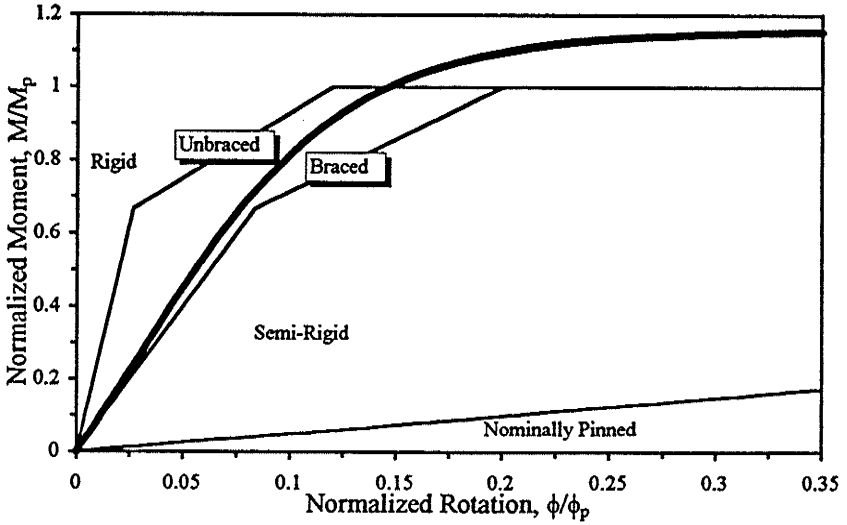


Figure A.253 (b) Eurocode3 Classification of Bailey: B7-R

Table A.254 M-ϕ data for Bailey: B8-L (1970)

Moment, M kN-m	Rotation, ϕ radians	Moment, M kN-m	Rotation, ϕ radians
0	0	106.891	0.0086
4.474	0.0002	108.329	0.0093
8.948	0.0003	109.287	0.0101
13.421	0.0005	110.246	0.0109
17.575	0.0006	110.725	0.0116
21.730	0.0007	111.204	0.0122
25.884	0.0008	111.843	0.0129
31.636	0.0010	112.482	0.0136
37.388	0.0011	113.121	0.0143
42.181	0.0013	113.601	0.0150
46.974	0.0015	114.080	0.0157
51.767	0.0016	114.720	0.0164
56.561	0.0017	115.359	0.0170
61.354	0.0017	115.999	0.0177
66.148	0.0018		
71.421	0.0021		
76.693	0.0023		
82.445	0.0031		
88.197	0.0039		
91.073	0.0044		
93.949	0.0049		
96.825	0.0054		
99.700	0.0059		
100.659	0.0065		
101.617	0.0071		
105.453	0.0079		

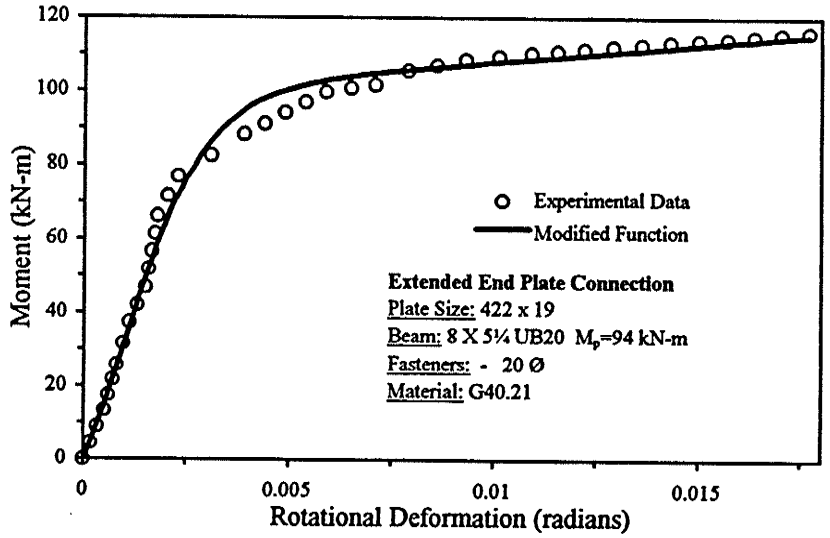


Figure A.254 (a) M-ϕ curve for Bailey: B8-L

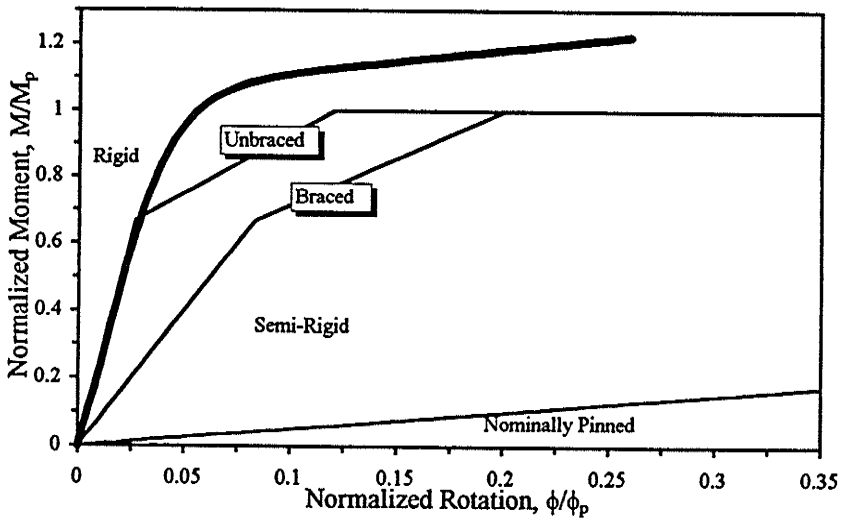


Figure A.254 (b) Eurocode3 Classification of Bailey: B8-L

Table A.255 M-ϕ data for Bailey: B8-R (1970)

Moment, M kN-m	Rotation, ϕ radians	Moment, M kN-m	Rotation, ϕ radians
0	0	96.164	0.0129
3.588	0.0005	98.077	0.0137
7.176	0.0009	99.991	0.0148
11.004	0.0012	101.905	0.0158
14.831	0.0016	102.861	0.0167
18.659	0.0019	103.818	0.0175
22.486	0.0021	105.253	0.0184
26.314	0.0024	106.688	0.0193
30.141	0.0026	108.124	0.0202
34.606	0.0029	109.560	0.0210
39.072	0.0031	109.560	0.0220
43.537	0.0034	109.560	0.0230
47.364	0.0039	110.516	0.0238
51.192	0.0043	111.473	0.0245
56.454	0.0048	111.951	0.0254
61.717	0.0053	112.430	0.0263
66.980	0.0058	112.908	0.0273
72.242	0.0062	113.386	0.0282
75.112	0.0068		
77.983	0.0074		
81.332	0.0082		
84.680	0.0089		
87.551	0.0095		
90.422	0.0100		
92.336	0.0111		
94.250	0.0121		

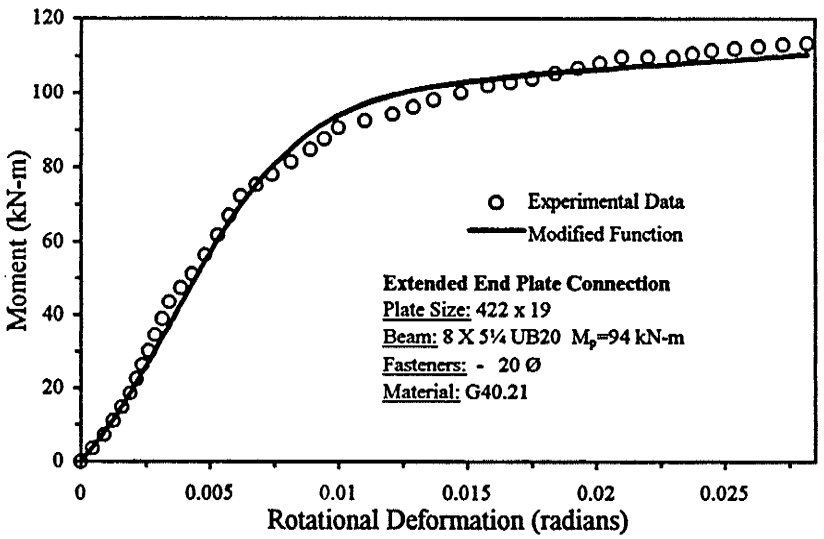


Figure A.255 (a) M-ϕ curve for Bailey: B8-R

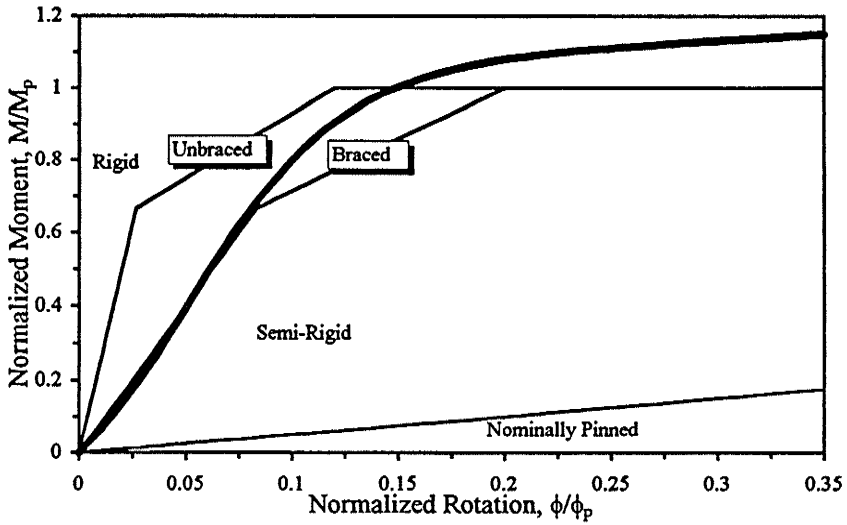


Figure A.255 (b) Eurocode3 Classification of Bailey: B8-R

Table A.256 M-ϕ data for Bailey: C9-L (1970)

Moment, M kN-m	Rotation, ϕ radians	Moment, M kN-m	Rotation, ϕ radians
0	0	70.462	0.0076
3.835	0.0004	71.660	0.0079
7.670	0.0007	72.858	0.0082
11.504	0.0010	74.056	0.0087
15.338	0.0013	75.255	0.0092
18.694	0.0016	76.453	0.0098
22.050	0.0019	77.652	0.0103
24.446	0.0021	78.610	0.0108
26.843	0.0022	79.569	0.0112
29.479	0.0023	80.528	0.0117
32.115	0.0024		
34.991	0.0027		
37.867	0.0030		
40.503	0.0032		
43.139	0.0033		
46.016	0.0036		
48.892	0.0038		
51.289	0.0040		
53.685	0.0042		
55.602	0.0045		
57.519	0.0048		
60.396	0.0052		
63.272	0.0056		
65.189	0.0061		
67.106	0.0066		
68.784	0.0071		

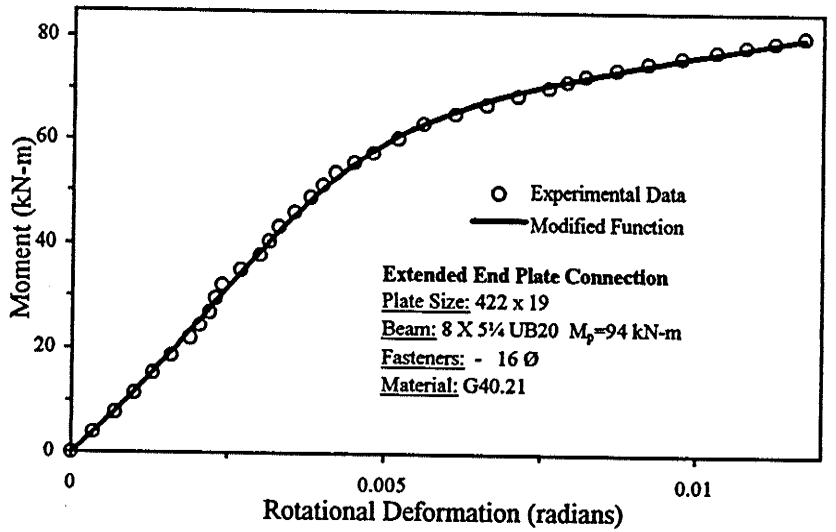


Figure A.256 (a) M-ϕ curve for Bailey: C9-L

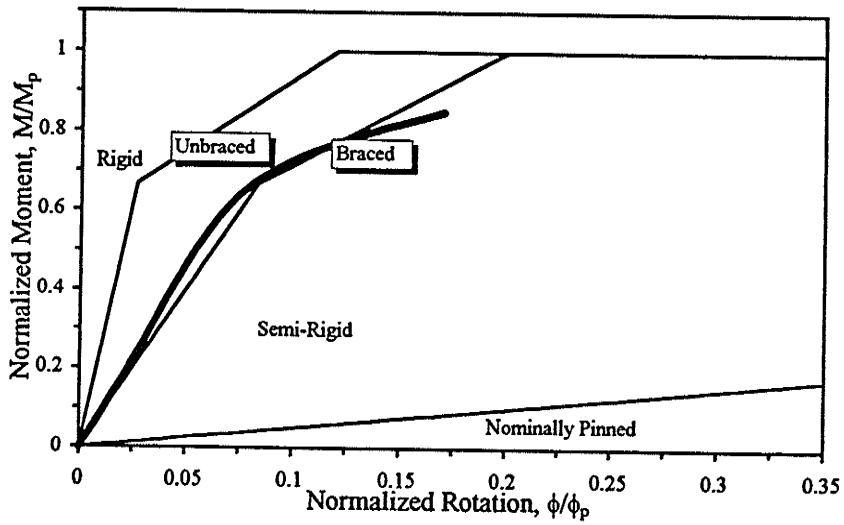


Figure A.256 (b) Eurocode3 Classification of Bailey: C9-L

Table A.257 M-ϕ data for Bailey: C9-R (1970)

Moment, M kN-m	Rotation, ϕ radians	Moment, M kN-m	Rotation, ϕ radians
0	0	72.139	0.0104
2.876	0.0003	73.338	0.0110
5.751	0.0006	74.776	0.0116
8.867	0.0009	76.213	0.0122
11.983	0.0011	77.172	0.0131
15.338	0.0014	78.130	0.0139
18.694	0.0017	79.089	0.0147
21.570	0.0020	80.048	0.0155
24.445	0.0022	80.288	0.0163
27.082	0.0025	80.528	0.0171
29.718	0.0027	81.007	0.0180
32.115	0.0029	81.486	0.0188
34.512	0.0031	81.726	0.0195
37.867	0.0034	81.966	0.0202
41.222	0.0037	81.966	0.0212
44.338	0.0040		
47.454	0.0042		
50.569	0.0045		
53.685	0.0048		
56.561	0.0053		
59.436	0.0058		
62.073	0.0066		
64.709	0.0073		
68.545	0.0083		
69.743	0.0091		
70.941	0.0098		

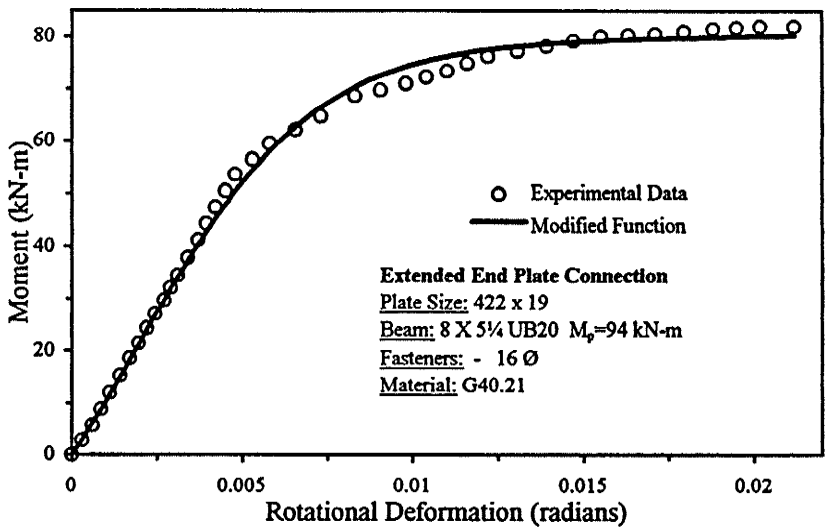


Figure A.257 (a) M-ϕ curve for Bailey: C9-R

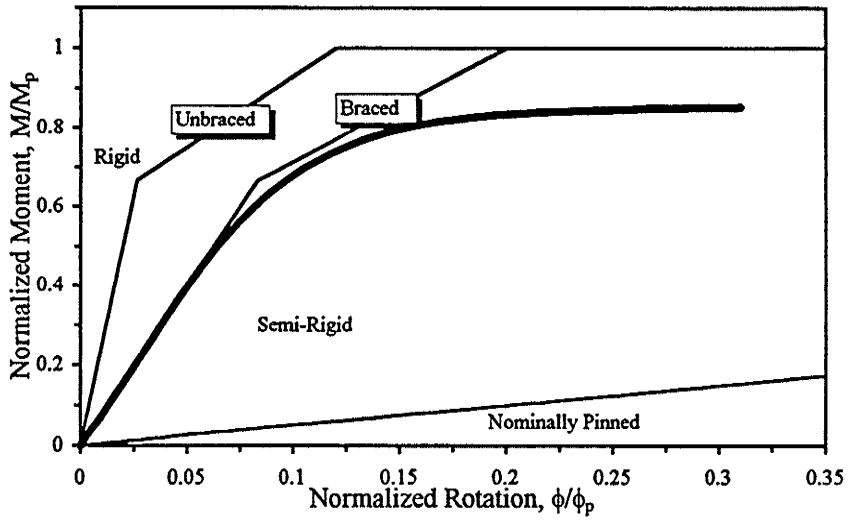


Figure A.257 (b) Eurocode3 Classification of Bailey: C9-R

Table A.258 M-ϕ data for Bailey: C10-L (1970)

Moment, M kN-m	Rotation, ϕ radians	Moment, M kN-m	Rotation, ϕ radians
0	0	181.604	0.0077
10.626	0.0002	186.433	0.0082
21.251	0.0004	189.009	0.0087
29.945	0.0006	191.586	0.0093
38.640	0.0007	194.162	0.0098
45.401	0.0008	198.026	0.0105
52.162	0.0009	201.890	0.0112
59.407	0.0011	204.466	0.0118
66.652	0.0013	207.042	0.0123
74.380	0.0014	209.618	0.0129
82.108	0.0014	212.033	0.0136
90.319	0.0016	214.447	0.0143
98.530	0.0018	216.862	0.0151
105.292	0.0021	219.277	0.0158
112.053	0.0023		
118.332	0.0024		
124.611	0.0025		
132.339	0.0030		
140.067	0.0035		
145.863	0.0040		
151.659	0.0045		
160.353	0.0052		
164.700	0.0056		
169.046	0.0060		
172.910	0.0066		
176.775	0.0071		

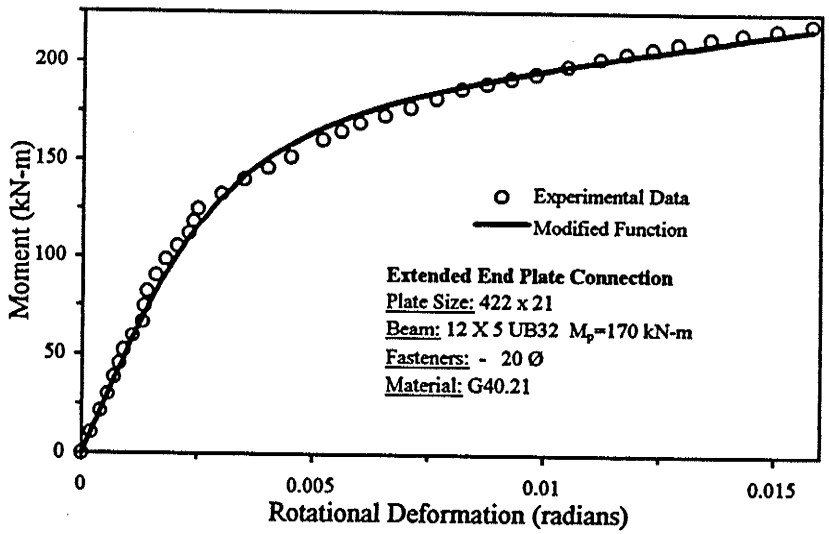


Figure A.258 (a) M-ϕ curve for Bailey: C10-L

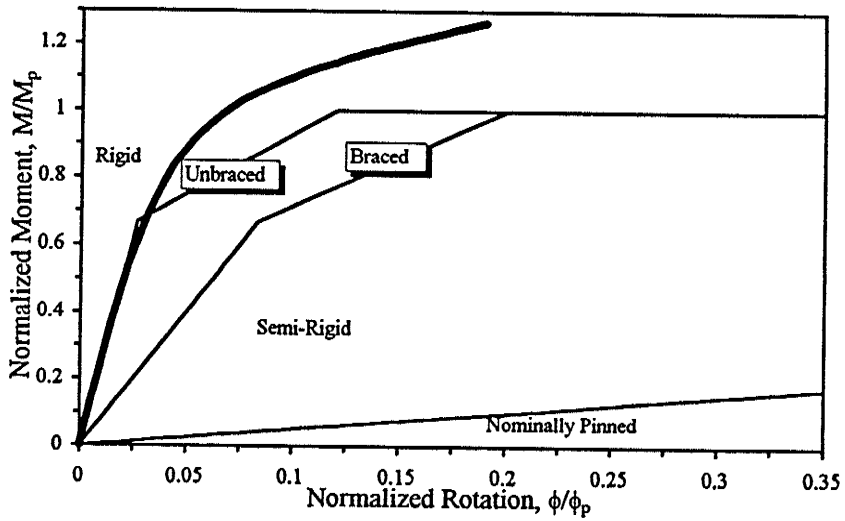


Figure A.258 (b) Eurocode3 Classification of Bailey: C10-L

Table A.259 M-ϕ data for Bailey: C10-R (1970)

Moment, M kN-m	Rotation, ϕ radians	Moment, M kN-m	Rotation, ϕ radians
0	0	180.639	0.0092
8.372	0.0002	183.053	0.0099
16.743	0.0004	185.468	0.0105
25.115	0.0006	189.332	0.0113
34.292	0.0008	193.196	0.0120
43.469	0.0010	196.577	0.0130
51.197	0.0013	199.958	0.0139
58.925	0.0016	202.372	0.0149
69.551	0.0017	204.787	0.0159
76.312	0.0020	206.719	0.0168
83.074	0.0022	208.651	0.0177
89.353	0.0024	210.583	0.0187
95.631	0.0025	212.515	0.0197
102.876	0.0028	212.515	0.0205
110.121	0.0030	212.515	0.0212
115.435	0.0032		
120.748	0.0033		
126.543	0.0036		
132.339	0.0038		
139.584	0.0044		
146.829	0.0049		
152.625	0.0055		
158.421	0.0061		
164.216	0.0068		
170.012	0.0075		
175.325	0.0084		

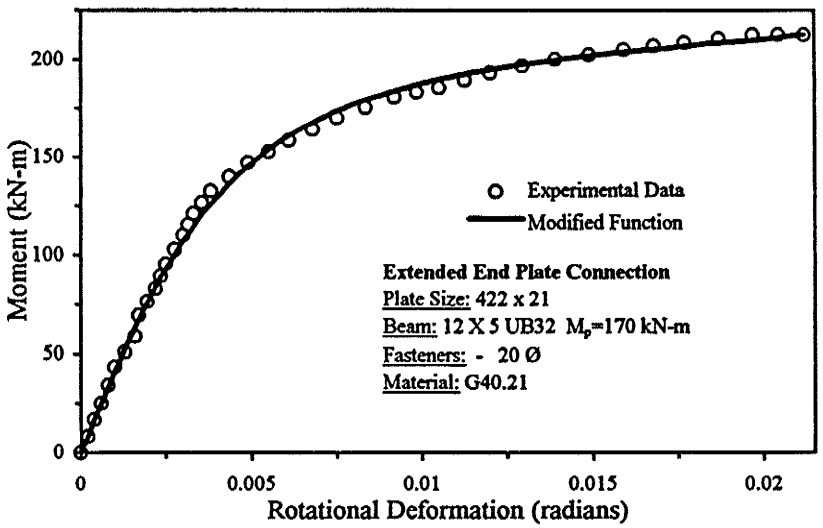


Figure A.259 (a) M-ϕ curve for Bailey: C10-R

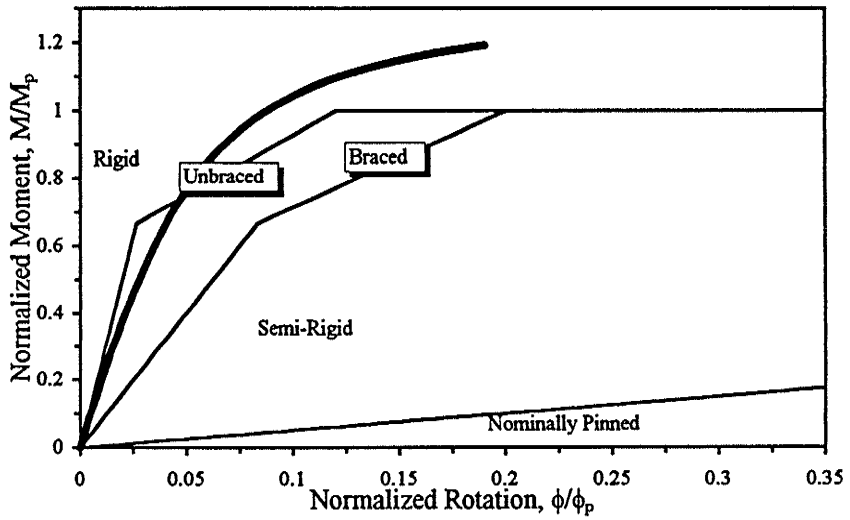


Figure A.259 (b) Eurocode3 Classification of Bailey: C10-R

Table A.260 M-ϕ data for Bailey: C11-L (1970)

Moment, M kN-m	Rotation, ϕ radians	Moment, M kN-m	Rotation, ϕ radians
0	0	140.710	0.0047
6.963	0.0002	142.631	0.0050
13.927	0.0003	143.591	0.0053
20.650	0.0006	144.552	0.0055
27.374	0.0008	145.512	0.0058
33.617	0.0010	148.394	0.0062
39.860	0.0011	151.276	0.0065
46.103	0.0013	153.197	0.0068
52.345	0.0014	155.118	0.0071
58.589	0.0017	156.078	0.0075
64.833	0.0019	157.038	0.0078
69.635	0.0020		
74.437	0.0021		
80.200	0.0023		
85.963	0.0024		
92.206	0.0026		
98.449	0.0028		
102.771	0.0030		
107.094	0.0032		
111.416	0.0033		
115.738	0.0033		
120.541	0.0035		
125.343	0.0037		
132.066	0.0040		
135.428	0.0042		
138.790	0.0044		

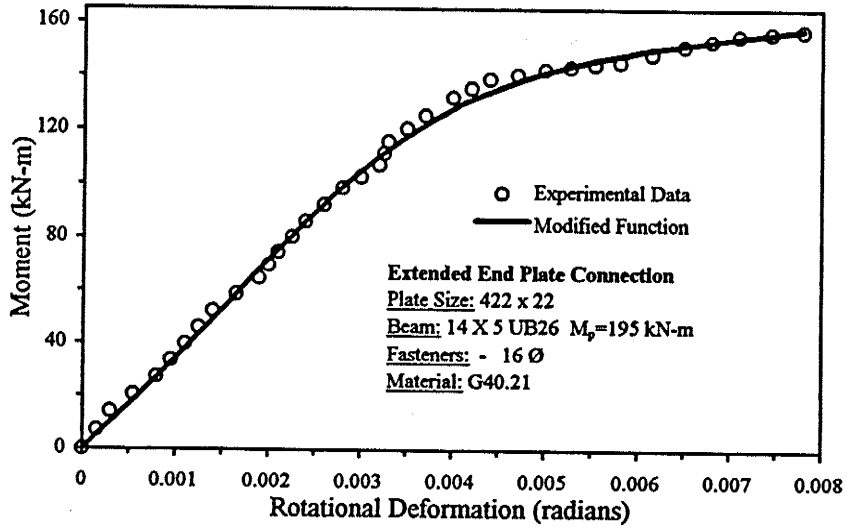


Figure A.260 (a) M-ϕ curve for Bailey: C11-L

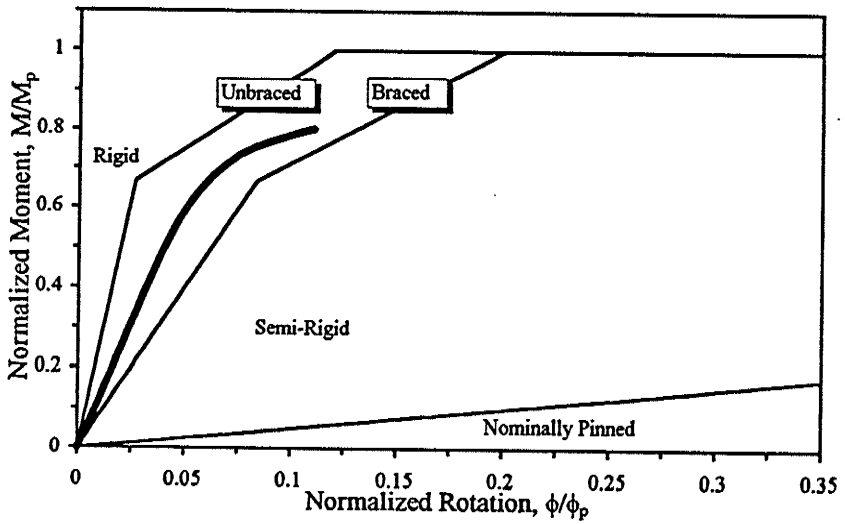


Figure A.260 (b) Eurocode3 Classification of Bailey: C11-L

Table A.261 M-ϕ data for Bailey: C11-R (1970)

Moment, M kN-m	Rotation, ϕ radians	Moment, M kN-m	Rotation, ϕ radians
0	0	139.750	0.0054
7.203	0.0003	142.151	0.0057
14.407	0.0005	144.552	0.0060
21.610	0.0008		
27.694	0.0010		
33.777	0.0012		
39.860	0.0014		
46.583	0.0017		
53.307	0.0019		
58.589	0.0021		
63.871	0.0022		
69.154	0.0024		
74.437	0.0026		
79.240	0.0028		
84.042	0.0030		
91.245	0.0032		
98.449	0.0033		
104.692	0.0036		
110.936	0.0038		
114.778	0.0040		
118.620	0.0042		
122.462	0.0044		
127.264	0.0046		
132.066	0.0047		
134.628	0.0049		
137.189	0.0052		

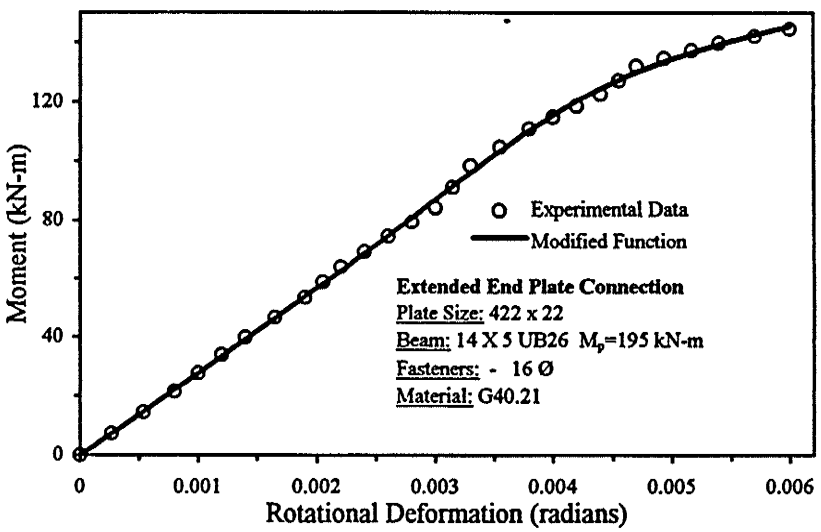


Figure A.261 (a) M-ϕ curve for Bailey: C11-R

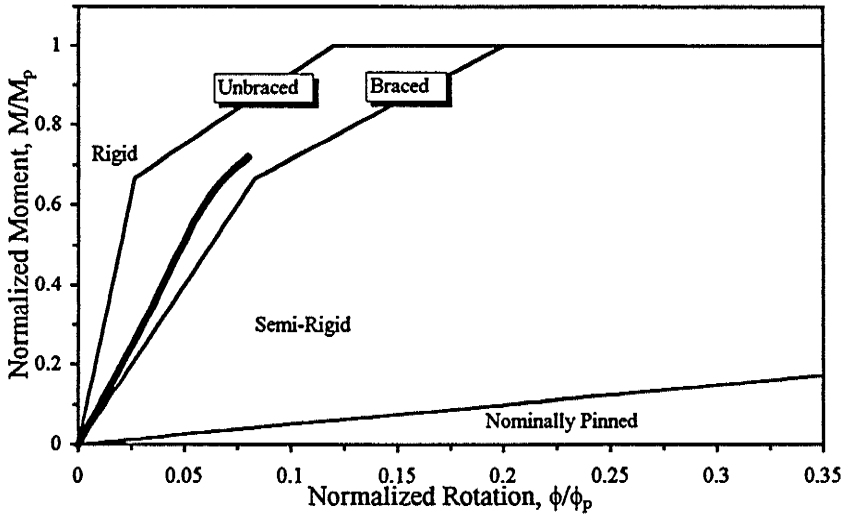


Figure A.261 (b) Eurocode3 Classification of Bailey: C11-R

Table A.262 M-ϕ data for Bailey: C12-L (1970)

Moment, M kN-m	Rotation, ϕ radians	Moment, M kN-m	Rotation, ϕ radians
0	0	293.752	0.0212
10.525	0.0004	293.752	0.0233
21.050	0.0007	299.494	0.0251
31.576	0.0011	301.407	0.0274
44.972	0.0014	303.321	0.0296
58.368	0.0017	305.234	0.0311
69.850	0.0021	306.192	0.0324
81.332	0.0025	307.149	0.0336
94.728	0.0030	307.149	0.0355
108.124	0.0034	309.062	0.0373
120.563	0.0037	309.062	0.0392
133.002	0.0040	309.062	0.0412
144.484	0.0045	312.889	0.0434
155.967	0.0049	310.976	0.0452
170.319	0.0054	314.804	0.0474
184.672	0.0059	312.889	0.0485
195.197	0.0065		
205.723	0.0070		
215.291	0.0077		
224.860	0.0084		
240.169	0.0099		
255.479	0.0115		
265.047	0.0133		
274.616	0.0156		
280.356	0.0177		
288.011	0.0195		

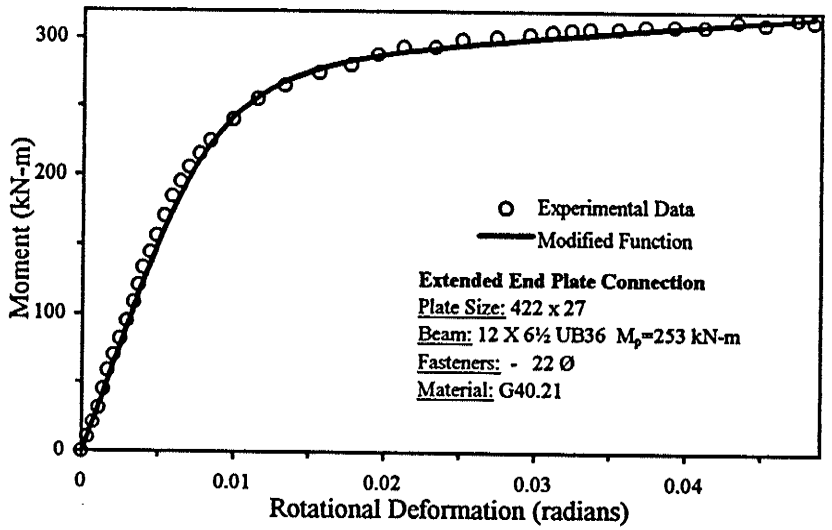


Figure A.262 (a) M-ϕ curve for Bailey: C12-L

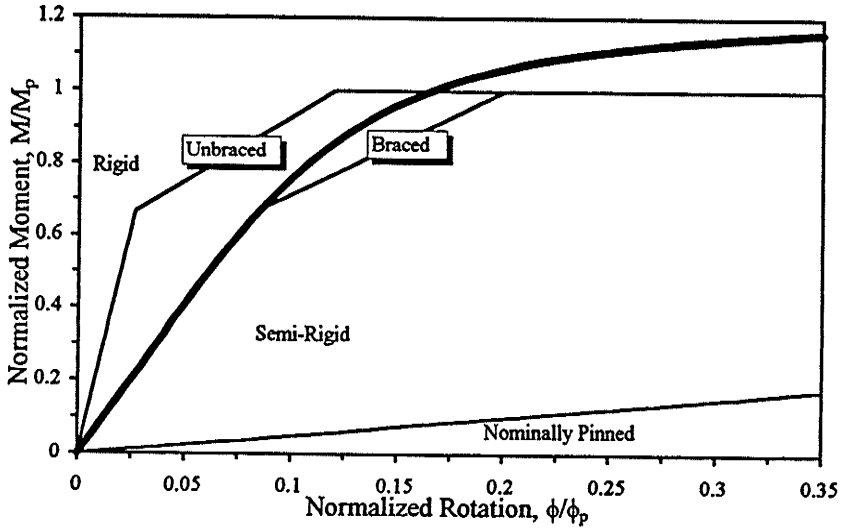


Figure A.262 (b) Eurocode3 Classification of Bailey: C12-L

Table A.263 M-ϕ data for Bailey: C12-R (1970)

Moment, M kN-m	Rotation, ϕ radians	Moment, M kN-m	Rotation, ϕ radians
0	0	315.636	0.0179
16.359	0.0004	321.411	0.0201
32.719	0.0007	322.373	0.0213
48.115	0.0011	323.335	0.0225
63.512	0.0014	329.109	0.0247
77.947	0.0017	331.033	0.0268
92.382	0.0019	332.958	0.0286
106.816	0.0022	332.958	0.0304
121.251	0.0025	332.958	0.0324
132.799	0.0028	336.807	0.0342
144.346	0.0030	336.807	0.0365
154.932	0.0034	338.731	0.0383
165.517	0.0038	338.731	0.0402
179.951	0.0041	336.807	0.0421
194.385	0.0043	340.657	0.0442
205.933	0.0048	340.657	0.0459
217.482	0.0053	340.657	0.0472
226.142	0.0059		
234.802	0.0065		
246.350	0.0074		
257.897	0.0082		
266.558	0.0090		
275.219	0.0098		
290.616	0.0119		
300.240	0.0137		
307.938	0.0159		

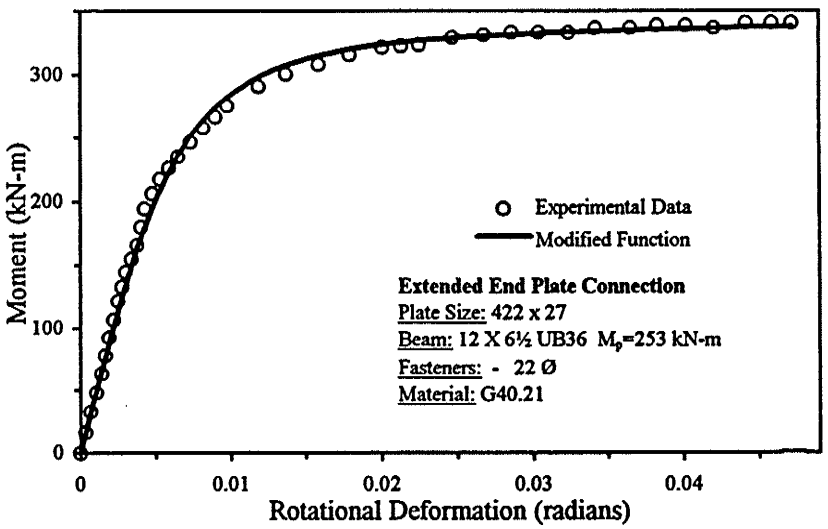


Figure A.263 (a) M-ϕ curve for Bailey: C12-R

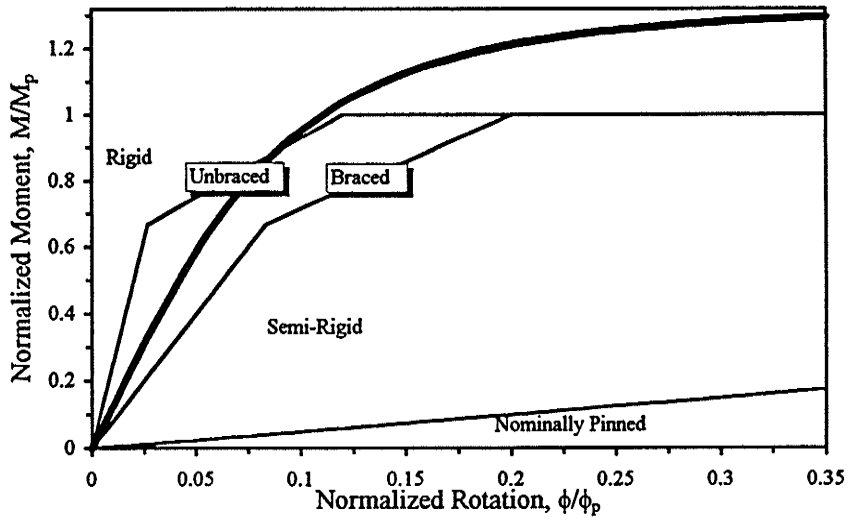


Figure A.263 (b) Eurocode3 Classification of Bailey: C12-R

Table A.264 M-ϕ data for Bailey: C13-L (1970)

Moment, M kN-m	Rotation, ϕ radians	Moment, M kN-m	Rotation, ϕ radians
0	0	273.142	0.0082
4.775	0.0001	284.603	0.0090
9.550	0.0002	291.288	0.0096
14.326	0.0003	297.974	0.0102
19.101	0.0004	302.749	0.0107
23.876	0.0005	307.524	0.0112
28.651	0.0006	311.344	0.0117
33.017	0.0007	315.164	0.0122
37.383	0.0008	318.984	0.0128
46.116	0.0010	322.804	0.0134
59.213	0.0013	325.669	0.0140
72.583	0.0017	328.534	0.0145
85.954	0.0021	329.489	0.0151
101.234	0.0025	330.445	0.0157
116.515	0.0029	331.400	0.0163
131.796	0.0033	332.355	0.0168
147.077	0.0037		
160.447	0.0040		
173.817	0.0043		
186.233	0.0046		
198.649	0.0048		
213.929	0.0053		
227.301	0.0058		
240.670	0.0066		
249.266	0.0070		
257.862	0.0074		

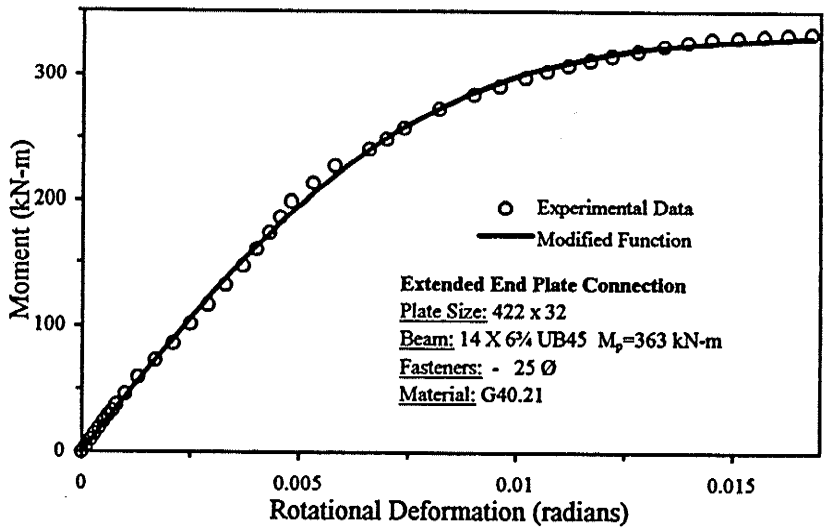


Figure A.264 (a) M-ϕ curve for Bailey: C13-L

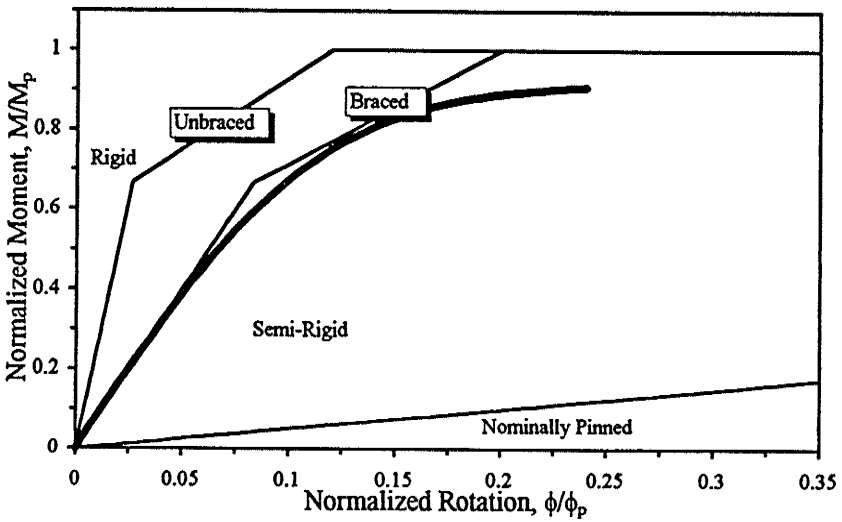


Figure A.264 (b) Eurocode3 Classification of Bailey: C13-L

Table A.265 M-ϕ data for Bailey: C13-R (1970)

Moment, M kN-m	Rotation, ϕ radians	Moment, M kN-m	Rotation, ϕ radians
0	0	293.448	0.0115
14.720	0.0002	299.145	0.0122
29.440	0.0004	302.944	0.0131
43.685	0.0008	306.742	0.0139
57.930	0.0012	310.541	0.0147
72.175	0.0015	314.340	0.0154
86.420	0.0018	316.240	0.0162
100.665	0.0021	318.139	0.0170
114.910	0.0023	319.089	0.0179
126.305	0.0026	320.039	0.0187
137.701	0.0029	320.039	0.0195
149.097	0.0032	320.039	0.0203
160.494	0.0034		
175.689	0.0037		
184.236	0.0040		
192.783	0.0042		
202.279	0.0048		
215.574	0.0054		
226.971	0.0059		
242.166	0.0069		
251.662	0.0076		
261.158	0.0083		
267.806	0.0090		
274.455	0.0096		
281.102	0.0102		
287.750	0.0107		

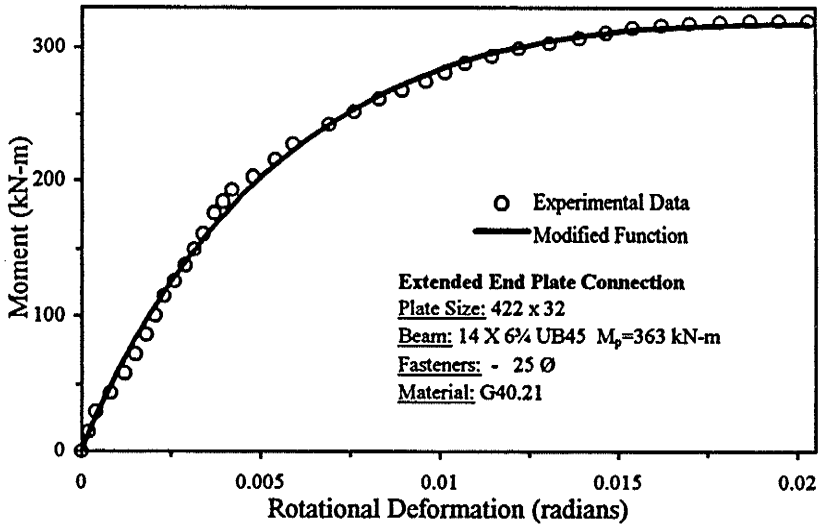


Figure A.265 (a) M-ϕ curve for Bailey: C13-R

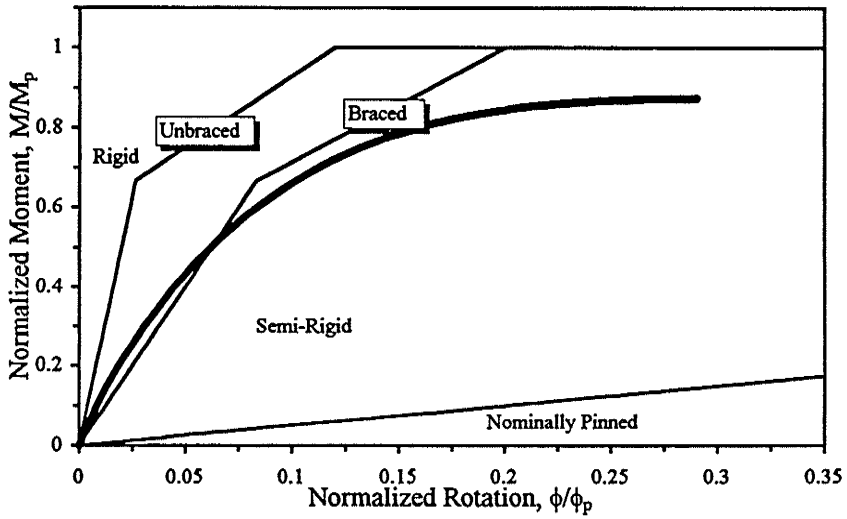


Figure A.265 (b) Eurocode3 Classification of Bailey: C13-R

Table A.266 M-ϕ data for Surtees: Test C6 (1970)

Moment, M kN-m	Rotation, ϕ radians	Moment, M kN-m	Rotation, ϕ radians
0	0	548.191	0.0071
23.452	0.0002	558.451	0.0084
46.905	0.0003	564.314	0.0099
64.494	0.0005	571.644	0.0115
82.083	0.0007	574.575	0.0132
108.466	0.0010	580.437	0.0148
134.850	0.0012	584.834	0.0161
156.103	0.0014	589.233	0.0176
177.356	0.0016	590.698	0.0191
196.411	0.0018	593.630	0.0209
215.466	0.0020	595.095	0.0222
239.651	0.0023	596.561	0.0237
263.836	0.0025	598.026	0.0257
285.089	0.0027	602.423	0.0272
306.342	0.0029	603.889	0.0289
327.595	0.0031	605.356	0.0302
348.848	0.0033	608.287	0.0313
364.972	0.0035	609.753	0.0326
381.095	0.0037	611.219	0.0339
400.150	0.0039	612.684	0.0351
419.205	0.0040	615.615	0.0363
440.458	0.0042	617.081	0.0375
461.711	0.0044	618.547	0.0386
489.561	0.0048	621.478	0.0400
510.081	0.0052		
530.602	0.0061		

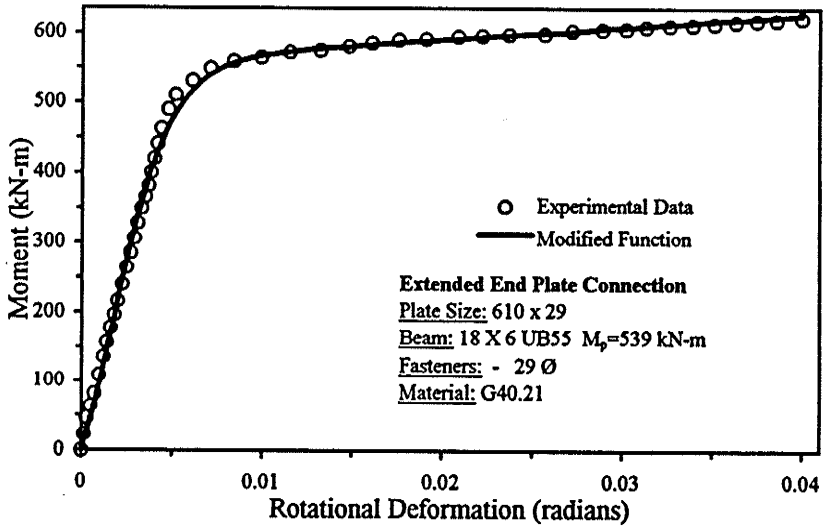


Figure A.266 (a) M-ϕ curve for Surtees: Test C6

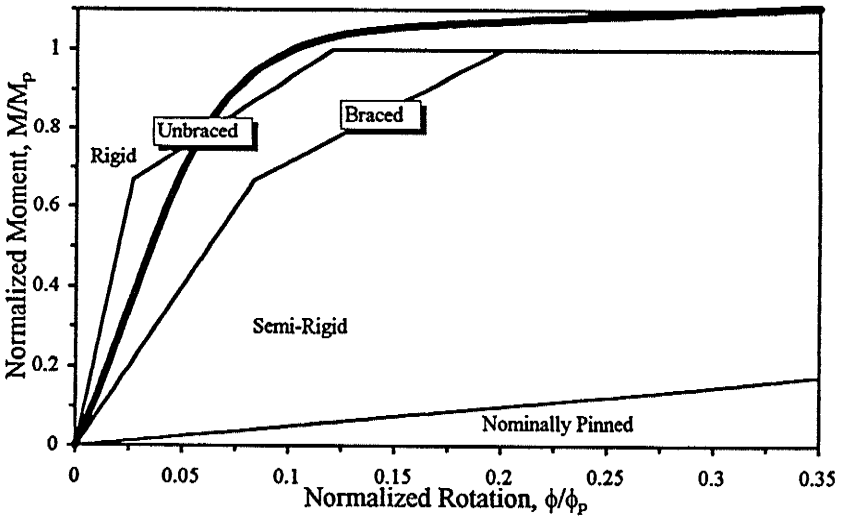


Figure A.266 (b) Eurocode3 Classification of Surtees: Test C6

Table A.267 M-ϕ data for Johnstone: Test 1-L (1981)

Moment, M kN-m	Rotation, ϕ radians	Moment, M kN-m	Rotation, ϕ radians
0	0	260.207	0.0240
11.375	0.0001	263.051	0.0263
22.751	0.0001	265.183	0.0286
34.125	0.0004	267.316	0.0309
45.500	0.0006	268.027	0.0330
56.875	0.0009	268.738	0.0351
68.251	0.0011	270.159	0.0387
79.626	0.0014	273.004	0.0420
93.134	0.0014	273.714	0.0439
106.642	0.0013	274.425	0.0458
117.306	0.0015	275.847	0.0494
127.970	0.0017	277.269	0.0531
140.056	0.0023	278.691	0.0555
152.142	0.0029	280.112	0.0578
162.806	0.0035	282.957	0.0613
173.470	0.0041	283.668	0.0637
184.846	0.0047	284.379	0.0661
196.221	0.0052	285.090	0.0684
204.041	0.0061	285.800	0.0706
211.862	0.0069	286.511	0.0726
224.659	0.0097	287.222	0.0746
233.190	0.0120		
240.300	0.0147		
247.410	0.0173		
252.387	0.0195		
257.363	0.0217		

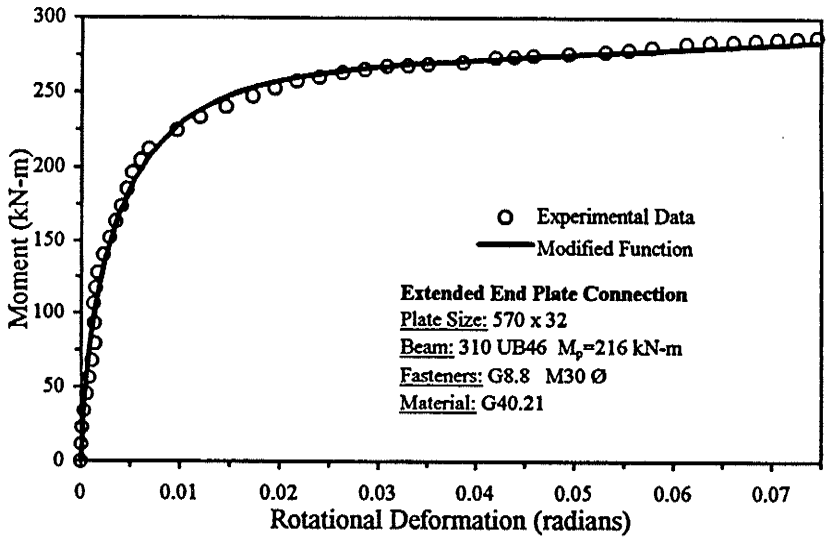


Figure A.267 (a) M-ϕ curve for Johnstone: Test 1-L

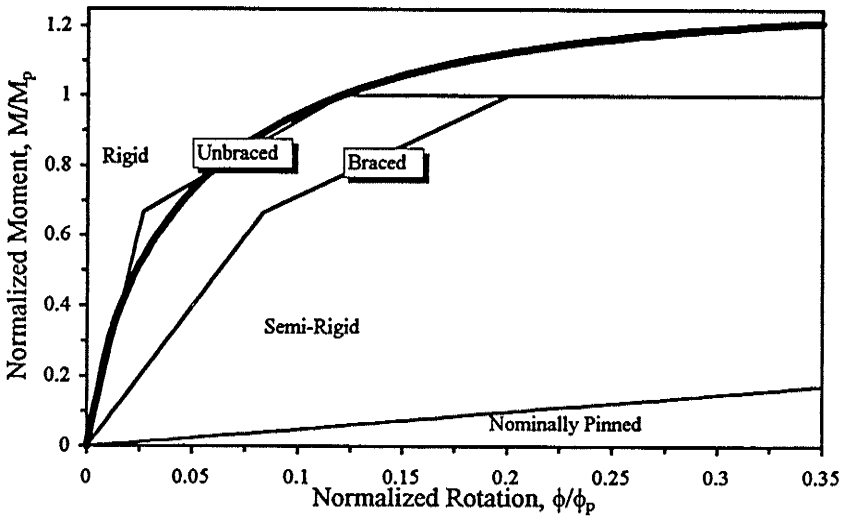


Figure A.267 (b) Eurocode3 Classification of Johnstone: Test 1-L

Table A.268 M-ϕ data for Johnstone: Test 1-R (1981)

Moment, M kN-m	Rotation, ϕ radians	Moment, M kN-m	Rotation, ϕ radians
0	0	271.546	0.0256
12.971	0.0001	272.972	0.0279
25.943	0.0002	274.398	0.0301
38.914	0.0004	276.536	0.0323
51.886	0.0005	278.674	0.0344
64.857	0.0006	280.099	0.0363
78.399	0.0008	281.524	0.0381
91.941	0.0009	284.375	0.0404
104.057	0.0011	287.226	0.0426
116.173	0.0013	290.077	0.0445
126.152	0.0016	292.928	0.0464
136.130	0.0018	295.778	0.0487
151.097	0.0023	298.629	0.0510
166.064	0.0027	301.480	0.0535
181.030	0.0034	304.331	0.0559
195.997	0.0041	305.044	0.0581
206.689	0.0048	305.756	0.0603
217.380	0.0054	311.459	0.0639
227.357	0.0073	311.459	0.0675
237.335	0.0091	309.321	0.0704
251.590	0.0123	307.183	0.0733
255.866	0.0143		
260.143	0.0163		
262.993	0.0185		
265.844	0.0207		
268.695	0.0232		

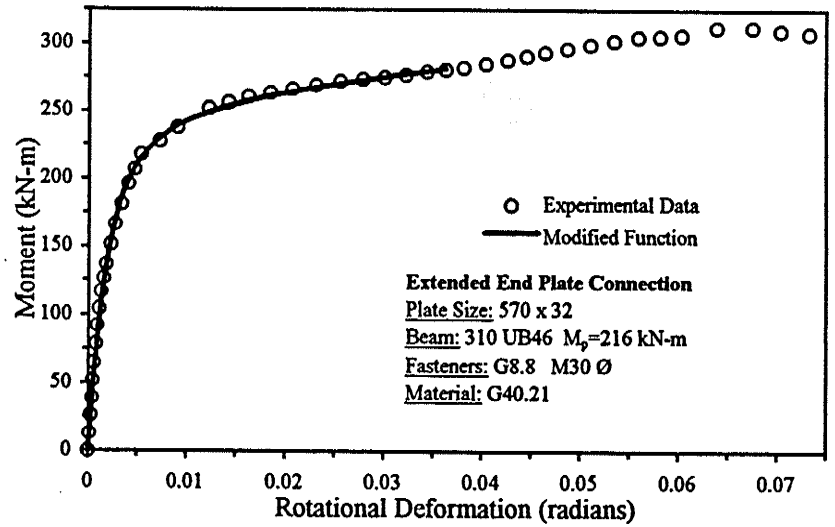


Figure A.268 (a) M-ϕ curve for Johnstone: Test 1-R

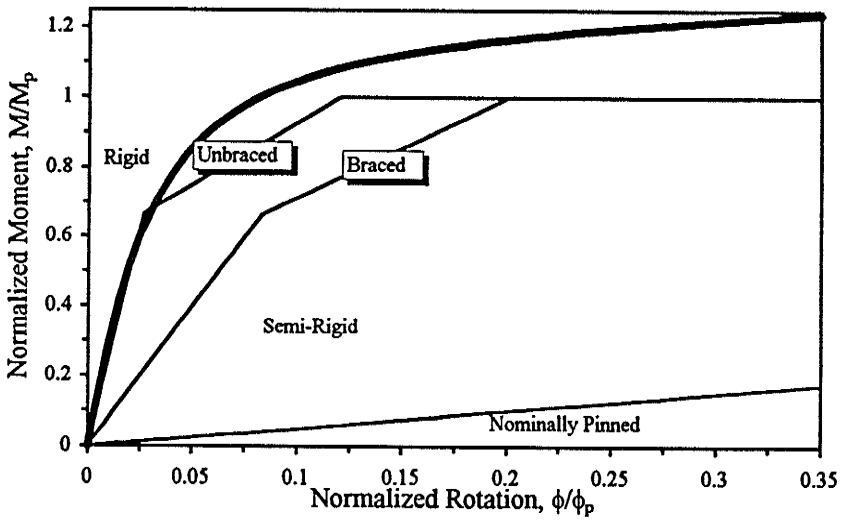


Figure A.268 (b) Eurocode3 Classification of Johnstone: Test 1-R

Table A.269 M-ϕ data for Johnstone: Test 2-L (1981)

Moment, M kN-m	Rotation, ϕ radians	Moment, M kN-m	Rotation, ϕ radians
0	0	265.844	0.0310
13.898	0.0004	268.695	0.0343
27.796	0.0008	271.546	0.0375
39.674	0.0010	272.259	0.0405
51.553	0.0012	272.971	0.0434
63.432	0.0014	274.397	0.0466
76.261	0.0018	275.823	0.0497
89.090	0.0022	277.961	0.0527
101.918	0.0026	280.099	0.0556
113.322	0.0029	281.049	0.0585
124.726	0.0032	282.000	0.0613
136.130	0.0035	282.950	0.0642
146.108	0.0039	284.851	0.0669
156.086	0.0043	286.751	0.0695
166.064	0.0047	288.651	0.0722
178.892	0.0053	290.077	0.0752
191.721	0.0058	291.503	0.0781
204.551	0.0068	292.928	0.0800
217.380	0.0077		
229.496	0.0105		
241.613	0.0132		
247.314	0.0161		
253.016	0.0190		
258.718	0.0219		
261.093	0.0249		
263.468	0.0280		

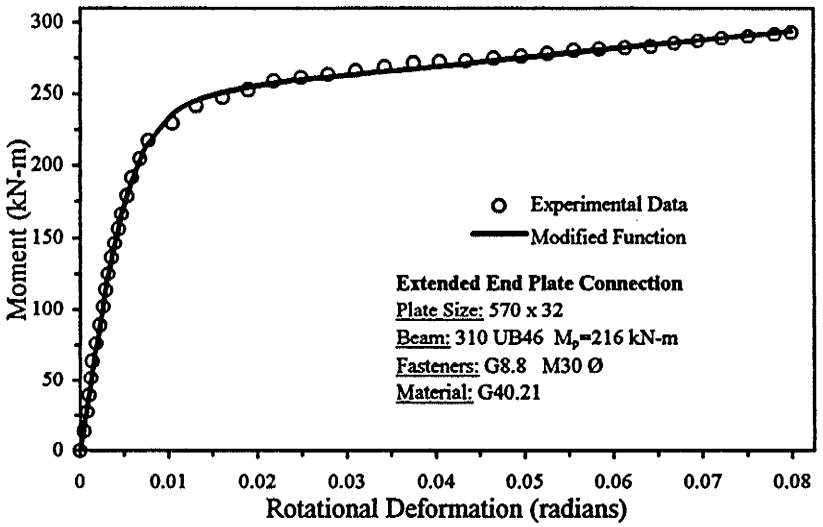


Figure A.269 (a) M-ϕ curve for Johnstone: Test 2-L

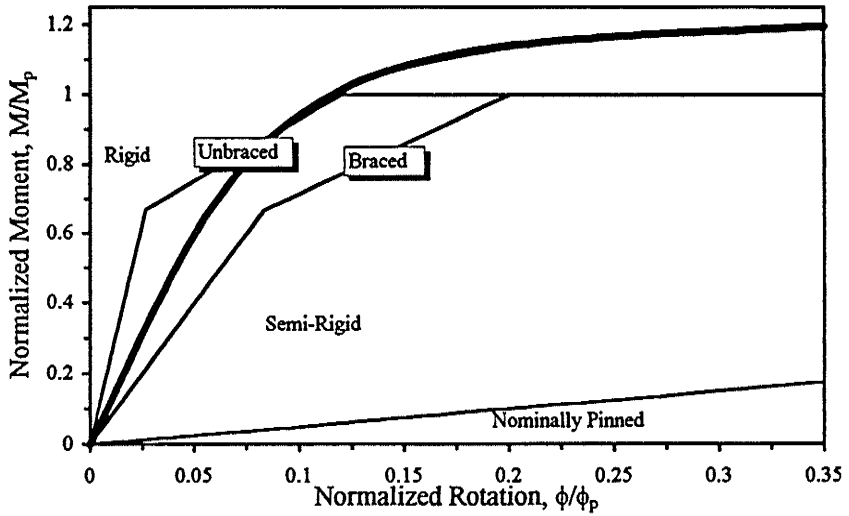


Figure A.269 (b) Eurocode3 Classification of Johnstone: Test 2-L

Table A.270 M-ϕ data for Johnstone: Test 2-R (1981)

Moment, M kN-m	Rotation, ϕ radians	Moment, M kN-m	Rotation, ϕ radians
0	0	245.688	0.0245
12.750	0.0002	248.553	0.0274
25.500	0.0004	251.418	0.0303
38.250	0.0006	253.567	0.0333
51.001	0.0008	255.716	0.0363
63.751	0.0010	257.149	0.0400
73.301	0.0014	258.582	0.0437
82.851	0.0019	260.014	0.0465
92.402	0.0023	261.447	0.0493
102.907	0.0028	260.014	0.0523
113.413	0.0033	258.582	0.0553
123.918	0.0038	258.104	0.0584
133.469	0.0043	257.627	0.0615
143.020	0.0049	257.149	0.0646
152.570	0.0054	257.865	0.0684
164.031	0.0060	258.582	0.0721
175.492	0.0065	260.014	0.0744
184.565	0.0072	261.447	0.0766
193.637	0.0080	261.447	0.0799
202.710	0.0087		
214.887	0.0110		
227.065	0.0132		
232.795	0.0159		
238.525	0.0185		
242.107	0.0215		
245.688	0.0244		

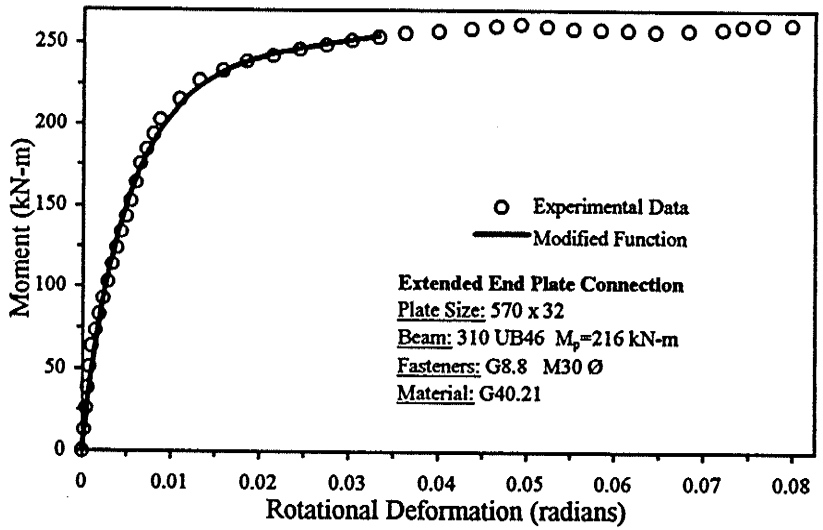


Figure A.270 (a) M-ϕ curve for Johnstone: Test 2-R

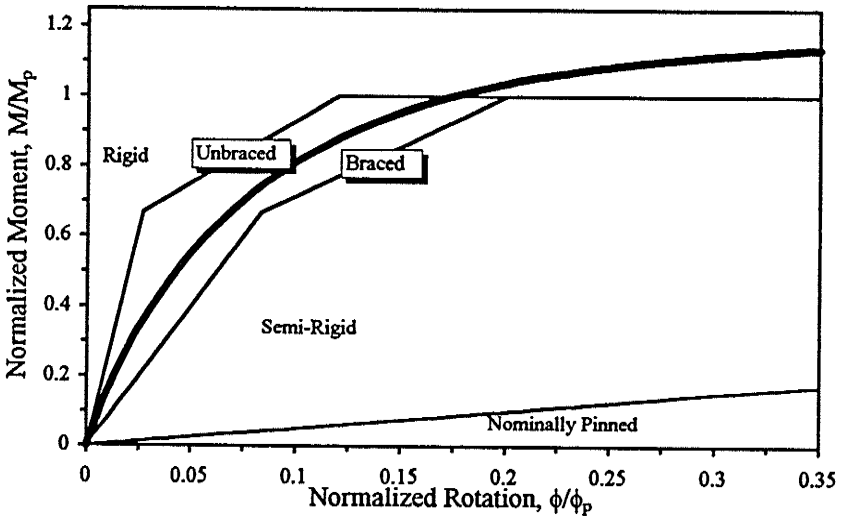


Figure A.270 (b) Eurocode3 Classification of Johnstone: Test 2-R

Table A.271 M-ϕ data for Johnstone: Test 3-L (1981)

Moment, M kN-m	Rotation, ϕ radians	Moment, M kN-m	Rotation, ϕ radians
0	0	243.038	0.0410
9.741	0.0002	245.888	0.0468
19.481	0.0005	248.739	0.0525
29.222	0.0007	250.877	0.0581
39.675	0.0009	253.015	0.0636
50.128	0.0010	253.728	0.0673
60.581	0.0012	254.441	0.0710
70.559	0.0017	257.292	0.0773
80.538	0.0022	260.143	0.0835
90.516	0.0027	261.568	0.0883
100.019	0.0032	262.993	0.0932
109.522	0.0038	264.419	0.0980
119.025	0.0043	267.983	0.1037
128.528	0.0050	271.546	0.1093
138.031	0.0057	272.259	0.1141
147.534	0.0064	272.971	0.1188
160.362	0.0079	272.496	0.1233
173.191	0.0093	272.021	0.1278
183.882	0.0109	271.546	0.1323
194.572	0.0124		
205.976	0.0156		
217.380	0.0188		
230.209	0.0247		
233.772	0.0282		
237.335	0.0316		
240.186	0.0363		

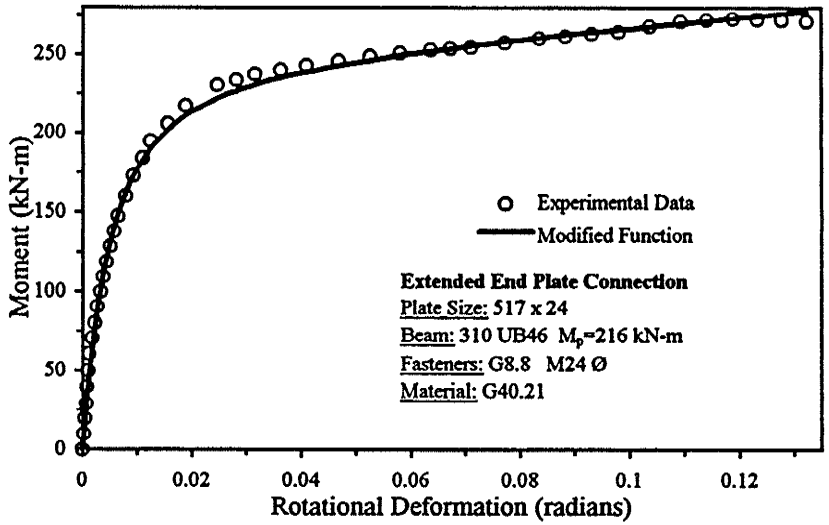


Figure A.271 (a) M-ϕ curve for Johnstone: Test 3-L

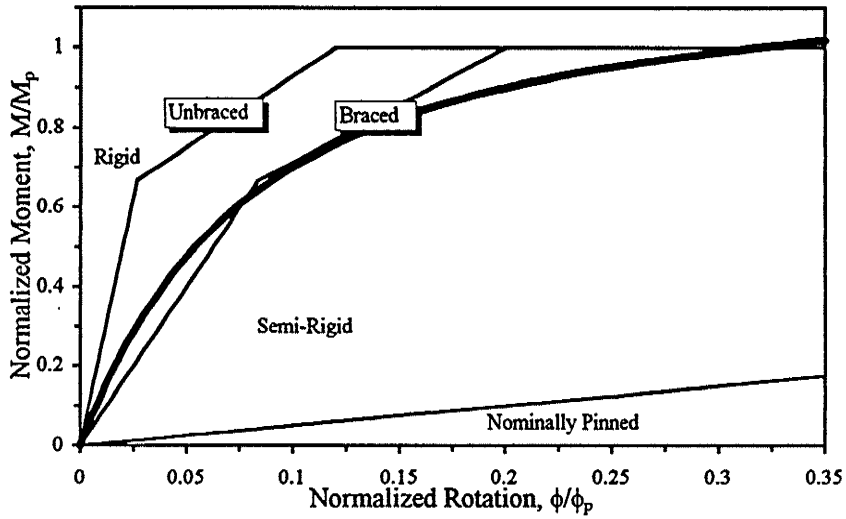


Figure A.271 (b) Eurocode3 Classification of Johnstone: Test 3-L

Table A.272 M-ϕ data for Johnstone: Test 3-R (1981)

Moment, M kN-m	Rotation, ϕ radians	Moment, M kN-m	Rotation, ϕ radians
0	0	221.815	0.0250
9.005	0.0002	225.133	0.0273
18.011	0.0004	228.450	0.0297
27.016	0.0006	231.768	0.0320
35.073	0.0007	234.138	0.0341
43.130	0.0008	236.508	0.0363
51.188	0.0009	238.878	0.0384
62.563	0.0014	238.878	0.0402
73.938	0.0018	238.878	0.0420
84.602	0.0027	238.404	0.0438
95.267	0.0035	237.930	0.0456
106.642	0.0042	237.456	0.0474
118.017	0.0049	238.878	0.0485
126.075	0.0054		
134.132	0.0059		
142.189	0.0064		
152.143	0.0077		
162.096	0.0089		
172.049	0.0103		
182.003	0.0116		
190.534	0.0134		
199.066	0.0152		
205.464	0.0173		
211.862	0.0194		
215.179	0.0213		
218.497	0.0231		

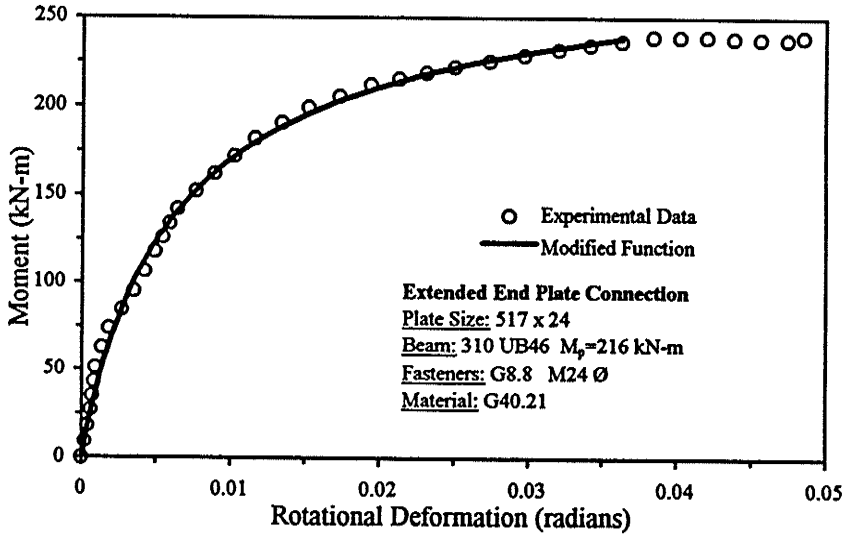


Figure A.272 (a) M-ϕ curve for Johnstone: Test 3-R

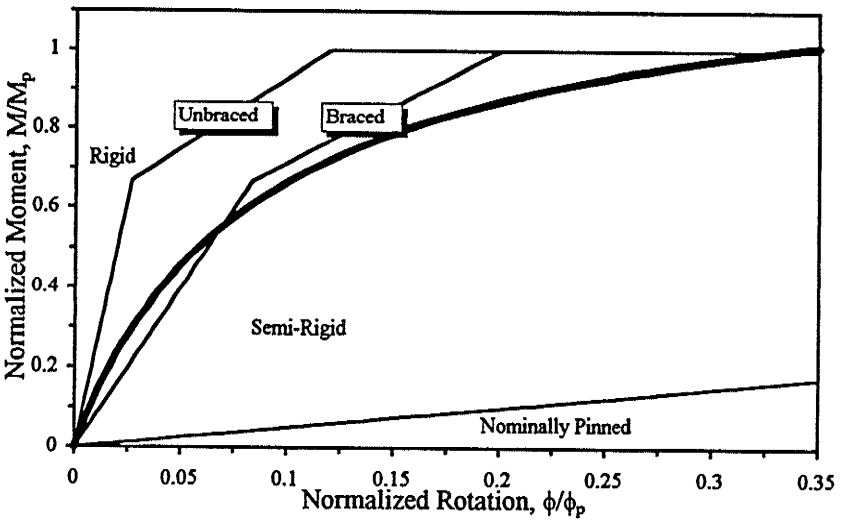


Figure A.272 (b) Eurocode3 Classification of Johnstone: Test 3-R

Table A.273 M-ϕ data for Johnstone: Test 4-L (1981)

Moment, M kN-m	Rotation, ϕ radians	Moment, M kN-m	Rotation, ϕ radians
0	0	233.546	0.0448
11.020	0.0001	237.812	0.0486
22.039	0.0003	243.677	0.0526
33.059	0.0004	249.543	0.0565
46.389	0.0011	251.675	0.0602
59.720	0.0017	253.808	0.0638
68.962	0.0022	257.541	0.0684
78.204	0.0028	261.273	0.0730
87.446	0.0033	265.006	0.0770
99.710	0.0039	268.738	0.0810
111.974	0.0044	270.338	0.0844
119.972	0.0055	271.937	0.0878
127.970	0.0065	270.870	0.0926
137.035	0.0082	269.804	0.0974
146.099	0.0098	269.804	0.1001
155.164	0.0114	269.804	0.1028
164.229	0.0129		
173.827	0.0153		
183.425	0.0176		
195.155	0.0218		
201.553	0.0245		
207.952	0.0271		
214.350	0.0306		
220.749	0.0340		
225.015	0.0375		
229.280	0.0409		

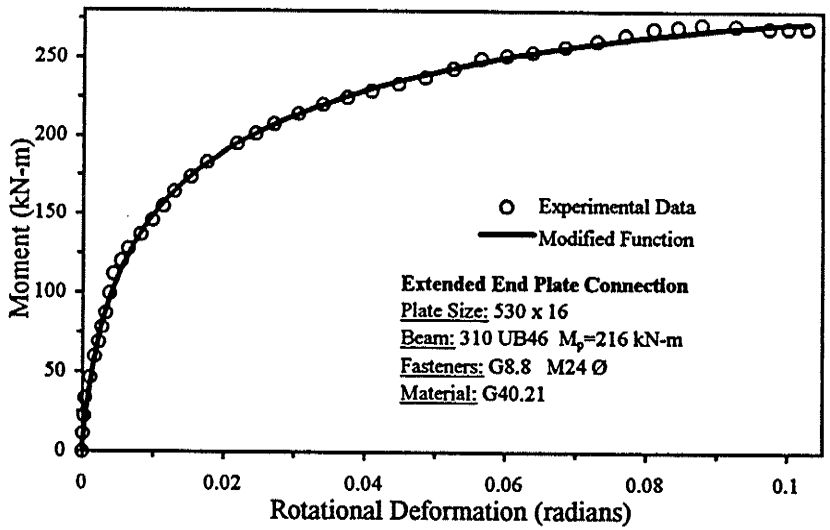


Figure A.273 (a) M-ϕ curve for Johnstone: Test 4-L

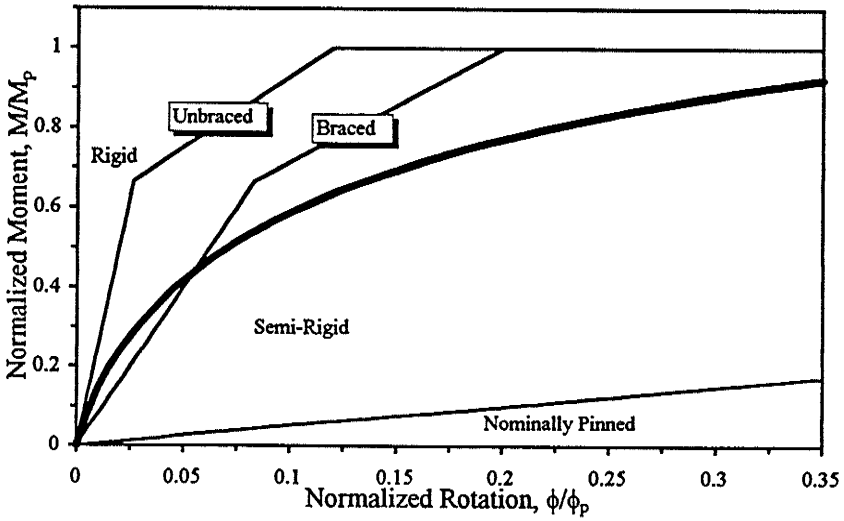


Figure A.273 (b) Eurocode3 Classification of Johnstone: Test 4-L

Table A.274 M-ϕ data for Johnstone: Test 4-R (1981)

Moment, M kN-m	Rotation, ϕ radians	Moment, M kN-m	Rotation, ϕ radians
0	0	185.346	0.0280
9.124	0.0006	187.135	0.0298
18.248	0.0012	188.924	0.0316
27.372	0.0018	191.429	0.0339
36.496	0.0024	193.933	0.0363
45.441	0.0029	196.438	0.0386
54.386	0.0035	197.153	0.0403
63.332	0.0040	197.869	0.0419
71.204	0.0047	198.584	0.0436
79.075	0.0054	195.364	0.0458
86.947	0.0061	192.144	0.0479
94.461	0.0070		
101.975	0.0078		
109.489	0.0087		
116.646	0.0098		
123.802	0.0109		
130.959	0.0120		
137.399	0.0126		
143.840	0.0133		
150.280	0.0139		
157.257	0.0156		
164.235	0.0172		
170.138	0.0195		
176.042	0.0218		
179.799	0.0240		
183.556	0.0262		

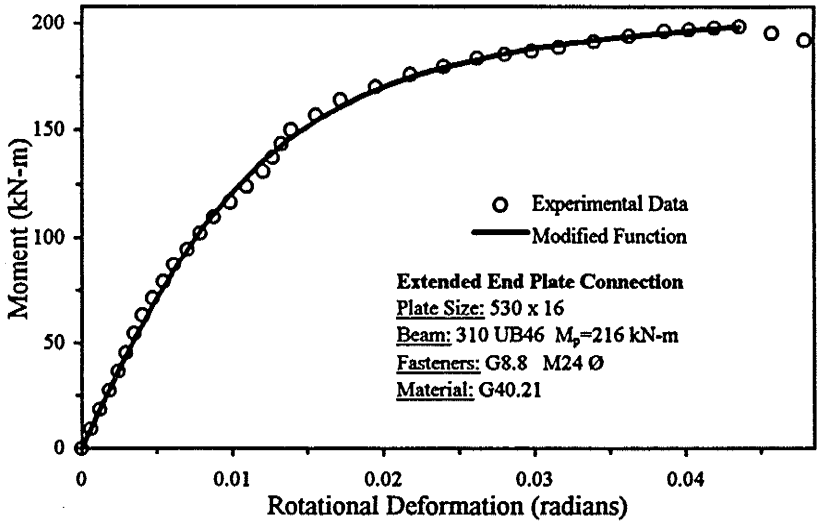


Figure A.274 (a) M-ϕ curve for Johnstone: Test 4-R

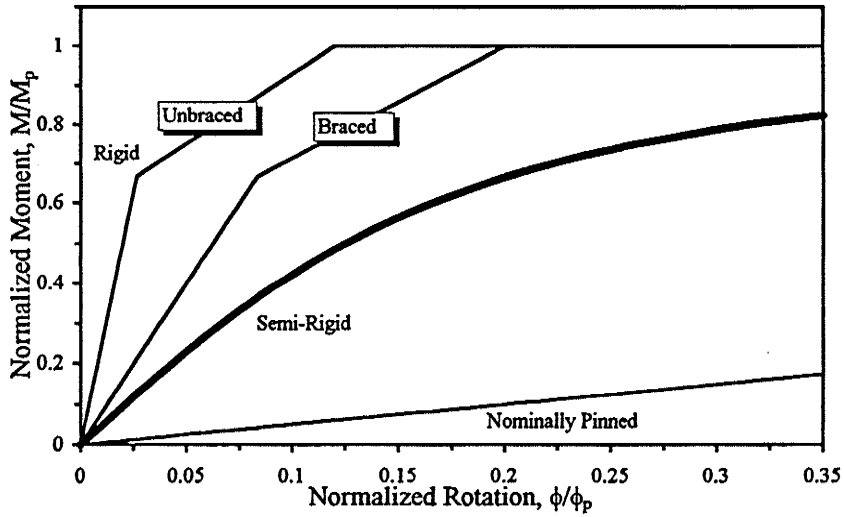


Figure A.274 (b) Eurocode3 Classification of Johnstone: Test 4-R